



Kent Academic Repository

Schlichtner, Stephanie (2022) *Fundamental immunosuppressive pathway determining ability of cancer and embryonic cells to escape cytotoxic immune attack*. Doctor of Philosophy (PhD) thesis, University of Kent,.

Downloaded from

<https://kar.kent.ac.uk/99185/> The University of Kent's Academic Repository KAR

The version of record is available from

<https://doi.org/10.22024/UniKent/01.02.99185>

This document version

UNSPECIFIED

DOI for this version

Licence for this version

CC BY (Attribution)

Additional information

Versions of research works

Versions of Record

If this version is the version of record, it is the same as the published version available on the publisher's web site. Cite as the published version.

Author Accepted Manuscripts

If this document is identified as the Author Accepted Manuscript it is the version after peer review but before type setting, copy editing or publisher branding. Cite as Surname, Initial. (Year) 'Title of article'. To be published in **Title of Journal**, Volume and issue numbers [peer-reviewed accepted version]. Available at: DOI or URL (Accessed: date).

Enquiries

If you have questions about this document contact ResearchSupport@kent.ac.uk. Please include the URL of the record in KAR. If you believe that your, or a third party's rights have been compromised through this document please see our [Take Down policy](https://www.kent.ac.uk/guides/kar-the-kent-academic-repository#policies) (available from <https://www.kent.ac.uk/guides/kar-the-kent-academic-repository#policies>).

**Fundamental
immunosuppressive pathway
determining ability of cancer and
embryonic cells to escape
cytotoxic immune attack**

Thesis by
Stephanie Schlichtner

A thesis submitted in partial fulfilment of the requirements of the
University of Kent and University of Greenwich for the Degree of Doctor
of Philosophy

September 2022

DECLARATION

“I certify that this work has not been accepted in substance of any degree, and is not concurrently submitted for any degree other than that of Doctor of Philosophy being studied at the Universities of Greenwich and Kent. I also declare that this work is the result of my own investigations except where otherwise identified by references and that I have not plagiarized the work of others.”

X

The Candidate

Date

X

The Supervisor

Date

ACKNOWLEDGEMENTS

First, I want to thank our collaborators for their aid in this project to perform the experiments necessary to achieve the results and publish these in journals. A big thank you to our collaborators, Luca Varani for the anti-Tim-3 antibody used in the experiments performed, Yuri Kvach for providing *M. galloprovincialis* samples, Elizaveta Fasler-Kan and Nijas Aliu for the primary embryonic samples and primary keratinocytes, Bernhard Gibbs for providing primary T cell samples and Prof. Ruslan Medzhitov for the CD4-hTLR4 constructs.

I also want to thank my colleagues Anette Teo Hansen Selnø and Inna M. Yasinska and Svetlana Sakhnevych for their results produced and published in Figures 19, 28, 34, 35, 41, 42, 49, 55, 57, 60, 63 supporting this work. Thanks also to our collaborators Elizaveta Fasler-Kan and her team for providing supporting results in Figures 25 and 27 as well as Helge Meyer and his team for the results in Figure 90 and 91.

A heartfelt Thank you also to my supervisor Dr Vadim Sumbayev for the guidance, and encouragement during my PhD programme, as well as his support in the challenges we had to endure outside of the lab. Thank you very much!

I also thank my family and friends, long-known and newly found, for their support and encouragement during the studies. It was a challenging time and without their support I wouldn't have been able to keep my focus as I did. Thank you all so very much!

Lastly, I want to dedicate this work to my grandfather, who was always there to push me through my doubts and solidify my decisions. I will always be grateful for your help and support, and I dearly miss you. Thank you so much and I will always remember you!

ABSTRACT

Nowadays rapid gaining of knowledge on cancer progression and mutagenesis has enabled the development of improved diagnostics and therapeutic approaches to be used in medicine. Yet, cancer is still one of the most dangerous diseases, especially in Europe, Asia, and America. This is due to rapid mutation of cancer cells and high costs of most therapies. A change in application of treatments is necessary to improve the survival of cancer patients, especially the development of personalized cancer therapy and establishment of easily accessible targets are needed.

In the last 20 years the proteins Tim-3, galectin-9 and VISTA have been investigated regarding their influence on cancer development. While a significance was determined in their ability of suppressing immune responses, the exact mechanisms have not been researched yet. Structural analysis has deemed these proteins as being able to interact with each other and results so far indicate that by formation of protein complexes these proteins are able to efficiently inhibit cytotoxic immune responses.

To investigate the immunosuppressive effects induced by interactions between these proteins and the ability to form such multi-protein complexes as receptors and ligands we used quantitative and qualitative experimental approaches. We analyzed a variety of cancer cell lines and primary cancer samples as well as embryonic cell lines and primary fetal samples.

We were able to not only verify for the first time that galectin-9 is a ligand of VISTA, but we were also able to determine that the same mechanisms used by embryonic cells to adapt to the mother's immune system can be reused later in life by cancer cells to inhibit cytotoxic immune responses. Furthermore, we were able to prove that each of these proteins is supported by the TGF- β – Smad-3 pathway, which is also able to self-sustain the production of TGF- β in an autocrine/paracrine fashion. Data gained during the investigation of galectin-9 expression levels within other organisms also indicate that this protein is evolutionary conserved.

Our results clearly show that understanding the exact mechanisms of this pathway will allow us to develop targeted, personalized and easily applicable immunotherapy in the future by determining the key factors in individual tumour types focusing on the Tim-3 – galectin-9 – VISTA pathway.

CONTENTS

DECLARATION	I
ACKNOWLEDGEMENTS	II
ABSTRACT	III
FIGURES	VIII
TABLES	XX
ABBREVIATIONS	XXI
1 Introduction.....	1
1.1 Cancer Diversity leading to therapeutic challenges	2
1.1.1 Cancer statistics	3
1.1.2 Cancer Hallmarks.....	5
1.1.3 General biomedical characterization of human cancers presented by solid tumours	7
1.1.4 Haematological malignancies as human cancers presented by “non-solid” tumours	9
1.2 Introduction to a variety of cancer therapies.....	14
1.2.1 Chemotherapy	14
1.2.2 Immunotherapy targets	15
1.2.3 Significance of hypoxia and angiogenesis for malignant tumour growth	16
1.2.4 Chimeric antigen receptor T cells (CAR T cells).....	20
1.2.5 Current therapeutic outlook	23
1.3 Functional role Tim-3, Galectin-9, and VISTA immune checkpoint proteins in cancer progression	24
1.3.1 T cell immunoglobulin and mucin domain -3 (TIM-3)	24
1.3.2 Galectin-9.....	30
1.3.3 V-domain Ig suppressor of T cell activation (VISTA).....	35
1.4 The conflict between the embryo and mother’s immune system and immune evasion strategy operated by foetal cells	41
1.5 Similarities of immune regulation in cancer and Embryonic development.....	43
1.6 Hypotheses researched in this PhD programme in light of lack of conceptual development outlined in the literature review.....	45
2 Materials and Methods:.....	48
2.1 Tissue cultures	48
2.1.1 Thawing cells:	48
2.1.2 Splitting cells:.....	49
2.1.3 Freezing cells:.....	50
2.1.4 Cell types and media used:	50
2.1.5 Smad-3 and HIF-1 α knockdown:	54
2.2 THP-1 vs. E. coli	54

2.2.1	On cell stain:	55
2.2.2	Fixed cell staining:	55
2.3	Preparing cell lysates	55
2.4	Mice:	56
2.5	Measurement of intracellular calcium	57
2.6	Western Blot	57
2.6.1	Preparation of the polyacrylamide gel:	57
2.6.2	Sample preparation:	59
2.6.3	Transfer to membrane:	60
2.6.4	Staining with antibodies:	62
2.7	Coomassie stain	63
2.8	Total protein stain	64
2.9	Enzyme-linked immunosorbent assay (ELISA)	64
2.9.1	Coating with capture antibody and blocking:	65
2.9.2	Sample preparation and Standard dilution:	65
2.9.3	Detection antibody and Streptavidin:	66
2.9.4	O-phenylenediamine (OPD) reaction:	66
2.10	Xanthine oxidase assay	67
2.11	In-vitro assays of protein interactions	67
2.12	Thiobarbituric acid reactive substance (TBARS) assay:	68
2.13	NADPH oxidase (NOX) assay	68
2.14	Flow cytometry	69
2.15	Caspase 3 assay	69
2.16	Granzyme B assay	70
2.17	Protein quantification ("Bradford assay")	70
2.18	May-Grünwald cell staining	70
2.19	Quantitative Real Time Polymerase Chain Reaction (q-RT PCR)	71
2.19.1	RNA isolation	71
2.19.2	DNA decontamination	72
2.19.3	DNA template preparation	72
2.19.4	QPCR	73
2.20	DNA agarose gel	74
2.21	Glycolysis assay	74
2.22	Nuclear extraction	75
2.23	PI3K assay	75
2.24	MTS assay	75
2.25	Chromatin immunoprecipitation (ChIP) assay	76
2.26	Primer design	77

2.27	Statistical Analysis	77
2.28	Measurement of galectin-9 in bacterial cell extracts.....	77
2.29	Determination of galectin-9 binding specificity to LPS and PGN.....	78
2.30	Nanocomplex-design for immunoprecipitation of proteins	78
2.31	ELISA immunoprecipitation for characterizing interactions between galectin-9 and Tim-3/VISTA	79
3	Results.....	80
3.1	Galectin-9 determined for the first time as a ligand of VISTA	80
3.1.1	Galectin-9 released by cancer progression binds to VISTA with high affinity	80
3.1.2	Galectin-9 binding to VISTA leads to inhibition of granzyme B release within T cells inducing apoptosis off-target.....	84
3.1.3	VISTA secretion leads in combination with galectin-9 to activation of apoptotic cascades in T cells.....	94
3.1.4	Discussion.....	99
3.2	Biochemical regulation of galectin-9 and VISTA expression are performed by similar pathways.....	103
3.2.1	Galectin-9 master regulators in cancer and embryonic cells consist of transforming growth factor beta type 1 (TGF- β) and hypoxia-inducible factor 1 (HIF-1) ..	103
3.2.1.1	High upregulation of HIF-1, TGF- β , Smad-3 as well as galectin-9 are detectable in primary human cancer and embryonic cells.....	104
3.2.1.2	TGF- β and galectin-9 expression are dependent on Redox mechanisms.....	110
3.2.1.3	HIF-1 transcription induces galectin-9 upregulation by TGF- β production in a Smad-3 dependent manner.....	113
3.2.1.4	Galectin-9 expression is regulated by TGF- β in human cancer as well as embryonic cells.....	116
3.2.1.5	Discussion.....	120
3.2.2	Regulation of immune checkpoint protein VISTA expression is achieved differentially in rapidly proliferating human cells and T lymphocytes by TGF- β and Smad-3 signalling.....	125
3.2.2.1	TGF- β leads to differential regulation of VISTA dependent on cell type.....	126
3.2.2.2	Discussion.....	136
3.3	Danger signal high mobility group box 1 (HMGB1) leads to activation of immune evasion pathways in cancer cells by upregulating galectin-9 production.....	140
3.3.1	Preparation and analysis of gold-nanoparticles.....	141
3.3.2	HMGB1 induced upregulation of TGF- β and galectin-9 in TLR4-positive cells.....	142
3.3.3	Discussion.....	151
3.4	Fundamental biochemical functions of galectin-9 and VISTA in immune evasion checkpoint pathways.....	153
3.4.1	Conservation of galectin-9 detectable in other organisms.....	153
3.4.2	Biochemical function of galectin-9 directing innate immune reactions against gram-negative bacteria as well as T cell apoptosis.....	155

3.4.2.1	Opsonization of gram-negative bacteria via LPS galectin-9 enables their phagocytosis leading to the enhancement of innate immune responses against bacteria.	156
3.4.2.2	Galectin-9 bound on cell surface of embryonic cells is capable of protecting against cytotoxic T cells but does not lead to colonization of these cells with bacteria.	162
3.4.2.3	Macrophages phagocyte galectin-9 “opsonized” T cells.	166
3.4.2.4	Discussion.	169
3.5	Fundamental pathological functions of galectin-9 and VISTA in immune evasion checkpoint pathways.	172
3.5.1	Interaction with T lymphocytes leads to solid tumour secreting galectin-9 and therefore induces immunosuppression by interaction with other checkpoint proteins.	172
3.5.1.1	Interaction between human solid cancer cells and T cells lead to secretion of galectin-9.	174
3.5.1.2	Secretion of galectin-9 is performed by solid tumour cells using two different mechanisms after induction by T cells.	181
3.5.1.3	Secreted galectin-9 interacts with VISTA expressed on T cells to suppress their anti-cancer activity.	184
3.5.1.4	In vivo studies confirm the ability of solid cancer cells to secrete galectin-9 to suppress the activity of cytotoxic T cells.	190
3.5.1.5	Discussion.	192
3.5.2	Differentiation and Polarization of macrophages enables them to release VISTA as a checkpoint immune protein	196
3.5.2.1	Monocytes express high levels of VISTA and release it into the microenvironment by metalloproteinases cleavage.	197
3.5.2.2	VISTA secretion can be detected in differentiating macrophages but not fully differentiated ones.	198
3.5.2.3	VISTA released into the microenvironment is able to inhibit the functions in TALL-104 and Jurkat T cells but does not induce apoptosis.	199
3.5.2.4	Discussion.	202
4	Future Outlook.....	204
5	Bibliography.....	205
6	Publication list.....	219

FIGURES

Figure 1 Cancer statistics (A) GLOBOCAN fact sheet 2018, (B) All Cancers Fact sheet from GLOBOCAN 2020, Ferlay J, et.al. (2020). Global Cancer Observatory: Cancer Today. Lyon, France: International Agency for Research on Cancer. Adapted from: <https://gco.iarc.fr/today>, accessed 16.03.2022. 4

Figure 2 Cancer hallmarks. Adapted from: Douglas Hanahan; Hallmarks of Cancer: New Dimensions. Cancer Discov 1 January 2022; 12 (1): 31–46.<https://doi.org/10.1158/2159-8290.CD-21-1059> 5

Figure 3 MCF-7 breast cancer cell visualized in low and high density. Adapted from the cell line bank ATCC. 22/07/2022. <https://www.atcc.org/products/htb-22> 9

Figure 4 Reed-Sternberg cells (left), Popcorn cells (right). This image was originally published in ASH Image Bank. Reed Sternberg cells: Girish Venkataraman, 2016, #00060568. Popcorn cells: Timothy C. Carll et.al, 2018, #00061372 © the American Society of Hematology 11

Figure 5 THP-1 acute myeloid leukaemia cells visualized in low and high density. Taken from the cell line bank ATCC. 22/07/2022. <https://www.atcc.org/products/tib-202> 12

Figure 6 Schematics visualizing the PI3K pathway activating AKT and inducing various effects within cells is shown. The general effects on activation of PI3K within for example cancer cells is shown. This pathway can lead to increased cell cycle turnover, increased biogenesis of ribosomes as well as upregulation of synthesis of proteins. Furthermore, it can enable prolonged cell survival. Schematic was made by using biorender. 19

Figure 7 Schematics visualizing the development of CAR-T cells over the last 30 years. T cells are modified using artificial receptors against specific targets expressed on cancer cells. Over time these receptors have been further modified to co-express signals needed to properly induce immune responses within the T cells if the corresponding ligand was detectable on the targeted cancer cells. Figure was prepared with biorender. 22

Figure 8 General structure of the human Tim-3 protein shown. (Left) The structure of the human form of the Tim-3 protein is shown including the cytoplasmic tail with potentially 5 tyrosine phosphorylation sites, transmembrane domain, and stalk with two N-glycosylation structures, mucin domain with potentially 5 O-glycosylation structures as well as the IgV domain containing the binding structures for corresponding ligands. (Right) Visualization of the 3D structure of Tim-3 made by using the Swiss PBD viewer and further explained in chapter 1 of the results. Left figure was prepared with biorender. 27

Figure 9 Structures of each subgroup of the galectin family shown. (Left) Most members of the galectin family are produced as simple monomers which are able to form dimers by non-covalent binding, this group is called prototypical galectins. (Middle) One specific type of galectin, galectin-3, is found as monomers with a single binding structure and a linker component. This structure is able to form pentamers and is referred to as chimeric galectin. (Right) Lastly, a group consisting of five different galectins is known as tandem-repeat galectin group. These are consisting of two binding sites connected with a linker. Dependent on the version of galectin this linker varies in size. In this subgroup the proteins are determined to be able to form dimers. Figure was prepared with biorender. 31

Figure 10 General structure of the human galectin-9 protein shown. (Left) The structure of the human form of the Tim-3 protein is shown including the variation with linker length. The binding domains recognize the galectin-9 binding site on Tim-3 without interfering with other proteins being able to bind to the loops of the Tim-3 proteins (Right) Visualization of the 3D structure of galectin-9 made by using the Swiss PBD viewer and further explained in chapter 1 of the results. Left figure was prepared with biorender. 34

Figure 11 General structure of the human VISTA protein shown. (Left) The schematic of the structure of human VISTA is shown including the cytoplasmic tail with potentially Src homology 2 and 3 binding motif binding sites, a transmembrane domain, and stalk as well as an extracellular IgV domain attached to a signal peptide. (Right) Visualization of the 3D structure of VISTA made by using the Swiss PBD viewer and further explained in chapter 1 of the results. Left figure was prepared with biorender. 39

Figure 12 Interaction between the foetal cells and surrounding immune cells. To support the embryonic development a variety of immune cells need to be recruited. Such cells include macrophages specific for the maternal-foetal-interface which can secrete immunosuppressive cytokines and proteins such as IL-10 or IDO. Other cells are supporting implantation as well as removal of debris in the surrounding. This interaction has to be regulated very thoroughly as a shift to one side or another leads to the risk of miscarriage. The figure was prepared with biorender. 43

Figure 13 Tim-3-galectin-9 secretory pathway operated by human AML cells in order to suppress cytotoxic immunity. The pathways shown are associated with acute myeloid leukemia cells and visualizes the biochemical features activated by LPHN-1 leading to further downstream activation of PKC α enabling translation of Tim-3 and galectin-9 onto the cell surface and their secretion. PKC α can be either activated by FLRT3 found on the surface of endothelial cells interacting with LPHN1 and the induction of the classic Gq/PLC/Ca $^{2+}$ pathway or PKC α is induced by DAG with upregulated Ca $^{2+}$ activating the classic mTOR translational pathway. Translation by mTOR controls the production of Tim-3 and galectin-9. PKC α can also pre-activate certain release machineries which together with elevated cytosolic Ca $^{2+}$ increases exocytosis of either free or galectin-9-complexed Tim-3. 46

Figure 14 Set-up of the semidry transfer. Using the Trans-Blot® SD Semi-Dry Transfer Cell from Bio-Rad the anode is on the bottom plate; therefore, proteins will move from top to bottom during the run. 60

Figure 15 Set-up of the wet transfer. Shown is the setup for two gels, for one gel it is a similar setup of 2 blotting pads, filter paper, membrane gel and 2 blotting papers. The current is moving from the box to the lid and therefore the membrane needs to sit atop of the gel. 60

Figure 16 Set-up of the semidry transfer. Using the Trans-Blot® SD Semi-Dry Transfer Cell from Bio-Rad the anode is on the bottom plate; therefore, proteins will move from top to bottom during the run. 63

Figure 17 OPD reaction. 65

Figure 18 Expression levels of VISTA within hematopoietic and primary cell types. Western Blot analysis of VISTA levels normalised against total protein (β -actin). Data of five independent experiments include mean values +/- SEM. N.D. referring to "non-detectable". 81

Figure 19 Determination of VISTA – galectin-9 binding ability. By coating wells on a 96-well plate with anti-VISTA antibody and co-incubation with galectin-9 derived from THP-1 complex formation has been detected by Western Blot (A) as well as ELISA approach (B). MCF-7 was used as a negative control. VISTA expression levels were measured on natural killer (NK) and Jurkat T cells (C). Binding affinity (D) was analysed by subsequently checking VISTA – galectin-9 (E) and galectin-9 in complex with human Ig-Fc (F). Data obtained include five individual experiments (mean +/- SEM), SRCD six repeats, average presented * $p < 0.05$ vs. control. 83

Figure 20 Determination of galectin-9 interaction with VISTA. Galectin-9 immobilization on CM5 sensor chip via Biacore amino-coupling kit and co-incubation with either Fc-VISTA or human Ig-Fc flow-through was used to confirm the binding ability of these two proteins in form of ligand-receptor interaction. Left diagram indicates the binding affinity constant by Lineweaver-Burke plot. Middle diagram consists of curves reporting binding affinity of 100 pM VISTA-Fc and 100 pM Ig-Fc (calculated by using Biacore T200 software) Right curve is obtained by

increased concentrations of VISTA-Fc applied to the CM5 sensor chip containing galectin-9. Fc values have been subtracted from values gathered in VISTA-Fc flow-through experiment. GraphPad Prism has been used for curve fitting (including exponential decay, association/dissociation) 84

Figure 21 Analysis of granzyme B expression levels within different human cell types. Comparison of granzyme B levels within THP-1 AML cells, non-stimulated Jurkat T cells, Jurkat T cells stimulated with 100 nM PMA for 24 h and primary human natural killer cells as positive control. Image used as a representation of four experiments with similar, independent results (mean +/- SEM shown) 85

Figure 22 VISTA interaction with galectin-9 inhibits granzyme B release. Co-culture of THP-1 and Jurkat cells was performed after stimulation with PMA in presence and absence of VISTA neutralising antibody. Granzyme B levels within cells and galectin-9 release in the medium were analysed (A). Galectin-9 levels were measured using the ELISA approach (B), granzyme B localized by using Western Blot as well as granzyme B assays (C). Data used mean +/-SEM to represent four individual experiments; *p<0.05, **p<0.01 vs control or indicated events. 86

Figure 23 Inhibition of granzyme B activity by addition of inhibitor Z-AAD-CMK. Jurkat T and human AML THP-1 cells were pre-treated with 100 nM PMA for 24 h. After removal of PMA co-culture was performed in presence or absence of 100 µM of the inhibitor for granzyme B activity Z-AAD-CMK. Granzyme B activity was measured according to protocol. Data is representative of four independent experiments (mean +/-SEM). 87

Figure 24 Galectin-9 produced by AML cells influences T cell response in a VISTA-dependent mechanism. Influence of human AML cell line THP-1 on immune responses was investigated in co-culture with Jurkat T cells using anti-VISTA neutralising antibody. THP-1 cells were co-cultured with Jurkat T cells and observed (A). Granzyme B activity within Jurkat T cells after co-culture at a ratio 1:1 with AML cell line was investigated using granzyme B assay kit. Data shown represent four individual experiments, mean +/-SEM. **p<0.01 vs. control. 88

Figure 25 Jurkat expression levels of galectin-9 receptors and influence of galectin-9 binding. Jurkat T cells were used to study upregulation of galectin-9 receptors and effect of galectin-9 binding onto these proteins. Jurkat were stimulated with 100 nM PMA for 24h and expression levels of Tim-3 as well as VISTA were investigated (A). VISTA expression was visualised on T cells using fluorescent microscopy (B). Expression levels of VISTA and Tim-3 were measured after permeabilization of T cells by FACS (C). Granzyme-B activity in T cells and the influence of galectin-9 and its corresponding receptors were analysed using granzyme B assays (D). To determine if granzyme B leads to further activation of pro-apoptotic processes in T cells caspase 3 and PARP cleavage were analysed using ELISA and Western Blot (E). 90

Figure 26 Caspase 3 activation and induction of cell death is granzyme B-dependent. PMA pre-treated Jurkat T cells were used to study granzyme B dependency of caspase 3 activation and induction of apoptosis upon galectin-9 stimulation. Jurkat were stimulated with 100 nM PMA for 24h and cell-viability after exposure to 2.5 µg/ml galectin-9 with or without granzyme B inhibition was determined with MTS assay. Percentage of apoptotic cells were determined using annexin V/propidium iodide assay. Caspase 3 activity significantly decreased in presence of granzyme B inhibition, measured with colorimetric assays. Data represent three individual experiments, mean +/- SEM. *p<0.05, **p<0.001 vs. control. 91

Figure 27 Lack of granzyme B inhibits increase of pro-apoptotic activity after galectin-9 stimulation. HaCaT cell line was studied to determine the VISTA and Tim-3 expression levels. (A-C). This cell line does not show any granzyme B activity (D). Caspase 3 activity and PARP cleavage did not increase significantly after galectin-9 exposure (E). Data represent four independent experiments, mean +/- SEM. *p<0.05 vs. control. 93

Figure 28 Difference in VISTA expression in T cells and natural killer cells leading to induction of pro-apoptotic process in T cells and not in NK cells. Natural killer cells and PMA pre-treated Jurkat T cells were co-

cultured with PMA pre-treated THP-1 AML cells in presence and absence of anti-galectin-9 antibody. In Jurkat T cells expressing VISTA galectin-9 led to increase in caspase 3 activity and PARP cleavage. Natural killer cells do not express VISTA and did not show any pro-apoptotic activity after galectin-9 exposure. Anti-galectin-9 antibody leads to significant decrease of such processes in T cells. Data represent four individual experiments, mean +/- SEM. * $p < 0.05$ vs control. 94

Figure 29 High levels of VISTA is released by malignant human primary cells. Human primary samples of healthy patients and AML patients were kept in culture for 24 h. Release of VISTA was measured in cell culture medium by ELISA (A). VISTA was analysed by deglycosylation to determine glycosylation levels using Western Blot (B). Data are representing five individual experiments with similar results, mean +/- SEM are shown. ** $p < 0.01$ vs. PHL. 95

Figure 30 Elevated levels of VISTA released by AML cells were attenuated by metalloproteinases inhibitors. Human primary samples of healthy patients and AML patients show an increased release of galectin-9 (A) and VISTA (B) upon malignant transformation, with a clear correlation of both proteins released simultaneously (C). Metalloproteinase inhibitors similar to the studies of Tim-3 release were used to investigate VISTA release by AML cells. In both cases the release was significantly reduced, especially by inhibition of ADAM 10/17. PMA pre-treated THP-1 AML cells (D) and primary AML cells (E) were investigated. Significant differences to control detectable; $p < 0.05$ vs. healthy donors without proteinase inhibitor exposure. 97

Figure 31 Exposure to a combination of galectin-9 and VISTA significantly increased activation of pro-apoptotic cascade. Jurkat T cells express both types of receptors for galectin-9 (A). Exposure for 16 h to galectin-9, VISTA or both proteins increased PARP cleavage, measured by Western Blot (B) and granzyme B accumulation, measured by fluorometric assays (C). Stimulation for 30 min with VISTA and galectin-9 protein led to changes in membrane potential in T cells (D). Studying primary T cells showed same effects upon exposure to VISTA, galectin-9 or both proteins for 16 h as seen in Jurkat T cells. VISTA, Tim-3, CD-3, and PARP cleavage were measured by Western Blot. Data represent one experiment with three repetitions, mean +/- SEM included. * $p < 0.05$ vs control. 98

Figure 32 Multi-complex formation observed by interaction between Tim-3, galectin-9, and VISTA. 3D structures formed using Swiss PDB viewer (A). SRCD spectra analysis, average of six curves. 98

Figure 33 Schematics depicting the formation of possible barrier formation and its consequences by Tim-3, galectin-9, and VISTA. Galectin-9 released by malignant cells can bind onto the surface of T cells by interacting with its receptors Tim-3 and VISTA. Further soluble VISTA produced by the same malignant cells binds onto the other side of galectin-9 creating a dense barrier on the T cells. Galectin-9 binding increases the granzyme B production in T cells, yet release is inhibited due to the barrier formed. This will consequently lead to activation of accumulated granzyme B within the T cell itself and induce pro-apoptotic activities such as caspase 3 and PARP cleavage. 103

Figure 34 Comparative studies of malignant and healthy primary breast tissue. Schematics of the hypothesis studied in this chapter includes the effect of NADPH oxidase and xanthine oxidase inducing HIF-1 upregulation leading to increased TGF- β and Smad-3 activity which will sustain itself in an autocrine fashion later on and leads to galectin-9 production to suppress immune responses towards the cancer cells (A). In malignant tissue xanthine oxidase, NADPH oxidase and TBARS levels are significantly increased due to hypoxic stress (B). HIF-1, TGF- β and phosphor S423/S425 Smad-3 are also highly upregulated in comparison to healthy tissue (C). As seen in prior studies both galectin-9 and Tim-3 are detectable in increased amounts in tumour tissue. Quantities are respectively compared to 1 gram of tissue each. Western Blot normalization includes Licor total protein assay, enzyme activities and TBARS are normalized per mg of total protein (shown in figure 35). Data included from five individual experiments, mean +/- SEM shown. * $p < 0.05$ and ** $p < 0.01$ vs. healthy tissue. 106

Figure 35 Normalization of values in Figure 34. Western Blot values were normalized against total protein. Enzyme activity as well as TBARS measurement against 1 mg of total tissue protein. Data included from five individual experiments, mean +/- SEM shown. * $p < 0.05$ and ** $p < 0.01$ vs. healthy tissue. 107

Figure 36 Comparative studies of primary acute myeloid leukaemia vs. healthy leukocytes. Cells were kept for 24 h in culture. Activity of xanthine oxidase, NADPH oxidase and TBARS levels were significantly increased in malignant samples compared to primary healthy leukocytes (A). Similar to solid tumour breast cancer samples, HIF-1 and phosphor-S423/425-Smad-3 were highly upregulated in malignant cells (B). Levels of secreted TGF- β , galectin-9 and Tim-3 in cell culture medium were analysed using ELISA (C). Data include mean +/-SEM of five individual experiments. * $p < 0.05$ and ** $p < 0.01$ vs. healthy donor samples. 108

Figure 37 Investigation of TGF- β release in blood circulation, solid vs. non-solid tumour. TGF β levels were determined in blood samples received from healthy donors, primary breast cancer donors, metastatic breast cancer patients and AML patients (n=6 in each set). Data include mean +/- SEM. * $p < 0.05$ vs. healthy samples. 109

Figure 38 Up-regulation of oxidative burst, HIF-1, TGF- β /Smad-3 and galectin-9/Tim-3 in early developmental stages. Primary embryonic samples from two different stages during human development were analysed. Stages chosen were chorionic (Ch) at about 13 weeks of development and amniotic (Am) ranging between 20 – 25 weeks of development. Measurements of xanthine oxidase, NADPH oxidase and TBARS levels are shown (A). Followed by analysis of HIF-1 (B), TGF- β and Smad-3 (C). Lastly, expression of galectin-9 and Tim-3 on and surrounding embryonic cells were analysed (D, E). Seven representatives investigated in one experiment: examples shown. * $p < 0.05$ vs amniotic stage. 110

Figure 39 Influence of NADPH oxidase pathway in TGF- β and galectin-9 production. Pathway with proteins investigated and their corresponding inhibitors shown (A). Inhibition of ASK1 (by Δ N-ASK1), AP-1 (by SR11302) or NADPH oxidase (by DPI) led to reduction of TGF- β , and galectin-9 release after HMGB1 stimulation in comparison to cells with no inhibition. HMGB greatly increases levels of proteins released in comparison to control. Data include four independent experiments, mean +/- SEM. * $p < 0.05$ or ** $p < 0.01$ vs. control. 111

Figure 40 Investigation of xanthine oxidase verifies its influence on galectin-9 and TGF- β expression. For analysing the effects of xanthine oxidase, we used MCF-7 cells exposed to 250 μ g/ml ammonium molybdate for 24 h with or without a xanthine oxidase inhibitor (allopurinol). Pathway of xanthine oxidase downstream activation shown (A). TBARS levels, influence of xanthine oxidase on HIF-1 α and TGF- β (A) as well as galectin-9, Tim-3 and Smad-3 were analysed by activity assays, ELISA, and Western Blot. Data represent four independent results, mean +/- SEM. * $p < 0.05$, ** $p < 0.01$ vs. shown events. 113

Figure 41 Involvement of HIF-1 and Smad-3 in TGF- β autocrine production and galectin-9 regulation. Induction of HIF-1 by cobalt chloride led to increased cell-associated TGF- β levels, DNA-bound HIF-1 increase and increased galectin-9 production (A). Regulation of HIF-1 – TGF- β – galectin-9 pathway is time-dependent with increased HIF-1 binding to DNA after 1 h, upregulation of TGF- β at 3 h and induction of galectin-9 production following lastly at 6 h (B). Inhibition of TGF- β activity by neutralizing antibodies led to lack of galectin-9 upregulation in presence of cobalt chloride after 6 h (C). Shown is a scheme proposing the influence of TGF- β and Smad-3 in galectin-9 production (D). Smad-3 knock-down led to decreased TGF- β levels after stimulation with external TGF- β and therefore also decreased galectin-9 levels in comparison to wild-type cells and random knock-down cells (E). Three individual experiments represented by images, mean +/- SEM. * $p < 0.05$, ** $p < 0.01$. 116

Figure 42 Investigation of different cell lines determined the influence of TGF- β on galectin-9 levels to be mainly found in cancer and embryonic cells. Cell lines investigated include THP-1 AML human leukaemia cells, Colo205 colorectal cancer cell line, MCF-7 breast cancer cell line, HaCaT non-malignant human keratinocyte cell

line, primary keratinocytes (prim KC) and as a representative for the embryonic development we used the HEK293 human embryonic kidney cell line. In malignant cell lines as well as the embryonic cell line TGF- β increased galectin-9 expression on cell surface, while Tim-3 levels did not change significantly. In non-malignant cells (HaCaT and primary keratinocytes) we did not see any increase in galectin-9 expression. Shown are representative of four independent experiments, mean +/- SEM included. * $p < 0.05$ vs. control samples. 118

Figure 43 K562 human cancer cells express galectin-9 levels after TGF- β exposure. K562 is a human chronic myeloid leukaemia cell line that expresses very low levels of galectin-9 without TGF- β treatment. Exposure to TGF- β at different concentrations (0, 2, 4, 8 ng/ml) for 24 h led to an increase in active phosphor-S423/425-Smad-3 and caused upregulation of galectin-9 expression, investigated by Western Blot analysis. ELISA analysis did not indicate any galectin-9 release after stimulation with TGF- β . Data represent one experiment with three repetitions, mean +/- SEM included. 119

Figure 44 Induction of Smad-3 by TGF- β exposure only detectable in malignant cells. MCF-7 breast cancer cells, HaCaT non-malignant human keratinocytes and primary keratinocytes were exposed to 2 ng/ml TGF- β for 24 h. Increase of active phosphor-S243/245-Smad-3 only detectable in malignant cells (A), while levels of active Smad-3 did not change in healthy cells (B, C). Data include four experiments, representative and mean +/- SEM included. * $p < 0.05$ vs non-treated cells. 120

Figure 45 Scheme depicting TGF- β in low and high oxygen availability stages. TGF- β is activated in low oxygen stage by HIF-1 induction. Later when new blood vessels are formed by angiogenesis and oxygen levels are returned to a normal stage TGF- β is maintained by autocrine support and Smad-3 upregulation. 125

Figure 46 Investigation of different types of human T lymphocytes after TGF- β exposure. In resting Jurkat T cells and PMA-activated Jurkat T cells (A) TGF- β led to an increase in phospho-S423/S425-Smad-3 levels. In TALL-104 TGF- β did not increase Tim-3 and galectin-9 levels significantly (B left side). Granzyme B levels were reduced while phospho-S423/S425-Smad-3 has been significantly upregulated (B right side). In primary T cells (C) a slight increase in galectin-9 and a significant increase in phospho-S423/S425-Smad-3 levels were detectable while levels of Tim-3 did not rise. Data include four experiments, one visual representative and mean +/- SEM included. * $p < 0.05$ and ** $p < 0.01$ vs non-treated cells. 128

Figure 47 Levels of VISTA mRNA analysed using qRT-PCR in two different cell lines, TALL-104 with high levels of VISTA expressed and MCF-7 with no detectable amounts. Data included are showing mean values +/- SEM of three experiments. 129

Figure 48 Study of the Wilms tumour cell line WT3ab after exposure to TGF- β . WT3ab cells are stimulated for 24 h with 2 ng/ml TGF- β and shown proteins have been analysed using Western blot approach. Pictures represent four repetitions in one experiment with similar results. Mean +/- SEM included. * $p < 0.05$ vs. control. 130

Figure 49 Effects of TGF- β on VISTA expression studied in a variety of cell types. Naïve Jurkat T cells (A) and PMA-activated Jurkat T cells (B), TALL-104 (C), primary T lymphocytes (D), the AML cell line THP-1 (E), primary AML cells (F), MCF-7 breast cancer cell line (G), primary human embryonic cells from two different developmental stages, chorion and amnion (H), Wilms tumour cell line WT3ab (I), non-malignant keratinocyte cell line HaCaT (J), K562 cell line (K) were exposed to 2 ng/ml TGF- β for 24 h (cell lines) or 16 h (primary samples) and expression levels of VISTA were investigated using Western blot approach. The K562 cell line has been further exposed to different concentrations of TGF- β to investigate if higher concentration immediately also leads to an increase in VISTA expression. Lastly, we used siRNA to knockdown Smad-3 activity and determined its influence similar to the galectin-9 studies on VISTA expression levels (L). Visual representatives were chosen from either 4-

7 individual results. Data include mean values +/- SEM from 4-7 experiments. *p<0.05 and **p<0.01 vs. non-stimulated control samples. 132

Figure 50 Analysis of TGF- β in cell-associated VISTA expression and secretion. (A) Jurkat T cells and TALL-104 cells were stimulated for 24 h with 2 ng/ml TGF- β , RNA has been isolated and mRNA levels investigated with and without stimulation using qRT-PCR. (B) To determine Smad-3 binding to the VISTA gene VSIG Jurkat T cells, resting, and stimulated with TGF- β , were investigated using ChIP and qRT-PCR. (C) Cell-surface bound VISTA has been investigated in PMA-treated Jurkat T cells, TALL-104 and THP-1 cells after exposure to TGF- β . (D) Jurkat T cells, (E) primary T lymphocytes, (F) THP-1 AML cell line, (G) primary AML blasts as well as (H) non-malignant HaCaT keratinocytes were treated with TGF- β for 24 h and differences in cell-bound (grey) and secreted (black) VISTA levels were investigated. Examples of five individual experiments shown, including mean +/- SEM. *p<0.05 vs control shown. 134

Figure 51 Investigation of VISTA expression in correlation with Smad-3-co-activator recruitment. Effects on co-activators to Smad-3 were investigated in different cell types including (A) Jurkat T cells, (B) THP-1 AML cell line, (C) MCF-7 breast cancer line, (D) non-malignant keratinocyte cell line HaCaT. Images are representative of four individual experiments, mean +/- SEM included. *p<0.05 and **p<0.01 vs. non-stimulated samples. 136

Figure 52 Schematic of different regulatory mechanisms for VISTA expression shown. (A) TGF- β receptor levels change dependent on if a protein is up- or downregulated. This can be achieved by TGF- β -Smad-3 regulation and the recruitment of co-activators Smad4 and TRIM33. "a" and "b" are used to represent protein molecules involved in the mechanism. (B) ATF1 or other transcription factors might be used to repress VISTA production. (C) Most likely nuclear compartmentalisation is used to translocate the VSIG-locus to the periphery leading to downregulation of VISTA during TGF- β exposure. 140

Figure 53. Gold nanoparticles used for HMGB1 immunoprecipitation visualized using Transmission Electron Microscopy (TEM). 142

Figure 54. Process of gold nanoparticles HMGB1 immunoprecipitation visualized. 142

Figure 55. Analysis of antibody bound to gold-nanoparticles. Gold-nanoparticles with anti-HMGB1 antibody and naïve nanoparticles were exposed to HRP-conjugated streptavidin and analysed using OPD (A). gold-nanoparticles containing mouse anti-human TGF- β antibodies were exposed to anti-mouse and anti-rabbit secondary antibodies. Analysis was performed by detecting fluorescence with Odyssey CLx imager (B). Each results contains a representative of three individual experiments, mean +/- SEM included. 143

Figure 56 Investigation of THP-1 cells regarding HMGB1 exposure. In the human AML cell line exposure to HMGB1 led to an increase in TGF- β expression as well as Smad-3 phosphorylation (A). Overall galectin-9 levels increased with most of the protein being secreted (B), therefore, reducing cell-surface bound galectin-9 levels (C). Tim-3 release increased significantly (D). Data include values and representatives from four independent experiments, mean +/- SEM included. *p<0.05, **p<0.01 vs. control. 144

Figure 57 Study of various cells regarding their HMGB1 receptor expression. Each receptor – TLR2, TLR4, Rage and Tim-3 – has been detected using Western Blot; values and representatives from four independent experiments, mean +/- SEM included. *p<0.05, **p<0.01 vs. control. 144

Figure 58 Investigation of TLR negative primary AML samples. Samples were chosen regarding their lack of expression of TLR2 and TLR4. In these samples stimulation with HMGB1 did not lead to significant increase of TGF- β and galectin-9 levels as well as release. Data contains representatives for four independent experiments, mean +/- SEM included. 145

Figure 59 Investigation of primary AML samples expressing TLR4. 2.5 µg/ml HMGB1 induces increased galectin-9 and Tim-3 release in primary human AML samples expressing TLR4 and TLR2 as well as Tim-3 and RAGE after 16 h exposure. Receptor expression was investigated using Western Blot approaches (A). Changes in Tim-3 and galectin-9 expression levels and increased secretion has been determined using Western Blot and ELISA (B). Representative images included from three individual experiments, mean +/- SEM. 146

Figure 60 Investigation of HMGB1 influence on TLR2-expressing human colorectal cancer cells (Colo 205). Cells were exposed to 1 µg/ml HMGB1 for 24 h. Galectin-9 expression and secretion levels remained same during HMGB1 treatment (B) but led to translocation onto the cell surface (C). TGF-β (A) and Tim-3 (D) did not increase indicating a need for TLR4 to be expressed. Data include representative images of four individual experiments, mean +/- SEM shown. **p<0.01 vs control. ND stands for non-detectable. 147

Figure 61 Investigation of HMGB1 influence on human breast cancer cell line MCF-7. Cells were exposed to 1 µg/ml HMGB1 for 24 h. Galectin-9 expression remained same and secretion levels were not detectable during HMGB1 treatment (B), yet a slight increase in translocation on cell surface has been determined (C). TGF-β (A) and Tim-3 (D) did not increase. Data include representative images of four individual experiments, mean +/- SEM shown. ND stands for non-detectable. 148

Figure 62 Investigation of HMGB1 influence on human embryonic kidney cell line HEK293. Cells were exposed to 1 µg/ml HMGB1 for 24 h. Galectin-9 expression levels remained same during HMGB1 treatment, and no secretion has been detectable (B). Furthermore, no increased translocation onto the cell surface was determined (C). TGF-β (A) and Tim-3 (D) did not increase significantly. Data include representative images of four individual experiments, mean +/- SEM shown. ND stands for non-detectable. 148

Figure 63 HMGB1 release triggered by exposing cells to apoptosis inducer BH3I-1. Cells were exposed to 100 µM BH3I-1 for 24 h (A), cell lines used were AML cell line THP-1, breast cancer cell line MCF-7 and colorectal cancer cell line Colo 205. HMGB1 release has been investigated using ELISA (B). Data set include three individual experiments, mean +/- SEM shown. *p<0.05 and **p<0.01 vs control. 149

Figure 64 HMGB1 level investigation in primary samples. Five samples of either healthy donors, primary breast cancer patients or acute myeloid leukaemia patients were investigated. Data include mean +/- SEM of five independent measurements as well as each sample is shown individually. *p<0.05 vs. healthy donor. 150

Figure 65 HMGB1 stimulation of TLR4-positive cells leads to induction of TGF-β expression and consequently to galectin-9 upregulation by cancer cells. Transfection with active TLR4 causes same effects as seen with HMGB1 stimulation. (A) THP-1 AML cell line has been stimulated for 24 h with 1 mM H₂O₂ inducing HMGB1 production, medium was collected for further use. The medium was treated with horseradish peroxidase to remove any H₂O₂ left and separated into two parts. In one part HMGB1 was immunoprecipitated and both mediums with and without HMGB1 were used to stimulate PMA-pre-treated THP-1 cells for 24 h. This medium was collected and one part immunoprecipitated against TGF-β. MCF-7 breast cancer cells were incubated with or without immunoprecipitated medium for 24 h. Galectin-9 levels were investigated after incubation. (B) Colo 205 cells were transfected with active TLR4 and incubated for 24 h afterwards. Galectin-9 release increased significantly, as well as Tim-3 analysed by Western Blot and ELISA. (C) Transfection with active TLR4 also increased TGF-β and phosphorylation of Smad-3. Data include representatives of four independent experiments, mean +/- SEM shown. *p<0.05 and **p<0.01 vs. control. 151

Figure 66 Schematics visualizing the proposed pathway of HMGB1 influencing immune suppression. Damaged cancer or immune cells release HMGB1 as a “danger signal” leading to further recruitment of immune cells. Yet, HMGB1 is able to bind to TLR4-positive cancer cells and cancer-associated cells such as tumour-

associated macrophages leading to the production of TGF- β . Increased levels of TGF- β in the tumour microenvironment causes on the one hand a para- and autocrine regulation of further TGF- β production as well as induction of galectin-9 secretion. On the other hand, does TGF- β also induce the suppression of granzyme B production within cytotoxic T cells and induces the differentiation of naïve T cells into regulatory T cells enabling further suppression of immune responses towards the cancer cells. Taking these processes together HMGB1 is most likely to support further tumour growth. 153

Figure 67 Investigation of galectin-9 expression in molluscs in presence and absence of malignant cells.

(Up) Healthy molluscs were exposed to malignant cells in presence and absence of lactose and reactivity of these organisms towards such cells were investigated. (Lower, A) Visual changes of immune cells within molluscs after exposure. (Lower, B) Smad-3 and galectin-9 were upregulated in presence of malignant cells, effects which were attenuated by lactose. mean +/- SEM shown. * $p < 0.05$ and ** $p < 0.01$ vs. control. 155

Figure 68 Scheme of experimental approach to determine if VISTA and Tim-3 are capable to associate with bacteria in absence of galectin-9.

Bacteria were incubated with target-specific antibodies (against galectin-9 in its presence and absence, against Tim-3 and against VISTA) and signal was detected similar to ELISA analysis. To verify the binding capability of VISTA and Tim-3 in presence of galectin-9 a combination of these proteins was also used for incubation. 159

Figure 69 Tim-3 and VISTA are capable of interacting with bacteria only in presence of galectin-9.

E. coli bacteria were exposed to either 0.1 μ M galectin-9, VISTA, Tim-3, or a combination of these proteins for 1 h. After exposure bound protein was detected similar to ELISA approach. Representative picture shown of three individual experiments, mean +/- SEM included. ***- $p < 0.001$ vs. control 159

Figure 70 Galectin-9 induces opsonization of gram-negative bacteria via LPS binding, leading to phagocytosis of the marked bacteria and induction of innate immune system cells secreting cytokines

(A) PMA induces differentiation of THP-1 monocytes to macrophages. These cells were kept in culture with *E. coli* bacteria for 16 h in presence and absence of 10 mM lactose. (B) In-cell Western was used to determine phagocytosis of bacteria. (C) Release of innate immune cytokines IL-1 β , IL-6 and TNF- α has been assessed by ELISA. (D, left) Bacteria collected after co-culture were lysed and galectin-9 was investigated in cytosol. (D, right) The pellet containing bacterial cell wall was investigated regarding bound galectin-9 and its corresponding partners Tim-3 and VISTA. (E) LPS-specific binding of galectin-9 and its associated proteins Tim-3 and VISTA was analysed. Results included of five independent experiments, mean +/- SEM *- $p < 0.05$ and **- $p < 0.01$ vs control. 160

Figure 71 Galectin-9 found in human blood plasma is able to opsonise gram-negative bacteria.

Human blood plasma of healthy donors was used to co-incubate *E. Coli XL10 Gold*[®] cells in presence or absence of lactose (30 mM). These bacterial cells were investigated regarding the binding of galectin-9, Tim-3, and VISTA on their surface. Five individual experiments were performed with a representative as well as mean +/- SEM shown. **- $p < 0.01$ vs. control. 161

Figure 72 Galectin-9 in human blood plasma does not opsonise gram-positive bacteria by PGN.

PGN retrieved from the gram-positive bacteria *S. aureus* was immobilized in wells of an ELISA plate and incubated with either galectin-9 from human blood plasma, recombinant galectin-9, or as positive control TLR2 from THP-1 cell line. Five individual experiments were performed, a representative image and mean +/- SEM is shown. **- $p < 0.01$ vs. control. 162

Figure 73 Visual scheme showing the ELISA approach used to determine the binding association of Tim-3 and VISTA to galectin-9 found on human embryonic cells.

(A) The binding of galectin-9 to the ELISA plates was measured using mouse anti-galectin-9 capture antibody and rabbit anti-galectin-9 detection antibody. The

signal was detectable due to a goat anti-rabbit antibody containing a fluorescent label. (B) For determining Tim-3 binding the capture antibody against galectin-9 has been originating from rabbit and the anti-Tim-3 detection antibody mouse. Signal was achieved by using goat anti-mouse antibody with fluorescent labelling. (C) VISTA was detected using a mouse anti-galectin-9 capture antibody, rabbit anti-VISTA detection antibody and goat anti-rabbit fluorescent labelled antibody.

164

Figure 74 Suppression of immune responses towards embryonic cells are heavily influenced by galectin-9 and VISTA levels. As described in Materials and methods we were able to culture primary human embryonic cells for co-culture purposes. (A, B) These cells were investigated regarding their expression levels of galectin-9, Tim-3, and VISTA in two different developmental stages. The chorion (Ch) stage ranges from 13-14 weeks of development and the samples of the amnion (Am) stage were retrieved at 20 weeks. (C) Association of these proteins with each other were detected by using ELISA approaches and analysing signals gained from proteins at the same time. (D) On embryonic cells the co-localization of VISTA and galectin-9 was determined by on-cell Western Blotting. Close proximity of VISTA and galectin-9 is shown by merging both signals. (E) Jurkat T cells were activated with 100 mM PMA for 24 h and expression levels of Tim-3, VISTA and granzyme B was analysed. (F) Apoptotic activity such as accumulation of granzyme B and increased caspase 3 activity were analysed in co-cultured Jurkat T cells in presence and absence of neutralization antibodies against VISTA, galectin-9, or both. Images shown are representing seven individual experiments. Mean +/- SEM is included. *-p<0.05 and **-p<0.01 vs. control shown.

165

Figure 75 No colonization of galectin-9 expressing embryonic cells by Gram-negative bacteria was detectable. Primary embryonic cells originating from the chorion stage were exposed to E. coli cells for 16 h with or without 10 mM lactose. After bacterial colonization these cells were co-cultured with THP-1 cells for 16 h to determine cytokine levels corresponding to an immune response. The levels of IL-1 β , IL-6 and TNF- α were analysed using ELISA approach. Results are representative of four experiments including mean +/- SEM. *-p<0.05 and **-p<0.01 vs. control.

166

Figure 76 Phagocytosis of T cells by macrophages is triggered by opsonization with secreted galectin-9. (A) PMA-treated Jurkat T cells were exposed to galectin-9 for 16 h and co-cultured with THP-1 macrophages for 3 h. PC- phosphatidylcholine, PS- phosphatidylserine and SM – sphingomyelin. (B) Viability, HMGB-1, TGF- β secretion and PS expression of the Jurkat T cells were analysed. (C) In-cell Western of CD3 in THP-1 cells was used to determine phagocytosis of T cells (top panel). Effects were attenuated with Tim-3 neutralizing antibody (bottom panel). (D) To verify effects in physiological conditions Jurkat T cells were exposed to AML blood plasma containing high levels of galectin-9 for 16 h increasing phagocytosis (top panel). Opsonization by galectin-9 after AML exposure was verified using on-cell Western (bottom panel). Representative images from one out of five experiments shown, including mean +/-SEM. *-p<0.05 and **-p<0.01 vs. control.

168

Figure 77 Galectin-9 induce PS expression and translocation on the cell surface in T helper and cytotoxic T cells. CD4⁺ T helper cells and CD8⁺ cytotoxic T cells were exposed for 16 h to 2.5 μ g/ml galectin-9. The translocation of PS was determined using annexin V staining. Data include results of eleven independent experiments as well as mean +/- SEM. **-p<0.01 vs. no stimulation.

169

Figure 78 G401 human kidney rhabdoid tumour cell line was investigated regarding its expression levels of galectin-9, VISTA, and Tim-3. Analysis was performed using Western Blot approach. Data was gathered from four independent experiments including representative images, mean +/- SEM.

176

Figure 79 Human glioblastoma cell line LN-18 was studied to determine galectin-9, VISTA, and Tim-3 expression levels after TGF- β induction. After exposure of LN-18 cells to 2 ng/ml TGF- β for 24 h Western Blot

analysis was used to determine the expression levels of galectin-9, VISTA, and Tim-3 as well as their mRNA levels. Data include representative images of one out of four experiments with similar results, mean +/- SEM shown. 176

Figure 80 Interaction with T cells leads to secretion of galectin-9 by solid human cancer cells as well as keratinocytes. At a ratio of 1:1 we co-cultured Jurkat T cells and a variety of solid cancer types, keratinocytes, or primary human embryonic cells for 16 h. The cells were separated from each other, and the adherent cells washed twice with PBS before adding again fresh medium culturing them for another 4 h. The release of galectin-9 was measured in samples taken at 2, 3 and 4 h. Jurkat T cells themselves did not release significant levels of galectin-9 on their own (A). To determine if these effects are seen while contact with any type of T cell, we used MCF-7 breast cancer cells and co-incubated them with either primary CD3-positive T cells, Jurkat (CD4⁺) or TALL-104 cytotoxic (CD8⁺) T cells for 16 h again at a ratio of 1:1 (B). Adherent cells were investigated regarding galectin-9 release in resting state (C). Data includes mean +/- SEM of four independent experiments. 177

Figure 81 Investigation of trafficker protein for galectin-9 in different cell lines. After co-culture with Jurkat T cells at a ratio of 1:1 for 16 h we investigated with which potential carrier/trafficker – VISTA or Tim-3 – was used to secrete galectin-9 by MCF-7 breast cancer cells (A), WT3ab paediatric kidney cancer cells (B) or LN-18 glioblastoma cells (C). The cells were washed after co-culture and the solid cells kept in fresh medium before immunoprecipitation of secreted galectin-9. The analysis was performed using Western Blotting with non-boiled samples. Images are used to visualize effects seen and are representative for four independent experiments. 179

Figure 82 Galectin-9 derived from solid cancer cells leads to opsonization of cytotoxic T cells. We co-cultured for 16 h at a ratio of 1:1 MCF-7 breast cancer cells with TALL-104 T cells (A). As control resting TALL-104 cells were used, both co-cultured and resting were lysed, and samples were analysed using Western Blot approach without boiling to detect galectin-9 and Tim-3 in these samples (B). Medium was collected after co-culture and galectin-9 immunoprecipitated. The amount of released galectin-9 as well as TGF- β mRNA levels were analysed in samples from TALL-104 (C) and MCF-7 (D) using qRT-PCR. Granzyme B found in both TALL-104 and MCF-7 were analysed quantitative (E) and its activity (F). Representative images were chosen from one out of four independent experiments, mean +/- SEM included. 181

Figure 83 Two mechanisms are involved in galectin-9 secretion by MCF-7 human breast cancer cells after induction by T cells. Scheme shown including a variety of biochemical mechanisms involved in the galectin-9 secretion by cancer cells induced by interaction with T cells. We investigated two most prominent mechanisms in our studies. One mechanism is the calcium/PKC-dependent translocation of the galectin-9 – Tim-3 complex onto the cell surface followed by matrix metalloproteinases causing proteolytic shedding. Another possibility is by galectin-9 in complex with a trafficker being integrated into an autophagosome, which then merge with lysosomes. In such the galectin-9 protein is shed and secretion is performed by lysosomal exocytosis (A). To investigate this MCF-7 human breast cancer cells were co-cultured with Jurkat T cells at a ratio of 1:1 for 16 h. As described before, the adherent breast cancer cells were washed and given fresh medium, which was kept for 4 h and samples were taken after 2, 3, 4 h. The medium we used as replacement would contain certain inhibitors for specific processes needed for shedding galectin-9 in regard to the two mechanisms investigated. The inhibitors used were: AZD2014 – 10 μ M, EDTA – 200 μ M, Gö6983 – 70 nM, PIC – 30 μ M, U73122 – 30 μ M, and Vacuolin-1. Data included are mean +/- SEM of five independent experiments 183

Figure 84 Interactions with T cells led to increased calcium levels in MCF-7 human breast cancer cells. We co-cultured MCF-7 cells with Jurkat T cells for 2 h at a ratio of 1:1 and investigated calcium levels found within using Fluo4 reactive dye. Data include mean +/- SEM of six independent experiments. 184

Figure 85 Galectin-9 derived from solid tumours can induce increased IL-2 secretion and PI3K activity in T helper cells. MCF-7 cells were co-cultured with CD4⁺ Jurkat T cells at a ratio of 1:1 with or without galectin-9

neutralizing antibodies or isotype control for 16 h. We measured IL-2 levels with ELISA in medium and within T cell lysates, as well as PI3K activity within the lysates. Five independent experiments were performed, mean +/- SEM included. 186

Figure 86 Expressing both galectin-9 and VISTA enables cancer cells to inhibit anti-cancer immunity of T helper and cytotoxic T cells. We cultured LN-18 glioblastoma cancer cells with Jurkat T cells (A) or primary CD3⁺ human T cells (B) for 16 h at a ratio of 1:1. We analysed the secreted levels of galectin-9, (if applicable) granzyme B, IL-2 and TGF- β using ELISA. The Data are acquired in six independent experiments, mean +/- SEM are shown. 187

Figure 87 VISTA translocated onto the surface of LN-18 cells after induction by T cells. The glioblastoma cell line was kept in culture with either Jurkat T cells or primary T cells at a ratio of 1:1 for 16 h. We analysed the levels of VISTA on the cell surface using on-cell Western. Images shown are representatives of five independent experiments with similar results, mean +/- SEM shown 188

Figure 88 Suppression of T helper and cytotoxic T cells activity is achieved by interaction between VISTA and galectin-9 on T cell surface. We used a co-culture of LN-18 glioblastoma cancer cells with Jurkat T cells at a ratio of 1:1 for 16 h with or without VISTA and galectin-9 neutralizing antibody to study the effects of VISTA and galectin-9 on cell responses. We measured the PI3K activity within T cell lysates and the release of IL-2 in medium (A). Next, we repeated the experiment using primary mouse T cells instead of Jurkat T cells using also neutralizing antibodies. In cell culture medium we measured the release of granzyme B and IL-2 levels. LN-18 viability was measured using MTS assays, cell-associated human galectin-9 on mouse T cells was measured using the ELISA method. Data are included of six independent experiments, with mean +/- SEM shown. 190

Figure 89 Detection of in vivo secretion of galectin-9 by solid cancer cells We used C57 BL16 mouse, which had tumorigenic LN-18 cells injected subcutaneously at 2×10^6 cells per mouse. We measured the presence of CD3 proteins as well as human galectin-9 and VISTA in the direct microenvironment of the injection site (A). We also investigated the levels of human galectin-9 and TGF- β in the blood plasma of these mice and the presence of human galectin-9 on the primary mouse T cell lysates (B). Lastly, we used a co-culture of K562 cells with primary mouse T lymphocytes taken from both control and LN-18 injected mice to determine their efficiency. We analysed the viability of these K562 cells using MTS assay, including images taken (C). Shown are images from five independent experiments, included are also mean +/- SEM values of these experiments. 192

Figure 90 Analysis of monocytes regarding VISTA expression. A scheme was made to show the functions of metalloproteinases in regard of VISTA shedding from monocytes and the position on which the inhibitors used act (A). Primary human monocytes were investigated by our collaborators regarding their VISTA expression by flow cytometry (B). Our collaborators were able to verify the release of VISTA is dependent on metalloproteinases by incubating monocytes with inhibitors (C). 198

Figure 91 Determination of VISTA within M1 and M2 macrophages. Analysis was performed by our collaborators. Staining was performed by using monoclonal anti-human VISTA antibody (mouse) and secondary Alexa Fluor 594-coupled antibody. The lower part shows deconvolution of a z-stack. 199

Figure 92 Soluble VISTA released into the microenvironment does not lead to activation of intracellular granzyme B activity in cytotoxic T cells and prevents T helper cells from releasing IL-2. (A) TALL-104 cells were kept in culture with either 5 μ g/ml VISTA-Fc or as control solely Fc for 16 h. (B) Viability of TALL-104 was determined after exposure. (C) For further studies we used K562 human chronic myeloid leukaemia cells, which do not express and release detectable amounts of VISTA and IL-2. These cells were treated with 100 nM PMA for 24 h to immobilize them onto wells of a Maxisorb plates followed by a co-culture with Jurkat T cells at a ratio of 1:1.

(D) In some of the Jurkat co-culture wells we added either 5 µg/ml VISTA-Fc or control Fc for 24 h before being separated. In these co-cultures, IL-2 secretion was measured (E) within the medium and (F) within cell lysates by ELISA approach. (G) Total amount of IL-2 found within the cells were calculated. (H) Measurement of PI3K activity was performed. (I) Jurkat T cells pre-treated with 100 nM PMA were exposed to either VISTA-Fc or control Fc for 24 h. Again IL-2 was measured in (J) medium and (K) cell lysates. (L) Total amount of IL-2 detectable was calculated and (M) PI3K activity analysed within these cells. The data shown include mean +/- SEM of four independent experiments. *p<0.05 vs. control samples. 201

Figure 93 Soluble VISTA influences the granzyme B release into target cells (e.g. chronic myeloid leukaemia cells) but does not induce cell death in cytotoxic T cells. (A) K562 cells were immobilized onto wells of a maxisorp plate by exposure to 100 nM PMA for 24 h. These cells are known to not express and release any significant levels of galectin-9. After immobilization the medium in each well was replaced with Iscove's Modified Dulbecco's medium formulated by ATCC containing 2.5 µg/ml human albumin, 0.5 µg/ml D-mannitol and foetal bovine serum as well as 100 units/ml recombinant human IL-2. To some of these wells TALL-104 cells were added at a ratio of 1:1. Some co-cultured wells were supplied with either VISTA-Fc or control Fc for 16 h. (B) In co-cultured TALL-104 cells in-cell granzyme B activity was measured, and (C) cell viability was analysed. (D) In K562 cells in-cell activity of granzyme B was determined as well as (E) cell viability. Data set includes mean +/- SEM of four independent experiments. *p<0.05, **p<0.01 vs. control. 202

TABLES

Table 1 Tris Buffer composition	58
Table 2 Running gel volumes for two gels	58
Table 3 Stacking gel volumes for two gels	58
Table 4 Antibodies used for Western Blot analysis	61
Table 5 Values of cell-associated and secreted VISTA levels in a variety of cell types. Ctrl refers to non-stimulated samples as a control. ND refers to non-detectable and NA to non-applicable.	133

ABBREVIATIONS

ACT therapy	adoptive T cell therapy	DNA	deoxyribonucleic acid
ADAM	A disintegrin and metalloproteinase	DOTAP	1,2-dioleoyl-3-trimethylammonium propane
ALL	acute lymphocytic leukemia	DPI	diphenyleneiodonium chloride, NADPH oxidase inhibitor
AML	acute myeloid leukaemia	DTT	Dithiothreitol
AMV	Avian Myeloblastosis virus	EAE	experimentally autoimmune encephalomyelitis
AP-1	activator protein 1	ECACC	European Collection of Cell Cultures
APS	Ammonium persulfate	EDC	1-ethyl-3-(3-dimethylpropyl)-carbodiimide
ASK1	apoptosis signal regulating kinase 1	ELISA	Enzyme-linked immunosorbent assay
ATCC	American Type Culture Collection	FACS	fluorescence-activated cell sorting
ATF1	activating transcription factor 1	Fc	fragment crystallizable
ATP	adenosine triphosphate	FDA	Food and Drug Administration
BH3I-1	(5-[(4-bromophenyl) methylene]-a-(1-methylethyl)-4-oxo-2-thioxo-3-thiazolidineacetic acid)	FoxO1	forkhead box protein O1
BSA	bovine serum albumin	GSH	glutathione
BTN	bivalve transmissive neoplasia	GSK3 β	glycose synthase kinase 3 beta
CAR T cells	chimeric antigen receptor T cells	H2SO4	Sulfuric acid
CEACAM-1	carcinoembryonic antigen cell adhesion molecule 1	HAVCR-1	hepatitis A virus cellular receptor 1
ChIP	chromatin immunoprecipitation	HBV	hepatitis B virus
CLL	chronic lymphocytic leukemia	HCL	hydrochloric acid
CM	costimulatory molecule	HCV	hepatitis C virus
CML	chronic myeloid leukemia	HEPES	4-(2-hydroxyethyl)-1-piperazineethanesulfonic acid
CoCl ₂	cobalt chloride	HIF-1	hypoxia-inducible factor 1
CTLA-4	cytotoxic T lymphocyte antigen-4	HMGB1	high-mobility-protein B1
DAG	diacyl glycerol	HMGB-1	high-mobility group protein B-1
DAP	2, 3-diaminophenazine	HRP	horseradish peroxidase
DMSO	dimethyl sulfoxide		

IDO	indoleamine 2, 3-dioxygenase	NHS	N-hydroxysuccinimide
IFN- γ	Interferon- γ	NK	natural killer cells
Ig	Immunoglobulin	Nrp	neurophilin
IgSF	Immunoglobulin superfamily	NSCLC	non-small cell lung carcinoma
IgV	variable immunoglobulin domain	OPD	o-Phenylenediamine dihydrochloride
IKK	I κ B kinase	PARP cleavage	poly-ADP-ribose polymerase cleavage
IL-12	interleukin-12	PBS	phosphate buffered saline
IL-1 β	interleukin-1beta	PC	phosphatidylcholine
IL-2	interleukin-2	PD-1	programmed cell death protein-1
IL-23	interleukin-23	PD-L1	programmed cell death protein ligand 1
IL-6	interleukin-6	PGN	peptidoglycan
ITAM activation motif	immunoreceptor tyrosine-based activation motif	PHL	primary healthy leukocytes
KCl	Kalium chloride	PI3K	phosphatidyl inositol 3 kinase
Kd	dissociation constant	PIC	proteinase inhibitor cocktail
kDa	kilodalton	PKC	protein kinase C
KIM-1	kidney injury molecule 1	PLC	phospholipase C
LPS	lipopolysaccharides	PIGF	placental growth factor
MACS	magnetic-activated cell sorting	PMA	phorbol 12-myristate 13-acetate
MAPK	mitogen-activated protein kinases	PMSF	Phenylmethylsulphonyl fluoride
MDA	malondialdehyde	Prim. KC	primary keratinocytes
MMP	matrix metalloproteinases	PS	phosphatidylserine
mRC	metastatic colorectal cancer	PSGL-1	P-selectin glycoprotein ligand-1
mTORC2	mechanistic target of rapamycin complex 2	PTEN	phosphatase and tensin homolog
N.A.	non-applicable	q-RT PCR	quantitative real time polymerase chain reaction
N.D.	non-detectable	RAGE	receptor of advanced glycation end products
NADPH	nicotinamide adenine dinucleotide phosphate	RECIST	response evaluation criteria in solid tumour
NaOH	sodium hydroxide		
NF- κ B	nuclear factor kappa-light-chain-enhancer of activated B cells		

RISC	RNA-induced silencing complex	TIL	tumour-infiltrating lymphocytes
RNA	ribonucleic acid	Tim-3	T cell immunoglobulin and mucin domain containing protein 3
ROS	reactive oxygen species	TLR2	toll-like receptor 2
RTK	receptor tyrosine kinase	TLR4	toll-like receptor 4
SCF	stem cell factor	TNF- α	tumour necrosis factor 1
SDS	Sodium dodecyl sulphate	Treg	regulatory T cell
SEM	standard error of mean	TRIMM33	tripartite motif-containing factor 33
siRNA	small interfering RNA	Tris	Tris(hydroxymethyl)aminomethane
SM	sphingomyelin	UK	United Kingdom
SPR	surface plasmon resonance	VEGF	vesicular endothelial growth factor
SR11302	AP-1 inhibitor	VEGFR	VEGF receptor
SRCD	synchrotron radiation circular dichroism	VISG	VISTA gene
TBARS	Thiobarbituric acid reactive substances	VISTA	V-domain Ig suppressor of T cell activation
TBS	Tris buffered saline	VSIG3	V-set and immunoglobulin domain containing 3
TBST	Tris buffered saline with Tween	VSIR	V-set Immunoregulatory Receptor
TCA	Trichloroacetic acid	WHO	World health organization
TEM	transmission electron microscope	WT3ab	Wilms' tumour 3ab
TEMED	Tetramethylethylenediamine	Xkr8	Xk-related Protein 8
TGFBR	TGF- β receptor	Z-AAD-CMK	benzyloxycarbonyl-ala-ala-asp-chloromethylketone
TGF- β	transforming growth factor β	Δ N-ASK1	dominant-negative ASK-1
TIF-1 γ	transcription intermediary factor 1-gamma		

1 INTRODUCTION

Cancer has always been and will always be a challenge in therapeutic approaches. Swift changes in the expression levels of de-novo targets cause difficulties in achieving proper treatment as well as lead to accelerated cancer progression later in life. Furthermore, due to the high diversity of cancer types and their origin as well as its progression a single therapeutic approach to be sufficiently efficient is highly unlikely. So far, a combination of different antibody targets, with focus on stable, fundamentally conserved ones might be the best approach for creating a less harmful way of treating cancer than e.g. chemotherapy. In my dissertation I am focusing on a pathway conserved throughout evolution, which is used primarily to protect the embryo during development in the mother's body yet can be reactivated in cancer as means to ensure tumour progression. This pathway, known as Tim-3 – galectin-9 – VISTA pathway, might provide a target for a variety of therapies as it can be found in most cancer types and might even be applicable to inhibit miscarriages caused by the mother's immune system. In the following introduction I will give an insight of antibody targets for cancer therapy nowadays as well as an overview of the known mechanisms and protein structures of the Tim-3 – galectin-9 – VISTA pathway. Regarding the influence of this pathway and prior research showing that some of these proteins are originating from the embryonic development I also summarize the comparison between the protection of the embryo against the immune system and similarities to inhibition of anti-cancer immunity.

1.1 CANCER DIVERSITY LEADING TO THERAPEUTIC CHALLENGES

The term “cancer” refers to an accumulation of malignant cells within a specific area or from a specific origin of the body (either an organ or a very specific cell type). The accumulation often leads to a series of interferences in the function and viability of healthy cells. Cancer cells are highly relying on an increased dependency of energy, eventually inducing malnutrition of surrounding healthy cells. In combination with high demand in space, this growth of malignant cells can lead to loss of function of healthy cells either due to this lack of nutrition or due to the take up of most of the space previously occupied by such healthy cells. Either way, a growth of malignant cells can, depending on how aggressive the tumour is, lead to diverse complications for patients, such as higher risk of infections and fatigue in everyday life to ultimately causing serious life-threatening conditions.

Cancer therapy is nowadays relying on many factors such as size, mutations, and time of diagnosis; yet the main diagnostic aim is to determine the type of cancer to be treated (Merlo, 2006) It can be either a mass accumulation of cells in a specific organ referred to as a solid tumour or it arises as hematopoietic cancers in a non-solid form. A non-solid form of cancer is an accumulation of cancer cells within the bloodstream. Hereby cells are often originating from immune cells, such as B and T cells and therefore tend to interfere with appropriate immune responses towards infections. Another form of cancer is the rise of malignant cells originating from one organ within another, due to metastasis. By angiogenesis, new blood vessels are formed for better nutrient and oxygen supply for solid cancers. The new rise of blood vessels can also lead to the spread of the malignant cells through the bloodstream to new locations within the body (Tak, 2014).

During the application of treatments further mutations can arise within cancer cells as these cells adapt to the changes within the microenvironment. This can lead to an onset of complications, especially as a high mutational rate might cause the loss of targets for antibody therapy. These changes can also induce the upregulation of anti-apoptotic features and together with other complications can severely influence the application of appropriate therapies. The high mutation rate might further decrease specific receptor expression during treatment progression, causing a therapy to be efficient in one cycle but losing any effect in a follow-up. This clearly indicates that the

application of combinations of antibodies to efficiently attack more than one cancer-specific checkpoint might be the most appropriate approach for the future (Shao, 2020).

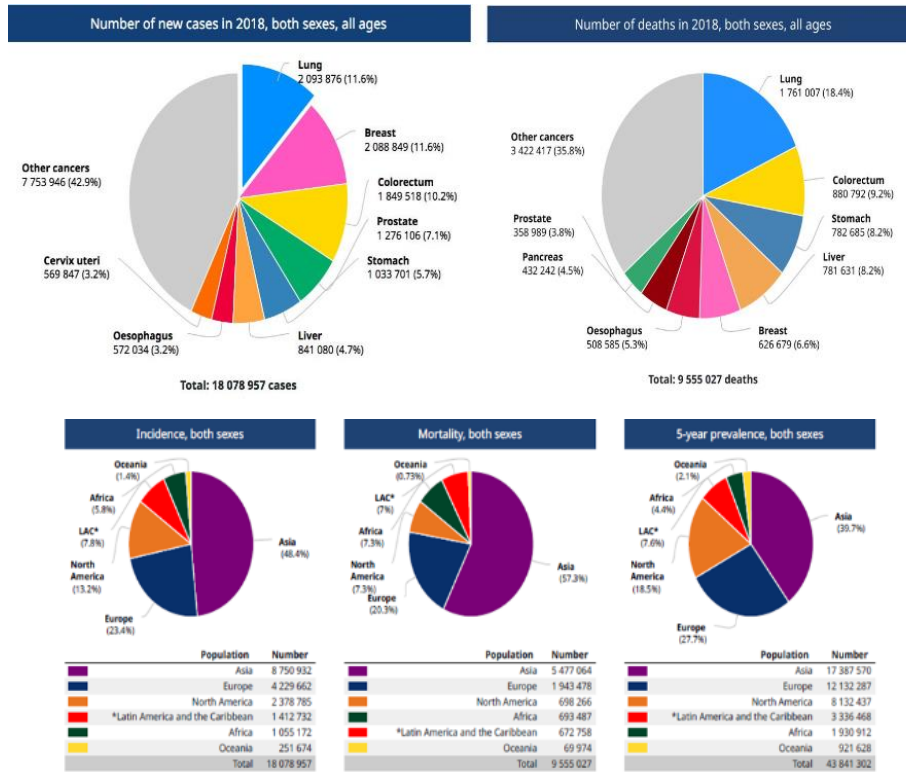
1.1.1 Cancer statistics

Cancer statistics provided by GLOBOCAN 2020 established by the World Health Organization (WHO) show that cancer still has a significant influence on the mortality rate especially in Asia, Europe, and North America. Most prominent are lung, breast, and colorectal cancer with about 2 million new cases each in 2020. Altogether the raise of cancer diagnosis will reach 50.5 million incidences within the next five years. Dependent on the type of cancer, treatment often includes either surgery, chemotherapy or immunotherapy enabling an average ten-year survival rate of about 50% in the UK with big discrepancies depending on the type of cancer. The statistic is updated in a regular basis about every two years to investigate further development.

Analysing the main incidence graph between the two statistics from 2018 and 2020 it is shown that the numbers of cancer cases of the commonly diagnosed types has not changed in percentages; such common types of cancer are lung (11.6% to 11.4%), breast (11.6% to 11.7%) and colorectal cancer (10.2% to 10%). Yet, the overall numbers of new cases have raised within the two years from about 18.1 million to 19.3 million indicating a clear increase in new malignant tumour diagnosis. The rise in new cases number does not necessarily mean an increase in cancer incidences due to outside factors or genetic mutations but is clearly also an indicator of improvement of cancer diagnosis in the last few years by routine check-ups and determining the risk of people with family history of cancer to ensure an early diagnosis (Figure 1).

Comparing the mortality between 2018 and 2020 has, unfortunately, also not shown a significant shift towards improved survival rates, especially in the three most common lethal cancer types: lung (18.4% to 18%), colorectal (9.2% to 9.4%) and stomach cancer (8.2% to 7.7%). We see a slight increase in the overall number of cancer patient mortality from 9.6 million deaths recorded in 2018 to 9.9 million deaths in 2020. Taking in consideration that depending on the severity and type of cancer the 5-year survival rate can be in average ranging between 7 – 84% this minimal increase in mortality rate next to an increased number of new diagnoses might indicate an improvement of cancer therapy (GLOBOCAN, 2020).

A)



B)

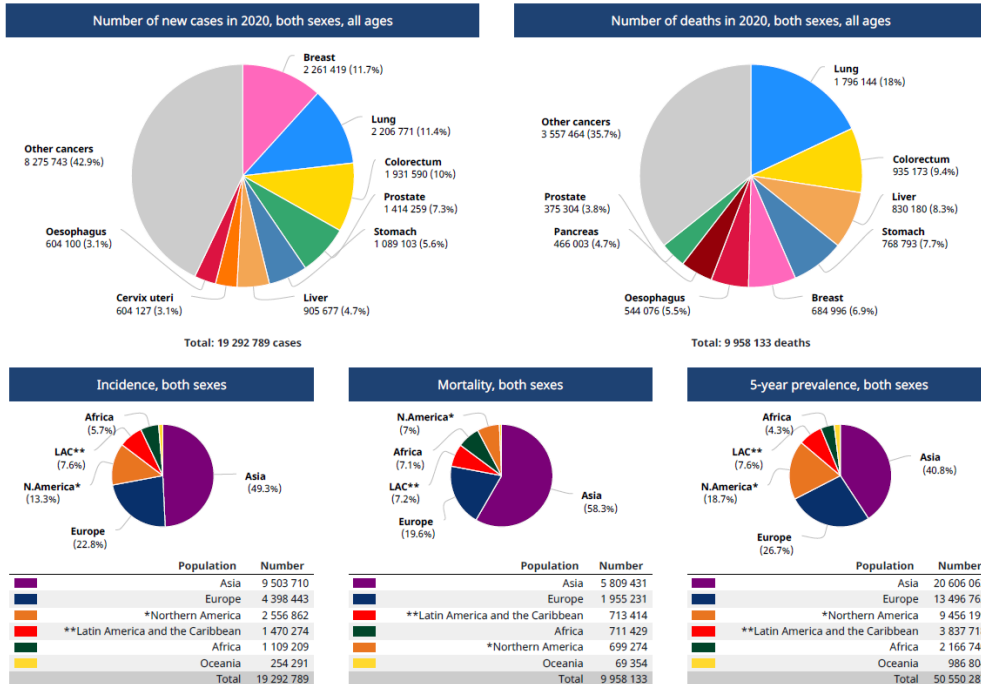


Figure 1 Cancer statistics (A) GLOBOCAN fact sheet 2018, (B) All Cancers Fact sheet from GLOBOCAN 2020, Ferlay J, et.al. (2020). Global Cancer Observatory: Cancer Today. Lyon, France: International Agency for Research on Cancer. Adapted from: <https://gco.iarc.fr/today>, accessed 16.03.2022.

1.1.2 Cancer Hallmarks

Concerning research on cancer mechanisms new influences and major events have been investigated in the last 50 years which led to the introduction of hallmarks in cancer development. While at the beginning in 2000 six major hallmarks were known, due to new research and further knowledge gathered about the development and survival of cancer cells the amount of hallmarks has continuously increased. These hallmarks nowadays consist of already 14 different categories in which a variety of events taking place during the cancer progression can be separated (Figure 2) (Hanahan, 2022).

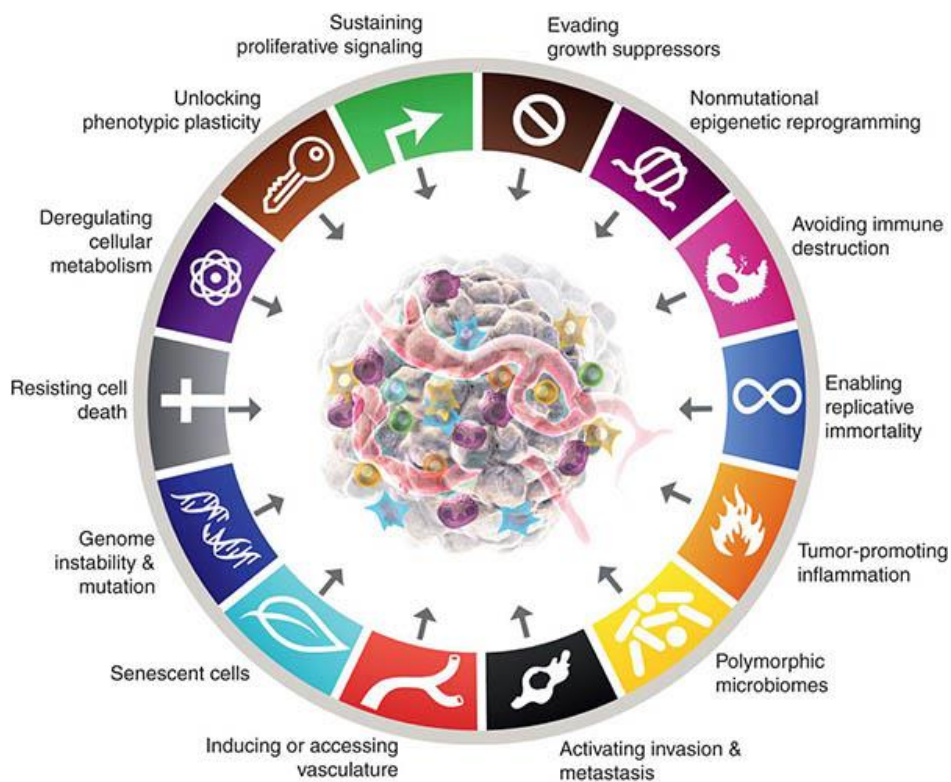


Figure 2 Cancer hallmarks. Adapted from: Douglas Hanahan; Hallmarks of Cancer: New Dimensions. Cancer Discov 1 January 2022; 12 (1): 31–46. <https://doi.org/10.1158/2159-8290.CD-21-1059>

As mentioned at the beginning, the formation of a new vascular system and the deregulation of the cellular metabolism are common features found in the majority of cancer types investigated and are therefore mentioned as hallmarks in cancer development. Also, the adaptation of new vesicles enabling proper nutritional support for the malignant cells can further support the invasion and development of metastatic growths in other organs.

In this thesis, we concentrate on specific pathways which can be categorized in the “avoiding immune destruction” hallmark. While to a certain extent they might also correlate with the hallmark “resisting cell death” our specific topic consists mainly of the disabling of cytotoxic lymphocytes attacking the cancer cells. Malignancies do not only need to adapt to external influences inducing cell death but might also need to resist internal influences due to increased genetic and metabolic changes, therefore these hallmarks were separated in two unique categories.

Lastly, genetics also play a significant role in the development of cancers. The human genes that might lead to cancer can be differentiated in either cancer-specific genetics that are inherited throughout generations and lead to a possible elevated risk of developing such cancers later in life, or genetic abnormalities following for example the exposure to radiation which raises the risk of malignancy formation within one individual if another cancer-inducing factor is introduced to the body (Das, 2015). Such genetic risk itself might lead to cancer development especially later in life after the body has been dealing with diverse outside factors but is theoretically not able to induce cancer on its own. Cancer types that can be inherited are a variety of solid cancers such as lung, breast, colon, uterine and others. Leukaemia is so far seen as non-inheritable by genetics, but genetic abnormalities can be found to lead to a higher risk (Tak, 2014). Depending on the stability of certain genes, they might be easily adapted by cancer cells during the progression to induce continuous immunosuppressive function, or some genes are too stable to be significantly modified but do offer already strong immune-adaptive functions that can be reused by cancer cells. While the first category of genes is causing difficulties to target a structure, the second category enables stable approaches in therapy.

Taking all this in consideration the development of a variety of different approaches of cancer therapy, such as personalized therapy, as well as determining further targets should be the main focus in the fight against malignancies. Not only is the improvement in therapies and discovery of new treatment approaches helpful to support the patient’s survival, but also the aim of generating better diagnosis for early detection can help to treat cancer types before severe side effects and complications arise.

1.1.3 General biomedical characterization of human cancers presented by solid tumours

Solid tumours can either be benign or malignant and are named generally according to the organ they are originating from. Benign forms are localized in a specific tissue without showing signs of growth or interference in the patient's survival. In some cases, it does cause some inconvenience depending on the location, e.g. interfere with motility if growing near joints or if the area is sensitive to pressure it can lead to pain, as seen within the brain. If a form of abnormal cell accumulation is determined as malignant it is referred to as cancer and treated depending on the diagnosis of a variety of features (size, localization, stage). As an abnormal growth of cells, cancers are prone to introduce further mutations leading to both increased cell cycle turnover for accelerated growth as well as inhibition of immune responses. Solid tumours are restricted at first to a specific area, which will be assigned as its origin and grow within such a specific organ (lung, stomach, colorectal). By increased angiogenesis, the cancer cells might be able to further spread such organ-specific malignant cells into other areas within the body, introducing so-called metastasis (Maccalli, 2013, Anand, 2008).

Tumour cells tend to arise from mutational burden within the body either by heritage of genetic abnormalities or by outside influences such as smoking, environmental impact, alcohol, and infections (Preetha, 2008). Most common are solid tumours in areas that are open to such environmental influences. These types of malignancies tend to be one of the most difficult to treat and arise with a variety of side effects leading to further complications in everyday life. Especially lung, colorectal, stomach, liver and pancreatic cancers have a high mortality rate due to complications in diagnosis and treatment (GLOBOCAN, 2020). Furthermore, cancer cells tend to vary within a single tumour growth, leading to different mutational states of malignant cells within one solid tumour. Such differential adaptations within a specific cancer type can lead to a recurrence of tumour growth even after the successful application of therapy if the surviving cells might be more aggressive and non-responsive to therapy than the treated ones (Mroz, 2016).

To determine the efficiency of therapy in solid malignancies the "response evaluation criteria in solid tumours" (RECIST) has been introduced as a diagnostic guideline during the development of new drugs. RECIST was developed by the RECIST working

group consisting of clinicians, academic researchers, government, industry, and statisticians as well as imaging specialist and its main focus is to be used in the early development of cancer therapy drugs; mainly in the phase II trials. The diagnosis for individual patients in applied therapy depends on similar approaches, yet these specific guidelines were intended to mainly focus on the development of new therapy against solid tumours. The focus hereby is to determine changes of the size of lesions, a single solid cancer type within the organ during the treatment (Eisenhauer, 2009). These measurements can be also used in the actual treatment considering one specific, important factor if applied: As soon as the immune system gets an advantage to attack a solid tumour due to the therapy, the immune cells attach to a certain extent to the solid tumour, which sometimes leads to an increase in size during regular visual check-ups. This increase in size does not indicate immediately a growth of the tumour but is actually a so-called “pseudo-progression” and is sometimes even favourable right after treatment as it does clearly indicate an increased response of the immune system towards the cancer (Ma, 2019). As follow-up an example of a solid cancer type regularly treated by immune therapy and other approaches is given. Breast cancer is one of the most prominent solid tumours to be diagnosed and often demands very invasive therapeutic approaches, with complete removal of breast tissue by surgery being regularly decided upon (Kamińska, 2015). As such it is still dependent on development of non-invasive approaches.

4.1.1.1 Breast cancer

A short introduction to the breast cancer development is further described, due to the fact that in our studies we will apply the MCF-7 breast cancer cell line (Figure 3) as a commonly used breast cancer model. Breast cancer can be differed according to its developmental stages, which are determined by certain key factors such as the size and the type of receptors the cancer developed.

As an example, stage 0 is determined as carcinoma in situ and refers to a locally encapsulated cancer with no spreading to immediate neighbouring tissue. It can be treated by mastectomy or lumpectomy with or without radiation. In comparison stage IV breast cancer cells tend to spread to surrounding tissue and further organs forming metastasis. This form of metastasis is referred to as secondary breast cancer and often occurs in liver, lung, bone marrow or even the brain. In such cases treatment decided upon is a universal approach such as hormone therapy, chemotherapy, radiation

therapy as well as antibody therapy. Surgery is often not an option in secondary breast cancer due to its spreading (Giuliano 2018, Cancer Research UK).

Breast cancer clearly visualizes the difficulty of solid tumour treatment approaches. While stage 1 has a high survival rate of 90% up for more than 20 years, in stage IV breast cancer therapy consists mainly of treating the symptoms as the spreading lowers the survival rate for the next 5 years to 25% (Giuliano 2018, Cancer Research UK).

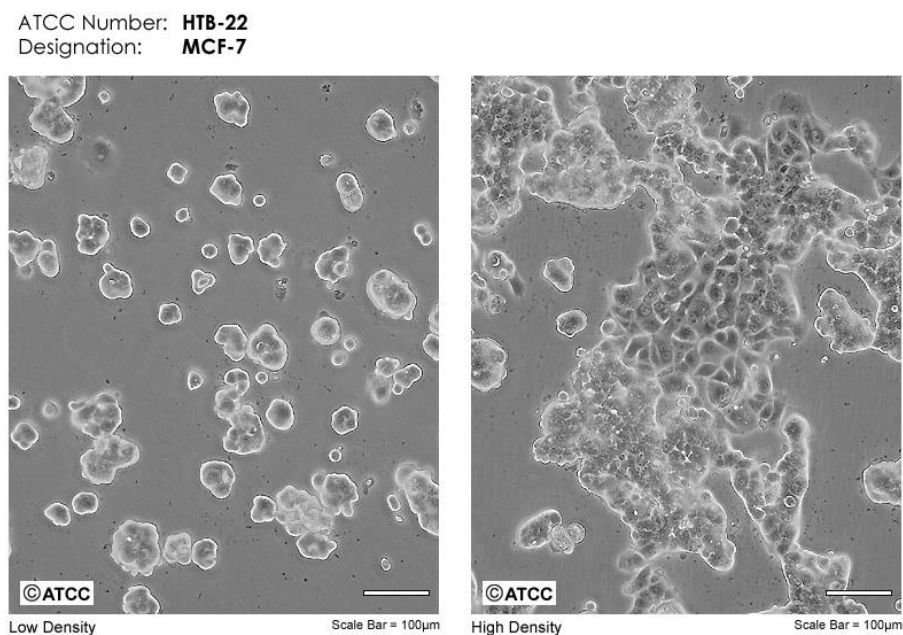


Figure 3 MCF-7 breast cancer cell visualized in low and high density. Taken from the cell line bank ATCC. 22/07/2022. <https://www.atcc.org/products/htb-22>

1.1.4 Haematological malignancies as human cancers presented by “non-solid” tumours

“Non-solid” tumours, also called “liquid” or hematopoietic cancers arise from immune cells, either directly from a malignant precursor stem cell in the bone marrow or by mutational changes within the developmental stages of mature immune cells. Dependent on their pre-cursor form non-solid tumours can be differentiated in three main categories, leukaemia, lymphoma, myeloma. Hereby, important to mention is that the term “non-solid” cancer is being used as a collective term for blood cancer, but dependent on their category these cancer types can also take on a solid form especially in case of lymphomas and myelomas (Tak, 2014).

In non-solid growths a benign form is not detectable, there are the possibilities of diagnosing some blood disorders that can be a predisposition for certain leukaemia forms but do not account for a malignancy themselves prior to further changes. An issue in cancer therapy is that some of these blood disorders can actually arise after the treatment of another malignancy with e.g. chemotherapy. These after-effects of cancer therapies are monitored closely to enable early diagnosis (Forman, 1979).

4.1.1.2 Multiple Myelomas

Myelomas are deriving from plasma cells. In the healthy human plasma cells are not able to further divide after development and are determined to simply produce antigen-specific antibodies for a limited time. By malignant mutations plasma cells are able to proliferate within the blood stream and start to produce paraproteins similar to for example IgM, which might consist of either light chain, heavy chain or fully formed immunoglobulins. Due to the high number of plasma cells proliferating it can lead to bone marrow “clogging” as they take up space and can further impair the B cell production leading to risk of infection and overall impaired immune responses (Tak, 2014).

4.1.1.3 Lymphomas

Lymphomas arise from lymphocytes, which underwent malignant transformation. Such lymphocytes tend to travel through the body via the blood stream, yet, in malignant forms they often accumulate within lymph nodes, thymus, or spleen similar to a solid tumour and are classified as either Hodgkin Lymphomas or non-Hodgkin Lymphoma.

The difference of Hodgkin and non-Hodgkin lymphomas is determined by their structural diversity, which is investigated by using a biopsy sample and performing analysis with a simple field stain consisting of Field stain A (methylene blue and Azure 1 dissolved in PBS) and Field stain B (Eosin Y in buffer solution). Hereby, Hodgkin Lymphoma diagnosis is fixed on the presence of either Reed-Sternberg cells (classic HL; 95%, Figure 4, left) or “popcorn” cells (nodular lymphocyte predominant HL; 5%, Figure 4 right). Non-Hodgkin lymphoma is more commonly diagnosed and consists of malignant lymphocytes without the presence of such specific cells mentioned before. Dependent on the cell of origin, either T or B cells, non-Hodgkin lymphoma can be further subcategorized in a variety of classes dependent on genetic aberrations, clinical characteristics or immunophenotypic changes (Tak, 2014).

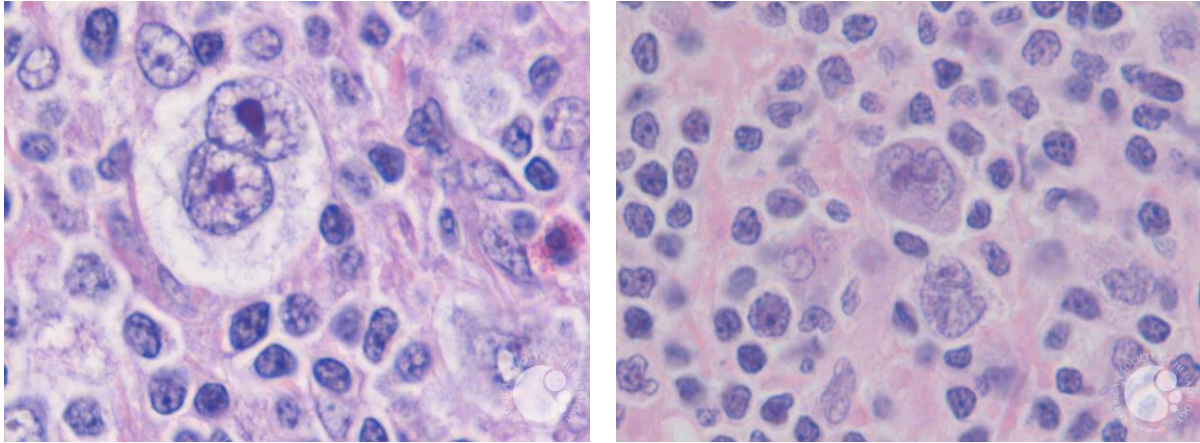


Figure 4 Reed-Sternberg cells (left), Popcorn cells (right). This image was originally published in ASH Image Bank. Reed Sternberg cells: Girish Venkataraman, 2016, #00060568. Popcorn cells: Timothy C. Carll et.al, 2018, #00061372 © the American Society of Hematology

4.1.1.4 Leukaemias

Leukaemia cells are derived from either myeloid or lymphoid cells and can differ in their onset as either chronic (long-termed development often diagnosed from age 50 or older) or acute (sudden development, with cases arising often in children and teenagers) leukaemia. Dependent on these factors leukaemia is differentiated as either acute myeloid leukaemia (AML), chronic myelogenous leukaemia (CML), acute lymphoblastic leukaemia (ALL) or chronic lymphocytic leukaemia (CLL). Altogether the occurrence for leukaemia is relatively low ranging at about 3% of diagnosed malignancies and the pre-disposition of developing childhood leukaemia is determined by genetics. This can include family history of leukaemia cases, genetic disorders such as Down Syndrome, or simply outside influences including previously applied chemotherapy as well as possible exposure to radiation of any kind (Stieglitz, 2013; Tak, 2014). In our research, we used mostly the AML cell line THP-1 to investigate effects of our protein of interests on non-solid tumour forms. We were also able to gather primary samples of AML patients to verify the effects seen, therefore a short introduction on the development of acute myeloid leukaemia is given below.

4.1.1.4.1 Acute myeloid leukaemia as a typical example of severe haematological malignancy

As mentioned before, for non-solid cancer, we used acute myeloid leukaemia in our studies. Either primary AML samples directly taken from patients by our collaborators in Switzerland or we cultured the THP-1 AML cell line (Figure 5).

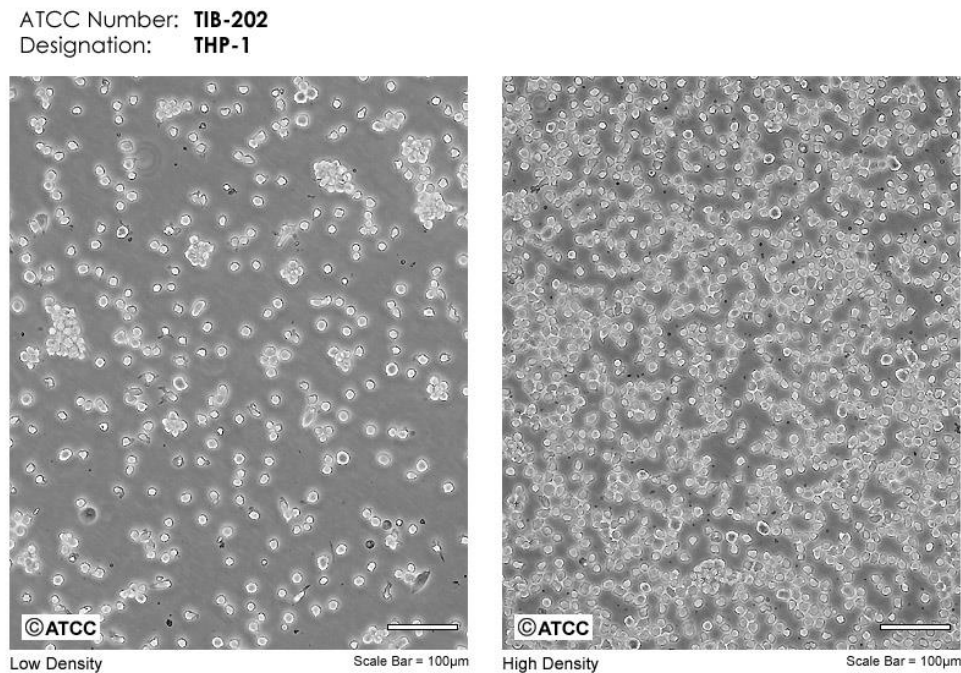


Figure 5 THP-1 acute myeloid leukaemia cells visualized in low and high density. Taken from the cell line bank ATCC. 22/07/2022. <https://www.atcc.org/products/tib-202>

AML arises from either a hematopoietic stem cell or a progenitor cell within the bone marrow. Accumulation of such cells lead to interference of production of “normal” blood cells and induces a diverse range of symptoms such as rapid weight loss, bone pain, fatigue, and difficulties in the healing process of either infections or wounds. The exact cause of AML development is yet to be known but a variety of genetic mutations is associated with an increased risk of developing acute myeloid leukaemia (Cai, 2019). The cells leading to such effects are referred to as myeloblasts, short *blasts*, and while structural changes are often not easily detectable the increased number of blasts within the bone marrow is an indicator of malignancy (Welch, 2012, Czeh, 2016, Kumar, 2011). The WHO has determined the amount necessary for proper diagnosis is about 20% - 30% of myeloblasts found within the bone marrow or as circulating white blood cells and the analysis should be performed with Wright or Wright-Giemsa-stained smears. (Hwang, 2020)

AML is difficult to categorize as different factors enable a variety of combinations and two different systems are in place: The WHO system and the French-American-British system, which of those are used is decided upon by each country. The WHO has determined some categories in which AML blasts can be differed and which can be further divided in subcategories (Hwang, 2020):

- Chromosomal (genetic) changes such as translocation, fusion genes, or mutation in genes for specific proteins.
- Cause of development, such as previous blood disorders that lead to AML
- How many cell types and which specifically show malignant transformations.
- Previous cancer therapy of another malignancy inducing AML development (e.g., chemotherapy)

Furthermore, due to the high variety of AML subcategories a patient is classified in relapse risk groups after treatments, which are dependent on such factors as changes in the chromosomes or genes, mutational markers on leukaemia cells, cell count, age of patient or also if the central nervous system has been affected. Depending on the risk group and the progression of AML at time of diagnosis the three risk groups are:

- Low risk group → relapse is at low risk, after chemotherapy patient is stated as cured
- Intermediate risk group → chances of relapse exist, to minimize the risk patients might need stem cell transplants after chemotherapy
- High risk group → the risk of relapse is in such cases particularly high, therapy consists of chemotherapy and early stem cell transplants.

Due to the high variations of AML occurring in patients a similar high diversity of therapies is available to counter the malignancy. To ensure the best possible outcome a proper diagnosis of the genetic composition, translocations, and mutations, has to be performed in an analytics lab beforehand (Hwang, 2020).

Cancer therapy nowadays has a high variety of approaches available ranging from different compositions of chemotherapy, surgeries, stem cell transplantation to newer techniques including antibody therapies and chimeric antigen receptor T cell (CAR T cell) development. In the following chapter a few of the most common therapies and therapeutic targets are explained.

1.2 INTRODUCTION TO A VARIETY OF CANCER THERAPIES

As the human body is dependent on cell renewal for its survival the probability of malignant cell formation at a certain time in life is very high. These cells are normally checked and upon recognition of failing abilities or fatal mutations the immune system is able to remove such mutated cells. With increasing age or genetic changes, the risk of such a malignant cell being able to evade the check-up and subsequently promoting cancer formation is significantly high. Due to tumour growth and further mutations, the immune system often ends up in a deficiency to remove malignant cells (Lynch, 1979).

To support the immune system a high variety of therapies have been developed over time focussing on different aspects of tumour growth. In this chapter I give a short overview of common treatments used in cancer therapies. Three main aims are put in focus to treat malignancies: a) support of the immune system in its function (immunology), b) suppression of the formation of new blood vessels during tumour development (angiogenesis) and c) to suppress altogether the tumour growth (growth factors). A combination of such therapies can be used to a certain extent to support remission and prolong the patient's life.

1.2.1 Chemotherapy

The most common approach in cancer therapy is nowadays still chemotherapy. Established as a treatment against malignant cells at the beginning of the twentieth century it can be used against most types of cancer. It is often combined with either surgery or stem cell transplantation from either the patient themselves taken before the application of the chemotherapy or a donor (Wu, 2018, Tormey 1975). The term chemotherapy includes any drug or chemical treatment that can be used as a cytotoxic approach against cancer cells. Such therapies can be deployed either as single agent therapy or as a combination of two or more drugs depending on the type and stage of the cancer development at the time of diagnosis. Hereby it is important to keep focus on the risk of patients acquiring low-dosage drug resistance or complications due to the toxicity of the drugs.

The main difference of chemotherapy to the following immunotherapy is the way it interacts with the tumour. Chemotherapy is applied to directly attack the tumour and leads to reduced survival by interfering with cell replication and metabolism (Conklin, 2004), while immunotherapy is meant to be a supportive mechanism for the patient's immune system to take on the cancer cells during application in a less toxic way. While

immunotherapy and immunomodulation seem to be the right way to treat cancer, it is still in focus of further research regarding efficiency and so far, the more common approaches are still chemotherapy, stem cell transplantation or surgery (Raza, 2019).

1.2.2 Immunotherapy targets

Immunological targets are used to aid the immune system dealing with cancer by either improving the functions of specific immune cells, such as natural killer (NK) cells, T cells (either CD8⁺, CD4⁺) or dendritic cells or to reverse inhibitory functions of cancer cells towards such immune cells (Kennedy, 2020). The immune system can be supported by inhibitors that interact directly with receptors expressed on the cell surface and hinders the binding of these receptors with certain ligands (example as follows: PD-1/PD-L1) or they interact within the cells to stop the main adaptors of often highly up-regulated production pathways of certain immunosuppressive proteins (example: AKT). Another approach that is in research focus nowadays is a modulation of T cells against specific targets outside of the patient's body, CAR T cells, which are adapted to either up-regulate or even regain certain functions useful against cancer and are introduced into the patient's body again after such modulation for better performance against the malignancy (Haslauer, 2021).

1.2.2.1 Programmed cell death receptor (PD-1) and ligand (PD-L1)

One of the most prominent targets to be used in immune therapy is the interaction of PD-1 and PD-L1. PD-1 is a receptor expressed on T cells, natural killer cells and B cells and is able to attenuate the activation of T cells by interacting with the T cell receptor (TCR) in the tumour environment. Hereby the cancer cell is expressing and releasing in high volume the ligand PD-L1 to suppress anti-cancer immune responses. The expression of PD-1/PD-L1 is dependent on a variety of cell signalling pathways and therefore can be difficult to properly target as cancer cells can adapt quickly to environmental changes as well as the sudden occurrence of specific inhibitors (Biotechne; Marshall, 2017).

The PD-1/PD-L1 interaction has been determined as an important target in mostly solid cancer types such as breast, pancreatic, colorectal, lung and gastric cancer. Due to the significantly high variety of pathways within cells influencing the expression of PD-1/PD-L1 the best target in such cancer types is to block the actual binding of ligand to receptor. Hereby a significant number of therapeutic components are available, such as Nivolumab, Pembrolizumab, JQ1, Atezolizumab, Avelumab and since September

2018 also Cemiplimab. Each of these PD-1/PD-L1 inhibitors has different efficiency depending on the type of cancer and the expression levels of the specific target (Marshall, 2017; Zhu, 2016; Huang, 2021; Migden, 2020).

Unfortunately, therapies with PD-1/PD-L1 inhibitors are sometimes not efficient in patients with high expression levels, which can be either caused by choosing an inhibitor lacking targets or due to the patient developing resistance. Furthermore, new studies also indicate that patients diagnosed to be PD-1/PD-L1 negative and therefore to be expected to not react to the inhibitor at all, have shown an improvement in anti-cancer immunity (Madore, 2014). Regarding the interaction of the PD-1 receptor and its potential ligands as well as the efficiency of their inhibitors, more studies are necessary.

1.2.3 Significance of hypoxia and angiogenesis for malignant tumour growth

While the main interaction leading to health issues in cancer development is the insufficient immune response, some other factors are just as important to target to hinder the progression of the tumour progression. On the one hand the induction of new blood vessel formation by angiogenesis is a main feature of most solid tumours to ensure proper delivery of any kind of supplements needed for growth. On the other hand, another issue that arises with the formation of new blood vessels is the risk of metastasis, the ability of a solid cancer to move from its original organ of development to other organs inducing there the formation of an organ-foreign tumour. This spread is one of the main indicators of poor survival prognosis, as the cancer as soon as it is able to leave its primary space can spread to any kind of organ and develop further mutations as well as severely influence the overall functions of organs (Zetter, 1998).

Next to the inhibition of blood vessel formation, the growth of a tumour is also a significant target to disable as it not only causes issues with immune cells to target the individual cancer cell properly but the more space a tumour takes up the less support of any healthy cell within the specific organ is able. Not only does the tumour simply take over space, it also interferes with nutrition and support to maintain such healthy tissue which might lead in worst cases to organ failure (López, 2014)

1.2.3.1 Targeting Angiogenesis option: Vascular endothelial growth factor (VEGF)

The formation of new blood vessel is a process that is needed in different situations during the human life. Beginning with the embryo growth to ensure survival as well as during wound healing and menstruation, the formation of new vessels is depending on a balance between activation and inhibition of specific proteins responsible for these procedures. This change of balance is referred to as “angiogenic switch” in which the endogenous activating factors are more prominent than endogenous inhibitory factors (Maas, 2001).

VEGF refers to a protein family responsible for the growth of blood vessels and consists of VEGF-A (commonly referred to VEGF), VEGF-B, VEGF-C, VEGF-D, and the placental growth factor (PlGF) responsible for new vessels during embryo development. Interaction on endothelial cells is maintained by binding to the receptor tyrosine kinase VEGF receptor 1 (VEGFR1), VEGFR2 or VEGFR3, which together with the co-receptors neuropilin 1 (Nrp-1) and Nrp-2 lead to downstream activation of angiogenesis and vasculogenesis (Sullivan, 2010).

To inhibit the formation of new blood vessels the VEGF protein family is a prominent target as it is one of the main interactors when developing such new structures. An approved approach to inhibit the formation of new blood vessels is the usage of Bevacizumab, a therapeutic antibody used to inhibit the binding of VEGF to VEGFR1 and 2. This treatment is performed on a variety of cancers from gastrointestinal to lung cancer and has been developed performing studies on mice. While the binding of VEGF does inhibit the formation of blood vessels to a certain extent, it has been determined as a treatment prolonging the patient’s life for only a few months and it can further lead to excessive bleeding if not observed closely. Bevacizumab is either applied as a single therapy or in combination with chemotherapy (Ferrara, 2005).

Another possibility to inhibit the interaction between VEGF and VEGFR is targeting the receptor. The VEGFR2 binding inhibitor therapy called Ramucirumab has been determined to prolong patients’ life in metastatic gastric, gastroesophageal junction cancer, metastatic non-small cell lung cancer (NSCLC) and metastatic colorectal cancer (mCRC) and has been approved in the U.S. by the Food and Drug Administration (FDA) as therapy (Vennepureddy, 2016). Lastly, targeting VEGF, a

decoy version of VEGF receptors is tested to inhibit binding as so-called VEGF traps, one so far approved is Aflibercept (Zirlik, 2018).

The formation of blood vessels is an early step within the cancer development, therefore treatment with such a therapeutic agent should be applied in early-stage solid cancers to suppress the formation of such new blood vessels and hopefully inhibit the support with nutrients and oxygen, also to avoid the possibility of cancer cells spreading to other organs and metastasising there. This naturally pre-sets an early diagnosis of cancer development and causes difficulties with this therapeutic target in late diagnostics.

1.2.3.2 Growth factor option: Protein kinase B (also known as AKT)

Protein kinase B, also known as AKT serine/threonine kinase is a protein that influences a variety of pathways regarding cell survival. In cancer, this protein is overexpressed to adapt to the high maintenance the cancer cell has to keep up for survival and proliferation. AKT can be induced by different approaches, such as extracellular stimuli, for example insulin, which will enable the activation of AKT via receptor tyrosine kinases (RTK) or intracellular stimulation by mechanistic target of rapamycin complex 2 (mTORC2). Due to the variety of pathways that are influenced by AKT and the increased activation, it has been determined as a useful target to influence cancer cells from within and diminish their survival (Marshall, 2017; Madhunapantula, 2011).

Pathways that are activated by AKT are for example I κ B kinase (IKK) responsible for nuclear factor kappa-light-chain-enhancer of activated B cells (NF- κ B) transcription factor activation and the mTORC1 complex responsible for ribosome biogenesis and protein synthesis. It can also enable the inhibition of forkhead box protein O1 (FoxO1) to ensure continuous cell survival and inhibition of WEE1 and glycose synthase kinase 3 beta (GSK3 β) for continuous cell cycle proliferation. Each of these pathways is highly active within cancer cells and might lead to complications during applied cancer therapies. Therefore, the AKT protein in its activated (phosphorylated at positions Thr308 and Ser473) form is a significant target to ensure the patients survival by counteracting its elevated functions during cancer progression (Nitulescu, 2018). A scheme of the general pathway including the previously mentioned proteins is shown in Figure 6.

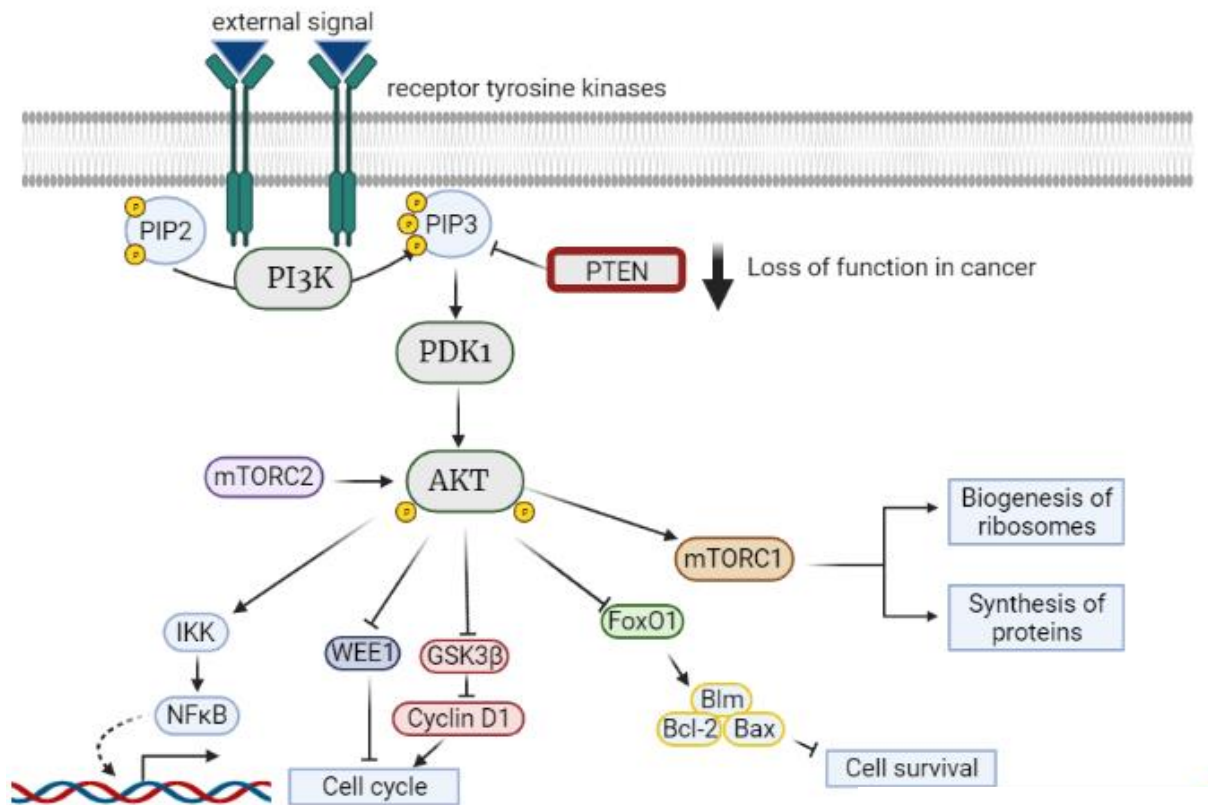


Figure 6 Schematics visualizing the PI3K pathway activating AKT and inducing various effects within cells is shown. The general effects on activation of PI3K within for example cancer cells is shown. This pathway can lead to increased cell cycle turnover, increased biogenesis of ribosomes as well as upregulation of synthesis of proteins. Furthermore, it can enable prolonged cell survival. Schematic was made by using biorender.

The issue arising hereby is that a multitude of downstream targets activated by AKT also means a multitude of chances of mutations to occur and influence this pathway. In some cases, targeting a specific protein to be either inhibited or up-/downregulated can lead to a shift within the cancer cell towards new mutations circumventing the primary target. Nowadays, a first approach is to aim for the primary activators of the PI3K/AKT/mTOR pathway, mainly the increased activity of the PI3K. To do so, two ways in which PI3K overexpression is induced can be targeted, this can either be the increased activation of PI3K components or the inactivation sometimes even loss of function of the PI3K inhibitor phosphatase and tensin homolog (PTEN) located on chromosome 10 (Dillon, 2014).

Loss of PTEN function can be inherited via germline mutation but tend to arise in all types of cancer in a variety of mutations, such as miss-/nonsense mutation as well as insertion and deletion. Each type of mutation in consequence lead to hyper-activation

of the AKT protein and its function of supporting cancer survival. To counter these effects, a therapy using an inhibitor performing in the same aspect as PTEN is needed and so far, a high number of possible drugs to do so are tested and investigated in just as many different tumour types. (Yang, 2019). AKT is found deeper within the pathway which further leads to challenges in drug delivery to ensure specific targeting. In both cases, aiming for AKT and mTOR, the best approach is so far to inhibit the usage of adenosine triphosphate (ATP) to basically starve the tumour. Drugs enabling this approach are currently in phase I or phase II trial studies to determine their overall efficiency (Lazaro, 2020).

1.2.4 Chimeric antigen receptor T cells (CAR T cells)

While new antibody therapies are tested in a high variety the most difficult part in cancer therapy is yet to elicit a proper immune response by the patient's very own immune system. Especially T cells are meant as one of the main interactors with malignant cells, but due to the mutations within cancer cells it is often difficult for such cells to recognize them as targets. To enhance T cell specific immune response towards cancer, a new form of therapy is developed using the patients T cells to induce a tumour-specific immune response. This process is called adoptive T cell therapy (ACT). Three ways on how this can be achieved are used:

First, extraction of tumour-specific T cells (also called tumour-infiltrating lymphocytes, TIL's), which are cultured in vitro to allow proliferation and are returned into the patient, the focus hereby is to increase the number of tumour-specific T cells.

The second approach is to isolate peripheral T cells from the patient's blood and genetically engineer the TCR recognizing a tumour-specific antigen, before returning them back into the patient's body.

Nowadays as a third option a new approach of T cell modulation is used in therapy against mostly haematological cancer forms. Hereby, the T cells are extracted from the patient's body and adapted to express a fully synthetic antigen receptor called chimeric antigen receptor (CAR) to allow them to recognize a cancer-specific antigen.

In this version of T cell modulation, more thoroughly explained below, the endogenic part of the receptor is also changed depending on the signalling it might need. The generation of such a receptor is being constantly improved based on new research and the outcome of patient's responses towards the cancer in co-culture with this

therapy. By using the approach of CAR's signalling via major histocompatibility complex (MHC), one of the primary targets for this complex that has its expression suppressed by cancer, is not needed. Hereby different developmental strategies have been performed, each building up on the information gather in the prior steps (Tokarew, 2019, Haslauer, 2021).

The production is currently a five generation-based strategy which arose within the last 30 years and requires a multitude of steps to ensure the best immune response within the human body.

To do so, the first approach was dependent of a single CD3 ζ - based receptor interacting with a simple immunoreceptor tyrosine-based activation motif (ITAM) domain for downstream signalling, which introduced a combination of not only the primary downstream domain needed but also additional domains for co-stimulatory signals for an appropriate T cell response (Figure 7, first generation CAR).

The second generation developed contained a costimulatory molecule (CM), often either a CD28 or CD137 co-stimulatory domain, next to the ITAM domain in the endodomain structure (Figure 7, second generation CAR). In the third generation two CMs were combined (Figure 7, third generation CAR).

Right now, a fourth-generation CAR is commonly used which is based on the additions of the second generation as well as another signalling domain for IL-12, which is activated upon binding and activation of the main CAR (Figure 7, fourth generation CAR).

The fifth-generation is still currently under development and is meant to combine the signals necessary to develop a proper T cell response similar to the natural response within the body. To do so, the aim is to achieve a combination of the CAR with second generation additions and a truncated cytoplasmic IL-2 receptor β -chain domain. This allows the same main processes as in a natural immune response to be activated: TCR-dependent, co-stimulatory (CD28 or CD137) and cytokine signalling (IL-2) (Figure 7, fifth generation CAR).

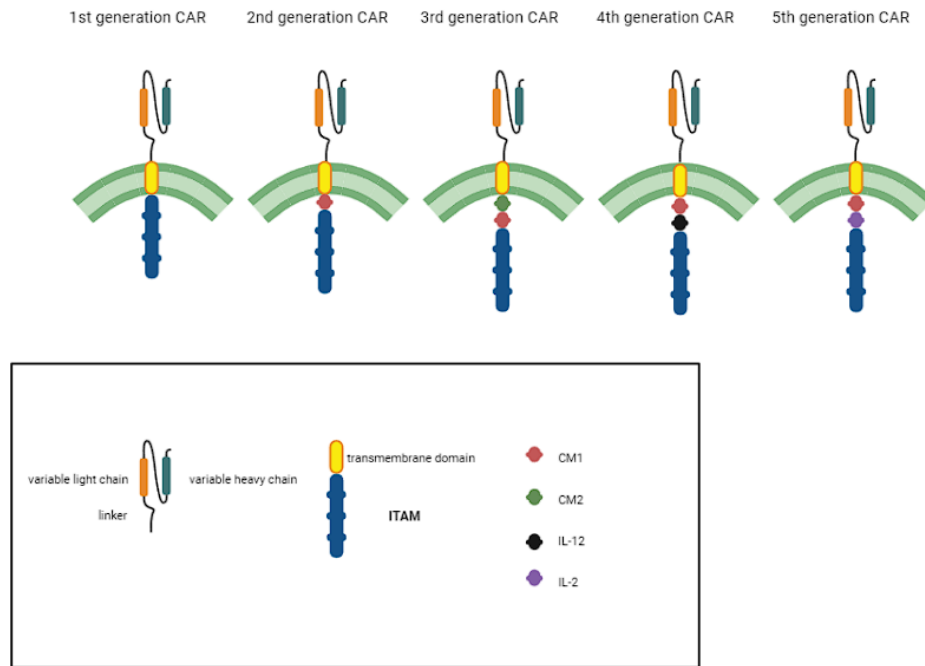


Figure 7 Schematics visualizing the development of CAR-T cells over the last 30 years. T cells are modified using artificial receptors against specific targets expressed on cancer cells. Over time these receptors have been further modified to co-express signals needed to properly induce immune responses within the T cells if the corresponding ligand was detectable on the targeted cancer cells. Figure was prepared with biorender.

To produce CAR T cells, a variety of steps need to be performed before achieving the appropriate type; first the T cells are taken from the patient by a process called leukapheresis, in which white blood cells are extracted from the patient or a donor for therapy. To gain a specific subset of T cells (CD8 or CD4 positive), the T cells are isolated and further sorted using magnetic beads against specific markers. This technique is called magnetic-activated cell sorting (MACS) and deploys nanoparticles with a specific antibody to do either positive or negative selection by adding the cells bound with magnetic nanoparticles to a column with a sufficiently strong magnetic field. In case of CD4 and CD8 positive T cells the preferred method is positive selection.

After isolation of the specific T cell subtypes, T cells need to be sustained and activated for further procedures. Hereby it is important to induce proper signalling either by antigen presenting cells (APCs) or by using beads coated with monoclonal antibodies presented as CD3/CD28 signal. Another stimulation added to culture for proper T cell activation is the interleukin 2 (IL-2). The CAR version to be added to the T cell is encoded in a vector, which is transfected into the T cells either by lentiviral approach,

mRNA transfection or a Sleeping Beauty transposon system. After incubation for about 10 -14 days the T cells are returned into the patient's body to perform the task of fighting the malignant cells (Zhang, 2017; Magnani, 2020).

CAR T cells do encounter nowadays a few challenges while being applied for cancer therapy. First and foremost, the mutation of cancer cells towards immune responses can be a rapid one and during the procedure of creating the CAR T cells against a very specific antigen, this target might have been lost by the cancer cells. Another issue is that some of the markers can be expressed to a certain extent by healthy cells and might cause a so-called on-target off-tumour effect leading to an immune response towards healthy cells similar to autoimmunity (Sterner, 2021; Haslauer, 2021).

1.2.5 Current therapeutic outlook

Each of the approaches used currently for cancer therapy has its advantages as well as disadvantages. Chemotherapy is the most common applied version of therapy in most of the targets, yet it can lead to severe side effects dependent on the concentration as well as the combinations applied. Chemotherapy has to be adapted on how severe the progress of the malignancy has been at the time of diagnosis. Another option, if diagnosed early is the removal of the tumour by surgery and application of chemotherapy to ensure all malignantly transformed cells are destroyed. This process is only applicable if the tumour hasn't reached a certain size and is approachable by surgical methods. In other cases, in which the tumour is found in difficult locations (such as brain), has reached a certain growth or within a non-solid version, a combination of newly developed immunotherapy and chemotherapy is the most common approach. These therapies are most of the time improving the overall survival rate for the next five to ten years. Lastly, the approach of CAR-T cells has yet to be established as a routine treatment for patients, due to high costs and some hurdles during the development, mainly the time-consuming process.

Due to a variety of difficulties in the therapeutic approaches nowadays other more mutation-resistant and easily-approachable targets expressed in high levels by cancer cells are needed to ease treatments, especially in regards of developing personalized therapies.

1.3 FUNCTIONAL ROLE TIM-3, GALECTIN-9, AND VISTA

IMMUNE CHECKPOINT PROTEINS IN CANCER PROGRESSION

The previously mentioned therapeutic approaches towards cancer tend to aim for targets that are often newly created in tumours due to mutational burden and can be ever so often circumvented if T cells attack such specific *de-novo* targets by permanent introduction of new mutations regulating the protein expression. Furthermore, the more approaches are necessary to modify immune cell responses the more likely are adverse effects either by toxicity or by unwanted autoimmunities. Due to these challenges, it's often difficult to ensure a proper, stable treatment that can be applied easily to a variety of cancer types. A possibility to circumvent this problem is to find a more stable, possibly even evolutionary conserved target that might not be as easily hidden from T cell recognition, due to it being a main factor of overall human survival. Such potential targets, either the proteins themselves or their expression pathways, are explained in the next few pages and is the main focus of my thesis.

1.3.1 T cell immunoglobulin and mucin domain -3 (TIM-3)

One of the proteins this thesis is focussing on is the TIM-3 protein expressed in a variety of cells, which exhibits two functions as either a receptor on immune cells for potential ligands or as a transporter of mainly another protein called galectin-9, which is produced by cancer cells in high levels and is another important focus in future research (He, 2018). This chapter consists of an introduction to the protein family, the function of TIM-3 and its structure.

1.3.1.1 Protein family

The TIM protein family came first in focus during studies of kidney ischemia. The kidney injury molecule 1 (Kim-1) was discovered as the first member of this protein group in studies with rats. Further research introduced similarities between Kim-1 and Tim-1, an equivalent discovered within mice. In follow-up studies the Kim-1/Tim-1 protein was determined as a receptor for the hepatitis A virus within primates and therefore is also known as hepatitis A virus cellular receptor 1 (HAVCR-1). The TIM-3 protein is a member of the TIM family and one out of three known members in humans (TIM-1, TIM-3, and TIM-4) located on chromosome 5q33.2. In comparison to mice eight different variations of TIM proteins can be found (TIM-1 – TIM-8). While each of the TIM proteins was determined as regulatory component in responses of helper T cell

subsets Th1 and Th2, the TIM-3 member can especially be found to be expressed on a variety of immune regulatory cells (Kane, 2010; Hu, 2016).

The TIM family was not placed in focus for time being until the influence of TIM-1 came in focus in mice during studies focussing on the development of allergic asthma. Hereby, using the mouse models BALB/c and DBA/2 these studies were enabling researchers to detect polymorphisms of TIM-1 and TIM-3 within those mouse models. Such investigations have shown that polymorphisms in TIM-1 in humans can induce an increased risk of differential asthmatic developments. Interestingly, in such cases the risk of developing asthma has been decreased by insertion approaches but only in patients displaying positive diagnosis regarding to exposure to the hepatitis A virus. How the infection with the hepatitis virus leads to a change in asthma susceptibility is yet to be understood (Kane, 2010).

1.3.1.2 *TIM-3 background in research*

Around the same time as TIM-1 came into focus, in 2002, TIM-3 was discovered as an immune receptor with its function being first determined to be dependent on the binding of ligands and inducing immunosuppression on B cells, macrophages, NK cells, dendritic cells, T cells (including regulatory) and mast cells (Hu, 2016). Studies in different aspects of life, not only in cancer development, have shown that TIM-3 can also influence to a certain extent e.g. autoimmune disorders such as experimentally autoimmune encephalomyelitis in mice (EAE model) and virally induced hepatitis. To further this idea, TIM-3 was also tested in cases of autoimmune diabetes mouse models using Tim-3-Ig fusion proteins leading to the production of necessary cytokines and enabling proliferation. In such cases the blocking of TIM-3 /TIM-3 ligand interaction caused an inhibition of developing tolerance (Kane, 2010; Anderson, 2006).

Another interesting factor that came up in research of TIM-3 was the fact that interaction with TIM-3 on specific cells can lead to exhaustion of immune responses. These pathways were primarily studied during infections, and indicated that these can also be up-regulated during cancer development and the embryonic development as one of the main immunosuppressive responses (Wolf, 2020).

1.3.1.3 Structure

The structure of TIM-3 proteins is reconstructed using protein purification and crystallization. This led to the visualisation of a structural combination containing an extracellular domain consisting of an Immunoglobulin V domain and the mucin domain in the proximity of the membrane; a transmembrane domain and an intracellular stem with five phosphorylation sites, of which two are fixed on positions Tyr265 and Tyr272 and phosphorylated during activation (Figure 8, left). Comparing the human structure consisting of 302 amino acids to the mouse version the TIM-3 proteins share 63% similarity (Das, 2017).

The gene of the human TIM-3 protein includes six exons. By investigating mouse spleens, studies show that the mTIM-3 protein on the other hand is lacking the exons 3-5 in the spliced version. Assuming as those exons encode the transmembrane and mucin domain, this form is a soluble version enabling trafficking of signals to a target cell. A human homolog of the spliced version is yet to be found. Studies show that in case of a soluble form in humans the TIM-3 protein is preferably shedded from the surface using ADAMs (a desintegrin and metalloproteinase), mainly ADAM17 and ADAM10. Studies further indicate that human TIM-3 shedding is controlled by signalling pathways and cannot be induced at random. A possibility of activating such shedding is by binding a ligand such as galectin-9 for example (Banerjee, 2018).

Lastly, the IgV domain of the Tim-3 protein consists of six invariant cysteines, two of them forming a hallmark disulfide bond found in most of the Immunoglobulin superfamily (IgSF) proteins connecting the B and F strand. The C-C' loop is formed in all currently known Tim proteins in humans, yet these proteins show next to two conserved cysteines within the loop a high structural variability. Yet in all three human versions of the TIM protein this area does enable each to form a uniquely structured cleft, which most likely is responsible for binding as an example phosphatidylserine. In the B-C loop region as well as in the C"-D region the Tim-3 protein contains a heightened flexibility. This structural flexibility in the binding area does enable Tim-3 to interact with different ligands such as galectin-9 either as a receptor or as a trafficker (Figure 8, left) (Gandhi, 2018).

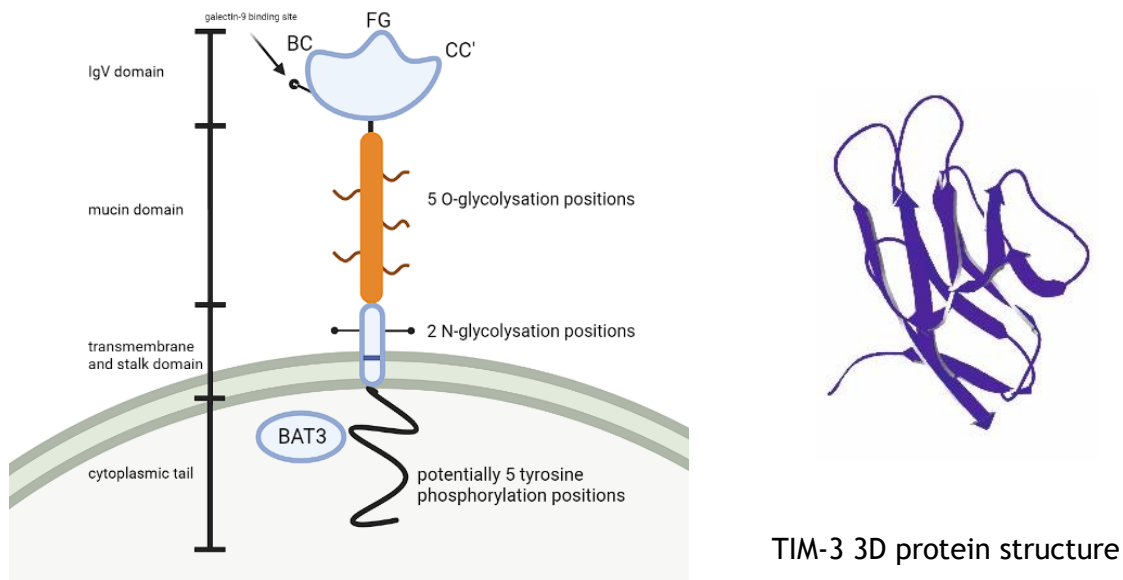


Figure 8 General structure of the human Tim-3 protein shown. (Left) The structure of the human form of the Tim-3 protein is shown including the cytoplasmic tail with potentially 5 tyrosine phosphorylation sites, transmembrane domain, and stalk with two N-glycosylation structures, mucin domain with potentially 5 O-glycosylation structures as well as the IgV domain containing the binding structures for corresponding ligands. (Right) Visualization of the 3D structure of Tim-3 made by using the Swiss PBD viewer and further explained in chapter 1 of the results. Left figure was prepared with biorender.

1.3.1.4 Ligands

Known ligands for Tim-3 are galectin-9, carcinoembryonic antigen cell adhesion molecule 1 (CEACAM-1), high-mobility group protein B-1 (HMGB-1) as well as phosphatidylserine (PS). Tim-3 can be found in either the cell-bound stage (acting as a receptor) or as a soluble form binding a ligand lacking a specific transmembrane and mucin domain. The binding therefore enables the ligand to be shedded from the cell surface with Tim-3 acting as its transporter. Upon binding of a ligand as a receptor, the downstream signalling pathway consisting of the large proline-rich protein BAT3 (known either as BAT3 or BAG6) and the lymphocyte-specific protein tyrosine kinase (LCK) pathway is activated (Das, 2017).

CEACAM-1 is excessively studied in different types of cancers, such as lung, breast, and pancreatic cancers and as the full name indicates is also found in the embryonic development. CEACAM-1 has been researched thoroughly as a ligand for Tim-3 and was determined to share structural similarities with Tim-3 regarding to their IgV domain, enabling an interaction with their GF-CC' interface. Furthermore, there is clear

evidence that the glycosylation of Tim-3 is dependent on the co-expression of CEACAM-1 therefore also warrant protein stability. This is achieved by the interaction between these proteins in a *cis* formation. If *trans* formation is used for such interactions, it leads to inhibition of T cell activity. As seen in Figure 8 the Tim-3 structure consists of different structural binding sites enabling both CEACAM-1 as well as galectin-9 to bind at the same time (Huang, 2015).

HMGB-1 has been investigated and determined only recently as a binding partner to Tim-3. Generally, within cells HMGB-1 is able to bind to the DNA within the nucleus inducing specific transcription processes. HMGB-1 is further associated with, damaged, dead as well as dying cells and released as a so-called “danger signal” to interact with either T or B cells inducing the corresponding immune responses. In cancers, especially non-solid cancer such as acute myeloid leukaemia, a high amount of HMGB-1 can be detected within the blood stream. Regarding to the interaction with Tim-3 our research group was already able to verify the binding ability of HMGB-1 as a ligand. Interaction between HMGB-1 and Tim-3 can support the survival of cancer cells by blocking the endosomal transportation of nucleic acids furthering the suppression of innate immune responses towards such normally released tumour-associated nucleic acids. In regard to binding, there are indications of competition between HMGB-1 and CEACAM-1 interacting with the epitopes found on the FG-CC’ loop in the IgV domain (Yasinska, 2018).

Studies with Tim-3-positive cytotoxic T cells derived from liver during infection with adenovirus indicated them to express similar functions as regulatory T cells. These cells are able to connect with released HMGB-1 disabling the activation of other CD8⁺ T cells found within the environment (Das, 2017).

Phosphatidylserine (PS) is a binding partner to Tim-3 which does not originate from the protein class. As a fatty acid is known to be associated with the beginning of cell death as changes within the cells lead to translocation of it on the outer cell membrane. As seen with CEACAM-1 and HMGB-1 PS is also binding onto the FG-CC’ loop on the IgV domain. How exactly cells differ which ligand should be targeted by the Tim-3 receptors expressed on the surface has yet to be understood. Recent research has shown that if macrophages, dendritic cells as well as fibroblasts expressing Tim-3 the interaction with PS can induce an increase in their ability to phagocytose dying cells.

Regarding T cells the exact correlation of PS binding to Tim-3 has yet to be understood (Das, 2017).

1.3.1.5 Functions

Tim-3 has so far been shown to be responsible for different immune response approaches in a variety of diseases as well as other bodily adaptations. Dependent on the usage and the ligand bound, the function of Tim-3 can differ just as much.

Activation of Tim-3 by binding of ligands leads to an induction within certain positions in the cytotoxic tail, which are occupied by BAT3. BAT3 can be activated during cell survival induction, by phosphorylation of those specific positions leading to the TIM-3 cytotoxic tail losing the connection with BAT3. This process is the beginning of T cell exhaustion advanced by induction of FYN recruitment, synapse disruption, further phosphatase recruitment and finally apoptosis of the T cell. Furthermore, it has been shown that TIM-3 also interferes with cytokine production such as IL-2 and Interferon- γ (IFN- γ). Investigation of various tumour types has proven that the interference of Tim-3 bound with specific ligands causes the activation of cell-death-inducing processes in cytotoxic T lymphocytes and consequently leads to a diminishing of patient survival. (He, 2018)

Similar to studies in cancer, the over-expression of TIM-3 during the hepatitis C virus (HCV) and hepatitis B virus (HBV) infection causes the inhibition of T cell responses by interfering with the IFN- γ production and inducing T cell depletion. By blocking the binding of galectin-9 to Tim-3 the T cell response can be restored in such infections. In autoimmune diseases associated with the liver regulatory T cells are expressing galectin-9 as an ligand to inhibit the function of T helper 1 cells. (Liu, 2016; Zhao, 2020)

While Tim-3 is clearly indicating an influence in certain disease progression, studies show that after transplantation of an organ a certain threshold of TIM-3 is needed to ensure that the organ will not be rejected. A study in mice by Olaf Boenisch et.al showed that the expression levels of Tim-3 are responsible for inhibiting the rejection of the organ by influencing the CD4⁺ cell activity. Using an inhibitor against Tim-3 during studies clearly indicated that disabling binding led to an increased rejection of the transplant (Boenisch, 2010).

1.3.2 Galectin-9

In studies so far, a clear indication has been shown that a prominent binding partner for Tim-3 is the protein galectin-9. This protein is detected in high levels within either the tumour microenvironment in solid cancer growth or within the blood stream if it is a non-solid cancer type. As it is produced in high levels by such cancer cells there is a clear demonstration that the interaction of high levels of galectin-9 with its corresponding receptors found on immune cells such as cytotoxic T cells and NK cells is used to suppress appropriate immune responses (Sun, 2019). As such the interactions between Tim-3 and galectin-9 are specifically investigated recently. In this chapter I shortly describe the structural and functional components of galectins, with special focus on galectin-9.

1.3.2.1 *Galectin protein family*

Galectins are a protein family that are already heavily researched in cancer studies with galectin-9 coming in focus later than others. Galectin-9 has been shown to be a protein that is highly expressed on embryonic cells as well as cancer cells and can be released in just as high amounts during cancer development to keep cytotoxic T cells as well as NK cells at bay (Blois, 2020).

The galectin protein family consists of up to 15 known proteins with differences in structure, but all collectively expressing binding capabilities to galactose. These structural differences can be divided in three subgroups (Hara, 2020).

Group 1 consists of galectin-1, -2, -5, -7, -10, -11, -13, -14 and -15 as so-called prototypical galectins, which are simple carbohydrate binding units that can either stay as a single component or enhance binding by their formation of a complex consisting of homodimers via non-covalent binding, with the carbohydrate recognition sides facing in opposite directions (Figure 9, left).

The second group of galectins includes solely galectin-3 which is forming a chimera-type structure. This structure allows it to form pentamers with its tail containing tandem repeats of amino acid sequences on its N-terminus (Figure 9, middle).

Last group contains galectin-4, -6, -8, -9 and -12. Hereby the two carbohydrate recognition sides are linked with a linker structure; this version of galectin proteins are called tandem-repeat-type galectins (Figure 9, right).

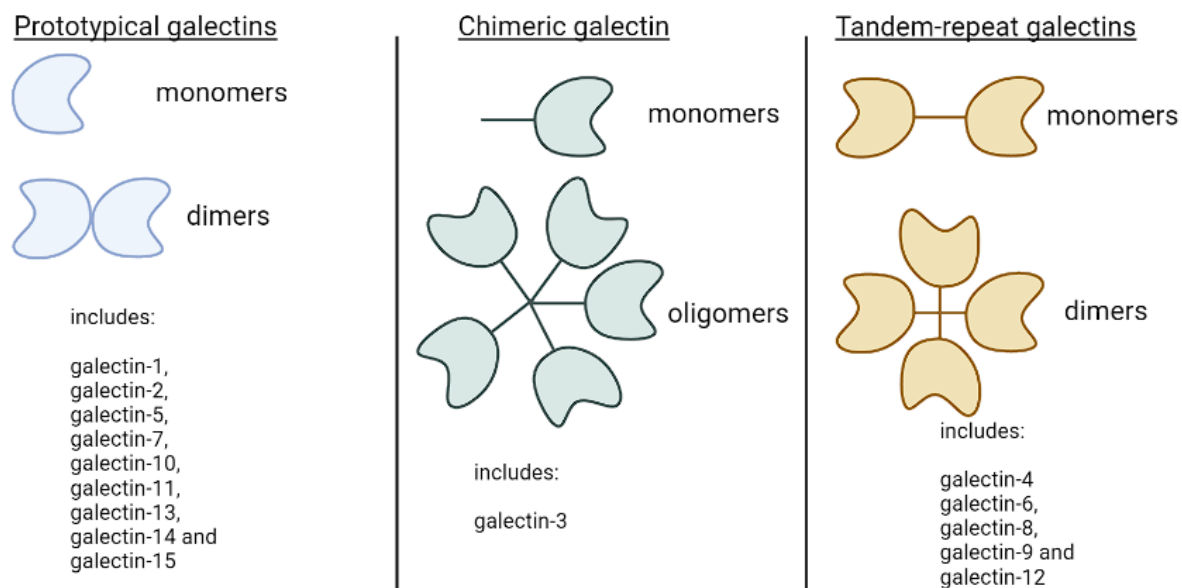


Figure 9 Structures of each subgroup of the galectin family shown. (Left) Most members of the galectin family are produced as simple monomers which are able to form dimers by non-covalent binding, this group is called prototypical galectins. (Middle) One specific type of galectin, galectin-3, is found as monomers with a single binding structure and a linker component. This structure is able to form pentamers and is referred to as chimeric galectin. (Right) Lastly, a group consisting of five different galectins is known as tandem-repeat galectin group. These are consisting of two binding sites connected with a linker. Dependent on the version of galectin this linker varies in size. In this subgroup the proteins are determined to be able to form dimers. Figure was prepared with biorender.

Function-wise galectin proteins are seen mainly to be responsible for immune suppression of T cells as well to a certain extent those of macrophages. Some types of galectins are determined to even be able to induce apoptosis in T cells or enhance the function of regulatory T cells. Furthermore, galectins are found to be elevated in tumour microenvironment indicating its influence on cancer survival by immune suppression. As an example, galectin-1 has also been determined to induce tolerance in the maternal-placenta interface enabling the mother's immune system to perform surveillance within the surrounding of the embryo during its development without risking an immune reaction to the embryo (Kopcow, 2008).

1.3.2.2 *Galectin-9 background in research*

Galectin-9 has been first identified and characterized in embryonic mice kidneys in 1996 by Jun Wada and Yashpal S. Kanwar. Determining the biochemical functions, they hypothesized that as galectins generally depend on non-classical secretion pathways galectin-9 might be released into the surrounding by a carrier protein as it lacks an appropriate signal sequence for conventional transport. They were also able to find a variant with different linker length in the small intestine. This indicates that there galectin-9 might have a different function or developmental origin influenced by the size variation than the version found in the kidney. The high upregulation of galectin-9 in embryonic samples indicated in these studies also that galectin-9 might be a regulatory protein during the embryonic development (Wada, 1997).

At the same time in Germany a protein with similarities to other galectin proteins was found within samples of Hodgkin's disease at a significantly similar size of the mouse galectin-9. They were able to determine that the C-terminal carbohydrate recognition unit showed 70% similarity to galectin-5 while the N-terminal did only compare to others in very low levels. Furthermore, after sequencing the galectin-9 protein found in Hodgkin's disease they were able to detect and analyse lower amounts of the same protein in healthy leukocytes. This led to an investigation if this protein has been upregulated within the disease by mutational burden. No difference has been found, leading to the conclusion that the response of producing galectin-9 is upregulated in a different approach (Ölzem, 1997).

Since the early 2000's galectin-9 has been rapidly gaining influence in the research of cancer but has also been deemed in a certain extent to be responsible for some allergy responses, autoimmunities, asthma, as well as influencing immune responses towards bacterial infections and transplantation rejection. It is further hypothesized that galectin-9 can be used to detect diseases and determine their severity, as an elevated level of galectin-9 in the blood can be an indicator of infections or in worse case of cancer growth. Galectin-9 might be able to be used in regular health checks, especially in cancer patients, to determine if the body shows any signs of disease progression even though from the outside the patient primarily looks healthy (Yu, 2020; Zhang, 2019).

The focus regarding galectin-9 studies should be put, as mentioned before, especially on cancer, due to galectin-9 seemingly being released from a very early stage in cancer

progression keeping the immune system under control. Therefore, while elevated galectin-9 levels do not have to automatically preface a cancer diagnosis, it can be an indicator to check the patient further with other diagnostic approaches. Cancer therapy is dependent on early diagnosis as the chances of treatment success are higher the earlier the cancer is detected.

1.3.2.3 Structure

As a tandem-repeat member of the galectin protein family galectin-9 consists of two carbohydrate-recognition domains, a N-terminal version with a size of about 145 amino acids and a C-terminal of 149 amino acids. By performing X-ray crystallography, studies show that the N-terminal domain contains a β -sandwich motif with either six-stranded (S1-S6) or five-stranded β -sheets (F1-F5). Another β -strand was detected later in research and has been determined to run anti-parallel to the C-terminal F1 strand, it has been therefore named F0. Comparing the C-terminal structure to the N-terminal domain significant similarities were detectable with two anti-parallel β -sheets found, these contain either S1-S6 or F1-F5 β -strands and a α -helix. Major differences in the domains are detectable in the loops due to insertions as well as deletions of amino acids. These differences in the loop are determining the binding-specificity of each carbohydrate unit (Wiersma, 2011).

By studying galectin-9 proteins more thoroughly it has been shown that three different isotypes are so far detectable within the human body. This difference is due to a variation of size found in the linker structure and the isoforms are commonly described as Gal-9(S) if the linker is small-sized, Gal-9(M) if middle-sized and Gal-9(L) if large-sized (Figure 10). The exact influence of the different linker sizes is yet to be understood, but research so far has shown that T cells mainly bind either Gal-9(M) or Gal-9(L), while small-sized linker protein are not commonly detectable on T cells. Another influence the linker size might have is the possibility of forming dimers, which are dependent on longer-sized linkers (Roy, 2013).

Furthermore, both structures, C-terminal, and N-terminal domain, enable a selection of branched N-glycans, repeated oligolactosamines and carbohydrate to be binding partners which can approach both domains to enable high binding affinity. As these domains have unique structures for binding it indicates that each of them has a specification regarding which proteins they interact with. One domain might be bound

to a carrier for release enabling the second domain to bind a corresponding receptor on the targeted cell (Wiersma, 2011).

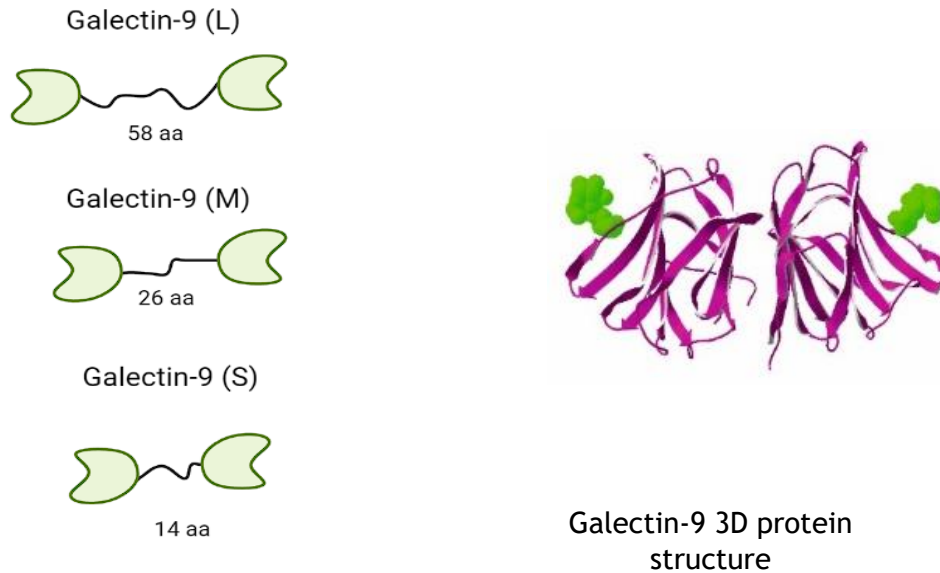


Figure 10 General structure of the human galectin-9 protein shown. (Left) The structure of the human form of the Tim-3 protein is shown including the variation with linker length. The binding domains recognize the galectin-9 binding site on Tim-3 without interfering with other proteins being able to bind to the loops of the Tim-3 proteins (Right) Visualization of the 3D structure of galectin-9 made by using the Swiss PBD viewer and further explained in chapter 1 of the results. Left figure was prepared with biorender.

1.3.2.4 Receptors

Galectin-9 has been only researched within the last 20 years more intensely regarding its influence on immune responses. Besides the known receptor Tim-3 recent studies have shown that a variety of binding partners inducing different functions are available for galectin-9. Such receptors include CD44, glucose transporter 2, immunoglobulin E, glucagon receptor, and the Epstein-Barr virus latent membrane protein-1 (Golden-Mason, 2017).

CD44, cluster of differentiation 44, is able to bind galectin-9 directly and further interaction with the TGF- β receptor I leads to the formation of a three-protein complex. As this receptor is expressed mainly on regulatory T cells it has been investigated if galectin-9 upon binding on CD44 affects their function. Studies indicate that the function of Tregs are stabilized if galectin-9 binds onto the CD44 receptor. As CD44 is also able to bind hyaluronic acid (HA) research indicates that the interactions with

galectin-9 enables modulation of CD44-HA binding therefore permitting the migration of leukocytes for example during allergic lung inflammations (Wu, 2014).

While galectin-9 studies indicate that other potential receptors are available on different cell types, it has yet to be investigated if galectin-9 is able to bind to them specifically or other more prominent receptors are to be found tied with galectin-9 functions. As an example, in the Epstein-Barr virus infections studies indicate nowadays that the infection itself induces the release of galectin-9 which then again binds preferably on Tim-3 expressed on T cells (Klibi, 2008).

1.3.2.5 Functions

The main function of galectins is to regulate immune responses by binding to specific receptors expressed on a variety of immune cells such as natural killer, T cells and monocytes. If these proteins within the galectin protein family are dysregulated in their release by for example by cancer cells it leads to a severe inhibition of normal immune cell functions, disabling any proper immune responses towards malignancies. On the other hand, in autoimmune disease, in which a suppression of increased immune responses would be beneficial the lack of galectin-9 might enhance the severity of such disorders.

Furthermore, studies indicate the influence of galectin-9 expression in regard to the adaptation of the mother's immune system against the embryo is crucial for the survival of the foetus (Li, 2016).

Understanding the exact influence of galectin-9 and its corresponding receptors is crucial to develop therapeutic approaches for a variety of diseases and disorders but so far research is still lacking regarding the exact function of galectin-9.

1.3.3 V-domain Ig suppressor of T cell activation (VISTA)

Cancer cells are highly adaptive in suppressing the immune response by lymphocytes, therefore a variety of checkpoint molecules to lead to such immune suppression is needed to be produced or expressed by each type of cell. A newly researched molecule proposing a significant target for cancer therapy is V-domain Ig suppressor of T cell activation (VISTA). In research, the corresponding gene constituting the VISTA protein is known as V-set Immunoregulatory Receptor (VSIR). This protein is detectable on T cells, either helper T or cytotoxic T cells, but expression is lacking on NK cells. It belongs to the protein family B7 which includes other factors known to

inhibit immune responses such as PD-L1. As this protein is within a family of proteins used as potential therapeutic targets in cancer treatments, it clearly indicates that further research is necessary to understand its functions properly and to enable it to become a new aimed protein on malignancies (Mohamed, 2019; Yuan, 2021).

1.3.3.1 B7 Protein family

The B7 protein family is consisting so far of seven investigated ligands known to influence immune responses. The seven known members are currently: PD-L1, CD86, CD80, ICOS-L, PD-L2, B7-H3 and B7-H4. Structural similarities between VISTA and PD-L1 indicates that it also belongs to this family of proteins. Each of these proteins is either a transmembrane or glycosylphosphatidylinositol-linked protein with either an IgV or IgC domain. These proteins can be found as monomers on the cell surface or tend to form homodimers and interact with specified receptors leading to the induction of either co-stimulatory or co-inhibitory activation of immune cells. CD80 and CD86 expressed on dendritic cells are for example able to interact with CTLA-4 found on T cells. This interaction induces the production of indoleamine 2, 3-dioxygenase (IDO) enabling the suppression of T cell activity (Collins, 2005).

These functions, especially the inhibition of T cells, as seen with PD-L1 and CD80/CD86 and similarities in structure between VISTA and B7 family proteins, indicate that this specific protein is also able to be targeted in cancer therapy depending on the result of further research performed.

1.3.3.2 VISTA background in research

As VISTA just arose as a protein of interest for research there have been made a variety of general discoveries regarding structure and potential effects, yet an overall insight in its functions is still lacking. There are indications that VISTA can be released by a variety of cells into the environment and a collective understanding is maintained that it is mainly responsible for suppressing immune responses. It is seen in most studies to act as either ligand or receptor, yet an exact description on these functions is still to be settled (Lines, 2014).

As far as research has been performed, the general influence of VISTA in the tumour environment is to be a negative checkpoint regulator. While VISTA is primarily expressed on hematopoietic cells, in the tumour microenvironment it is also found on infiltrating cells such as myeloid DC's and MDSC's. Studies have also shown a 10-fold

increase of expression on leukaemia cells, indicating a possible correlation with the hypoxia stage established during tumour growth (Nowak, 2017).

VISTA expression levels within cells have been determined by mRNA testing. It clarifies that VISTA is high expressed in embryonic cells as well as in the human placenta (Kakavand, 2017). The level in a healthy adult mouse is quite low within hematopoietic cells as well as in tissues such as lung, spleen, brain, heart, and muscle. Comparing the human VISTA levels to mice, it has been shown that human CD4⁺ and CD8⁺ T cells are expressing similar VISTA levels while in mice the CD4⁺ T cells tend to have higher VISTA levels than CD8⁺. Furthermore, studies have verified that VISTA expression is rising in cancer after treatment with anti-PD1 and anti-CTLA4 therapy. Performing flow cytometry using the monoclonal VISTA antibody GA1 has also clarified that VISTA is expressed on CD4⁺ and CD8⁺ T cells but not on B cells and CD56^{high} NK cells. CD56^{low} NK cells showed only a small non-significant level of VISTA expression. Histological distinction of cells stained for VISTA has indicated a relation of VISTA expression with CD11b expression (Nowak, 2017; Gao, 2017).

Next, dependency of VISTA expression on methylation levels has also been tested, by bisulfite sequencing of two different cell lines, JHUEM1 (high VISTA levels) and JHUEM7 (low VISTA levels), after treatment with decitabine. JHUEM1 clearly showed low methylation levels, while JHUEM7 contained a high level of methylation. In patient data showing either high or low expression of VISTA, a difference in methylation levels has also been confirmed (Mulati, 2019).

1.3.3.3 Structure

Structure-wise the VISTA protein is a type I membrane protein with a single N-terminal immunoglobulin V domain. The amino acid sequence is still currently investigated but so far is determined as about 279 aa in length consisting of an extracellular domain of about 162 aa, a transmembrane domain of about 20-21 aa and a cytoplasmic domain of about 96 aa. The extracellular domain can further be divided into a 30 – 32 aa long signal peptide and a 130 aa long extracellular IgV domain (Figure 11).

The protein is encoded for on a large intron on the CDH23 gene, which can be found in a high variety of lifeforms, far back throughout evolution - even in the primitive ray-finned fish. The encoded area for the IgV domain show similarities to the PD-1 domain at about 23%. Furthermore, the conserved cytotoxic tail does not contain any ITAM

motif, rather it includes a Src homology 2 binding motif. The recruitment of specific proteins is yet to be researched (Nowak, 2017).

Depending on the state, either bound to the cell or in soluble form, the VISTA protein can be detected in different glycosylation levels. So far research has indicated up to five different glycosylation sites, but as the structure of the VISTA protein is a newly researched topic this number might further vary. Glycosylation is a co- or post-translational modification influencing the attachment ability of glycan structures to other corresponding domains. In case of VISTA this is found at the N-glycosylation domain indicating an attachment of glycans to the nitrogen found within asparagine or arginine by dolichol phosphate. In comparison to other B7 superfamily protein VISTA seem to be higher glycosylated, especially in cancer cells and in the soluble form. Using analytical measurement such as Western Blot it was shown that the size of the VISTA protein averages at 35 kDa dependent on these glycosylation levels (Nishant, 2019).

The binding structure of the VISTA protein consists of three disulfide bonds formed in the extracellular domain between six cysteine residues. It is folded in a canonical beta sandwich conformation with 10 beta strands and 3 alpha helices. The structure can be separated into two coplanar surfaces, one is facilitated out of 6 beta strands and the other out of four. A protein structure between the C and C' strand consists of 21 residues forming an extended loop and 4 residues within the alpha helix. The surface charge of the VISTA protein is mainly positive with 6 positive residues and only three negative ones. (Nishant, 2019)

Lastly, comparing the VISTA protein to proteins of the B7 superfamily shows that the VISTA protein does not contain any constant immunoglobulin area. The most similar B7 protein is PDL-1; by comparing VISTA to this protein the most prominent difference is that VISTA contains 10 beta strands instead of 9. Furthermore, within the C' region as an alternative to a beta strand it contains an extra alpha helix. The structure within the C-C' position is extended to 21 residues instead of four as in the B7 superfamily proteins, and within the VISTA structure 2 more disulfide bonds are contained (Nishant, 2019).

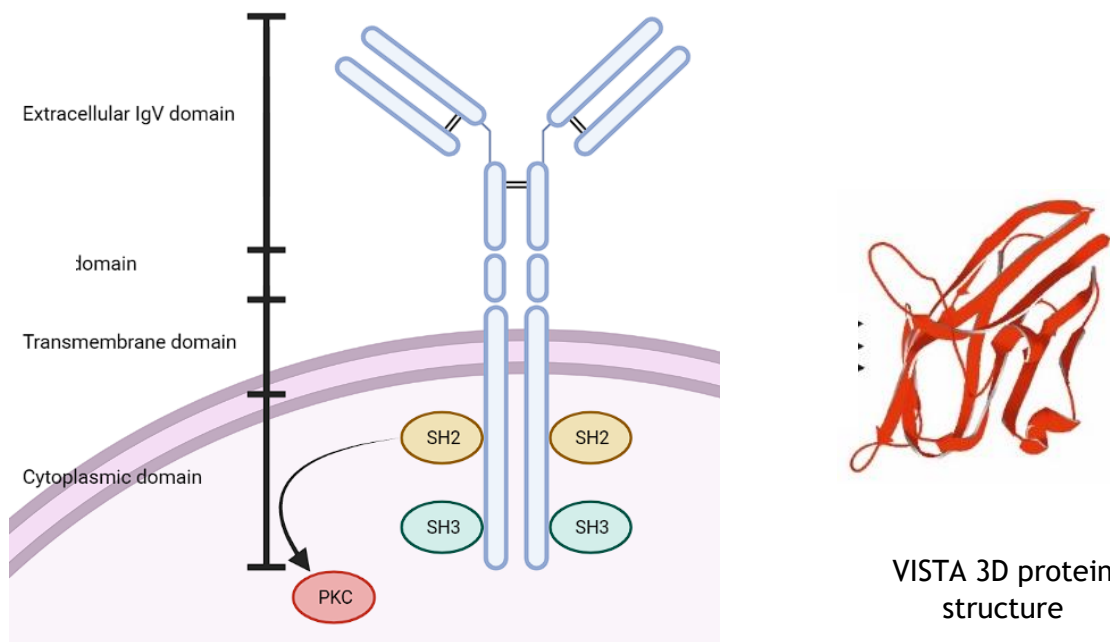


Figure 11 General structure of the human VISTA protein shown. (Left) The schematic of the structure of human VISTA is shown including the cytoplasmic tail with potentially Src homology 2 and 3 binding motif binding sites, a transmembrane domain, and stalk as well as an extracellular IgV domain attached to a signal peptide. (Right) Visualization of the 3D structure of VISTA made by using the Swiss PBD viewer and further explained in chapter 1 of the results. Left figure was prepared with biorender.

1.3.3.4 Functions

To investigate the function of VISTA, the phenotype of VISTA deficient mice for studies is created in two ways. It can be achieved by deletion of exon 1 which led to an elevated level of activated T cells. Crossing these mice with a C57BL/6 line caused no increase of T cell numbers in the spleen but an elevated levels of activated T cells. Another way of achieving a phenotype of VISTA deficient mice is by floxing the exon2 and exon3 by loxP sites. Crossing these mice further with E1a-cre mice might cause the deletion of VISTA. Altogether, the deletion of VISTA has shown that these mice increasingly developed an autoimmunity (Nowak, 2017)

The accurate function of VISTA in an immune response has yet to be properly researched. So far, the idea is that VISTA can work as mentioned beforehand as either receptor or ligand. As ligand it has been seen to suppress proliferation within the T cells, particularly it inhibited CD4⁺ T cells activation. While as receptor it leads within CD14⁺ monocytes to increased expression of IL-6, IL-8, IL1 β and TNF α by VISTA overexpression. Further, while VISTA lacks ITIM and ITAM domains it contains kinase

C binding sites and proline rich motifs, which can lead to transduction of intracellular inhibitor signals in T cells (Nowak, 2017).

The effect of VISTA on T cells has been tested with Ig proteins synthesized by combining the extracellular domain of VISTA with the Fc region of the human IgG. These proteins were stabilized on a CD3 coated plate and the bound VISTA complex led to suppression of the CFSE dilution, therefore proliferation of CD4⁺ and CD8⁺ T cells. It also clearly indicated an influence on memory and effector CD4⁺ T cell subsets. The cytokine production in case of IL-10, TNF α , INF- γ and IL-17 has been diminished. Continuous study of the effect led to the conclusion that VISTA influence is long lasting, as no recovery of T cells was detected even after cultivation without VISTA. The suppressive effect of VISTA on T cells can be reversed if VISTA itself is present in low dosage. High amount of VISTA would need a supra-physiological concentration of either anti-CD28 co-stimulation or cytokines to be reversed. Further results showed that VISTA can induce Treg cells by FoxP3 in case T cells continue to proliferate. How exactly these mechanisms are induced, and which intracellular pathways are included still needs to be investigated (EITanbouly, 2020; Suriawinata, 2014).

1.3.3.5 Ligands

In regard to VISTA the binding to specific ligands or receptors is not yet properly verified. It is known that VISTA must be interacting with proteins found within the surrounding of cancer cells as it can be detected in high levels within the tumour microenvironment. Currently, two binding partners are investigated regarding their interaction with VISTA, on the one hand VSIG3 and on the other P-selectin glycoprotein ligand-1 (PSGL-1) (Long, 2021).

VSIG3 structure has been known already for a few years, as well as its expression on a variety of non-hematopoietic cells as a member of the Ig superfamily. Studies with human T cells indicated that the interaction between VSIG3 and VISTA might lead to a reduced release of certain cytokines by T cells, such as chemokine ligand 5 and 3 (CCL5, CCL3), interleukin-2 and -17 (IL-2, IL-17) as well as interferon γ (IFN- γ). VSIG3 is expressed in healthy tissue most commonly in testis and ovary, yet studies have shown that it can also be found within different forms of cancer such as hepatoma and gastric cancers. Further investigations are needed to determine the effects of VSIG3 – VISTA binding (Wang, 2019).

Another potential influence on VISTA activity is the binding of the ligand PSGL-1, which is associated primarily with hematopoietic cells and is known to act as an adhesion molecule to enable leukocyte trafficking. The binding of PSGL-1 to VISTA is facilitated by the presence of glycosylation and tyrosine sulfation activity, which need to be induced before any effect of PSGL-1 on T cells can be taking place. In chronic infectious diseases the activity of PSGL-1 is clearly associated with exhausted T cells, both CD4⁺ and CD8⁺, yet the exact pathway is still currently investigated. In malignancies the presence of PSGL-1 is interconnected with a low pH environment ranging from 5.85 – 6.5, which can also be found within the tumour microenvironment. This indicates that in cancer growth the presence of VISTA and a low pH environment enables PSGL-1 to bind and induce immunosuppressive effects. These effects still need to be evaluated (Long, 2021).

As mentioned, the studies regarding VISTA and its effects on immune responses are still mainly speculations or primary data gathered studying binding efficiencies of known ligands. The VISTA protein needs further research to understand the exact effects on immune cells as well as determining a specific binding partner.

1.4 THE CONFLICT BETWEEN THE EMBRYO AND MOTHER'S IMMUNE SYSTEM AND IMMUNE EVASION STRATEGY OPERATED BY FOETAL CELLS

The survival of an embryo is dependent on the protection against infectious diseases by the mother's immune system without the induction of a response against the foetus. The embryo is consisting not only of the mother's DNA but also the father's raising the risk of it being recognized as non-self. The studies regarding this immune regulation are referred to as maternal-foetal immunology and contribute to the understanding how these mechanisms are regulated (Robertson, 2010, Alijotas-Reig, 2015).

The introduction of an embryo-specific immune system takes place at about 27 days of development and begins within the yolk sac sustaining the embryo from the earliest stages of progression. Continuation of the immune system development is found within the liver as studies indicate that the haematopoiesis within the yolk sac is reduced and new activity of progenitors formed can be found within the embryonic liver. After the first trimester more progenitors can be detected within the liver expressing CD34 as a marker. Following the migration from the liver and development of progenitors, the next

steps take place in the bone marrow, which then consequently is the main compartment of the human body responsible for the production of immune cells. In early studies with mice, cells produced in the bone marrow of the embryo were still seen as progenitors of immune cells and were not associated with significant activity prior to birth. Studies nowadays clearly verify that the hematopoietic cells arising in the yolk sac do not migrate as progenitors into the liver. This organ rather begins at about 5 weeks development to produce progenitors independently. While research indicate that an immune system is formed during the embryonic development, specifications of such cells and activity is dependent mostly on post-natal exposure to environmental influences (Tavian, 2005; Tavian, 2010).

The beginning of pregnancy is associated with the same risk of infections as an open wound, as both the epithelial tissue of the uterus and the endometrial tissue need to be damaged to enable the blastocyst to be implanted. These damages naturally require a variety of cells to be recruited for repairs as well as protection against infections. Also, the growth of the embryo is supported by angiogenesis to further progression by appropriate nutrition and oxygen transportation (Dekel, 2014). A schematic regarding of cells recruited and their effects during the development of the foetus is shown in Figure 12.

Furthermore, as the embryo is only expressing specific hematopoietic cells later in development, at the beginning it is severely dependent on the mother's immune system to protect against any bacterial and viral infections. Such high activity of immune cells in the immediate surrounding of the foetus naturally also increases the risk of interaction between the mother's T cells and the embryonic cells and therefore might lead to recognition of non-self-structures. To regulate this interaction, the mother's lymphocytes need to be able to approach the foetus while a potential interaction is being suppressed. The exact mechanisms are yet to be understood on how this very fragile balance is managed.

Recent studies performed a dependency on cells expressing Tim-3 to regulate decidual NK cell responses as well as increased levels of galectin-9 indicating that this specific interaction is included in the embryonic development (Li, 2017, Li, 2016).

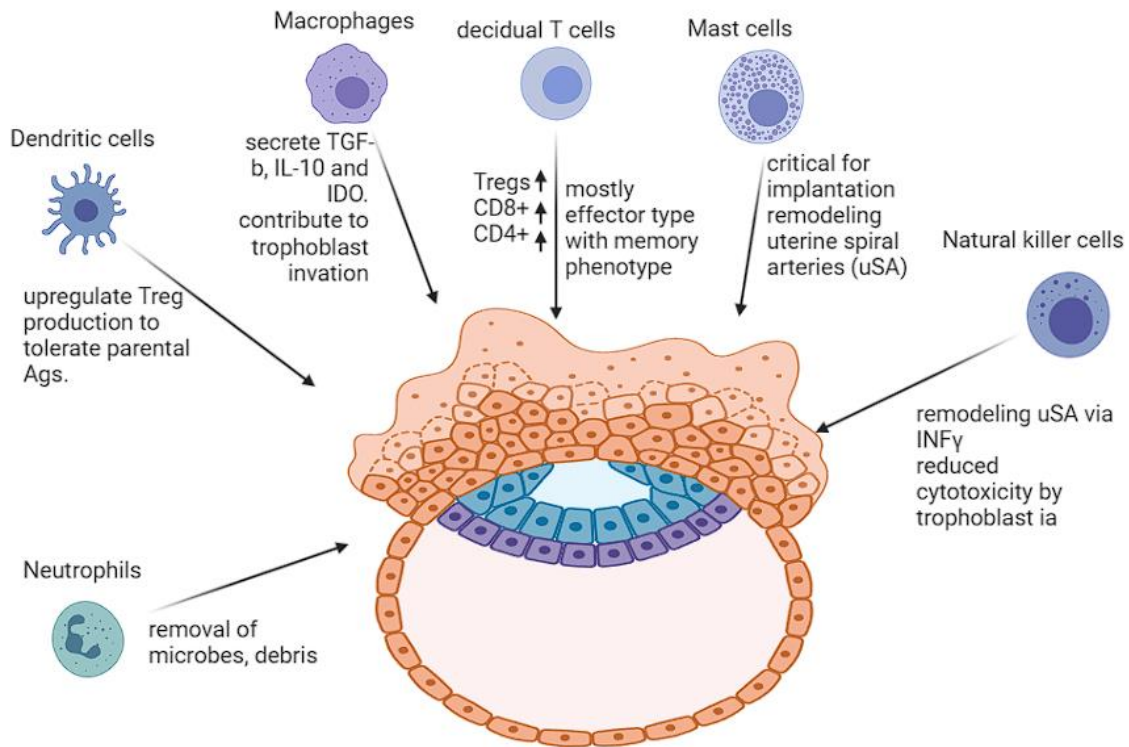


Figure 12 Interaction between the foetal cells and surrounding immune cells. To support the embryonic development a variety of immune cells need to be recruited. Such cells include macrophages specific for the maternal-foetal-interface which can secrete immunosuppressive cytokines and proteins such as IL-10 or IDO. Other cells are supporting implantation as well as removal of debris in the surrounding. This interaction has to be regulated very thoroughly as a shift to one side or another leads to the risk of miscarriage. The figure was prepared with biorender.

1.5 SIMILARITIES OF IMMUNE REGULATION IN CANCER AND EMBRYONIC DEVELOPMENT

Studying the embryonic development and cancer progression are two different categories and tend to not be regularly intertwined. Cancer cells are originating from prior healthy human cells, which were all arising from stem cells present since the embryonic development. These cells do contain mechanisms, which have been downregulated after the foetal development and tend to stay dormant the rest of the life cycle (Ridolfi, 2009). Interestingly, when malignancies converge with similar situations in the environment, same defensive mechanisms arise as seen in the embryonic development. The survival success of embryonic cells achieved by the application of such pathways in each human, is also determining the efficiency of these pathways if employed by cancer cells.

One of such situations is a hypoxic condition at the very beginning of growth of both cancer and the embryo. Due to the accelerated rate of a mass growing the present support system cannot provide enough oxygen leading to increased reactive oxygen species (ROS) and a general lack of oxygen to be present. In both cases this induces the recruitment of pathways to enable hypoxia tolerance. Mainly, this is achieved by recruitment of hypoxia inducible factor 1 (HIF-1), which does not only enable the survival of such an unfavourable condition but can also induce regulatory mechanisms responsible for morphogenesis. While in the embryonic development this is favourable, the recruitment of HIF-1 members in the cancer growth also can lead to quick adaption of malignancies to hypoxia (Kim, 2016; Brahim-Horn, 2007).

By activation of mechanisms to counter the hypoxic stage one of the most prominent protein to be recruited is the vascular endothelial growth factor (VEGF), which induces the formation of new blood vessels, supporting accelerated oxygen transport as well as sustaining nutrition. In the embryonic development a similar protein to the VEGF can be found to also support the proper sustenance of the embryo, called placenta growth factor (PlGF). The lack of PlGF can lead to lowered survival chances of the foetus. As mentioned in the prior chapter on therapeutic targets in cancer, the angiogenesis factor VEGF is a prominent target in cancer treatments, as it is one of the main proteins recruited from a very early stage in cancer development (Dunwoodie, 2009; Berra, 2000; De Falco, 2012).

Next, a supporting cell type recruited in both embryogenesis as well as cancer growth are macrophages. Studies show a specific subtype of macrophages to be found within the surrounding of the foetus, called decidual macrophages which are known to produce immunosuppressive cytokines and other proteins such as IL-10 and IDO as well as a factor to support the growth of the embryonic cells, TGF- β . These macrophages are crucial to enable the survival of the foetus. In comparison cancer cells are also able to recruit tumour-associated macrophages, which are currently investigated more thoroughly but are most likely to have similar functions as macrophages found in the embryonic development (Jiang, 2020; Miwa, 2005, Chen, 2019).

Lastly, one of the most common features found in all cancer types is the up-regulation of immunosuppressive features such as downregulation of specific receptors targeted by immune cells and recruitment of regulatory T cells enhancing these suppressive

immune responses by the cancer cells. Such components produced are able to induce downregulation of immune responses, or worse, even lead to cell death of approaching lymphocytes. Some of these targets for immunotherapy have been newly formed by mutations, e.g. point-mutations, while others seem to arise from the foetal formation as these proteins can already be detected in high levels at the beginning of the embryonic development. Such proteins include Tim-3 and galectin-9 which are highly upregulated in both types of growing tissues, indicating that the cancer cells are able to re-activate pathways which were dormant after the embryonic development. While this naturally introduce a more complex mechanism on how cancer cells are able to adapt to the immune system, such targets conserved within the genes are often very stable and difficult to mutate without causing severe complications further in cell progression. This clearly shows that by understanding the regulation of such pathways these proteins might provide more stable targets for cancer therapy. Furthermore, study of these pathways might also enable further understanding of miscarriages caused by the mother's immune system, indicating that it is a versatile mechanism to be targeted in a variety of complications (Fridlaender, 2019; Nakajima, 2019).

1.6 HYPOTHESES RESEARCHED IN THIS PHD PROGRAMME IN LIGHT OF LACK OF CONCEPTUAL DEVELOPMENT OUTLINED IN THE LITERATURE REVIEW

To summarize the introduction, cancer still is a challenge in regard to both diagnosis and therapy, especially due to the increased life expectancy and the corresponding health problems arising. While nowadays a variety of treatments are available to target cancer cells, they often tend to be either time or money consuming and are able to introduce further challenges during the application. Such challenges can include severe toxicity of chemotherapy, which induce complications during the treatment varying from common, reversible ones such as hair loss and weakness, to more severe complications such as a higher risk of infections and after the application can even lead to induced life-long difficulties such as blood disorders. This can consequently increase the risk of blood cancers later in life. Newer approaches of therapy tend to be more specific to a single target enabling a very directed approach to a very specific subtype of cells without causing off-target effects on healthy cells (Madhu, 2015). This can lead to the necessity of applying a variety of therapeutic methods at the same time,

which also are prone to lose their target in further progression of the cancer due to mutations if it is applied over a long time-period. In our research we focus now on understanding the interactions of the three beforementioned proteins: Tim-3, galectin-9, and VISTA. Tim-3 and galectin-9 binding abilities have been already proven by prior published results of our research group.

A schematic of the interaction of Tim-3 with galectin-9 and their downstream signalling as already proposed shown below. Visualized in Figure 13, a variety of downstream pathways are induced upon the interaction of galectin-9 with Tim-3, which are determined to further inhibit killing of cancer cells by either natural killer or cytotoxic T cells (Gonçalves-Silva, 2017)

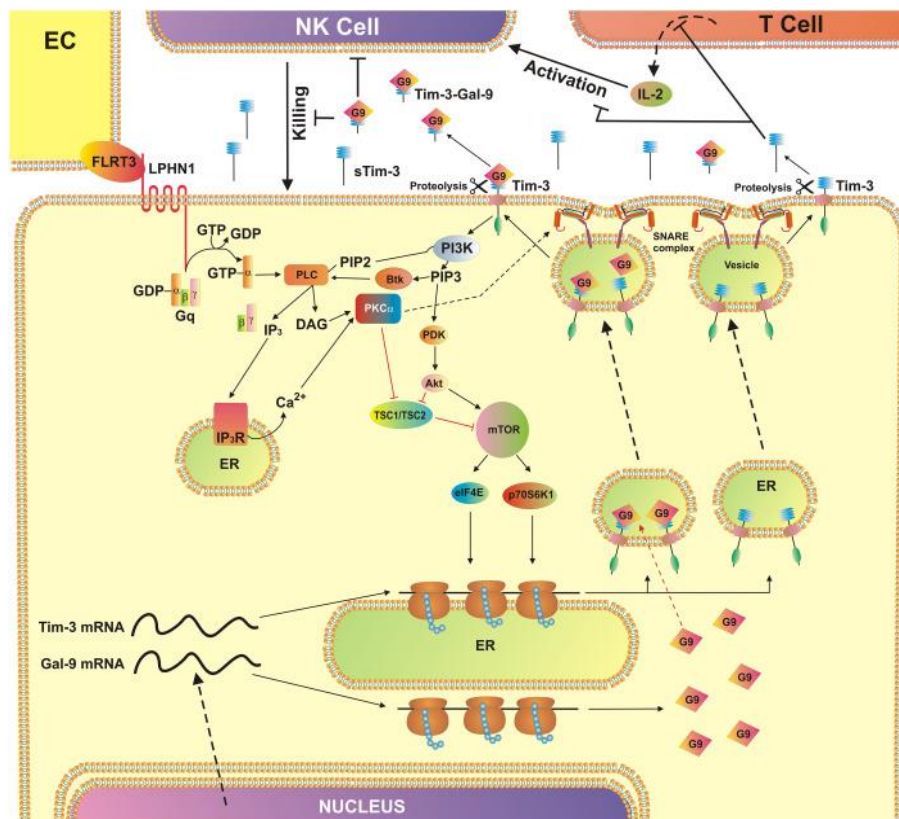


Figure 13 Tim-3-galectin-9 secretory pathway operated by human AML cells in order to suppress cytotoxic immunity. The pathways shown are associated with acute myeloid leukemia cells and visualizes the biochemical features activated by LPHN-1 leading to further downstream activation of PKC α enabling translation of Tim-3 and galectin-9 onto the cell surface and their secretion. PKC α can be either activated by FLRT3 found on the surface of endothelial cells interacting with LPHN1 and the induction of the classic Gq/PLC/Ca $^{2+}$ pathway or PKC α is induced by DAG with upregulated Ca $^{2+}$ activating the classic mTOR translational pathway. Translation by mTOR controls the production of Tim-3 and galectin-9. PKC α can also pre-activate certain release machineries which together with elevated cytosolic Ca $^{2+}$ increases exocytosis of either free or galectin-9-complexed Tim-3.

Next, to determining the exact effects induced by galectin-9 binding on Tim-3 we will investigate the interaction of T cells with cancer cells via the receptor/ligand VISTA. Investigating further proteins expressed on T cell surface a similarity in structure between Tim-3 and VISTA has been detected (Qin, 2019). As no specified ligand for VISTA has been found yet we will investigate the possibility of it interacting with galectin-9 released by cancer cells. First, we will analyse if and how galectin-9 is able to bind to VISTA, as well as understanding the mechanisms activated if galectin-9 is able to interact with VISTA. As VISTA is mainly found on T cells but no significant amount has been found on natural killer cells, which do express Tim-3, we were also interested to understand the differential responses of galectin-9 binding to either of those two proteins. Research further indicates that by induction of hypoxia in the environment of cancer cells an increased production of VISTA, next to galectin-9 and TGF- β , is detectable. TGF- β is known to support itself either by autocrine or paracrine effect and has already been established to be present in very high levels in the tumour microenvironment. This protein is commonly known to upregulate the Smad-3 production within a variety of cells, which further induces an increase in the production of a diversity of immunosuppressive and proliferating proteins (Deng, 2019; Ungefroren, 2021). We theorized that this TGF- β -Smad-3 pathway might be corresponding also with the suppression of anti-cancer immunity by the Tim-3 – galectin-9 – VISTA pathway. Altogether this pathway including Tim-3, galectin-9 and VISTA might be a new target for combinational therapies in cancer combined with already known targets such as CTLA-4 and PD-1.

This thesis focusses on the following points:

1. Determining expression levels of VISTA, galectin-9, and Tim-3 in both cancer cells as well as embryonic cells.
2. Determining the binding ability of galectin-9 to VISTA expressed on T cells and understand the exact effects of this interactions.
3. Understanding on how these proteins are regulated and which components commonly found in the tumour environment and within the cells are inducing the production in the first place.
4. Determining the origin of galectin-9 and its corresponding receptors/traffickers.
5. Investigating the differences of this mechanism in a fundamental and pathological context.

2 MATERIALS AND METHODS:

Most chemicals used were purchased either from Sigma (Suffolk, UK) or from Thermo Fisher Scientific (Loughborough, UK). Cells were bought from the European Collection of Cell Cultures (ECACC), Cell Line Services (CLS, Germany) or American Type Culture Collection (ATCC), primary cells were provided from collaboration partners in Switzerland, Germany and WT3ab cells were immortalized in Austria.

2.1 TISSUE CULTURES

To check on protein expression, biochemical pathways, and to determine therapeutic approaches the first step is to analyse each of those using cell lines. Cell lines are specific cell types that have been immortalized in a way that they can survive for a given time in an incubator and can be used to check upon specific research interests. The cell types can be differentiated into adherent and non-adherent cells. Adherent cells are cell lines originating from solid tissue types such as skin, breast, pancreas, and brain, while non-adherent cells consist mostly of cell types that are found in the blood such as T cells, B cells, macrophages, and natural killer cells. Dependent on the cell type and their originating tissue these cells have different requirements to be able to survive and proliferate in the tissue culture. Different preparation steps need to be taken in consideration for culturing cells.

2.1.1 Thawing cells:

Cells can be stored for a certain time in frozen form at -80 °C; liquid nitrogen is preferred for long-time storage to ensure proper conservation of cells. As cells are frozen using DMSO (AnalaR NORMAPUR®) the thawing of cells should be done quickly to ensure a high number of cells are viable. Media is therefore preheated at 37 °C and an aliquot of about 20 ml is prepared in a 50 ml tube for washing. The cells are quickly thawed in the water bath and transferred in the aliquoted media to dilute the DMSO used during freezing. The cells are centrifuged at 1200 rpm for 5 min and the supernatant containing the DMSO tossed. The cells are resuspended in fresh media and transferred into a flask suitable for the incubator (FisherBrand™). The condition of the incubator consists of 37 °C as ideal temperature and 5% CO₂ supply. Cells should be checked daily and taken care of as soon as they reach about 70-80% confluency.

2.1.2 Splitting cells:

Dependent on whether the cells are adherent or non-adherent different approaches are needed to split cells. Non-adherent cells will be transferred in a 50 ml Greiner tube with their media and centrifuged at 1200 rpm for 5 min. The supernatant consisting of old media and debris is tossed and the pellet resuspended in fresh media. An aliquot of that is transferred into a new flask and up to 30 ml of fresh media is added to ensure proper nutrition and space for the cells to proliferate.

Adherent cells need to be trypsinized before splitting. Trypsinization is a process to break connections between cells and the surface of the flask. Cells attach to the flask via surface proteins such as surface integrin receptors; these connections can be quite difficult to break. The process called trypsinization is induced by the usage of a proteolytic enzyme which removes these connecting proteins and leads to the cells detaching from the surface. This process takes, depending on cell type and confluency, between five to ten minutes. Cells should not be kept too long in trypsin as, while the main target is the proteins causing the cells to attach to the surface, the proteolytic enzyme can also cleave other proteins and structures responsible for the cell's survival. Cell culture media can be used to stop this process after the cells are detached, it can also hinder the process from performing properly if some is left after the media is poured off and trypsin is added.

The used media is collected prior trypsinization in a 50 ml tube. To ease the process of detaching the cells can be washed with filtered PBS prior trypsinization, once or twice, to remove any excess media and ensure that the trypsin can perform the detachment properly. For a T75 flask 5 ml of 1x trypsin (Sigma) is added and the flask kept in the incubator for 5 – 10 min. After incubation with the trypsin add the collected media back into the flask to stop any further proteolytic activity. The detached cells are poured back in the 50 ml tube and centrifuged at 1200 rpm for 5 min. Same as with non-adherent cells, the supernatant is poured off the cell pellet resuspended in fresh media and an aliquot transferred in a new T75 flask (Thermo Fisher Scientific). Up to 20 ml of media is added to ensure proper nutrition of the cells. As they are adherent to the surface of the flask their growth is dependent on the size of the flask and not on the amount of media added.

2.1.3 Freezing cells:

To store cells for further experiments in the future, a certain amount is frozen while the cells are most active. These aliquots are stored in -80 °C and can be thawed when the cell line is needed again. The process of freezing is mainly dependent on DMSO, dimethyl sulfoxide, as it enables a controlled freezing. Without DMSO at -80 °C the water within the cells would freeze rapidly and lead to the cells bursting, therefore none of them would survive. With DMSO this process is slow enough to avoid the cells bursting but still fast enough to ensure a high number of cells surviving. To do so a dilution of 1:10 DMSO in media is prepared and the cells are centrifuged at 1200 rpm for 5 min. The supernatant is removed, and the pellet is resuspended in an appropriate amount of DMSO/media solution. The cells should not be diluted too much as DMSO, while helpful for freezing, is a cell poison and will lead to some of the cells dying rather than being frozen. So, to ensure that sufficient cell number will survive the freezing and also the thawing process the amount of cells per vial should be high. The freezing process should be quick as the DMSO is mainly an active poison at RT.

2.1.4 Cell types and media used:

2.1.4.1 Media:

RPMI-1640 with 10% FBS and 7.5 ml Penicillin and Streptomycin **Sigma (Suffolk, UK)**

DMEM with 10% FBS and 7.5 ml Penicillin and Streptomycin **Sigma (Suffolk, UK)**

Keratinocyte SFM (serum-free media) **(Gibco)**

Chang Media **FujiFilm Irvine Scientific Inc.**

McCoy's media with 10% FBS and Penicillin and Streptomycin **(ATCC)**

2.1.4.2 Cell lines

To study the fundamental biochemical pathways within cells, responses to cancer cells, as well as determining efficiency of possible therapeutic approaches the first preliminary steps need to be performed in cell culture. Primary cells derived from patients are not able to survive sufficiently long outside of the human body to study each detail very thoroughly. Furthermore, taking samples from different timepoints or different patients might be inconclusive. Some might carry unique mutations that cannot be found within most of the population, or some have started therapy prior the first sample was taken leading to the cells to be weak or stressed which leads to

continuous issues with keeping them alive and well outside of the human body. To enable science to study biochemical pathways and cell responses the idea of immortalizing cells came up. Hereby, a cell type is taken from a patient and treated in such a way that these cells are not only able to survive for a given time outside of the body but also are able to proliferate simulating therefore the possible growth of cancer cells in the human body as well as allowing the storage and reuse of cells in laboratories. Most of the cell lines that are well established have been immortalized in the 1970s. Information for each cell line was taken from the ATCC database.

2.1.4.2.1 Colo-205:

The Colo-205 cell line was taken and modified from a 70-old Caucasian male patient and represents mainly an adenocarcinoma with Dukes' type D specificity (ATCC). Colo-205 is preferably cultured in RPMI-1640 media and has been acquired from the European Collection of Cell Cultures.

2.1.4.2.2 HaCaT:

The HaCaT cell line is consisting of immortalized keratinocytes that do not derive from cancer. The cells were taken from a 62-year-old male and is used to study biochemical pathways in non-cancerogenic, tissue-forming cells (ATCC). This cell line is kept in RPMI media and was obtained from Cell Line Service (Germany).

2.1.4.2.3 HEK293:

Human embryonic kidney cells (HEK) are derived from a foetus and are adherent (ATCC). Due to inconsistencies in the origin and process of immortalization these cells are mainly used to just investigate biochemical pathways and might not be completely consistent with natural responses for therapeutic development. HEK are kept in RPMI media.

2.1.4.2.4 Jurkat cells:

The Jurkat cell line is immortalized T cells used for the study of immune responses. It is derived from the peripheral blood of a 14-year-old boy with T cell leukaemia in the 1970s (ATCC). By stimulation with PMA these cells are able to produce granzyme B and simulate therefore CD8⁺ T cells. This cell line can be used to determine the immune response towards cancer in cell cultures and is a model for researching possible adaptations to insufficient cancer immune response. Jurkat T cells were acquired from the European Collection of Cell Cultures (Salisbury, UK) and are kept in RPMI.

2.1.4.2.5 K562:

As the first myelogenous leukaemia cell line derived from a 53-old patient and immortalized, these cells are used mainly as a representative for natural killer activity during immune response. Cells were obtained from the European and American Tissue and Cell collection and are cultured mainly in RPMI.

2.1.4.2.6 LN-18:

LN-18 is a glioblastoma cell line taken from a male patient, 65 years old, from his right frontal temporal lobe in 1976 (ATCC). These cells have a mutation at the TP53 gene as well as a wild-type PTEN gene. In culture they are kept in DMEM media and are adherent.

2.1.4.2.7 MCF-7:

MCF-7 cells are a breast cancer cell line derived from a 69-year-old woman, who had metastatic adenocarcinoma (ATCC). This model is fast growing and a good example of adherent cancer cell lines. Dependent on the target of research it is a good model to study biochemical pathways. These cells are also kept in RPMI media but can also be incubated in DMEM media and have been obtained from the European Collection of Cell Cultures (Salisbury, UK).

2.1.4.2.8 TALL-104:

TALL-104 is a cell line consisting of T lymphoblasts derived from the peripheral blood of a 2-year-old boy with acute lymphoblastic leukaemia (ATCC). These cells are cytotoxic and can therefore be used to study the similarities of biochemical reactivity of CD8⁺ T cells on tumours. Furthermore, with PMA stimulation these cells are able to attach to the surface and allow the study of T cell to T cell response, similar to mechanisms that might be found in the blood of leukaemia patients.

2.1.4.2.9 THP-1

The THP-1 cells have been derived from a 1-year-old male patient and represent an acute monocytic leukaemia cell type (ATCC). These cells are non-adherent and can be cultured in RPMI-1640 media. THP-1 are able to perform phagocytic activity and produce IL-1, upon stimulation with LPS as well as IFN- γ they can be polarized into M1 macrophages. The cell line was obtained from the European Collection of Cell Cultures.

2.1.4.2.10 WT3ab:

Wilm's tumour cells are derived from an early-age kidney cancer and are used to study this aggressive form of cancer. The cells are adherent and contain a TP53 mutation. For our research these cells were immortalized and provided by Dr. C. Stock from the Children's Cancer Research Institute in Vienna, Austria.

2.1.4.2.11 Primary cells:

Primary cells are used just for the time being and to revalue the results gathered using cell lines. Such cells are able to indicate if the cells obtained from the human bodies will react in similar ways to therapies or are producing a specific target that has been investigated in corresponding cell lines. These checks ensure that the results gathered using cell lines that have been modified are also found in non-modified cells. Preferably primary samples from different donors are used to verify the cell line experiments to avoid any issues arising from a person's genetic profile. As primary cells are kept just for a particularly short time period the media is chosen according to the most similar cell line. This also ensures that the results are gathered in the same environment as the cell line.

Healthy donor ethics approval: EC reference: 16-SS-03, buffy coat was bought from the National Health Blood and Transfusion Service.

AML donor sample ethics approval: reference: PV3469, samples were obtained from the bank of University Medical Centre Hamburg-Eppendorf.

Breast cancer samples ethics approval references: MH 363 (AM03) and 09/H0301/37, obtained from the NRES Essex Research Ethics Committee and the Research and Innovation Department of the Colchester Hospitals.

Primary T cell ethics were approved by "Medizinische Ethikkommission der Carl von Ossietzky Universität " Oldenburg".

2.1.4.2.12 Primary Keratinocytes:

Primary Keratinocytes are dependable on the Keratinocyte SFM media to be cultured and therefore enabling proper growth. Ethic approval was given by the Kantonale Ethikkommission of Bern, Switzerland, (2017-01394).

2.1.4.2.13 Primary embryonic cells:

In our research we used different types of primary embryonic cells from two different stages during the development. Chorionic and amniotic cells were taken as samples from our collaboration partners in Switzerland and sent to us for further investigation. For cell culture these cells are kept in Chang media *In Situ* provided by our collaboration partner and bought from FUJIFILM.

2.1.5 Smad-3 and HIF-1 α knockdown:

To determine the effects of Smad-3 or HIF-1 α on the regulation of protein expression such as VISTA and galectin-9 and their influence upon TGF- β stimulation a knock-down has been performed. The gene expression is hereby inhibited during stimulation with TGF- β and a correlation in biochemical activity investigated. To ensure that the process of knock-down is showing results due to proper targeting and not due to the knockdown process itself an isotype control is applied. The knockdown is performed using small interfering double-stranded RNA's targeting the gene in question. Being processed by the RNA-induced silencing complex (RISC) the gene is targeted and cleaved by ribonucleases inhibiting further expression during cell cultivation.

1.5 ml of the designated cells are added into each well of a six well plate. The following transfection protocol consists of using DOTAP. 30 μ l per well is planned, for 3 replicates a master mix consisting of 40 μ l of HEPES, 5 μ l of RNA and 80 μ l of a DOTAP mix (30 μ l DOTAP and 70 μ l HEPES) is prepared. This master mix is kept on ice for 30 min and shaken every 5 min. The mix is added to the cells and incubation is performed overnight. Dependent on the treatment the media is changed on the next day and the experiment continues with, for example, stimulation with TGF- β (Smad-3 knockdown) or investigation of galectin-9 and TGF- β expression (HIF-1 α knockdown).

2.2 THP-1 VS. E. COLI

In a small flask 10 ml of THP-1 cells were seeded and treated with PMA for 24 h. Media is exchanged afterwards adding fresh one containing E. coli and no Penicillin and Streptomycin, the cells are co-cultured with E. coli for 16 h. Media is collected, and cells are scraped off. The 1 ml of PBS containing the cells is separated into to tubes each 500 ml for further investigation, either on cell stain or fixed cell staining.

2.2.1 On cell stain:

To the cell pellet 10 µl of the primary antibody against the targeted protein is added and the pellet is incubated at the shaker for 2 h. The pellet is washed with PBS and a secondary antibody added for another 2 h at RT.

2.2.2 Fixed cell staining:

The pellet is centrifuged at 1200 rpm for 5 min, and the PBS removed. The cells are resuspended in 100 µl of ice-cold ethanol and kept in the freezer for 10 min. The cells are spun again and resuspended in 500 µl PBS containing the primary antibody. Incubation period is 2 h at RT. Cells are washed with fresh PBS and resuspended in 500 µl of PBS containing the secondary antibody.

In both staining the cells are washed again after 2 h incubation with secondary antibody with 300 µl of fresh PBS. After the wash each pellet is resuspended in 300 µl PBS and cells are counted. To have a comparative value for on and fixed cell stain the cell number in each well should be the same. On a plate 100 µl of the stained and diluted cells are added and fluorescence is measured at the Odyssey machine.

2.3 PREPARING CELL LYSATES

Activity after stimulation or co-culture of cells can be measured in two ways. Changes in the release of proteins such as immune activating factors or immunosuppressive ones can be measured in the media collected after the designated incubation time period has passed. This enables an insight on how the proteins are for example either released massively upon recognition of danger signals, or the exact mechanisms for the suppressive functions of cancer cells to inhibit T cells signalling. Another way is to determine the production of specific proteins. While release itself might be reduced it can also indicate that the biochemical pathway leading to the protein production itself is down- or upregulated. To do so, cells are collected and lysed leading to the proteins stored within the cells to be released into the lysis buffer allowing diagnostics on their activity.

Lysis buffer:

- 930 mg EDTA
- 4350 mg NaCl
- 3028.5 mg Tris
- 2.5 ml NP-40
- 497.5 ml bidistilled H₂O

Before using the lysis buffer on cells, 1 mM Phenylmethylsulphonyl fluoride (PMSF) is added to ensure that the proteins of interest are not destroyed during the lysis process by inhibiting proteinase activity such as trypsin or acetylcholinesterase.

Cells are centrifuged at 1200 rpm for 5 min to obtain a pellet at the bottom of the tube; the media is removed into another tube to store for other analytical approaches. Dependent on the size of the pellet an aliquot of lysis buffer is added, medium sized pellet can be incubated with about 300-400 µl. The lysis is taking place on ice to ensure a controlled degradation of the cells while keeping the proteins safe. The pellet is dissolved in the lysis buffer by pipetting up and down and left for about an hour on ice. Every 10 minutes the tube is vortexed or shaken to ensure that all cells are properly digested.

After the lysis the samples are centrifuged again at full speed for 5 min to collect the debris consisting of e.g. cell walls at the bottom. Within the supernatant the proteins that have been stored in the cells can be found. These lysates can be used for analytical steps such as for western blot analysis or ELISA's.

2.4 MICE:

To study immune responses in vivo we used C57 BL16 mice at 6 weeks of age after approval by the Institutional Animal Welfare and Ethics Review Body. The animals were taken care of by authorized personnel according to the Declaration of Helsinki protocols. The mice were injected with cancer cells and blood samples were taken after 6 h. Injection sites were homogenized for further analysis.

2.5 MEASUREMENT OF INTRACELLULAR CALCIUM

Cells to investigate were washed with a recording buffer containing Glucose – 5.6 mM, MgCl₂ – 1 mM, HEPES – 15 mM, NaCl – 145 mM, KCl – 5.6 mM, 0.5 mg BSA and pH 7.4. Into this buffer 0.25 mM sulfinpyrazone was added to avoid the removal of dye from stained cells. Next, cells were stained using 2 µM acetoxymethyl (AM) ester of Fluo4 dye and incubated it at RT in the dark for 30 min. After staining the cells were washed twice with the RB buffer and for degradation of AM ester the cells were incubated for 30 min in RB. Measurement was done using a microplate fluorometer at wavelengths: excitation = 485 nm and emission = 538 nm.

2.6 WESTERN BLOT

Western Blot is a method to separate proteins according to their size (weight). Dependent on the size of the protein of interest the gel percentage of the running gel needs to be adjusted to allow proper separation. This leads to restrictions on detection range and while Western Blot can be used to study more than one protein per membrane, due to this separation range some samples have to be run a few times at different gel percentages.

Gel percentages we used:

7.5 % for proteins at sizes ranging from 200 kDa to 50 kDa.

10 % for 120 kDa to 35 kDa

12 % for 90 kDa to 20 kDa

15 % for 70 kDa to very small sizes.

Gel percentage should be chosen according to the size of the protein of interest. If more than one protein is required for analysis the percentage should be chosen so both are well separated but still easily detected within the membrane.

The protocol for Western Blot analysis includes following steps.

2.6.1 Preparation of the polyacrylamide gel:

Depending on how many experiments are planned a stock of the gel can be produced and stored for about two months at 4 °C. Longer storage will lead to decrease of acrylamide content within the gel and therefore lead to a decrease in the percentage.

Using gel components with inadequate percentage might lead to issues with separating the proteins accordingly. In worst case it will cause the loss of smaller sized proteins.

	Lower Tris Buffer (1.5 M)	Upper Tris Buffer (0.5 M)
Tris	181.5 g	60.5 g
H₂O	1 L	1 L
pH	8.8	6.8

Table 1 Tris Buffer composition

Running gel (for two gels):

Per 10 ml	7.5%	10%	12%	15%
H₂O	5.525 ml	4.9 ml	4.4 ml	3.65 ml
1.5 M Lower Tris-Buffer (pH 8.8)	2.5 ml	2.5 ml	2.5 ml	2.5 ml
40% Acrylamide (37.5% = 1% w/v)	1.875 ml	2.5 ml	3.0 ml	3.75 ml
10% (w/v) SDS	100 µl	100 µl	100 µl	100 µl

Table 2 Running gel volumes for two gels

- 10 ml of the chosen percentage
- 120 µl of 10% Ammonium persulfate (APS)
- 25 µl N,N,N',N' Tetramethylethyldiamine (TEMED)

Stacking gel (for two gels):

Per 10 ml	4%
H₂O	6.4 ml
0.5 M Upper Tris-Buffer (pH 6.8)	2.5 ml
40% Acrylamide (37.5% = 1% w/v)	1 ml
10% (w/v) SDS	100 µl

Table 3 Stacking gel volumes for two gels

- 5 ml of upper gel (4%)
- 100 µl of 10% APS
- 20 µl TEMED

Each part of the gel will be setting for 25 min at room temperature in the spacing between glasses referring to it as a slab gel. Important is to avoid any bubbles forming in between the two gel parts as it can hinder the protein to move from the stacking gel into the running gel during the run. In the stacking gel a comb for 10 wells is inserted, in these wells the samples will be loaded. While the gel is solidifying the gel tank, running buffer and samples are prepared.

Running buffer (10x) (pH should range at about 8.3, no adjusting!)

- 30.0 g Tris(hydroxymethyl)aminomethane (Tris)
- 144.0 g Glycine
- 10.0 g Sodium dodecyl sulphate (SDS)
- 1 L H₂O

For a single run ~1.3 L of 1x Running buffer is needed.

2.6.2 Sample preparation:

Samples are prepared by mixing each one of them with sample buffer in a 1:2 dilution and heating on the heating block for 5 min at 95 °C. In general, 2x sample buffer is used, should the protein concentration be small and might not be detectable with 2x sample buffer 4x can also be used. By mixing with sample buffer and heating the proteins are denatured and can be bound in a linear form by the sample buffer.

2x Sample buffer (10ml)

- 1.25 ml Upper Tris buffer
- 2.0 ml 10% SDS
- 2.5 ml Glycerol
- 10.0 mg Bromophenol Blue
- 3.75 ml H₂O

Before use of the sample buffer add Dithiothreitol (DTT). DTT ensures that the protein stay in a single form by acting as “reducing” agent. Hereby it keeps the thiolated protein stable together with SDS within the sample buffer. Heating ensures that also disulphide bonds deeper in the protein structure is accessible due to denaturation. Furthermore, SDS ensures that all protein structures are negatively charged as the separation of proteins is dependent solely on size/weight by using an electric current running from a negative pole at the top of the gel to a positive pole at the bottom of the gel. Dependent

on the gel percentage, bigger proteins will take more time to move through the gel while smaller proteins can separate faster. Using an adequate percentage ensures that the protein of interest can move efficiently through the gel to be detectable. If the wrong percentage is used it might lead to either big proteins stuck at the top without proper separation or smaller proteins accumulating at the bottom of the gel with other debris.

After the gel and samples are prepared the comb is removed from the stacking gel and the samples are loaded into the wells. To ensure that proper separation is performed as well as being able to prove the proper size of the protein of interest a marker is added to one of the wells. In our case we are using a Rainbow marker from GE Healthcare Life Sciences (RPN800E). When the samples and the marker are loaded (20 µl/well) the gel is set to start the run. At the beginning the run takes 5 min at 50 V to ensure that the samples are collected properly within the well. After those 5 min the voltage of the run is increased to 100 V for 45 – 90 min dependent on how fast the samples are moving through the gel. Due to the sample buffer containing Bromophenol blue the position of the bottom of the samples can be determined and used as an indicator how far along the run is. In the last 5 min voltage is increased to 200 to collect the debris on the bottom. While the run is performing the membrane for the transfer is activated and the filter papers are soaked with transfer buffer. Hereby, the membrane needs to be handled with proper care (gloves and minimal touching of the membrane) as it will show at analysis everything it gets in contact with (for example fingerprints).

Transfer buffer (10x):

- 30.3 g Tris
- 144 g Glycine
- 1 L H₂O

Transfer buffer (1x):

- 100 ml 10x Transfer Buffer
- 200 ml Methanol
- 700 ml H₂O

2.6.3 Transfer to membrane:

To get accessibility for analysis of the proteins, these need to be transferred onto the nitrocellulose membrane that has been stored in transfer buffer during the gel run. After the transfer, corresponding antibodies to the protein of interest will be able to bind to them allowing detection. To do so two methods are available semi-dry transfer which is suitable for general approaches of transfer in case there is not a lacking amount of protein. Wet transfer on the other hand ensures proper transfer of protein that might be low in amount.

Semi-dry transfer

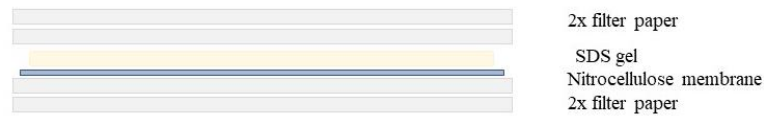


Figure 14 Set-up of the semidry transfer. Using the Trans-Blot® SD Semi-Dry Transfer Cell from Bio-Rad the anode is on the bottom plate; therefore, proteins will move from top to bottom during the run.

Semi-dry transfer is using just a minimal amount of transfer buffer, the filter papers keep the membrane and the gel wet enough for the transfer to perform while the rest of the machine stays dry. During the transfer proteins move due to an applied current through the gel and onto the membrane underneath. In our case we apply a constant current of 7 mA and set a limit to the voltage of 24 V. Due to the run by electricity heat is produced and this can be fatal to the transfer. The set limit for the voltage leads to a decrease of ampere in case it would be exceeded, this is to ensure that the proteins are safely transferred onto the membrane, the machine also has a voltage limit of 25 V for proper function.

Wet transfer:

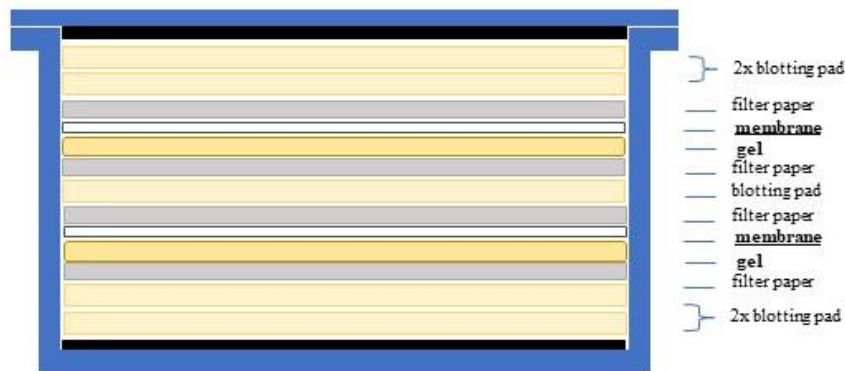


Figure 15 Set-up of the wet transfer. Shown is the setup for two gels, for one gel it is a similar setup of 2 blotting pads, filter paper, membrane gel and 2 blotting papers. The current is moving from the box to the lid and therefore the membrane needs to sit atop of the gel.

After the transfer the membrane is left in a blocking buffer (2 % BSA in TBST) for 1 h to ensure that the binding positions without any proteins do not lead to unspecific binding of the antibodies that will follow. Without blocking the membrane would be botchy during scanning and will not show the protein of interest as a specific band.

2.6.4 Staining with antibodies:

Target protein	kDa size	Amount	Secondary target	Incubation period
α LPHN2	~110 kDa	5 μ l	Rabbit	1h
Actin	~42 kDa	0.5 μ l	Mouse	30 min
AhR	~92 kDa	4 μ l	Rabbit	1h
ATF-2 total	~70 kDa	4 μ l	Rabbit	1h
CD3	~20 kDa	~50 μ l (1 drop)	Rabbit	2h
Galectin-9	~36 kDa	4 μ l	Rabbit	1h
Granzyme B	~30 kDa	5 μ l	Mouse	1h
HIF-1 α	~120 kDa	10 μ l	Mouse	1h
PARP	~116 kDa	1 μ l	Rabbit	1h
pATF2	~70 kDa	4 μ l	Rabbit	1h
pSMAD3	~52 kDa	4 μ l	Rabbit	1h
RAGE	~50 kDa	3 μ l	Rabbit	1h
SMAD3 total	~48 kDa	3 – 4 μ l	Rabbit	1h
Tim-3	~45 kDa	4 μ l	Mouse	1h
TLR2	~90 kDa	5 μ l	Mouse	1h
TLR4	~95 kDa	10 μ l	Mouse	1h
VISTA	~55 kDa	5 μ l	Rabbit	1h
HIF-1 β , ARNT	~86 kDa	1 μ l	Mouse	1h

Table 4 Antibodies used for Western Blot analysis

After the blocking specific antibodies aiming to bind to the proteins of interest are added to the membrane; a list of our most common antibodies used is shown above (Table 4). All antibodies are added to 10 ml of blocking buffer and the membrane is kept for the minimum incubation period on a shaker at RT or overnight in the fridge. After incubation with the primary antibody, excess is washed off using TBST 3 x for five minutes on the shaker.

Following the wash, secondary antibodies are used according to the animal model the primary was produced in. To visualize the staining the Odyssey Clx by Licor is used and therefore also the secondary antibodies are provided by them. In this specific setup either a green-fluorescent antibody detectable at 800 nm wavelength or a red-fluorescent antibody at 700 nm wavelength is available. The membrane is incubated with the secondary antibody for 1 h at RT on the shaker. After the incubation period the excess is washed off same as with primary and the membrane is ready for scanning.

Tris buffered saline (TBS) (10x) adjust pH to 7.4 with Hydrogen chloride (HCl):

- 12.11 g Tris
- 90 g Sodium chloride (NaCl)
- 1 L H₂O

Tris buffered saline with Tween (TBST):

- 100 ml 10x TBS
- 2 ml Tween20
- 900 ml H₂O

Dependent on how many proteins are checked this process can be repeated a few times as long as the proteins are not of similar size and the primary antibody differs in species produced. After analysing all proteins required the membrane can be stored for a certain time in TBS at 4°C.

2.7 COOMASSIE STAIN

For verification of certain protein amount, different ways of achieving this have been developed over time. One of such methods is staining the gel after electrophoresis with Coomassie. This leads to visualization of all protein bands within a gel and can be used to determine concentration differences in various cell types or treatments. The method hereby depends on the binding between the stain and proteins by ionic or van der Waals forces depending on the proteins. Coomassie tends to bind to amino acids such as lysine, tyrosine, histidine, and phenylalanine within the protein structure in acidic conditions and dependent on the dye used will produce a blue colour with an influence of either red (R-250) or green (G-250). To do so, a SDS gel is run at the preferred percentage and placed into a microwavable container after the run. The gel is covered in stain and microwaved for 45 seconds. Under the hood let the gel sit in the stain while

shaking it for 10 – 15 min. Afterwards, add the destainer to ensure that just protein stay coloured and microwave the membrane again for 45 seconds. Leave the membrane in with destainer overnight in the hood and check next day.

2.8 TOTAL PROTEIN STAIN

Coomassie staining is used on the SDS-gel after electrophoresis and is properly visible to the eye. Another staining is the total protein stain in which a Western Blot membrane after transfer is used and visualized by a machine such as the Odyssey CLx. This staining is especially helpful in cases that do not offer any other housekeeping proteins for total protein amount quantification such as β -actin. Revert total protein stain is dependent on the interaction between stain and proteins on a non-covalently level.

To do so, the membrane is covered for 5 min on a shaker in the solution and washed twice with TBST afterwards. It is once more washed with the given washing solution and TBST to remove any excess of the staining and scanned in the red channel afterwards at the Odyssey machine.

After detection the stain can be removed with a destaining process, and the membrane further used for analysis. In comparison to the Coomassie stain the total protein staining is therefore reversible and the membrane can be used for other analytical approaches.

2.9 ENZYME-LINKED IMMUNOSORBENT ASSAY (ELISA)

An ELISA is an analytical approach focused on determining the amount of a specific protein of interest, which can be found within samples. Hereby, different versions are available such as indirect or direct ELISA or in the experiments shown, a version called sandwich ELISA. This approach enhances the accuracy of the capturing of the protein of interest and enables a stable result. In the results provided in this thesis the ELISA form used is the direct sandwich ELISA using specific kits provided by R&D systems, a visual of the general procedure is provided on the next page.

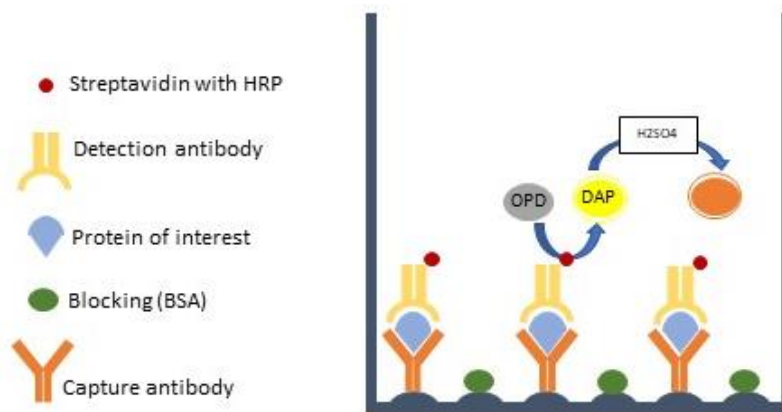


Figure 16 Set-up semidry transfer. Using the Trans-Blot® SD Semi-Dry Transfer Cell from Bio-Rad the anode is on the bottom plate; therefore, proteins will move from top to bottom during the run.

2.9.1 Coating with capture antibody and blocking:

The capture antibody is added to the plate overnight at RT to ensure efficient binding of it. The dilution is performed according to the manufacturer's instructions in filtered PBS to avoid contamination. Due to the fact that a specific amount of antibody is added to the plate certain binding areas might be still empty after incubation. These binding areas are prone to interact with any type of protein and therefore need to be blocked prior to adding the sample. Blocking is done for 1 h at RT using 1 % BSA in PBS.

2.9.2 Sample preparation and Standard dilution:

In most of the ELISA procedures performed the media collected during cell culture is used for determining the release of the protein of interest. In such cases, the media does not require any preparation besides thawing before use. In some cases, the protein extracted from within the cells was also analysed. Hereby, to allow proper binding the lysate samples were diluted with PBS in either 1:10 or 1:5 dilutions depending on how much protein is expected and how concentrated the lysate is. In case of TGF- β analysis the complete amount of TGF- β might be determined and not solely the active form, Hereby, the media needs to be pre-treated to ensure the complete amount is converted in its active form. It is firstly incubated for 10 min with 1 M HCL (20 μ l/100 μ l media) at RT, followed by 1.2 M NaOH (20 μ l/100 μ l media) neutralizing the HCl by another 10 min incubation period. The samples should be added onto the plate immediately after the NaOH incubation period.

During the blocking a standard dilution series of a known concentration of the protein of interest is prepared. With a known standard we are able to compare on how much protein has been produced/released in our samples. Hereby, the protein of interest is

provided by the company in a specific concentration and a dilution series is prepared with different reference values. The dilution values were normally chosen as 2000 pg/ml the highest concentration followed by 1:2 dilution up to 125 pg/ml and a 0 value as a blank reference. After 1 h blocking the blocking buffer is removed, the samples as well as the standard dilution is added to the wells (100 µl/well) and the plate is incubated for 2 h at RT on the shaker. During this incubation period the capture antibody attached to the bottom of the wells will be able to bind to our protein of interest.

2.9.3 Detection antibody and Streptavidin:

After the sample has been incubated on the plate the remaining liquid is tossed, and the plate will be washed 3x with TBST to remove any excess protein that has not been bound to the capture antibody on the plate. This ensures that the detection antibody added to the plate next will sufficiently bind to the protein located on the capture antibody and not on remaining loose proteins within the plate.

The detection antibody is diluted according to the manufacturer's manual and 100 µl is added to each well. The incubation period consists of another 2 h at RT on the shaker.

After the incubation with the detection antibody the next step is again washing 3x with TBST to remove any excess of detection antibody and streptavidin is added. Streptavidin is able to bind to a biotin linker on the detection antibody and contains horseradish peroxidase as an enzyme for the final step. Streptavidin is diluted according to the manual and 100 µl per well is added. The incubation period is at least 30- 45 min to ensure we have sufficient HRP bound onto the detection antibody for the final reaction.

2.9.4 O-phenylenediamine (OPD) reaction:

After the incubation with streptavidin the excess is washed off and the last step has to be done. Hereby, a visual confirmation that the experiment has worked is achieved with the standard as a positive control. For this part OPD and H₂SO₄ need to be prepared. 60 mg OPD is diluted in 10 ml ddH₂O and right before use 100 µl H₂O₂ is added. As the machine has a limit on high values that can be detected the reaction needs to be stopped when a certain time has passed, and sufficient visual confirmation is achieved. This is done by using H₂SO₄ (1 ml concentrated H₂SO₄ and 9 ml ddH₂O). After the reaction is stopped, the plate is analysed using the TECAN sunrise plate reader at a set wavelength of 492 nm.

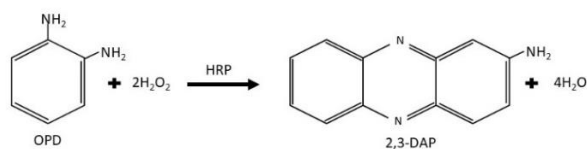


Figure 17 OPD reaction

2.10 XANTHINE OXIDASE ASSAY

Xanthine oxidase is a form of oxidoreductase that can be found highly within cancer tissue. The general process of this enzyme is to turn hypoxanthine into xanthine and further into uric acid leading to generation of reactive oxygen species. High activity within the body can lead to damages to tissue or even toxicity, which in worst cases can induce further cancer development. As cancer cells increase their metabolic activity and proliferation, they are dependent on a higher use of purine. In healthy human tissue the amount of purine is tightly regulated by using xanthine oxidase. In cancer this activity is therefore increased, and such an up-regulation might be an indicator for cancer development. Especially as in high-proliferating cancer types the activity shows higher percentage of increased function than slow growing cancers (Yin, 2018). The investigation of different types of cancer clearly shows that the increased activity of xanthine oxidase is an indicator on growth rate as well as stage of the cancer and might indicate already a survival rate dependent on its levels.

For each sample prepare following mix:

- 60 µl HRP reagent (TRIS buffer + HRP pH 7.5)
- 20 µl Xanthine
- 10 µl OPD
- 10 µl sample

Each sample is put in a well of a plate and incubated for 30 min at 40 °C. The reaction is stopped using H₂SO₄. The plate is analysed at a wavelength of 492 nm.

2.11 IN-VITRO ASSAYS OF PROTEIN INTERACTIONS

To determine the interaction between proteins and co-stimulating components or ligands as well as their receptors or carriers a type of ELISA can be performed in which one of the proteins is targeted with the capture antibody and another with the detection antibody. Hereby the specific ligand will be bound onto the plate and after washing a

detection antibody for the specific binding partner is used during incubation. By addition of HRP and performing the OPD reaction the amount of proteins interacting with each other can be determined.

An example is the interaction between Smad-3 and its co-stimulatory molecules SMAD-4 and TRIMM-33. The plate is incubated with the Smad-3 capture antibody overnight at RT. The next day after blocking the sample is added onto the plate and Smad-3 proteins in complex with their co-stimulatory interaction partners are bound and kept on the shaker for 2 h at RT. Next the detection antibody correlating with the targeted interaction partner is added and incubation is performed for another 2 h at RT. The next steps are following the ELISA protocol and finalize with development of a signal using OPD detectable at 492 nm on a plate reader.

2.12 THIOBARBITURIC ACID REACTIVE SUBSTANCE (TBARS)

ASSAY:

Due to the quick turnaround rate of reactive oxygen species and therefore a short half-life determining the amount of such is very difficult. To measure changes of the oxidative stress leading to cellular damage other components created as end products of decomposition can be investigated. One of such end products is malondialdehyde (MDA), which is either already contained in the sample or produced during the assay. MDA is procured by lipid peroxidation. Using the TBARS assay a red-coloured product consisting of an MDA-TBA₂ adduct is formed. Dilute sample 1:6 with H₂O and add 40 µl of 10 % TCA. Incubate the samples at RT for 5 min and centrifuge for 5 min at 12000 rpm. Transfer 90 µl of this mixture in a fresh tube and add 45 µl TBA. Incubate for 5 – 10 min at 95 °C. Transfer 100 µl into a well on a plate and analyse the plate using the reader at a wavelength of 532 nm.

2.13 NADPH OXIDASE (NOX) ASSAY

One of the processes responsible to produce oxygen-derived free radicals are a family of NADPH (nicotinamide adenine dinucleotide phosphate) oxidases with seven members found in a variety of tissues. These enzymes are able to transfer electrons onto oxygen from NADPH creating superoxide free radicals, one of the main produced is ROS, which leads in healthy tissue to an oxidative burst and can induce an upregulation of immune responses.

For the NOX assay PBS is combined with 1 mM EDTA as the reaction buffer. 200 μ l of the buffer are mixed with 50 μ l of NTB. In a 96-well plate 190 μ l of the NTB-buffer is added into each well and combined with 10 μ l of sample. Incubation takes 10 min at RT and the plate is measured at 525 nm.

2.14 FLOW CYTOMETRY

During the apoptotic process one of the mechanisms indicating to immune cells that the cell is a target for clearing is the externalization of phosphatidylserine (PS). PS can be also bound by a 36 kDa sized protein called Annexin V. This protein as a combination of fluorescent conjugates leads to separation of apoptotic cells from living using flow cytometry. Flow cytometry is a technique allowing the detection of single stained cells, analysing the fluorescence detected to separate cells according to the proteins of interest. In the Annexin V example cells are detectable and separated containing either the fluorescent marker for Annexin V or not indicating them to be apoptotic or viable cells.

Cells were collected after certain types of treatment or co-cultures and stained according to the protocol given by the Invitrogen kit for Annexin V and propidium iodide assays and measured using the BD FACSCalibur.

2.15 CASPASE 3 ASSAY

Cell death is measured by determining the activity of apoptotic factors such as caspase 3. Caspase 3 is activated by mediators inducing the caspase cascade and will lead eventually to programmed cell death. An increase of caspase 3 activity is an indicator that such cell death might be induced. To determine caspase activity a colorimetric kit from R&D Systems is used. Hereby caspase 3 is inducing the hydrolysis of a structure consisting of Ac-DEVD-pNA (acetyl-Asp-Glu-Val-Asp p-nitroanilide) which leads to the release of spectrometric detectable p-nitroanilide at a wavelength of 405 nm.

To be able to detect caspase-3 activity the samples are lysed in a special buffer and lysis is performed similar to the given lysis protocol. Dependent on the size of the pellet the incubation period on ice ranges from 30-60 min. Samples are centrifuged after incubation finished at 12000 rpm for 5 min. The supernatant containing caspase-3 is transferred in new tubes. In a 96-well plate 0.5 μ l of 1 M DTT solution, 50 μ l of reaction buffer as well as 5 μ l of the Ac-DEVD-pNA are combined with 50 μ l of sample. The

plate is incubated for 1-2 h at 37 °C in an incubator and analysed using a plate reader at 405 nm.

2.16 GRANZYME B ASSAY

Granzyme B is produced within cytotoxic lymphocytes such as T cell and NK cells to be released in combination with perforin into malignant or malfunctioning cells and induce programmed cell death upon activation. To determine the amount of activated Granzyme B and therefore the potential apoptosis activity within cells a substrate recognized and processed by the active form of Granzyme B can be used to determine this. A fluorescence-dependent kit is applied containing such a substrate, which after hydrolysis releases a component detectable at a wavelength of Ex/Em =380/500 nm. The samples hereby are lysed according to protocol and 25 µl were combined onto a plate with 2,5 µl buffer and 2.5 µl reagent. The plate is kept in the dark in the incubator for 30-60 min at 37 °C and measured accordingly with the plate-reader.

2.17 PROTEIN QUANTIFICATION (“BRADFORD ASSAY”)

To determine the protein concentration within a lysate one of the most common methods is the Bradford assay. The Bradford assay relies on the interaction between the protein contained in the sample and the dye Coomassie Brilliant Blue G-250. The higher the protein concentration the darker the colour turns as the interaction leads to binding between the protein and the dye by van der Waals forces and ionic interaction. To determine the protein concentration in the samples a standard curve of a known concentration of BSA is used.

Hereby, 150 µl of the Bradford reagent are mixed with 5 µl of the sample or standard and incubated for 10 min at RT while being covered. The plate is measured at 620 nm.

2.18 MAY-GRÜNWARD CELL STAINING

To visualize cells originating from bone marrow the application of the May-Grünwald staining leads to a blue-violet colourization of such cells, visible using light microscopy. The stain contains methylene blue colouring the nucleic acids found in chromosomes and either Eosin Y or Eosin B which leads to visualization of DNA-binding proteins. Due to this specific binding it allows to differ between cell type such as lymphocytes and monocytes for example and is used in cytopathology as a method to determine

the health of a patient. The stain is showing a correlation of different diseases ranging from inflammatory and infectious conditions inflicting changes within the body, yet the most common application is the early determination of malignancy formation.

The sample is transferred onto a slide and spread with the top glass along the bottom slide, for the stain to be fixated the sample needs to dry on the slide for 60 min at RT. 500 µl of the May-Grünwald stain is added onto the sample and incubated for 3 min. Next 500 µl of 10 mM of NaPi7.0 is added and left on the slide for 7 min. The excess is removed by lifting the slide and placing it for 1 min in ddH₂O. The stained sample is dried vertically for 5 min, and a cover slip is added.

2.19 QUANTITATIVE REAL TIME POLYMERASE CHAIN REACTION **(Q-RT PCR)**

While protein release and accumulation in the surrounding microenvironment is dictating the immune response by inducing the activation of lymphocytic cells and increased recruitment to the organ affected, analysing the overall production of proteins within the cells is as important as determining the release. To detect the activity of gene transcription responsible for producing the protein of interest a quantitative polymerase chain reaction with SYBR green is performed. Hereby, the more protein needs to be expressed the more DNA is turned into RNA as a genetic transcript. By performing a PCR, the amount of RNA is analysed, firstly by reverse transcriptase turning it back into individual DNA strands, which will be amplified. The more DNA is amplified the shorter is the time for the machine to detect a proper turnover rate of the DNA responsible for the protein production. Comparing these values to a control (in cancer research often healthy cells are acquired as such) leads to an understanding how efficiently cancer cells are producing anti-immunity inducing proteins.

2.19.1 RNA isolation

As the primary target is the RNA expressed within the cells and its levels, the first step for performing a PCR is isolating the RNA from within the samples. To do so the cell pellets are treated with components received within the kit “GenElute™ Mammalian Total RNA miniprep kit” from Sigma.

The cell pellet gathered after collecting the cells with the media and separated from supernatant via centrifugation is resuspended in 250 µl of lysis buffer. This is kept for a minute after which 70 % of ethanol in equal amount is added to stop the reaction. This will lead to just the membrane of the cell being lysed and therefore grants access to the RNA within. The mixture is added onto the binding column delivered by the company's kit. It is centrifuged at full speed for 15 seconds to remove the lysis buffer and ethanol mix. The RNA is bound onto the surface of the column. To ensure that the RNA is as pure as possible the column is washed twice using washing buffer 1 and 2, each time 500 µl are added followed by centrifugation at max speed for 15 seconds. After washing the column is spun dry for 1 min at max speed to ensure all the buffers are removed and the column is placed into a collection tube. Lastly, 20 µl of an elution buffer is added onto the column to remove the RNA by spinning it at full speed for 1 min.

2.19.2 DNA decontamination

To ensure that the samples are containing just the RNA of interest and has not been contaminated with DNA able to be bound by primers after RNA extraction a DNase is used to digest any remaining DNA within the samples.

For DNA decontamination each sample is mixed as follows

- 8 µl of sample
- 1 µl of 10x reaction buffer
- 1 µl of DNase I

The mixture is incubated for 15 min at RT to allow the DNase break down any leftover DNA within the sample. After the incubation 1 µl of a stop solution is added and the samples are incubated at 70 °C for 10 min. To continue with the next steps the samples are chilled on ice after incubation.

2.19.3 DNA template preparation

After any remaining DNA is removed the RNA contained in the samples has to be turned into DNA templates for the primers to bind onto. The process to achieve this is called reverse transcriptase and recreates the DNA from which the RNA is originating. Reverse transcriptases are processes normally found in viruses to entice the replication of their genome within the host as well as in eukaryotic cells to increase the

length of telomeres on linear chromosomes. The enhanced avian reverse transcriptase by Sigma Aldrich is retrieved from Avian Myeloblastosis virus (AMV).

To the 11 µl gained after the DNA decontamination the following steps are added.

- 1 µl Oligo-DT
- 1 µl Deoxy RN mix
- 2 µl Buffer
- 1 µl enhanced avian reverse transcriptase
- 1 µl of RNase inhibitor
- 3 µl H₂O

This mix is incubated at 42-50 °C for 50 min.

2.19.4 QPCR

After gaining the DNA templates of our protein of interest the final step is to amplify the gene determining the amount within specific cell types. If a cell type is due to stimulation or mutations prone to produce more protein in a cellular level the amplification to a detectable level takes less cycles than a healthy, non-stimulated cell. To quantify the amplification of the gene a certain threshold is set as zero value. Lastly, the PCR is performed. To do so a master mix containing the following components is prepared. For each sample 15 µl of the master mix is needed.

- 3 µl H₂O
- 2 µl Primer (1µl forward and 1µl reverse Primer)
- 10 µl Master mix 2x concentrated

The master mix is properly combined by pipetting and not vortexing. On a light cycler multiwell plate 15 µl of the master mix is added into each well and 5 µl of sample is added. The plate is spun for 1 min at 800 rpm before the PCR program is started.

In our case we decided for these primers:

- VISTA: forward – 5'-GATGCACCATCCAACCTGTGT-3',
reverse – 5'-GCAGAGGATTCCTACGATGC-3';
- actin: forward – 5'-TGACGGGGTCACCCACACTGTGCCCATCTA-3',
reverse – 5'-CTAGAAGCATTTGCGGTTCGACGATGGAGGG-3'.

2.20 DNA AGAROSE GEL

The DNA agarose gel is performed as separation of DNA strands similar to SDS electrophoresis separation of proteins. DNA can be used after extraction from cells or after the PCR run and further allows the recovery of a specific DNA sample for further analysis e.g., sequencing. In such cases the gel is cut after the run by visualizing the bands on an UV transilluminator and the gel surrounding the DNA is digested to extract the sample. For the DNA agarose gel a TBE buffer is needed.

5x TBE buffer:

- 27 g TRIS
- 13.75 g Boric acid
- 1.86 g (0.5 M) EDTA
- 500 ml H₂O

1.5 % Agarose gel is prepared by weighing in 1.5 g agarose in 100 ml of 1x TBE buffer. To do so the 1.5 g is melted in 20 ml buffer and filled up after. To melt the gel add it in the microwave in 1 min intervals and stir in between. After it is molten add 100 µl ethidium bromide and stir. When mixed pour the gel into the cassette and add the comb for wells. The gel has set fill the surrounding area with 1x TBE buffer for the run. Samples are prepared as 1:2 dilution with DNA sample buffer and 20 µl are added into each well. The run takes either about 30 min at 1.5% or 1- 1 ½ hours at 5% and a setting of 110 Volt. To visualize the result, an UV machine is used.

2.21 GLYCOLYSIS ASSAY

Cancer cells are depending on a high metabolism to ensure their increased growth and high production of immune-suppressive proteins. In such cases the processes responsible for energy production will be interchanged from mitochondrial respiration dependent on proper oxygen levels to glycolysis during hypoxia found in early stages of cancer development. Determining the glycolysis levels within cancer cells allows an insight in the energy production as well as speed of growth during malignant transformation. These processes are further kept in later stages lacking hypoxia providing an insight that cancer cells prefer glycolysis and its production of lactic acid.

To determine the glycolysis activity within cancer cells 60 µl of lysates are combined with 600 µl of 1% Glucose and filled up to 1 ml with PBS. Oil is added on top to create

an aerobic condition and the samples are incubated at 37 °C for 45 min. In fresh tubes either 300 or 600 µl of samples are added after incubation. The amount chosen is dependent on the amount of samples left and the oil contained needs to be avoided. Per 300 µl of sample 100 µl of 10 % TCA is added and the sample is spun for 5 min at 12000 rpm. After centrifugation 300 µl of sample are transferred into a fresh tube and 100 µl of copper sulphate and calcium chloride mix is added at a concentration of 23 µg/sample. Incubation for 5 min at RT takes place and the samples are centrifuged again at 12000 rpm for 5 min.

In fresh tubes 20 µl of sample are added and combined with 200 µl of concentrated H₂SO₄, the samples are incubated at 95 °C for 4 min and cooled down on ice afterwards. To each sample 10 µl of 1,2-DMB is added and the samples are measured on a plate at 492 nm.

2.22 NUCLEAR EXTRACTION

To study the interaction between transcription factors and DNA and as such specific proteins, a possibility is to extract the nucleus. During the activation process upon recognizing external signals the cell is inducing an asset of various pathways and upon phosphorylation or binding of transporters and such, these proteins are able to enter the nucleus. In the nucleus transcription factors are responsible to induce immune activation or suppression dependent on the factor activated. To determine the amount of an active version of such factors and if these factors are interacting with the DNA a nuclear extraction containing just the active forms within the innermost centre of a cell can be performed.

Buffer A:

- 20 mM TRIS pH 7.5 – 8.0
- 100 mM NaCl
- 300 mM Sucrose
- 3 mM MgCl₂
- PSMF added right before use

Buffer B:

- 20 mM TRIS pH 8.0
- 100 mM NaCl
- 2 mM EDTA pH 8.0
- PSMF added right before use

To safely analyse the samples each step is performed on ice or in cooled centrifuges. The cells are harvested in tubes and spun down at 500 rpm for 5 min. The media is collected for further experiments. The pellet is resuspended in 62,5 µl of Buffer A and

kept on ice for 10 min. After incubation, the samples are centrifuged at 3000 rpm for 10 min at 4 °C (pre-cool centrifuge). The supernatant is discarded, and the pellet is resuspended in Buffer B containing NaCl, the samples are homogenized using the pipette and left on ice for 30 min while regularly mixed with pipetting every 10 min. Samples are spun again at 4 °C for 20 min at 24000 rcf and the supernatant is stored at -80 °C for further analysis.

2.23 PI3K ASSAY

Members of the phosphoinositide 3-kinases or phosphatidylinositol 3-kinases (PI3K) family are one of the main interactors in signal transduction responsible for cell growth proliferation and differentiation. This pathway is dependent on a well-maintained approach for cell survival and can be highly up-regulated in cancer growth. To determine if a heightened amount of protein found within cells or released is dependent on the PI3K pathway an assay can be performed to analyse the output. Especially in release processes, it is an important diagnostic factor to determine if it is a constant release due to an increase on protein production or simply due to the release mechanisms themselves. To analyse the PI3K function within the samples acquired, we added to each 10 µl of sample 90 µl of PI3K substrate (already contained within buffer) and incubated the samples for 1 h at 37 °C while shaking. After the incubation 1 ml of Heptane/Isopropanol mix (7:3) and 200 µl potassium chloride is added to each tube. The samples are mixed by vortexing and left at RT till phase separation happened. 500 µl from the upper phase is taken and transferred to a fresh tube. The tubes are left open on the heating block (at a properly ventilated place) for about 10 min at 95 °C till the liquid has fully evaporated. After the samples are dried resuspend it in 120 µl H₂O each. In a plate 100 µl of the sample are mixed with 20 µl ammonium molybdate and 20 µl molybdate reagent. The plate is read at 492 nm.

2.24 MTS ASSAY

Most analytical approaches used nowadays tend to either compare protein output to total protein within the samples to get a comparative value between for example control and treatment or control and co-culture. Different aspects can influence how much protein is contained within the samples such as pipetting error and different conditions influencing the growth of cell types. Yet, due to treatments often consisting of chemicals at a certain concentration or due to the interaction between different cell

types influencing altogether the survival rate in cells a decrease in protein concentration might also be dependent on this. One of the methods to determine the survival rate is the MTS assay used to stain viable cells and MTS hereby stands for the component that is used to stain the cells called (3-(4,5-dimethyliazol-2-yl)-5-(3-carboxymethoxyphenyl)-2-(4-sulfophenyl)-2H-tetrazolium). For the MTS assay cells are treated and preferably kept in a 96 well plate. After incubation the cells are stained by adding the MTS reagent according to the manufacturers protocol. The plate is kept incubated for 1-4 hours and measured at the plate reader.

2.25 CHROMATIN IMMUNOPRECIPITATION (CHIP) ASSAY

To induce activation of specific genes regarding immune responses, adaption to hormonal changes or cell transformation, proteins acting as ligands are able to activate a cascade of response elements within the cells. These cascades tend to end by binding of different types of transcription-inducing proteins onto the chromatin in the nucleus. To determine where exactly these proteins bind onto the chromatin a technique was developed precipitating chromatin with the bound protein which then can be further analysed by either PCR or sequencing. Different types of immunoprecipitation assays were developed over time but in general each depends on shearing the DNA into smaller fragments and capturing the protein of interest bound to specific sequencing.

After precipitation the samples are purified and processed dependent on the next analytical steps necessary. ELISA plate is precoated with e.g. total Smad-3 antibody overnight. Next day blocking buffer is added to the wells (100 µl 1% BSA in PBS) and the plate is left on the shaker for 1 h. samples are added into the blocking buffer and the plate is incubated for another 2 hours. After incubation and therefore extraction of Smad-3 bound chromatin, the samples are transferred onto DNA binding tubes from Sigma-Aldrich DNA extraction kit using the given lysis buffer. The samples are washed and eluted in 30 µl of elution buffer each. These samples are than further treated according to the PCR protocol.

Primers used were forward: 5'-GCCTACCACATACCAAGCCC-3' and reverse: 5'-ATCGGCAGTTTAAAGCCCGT-3'.

2.26 PRIMER DESIGN

For different analytical approaches focusing on analysing sequences either leading to protein expression, mRNA, or understanding the binding ability to DNA, ChIP, a targeting approach needs to be created. This targeting approach is a specific sequence determined to be found within the gene of interest and allows continuous replication of this sequence in PCR. Hereby the important focus is that the primers are produced in forward and reverse with the sequence of interest found in the middle. The primers need to be created in such a way to ensure the target is properly included without risking loss. Furthermore, the sequence of interest needs to be specified to avoid unspecific binding. Preferably a size of about 18-30 nucleotides, and not more than 24 for efficiency, and a primer without highly repetitive sequences as repetition within the primer might lead to binding of self rather to the DNA templates. The NCBI primer-blast website offers a great variety of parameters to choose from when designing primers as well as allowing to check for primers used by other laboratories that have been published to ensure it encodes for the protein or sequence of interest.

2.27 STATISTICAL ANALYSIS

For each experiment the samples were analysed at a repetition of at least three times while statistical analysis for comparing two events at a time was regulated using a two-tailed Student's t-test. Multiple comparisons in case of high numbers of samples were performed by ANOVA. Post-hoc Bonferroni correction was applied, and statistical probabilities (p) are shown as * when $p < 0.05$; **, $p < 0.01$ and *** when $p < 0.001$.

2.28 MEASUREMENT OF GALECTIN-9 IN BACTERIAL CELL

EXTRACTS

Immune responses towards bacteria are dependent on the recognition of bacterial infections by immune cells. In some cases, this is achieved by the aid of proteins able to act as danger signals after binding specific bacterial structures. In case of gram—negative bacteria galectin-9 has been tested as such a component. To do so E. coli XL10 Gold® bacterial cells were sonicated after co-culture with Jurkat or THP-1 cells. Supernatant and cell pellet of E. coli were collected and stored for further analysis. To determine the process of bacterial binding of galectin-9 and influence of its cellular binding partners such as VISTA and Tim-3 both supernatant and cell pellet were

incubated with biotinylated antibodies against the targets and analysed in similar way as ELISA. After incubation with HRP the samples were visualized using OPD and analysed at 492 nm using plates.

2.29 DETERMINATION OF GALECTIN-9 BINDING SPECIFICITY TO LPS AND PGN

Determining the specificity of galectin-9 regarding the bacterial immune responses the binding capability to gram-negative as well as gram-positive signals found on bacteria is analysed. To do so LPS (1 µg/well *Pseudomonas aeruginosa* (Sigma)) and PGN (5 µg/well *Staphylococcus aureus*) are immobilized using anti-LPS or anti-PGN antibody onto an ELISA plate. The coated plate was co-cultured with human blood plasma, 500 ng/well recombinant human galectin-9 or TLR-2 as a positive control. Binding is visualized with OPD and analysed with a plate reader at 492 nm.

2.30 NANOCOMPLEX-DESIGN FOR IMMUNOPRECIPITATION OF PROTEINS

Proteins are produced in a cascade-like pathway, with one protein leading to the activation of the production of another signalling protein downstream. These proteins might cause an immune response leading in cell death of the target. A way to determine a difference in immune defences is to remove the intermediate protein within these immune pathways. To do so, the media collected from the first incubation period is treated in a way to remove the protein using an extraction method. A primary example of such an extraction method is the use of gold nanoparticles. These nanoparticles are combined with specific antibodies against the protein of interest, creating so-called nanoconjugates. Nanoconjugates are created using 30 nm of gold particles formed from 5 ml aqueous gold chloride trihydrate and 2.5 ml sodium citrate solution combined into 95 ml MilliQ-water using a magnetic stirrer. During stirring the solution is chilled to 4 °C and 1 ml of chilled sodium borohydride is added. These nanoparticles were analysed by using Transmission Electron Microscopy (TEM).

The particles are combined with the antibody at a ratio of 1:6. Sufficient coating of the nanoparticles supports the removal of all the targeted proteins. The antibody is connected to the particles by activated glutathione (GSH), which had been prepared by incubation of 0.05 M at RT for 2 h with a solution of 0.4 M 1-ethyl-3-(3-

dimethylpropyl)-carbodiimide (EDC) and 0.1 M N-hydroxysuccinimide (NHS). To determine how much antibody has to be added to the nanoparticles the amount of gold nanoparticles produced are calculated as followed using the constants for molar weight of antibodies 150, 000 g x mol⁻¹ and 1 mole antibody 6.02 x 10²³ molecules:

$$N_{AuNP} = m_{totalAu} / m_{AuNP} (m = mass; N = quantity);$$

$$m_{totalAu} = C_{Au} (mol \times l^{-1}) \times MW_{Au} (g \times mol^{-1}) \times V_{AuNP}$$

(*C* = molar concentration, *MW* = molecular weight, *V_{AuNP}* = the volume of the AuNP suspension used);

$$m_{1AuNP} = \rho_{Au} \times V_{1AuNP}; (\rho = density, V = volume; \rho_{Au} = 19.3 g cm^{-3});$$

$$V_{1AuNP} = 4/3 \pi R^3; (R = radius of a AuNP)$$

$$R = d_{1AuNP} / 2; (d = diameter of 1 AuNP expressed in cm)$$

Finally, the samples are co-cultured with the nanoparticles leading to the protein targeted within the media to be bound by the attached antibody. Removal of the nanoparticles lead to depletion of the protein of interest and the media can be used for the next steps.

2.31 ELISA IMMUNOPRECIPITATION FOR CHARACTERIZING INTERACTIONS BETWEEN GALECTIN-9 AND TIM-3/VISTA

To immunoprecipitate galectin-9 for analysing complex formation we used ELISA plates. These were coated with anti-galectin-9 antibodies overnight and blocked for 1 h with a blocking buffer containing 2 % bovine serum albumin (BSA). The media taken after cell culture is kept on the plate for 2 h at room temperature and washed three times with TBST afterwards. To extract the bound galectin-9 (in complex with other binding proteins) a HCl pH-lowering buffer at a pH of 2 was added. These extracted proteins were mixed with the same volume of lysis buffer at a pH of 7.5 first and then a 4x sample buffer at a ratio of 1:3 was added. These samples were analysed using Western Blotting and antibodies against galectin-9, Tim-3, and VISTA.

3 RESULTS

3.1 GALECTIN-9 DETERMINED FOR THE FIRST TIME AS A LIGAND OF VISTA

The VISTA protein has been put in focus regarding its immunosuppressive functions especially in correlation with cancer studies lately. VISTA has been first determined as an Ig superfamily ligand in mouse studies (Wang, 2011) expressed on hematopoietic cells inducing immune suppression in cancer patients. In further studies VISTA has been investigated as a ligand as well as a receptor similar to cytotoxic T-lymphocyte antigen-4 (CTLA-4) and programmed cell death protein-1 (PD-1) with binding affinity to a till then unknown ligand. In this chapter we investigate the ability of VISTA to bind galectin-9 as a ligand.

3.1.1 GALECTIN-9 RELEASED BY CANCER PROGRESSION BINDS TO VISTA WITH HIGH AFFINITY

Galectin-9 has been determined to be produced in high levels, and its ability to induce apoptosis is well established in mice since the 1990s (Wada, 1997). As a ligand to induce apoptosis within T lymphocytes galectin-9 needs to be able to bind to specific receptors. In studies prior the Tim-3 protein has been determined as a potential receptor and carrier of galectin-9. As VISTA is expressed on T cells in various levels and no specific ligand was known, galectin-9 binding affinity to VISTA has been tested. First, VISTA expression levels have been compared in a variety of hematopoietic and primary cell lines (Figure 18).

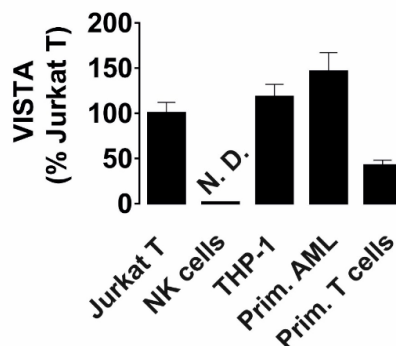


Figure 18 Expression levels of VISTA within hematopoietic and primary cell types. Western Blot analysis of VISTA levels normalised against total protein (β -actin). Data of five independent experiments include mean values \pm SEM. N.D. referring to “non-detectable”.

Next, we incubated Jurkat T cell lysates onto a 96 well ELISA plate coated with anti-VISTA antibody immunoprecipitating and analysing released VISTA (Goncalves-Silva, 2016). After incubation VISTA released from the Jurkat lysates was bound onto the plate and further exposed to medium collected from an AML cell line and MCF-7 breast cancer cells. The AML cell line, THP-1, has been incubated with 100 nM phorbol 12-myristate 13-acetate (PMA) treatment for 24 h activating intercellular pathways mimicking their induction similar to receptor stimulation and therefore leading to release of galectin-9 in increased levels. The negative control consisted of MCF-7 cells in presence of 100 nM PMA showing no indication of galectin-9 release after 24 h. The medium of both cell lines has been incubated with the bound VISTA for 2 h, galectin-9 binding to VISTA was measured using ELISA and Western Blotting (detectable at about ~36 kDa) according to Materials and Methods (Figure 19A, B). Upon co-incubation VISTA shows clear binding of galectin-9 as its ligand. In comparison investigating natural killer cell lysates no VISTA levels were detectable. Both cell types have been analysed at ~45-65 kDa using the Western Blot approach described prior for determining their ability to produce VISTA (Figure 19C).

The binding affinity of galectin-9 to VISTA has been tested using human recombinant galectin-9 binding to VISTA analysed by synchrotron radiation circular dichroism (SRCD) spectroscopy. By binding to each other conformational changes were detectable, furthermore, titration verified a high binding affinity at $K_d = 18$ nM (Figure 19E). VISTA has been procured as a Fc-VISTA complex, to verify that binding affinity has been solely by VISTA-galectin-9 interaction; the binding affinity between galectin-9 and Fc proteins were tested with no certain interaction (Figure 19F). Any observed interaction between Fc and galectin-9 has been subtracted from the VISTA-Fc binding (Figure 19D).

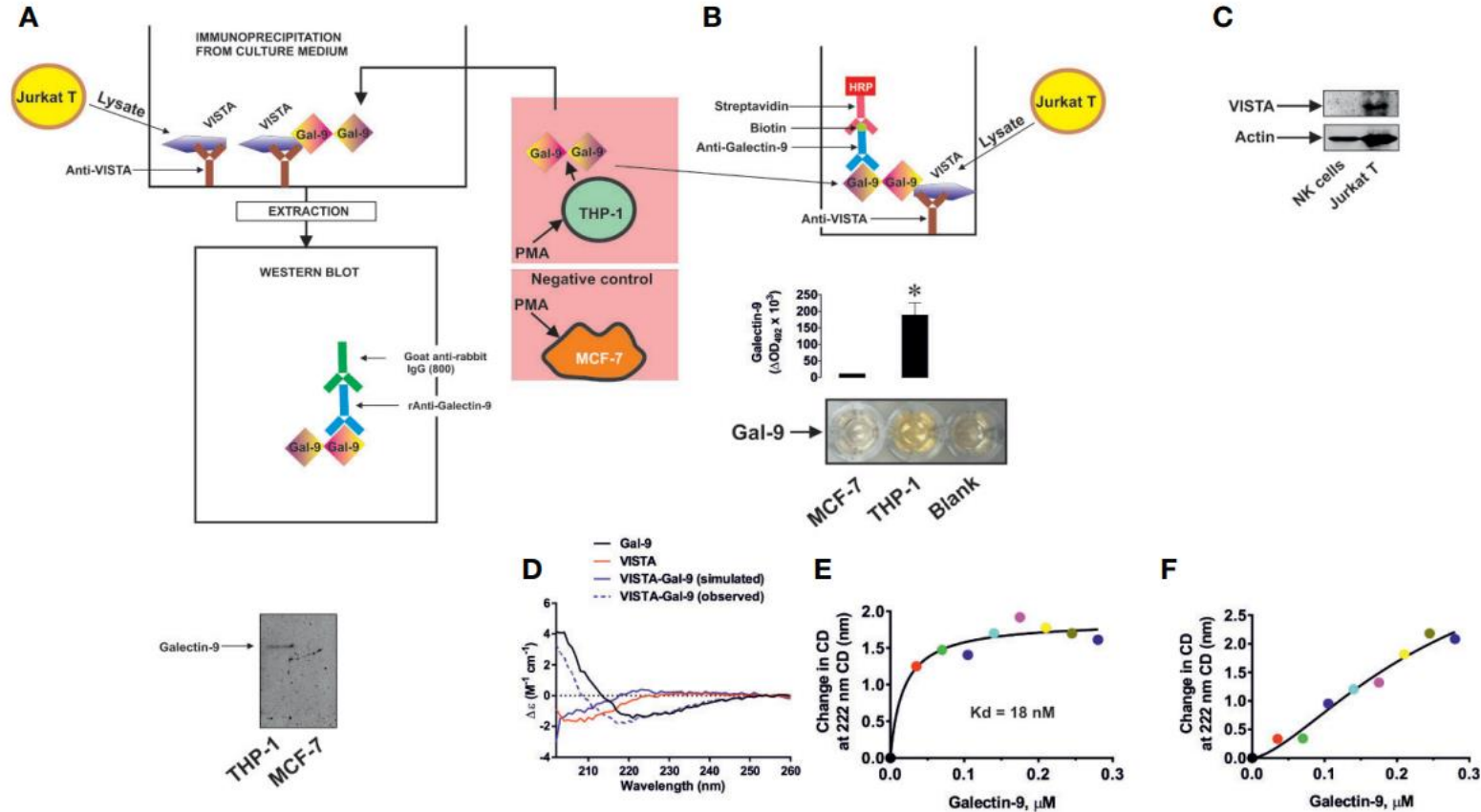


Figure 19 Determination of VISTA – galectin-9 binding ability. By coating wells on a 96-well plate with anti-VISTA antibody and co-incubation with galectin-9 derived from THP-1 complex formation has been detected by Western Blot (A) as well as ELISA approach (B). MCF-7 was used as a negative control. VISTA expression levels were measured on natural killer (NK) and Jurkat T cells (C). Binding affinity (D) was analysed by subsequently checking VISTA – galectin-9 (E) and galectin-9 in complex with human Ig-Fc (F). Data obtained include five individual experiments (mean +/- SEM), SRCD six repeats, average presented * $p < 0.05$ vs. control.

To appropriately determine the binding affinity K_d we performed analysis by immobilization of galectin-9 on a CM5 Biacore sensor chip and co-incubation with either Fc-VISTA complex or solely Fc flowing through the cell. Binding of VISTA to galectin-9 has been verified and binding affinity was calculated using Lineweaver-Burk type plot as well as Biacore T200 software and GraphPad prism for exponential decay, association/dissociation approach. An average binding affinity of $K_d = 100$ nM was calculated (Figure 20).

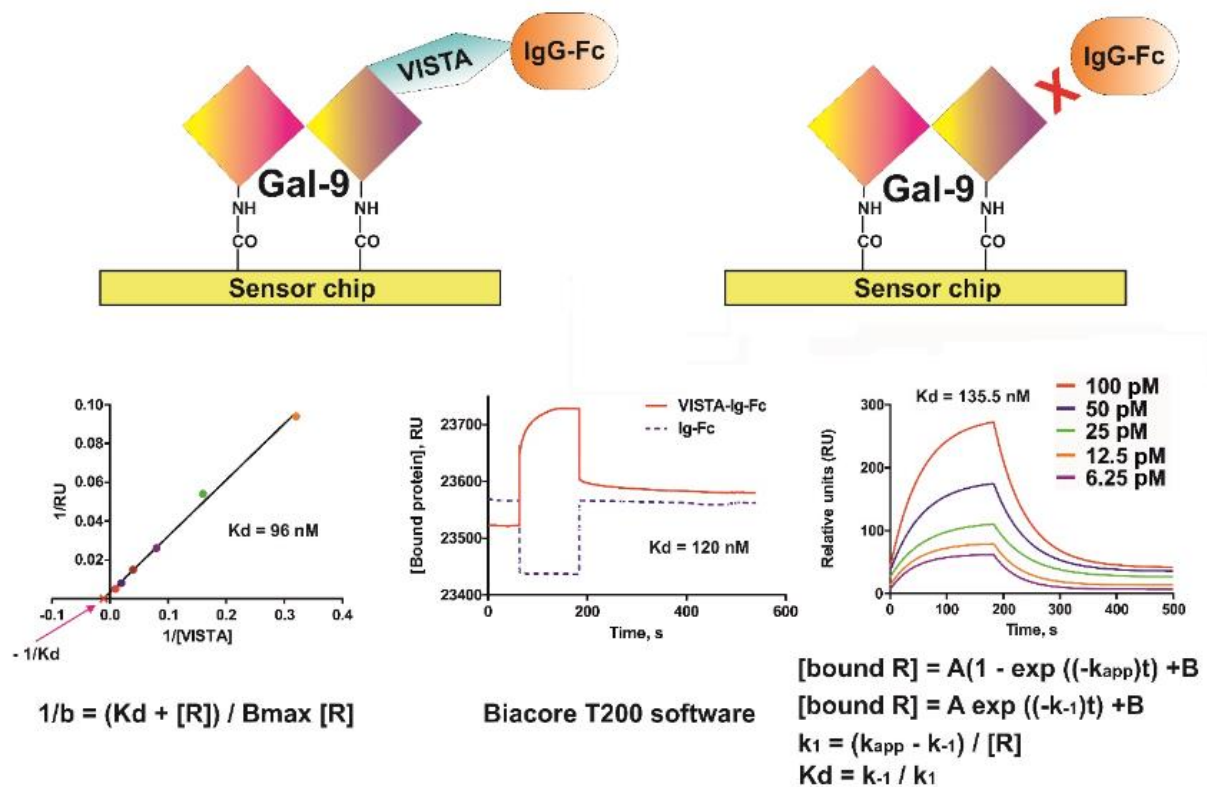


Figure 20 Determination of galectin-9 interaction with VISTA. Galectin-9 immobilization on CM5 sensor chip via Biacore amino-coupling kit and co-incubation with either Fc-VISTA or human Ig-Fc flow-through was used to confirm the binding ability of these two proteins in form of ligand-receptor interaction. Left diagram indicates the binding affinity constant by Lineweaver-Burke plot. Middle diagram consists of curves reporting binding affinity of 100 pM VISTA-Fc and 100 pM Ig-Fc (calculated by using Biacore T200 software) Right curve is obtained by increased concentrations of VISTA-Fc applied to the CM5 sensor chip containing galectin-9. Fc values have been subtracted from values gathered in VISTA-Fc flow-through experiment. GraphPad Prism has been used for curve fitting (including exponential decay, association/dissociation)

3.1.2 GALECTIN-9 BINDING TO VISTA LEADS TO INHIBITION OF GRANZYME

B RELEASE WITHIN T CELLS INDUCING APOPTOSIS OFF-TARGET.

To determine the influence of granzyme B produced by T cells upon binding of galectin-9 to their surface we co-cultured the human AML cell line, THP-1, with Jurkat T cells at a ratio of 1:1. Prior the co-culture Jurkat T cells were stimulated with PMA leading to a cytotoxic phenotype of these cells including increased granzyme B production. To ensure granzyme B has been produced upon stimulation with PMA and to determine the levels of granzyme B found within THP-1, both cell lines were tested while using natural killer cells as a positive control. THP-1 cells do not contain any detectable amount of granzyme B similar to non-stimulated Jurkat T cells containing just traces. Upon stimulation with PMA the granzyme B production is increased in Jurkat T cells. Levels within cells were determined by Western Blot and granzyme B assay. (Figure 21).

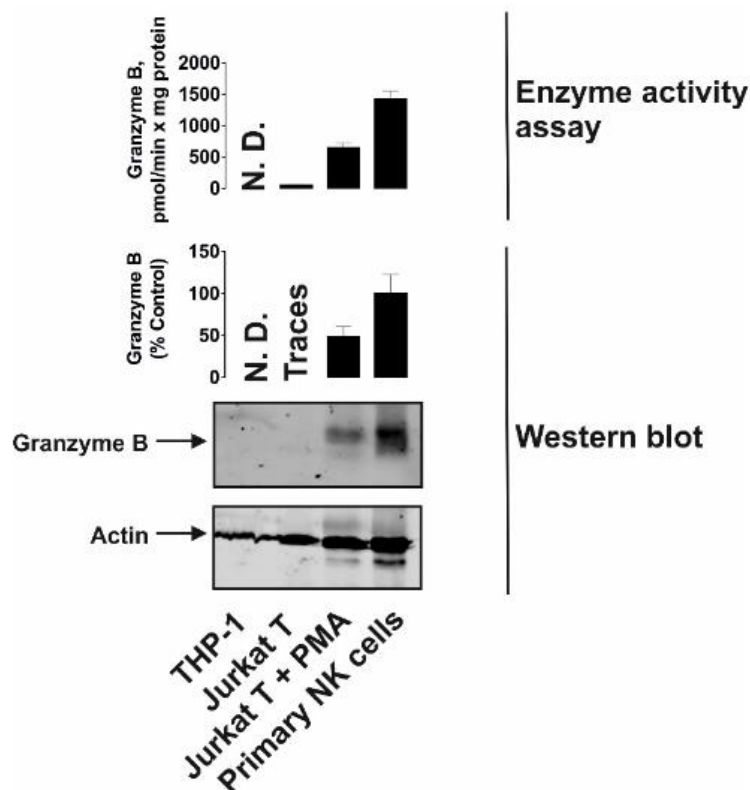


Figure 21 Analysis of granzyme B expression levels within different human cell types.

Comparison of granzyme B levels within THP-1 AML cells, non-stimulated Jurkat T cells, Jurkat T cells stimulated with 100 nM PMA for 24 h and primary human natural killer cells as positive control. Image used as a representation of four experiments with similar, independent results (mean +/- SEM shown)

THP-1 cells have been attached to the surface of cell culture plates by stimulation of 100 nm PMA for 24 h which further led to the increased, continuous release of galectin-

9 (>6 ng/10⁶ cells) into the cell culture medium after removal of PMA stimulation up to 16 h. Co-culture of Jurkat T and THP-1 cells was performed (Figure 22A) for 16 h, galectin-9 release and granzyme B within both cell types were analysed. A decrease of galectin-9 in the medium while co-culture indicates galectin-9 interaction with Jurkat T cells (Figure 22B). Granzyme B is equally distributed between Jurkat T and THP-1 cells during co-culture. By addition of 5µg/ml anti-VISTA antibody neutralizing binding capabilities of galectin-9 onto T cells, granzyme B was mainly found within the targeted AML cell line (Figure 22C). This indicates a clear correlation between galectin-9 binding and granzyme B release. Isotype control has been used to verify granzyme B release and uptake by THP-1 cells were elevated due to VISTA neutralization.

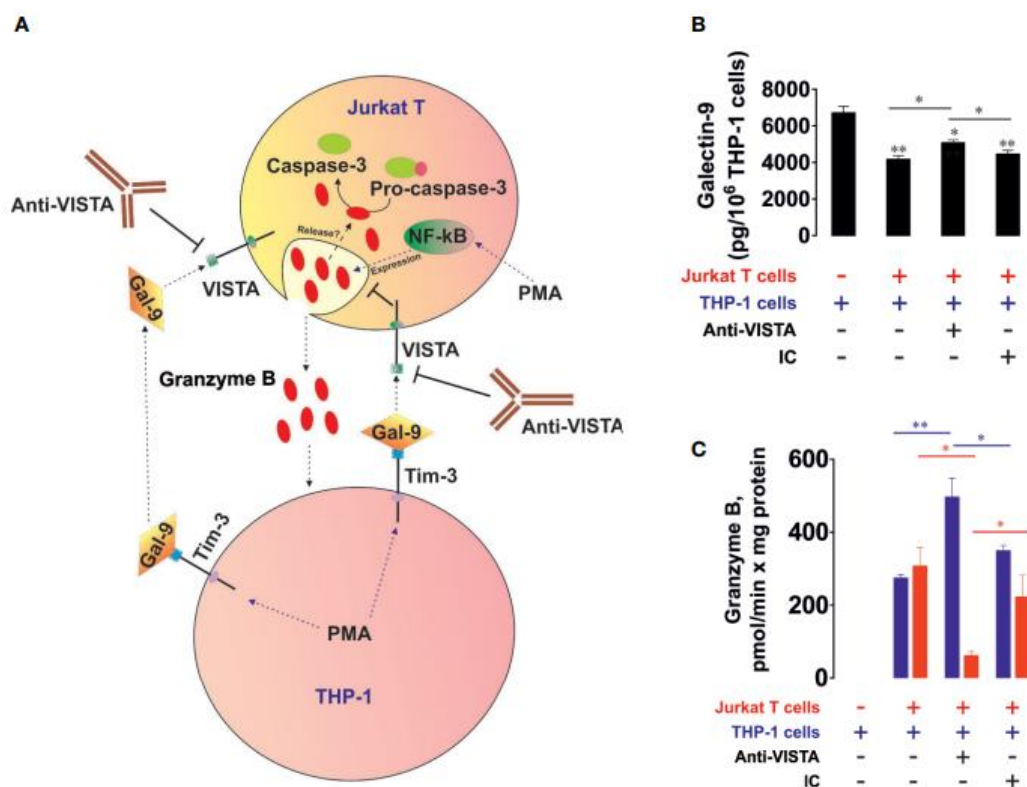


Figure 22 VISTA interaction with galectin-9 inhibits granzyme B release. Co-culture of THP-1 and Jurkat cells was performed after stimulation with PMA in presence and absence of VISTA neutralising antibody. Granzyme B levels within cells and galectin-9 release in the medium were analysed (A). Galectin-9 levels were measured using the ELISA approach (B), granzyme B localized by using Western Blot as well as granzyme B assays (C). Data used mean +/-SEM to represent four individual experiments; *p<0.05, **p<0.01 vs control or indicated events.

A variety of apoptosis-inducing processes can take place within a cell, one of such varieties besides granzyme B induction is caspase 8 activation via cleavage. The substrate used for granzyme B assays does include a similar amino acid sequence as

IETD used for determining caspase 8 activity leading to a possibility of binding for cleavage. To ensure the apoptosis-inducing effects we see in the samples measured are due to granzyme B and not caspase 8 an inhibitor for granzyme B has been used and values compared to the affected control. By addition of granzyme B inhibitor benzyloxycarbonyl-ala-ala-asp-chloromethylketone (Z-AAD-CMK) in a concentration of 100 μ M we eliminated any detectable proteolytic activity within both cell types used (Figure 23).

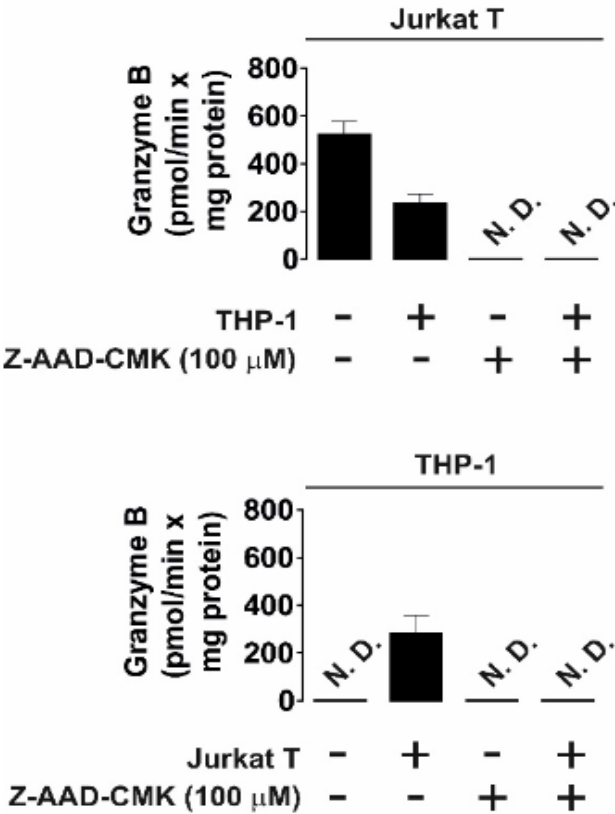


Figure 23 Inhibition of granzyme B activity by addition of inhibitor Z-AAD-CMK. Jurkat T and human AML THP-1 cells were pre-treated with 100 nM PMA for 24 h. After removal of PMA co-culture was performed in presence or absence of 100 μ M of the inhibitor for granzyme B activity Z-AAD-CMK. Granzyme B activity was measured according to protocol. Data is representative of four independent experiments (mean +/-SEM).

By addition of anti-VISTA neutralising antibody during co-culture a shift in granzyme B activity has been observed with main activation found within the THP-1 AML cell line. Isotype control did not influence the granzyme B activity shifting from one cell type to another, differences in granzyme B activity within the THP-1 cell line were observed within the different co-culture conditions (Figure 24A). To determine the effect of co-culture of PMA-treated Jurkat T cells and their activity upon recognition of THP-1 AML cells we measured granzyme B activity within cells in comparison to no co-culture. To do so the cells were co-cultured for 16 h after each were pre-treated with PMA for 24 h. Jurkat T cells were separated from the AML cell line after co-culture and incubated for 1 h at 37 °C with 150 μ M granzyme B substrate (Ac-IEPD-AFC). Fluorescence was measured comparing to Jurkat cells without substrate exposure after precipitation. Granzyme B activity was significantly increased after co-culture (Figure 24B).

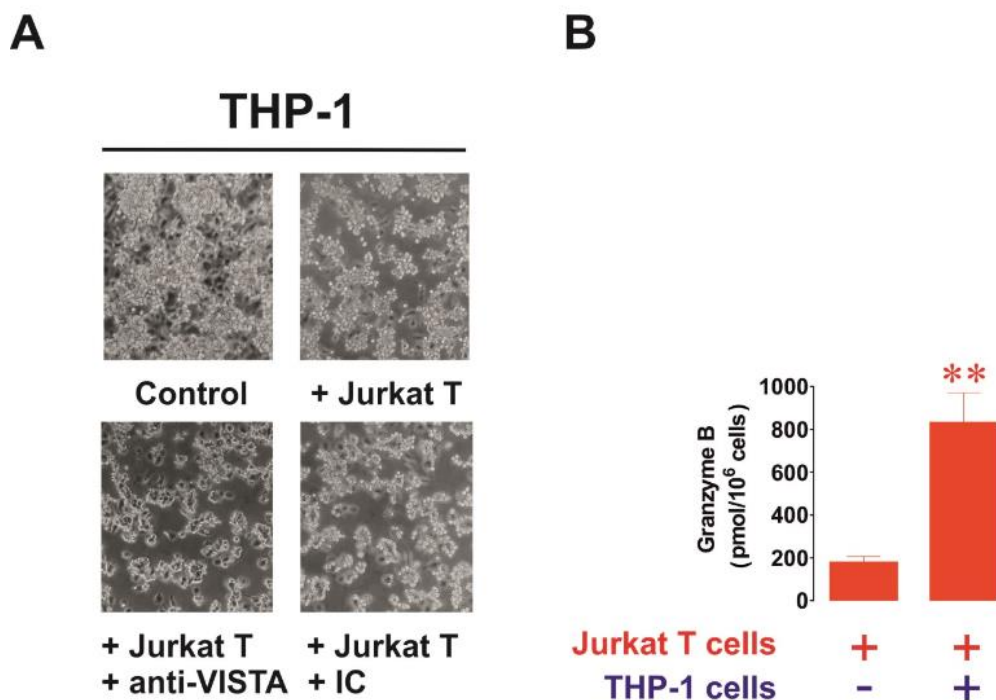


Figure 24 Galectin-9 produced by AML cells influences T cell response in a VISTA-dependent mechanism. Influence of human AML cell line THP-1 on immune responses was investigated in co-culture with Jurkat T cells using anti-VISTA neutralising antibody. THP-1 cells were co-cultured with Jurkat T cells and observed (A). Granzyme B activity within Jurkat T cells after co-culture at a ratio 1:1 with AML cell line was investigated using granzyme B assay kit. Data shown represent four individual experiments, mean +/-SEM. **-p<0.01 vs. control.

In these experiments we were able to gather observations suggesting that VISTA is a receptor on T cells, which by binding of galectin-9 induces a suppression of immune responses towards the targeted cancer cells. By blockage of VISTA or Tim-3, a known receptor and carrier of galectin-9, these effects were reversible. Both proteins were tested for their binding capabilities during exposure of each to galectin-9 for 2 h. Using ELISA, we immobilized either VISTA or Tim-3 onto the surface of plate wells after the exposure to galectin-9 and detected it in bound form while investigating both proteins. Incubation of the proteins with a neutralising antibody prior to galectin-9 exposure led to no detection of galectin-9 via ELISA. To study these effects on Jurkat T cells and their granzyme B production these cells were pre-treated with 100 nM PMA for 24 h and exposed to 2.5 µg/ml galectin-9 in presence and absence prior the incubation of either 5 µg/ml VISTA or Tim-3 neutralising antibodies. Granzyme B activity within Jurkat T cells was clearly influenced by the inhibition of galectin-9 binding to the respective receptors; VISTA and Tim-3 (Figure 25D).

Tim-3 and VISTA expression was analysed on Jurkat T cells before and after stimulation with PMA. Surface expression of both proteins increased after 24 h incubation with 100 nM PMA. VISTA has been expressed on the T cell surface prior to the stimulation and only increased slightly while Tim-3 expression increased significantly (Figure 25A). Presence of VISTA on the T cell surface was visualised using immunofluorescent microscopy (Figure 25B) as well as both proteins were quantified on T cells using fluorescence-activated cell sorting (FACS) (Figure 25C).

As granzyme B leads to the activation of the apoptotic cascade inducing cell death down-stream pro-apoptotic effects were analysed. After exposure of Jurkat T cells to 2.5 µg/ml galectin-9 for 16 h the activity of caspase 3 by caspase 3 activity colorimetric assay as well as poly-ADP-ribose polymerase (PARP) cleavage by Western Blot were measured, verifying the activation of the apoptotic cascade within cells upon galectin-9 binding (Figure 25E).

Jurkat T

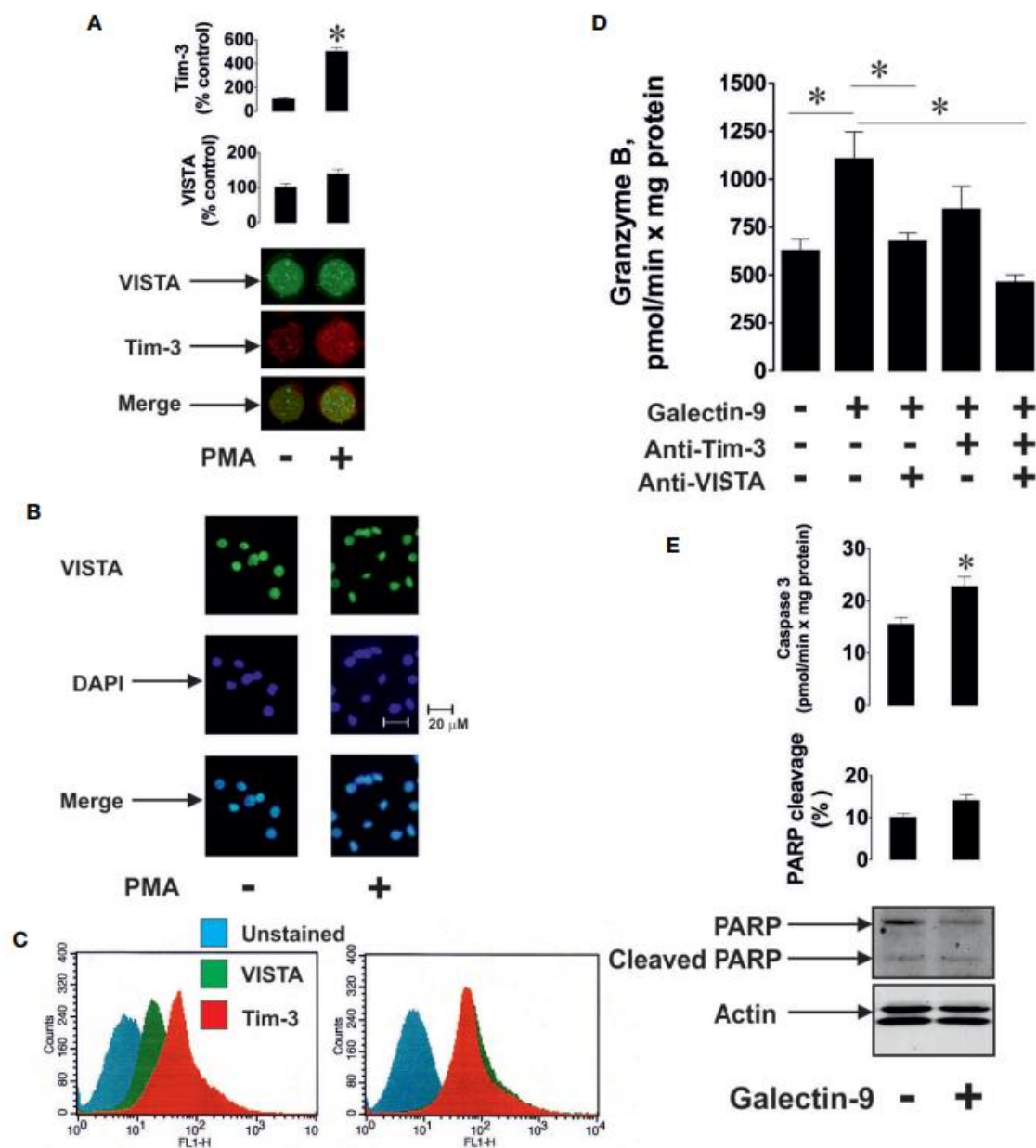


Figure 25 Jurkat expression levels of galectin-9 receptors and influence of galectin-9 binding.

Jurkat T cells were used to study upregulation of galectin-9 receptors and effect of galectin-9 binding onto these proteins. Jurkat were stimulated with 100 nM PMA for 24h and expression levels of Tim-3 as well as VISTA were investigated (A). VISTA expression was visualised on T cells using fluorescent microscopy (B). Expression levels of VISTA and Tim-3 were measured after permeabilization of T cells by FACS (C). Granzyme-B activity in T cells and the influence of galectin-9 and its corresponding receptors were analysed using granzyme B assays (D). To determine if granzyme B leads to further activation of pro-apoptotic processes in T cells caspase 3 and PARP cleavage were analysed using ELISA and Western Blot (E).

To ensure the activation of pro-apoptotic caspase 3 is due to the significant increase of granzyme B activity we analysed their expression levels after incubation of PMA-pre-treated Jurkat T cells with 2.5µg/ml galectin-9 in presence or absence of 100 µM Z-AAD-CMK granzyme B inhibitor. Caspase 3 activity has been significantly reduced by inhibition of granzyme B activation. The percentage of apoptotic cells also decreased, measured by annexin V/propidium iodide kit. Cell viability has been analysed using an MTS assay. This experiment further proved the influence of galectin-9 on cell survival (Figure 26).

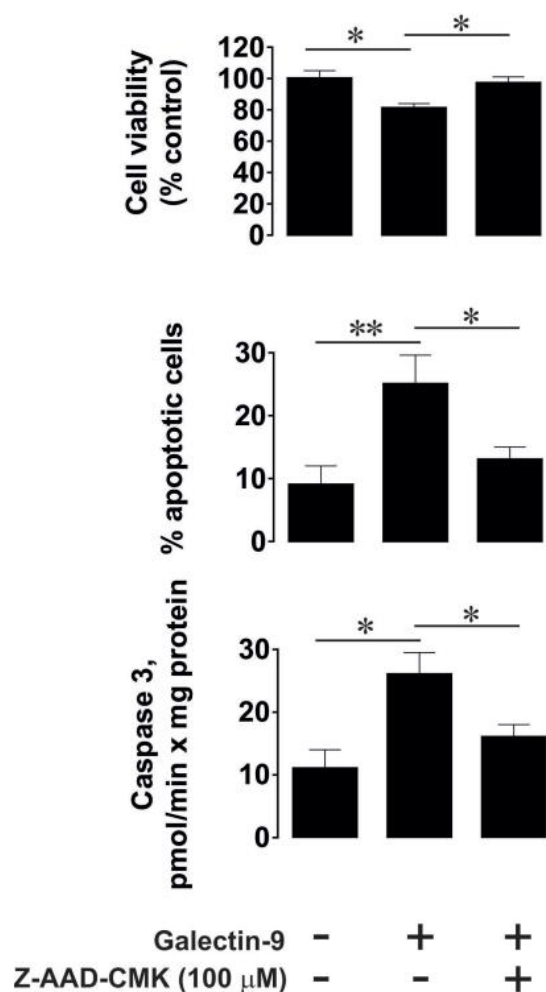


Figure 26 Caspase 3 activation and induction of cell death is granzyme B-dependent. PMA pre-treated Jurkat T cells were used to study granzyme B dependency of caspase 3 activation and induction of apoptosis upon galectin-9 stimulation. Jurkat were stimulated with 100 nM PMA for 24h and cell-viability after exposure to 2.5 µg/ml galectin-9 with or without granzyme B inhibition was determined with MTS assay. Percentage of apoptotic cells were determined using annexin V/propidium iodide assay. Caspase 3 activity significantly decreased in presence of granzyme B inhibition, measured with colorimetric assays. Data represent three individual experiments, mean +/- SEM. *p<0.05, **p<0.001 vs. control.

Furthermore, to ensure that granzyme B production is dependent on galectin-9 another cell line has been studied to determine the effects of galectin-9 binding to its receptors, VISTA, and Tim-3. HaCaT cells, a non-malignant form of human keratinocytes was used to determine if galectin-9 can independently from granzyme B induce apoptosis. These cells express both receptors for galectin-9, thoroughly visualized using fluorescent staining as well as flow cytometry (Figure 27A-C).

HaCaT cells do not express any significant granzyme B activity and further exposure to galectin-9 did not increase these levels (Figure 27D). Caspase 3 activity as well as PARP cleavage did increase after exposure to galectin-9 but did not reach significant levels to induce any apoptotic cascade leading to cell death (Figure 27E). Activity in caspase 3 would need to increase at about 10-fold than original levels to induce any pro-apoptotic processes.

To determine the difference in responses and inhibition of such in natural killer cells and cytotoxic T cells both were exposed to 24 h PMA pre-treated THP-1 AML cells with or without anti-galectin-9 antibody for 16 h. As cytotoxic T cells PMA pre-treated Jurkat T cells were used, NK cells shown consist of primary human natural killer cells. Levels of secreted galectin-9 were similar in both co-cultures with 4.2 +/- 0.3 ng/ml in Jurkat T cell co-culture and 3.9 +/- 0.2 ng/ml in NK co-culture. In the Jurkat T cells exposure led to increased caspase 3 activity and PARP cleavage, while in natural killer cells no changes were detectable. By addition of anti-galectin-9 antibody the effects on caspase 3 activity and PARP cleavage were reduced in Jurkat T cells. Natural killer cells do not produce any detectable VISTA levels, indicating a correlation on galectin-9 inducing apoptosis via binding to VISTA (Figure 28).

HaCaT

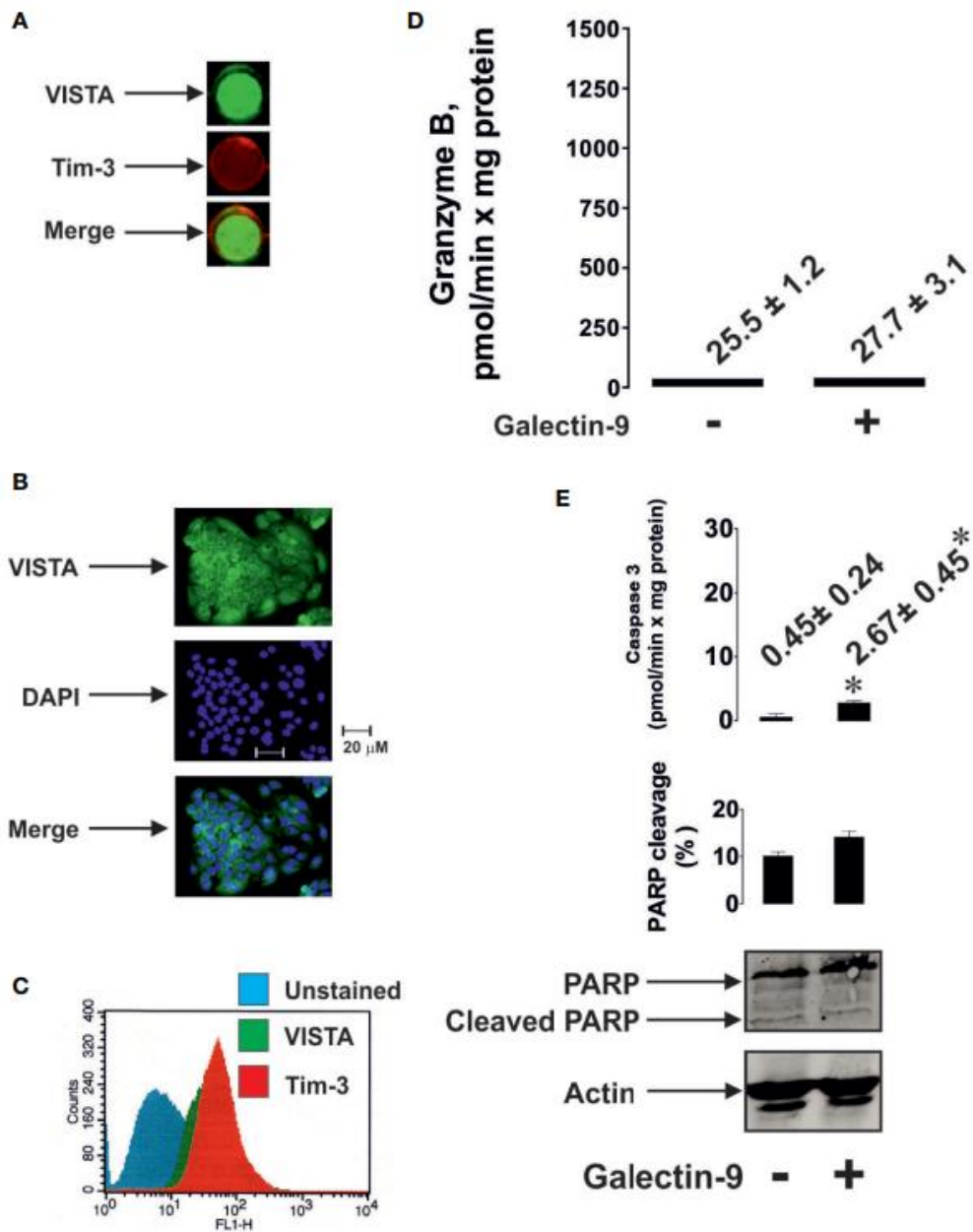


Figure 27 Lack of granzyme B inhibits increase of pro-apoptotic activity after galectin-9 stimulation. HaCaT cell line was studied to determine the VISTA and Tim-3 expression levels. (A-C). This cell line does not show any granzyme B activity (D). Caspase 3 activity and PARP cleavage did not increase significantly after galectin-9 exposure (E). Data represent four independent experiments, mean \pm SEM. * $p < 0.05$ vs. control.

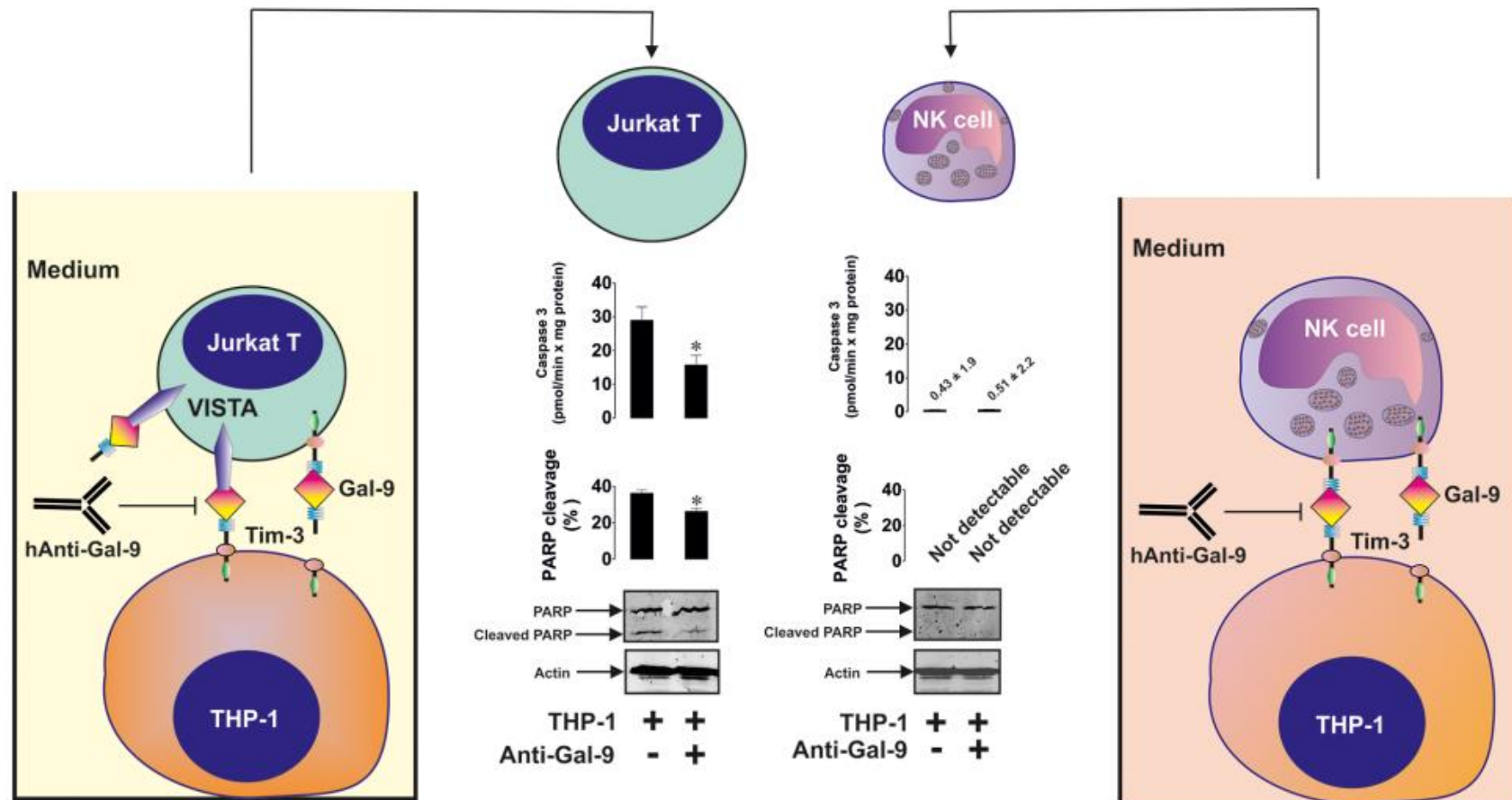


Figure 28 Difference in VISTA expression in T cells and natural killer cells leading to induction of pro-apoptotic process in T cells and not in NK cells. Natural killer cells and PMA pre-treated Jurkat T cells were co-cultured with PMA pre-treated THP-1 AML cells in presence and absence of anti-galactin-9 antibody. In Jurkat T cells expressing VISTA galectin-9 led to increase in caspase 3 activity and PARP cleavage. Natural killer cells do not express VISTA and did not show any pro-apoptotic activity after galectin-9 exposure. Anti-galactin-9 antibody leads to significant decrease of such processes in T cells. Data represent four individual experiments, mean +/- SEM. *p<0.05 vs control.

3.1.3 VISTA SECRETION LEADS IN COMBINATION WITH GALECTIN-9 TO ACTIVATION OF APOPTOTIC CASCADES IN T CELLS.

Recent studies indicate that human myeloid cells are able to release VISTA in a soluble form, therefore, we studied AML cells and their release of VISTA proteins into the blood stream. Firstly, we investigated the release of VISTA and galectin-9 in primary healthy human leukocytes (PHL) and primary human AML cells cultured for 24 h. A significant increase was detectable comparing healthy cells to malignant cells. PHL cells released about 220 +/- 24 pg/10⁶ cells galectin-9 and 89 +/- 12 pg/10⁶ cells VISTA. In primary AML cells the levels of galectin-9 ranged at 5980 +/- 626pg/10⁶ cells and VISTA release was significantly increased in comparison to healthy cells at a range of 707 +/- 154 pg/10⁶ cells detectable after 24 h in vitro culture (Figure 29A). Soluble VISTA was further investigated to determine the size after release, the protein was detectable by Western Blot at 40 kDa. This size is most likely corresponding to the extracellular domain being glycosylated. Exposure of VISTA proteins to deglycosylation using Promega deglycosylation kit led to the detection of new bands at 36 kDa and 28 kDa (Figure 29B). The incubation has been performed for 3 h, longer incubation up to 18 h leads to all proteins exposed being deglycosylated to 28 kDa.

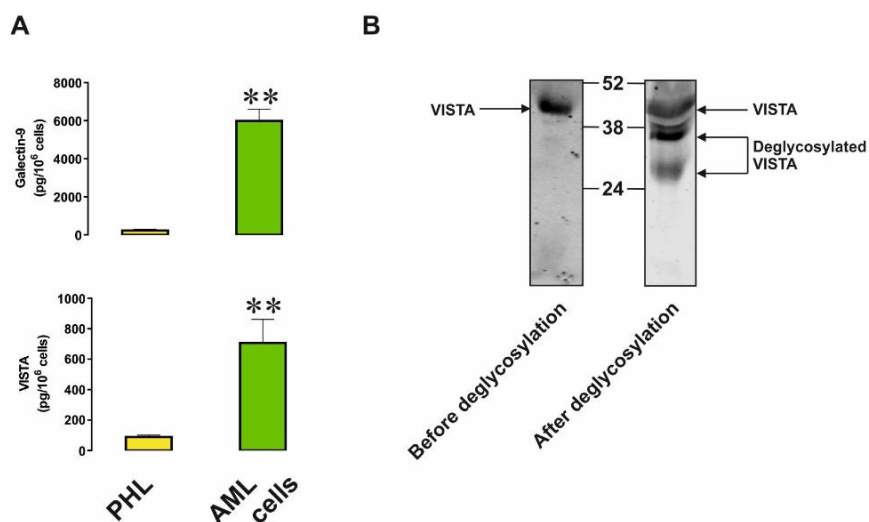


Figure 29 High levels of VISTA is released by malignant human primary cells. Human primary samples of healthy patients and AML patients were kept in culture for 24 h. Release of VISTA was measured in cell culture medium by ELISA (A). VISTA was analysed by deglycosylation to determine glycosylation levels using Western Blot (B). Data are representing five individual experiments with similar results, mean +/- SEM are shown. **-p<0.01 vs. PHL.

Blood samples of 5 diagnosed AML patients were compared to samples from 5 healthy blood donors and galectin-9 as well as VISTA release were investigated (Figure 30A, B). A correlation was clearly detectable between the release of both proteins from leukaemia cells and the inhibition of immune responses (Figure 30C). Furthermore, regarding the release of VISTA proteins into the blood stream the option of proteolytic shedding similar to Tim-3 release was investigated. To do so, the PMA pre-treated THP-1 cell line has been exposed to proteolytic shedding inhibitors GI254023X, inhibitor against the angiotensin and metalloproteinase domain-containing proteins 10/17 (ADAM 10/17), as well as batimastat, matrix metalloproteinase inhibitor (BB-94), each at a concentration of 100 μ M for 24 h. Both inhibitors greatly reduced the shedding of VISTA indicating the influence of metalloproteinases in the release of VISTA proteins similar to Tim-3 release (Figure 30D). To verify this effect primary AML cells were kept with both inhibitors leading to further attenuation of VISTA release in comparison to the cell line (Figure 30E). Release of the protein was measured by ELISA, VISTA protein within the cells were analysed by Western Blot, clearly indicating that VISTA highly accumulated within the cells. As the effect by ADAM 10/17 showed a stronger inhibition of VISTA release it is a clear sign that shedding, as seen with Tim-3, is mainly performed by these specific metalloproteinases.

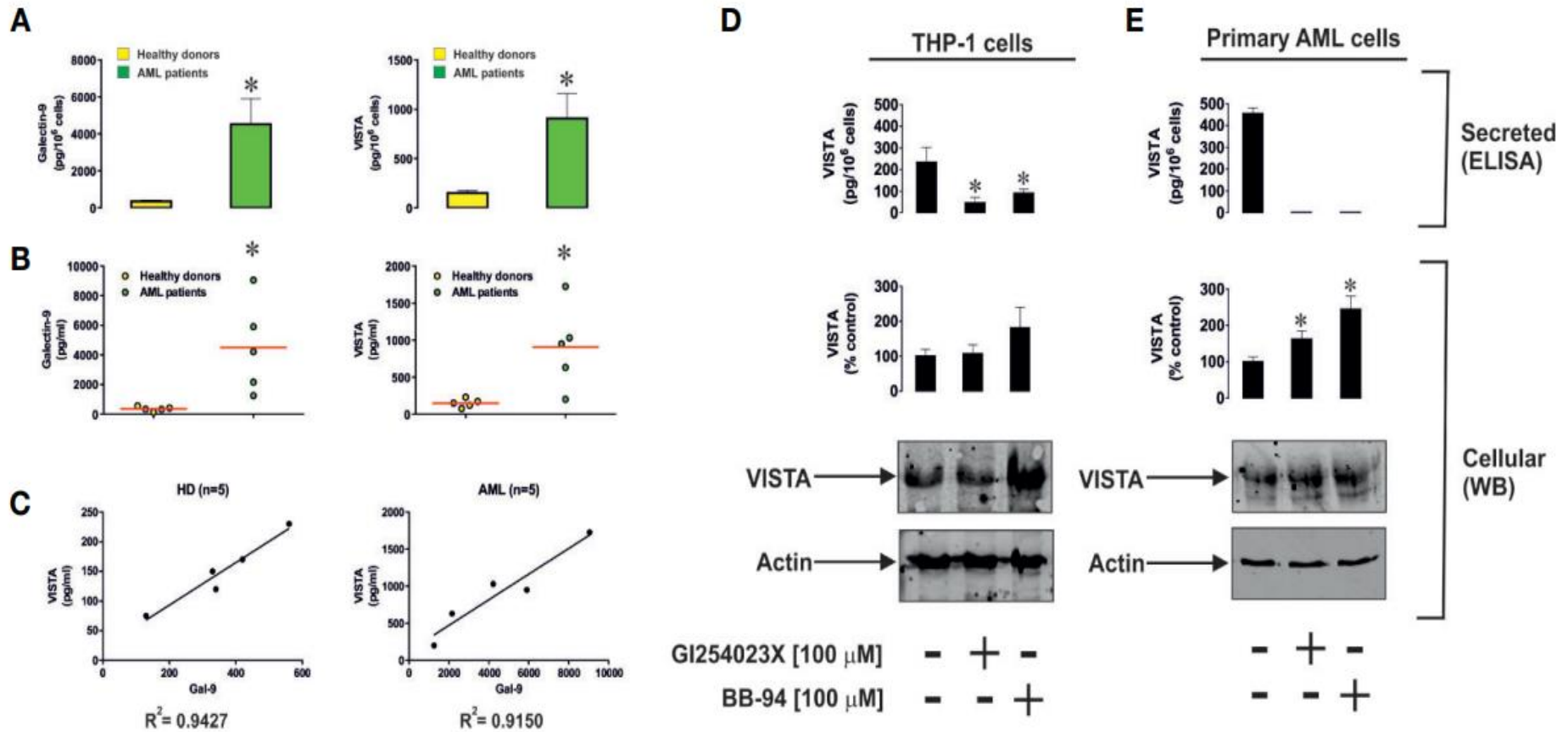


Figure 30 Elevated levels of VISTA released by AML cells were attenuated by metalloproteinases inhibitors. Human primary samples of healthy patients and AML patients show an increased release of galectin-9 (A) and VISTA (B) upon malignant transformation, with a clear correlation of both proteins released simultaneously (C). Metalloproteinase inhibitors similar to the studies of Tim-3 release were used to investigate VISTA release by AML cells. In both cases the release was significantly reduced, especially by inhibition of ADAM 10/17. PMA pre-treated THP-1 AML cells (D) and primary AML cells (E) were investigated. Significant differences to control detectable; $p < 0.05$ vs. healthy donors without proteinase inhibitor exposure.

To study the effects of VISTA interaction with galectin-9 on T cells, PMA pre-treated Jurkat T cells were exposed to either 2.5 µg/ml galectin-9, 5 µg/ml of VISTA, concentrations were chosen to ensure equalmolar amounts, or both proteins at the same time. Cells were exposed to each treatment for 16 h and effects on the activation of pro-apoptotic pathways were analysed. Jurkat T cells express both receptors for galectin-9, visualized by immunofluorescent microscopy (Figure 31A). In case of exposure with both proteins PARP cleavage (Figure 31B) as well as granzyme B activity (figure 31C) were highly upregulated within T cells; in both cases the exposure to one of the proteins already induced a significant increase in both pro-apoptotic activities.

Furthermore, using DiBAC4 reactive dye analysing the membrane potential changes after exposure of Jurkat T cells to galectin-9 and VISTA for 30 min indicates that a combination of both proteins might lead to changes in the membrane potential of T cells inhibiting the release of granzyme B into the environment and the targeted cells (Figure 31D).

Lastly, primary T cells derived from healthy donors were used to study the effects of VISTA and galectin-9 similar to the studies with the Jurkat T cell line. These cells were exposed to both proteins at the concentration mentioned beforehand for 16 h. Expression of VISTA, Tim-3 as well as PARP cleavage were analysed using Western Blot; to verify that the cells isolated were T cells CD-3 expression, as a T cell marker, was also investigated (Figure 31E). While VISTA levels on T cells did not change significantly after exposure to galectin-9, Tim-3 levels did increase. Similar to the Jurkat T cell line, the incubation with both proteins led to a significant increase of PARP cleavage in primary T cells.

To test multi-complex formation on T cells, these three proteins, Tim-3, galectin-9, and VISTA were exposed to each other and analysed by SRCD spectroscopy. A clear interaction of the three proteins was detectable as conformational changes were seen (Figure 32).

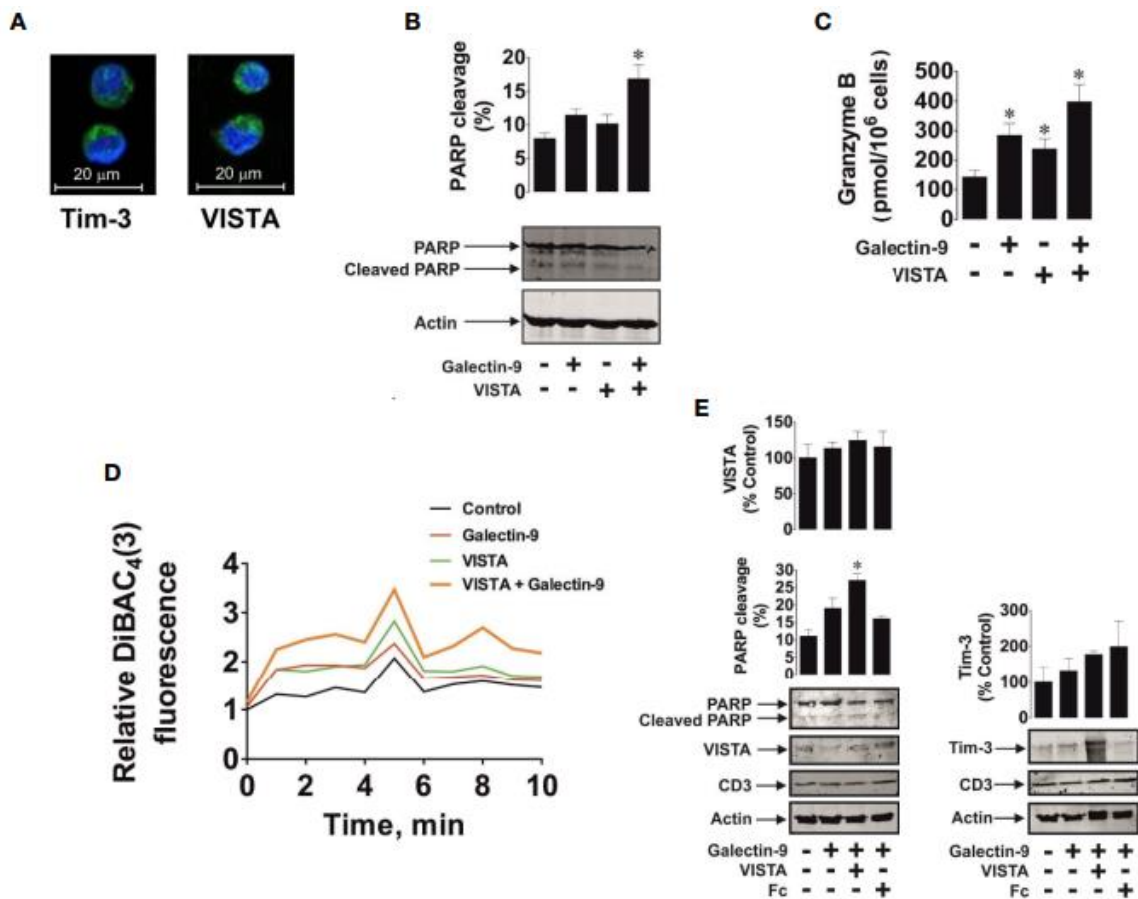


Figure 31 Exposure to a combination of galectin-9 and VISTA significantly increased activation of pro-apoptotic cascade. Jurkat T cells express both types of receptors for galectin-9 (A). Exposure for 16 h to galectin-9, VISTA or both proteins increased PARP cleavage, measured by Western Blot (B) and granzyme B accumulation, measured by fluorometric assays (C). Stimulation for 30 min with VISTA and galectin-9 protein led to changes in membrane potential in T cells (D). Studying primary T cells showed same effects upon exposure to VISTA, galectin-9 or both proteins for 16 h as seen in Jurkat T cells. VISTA, Tim-3, CD-3, and PARP cleavage were measured by Western Blot. Data represent one experiment with three repetitions, mean \pm SEM included. * $p < 0.05$ vs control.

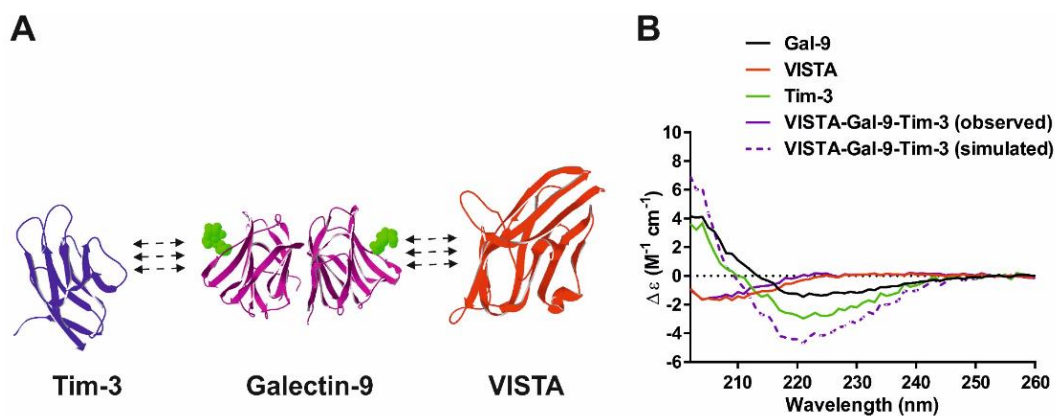


Figure 32 Multi-complex formation observed by interaction between Tim-3, galectin-9, and VISTA. 3D structures formed using Swiss PDB viewer (A). SRCD spectra analysis, average of six curves.

3.1.4 DISCUSSION.

This chapter focusses on understanding the differences in immune responses detected in cytotoxic T cells and natural killer cells. A protein in centre of this study is VISTA found to be highly expressed on T cells, but no significant amount detectable on natural killer cells (Figure 19C and Figure 31E). VISTA has been determined as an immunosuppressive protein found in soluble and bound form, especially in the tumour microenvironment interaction between malignant and T cells. Studying binding capabilities between VISTA and galectin-9 led the detection of a high binding affinity using immunoprecipitation and biophysical assays such as surface-free SRCD (~18 nM) spectroscopy and SPR immobilization on surface (100 nM). Galectin-9 is produced and released in high levels by primary AML cells as well as the AML cell line THP-1 after exposure to PMA for 24 h. Furthermore, upon release galectin-9 can bind to Jurkat T cells, which were transformed into a cytotoxic T cell variation producing granzyme B after stimulation for 24 h with PMA. By binding to these T cells galectin-9 inhibits the release of granzyme B into the surrounding, leading to accumulation within the T cell (Figure 20).

Induction of cell death pathways within T cells are shown in this chapter to be dependent on VISTA expression and active production of granzyme B. Such pathways induced include pro-apoptotic ones such as caspase 3 activation and PARP cleavage, which can be significantly suppressed using either granzyme B inhibitor (Z-AAD-CMK) or anti-VISTA and anti-galectin-9 antibodies attenuating the binding ability between these proteins. None of these pro-apoptotic pathways can be induced in NK cells upon stimulation with galectin-9 and inhibition of galectin-9 binding to VISTA did not influence granzyme B release of such cells, since they are not expressing any VISTA proteins as receptors (Figure 18 and 28) (Lines, 2014; Wang, 2011, Lines, 2014).

A primary cell type investigated is the acute myeloid leukaemia, which produced high amount of galectin-9 as well as soluble VISTA protein released into the blood stream (Figure 29). Furthermore, naturally produced VISTA and galectin-9 have a significantly higher influence on immunosuppression of T cells responses than recombinant proteins. Studying the released VISTA protein from AML patients and Jurkat T cells indicates that VISTA has different glycosylation levels, similar to another galectin-9 receptor/binding partner called Tim-3. Interestingly, both of these proteins able to

interact with galectin-9 are shed from the surface by proteolytic shedding, ADAM10/17 to be specific (Figure 30D and E).

In this chapter we also showed the influence of VISTA and galectin-9 binding onto the T cell surface to be able to change membrane potential/cell polarization (Figure 31D). These effects attenuate the capability of cytotoxic T cells to release granzyme B into the environment consequently targeting malignant cells. Accumulation of granzyme B in T cells can therefore lead to release of such into the T cells and activation of caspase 3 activity and PARP cleavage. Recognition of galectin-9 by T cells further leads to increased granzyme B production induced by NF- κ B (Huang, 2006).

The hypothesis formed after these observations is that Tim-3, galectin-9, and VISTA are able to form a multi-complex barrier on the surface of cytotoxic T cells, which on the one hand leads to stimulation of granzyme B production within the cells but inhibits on the other the release of such. Accumulation of acidic granules containing granzyme B might induce leakage of granzyme B within T cells inducing pro-apoptotic events, ultimately leading to cell death (Sumbayev, 2008; Kurschus, 2010). In myeloid cells no such processes were detectable (Prokhorov, 2015; Lhuillier, 2015). Release of granzyme B in T cells is most likely dependent on strong calcium mobilization and preservation of high calcium concentrations in these cells (Lhuillier, 2015). This calcium influence can also lead to calcium-calpain-caspase dependency in induction of apoptosis (Kashio, 2003). This theory is supported by studying HaCaT keratinocyte cell line, which do not express any detectable granzyme B amount, yet exposure to galectin-9 led to slight increase in caspase 3 activity and PARP cleavage (Figure 27E). These levels are barely able to cause any apoptosis in this keratinocyte cell line, but T helper cells might react more strongly to galectin-9 interactions.

Cytotoxic T cells express an endogenous inhibitor activity of granzyme B using serpin B9, protecting these cells to a certain extent from granzyme B activity from within. If a certain concentration of active granzyme B is reached within cytotoxic T cells serpin B9 might not be able to counter these pro-apoptotic effects taking place (Bird, 2014; Yasinska, 2020, Zhang, 2006). In Jurkat T cells serpin B9 expression is nearly lacking indicating that granzyme B activation cannot be sufficiently countered, consequently it might be an indication that in primary T cells the amount of granzyme B leaking into the cells may be significantly higher than available serpin B9. This would need further research to verify.

Efficient induction of apoptosis in targeted cells is induced by release of granzyme B by diffusion of it through transmembrane pores, which are formed by perforin released together with granzyme B upon recognition of a malignant or infected cell. In regulatory T cells (Tregs) and NK cells a similar effect of self-inflicted damage by granzyme B activation within can be described (Zhang, 2006).

This chapter indicates an influence of galectin-9 involvement in production and release of granzyme B within T cells by binding to its corresponding receptor called VISTA. This is the first time galectin-9 has been verified as a binding partner to VISTA at a high affinity. Furthermore, soluble VISTA produced by malignant cells can enhance immunosuppressive function of galectin-9 and consequently leading to cell death of cytotoxic T cells. Together with another galectin-9 receptor highly expressed on cytotoxic T cells, Tim-3, one could suggest that a multiprotein complex is formed on the T cell surface leading to changes in the membrane potential and preventing the release of granzyme B. This inhibition together with an increased production of granzyme B in T cells upon binding of galectin-9 can induce pro-apoptotic activity within the T cell itself and consequently lead to cell death.

Below a schematic visualizing this formation of a barrier on the T cell by Tim-3, galectin-9 and VISTA and the consequences following this barrier formation are shown (Figure 33).

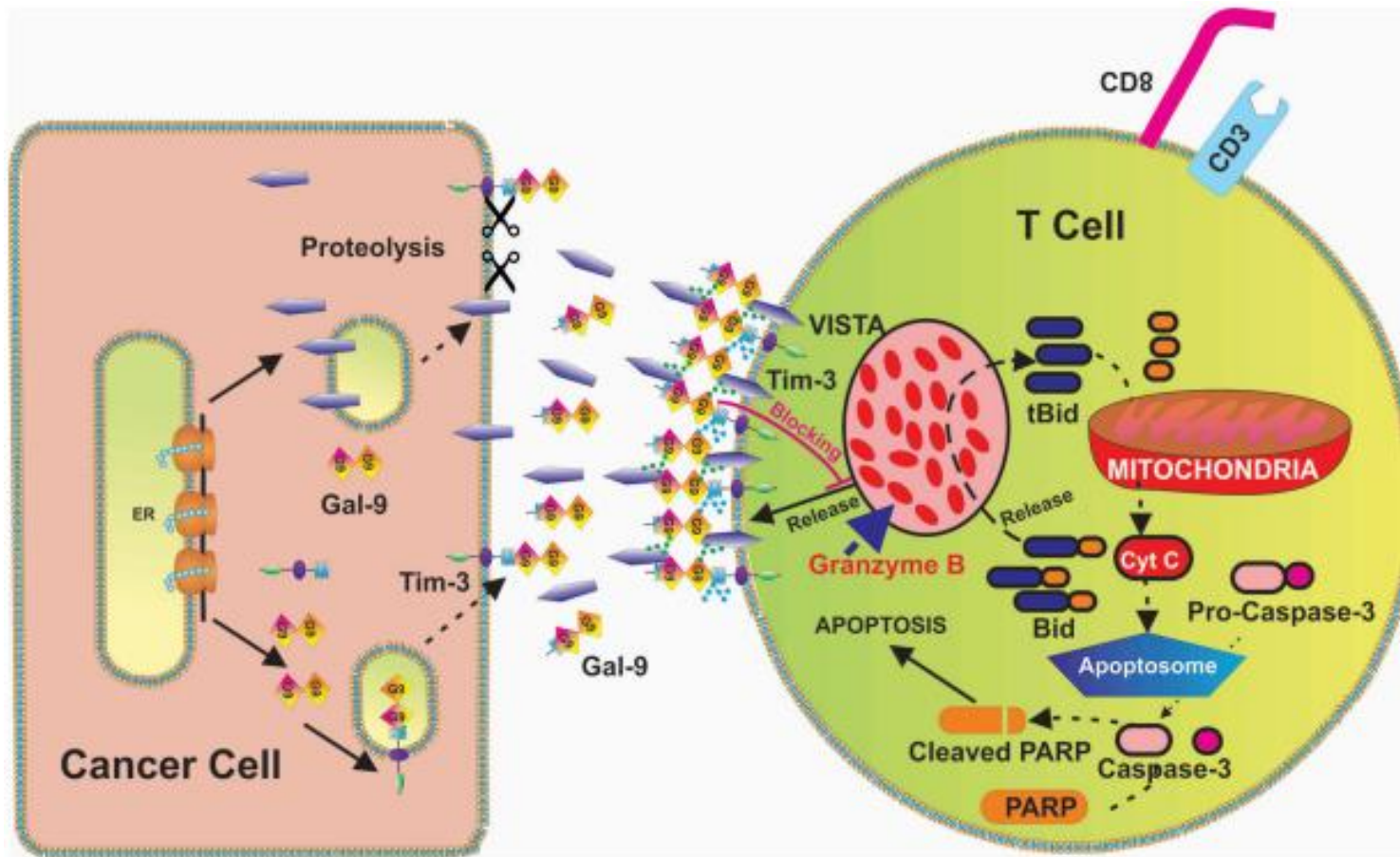


Figure 33 Schematics depicting the formation of possible barrier formation and its consequences by Tim-3, galectin-9 and VISTA. Galectin-9 released by malignant cells can bind onto the surface of T cells by interacting with its receptors Tim-3 and VISTA. Further soluble VISTA produced by the same malignant cells binds onto the other side of galectin-9 creating a dense barrier on the T cells. Galectin-9 binding increases the granzyme B production in T cells, yet release is inhibited due to the barrier formed. This will consequently lead to activation of accumulated granzyme B within the T cell itself and induce pro-apoptotic activities such as caspase 3 and PARP cleavage.

3.2 BIOCHEMICAL REGULATION OF GALECTIN-9 AND VISTA EXPRESSION ARE PERFORMED BY SIMILAR PATHWAYS.

Galectin-9 expression has been widely researched already in correlation with immune responses. Certain studies show that the corresponding gene, LGALS9, contains at least five Smad-3 response elements. This clearly indicates an influence of Smad-3 in the up-regulation of galectin-9 expression by malignant cells (Wu, 2014). In this chapter, we concentrate on the influence of Smad-3 in the induction of galectin-9 expression. Furthermore, as malignant cells are able to produce and release high levels of both galectin-9 and VISTA in response to immune cells attacking we also investigate the correlation of proteins being produced at the same time and which biochemical pathways lead to their expressions.

3.2.1 GALECTIN-9 MASTER REGULATORS IN CANCER AND EMBRYONIC CELLS CONSIST OF TRANSFORMING GROWTH FACTOR BETA TYPE 1 (TGF- β) AND HYPOXIA-INDUCIBLE FACTOR 1 (HIF-1)

As described in the prior chapter, cancer cells are able to produce high amounts of galectin-9 to suppress immune response by cytotoxic T lymphocytes and natural killer cells (Yasinska, 2019, 2018; Goncalves-Silva, 2017, Luhlilier, 2015). Dependent on the cancer cell this mechanism might be by secretion of galectin-9 or increased surface presentation. For secretion galectin-9 is forming a complex with its possible trafficker, Tim-3, which can also be found as a receptor on the targeted cells. Upon binding onto Tim-3 or VISTA, downstream signalling is activated leading to pro-apoptotic effects within the cytotoxic lymphocytes (Prokhorov, 2015, Goncalves-Silva, 2015, Kikushige, 2015). This high upregulation by malignant cells and its biochemical mechanisms has not been fully investigated and completely understood yet. A common factor that is also highly upregulated during the cancer development, sometimes referred to as tumour growth factor, is the transforming growth factor β (TGF- β), which can interact with its receptors expressed on cancer cells in an autocrine fashion (Kim, 1990; Duan, 2019). This leads to up-regulation of Smad-3 expression triggering specific target genes responsible for tissue growth and increased cell differentiation. As the gene encoding the galectin-9 protein also expresses Smad-3 response elements we were investigating the influence of TGF- β via Smad-3 on the upregulation of galectin-9 production (Massagué, 2005; Wu, 2014). Furthermore, the gene encoding for TGF- β itself also contains Smad-3 response elements (at least 9) and therefore increased production of TGF- β not only leads to upregulation of galectin-9 via Smad-3 but also self-supports its own production within cancer cells.

The primary activation of TGF- β production in cancer cells is dependent on the induction via hypoxia-inducible factor 1 (HIF-1). Due to rapid growth and lack of supporting blood vessels at the very early stages of cancer cell growth, these cells tend to be surrounded by a hypoxic environment leading to increased HIF-1 production. Two subunits are forming this complex, subunit α , which is inducible and the constitutive subunit β . As HIF-1 is an early response to the hypoxic state surrounding the malignant cells it might be one of the early inducers of TGF- β production leading consequently to an increase in galectin-9 production after autocrine stimulation of TGF- β is established. Hypoxia also leads to increased activation of NADPH oxidase and xanthine oxidase, causing accumulation of reactive oxygen species (ROS) (Sumbayev, 2010; Abogali, 2014). These elevated ROS levels induce the activation of apoptosis signal regulating kinase 1 (ASK1) followed by downstream signalling and activation of activator protein 1 (AP-1), a transcription complex upregulating TGF- β production (Sumbayev, 2005). As similar events can take place in the development of embryos, with high levels of galectin-9 inhibiting the rejection of the embryo by the mother's immune system, we also investigated this complex hypothesis indicating an origin of the galectin-9 pathway from the embryonic development and being reused later on by cancer cells (Manzo, 2019). In this chapter, we investigate if both AML cells as well as embryonic cells use HIF-1 and AP-1 to induce TGF- β upregulation consequently leading to autocrine action by increased Smad-3 levels. While no upregulation might be detectable in healthy mature human cells, this process could lead to increase of galectin-9 in cancer and embryonic cells.

3.2.1.1 High upregulation of HIF-1, TGF- β , Smad-3 as well as galectin-9 are detectable in primary human cancer and embryonic cells.

For testing the hypothesis on self-sustaining TGF- β regulation and its influence on galectin-9 expression we analysed primary AML cells, primary human breast cancer and primary embryonic cells. A schematic visualizing the hypothesis is shown in figure 34 A. The first finding shows that especially in all five samples of primary human breast cancer tissue both xanthine oxidase as well as NADPH oxidase were significantly upregulated. Furthermore, thiobarbiturate-reactive species, a product created by lipid peroxidation during increased oxidative burst, were clearly detectable in tumour tissue compared to healthy samples (Figure 34B). In line with the hypothesis both HIF-1 and active phospho-S423/S425-Smad-3 levels were significantly increased in malignant tissue as seen by Western Blot analysis. As shown in the prior chapter both Tim-3 and galectin-9 levels are highly increased in malignant tissue compared to healthy samples (figure 34D).

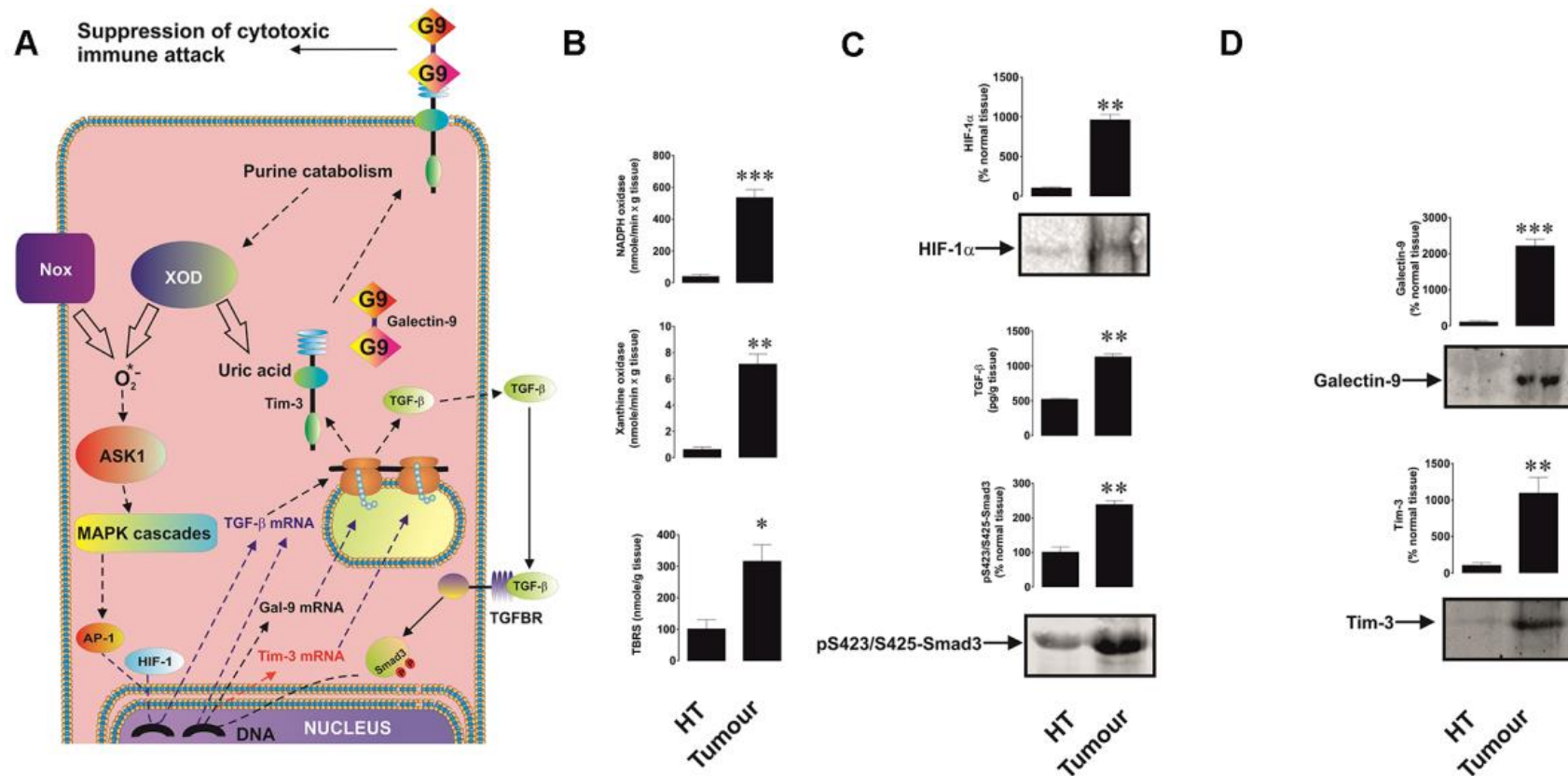


Figure 34 Comparative studies of malignant and healthy primary breast tissue. Schematics of the hypothesis studied in this chapter includes the effect of NADPH oxidase and xanthine oxidase inducing HIF-1 upregulation leading to increased TGF- β and Smad-3 activity which will sustain itself in an autocrine fashion later on and leads to galectin-9 production to suppress immune responses towards the cancer cells (A). In malignant tissue xanthine oxidase, NADPH oxidase and TBARS levels are significantly increased due to hypoxic stress (B). HIF-1, TGF- β and phosphor S423/S425 Smad-3 are also highly upregulated in comparison to healthy tissue (C). As seen in prior studies both galectin-9 and Tim-3 are detectable in increased amounts in tumour tissue. Quantities are respectively compared to 1 gram of tissue each. Western Blot normalization includes Licor total protein assay, enzyme activities and TBARS are normalized per mg of total protein (shown in figure 35). Data included from five individual experiments, mean +/-SEM shown. * - $p < 0.05$ and ** - $p < 0.01$ vs. healthy tissue.

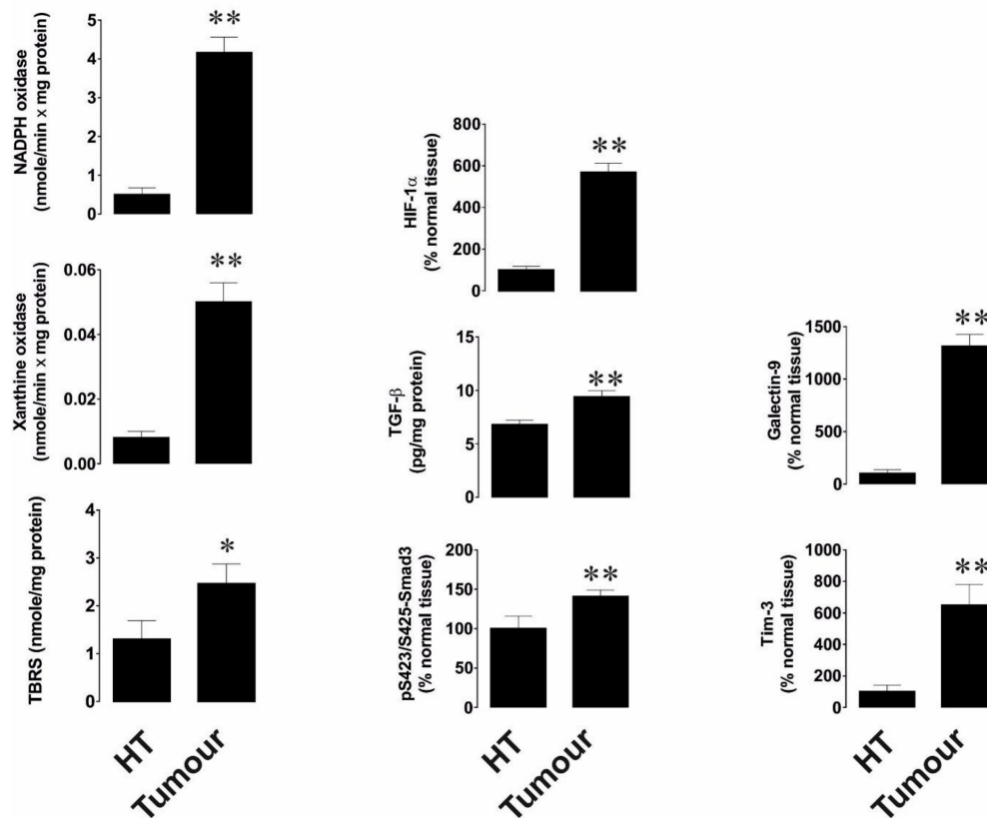


Figure 35 Normalization of values in Figure 34. Western Blot values were normalized against total protein. Enzyme activity as well as TBARS measurement against 1 mg of total tissue protein. Data included from five individual experiments, mean +/- SEM shown. * $p < 0.05$ and ** $p < 0.01$ vs. healthy tissue.

Next, we compared a non-solid malignancy, acute myeloid leukaemia, to the results gained from studying primary human breast cancer tissue. Similar to the breast cancer studies we used primary samples gained from newly diagnosed AML patients and compared these with primary healthy leukocytes from donors. Both cell types were cultured individually for 24 h in cell culture and activities of xanthine oxidase, NADPH oxidase as well as TBARS levels were measured. Each of these were significantly increased compared to the healthy leukocytes, implying a higher oxidative stress for this non-solid cancer in comparison to healthy cells (Figure 36A). While HIF-1 and phospho-S423/425-Smad-3 levels are very low in healthy tissue, the malignant cells showed a significant increase in both (figure 36B). Importantly, in healthy tissue Tim-3 and galectin-9 levels were non-detectable and TGF- β levels were low compared to the malignant cells. Primary AML samples produced significantly higher levels of galectin-9 and Tim-3 in comparison to healthy tissue and released these into the medium during the 24 h culture (Figure 36C).

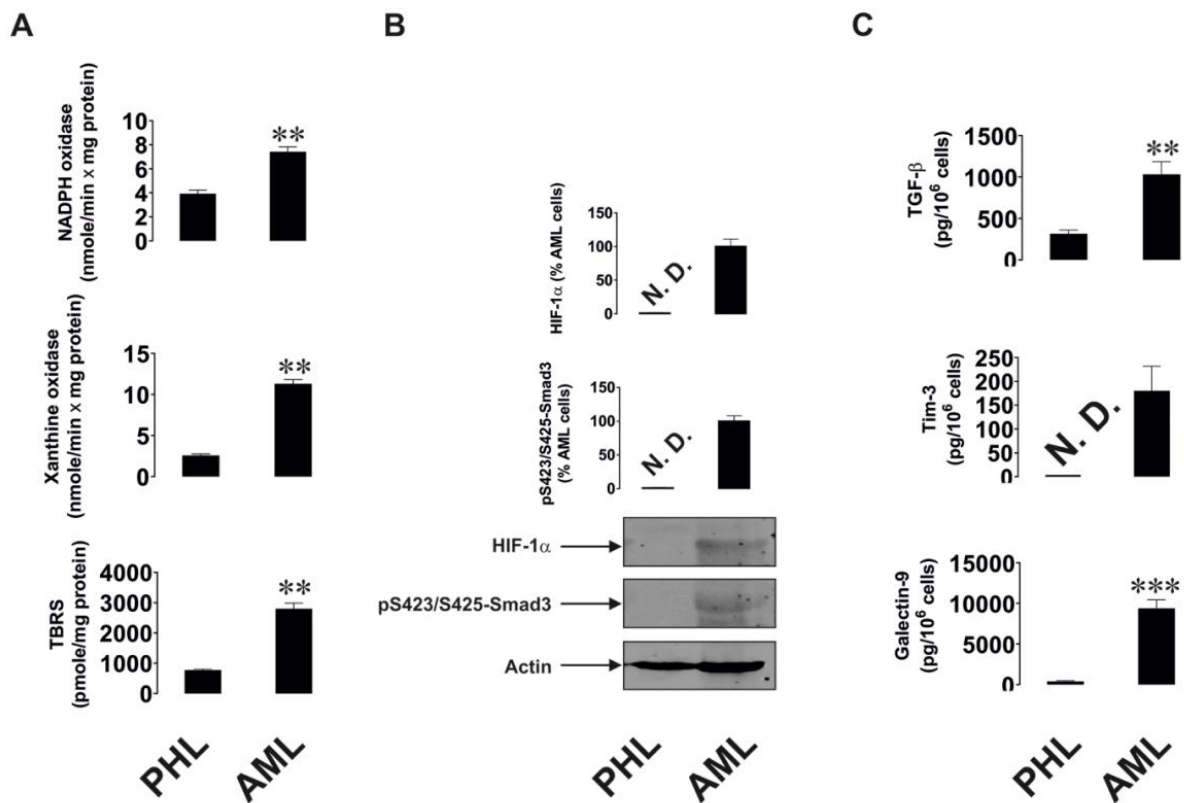


Figure 36 Comparative studies of primary acute myeloid leukaemia vs. healthy leukocytes. Cells were kept for 24 h in culture. Activity of xanthine oxidase, NADPH oxidase and TBARS levels were significantly increased in malignant samples compared to primary healthy leukocytes (A). Similar to solid tumour breast cancer samples, HIF-1 and phosphor-S423/425-Smad-3 were highly upregulated in malignant cells (B). Levels of secreted TGF- β , galectin-9 and Tim-3 in cell culture medium were analysed using ELISA (C). Data include mean \pm SEM of five individual experiments. *- $p < 0.05$ and **- $p < 0.01$ vs. healthy donor samples.

To determine the effects of TGF- β between solid tumour and non-solid tumours we investigated the TGF- β levels in blood samples from healthy donors, primary breast cancer samples, metastatic breast cancer samples and AML samples, each group including six donors. Strikingly, the primary breast cancer samples and metastatic breast cancer samples did not differ significantly from healthy donor samples, while AML patients showed an increased amount of TGF- β detectable in blood. These findings suggest that TGF- β in solid tumour samples remains in the microenvironment. As AML cells are circulating in the blood stream the release of TGF- β into circulation allows these cells to employ it against corresponding T cells (Figure 37).

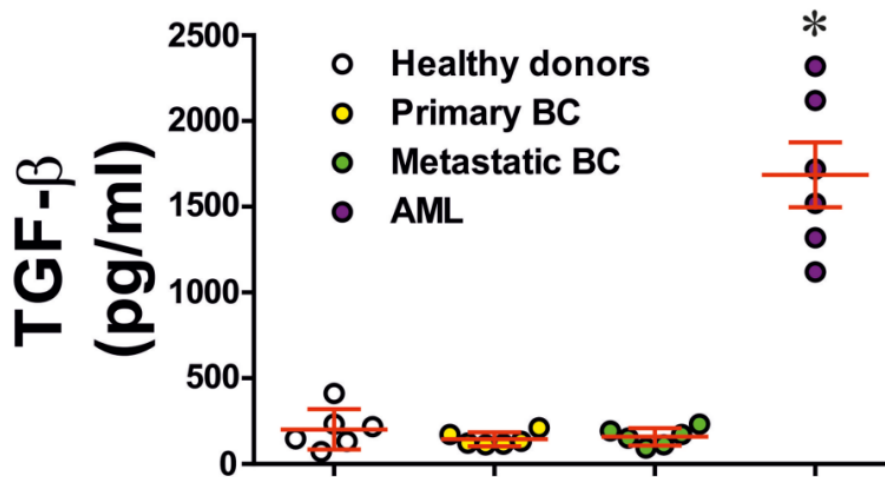


Figure 37 Investigation of TGF- β release in blood circulation, solid vs. non-solid tumour. TGF β levels were determined in blood samples received from healthy donors, primary breast cancer donors, metastatic breast cancer patients and AML patients (n=6 in each set). Data include mean +/- SEM. *- p<0.05 vs. healthy samples.

We were also able to investigate primary human embryonic samples gathered at two different developmental stages by our colleagues at the University Hospital Bern. The stages obtained were chorionic, found at about 13 weeks of development, and amniotic ranging between 20 to 25 weeks of development. By comparing these samples, we were able to detect high levels of xanthine oxidase and NADPH oxidase activity as well as significant increase in TBARS in the early (chorionic) development stage (Figure 38A). Next to this oxidative burst and HIF-1 were also significantly increased in the chorionic stage (Figure 38B), as well as TGF- β and phospho-S423/425-Smad-3 (Figure 38C). Lastly, we investigated galectin-9 and Tim-3 levels by Western Blot and ELISA. While both proteins were highly upregulated on the cell surface in the early developmental stage, no secretion of these proteins was detectable by ELISA indicating that they stay situated on the cell surface (Figure 38D, E).

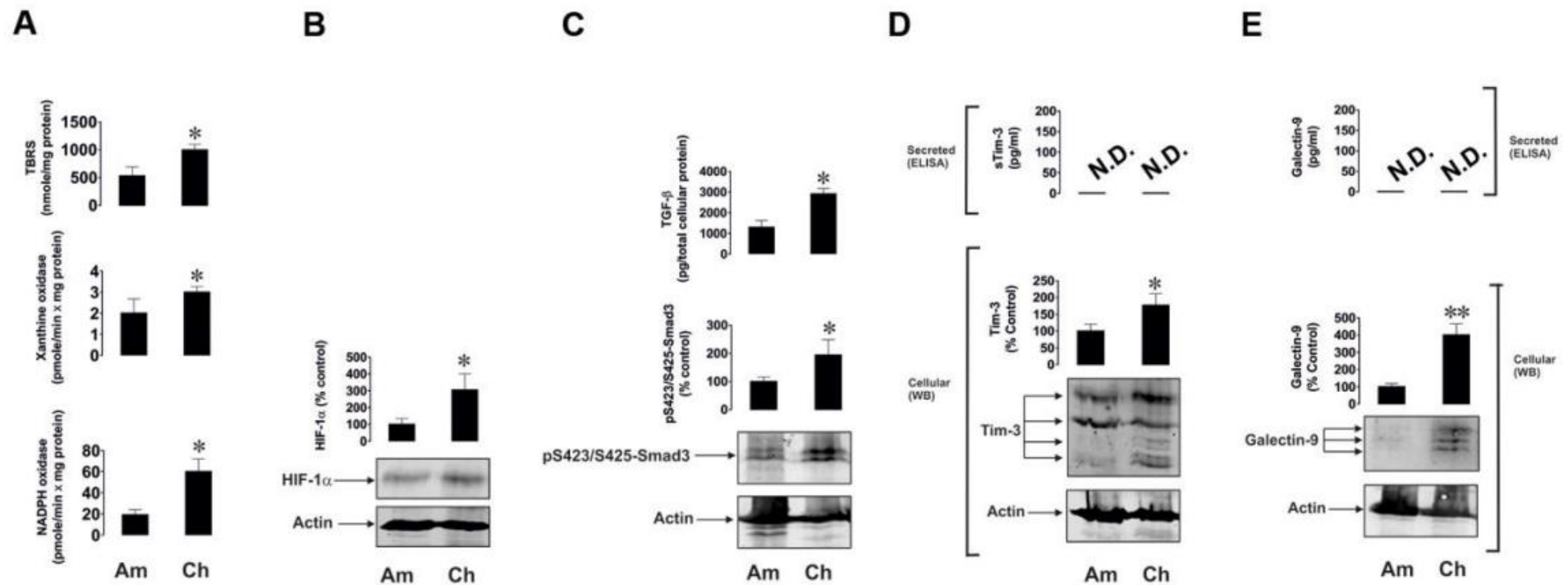


Figure 38 Up-regulation of oxidative burst, HIF-1, TGF- β /Smad-3 and galectin-9/Tim-3 in early developmental stages. Primary embryonic samples from two different stages during human development were analysed. Stages chosen were chorionic (Ch) at about 13 weeks of development and amniotic (Am) ranging between 20 – 25 weeks of development. Measurements of xanthine oxidase, NADPH oxidase and TBARS levels are shown (A). Followed by analysis of HIF-1 (B), TGF- β and Smad-3 (C). Lastly, expression of galectin-9 and Tim-3 on and surrounding embryonic cells were analysed (D, E). Seven representatives investigated in one experiment: examples shown. *-p<0.05 vs amniotic stage.

3.2.1.2 TGF- β and galectin-9 expression are dependent on Redox mechanisms.

To understand the influence of NADPH oxidase and AP-1 activation by ASK1 and MAPK cascades and its effect on TGF- β expression during redox conditions we studied the THP-1 acute myeloid leukaemia cell line expressing Toll-like receptor 4 (TLR4) (Figure 39A). These cells were exposed to 1 μ g/ml of high mobility group box 1 (HMGB1) protein for 24 h inducing increased galectin-9 and TGF- β secretion (Figure 39B). As the NADPH-oxidase pathway including ASK1 and AP-1 seems to be significantly influencing the TGF- β expression we pre-treated cells before the HMGB1 stimulation with either 30 μ M Diphenyleneiodonium chloride (DPI; an inhibitor of NADPH oxidase), 1 μ M SR11302 (an inhibitor of AP-1) or with dominant-negative ASK1 (Δ N-ASK1) for 1 h to block any activity of these components during HMGB1 stimulation. While HMGB1 significantly increased the production and release of TGF- β and galectin-9, each of these components greatly reduced the HMGB1 induction with AP-1 inhibition causing the biggest difference in galectin-9 and TGF- β levels.

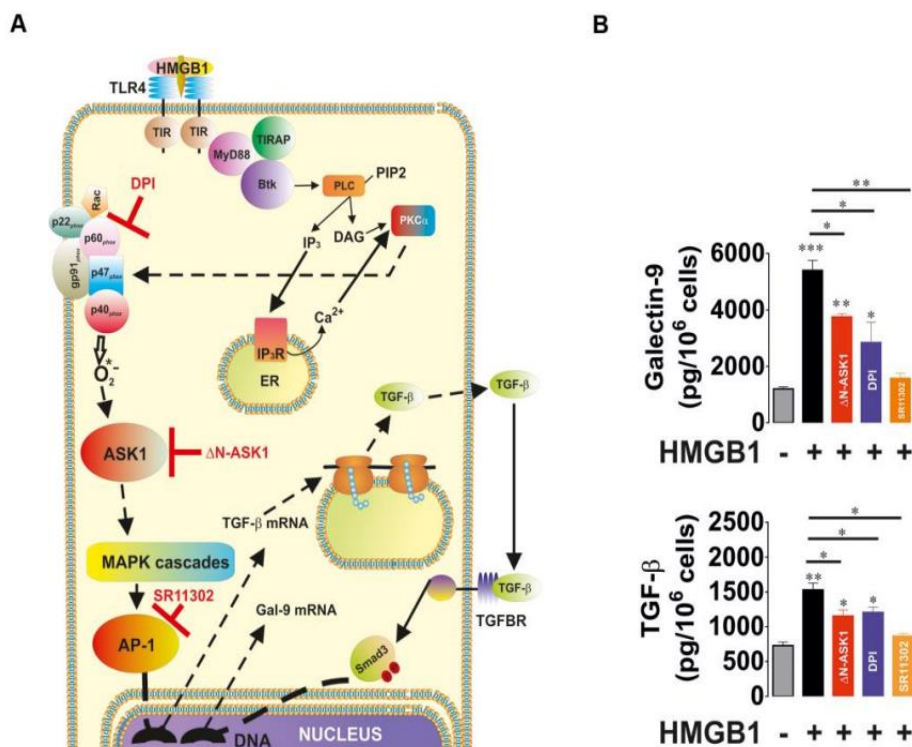


Figure 39 Influence of NADPH oxidase pathway in TGF- β and galectin-9 production. Pathway with proteins investigated and their corresponding inhibitors shown (A). Inhibition of ASK1 (by Δ N-ASK1), AP-1 (by SR11302) or NADPH oxidase (by DPI) led to reduction of TGF- β , and galectin-9 release after HMGB1 stimulation in comparison to cells with no inhibition. HMGB greatly increases levels of proteins released in comparison to control. Data include four independent experiments, mean \pm SEM. *- p <0.05 or **- p <0.01 vs. control.

Similar to NADPH oxidase we also investigated the effects of xanthine oxidase on TGF- β regulation. These effects were studied in MCF-7 breast cancer cells with high levels of xanthine oxidase being induced by using ammonium molybdate. As xanthine oxidase is an enzyme containing molybdenum, addition of further molybdenum leads to activation of each available xanthine oxidase molecule (figure 40A). The MCF-7 cells investigated were treated with 100 $\mu\text{g/ml}$ ammonium molybdate with or without 250 $\mu\text{g/ml}$ allopurinol, an inhibitor of xanthine oxidase activity. Hereby, we were able to clearly show that molybdate significantly increased xanthine oxidase activity which further led to increased TBARS levels and secretion of TGF- β . These effects took place independently from HIF- α accumulation (figure 40B). TGF- β increase induced Smad-3 activity causing increased levels of galectin-9 and Tim-3 expressed on the breast cancer cells.

By addition of allopurinol as a xanthine oxidase inhibitor TBARS levels, TGF- β release as well as expression of Smad-3 and galectin-9 were significantly reduced. Tim-3 levels on the cell surface were also slightly reduced.

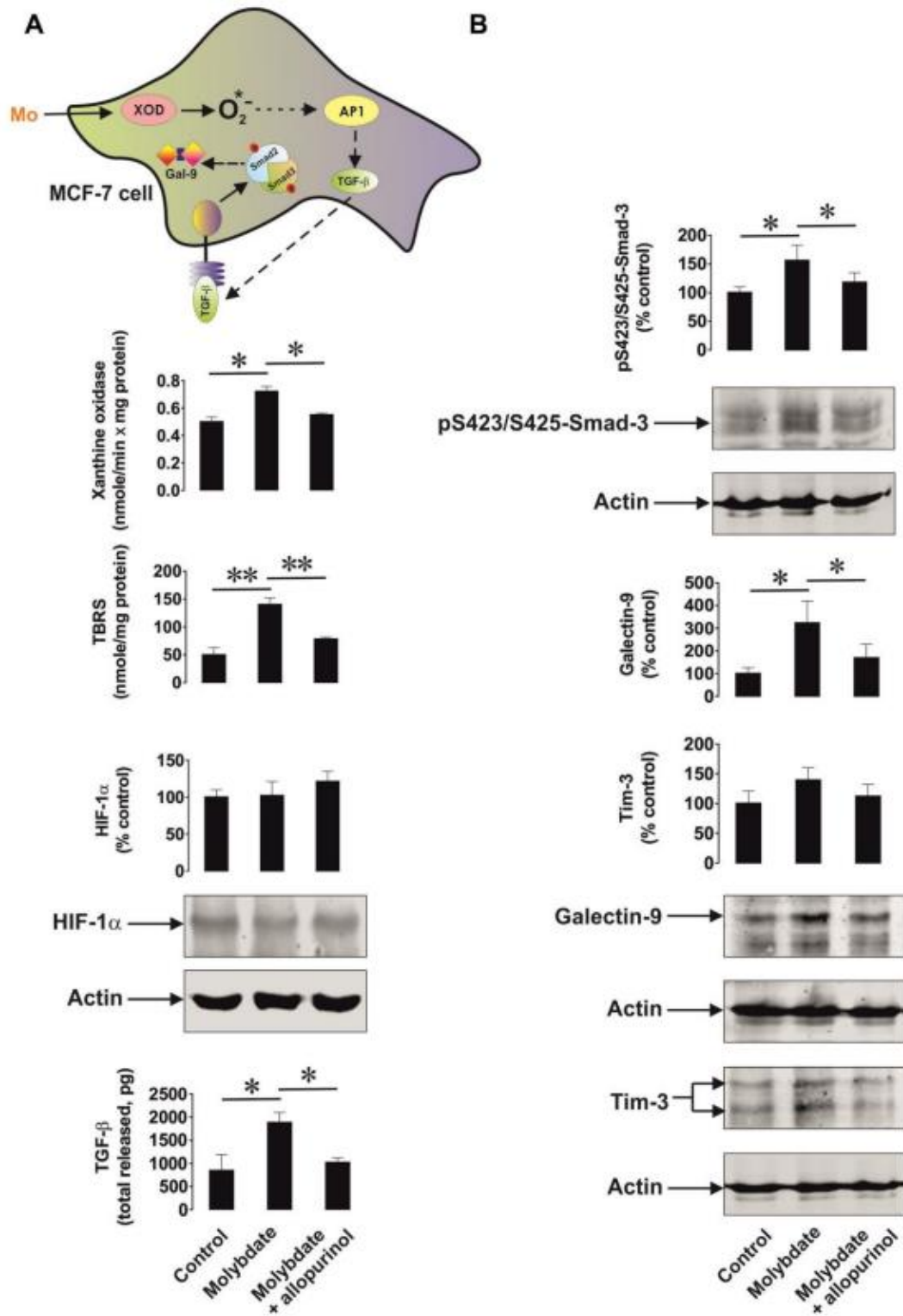


Figure 40 Investigation of xanthine oxidase verifies its influence on galectin-9 and TGF-β expression. For analysing the effects of xanthine oxidase, we used MCF-7 cells exposed to 250 µg/ml ammonium molybdate for 24 h with or without a xanthine oxidase inhibitor (allopurinol). Pathway of xanthine oxidase downstream activation shown (A). TBARS levels, influence of xanthine oxidase on HIF-1α and TGF-β (A) as well as galectin-9, Tim-3 and Smad-3 were analysed by activity assays, ELISA, and Western Blot. Data represent four independent results, mean +/- SEM. *-p<0.05, **-p<0.01 vs. shown events.

3.2.1.3 HIF-1 transcription induces galectin-9 upregulation by TGF- β production in a Smad-3 dependent manner.

Next, we investigated the influence of HIF-1 activation on TGF- β production followed by galectin-9 upregulation. To do so, we used MCF-7 cells, as control we chose wild-type breast cancer cells and to investigate HIF-1 influence we transfected these MCF-7 cells with HIF-1 α siRNA achieving knock-down. Both of these cells were exposed for 6 h to 50 μ M cobalt chloride (CoCl₂), which inhibits degradative hydroxylation of HIF-1 using Co⁺. Following incubation HIF-1 DNA-binding activity, secreted (ELISA) and cell-associated TGF- β (Western Blot) and cell-bound galectin-9 (Western Blot) were measured. In control MCF-7 as well as random-siRNA transfected cells the stimulation with CoCl₂ led to an increase in HIF-1 bound to DNA compared to the HIF-1 α knock-down cells. Furthermore, CoCl₂ induced upregulation of cell-bound and secreted TGF- β in control and random siRNA MCF breast cancer cells, while no difference was detectable in HIF-1 knock-down cells (Figure 41A). CoCl₂ also increased the levels of total TGF- β in random siRNA cells to similar values seen in the wild type MCF-7 cells, this increase is not detectable in HIF-1 knock-down cells (Figure 41A). Due to the application of DOTAP in the transfection procedure the process of TGF- β release has been slowed down in random siRNA knock-down cells, leading to levels of galectin-9 to be upregulated only in wild-type MCF-7 cells after CoCl₂ treatment (Figure 41A). Yet, by studies of the wild-type cells we were able to verify that HIF-1 increases TGF- β production and its release causing galectin-9 to be upregulated on cancer cells.

Further studies to verify the results included the investigation of time influencing DNA-binding of HIF-1, TGF- β secretion and expression of galectin-9 on the cell surface. To do so, we treated MCF-7 cells with 50 μ M CoCl₂ for 1 - 6 h and investigated the prior mentioned proteins in 1-hour intervals. The levels of HIF-1 bound to DNA showed a significant increase after the first hour of exposure to CoCl₂. TGF- β has been highly upregulated after 3 hours of exposure while galectin-9 followed suit after 6 hours (figure 41B). To verify that the induction of galectin-9 expression is dependent on prior upregulation of TGF- β we exposed MCF-7 cells to CoCl₂ for 6 h in presence and absence of TGF- β -neutralization antibody. Neutralization of TGF- β leads to similar galectin-9 levels found in non-CoCl₂-treated MCF-7 cells, the use of an isotype control antibody verified these results (Figure 41C).

Lastly, we investigated the influence of Smad-3 in TGF- β and galectin-9 induction by addition of a Smad-3 knock-down vs. control experiment. Reagent control has been performed by including a random siRNA knock-down treatment. To determine the influence of Smad-3 we

exposed MCF-7 cells, either wild-type, Smad-3 knock-down or random knock-down, to 2 ng/ml TGF- β for 24 h. TGF- β levels were analysed after exposure in cell culture medium as well as cell-associated in lysates. Furthermore, phosphor-S433/425-Smad-3 levels as well as galectin-9 were measured in lysates, which are, according to the shown schematics, influenced by TGF- β expression (Figure 41D). First, the exposure of MCF-7 to external TGF- β induced, in an autocrine mechanism, further production of TGF- β in wild-type and random knock-down cells, with very high levels being released into the environment. Following the release of TGF- β , galectin-9 has been also significantly upregulated in these cell types. In cells lacking Smad-3 no induction of TGF- β and galectin-9 production was measurable (Figure 41E).

Comparing random siRNA transfected cells in both experiments, CoCl₂ and TGF- β exposure, it is evident that while CoCl₂ induced TGF- β upregulation on cell-associated levels release has been inhibited. This might indicate that the interaction between DOTAP reagent and Co⁺ inhibits the ability of MCF-7 cells to properly secrete *de novo* produced TGF- β .

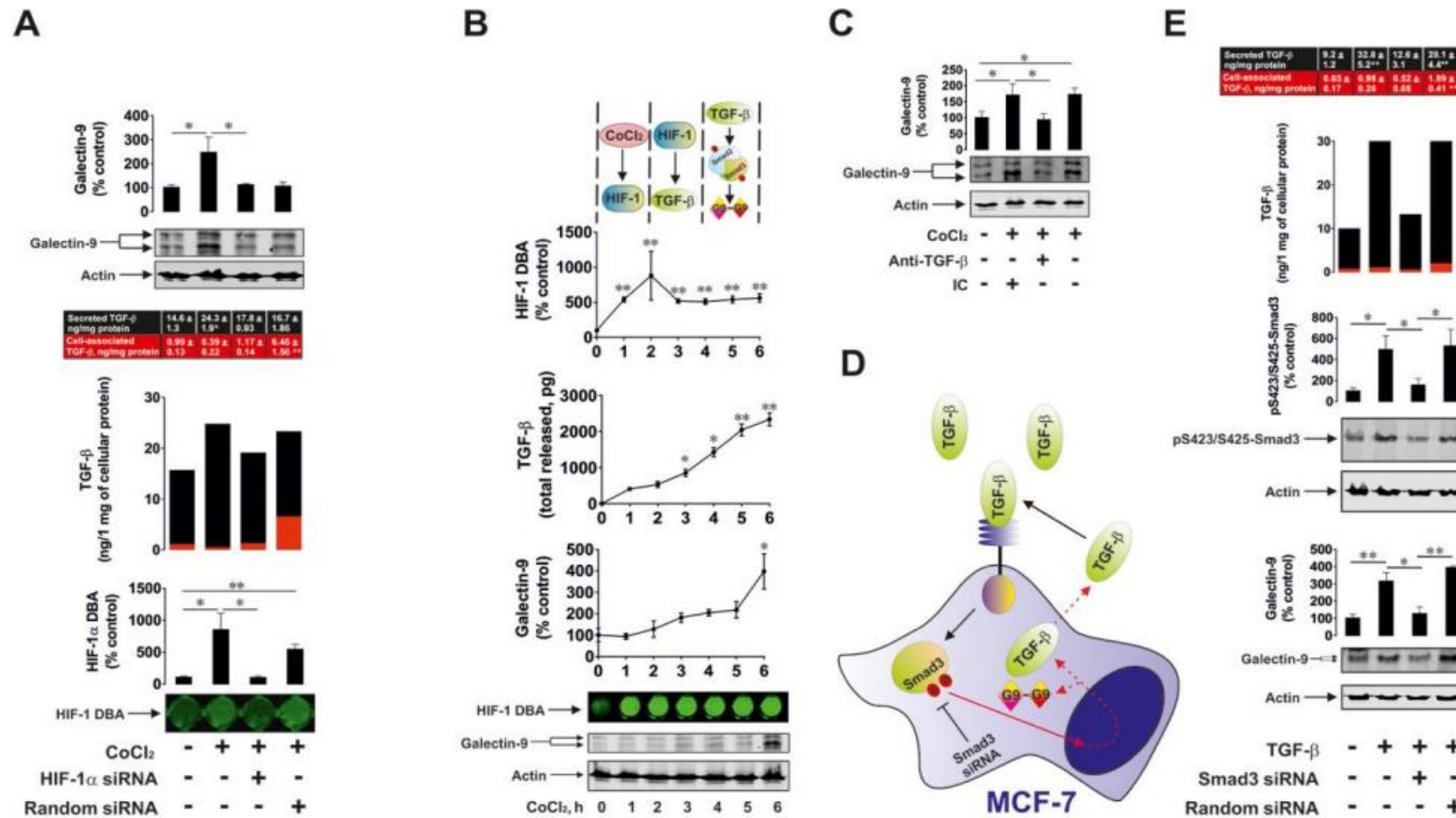


Figure 41 Involvement of HIF-1 and Smad-3 in TGF- β autocrine production and galectin-9 regulation. Induction of HIF-1 by cobalt chloride led to increased cell-associated TGF- β levels, DNA-bound HIF-1 increase and increased galectin-9 production (A). Regulation of HIF-1 – TGF- β – galectin-9 pathway is time-dependent with increased HIF-1 binding to DNA after 1 h, upregulation of TGF- β at 3 h and induction of galectin-9 production following lastly at 6 h (B). Inhibition of TGF- β activity by neutralizing antibodies led to lack of galectin-9 upregulation in presence of cobalt chloride after 6 h (C). Shown is a scheme proposing the influence of TGF- β and Smad-3 in galectin-9 production (D). Smad-3 knock-down led to decreased TGF- β levels after stimulation with external TGF- β and therefore also decreased galectin-9 levels in comparison to wild-type cells and random knock-down cells (E). Three individual experiments represented by images, mean \pm SEM. *- $p < 0.05$, **- $p < 0.01$.

3.2.1.4 Galectin-9 expression is regulated by TGF- β in human cancer as well as embryonic cells.

For the final investigation of galectin-9 expression we used different cell lines and exposed each of them for 24 h to 2 ng/ml TGF- β . The cell lines used were THP-1 AML cells, MCF-7 human breast cancer cells, Colo205 human colorectal cancer cells, primary healthy human keratinocytes and HaCaT human keratinocytes as well as human HEK293 embryonic kidney cells. Both Tim-3 and galectin-9 were analysed in expression on cell surface by Western Blot and secretion by ELISA. In cancer cell lines as well as the HEK293 embryonic cell line galectin-9 levels were significantly increased after exposure to TGF- β after 24 h, while Tim-3 levels did not change. In primary keratinocytes and HaCaT cells, used as non-malignant cells to study, the galectin-9 and Tim-3 levels did not increase in presence of TGF- β (Figure 42).

We investigated if the lack of galectin-9 induction by TGF- β can also be found in cancer cells using the K562 chronic myeloid leukaemia cell line, which initially only expresses traces of galectin-9. Upon stimulation with different concentrations of TGF- β for 24 h the galectin-9 levels increased significantly. Without stimulation K562 cells did not express active phospho-S423/425-Smad-3 levels, which clearly was upregulated during the stimulation with TGF- β . Galectin-9 levels were only increased on a cell-associated level and no release has been detectable by ELISA (Figure 43).

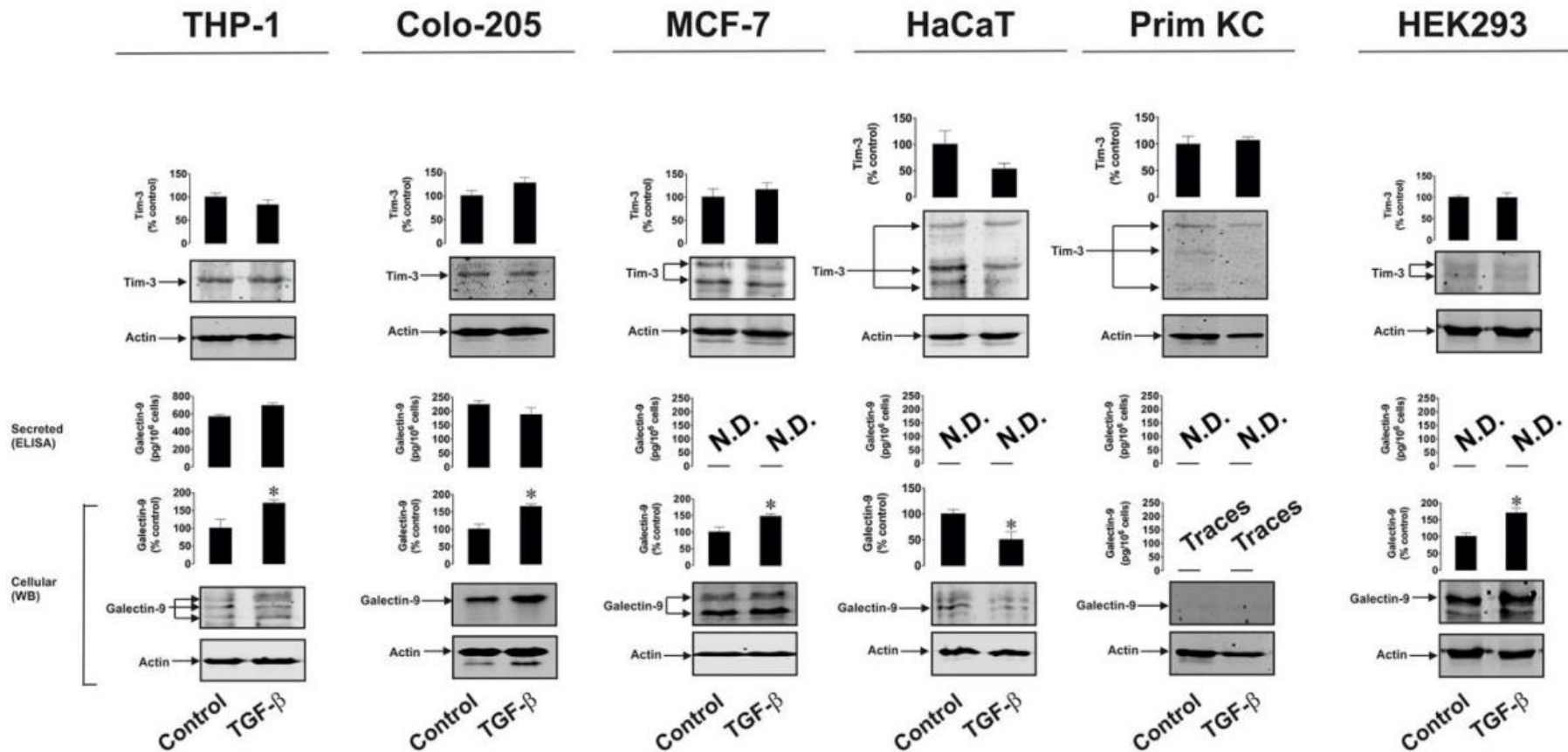


Figure 42 Investigation of different cell lines determined the influence of TGF-β on galectin-9 levels to be mainly found in cancer and embryonic cells. Cell lines investigated include THP-1 AML human leukaemia cells, Colo205 colorectal cancer cell line, MCF-7 breast cancer cell line, HaCaT non-malignant human keratinocyte cell line, primary keratinocytes (prim KC) and as a representative for the embryonic development we used the HEK2993 human embryonic kidney cell line. In malignant cell lines as well as the embryonic cell line TGF-β increased galectin-9 expression on cell surface, while Tim-3 levels did not change significantly. In non-malignant cells (HaCaT and primary keratinocytes) we did not see any increase in galectin-9 expression. Shown are representative of four independent experiments, mean +/- SEM included. *-p<0.05 vs. control samples.

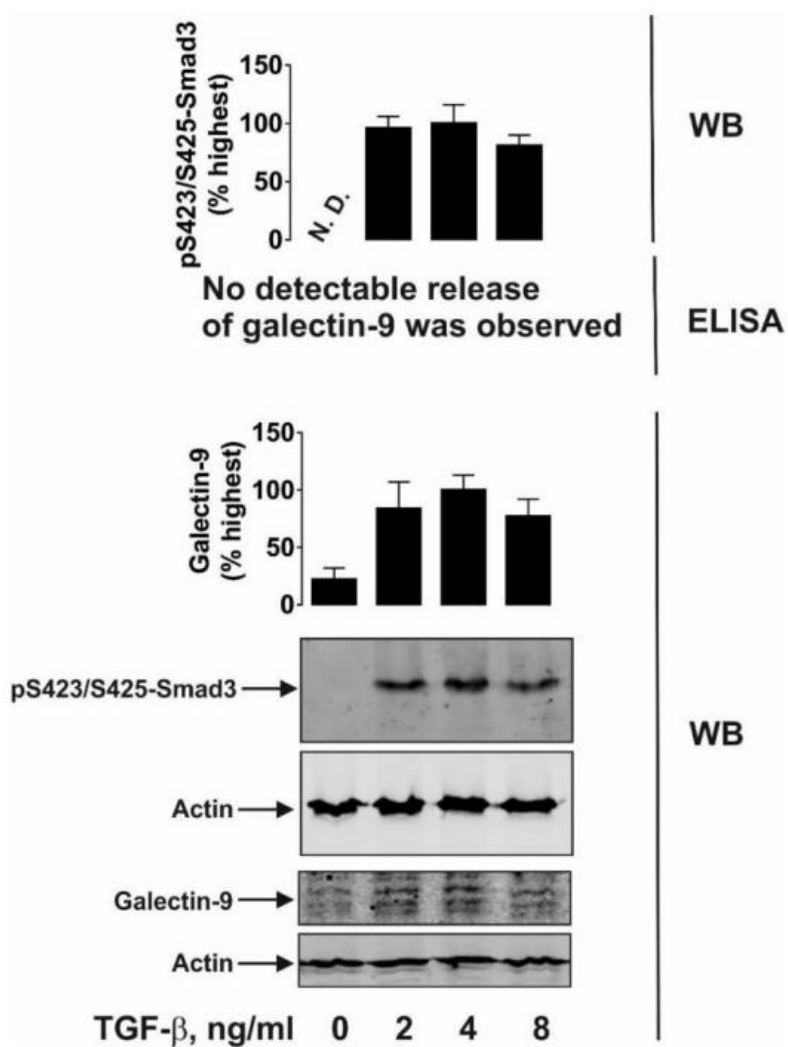


Figure 43 K562 human cancer cells express galectin-9 levels after TGF- β exposure. K562 is a human chronic myeloid leukaemia cell line that expresses very low levels of galectin-9 without TGF- β treatment. Exposure to TGF- β at different concentrations (0, 2, 4, 8 ng/ml) for 24 h led to an increase in active phosphor-S423/425-Smad-3 and caused upregulation of galectin-9 expression, investigated by Western Blot analysis. ELISA analysis did not indicate any galectin-9 release after stimulation with TGF- β . Data represent one experiment with three repetitions, mean +/- SEM included.

We further looked into the differences in the TGF-β induction of galectin-9 expression in healthy cells vs. malignant cells. As we were able to verify the influence of Smad-3 in the upregulation of galectin-9 we compared the MCF-7 cell line with HaCaT human keratinocytes and primary keratinocytes. After exposure to 2 ng/ml of TGF-β for 24 h phosphor-Smad-3 was significantly upregulated in MCF-7 cells but not in either non-malignant cell type. Furthermore, MCF-7 cells already expressed higher levels of Smad-3 in comparison to healthy cell lines. This indicates that galectin-9 expression is mainly found as a mechanism within cancer and embryonic cells and is influenced by TGF-β and Smad-3 expression (Figure 44).

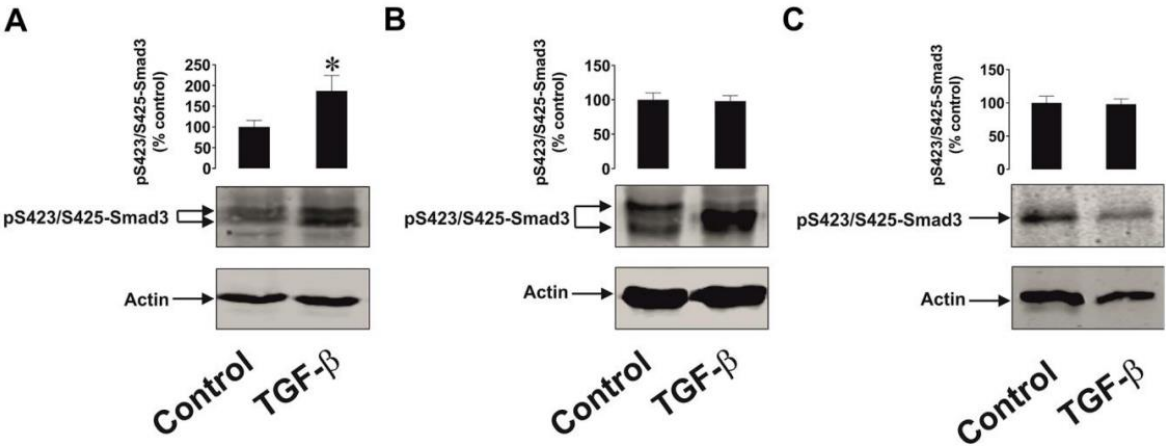


Figure 44 Induction of Smad-3 by TGF-β exposure only detectable in malignant cells. MCF-7 breast cancer cells, HaCaT non-malignant human keratinocytes and primary keratinocytes were exposed to 2 ng/ml TGF-β for 24 h. Increase of active phosphor-S243/245-Smad-3 only detectable in malignant cells (A), while levels of active Smad-3 did not change in healthy cells (B, C). Data include four experiments, representative and mean +/- SEM included. *-p<0.05 vs non-treated cells.

3.2.1.5 Discussion.

As investigated in the chapter prior, does the production of galectin-9 influence immune responses towards cancer by being discharged in high amounts by malignant cells. While galectin-9 is found in high amount in the surrounding microenvironment, it is lacking a secretion signal sequence. Therefore, to enable galectin-9 being released into the environment and bind to T cell surface it is discharged in a complex with Tim-3 as its carrier (Yasinska, 2019, Goncalves-Silva, 2016). By binding to the surface of cytotoxic immune cells such as cytotoxic T cells and natural killer cells, galectin-9 impairs their function to induce cell death within the malignant cell (Yasinska, 2019, Goncalves-Silva, 2017). Tim-3 is also a possible receptor on the targeted cells. Binding of galectin-9 on such receptors (Tim-3 as well as VISTA) leads to the induction of pro-apoptotic signalling in cytotoxic T cells.

While it is shown that malignant cells express and release high amounts of galectin-9 the exact mechanism on this biochemical regulation has not been investigated prior and was the focus of this chapter.

Here, we hypothesized that the regulation of galectin-9 expression is dependent on TGF- β , a growth factor highly produced by cancer cells and in later stages regulated in an autocrine fashion. By studying human breast cancer and acute myeloid leukaemia cell lines we detected significantly higher levels of TGF- β than in healthy tissue of the same origin. Furthermore, levels of NADPH oxidase as well as xanthine oxidase, responsible for producing reactive oxygen species (ROS), as well oxidative stress altogether were greatly increased during the development of cancer tissue. Such stress can induce the activation of high levels of the AP-1 transcription complex consequently leading to increased TGF- β production by down-stream signalling (Sumbayev, 2005; Birchenall-Roberts, 1990). Next to increased AP-1 activity HIF-1 α accumulation was also highly detectable in cancer cells. HIF-1 α can further the transcription activity of the HIF-1 complex leading to expression of TGF- β . By increase of TGF- β levels Smad-3 is also upregulated in its active, phosphorylated form (at S243/S245) in all of the studied tissue types. Furthermore, we were able to detect higher levels of Tim-3 and galectin-9 in these cancer cell types (Figure 34 and 36). Comparing the AML cell line (as a non-solid cancer) to the MCF-7 breast cancer cells (as a solid cancer) we were able to determine that TGF- β seems to be kept in solid tumours in their microenvironment while in the AML samples it can be found in high levels in the blood stream enabling TGF- β to be continuously used by circulating cells (Figure 37).

In our studies, we were able to detect the same pathway being used in embryonic development to control the mother's immune system to a certain extent (Figure 38). Hereby, in the earliest stages the levels of galectin-9 and Tim-3 were significantly increased on the surface of embryonic cells. Similar to the studies of solid tumours, in embryonic cells we were unable to detect a release of these proteins from their surface into the surrounding environment.

We were also able to confirm that TGF- β is upregulated by NADPH and xanthine oxidase. HMGB-1 is capable of inducing NADPH oxidase, which then furthered the TGF- β production followed by galectin-9 increase in the THP-1 cell line. Blocking either NADPH oxidase activity, AP-1 transcriptional activity or ASK1 kinase activity led to a decrease in such HMGB1-induced effects of galectin-9 and TGF- β (Figure 39). As already investigated previously HMGB1 is able to act by binding to Toll-like receptors 2 and 4 (TLR2 and 4) by inducing oxidative stress and HIF-1 activation (Yasinska, 2018). AP-1 is also known to correlate with TGF- β expression, yet it might not be by direct interaction with the TGF- β gene (Birchenall-Roberts, 1990). In our experiments, we were able to show that blockage of AP-1 does interfere with any HMGB1 effects regarding TGF- β and galectin-9 production. In regard to xanthine oxidase activation, we were able to detect upregulation of oxidative burst in MCF-7, yet, no sufficient HIF-1 α accumulation was detectable (Figure 40A). Upregulation of TGF- β , phospho-S423/425-Smad-3 and galectin-9 despite lacking accumulation does indicate a contribution of the AP-1 pathway.

By exposing MCF-7 cells to Cobalt chloride (CoCl₂) we were also able to confirm the role of HIF-1 inducing TGF- β expression by inhibition of degradative hydroxylation of HIF-1 α leading to it being stabilized and the HIF-1 complex activated. By CoCl₂ stimulation cells are exposed to oxidative stress due to increased ROS generation by interaction with the mitochondrial transition pore (Battaglia, 2009; Stenger, 2011). Free radicals are formed, which trigger activation of AP-1 through ASK1 mediation (Sumbayev, 2005). AP-1 is deemed to be required yet not fully important for TGF- β gene expression control, HIF-1 yet does seem to be directly in control. Using HIF-1 α -knockdown MCF-7 cells in comparison to wild-type cells we were able to determine that CoCl₂ was able to induce increased TGF- β and galectin-9 production in the wild-type confirming a HIF-1 dependency. In cells used as a method control consisting of a random knock-down, we were able to see that the combination of the DOTAP reagent from the method and the application of CoCl₂ led to accumulation of TGF- β on the surface reducing secretion, and galectin-9 regulation had been slowed down too (Figure 41A).

After exposure to CoCl₂ we were able to detect increased binding of HIF-1 to DNA after 1 h, increased levels of secreted TGF- β after 3 - 4 h and lastly galectin-9 levels were significantly

upregulated after 6 h. This clearly shows the regulatory pathway of HIF-1-induced TGF- β production which consequently leads to increased galectin-9 expression, as well as an autocrine induction of TGF- β stimulation. To specify that galectin-9 production was clearly dependent on TGF- β upregulation we used TGF- β -neutralising antibody and 50 μ M of CoCl₂ simultaneously. Using an isotype control we were able to verify that attenuation of TGF- β consequently leads to crucially reduced galectin-9 expression. Furthermore, we were able to verify the role of active phosphor-S423/425- Smad-3 in the autocrine TGF- β production and galectin-9 upregulation by using Smad-3 knockdown MCF-7 breast cancer cells.

In our study, we demonstrated that TGF- β is able to increase the galectin-9 production in embryonic cells as well as human AML, breast, and colorectal cancer cells, but did not lead to any significant changes in healthy, non-malignant cell types. Cancer cell lines, such as the K562 chronic myeloid leukaemia cell line, which only show traces of galectin-9 prior to TGF- β stimulation increased those level significantly after exposure (Figure 42 and 43). These findings are in correlation with prior research indicating differences in the TGF- β -Smad-3 signalling in malignant and healthy tissue, with TGF- β significantly inducing phosphor-S423/S2454-Smad-3 in malignant cell lines and primary cells but not in healthy samples (Brown, 2008; Kubiczkova, 2012). Using Western Blotting we were able to see high variation in active Smad-3 bands comparing malignant and embryonic samples to healthy ones, suggesting the influence of Smad-3 in the induction of significantly increased galectin-9 expression found in malignant and embryonic cells.

An indication for the difference in responses might be the receptor expression for TGF- β (TGFBR). In cancer and embryonic samples TGFBR might be kept at high levels corresponding with the autocrine production of TGF- β itself, while healthy tissue decreases them in case of high levels of TGF- β in the surrounding tissue. Furthermore, focussing on Smad-3 activation, it is known to recruit different co-activators depending on the response needed to stimuli. The main co-activators are transcription intermediary factor 1-gamma (TIF-1 γ , also known as TRIMM33 (tripartite motif-containing factor 33)) and Smad-4, which can also be used by other binding partners such as Smad2 and interact further with Smad-3 to trigger responses (He, 2006). To understand the influence of these co-activators further research has been performed. In clinical studies a high expression of TGFBR has already been associated with poor prognosis in case of AML patients impacting remission as well as long-term survival.

Our observations in this chapter indicate that in early stages of development, both cancer and embryo, the low oxygen availability leads to HIF-1 induced TGF- β activation followed by

significant increase of galectin-9. Low oxygen availability is countered in the human body by increased angiogenesis, in this stage TGF- β most likely established an autocrine support of its own production via Smad-3 upregulation, which in case of malignancies or the embryo can further induce galectin-9 expression. As TGF- β in theory can also activate tumour-suppressing biochemical activities, the increased acquisition of mutations in specific genes can lead to cancer cells inhibiting such anti-proliferative responses by TGF- β . A scheme indicating the different approaches of TGF- β activation in case of low and high oxygen availability is shown in Figure 45.

The results in this chapter clearly show a self-supportive mechanism regarding galectin-9 regulation in malignancies such as AML, breast, and colorectal cancer as well as during the embryonic development.

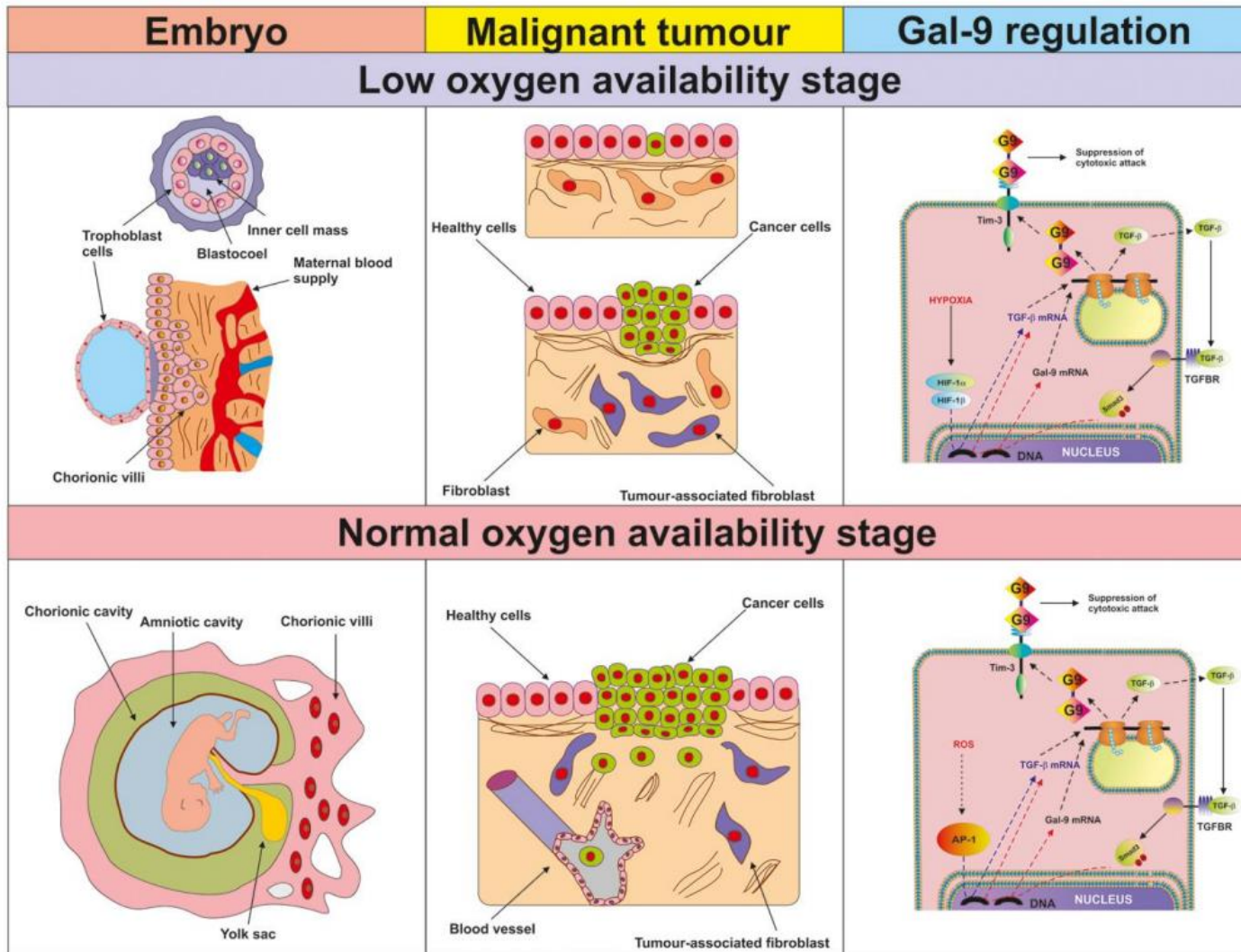


Figure 45 Scheme depicting TGF- β in low and high oxygen availability stages. TGF- β is activated in low oxygen stage by HIF-1 induction. Later when new blood vessels are formed by angiogenesis and oxygen levels are returned to a normal stage TGF- β is maintained by autocrine support and Smad-3 upregulation.

3.2.2 REGULATION OF IMMUNE CHECKPOINT PROTEIN VISTA EXPRESSION IS ACHIEVED DIFFERENTIALLY IN RAPIDLY PROLIFERATING HUMAN CELLS AND T LYMPHOCYTES BY TGF- β AND SMAD-3 SIGNALLING.

As galectin-9 is mainly regulated by the TGF- β – Smad-3 pathway and VISTA is one of the main receptors for galectin-9-induced immune suppression we decided to investigate the regulation of this receptor in rapidly proliferating cells, such as cancer cells, as well as T lymphocytes. VISTA belongs to a group of proteins that act as immune checkpoint proteins determining the regulation of cancer cells escaping immune responses. Such proteins are part of complex machineries inhibiting cytotoxic attacks by T lymphocytes and natural killer cells leading to fully suppressed immune responses in the long run. Pathways, such as the one including VISTA and galectin-9, are included fundamentally in the regulation of protection of human foetal cells against rejection by the mother's immune system. Checkpoint proteins such as programmed cell death protein 1 (PD-1) and the corresponding ligand (PD-L1), T cell immunoglobulin and mucin domain containing protein 3 (Tim-3) and its ligand galectin-9 and cytotoxic T-lymphocyte-associated protein 4 (CTLA4) have been thoroughly investigated to understand their regulation and expression (Buckle, 2021; Yoo, 2021; Yasinska, 2018). Other molecules have been found just recently and research the understanding of their functions is still lacking. To investigate these proteins and their biochemical regulation is crucial for further development in cancer treatments and to optimize these proteins as targets for immunotherapies. One of such potential targets is the V-domain Ig-containing suppressor of T cell activation (VISTA) and its ligands VSIG3 (V-set and immunoglobulin domain containing 3) and galectin-9 influencing the suppression of cytotoxic T cell responses (Xie, 2021). VISTA is found mainly in blood cells, with myeloid cells containing highest levels as well as in T lymphocytes in which it is used as receptor to inhibit their anti-cancer immunity (Lines, 2014; Wang, 2011; Lines, 2014). As seen in chapter 1, binding of either of the three isoforms of galectin-9 (varying in linker size) to VISTA leads to the prevention of granzyme B release by cytotoxic T lymphocytes increasing the induction of cell death within themselves. Interestingly, some cancer cell types also express high levels of VISTA on the cell surface (Im, 2021; Popp, 2021). The exact mechanisms how VISTA is regulated in different cell types has yet to be understood. Investigating the promotor region of the

human VISTA gene, response elements for the Smad-3 transcription factor able to be activated by TGF- β have been found. As galectin-9 is highly maintained by TGF- β -Smad-3 interaction in autocrine and paracrine fashion in human cancer and embryonic cells we decided to investigate the involvement of the same regulatory pathway in VISTA expression. In this chapter, we are interested to verify for the first time the influence of TGF- β and Smad-3 in VISTA expression. In T lymphocytes the upregulation of VISTA might only be detectable if these cells do not show any cytotoxic activity by granzyme B production. If such cells are expressing detectable proteolytic enzyme activity VISTA might be decreased after TGF- β stimulation. This could be achieved due to differential nuclear compartmentalization of the VISTA gene (VSIG).

3.2.2.1 TGF- β leads to differential regulation of VISTA dependent on cell type.

The first step on the investigation on VISTA expression was to observe if TGF- β is able to induce VISTA expression in human T lymphocytes similar to galectin-9 due to their combined effects on inducing programmed cell death in these cells. We compared non-stimulated Jurkat T cells and PMA-activated (24 h with 100 mM PMA) Jurkat T cells expressing similar activity as cytotoxic T cells. These cells were exposed for 24 h to 2 ng/ml TGF- β and expression levels of VISTA were analysed using the Western blot approach. In non-stimulated Jurkat T cells TGF- β led to an increase in VISTA levels (Figure 49A) yet in PMA-activated Jurkat T cells demonstrating cytotoxic activity TGF- β decreased VISTA levels (Figure 49B). Interestingly in both cell types TGF- β increased the phosphorylation of Smad-3 transcription factor (Figure 46A). To investigate these effects on cytotoxic T cells we analysed VISTA expression levels on TALL-104 after exposure to 2 ng/ml TGF- β for 24 h. As seen in the PMA-treated Jurkat T cells the exposure to TGF- β caused a downregulation of VISTA levels in TALL-104 (Figure 49C). Furthermore, we were able to detect again an increase in phospho-S423/S425-Smad-3 levels (Figure 46B right side). According to previous research we were also able to detect a downregulation of granzyme B expression after TGF- β exposure (Figure 46B right side). In this cell line Tim-3 and galectin-9 levels were detectable in low amounts and stimulation with TGF- β did not lead to a significant increase (Figure 46B left side). To further investigate the effects of TGF- β on VISTA regulation we isolated primary human T cells using CD3 as a detection marker. These cells were exposed to 2 ng/ml TGF- β for 16 h. Time has been reduced due to higher reactivity of primary T cells in comparison to cell lines. While stimulation with TGF- β

caused a slight increase in galectin-9 levels, both galectin-9 and Tim-3 are expressed at very low amounts in primary T cells (Figure 46C). Yet, TGF- β exposure did lead to a significant increase in phospho-Smad-3, as seen in the Jurkat T cell line and the TALL-104 cell line. In primary T cells the exposure to TGF- β yet again decreased VISTA and granzyme B levels (Figure 49D).

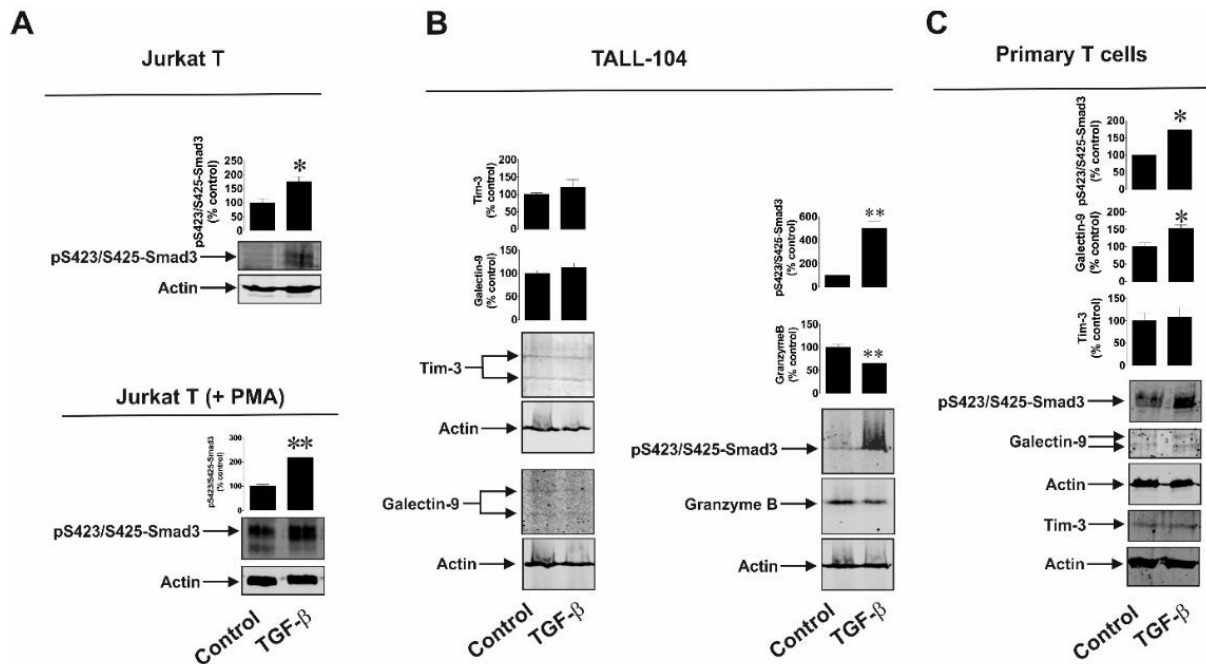


Figure 46 Investigation of different types of human T lymphocytes after TGF- β exposure. In resting Jurkat T cells and PMA-activated Jurkat T cells (A) TGF- β led to an increase in phospho-S423/S425-Smad-3 levels. In TALL-104 TGF- β did not increase Tim-3 and galectin-9 levels significantly (B left side). Granzyme B levels were reduced while phospho-S423/S425-Smad-3 has been significantly upregulated (B right side). In primary T cells (C) a slight increase in galectin-9 and a significant increase in phospho-S423/S425-Smad-3 levels were detectable while levels of Tim-3 did not rise. Data include four experiments, one visual representative and mean +/- SEM included. *-p<0.05 and **-p<0.01 vs non-treated cells.

Next, we investigated myeloid cell types in regard to VISTA expression, which are known to have high levels of VISTA already prior to stimulation with TGF- β . To do so we used the human acute myeloid leukaemia (AML) cell line THP-1 consisting of monocytic leukaemia, as well as primary human AML blasts. In chapter 3.1 we were able to show already that stimulation of the THP-1 cell line with TGF- β can induce a significant increase in galectin-9 expression by association with Smad-3 induction. These cells are further known to not express any levels of granzyme B and do not show any catalytic activity as such. In the THP-1 cell line the exposure to 2 ng/ml TGF-

β for 24 h induced a downregulation of VISTA expression (figure 49E), while 16 h stimulation of the primary AML cell line it has been upregulated significantly (figure 49F). As there was a differential response to TGF- β detectable in case of VISTA expression we decided to determine if TGF- β is able to induce the expression in cells that are known to not have any detectable levels of VISTA prior to stimulation. The cell line we have chosen is the human epithelial breast cancer cell line MCF-7, which after stimulation with TGF- β have been able to express galectin-9. Yet, in case of VISTA, stimulation with TGF- β did not induce any detectable levels of VISTA in the MCF-7 cell line (figure 49G). This has been further confirmed using qRT-PCR as no significant levels of VISTA mRNA is detectable in MCF-7 cells (Figure 47).

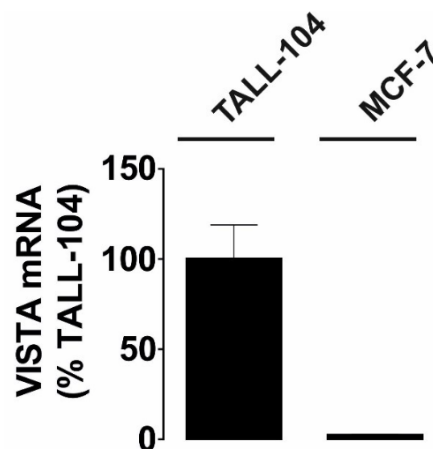


Figure 47 Levels of VISTA mRNA analysed using qRT-PCR in two different cell lines, TALL-104 with high levels of VISTA expressed and MCF-7 with no detectable amounts. Data included are showing mean values +/- SEM of three experiments.

In comparison to cancer cells embryonic cells are also able to produce high levels of TGF- β and have a significant amount of VISTA proteins on their surface. With progression of the foetal development the amount of TGF- β is reduced. In our studies we compare two different stages of embryo development, cells were taken either during the amnion stage (~20 weeks) or during the chorion stage (ranging from 13 to 14 weeks). Similar to the high levels of galectin-9, expression of TGF- β as well as VISTA was significantly higher in the chorion stage and has been reduced in the later, amnion stage (Figure 49H). In correlation to these studies the phosphorylation levels of Smad-3 were also significantly higher in the chorion stage. Similar to the foetal cells some solid cancer cells are able to express VISTA on their surface, which can be further upregulated by increased TGF- β levels. One cell line we investigated concerning VISTA expression on cell surface has been the human paediatric kidney

tumour cell lines WT3ab. These cells are known to express VISTA in non-stimulated form and with further exposure to TGF- β the VISTA levels also increased significantly (Figure 49I). Furthermore, these cells also express Tim-3 and galectin-9, with galectin-9 levels being raised after TGF- β stimulation. This correlates with the increase in Smad-3 phosphorylation after TGF- β exposure for 24 h (Figure 48).

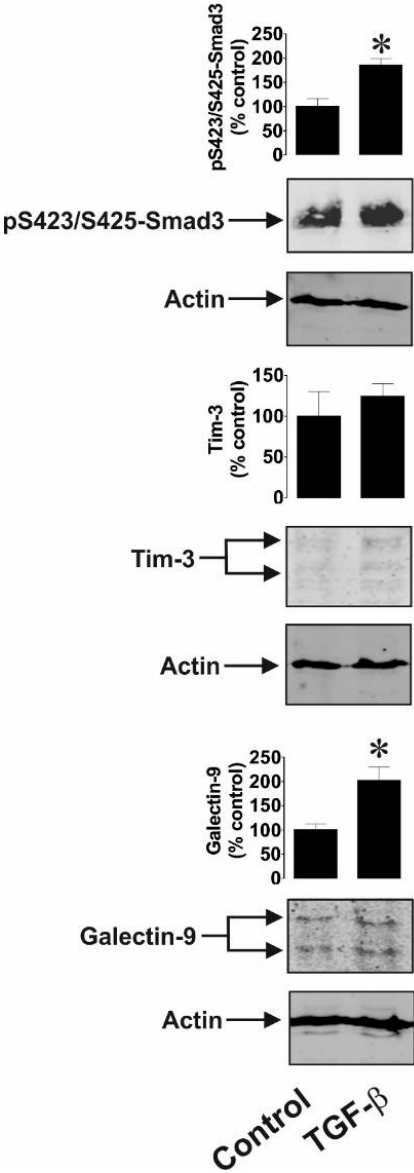


Figure 48 Study of the Wilms tumour cell line WT3ab after exposure to TGF- β . WT3ab cells are stimulated for 24 h with 2 ng/ml TGF- β and shown proteins have been analysed using Western blot approach. Pictures represent four repetitions in one experiment with similar results. Mean +/- SEM included. *-p<0.05 vs. control.

Interestingly, similar results were achieved studying the non-malignant human keratinocyte cell line HaCaT. These cells express detectable levels of VISTA and after exposure to TGF- β for 24 h the amount was further increased (Figure 49J). Furthermore, in cell lines that express even very low, barely detectable levels of VISTA, such as the human chronic myelogenous leukaemia cell line K562, TGF- β is able to significantly increase the expression (Figure 49K). Increased concentrations of TGF- β of either 4 or 8 ng/ml did not lead to even higher levels of VISTA in comparison of 2 ng/ml stimulation. Correlating to these findings resting K562 did only express low, barely detectable amounts of phosphorylated Smad-3 which has been highly increased in response to the TGF- β stimulation.

Differences in VISTA expression has been detected regarding the glycosylation levels. Most of the investigated cell lines express a glycosylated VISTA protein with an average molecular weight of 52 kDa, yet the K562 cell line as an example has a partly glycosylated VISTA protein and embryonic cells do not show any glycosylation with a molecular weight ranging at ~30 kDa. As VISTA is mainly functional at a molecular weight of 52 kDa, this might indicate that glycosylation is achieved gradually at different velocity depending on the cell type. Although embryonic cells might also store VISTA protein for further use in case of emergencies, the exact mechanisms and reasons still need to be investigated.

Lastly, as performed during the galectin-9 expression studies we used Smad-3 knockdown using Smad-3 siRNA, including random siRNA as a negative control, in Jurkat T cells and investigated the effects of Smad-3 correlating with stimulation with TGF- β . We analysed the cellular levels of VISTA, galectin-9 and phospho-Smad-3 using Western Blot approaches. TGF- β effects leading to increased VISTA expression were inhibited using the siRNA for Smad-3 knockdown (Figure 49L). This clearly indicates a dependency of VISTA expression on Smad-3 increase after TGF- β exposure.

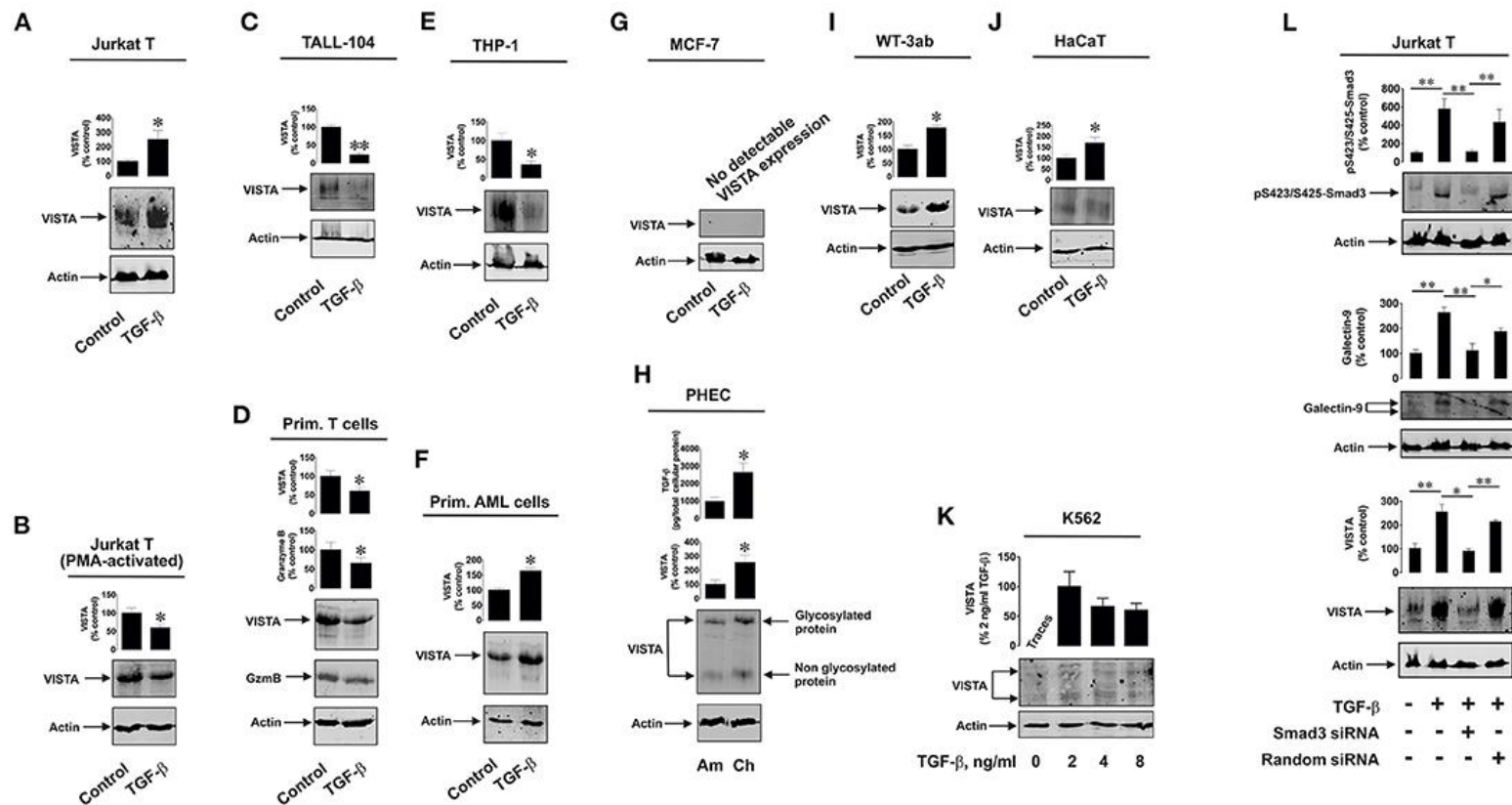


Figure 49 Effects of TGF-β on VISTA expression studied in a variety of cell types. Naïve Jurkat T cells (A) and PMA-activated Jurkat T cells (B), TALL-104 (C), primary T lymphocytes (D), the AML cell line THP-1 (E), primary AML cells (F), MCF-7 breast cancer cell line (G), primary human embryonic cells from two different developmental stages, chorion and amnion (H), Wilms tumour cell line WT3ab (I), non-malignant keratinocyte cell line HaCaT (J), K562 cell line (K) were exposed to 2 ng/ml TGF-β for 24 h (cell lines) or 16 h (primary samples) and expression levels of VISTA were investigated using Western blot approach. The K562 cell line has been further exposed to different concentrations of TGF-β to investigate if higher concentration immediately also leads to an increase in VISTA expression. Lastly, we used siRNA to knockdown Smad-3 activity and determined its influence similar to the galectin-9 studies on VISTA expression levels (L). Visual representatives were chosen from either 4-7 individual results. Data include mean values +/- SEM from 4-7 experiments. *p<0.05 and **p<0.01 vs. non-stimulated control samples.

Next, we investigated mRNA levels of VISTA in different cell lines to determine if the effects seen are correlating to these. We compared non-stimulated and TGF- β -stimulated Jurkat T and TALL-104 cells. As observed with VISTA on the surface of Jurkat T cells, increased VISTA expression levels correlated with significantly higher mRNA levels. TALL-104 which downregulated VISTA expression after exposure to TGF- β also showed clear decrease of mRNA levels (figure 50A). Using ChIP qRT-PCR approach we also verified that Smad-3 is able to bind to the VISTA gene, VSIG. Here we also were able to verify that TGF- β increased the enrichment of the gene with Smad-3 elements, clarifying that Smad-3 is directly interacting with the VSIG promotor region (Figure 50B).

We also investigated how TGF- β impacted the cell surface levels of VISTA as well as the possibility of secretion. Cell-surface bound VISTA was studied in resting Jurkat T cells, PMA-activated Jurkat T cells, TALL-104 and THP-1 cell line after exposure to 2 ng/ml of TGF- β for 24 h. Clearly in correlation with the studies performed before, TGF- β exposure lead a decrease of overall VISTA levels as well as to a decrease of VISTA expression on cell surface as seen in the TALL-104 and THP-1 cell lines. In the Jurkat T cell samples surface expression has not been significantly increased after TGF- β exposure indicating that increased VISTA levels in the cells did not lead to an automatic increase on the cell surface (Figure 50C). Cell-associated and secreted VISTA protein levels were compared using ELISA approach. We tested these levels in Jurkat T cells (Figure 50D), primary T cells (Figure 50E), THP-1 cell line (Figure 50F), primary AML samples (Figure 50G) as well as non-malignant keratinocyte cell line HaCaT (Figure 50H). Exact numbers are shown in the table below (Table 4).

Protein	Jurkat T		Primary T cells		THP-1		Primary AML cells		HaCaT	
	Ctrl	TGF- β								
VISTA (cell-associated), pg/mg cell protein	166 \pm 12	492 \pm 52	365 \pm 54	220 \pm 18	614 \pm 58	367 \pm 27	310 \pm 36	522 \pm 64	143 \pm 18	266 \pm 29
VISTA (secreted), pg/mg cell protein	ND \pm NA	ND \pm NA	50 \pm 7	45 \pm 4	10 \pm 2	55 \pm 8	108 \pm 17	524 \pm 73	59 \pm 8	21 \pm 3

Table 5 Values of cell-associated and secreted VISTA levels in a variety of cell types. Ctrl refers to non-stimulated samples as a control. ND refers to non-detectable and NA to non-applicable.

The only cell type that showed a significant increase of secretion of VISTA after stimulation with TGF- β has been the primary AML cells, while the total expression levels were similar to the levels detected prior by Western blot. This might be an indication that TGF- β is not responsible for the secretion of the VISTA protein in any of the cell types (Figure 2D- 2H).

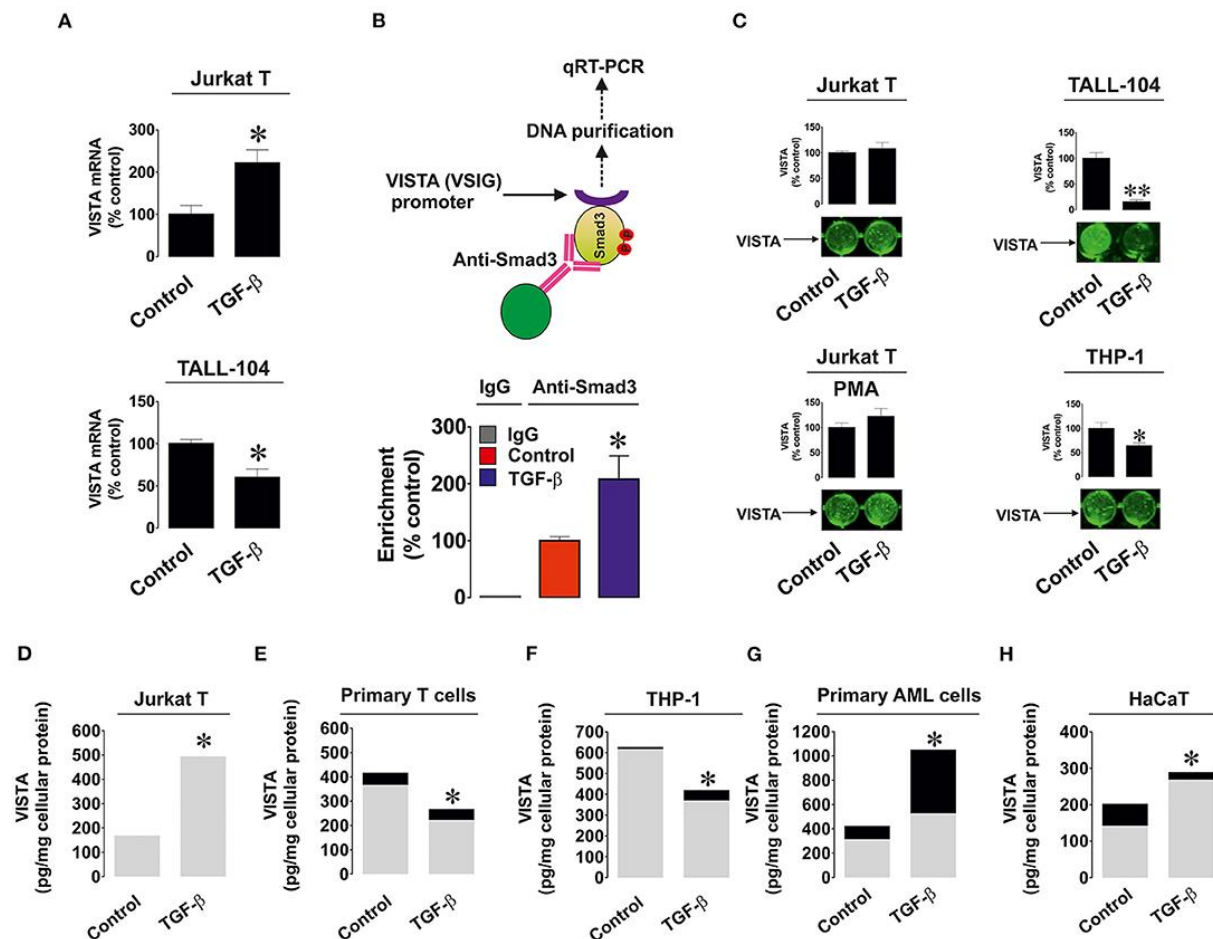


Figure 50 Analysis of TGF- β in cell-associated VISTA expression and secretion. (A) Jurkat T cells and TALL-104 cells were stimulated for 24 h with 2 ng/ml TGF- β , RNA has been isolated and mRNA levels investigated with and without stimulation using qRT-PCR. (B) To determine Smad-3 binding to the VISTA gene VSIG Jurkat T cells, resting, and stimulated with TGF- β , were investigated using ChIP and qRT-PCR. (C) Cell-surface bound VISTA has been investigated in PMA-treated Jurkat T cells, TALL-104 and THP-1 cells after exposure to TGF- β . (D) Jurkat T cells, (E) primary T lymphocytes, (F) THP-1 AML cell line, (G) primary AML blasts as well as (H) non-malignant HaCaT keratinocytes were treated with TGF- β for 24 h and differences in cell-bound (grey) and secreted (black) VISTA levels were investigated. Examples of five individual experiments shown, including mean \pm SEM. * p <0.05 vs control shown.

To further investigate the differences in VISTA expression in different cell types we investigated if co-activators able to bind to Smad-3, mainly Smad-4 and tripartite motif-containing protein 33 ((TRIM33) also known as transcriptional intermediary factor 1 gamma (TIF-1 γ)), influence these differential responses. TRIM33 is mainly known as an inducer of repressed gene activation by interaction with Smad-3, while Smad-4 mainly leads to induction of non-repressed genes. We studied these effects in non-stimulated Jurkat T cells, known to increase VISTA expression after TGF- β stimulation, in the THP-1 cell line, which downregulated VISTA expression in presence of TGF- β as well as MCF-7 cell line (no VISTA detectable at any time) and the non-malignant keratinocyte cell line HaCaT (upregulation of VISTA by TGF- β). We analysed the recruitment of both co-activators and determined if these had any effect on the VISTA expression. There was no detectable correlation found that indicate these co-activators influence VISTA regulation after TGF- β stimulation (Figure 51).

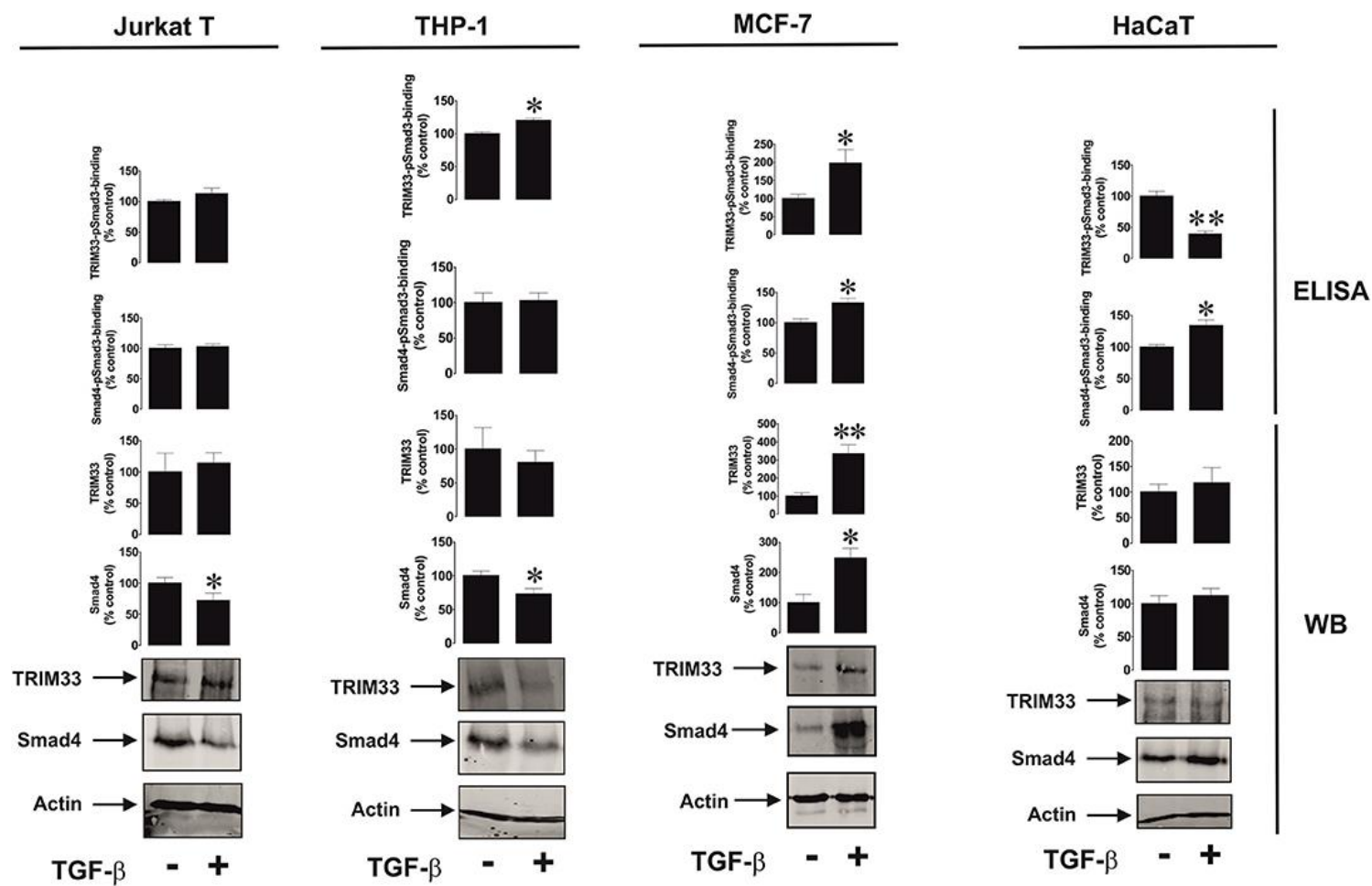


Figure 51 Investigation of VISTA expression in correlation with Smad-3-co-activator recruitment. Effects on co-activators to Smad-3 were investigated in different cell types including (A) Jurkat T cells, (B) THP-1 AML cell line, (C) MCF-7 breast cancer line, (D) non-malignant keratinocyte cell line HaCaT. Images are representative of four individual experiments, mean \pm SEM included. * p <0.05 and ** p <0.01 vs. non-stimulated samples.

3.2.2.2 Discussion.

The influence of VISTA on immunosuppression of cytotoxic T lymphocytes leading to anti-cancer immunity has been only reported recently. However, the exact biochemical mechanisms have yet to be understood (Lines, 2014; Yasinska, 2020). In this chapter we investigated how VISTA is expressed in different cell types. The gene encoding VISTA proteins, VSIR, has several response elements for Smad-3 to bind to. This caused the establishment of the hypothesis that similar to the regulation of galectin-9 expression, VISTA protein expression is induced by the TGF- β – Smad-3 autocrine/paracrine pathway. The experiments performed showed that in various cell types such as naïve Jurkat T cells, primary AML blasts, HaCaT keratinocytes, Wilms' tumour, and chronic AML cells TGF- β exposure induces an increase in VISTA proteins being expressed. Interestingly, other cell types including PMA-activated Jurkat T cells able to produce granzyme B, primary human T lymphocytes and cytotoxic TALL-104 as well as monocytic AML THP-1 cells downregulated the VISTA expression upon TGF- β stimulation.

A correlation between the ability of T cells to perform cytotoxic immune responses, mainly by the production and release of granzyme B, and a down-regulation of VISTA was observed. As mentioned in chapter 4.1 galectin-9 can interact with VISTA expressed on the surface of cytotoxic T cells leading to accumulation of granzyme B within the T cells themselves and activation. This indicates that the programmed cell death in cytotoxic T cells is dependent on VISTA expression. It is important to notice that in such cells the granzyme B production is downregulated after stimulation with TGF- β as seen in Figure 49D and 47. In monocytic AML cells with no detectable amounts of granzyme B a more complex biological response is the reason for these changes. The THP-1 cell line is hereby able to secrete high levels of galectin-9 after exposure to TGF- β , especially if these cells have been treated prior with triggers of exocytosis such as PMA (Selno, 2021). These cells are also able to secrete VISTA and a combination of both proteins in a certain ratio, which is most likely responsible for the inhibition of cytotoxic immune responses towards cancer cells. In THP-1 cells galectin-9 expression is upregulated by TGF- β stimulation, yet it does not cause secretion. The upregulation of VISTA might lead to a change in ratio of these two proteins as increased translocation to the surface might also induce shedding (Figure 50F). So, to ensure an appropriate ratio to inhibit immune responses this downregulation of VISTA is performed.

Furthermore, cells were only able to increase VISTA levels by TGF- β if they already expressed detectable amounts of it prior. MCF-7 cells do not express any VISTA in resting stage and therefore TGF- β applied does not lead to any expression of it (Figure 49G). As galectin-9 is Smad-3 dependent we also investigated its influence on VISTA expression. Knockdown of Smad-3 using siRNA attenuated the effects of TGF- β regarding VISTA upregulation. Investigating the mRNA levels, we were able to verify that Smad-3 binds directly to the promotor region of VISTA gene VSIG, which has been increased upon stimulation with TGF- β (Figure 50A and B).

Next, we were trying to understand how such differential responses to TGF- β is achieved in a variety of cell types. We investigated the influence of co-activators binding to Smad-3, mainly TRIM33 and Smad-4, but these were not responsible for such differences in VISTA expression. Cells like non-stimulated Jurkat T and THP-1 cells with opposing VISTA regulations did show a higher usage of Smad-4 leading to its reduction in quantity, yet TRIM33 recruitment by Smad-3 has not been affected. Analysis of MCF-7 also showed an increase in the amount and usage of both co-activators, but no detectable amounts of VISTA were found. In comparison HaCaT cells with a significant increase of VISTA levels after TGF- β exposure also showed an increase in Smad-4 recruitment while TRIM33 has been downregulated (Figure 51). Taking these results in consideration it is very unlikely that either of these co-activators influence VISTA expression levels after stimulation with TGF- β . If there is any correlation possible, it most likely is Smad-4 in combination with Smad-3 influencing the VISTA expression as TRIM33 is known to act in a de-repression way on target genes. As seen in Figure 49G, TGF- β has been unable to actively induce VISTA expression in MCF-7 breast cancer cells, in which VISTA is most likely repressed. Smad4 also applies most likely as a co-activator in the galectin-9 induction by TGF- β -Smad3 interactions in cells with very low levels prior stimulation.

Another option for regulation of responses to TGF- β might be the relocation of TGF- β receptors after the ligand has been bound. Dependent on the increased amount of ligands present, the number of active TGFBR might also increase on the cell surface. This phenomenon has already been reported regarding TGFBR as well as Toll-like receptors (TLRs) (Guglielmo, 2003; Mitchell, 2004; Barton, 2009). In such case cells with increased VISTA production might maintain a stable amount of TGFBRs on the cell surface or might even increase the levels after exposure to TGF- β . This would lead to the hypothesis that in cells downregulating VISTA the amount of TGFBR on the cell

surface is also decreased. A schematic showing this mechanism is found in Figure 52A. Yet, increased induction of Smad-3 phosphorylation was detectable in either down- or up-regulation of VISTA expression, indicating that this mechanism is most likely not applicable.

Another possibility is shown in Figure 52B regarding an involvement of ATF1 and other repressing transcription factors in VISTA expression. In granzyme B regulation ATF1 is known to be involved in a TGF- β and Smad-3-dependent downregulating effect (Thomas, 2005). ATF1 response elements are not found on the VISTA gene VSIR (response elements are ACGTAA and ACGTCC) in comparison to the granzyme B promoter region. So, if cells use ATF1 the stimulation with TGF- β causes the downregulation of granzyme B, while the effects on VISTA might be differential.

With the information gathered during the studies we conclude that most likely nuclear compartmentalisation, chromatin re-organization, is responsible for the regulation of VISTA expression in regard to TGF- β influence. This molecular mechanism is a recent phenomenon that came in focus regarding the regulation of differential gene expression and has been reported to influence T cell development (Meldi, 2011). In this mechanism the genes that are not needed at a specific timepoint are translocated to the periphery of the nucleus, while other genes needed are found at the centre. This could indicate that the down-regulation of VISTA is achieved by translocation to the periphery and the induction of genes by TGF- β and Smad-3 is concentrated on other genes, such as for galectin-9 to stay active within the centre of the nucleus. A schematic of this regulation is shown in Figure 52C.

T cell subsets that do not express granzyme B might use increased VISTA production to regulate immune responses of cytotoxic T cells. As apoptotic T cells release TGF- β into the environment an increase in VISTA production and shedding might be used to suppress cytotoxic T cells from uncontrollably attacking other cells, such as other malignantly transformed T cells (Chen, 2001).

To conclude in this chapter, we were able to show that both proteins negatively impacting anti-cancer immune responses are highly maintained by TGF- β and Smad-3 and malignant cells use this mechanism in significantly high levels. The interaction of both protein in a certain ratio leads to inhibition of cytotoxic immune responses and can in worst case induce cell death in cytotoxic T cells by accumulation and activation of granzyme B within themselves.

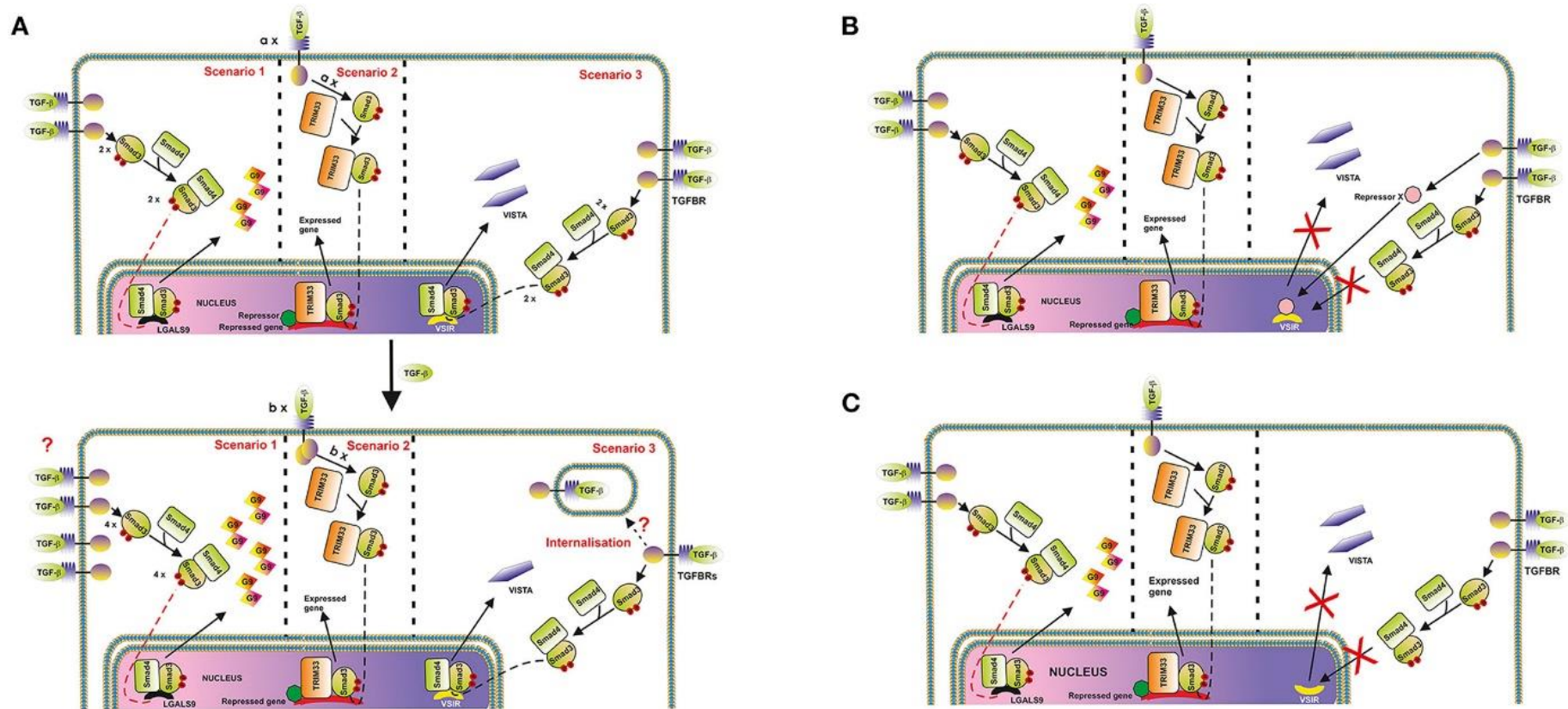


Figure 52 Schematic of different regulatory mechanisms for VISTA expression shown. (A) TGF-β receptor levels change dependent on if a protein is up- or downregulated. This can be achieved by TGF-β-Smad-3 regulation and the recruitment of co-activators Smad4 and TRIM33. “a” and “b” are used to represent protein molecules involved in the mechanism. (B) ATF1 or other transcription factors might be used to repress VISTA production. (C) Most likely nuclear compartmentalisation is used to translocate the VSIG-locus to the periphery leading to downregulation of VISTA during TGF-β exposure.

3.3 DANGER SIGNAL HIGH MOBILITY GROUP BOX 1 (HMGB1) LEADS TO ACTIVATION OF IMMUNE EVASION PATHWAYS IN CANCER CELLS BY UPREGULATING GALECTIN-9 PRODUCTION.

The non-histone protein high mobility group box 1 (HMGB1) is mainly located within the nucleus promoting specific nuclear transcription processes by DNA-interaction (Kang, 2013; He, 2017; Chiba, 2012). If a cell is damaged, dying or already dead HMGB1 can be released into the extracellular environment passively. Interestingly, cancer cells as well as certain immune cells are able to actively release HMGB1 due to endogenous or exogenous stimulation. In such cases HMGB1 acts as an “alarmin” also called “danger signal”, which can induce progression of malignant transformation. Furthermore, as reported already, HMGB1 is known to promote the production of interleukin-1beta (IL-1 β) as well as stimulating its secretion. This leads to the induction of stem cell factor (SCF) by competent cells, facilitating further progression of malignancies including AML (Yasinska, 2018).

Cells expressing immune receptors such as for example toll-like receptors 2 and 4 (TLR2 and TLR4) normally use these to recognize gram-negative and gram-positive bacteria by their molecular patterns and are able to bind HMGB1 as a ligand (Yasinska, 2018). Other known HMBG1 receptors also include receptor of advanced glycation end products (RAGE) and Tim-3 (Chiba, 2012, Yasinska, 2018). Binding such receptors causes activation of pro-inflammatory and -angiogenic processes. As already indicated by binding of HMGB1 to TLR4 an upregulation of TGF- β production is detectable, leading to paracrine and autocrine regulation of TGF- β , Smad-3 activation and lastly galectin-9 increase (Selno, 2020; Yasinska, 2020).

As the exact biochemical mechanism determining the influence of HMBG1 in its immunogenic form to escape cytotoxic immune responses remain poorly understood, we investigated these. The hypothesis refers to the ability of HMGB1 to induce TGF- β production after binding to TLR4 leading to increased galectin-9 levels. We investigate for the first time that the HMGB1-dependent anti-cancer immunity might be achieved mainly by it binding to TLR4 as a ligand. In cancer cells expressing TLR4 exposure to HMGB1 could increase TGF- β production and release inducing the galectin-9 production supporting the formation of an autocrine loop. In cancer cells lacking the corresponding receptor HMGB1 still might induce galectin-9 production by activating

for example tumour-associated macrophages and other TLR4-positive myeloid cells within the tumour microenvironment to produce TGF- β . Importantly, other HMGB1-associated receptors might not show any involvement in the induction of TGF- β upregulation.

3.3.1 PREPARATION AND ANALYSIS OF GOLD-NANOPARTICLES.

For immunoprecipitation gold-nanoparticles were prepared according to the procedure mentioned in Materials and Methods and visualized using transmission electron microscope, shown in Figure 53.

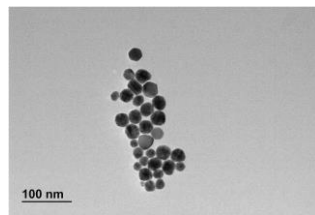


Figure 53. Gold nanoparticles used for HMGB1 immunoprecipitation visualized using Transmission Electron Microscopy (TEM).

These gold-nanoparticles were combined with antibody against HMGB1 to form nanoconjugates used to remove HMGB1 from medium, schematics shown in Figure 54.

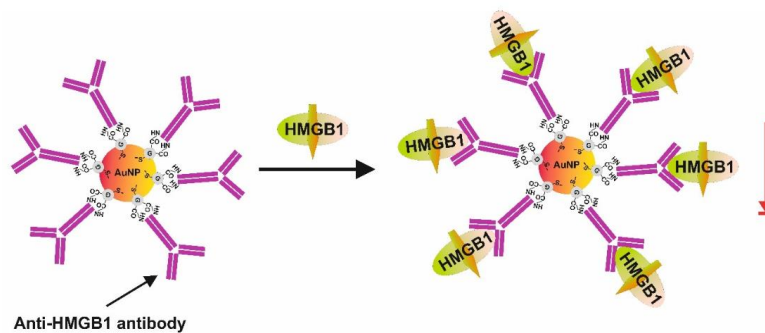


Figure 54. Process of gold nanoparticles HMGB1 immunoprecipitation visualized.

To test the efficiency of the immunoprecipitation, nanoparticles were analysed using either an ELISA-like approach with OPD and sulfuric acid to determine if antibody has bound onto the particles (Figure 55). In case of TGF- β -specific nanoparticles we exposed them to anti-mouse and anti-rabbit fluorescent dye from Licor and measured the fluorescence using the Li-Cor Odyssey CLX Imager (Figure 55)

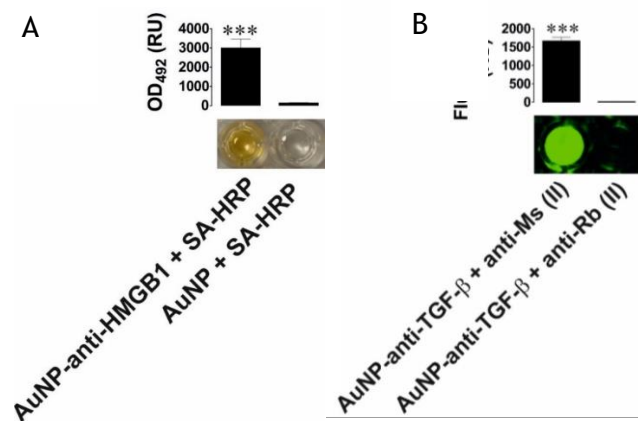


Figure 55. Analysis of antibody bound to gold-nanoparticles. Gold-nanoparticles with anti-HMGB1 antibody and naïve nanoparticles were exposed to HRP-conjugated streptavidin and analysed using OPD (A). gold-nanoparticles containing mouse anti-human TGF- β antibodies were exposed to anti-mouse and anti-rabbit secondary antibodies. Analysis was performed by detecting fluorescence with Odyssey C_{LX} imager (B). Each results contains a representative of three individual experiments, mean +/- SEM included.

3.3.2 HMGB1 INDUCED UPREGULATION OF TGF-B AND GALECTIN-9 IN TLR4-POSITIVE CELLS.

The first cell line we investigated regarding to HMGB1 was the AML cell line THP-1. The cells have been exposed to 1 μ g/ml of the immunogenic form of recombinant human HMGB1 for 24 h. Using the ELISA approach, we were able to detect significant increase in TGF- β as well as high levels of secreted galectin-9. By Western blot analysis we were able to also verify an increase in Smad-3 phosphorylation (Figure 56A) and a reduction of cell-bound as well as surface-associated galectin-9 (Figure 56B, C) due to the increased secretion. Altogether, we were able to determine an increase in galectin-9 production by combining values of cell-bound and secreted protein. Without stimulation, cells produced galectin-9 ranging at 890 +/- 48 pg/10⁶ cells. After HMGB1 stimulation levels rose to 2110 +/- 93 pg/10⁶ cells. The decrease in cell-bound galectin-9 clearly indicates that after increased exposure to TGF- β the proteolytic shedding activity of galectin-9 bound to Tim-3 as carrier also has been elevated. An increase in secreted Tim-3 has been detectable after induction of TLR-4 signalling by HMGB1 (Figure 56D). The THP-1 cell line contains four HMGB1 receptors – both TLR's, RAGE as well as Tim-3 (Figure 57).

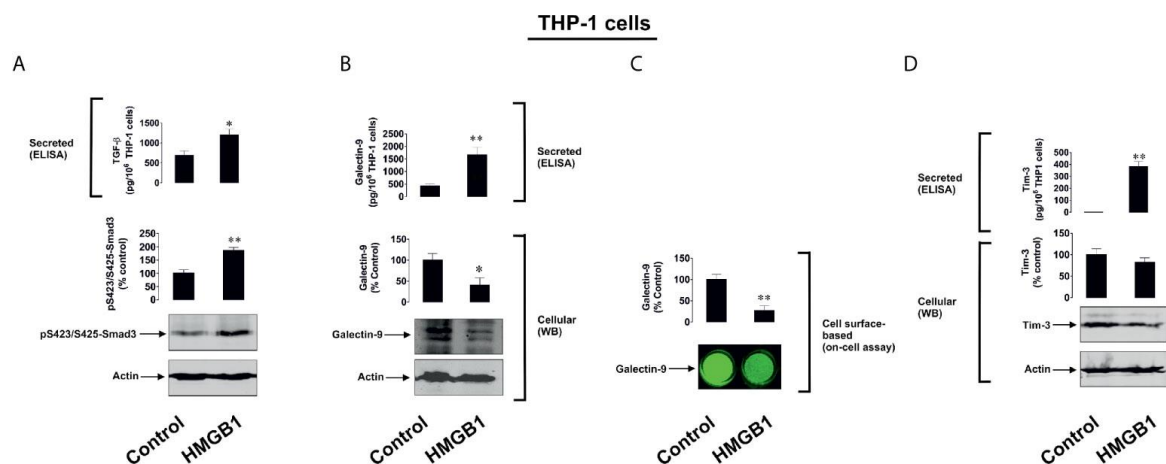


Figure 56 Investigation of THP-1 cells regarding HMGB1 exposure. In the human AML cell line exposure to HMGB1 led to an increase in TGF- β expression as well as Smad-3 phosphorylation (A). Overall galectin-9 levels increased with most of the protein being secreted (B), therefore, reducing cell-surface bound galectin-9 levels (C). Tim-3 release increased significantly (D). Data include values and representatives from four independent experiments, mean \pm SEM included. * $p < 0.05$, ** $p < 0.01$ vs. control.

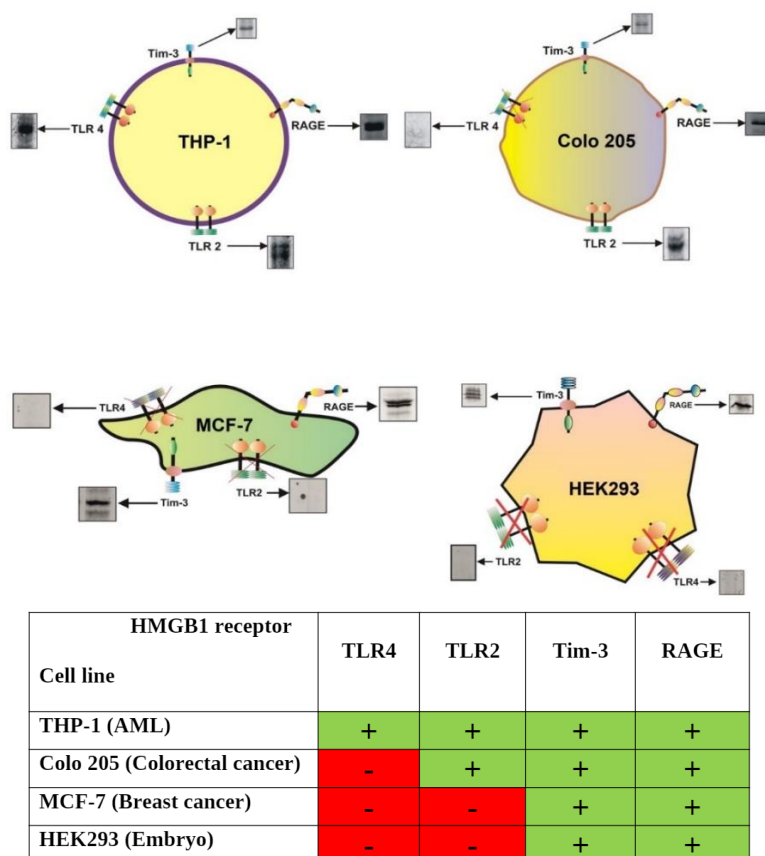


Figure 57 Study of various cells regarding their HMGB1 receptor expression. Each receptor – TLR2, TLR4, RAGE and Tim-3 – has been detected using Western Blot; values and representatives from four independent experiments, mean \pm SEM included. * $p < 0.05$, ** $p < 0.01$ vs. control.

To ensure that the results we have seen have been TLR-dependent we studied samples of primary AML cells from newly diagnosed patients. These cells were analysed using Western blotting and results have been taken in consideration for further investigation according to their receptor expression - only samples with RAGE and Tim-3 but none of the two TLR's – 2 and 4 – were chosen. These samples were exposed for 16 h to 2.5 $\mu\text{g/ml}$ HMGB1. None of the results seen in the studies of Figure 56 were found within those samples indicating that the effects seen are dependent on the interaction between HMGB1 and toll-like receptors leading to induction of TGF- β (Figure 58).

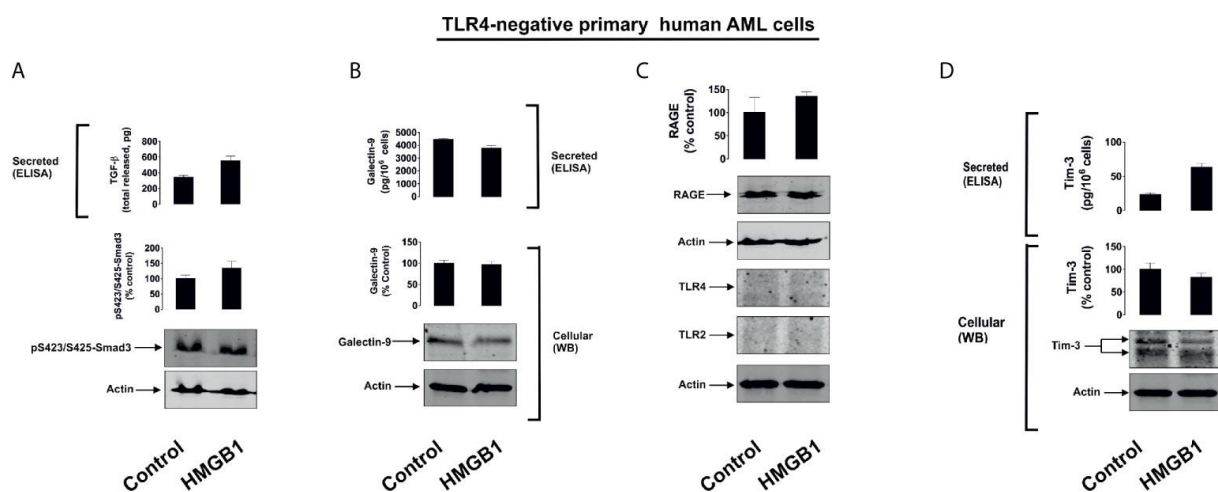


Figure 58 Investigation of TLR negative primary AML samples. Samples were chosen regarding their lack of expression of TLR2 and TLR4. In these samples stimulation with HMGB1 did not lead to significant increase of TGF- β and galectin-9 levels as well as release. Data contains representatives for four independent experiments, mean +/- SEM included.

Testing primary human AML cells expressing TLR's we were able to detect the same effects as in the THP-1 cell line after exposing these cells to 2.5 µg/ml HMGB1 for 16 h. Both Tim-3 and galectin-9 were significantly upregulated regarding to secretion (Figure 59).

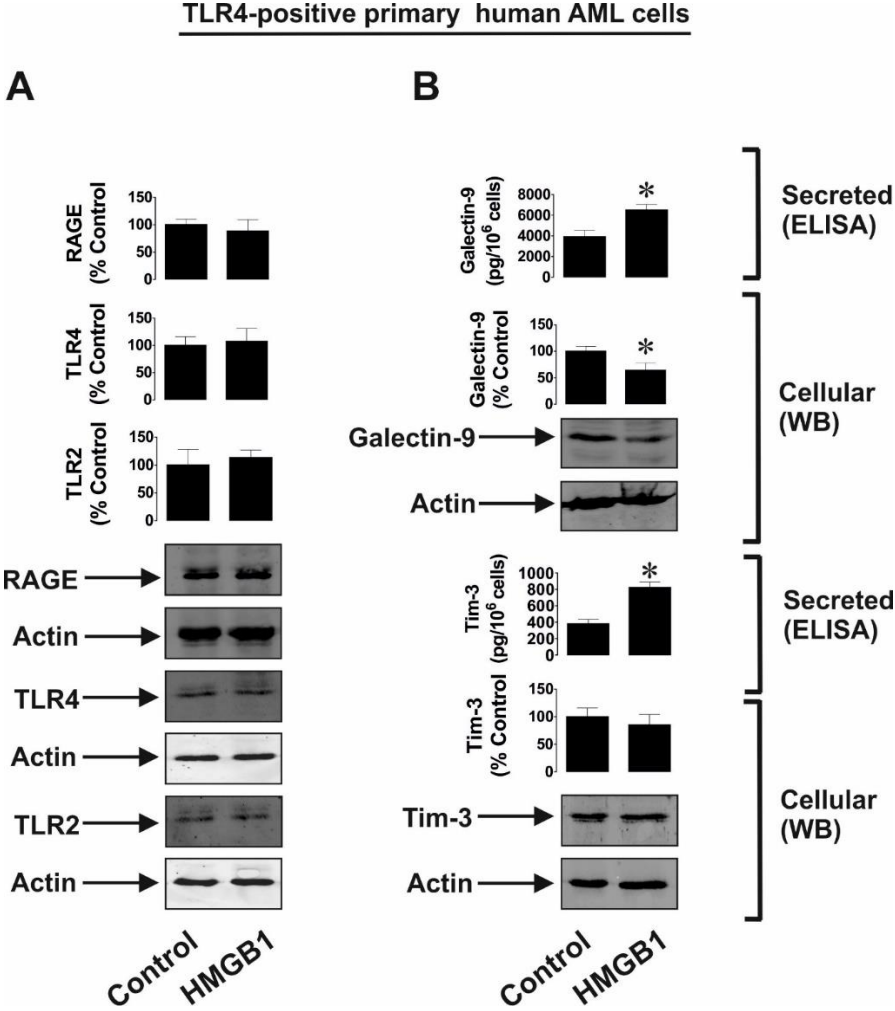


Figure 59 Investigation of primary AML samples expressing TLR4. 2.5 µg/ml HMGB1 induces increased galectin-9 and Tim-3 release in primary human AML samples expressing TLR4 and TLR2 as well as Tim-3 and RAGE after 16 h exposure. Receptor expression was investigated using Western Blot approaches (A). Changes in Tim-3 and galectin-9 expression levels and increased secretion has been determined using Western Blot and ELISA (B). Representative images included from three individual experiments, mean +/- SEM.

Next, we investigated the differential influences of TLR2 and TLR4 by using the following cell lines: human breast cancer cell line MCF-7, human colorectal cancer cell line Colo 205 and the human embryonic kidney cell line HEK293. As shown in Figure 57 MCF-7 and HEK293 express Tim-3 and RAGE but do not show any detectable levels of TLR2 and TLR4, while Colo 205 does express TLR2 as well as Tim-3 and RAGE. In these cell types investigated, only in the Colo 205 we were able to detect increased translocation of galectin-9 onto the cell surface after exposure to 1 μ g/ml of HMGB1 for 24 h (Figure 60C), yet the overall levels of expressed and secreted levels of galectin-9 did not increase significantly (Figure 60B). Furthermore, effects seen in the prior investigated AML cell line THP-1, such as increased TGF- β production and release as well as Smad-3 and Tim-3 upregulation were not detectable in Colo 205 (Figure 60A, D).

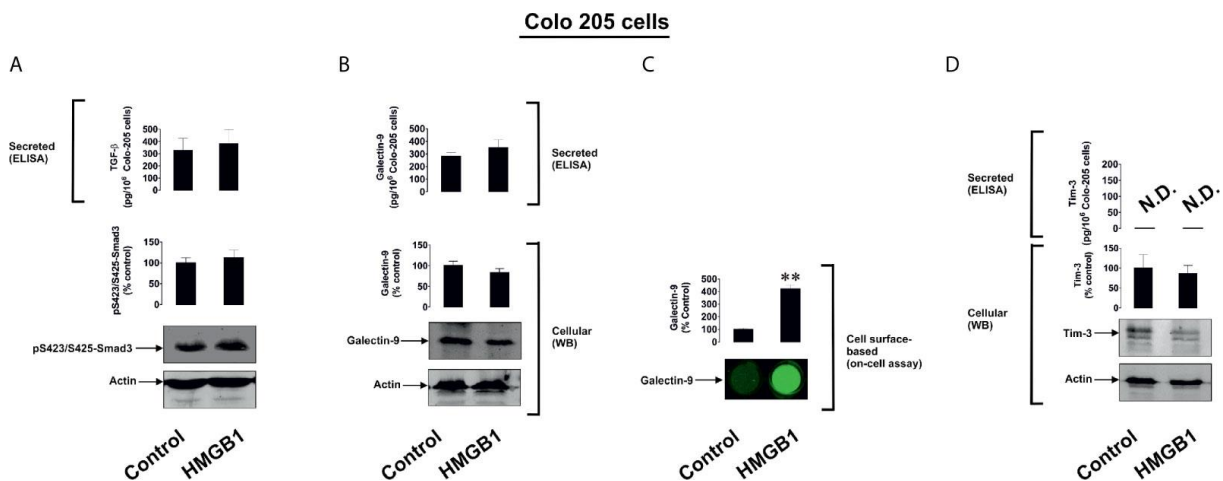


Figure 60 Investigation of HMGB1 influence on TLR2-expressing human colorectal cancer cells (Colo 205). Cells were exposed to 1 μ g/ml HMGB1 for 24 h. Galectin-9 expression and secretion levels remained same during HMGB1 treatment (B) but led to translocation onto the cell surface (C). TGF- β (A) and Tim-3 (D) did not increase indicating a need for TLR4 to be expressed. Data include representative images of four individual experiments, mean \pm SEM shown. ** $p < 0.01$ vs control. ND stands for non-detectable.

In other cell types investigated – MCF-7 (Figure 61) and HEK293 (Figure 62) – we did not see any change in the expression levels of either galectin-9, Tim-3 or TGF-β. These results clearly indicate that TLR4 expression and interaction with HMGB1 is needed for the expression changes seen in the AML cell line THP-1.

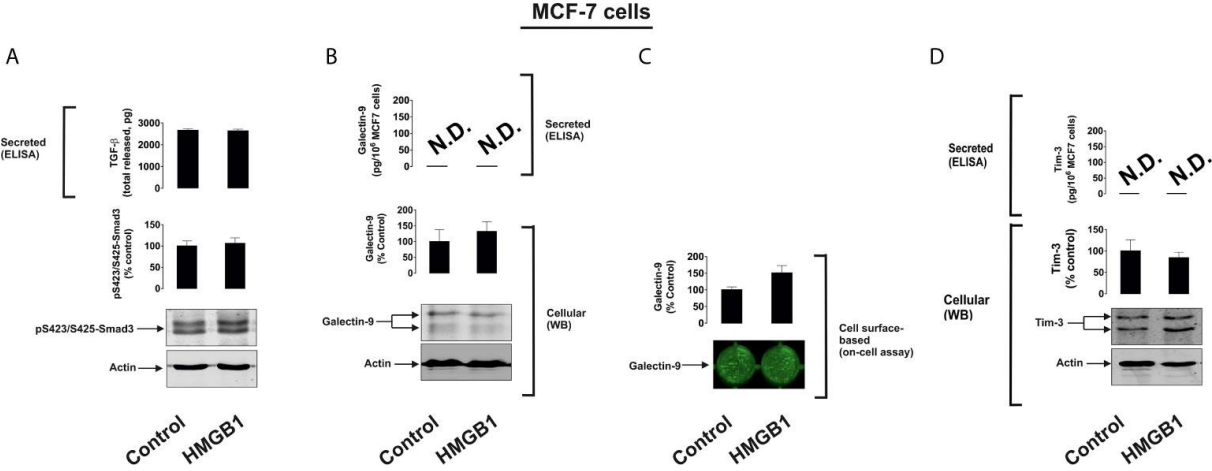


Figure 61 Investigation of HMGB1 influence on human breast cancer cell line MCF-7. Cells were exposed to 1 μg/ml HMGB1 for 24 h. Galectin-9 expression remained same and secretion levels were not detectable during HMGB1 treatment (B), yet a slight increase in translocation on cell surface has been determined (C). TGF-β (A) and Tim-3 (D) did not increase. Data include representative images of four individual experiments, mean +/- SEM shown. ND stands for non-detectable.

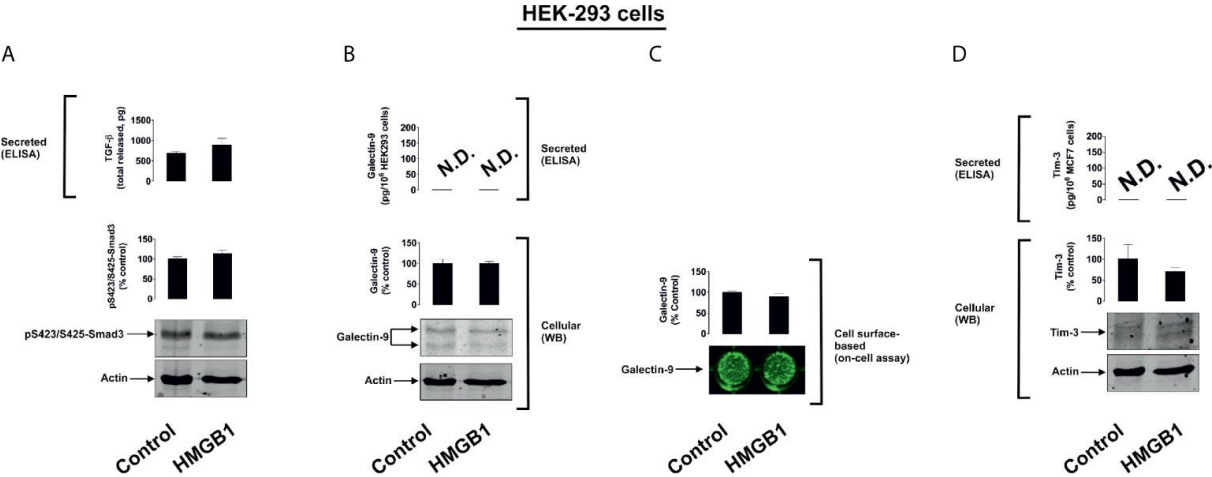


Figure 62 Investigation of HMGB1 influence on human embryonic kidney cell line HEK293. Cells were exposed to 1 μg/ml HMGB1 for 24 h. Galectin-9 expression levels remained same during HMGB1 treatment, and no secretion has been detectable (B). Furthermore, no increased translocation onto the cell surface was determined (C). TGF-β (A) and Tim-3 (D) did not increase significantly. Data include representative images of four individual experiments, mean +/- SEM shown. ND stands for non-detectable.

To verify that the effects seen were also caused by natural occurring HMGB1 in the human body, we studied this using TLR4-expressing cells. To do so we incubated several cell lines – MCF-7 breast cancer cell line, Colo 205 colorectal cancer cell line and THP-1 AML cell line – with 100 μ M BH3I-1 (5-[(4-bromophenyl) methylene]-a-(1-methylethyl)-4-oxo-2-thioxo-3-thiazolidineacetic acid) for 24 h. BH3I-1 is a synthetic, cell-permeable antagonist to Bcl-XL, causing loss of function within the mitochondria by inhibition of interactions between BH3 domain and Bcl-XL which will lead to apoptosis. Exposure to BH3I-1 caused the highest increase of HMGB1 release in THP-1 cells, an increase was detectable in the other cell lines, yet not in such levels as in the THP-1 cell line (Figure 63).

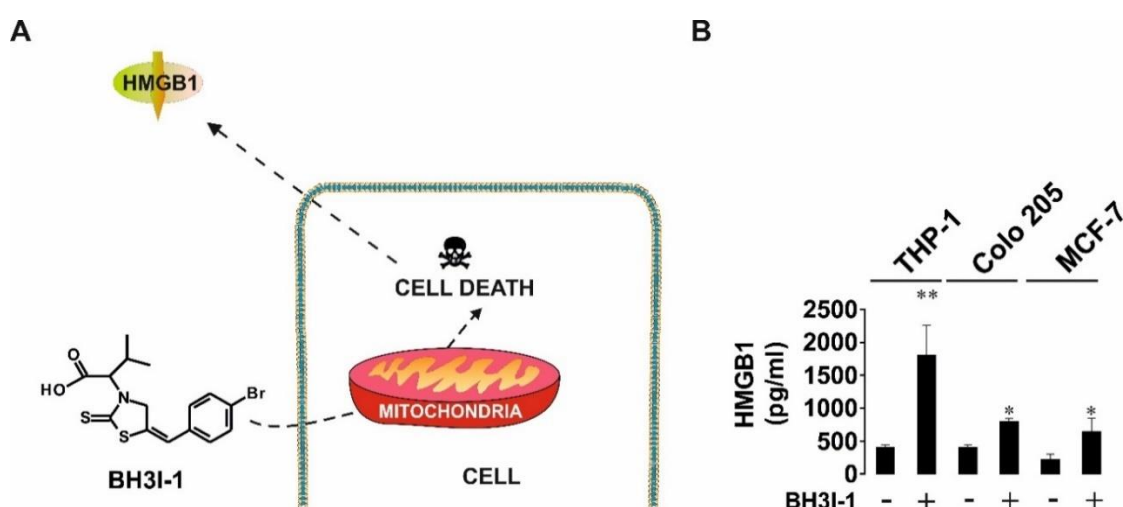


Figure 63 HMGB1 release triggered by exposing cells to apoptosis inducer BH3I-1. Cells were exposed to 100 μ M BH3I-1 for 24 h (A), cell lines used were AML cell line THP-1, breast cancer cell line MCF-7 and colorectal cancer cell line Colo 205. HMGB1 release has been investigated using ELISA (B). Data set include three individual experiments, mean +/- SEM shown. *-p<0.05 and **-p<0.01 vs control.

To ensure that these results physiologically correlate with detectable levels in cancer patients we compared primary samples gathered from healthy donors with primary cancer cell patients; breast cancer (as a solid tumour example) as well as acute myeloid leukaemia (as a non-solid tumour example) patients. For each set we analysed five samples, highest detectable levels within the blood plasma have been found in AML patients, suggesting that released HMGB1 stays in solid tumours within the tumour microenvironment (Figure 64).

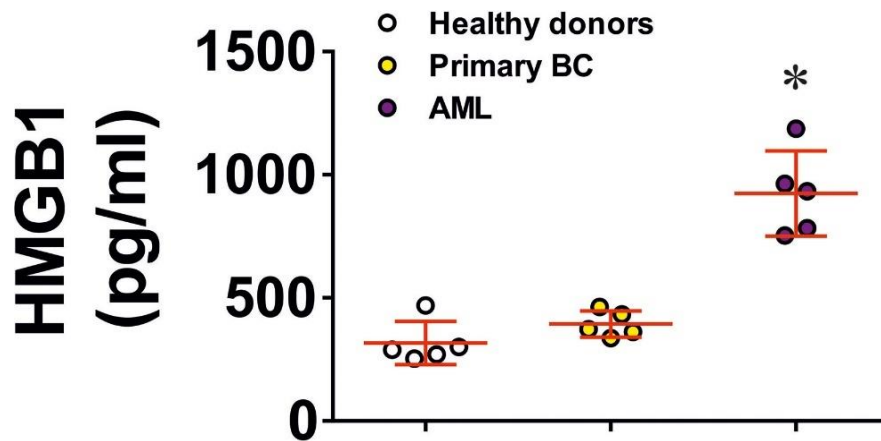


Figure 64 HMGB1 level investigation in primary samples. Five samples of either healthy donors, primary breast cancer patients or acute myeloid leukaemia patients were investigated. Data include mean \pm SEM of five independent measurements as well as each sample is shown individually. * $p < 0.05$ vs. healthy donor.

In consistency with results achieved so far, we chose the THP-1 AML cell line as most efficient HMGB1-releasing cells. These cells were treated for 24 h with 1 mM hydrogen peroxide and released about 13.14 \pm 0.37 ng/ml HMGB1, schematics of process shown in Figure 65A. Hydrogen peroxide was degraded in the medium using 5 mg/ml horseradish peroxidase and the medium has been used to treat macrophage-differentiated THP-1 cells expressing high levels of TLR4 (achieved by pre-exposing these cells to 100 nM PMA) for 24 h. For the control sample, we exposed the PMA-treated THP-1 cells with the same medium after precipitation of HMGB1 using gold-nanoparticles conjugated with anti-HMGB1 antibody as described in Materials and Methods. Exposure to medium containing HMGB1 led to an increase of TGF- β production ranging at ca. 15 ng/ml, clearly indicating that naturally produced HMGB1 caused higher biochemical activity than recombinant proteins. Medium containing naturally produced TGF- β was used to stimulate the MCF-7 breast cancer cell line, for control we immunoprecipitated TGF- β using again gold nanoconjugates with anti-TGF- β antibodies. Exposure to TGF- β significantly increased galectin-9 production in the breast cancer cells (Figure 65A).

To confirm the results seen being dependent on TLR4-expression we decided to use Colo 205 cells naturally lacking TLR4 and transfected these cells with active TLR4 using mCD4-hTLR4 constructs (human intracellular and transmembrane proteins of TLR4 fused with extracellular mouse CD4 domain) provided kindly by Prof. Ruslan Medzhitov, Yale University, USA. The induction of TLR4 presence lead to an increase of galectin-9 secretion and reduced the cell-associated levels. To verify these results,

we also measured the cell-associated levels by ELISA, as seen with Western Blot the cell-bound galectin-9 levels were greatly reduced while the total amount of galectin-9 produced significantly increased after transfection. An increase in Tim-3 secretion of about $95 \pm 9 \text{ pg}/10^6 \text{ cells}$ has also been detectable after transfection (Figure 65B), as well as an upregulation of TGF- β and Smad-3 phosphorylation (Figure 65C).

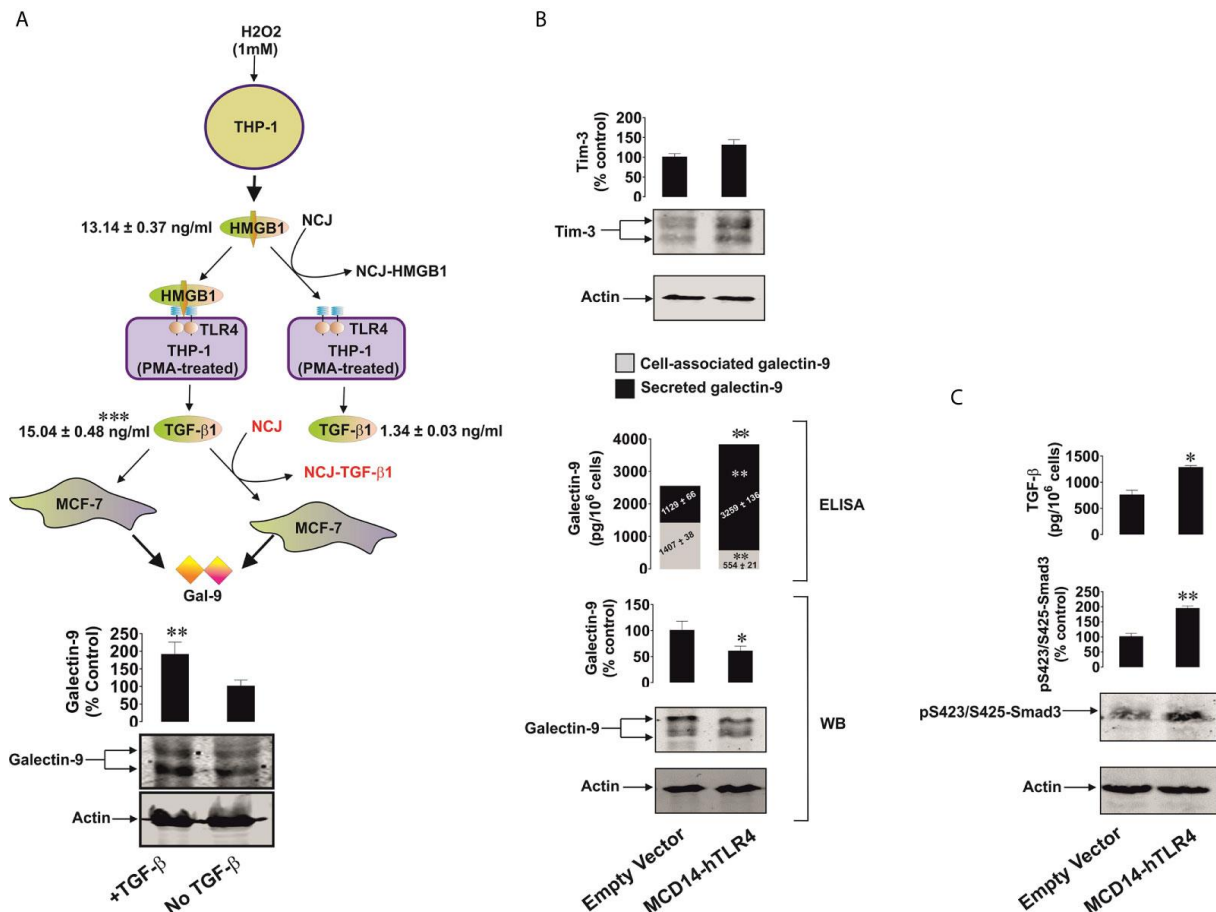


Figure 65 HMGB1 stimulation of TLR4-positive cells leads to induction of TGF- β expression and consequently to galectin-9 upregulation by cancer cells. Transfection with active TLR4 causes same effects as seen with HMGB1 stimulation. (A) THP-1 AML cell line has been stimulated for 24 h with 1 mM H_2O_2 inducing HMGB1 production, medium was collected for further use. The medium was treated with horseradish peroxidase to remove any H_2O_2 left and separated into two parts. In one part HMGB1 was immunoprecipitated and both mediums with and without HMGB1 were used to stimulate PMA-pre-treated THP-1 cells for 24 h. This medium was collected and one part immunoprecipitated against TGF- β . MCF-7 breast cancer cells were incubated with or without immunoprecipitated medium for 24 h. Galectin-9 levels were investigated after incubation. (B) Colo 205 cells were transfected with active TLR4 and incubated for 24 h afterwards. Galectin-9 release increased significantly, as well as Tim-3 analysed by Western Blot and ELISA. (C) Transfection with active TLR4 also increased TGF- β and phosphorylation of Smad-3. Data include representatives of four independent experiments, mean \pm SEM shown. * $p < 0.05$ and ** $p < 0.01$ vs. control.

3.3.3 DISCUSSION.

HMGB1 has been thoroughly studied in the last decade as a “danger signal” during cancer progression indicating its clearly significant role during cancer immune response evasion, yet the exact biochemical mechanisms leading to furthering cancer progression still need to be investigated (Kang, 2013, He, 2017, Chiba, 2012, Yasinska, 2018). We focussed our research in this chapter on investigating the effects of HMGB1 on TLR4-positive cancer cells and its ability to induce TGF- β production and secretion. Toll-like receptor 4 is known to be activated by the recognition of lipopolysaccharides (LPS) as well as endogenous stimuli like hyaluronic acid, leading to the production of TGF- β . Furthermore, it has also been proven that HMGB1 induces TGF- β production in TLR4-positive cells by activation of the transcription factor for activator protein 1 (AP-1) and its downstream signalling pathway (Selno, 2020). Similar to LPS, HMGB1 expresses ligand properties towards TLR4 and therefore can possibly act in a similar way. Studies have also indicated that the induction of TGF- β by HMGB1-mediated signalling can be dependent on the hypoxia-inducible factor 1 (HIF-1) transcription machinery, which is significantly upregulated downstream of the TLR4 receptor. By activation of HIF-1, TGF- β secretion is also upregulated causing auto- and paracrine self-maintenance of cancer cells inducing galectin-9 production by Smad-3 phosphorylation as reported in earlier chapters. This will lead to a galectin-9-dependent suppression of immune responses of natural killer and cytotoxic T cells. Such effects dependent on HMGB1 stimulation were seen in the human AML cell line THP-1 as well as primary, TLR4-positive AML samples. The results reported in this chapter also show that cells not expressing TLR4 but other HMGB1 receptors such as Tim-3, TLR2 and RAGE, did not increase the TGF β levels upon HMGB1 stimulation. This is seen in TLR4-negative, primary AML samples (Figure 58), MCF-7 (Figure 61), HEK293 (Figure 62) as well as Colo 205 (Figure 60). Due to the lack of TGF- β upregulation, no induction of galectin-9 production was detectable. Yet, in the tumour microenvironment other cells are present that express TLR4 such as tumour-associated macrophages. These cells can recognize HMGB1 as a ligand and continuously produce TGF- β leading to an induction of galectin-9 production by cancer cells, creating an immunosuppressive milieu surrounding these cancer cells (Suga, 2014). TGF- β not only leads to the suppression of granzyme B activity within cytotoxic T cells but can also induce the differentiation of naïve T cells into regulatory T cells (Treg) which are able to further

the suppression of cytotoxic T cell activity (Thomas, 2018). A schematic visualizing the proposed pathway is shown in Figure 66.

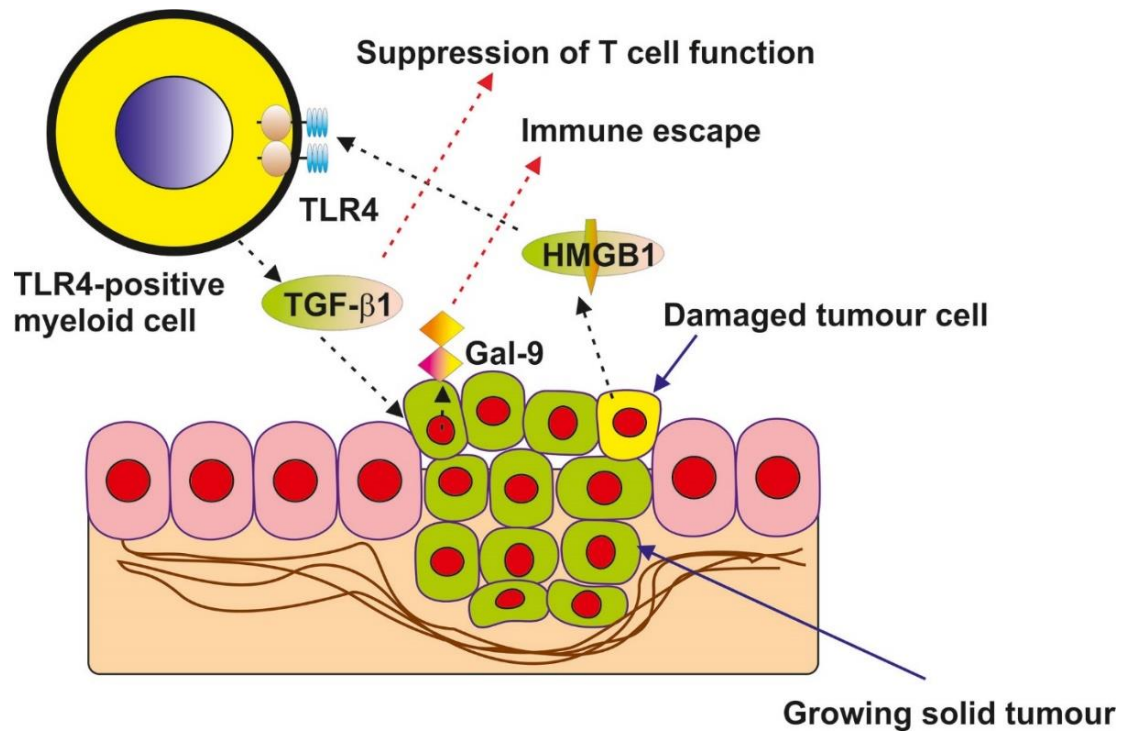


Figure 66 Schematics visualizing the proposed pathway of HMGB1 influencing immune suppression. Damaged cancer or immune cells release HMGB1 as a “danger signal” leading to further recruitment of immune cells. Yet, HMGB1 is able to bind to TLR4-positive cancer cells and cancer-associated cells such as tumour-associated macrophages leading to the production of TGF-β. Increased levels of TGF-β in the tumour microenvironment causes on the one hand a para- and autocrine regulation of further TGF-β production as well as induction of galectin-9 secretion. On the other hand, does TGF-β also induce the suppression of granzyme B production within cytotoxic T cells and induces the differentiation of naïve T cells into regulatory T cells enabling further suppression of immune responses towards the cancer cells. Taking these processes together HMGB1 is most likely to support further tumour growth.

3.4 FUNDAMENTAL BIOCHEMICAL FUNCTIONS OF GALECTIN-9 AND VISTA IN IMMUNE EVASION CHECKPOINT PATHWAYS.

In our studies we investigated the origin of galectin-9 as it has been found within not only cancer cells but in the human body also arises from the embryonic development. This indicates that this pathway consisting of galectin-9, Tim-3 and VISTA is a conserved way of survival. The galectin protein family, firstly identified to be able to bind to specific carbohydrates containing β -galactosides has been studied regarding its influence in suppressing immune responses; in focus are especially galectin-1, galectin-3, galectin-7 and recently also galectin-9 (St-Pierre, 2011). Furthermore, studies have shown the galectin family protein members to be expressed in vertebrates, invertebrates as well as protists (Cooper, 2002). In this chapter we specifically focussed on the expression of galectin-9, if it is to be found in other organisms which indicates that it is conserved throughout evolution. We also decided to investigate the function of galectin-9 regarding immune stimulation and its function prior the adaptation to cancer immunoregulation.

3.4.1 CONSERVATION OF GALECTIN-9 DETECTABLE IN OTHER ORGANISMS.

Galectin-9 is a protein consisting of a tandem structure with two very distinctive carbohydrate recognition domains found within one polypeptide linked by a peptide linker. As it is a very sturdy protein discovered already in a variety of organisms we will investigate when exactly it appeared within the evolutionary tree. One organism we investigated during this thesis were molluscs (*Mytilus galloprovincialis*), which are able to develop and transmit across the population a form of haemolympic malignancy on their own called bivalve transmissible neoplasia (BTN). Other organisms that are known to produce galectin-9 in a variety of situations are primates, including humans, as well as rodents, such as mice and rats.

Molluscs (from the Black Sea) were kept for 5 days in three 10 L tanks with each containing exactly 25 molluscs. In tank 2 and 3 we added 10 million malignant cells inducing BTN at the very beginning in presence of 10 mM lactose supplied to the third tank. After 5 days we collected haemolymph and subjected to investigations. These experiments were performed in collaboration with Dr Yuri Kvach from the Institute for Marine Biology, NAS of Ukraine (Odessa, Ukraine), who provided samples ready for

biochemical analysis. Galectin-9 is conserved in evolution – detectable by Western Blot in samples from molluscs as shown in Figure 67, which can be further induced by the presence of malignant cells in the surrounding water. Future research will be done to investigate other samples from organisms found throughout the evolutionary tree.

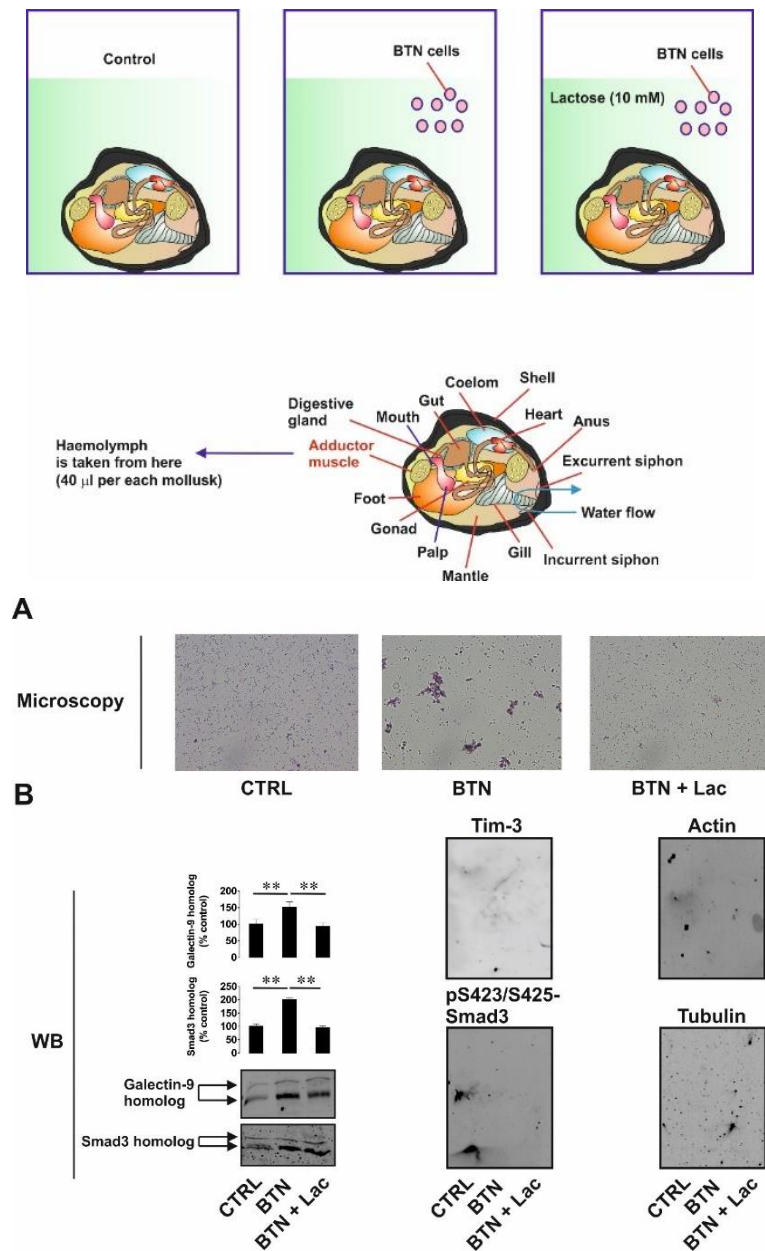


Figure 67 Investigation of galectin-9 expression in molluscs in presence and absence of malignant cells. (Up) Healthy molluscs were exposed to malignant cells in presence and absence of lactose and reactivity of these organisms towards such cells were investigated. (Lower, A) Visual changes of immune cells within molluscs after exposure. (Lower, B) Smad-3 and galectin-9 were upregulated in presence of malignant cells, effects which were attenuated by lactose. mean +/- SEM shown. * $p < 0.05$ and ** $p < 0.01$ vs. control.

3.4.2 BIOCHEMICAL FUNCTION OF GALECTIN-9 DIRECTING INNATE IMMUNE REACTIONS AGAINST GRAM-NEGATIVE BACTERIA AS WELL AS T CELL APOPTOSIS.

In the human immune system galectin-9 is one of the most important galectins due to its ability to suppress immune responses of cytotoxic T cells and NK cells. As reported in the previous chapters, galectin-9 acts on cytotoxic T cells by using its corresponding receptors such as Tim-3 and VISTA (Yasinska, 2020). This can induce the leakage of granzyme B within T cells themselves and consequently lead to programmed cell death. In regard to the embryonic development this process is used to inhibit natural killer cell activity by the interaction of galectin-9 with Tim-3 protecting the foetus from being rejected by the mother's immune system. Galectin-9 has also been investigated regarding its influence on the promotion of phagocytosis of gram-negative bacteria by neutrophils due to opsonisation (Vega-Carrascal, 2014). The exact role of galectin-9 influencing biochemically both anti-bacterial immune defence as well as inhibition of immune responses by T cells is yet to be understood. In this chapter we investigate the binding capability of galectin-9 to gram-negative bacteria and report LPS as the corresponding binding partner, a crucial component of the bacteria's cell wall. This opsonization leads to two effects: on the one hand, increased binding of galectin-9 causes decreased motility of gram-negative bacteria whilst on the other hand also enhances innate immune responses of macrophages such as the production of pro-inflammatory cytokines, including IL-1 β , IL-6 and tumour necrosis factor α (TNF- α). By investigating gram-positive bacteria, we are interested to determine if the ability to detect this opsonization process is dependent on gram-negative bacteria structures being present as no significant binding to the gram-positive bacteria wall component peptidoglycan (PGN) might be detectable. Cell-bound galectin-9, such as present on embryonic cells, should not show any bacteria-binding ability and therefore does not lead to colonization of bacteria on such cells. Yet, galectin-9 bound on cells e.g. cancer and foetal cells as well as secreted galectin-9 might be able to induce a similar way of "opsonization" of T cells by macrophages. The induction of TGF- β and especially HMGB1 by galectin-9 in embryonic and cancer cells also enhances phagocytosis of dying T cells by macrophages.

3.4.2.1 Opsonization of gram-negative bacteria via LPS galectin-9 enables their phagocytosis leading to the enhancement of innate immune responses against bacteria.

Direct interactions are needed for galectin-9 to opsonize gram-negative bacteria. To start we decided to investigate the reactivity of galectin-9 with the gram-negative bacteria wall component LPS and how it influences the ability of macrophages to phagocyte these bacteria. Macrophages were formed by treating THP-1 cells with 100 nM PMA for 24 h. After differentiation was achieved the medium was replaced with RPMI containing no PMA as well as no antibiotics. Next, the cells were co-cultured with 50 μ l *E. coli* XL10 Gold® in standard cell culturing conditions (37 °C, 5% CO₂) for 16 h with or without 10 mM lactose to inhibit the ability of galectin-9 to bind to sugar components (Figure 70A). 10 mM was a high enough concentration of lactose to block sufficiently binding of THP-1-originating galectin-9 without causing any effect on the overall survival of these cells, as tested using the MTS assay, or on the proliferation efficiency, determined by cell count.

After co-culture bacteria were removed by washing with sterile PBS and the THP-1 cells were permeabilized using methanol, bound LPS was detected using an LPS-directed in-cell Western approach (Figure 70B). Hereby, we found significant amount of LPS within the THP-1 macrophages, this effect has been highly inhibited if lactose was present during the co-culture (Figure 70B). Furthermore, presence of bacteria led to the cells producing high levels of cytokines such as IL-1 β , IL-6 and TNF- α , which also have been clearly attenuated by the presence of lactose (Figure 70C). We also investigated levels of galectin-9, Tim-3, and VISTA present after the co-culture. The values detected were 8.7 +/- 1.1 ng/10⁶ cells galectin-9 in presence of bacteria, 1.12 +/- 0,2 ng/10⁶ cells of Tim-3 and 0.91 +/- 0.14 ng/10⁶ cells of VISTA, which were not found in such levels if lactose was added to the culture.

We also investigated the bacteria removed from the co-culture by lysing them and analysing the extracted cytoplasmic components using Western Blot for galectin-9 presence. No galectin-9 was detectable in the cytoplasm (Figure 70D, left side).

Next, we analysed the cell pellet also containing the cell walls and therefore LPS by exposing it for 1 h to a biotinylated anti-galectin-9 antibody. The pellet was washed 3 times with PBS and streptavidin labelled with horseradish peroxidase (HRP) was added for another 1 h of incubation. After incubation the binding was visualized according to the method given in Materials and Methods. Lysed bacteria without co-

culture did not have any detectable amount of galectin-9 bound on the cell pellet, while the co-culture lead to a significantly high amount of galectin-9 found in the bacterial cell pellet. Lactose led to a reduction of this effect (Figure 70D, right side).

As Tim-3 and VISTA are corresponding interaction partners with galectin-9 we also investigated their presence in the bacterial cell pellet. The same detection approach as with galectin-9 was used with either anti-Tim-3 or anti-VISTA antibody instead. Both were clearly increased in presence of galectin-9 after co-culture and the effect was also reduced after exposure to lactose. To verify that the detection of Tim-3 and VISTA is dependent on galectin-9 presence and not by direct interaction with the bacteria itself we incubated bacteria with either 1 μ M of recombinant, human galectin-9, Tim-3, VISTA, or a combination of 1 μ M of galectin, VISTA, and Tim-3 for 1 h (visualized in scheme seen in Figure 68). The data collected clearly show that Tim-3 and VISTA are dependent on galectin-9 bound to LPS to be detectable, verifying that VISTA and Tim-3 only associate with bacteria in presence of galectin-9 (Figure 69).

Lastly, we decided to determine if galectin-9 is binding specifically LPS. This was achieved by preparing an ELISA plate with anti-LPS antibody at a concentration of 3 μ g/well and afterwards addition of immobilized 1 μ g/well LPS from *P. aeruginosa*. After LPS has been bound to the plate blood plasma from healthy donors was added to each well in presence and absence of 30 mM lactose, containing following protein concentrations: 520 pg/ml galectin-9, 335 pg/ml VISTA and 7990 pg/ml Tim-3. A high concentration of lactose had to be used due to the viscosity of plasma and other proteins potentially able to bind lactose. We investigated the concentration of bound galectin-9, VISTA, and Tim-3 in these wells. As seen prior galectin-9 enables the detection of LPS-associated Tim-3 and VISTA, which can be easily attenuated in the presence of lactose (Figure 70E).

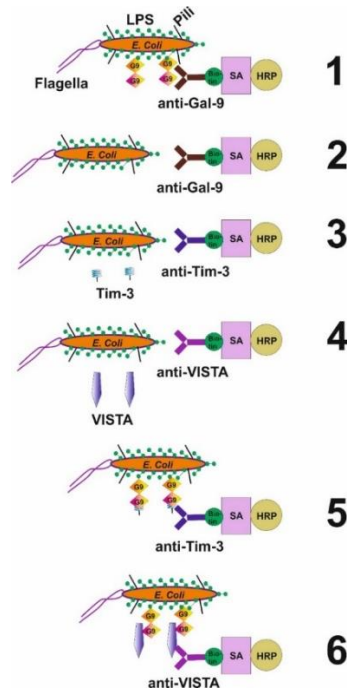


Figure 68 Scheme of experimental approach to determine if VISTA and Tim-3 are capable to associate with bacteria in absence of galectin-9. Bacteria were incubated with target-specific antibodies (against galectin-9 in its presence and absence, against Tim-3 and against VISTA) and signal was detected similar to ELISA analysis. To verify the binding capability of VISTA and Tim-3 in presence of galectin-9 a combination of these proteins was also used for incubation.

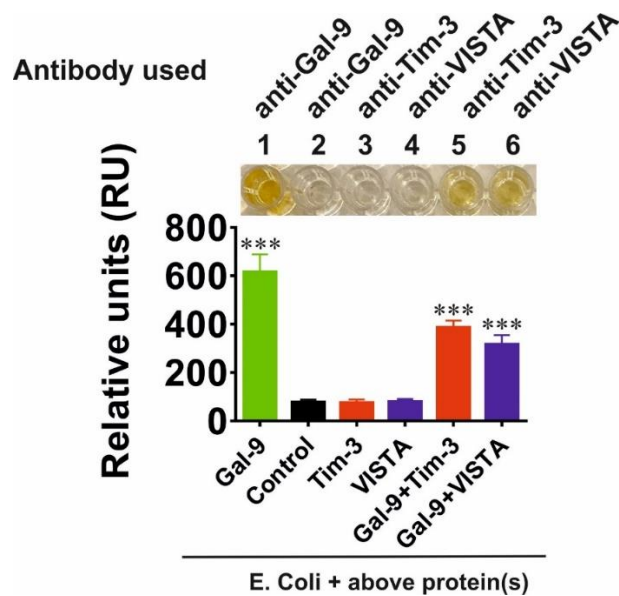


Figure 69 Tim-3 and VISTA are capable of interacting with bacteria only in presence of galectin-9. E. coli bacteria were exposed to either 0.1 μ M galectin-9, VISTA, Tim-3, or a combination of these proteins for 1 h. After exposure bound protein was detected similar to ELISA approach. Representative picture shown of three individual experiments, mean +/- SEM included. ***- $p < 0.001$ vs. control

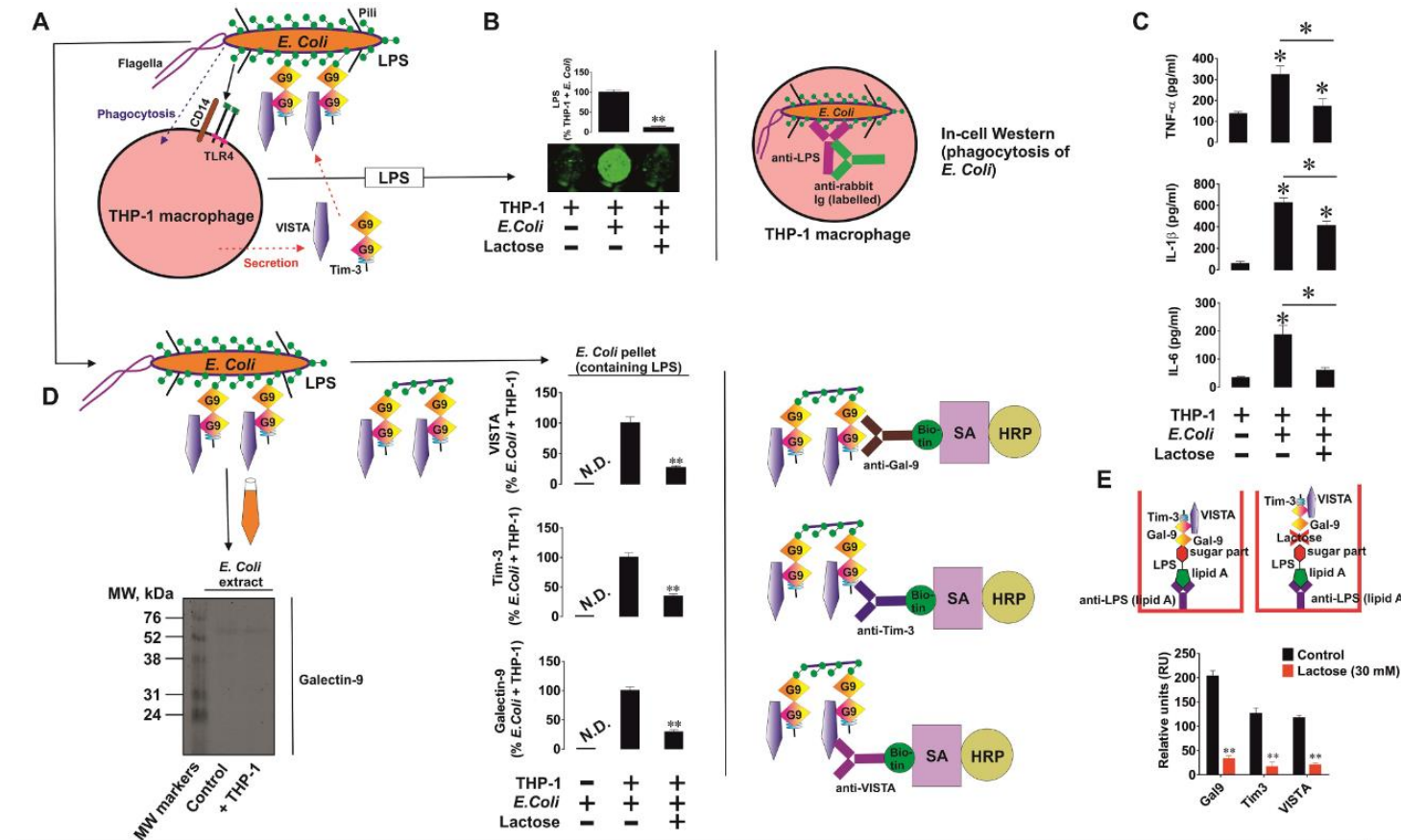


Figure 70 Galectin-9 induces opsonization of gram-negative bacteria via LPS binding, leading to phagocytosis of the marked bacteria and induction of innate immune system cells secreting cytokines (A) PMA induces differentiation of THP-1 monocytes to macrophages. These cells were kept in culture with E. coli bacteria for 16 h in presence and absence of 10 mM lactose. (B) In-cell Western was used to determine phagocytosis of bacteria. (C) Release of innate immune cytokines IL-1 β , IL-6 and TNF- α has been assessed by ELISA. (D, left) Bacteria collected after co-culture were lysed and galectin-9 was investigated in cytosol. (D, right) The pellet containing bacterial cell wall was investigated regarding bound galectin-9 and its corresponding partners Tim-3 and VISTA. (E) LPS-specific binding of galectin-9 and its associated proteins Tim-3 and VISTA was analysed. Results included of five independent experiments, mean \pm SEM *- p <0.05 and **- p <0.01 vs control.

To verify the effectiveness of galectin-9 binding to bacterial cell wall via LPS we incubated 50 μ l of whole *E. Coli XL10 Gold®* bacterial cells with 500 μ l of healthy donor blood plasma with or without 30 mM lactose consisting of 460 pg/ml galectin-9, 285 pg/ml VISTA and 410 pg/ml Tim-3. The bacteria were precipitated after incubation, and we investigated the levels of galectin-9, VISTA, and Tim-3. In absence of lactose the proteins were clearly associated with bacteria (Figure 71). This association was significantly downregulated in presence of lactose.

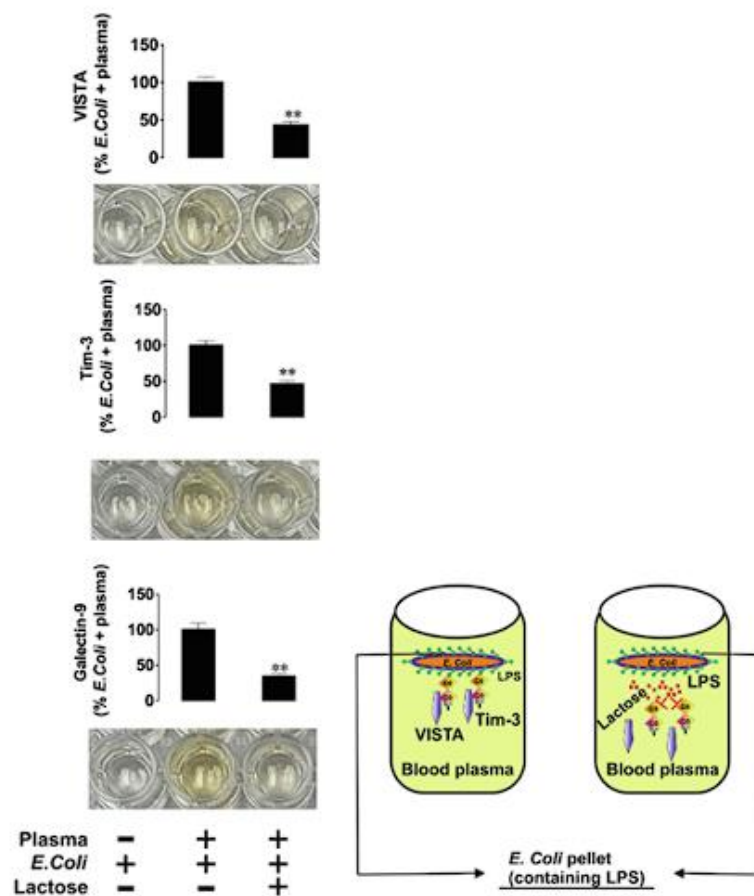


Figure 71 Galectin-9 found in human blood plasma is able to opsonise gram-negative bacteria.

Human blood plasma of healthy donors was used to co-incubate *E. Coli XL10 Gold®* cells in presence or absence of lactose (30 mM). These bacterial cells were investigated regarding the binding of galectin-9, Tim-3, and VISTA on their surface. Five individual experiments were performed with a representative as well as mean \pm SEM shown. **- $p < 0.01$ vs. control.

Lastly, we decided to verify that the binding of bacteria is only found by gram-negative expressing LPS and not gram-positive with peptidoglycans (PGN) on their surface. This was tested by coating wells of an ELISA plate with 5 μ g PGN in each and added blood plasma from a healthy donor containing 560 ng/ml galectin-9. We also incubated

some of the coated wells with 500 ng recombinant human galectin-9, which amounts to about 20 % of the added PGN values for each well. We chose such a high amount of galectin-9 to sufficiently enable any possible interaction between the substances within each well – galectin-9 and PGN. As a confirmation that each well was sufficiently coated with PGN we also incubated some with THP-1 cell lysates containing a PGN receptor, TLR2. The presence was verified using an ELISA approach. We were able to detect no significant interactions between galectin-9 from blood plasma and PGN (Figure 72), yet high amounts of recombinant galectin-9 (1000x higher as in the human blood plasma) did lead to traces of interactions. As a positive control regarding the coating of wells with PGN and its immobilization TLR2 was clearly detectable to be bound. These results verify that at a physiological concentration found in the human body galectin-9 is not able to interact with gram-positive bacteria and thus opsonization of bacteria by binding of galectin-9 can only be achieved at gram-negative bacteria.

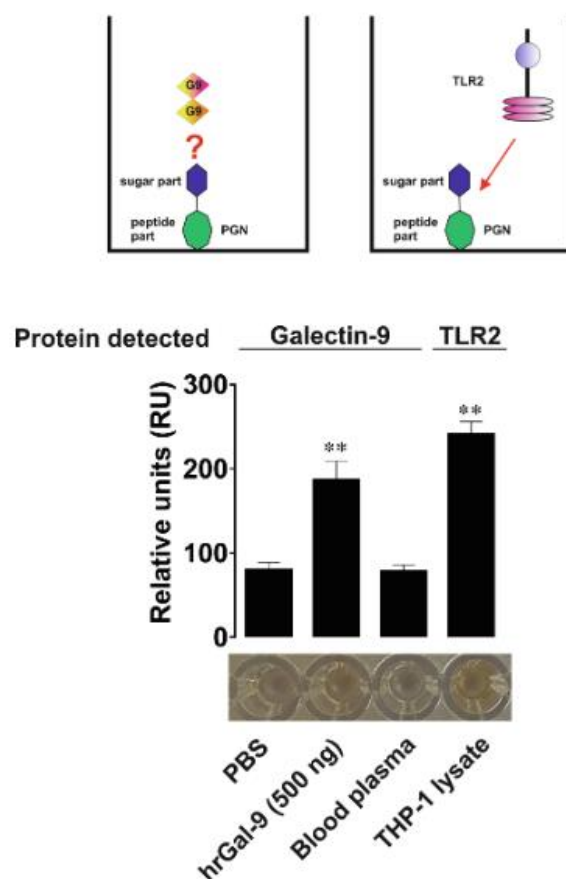


Figure 72 Galectin-9 in human blood plasma does not opsonise gram-positive bacteria by PGN. PGN retrieved from the gram-positive bacteria *S. aureus* was immobilized in wells of an ELISA plate and incubated with either galectin-9 from human blood plasma, recombinant galectin-9, or as positive control TLR2 from THP-1 cell line. Five individual experiments were performed, a representative image and mean +/- SEM is shown. **-p<0.01 vs. control.

3.4.2.2 Galectin-9 bound on cell surface of embryonic cells is capable of protecting against cytotoxic T cells but does not lead to colonization of these cells with bacteria.

As reported in previous chapters, embryonic cells express high levels of galectin-9 on the cell surface especially in early stages of development to suppress maternal cytotoxic immune cells from attacking the foetus. The levels of galectin-9, Tim-3 and VISTA are especially high in the earlier developmental stages for example in the chorion stage ranging from 13 – 14 weeks of pregnancy and are down-regulated in later development such as the amnion stage at 20 weeks (Figure 74 A – C). As galectin-9 does not possess the ability to be shed on its own we investigated the ability of Tim-3 and VISTA as carriers or traffickers allowing its translocation to the surface. We used an ELISA plate and coated wells with anti-galectin-9 antibody of either mouse or rabbit origin to capture galectin-9 contained in embryonic cell lysates originating from the chorion stage.

The capturing of galectin-9 was confirmed using an ELISA approach with mouse capture antibody and a rabbit anti-galectin-9 detection antibody, as shown in Figure 73A. These results were visualized using anti-rabbit antibody originating from goat, which is labelled with a detectable fluorescence signal. We also investigated bound Tim-3 (Figure 73B) and VISTA (Figure 73C) in these samples containing galectin-9. Both proteins were detectable, yet the signal found by investigating Tim-3 was at a much higher intensity than the samples with VISTA detection. This difference indicates that Tim-3 is preferable in regard to being a carrier or trafficker for galectin-9 to the cell surface and VISTA is most likely to simply associate with the formed complex on the surface. By performing an on-cell Western we were also able to measure the presence of galectin-9 and VISTA on the surface of embryonic cells. The signal gained clearly verifies the presence of both proteins on the cell surface and also visualizes by merging the individual fluorescence signals an overlap of both protein signals (yellow colour). This indicates a close co-location of both proteins on the foetal cell surface.

In our recent studies with acute myeloid leukaemia cells, we already were able to show interaction between galectin-9 and VISTA, especially in correlation to cytotoxic T cell-dependent immune responses. In this study with embryonic cells, we decided to verify this effect by co-culturing primary human embryonic cells expressing high levels of galectin-9 with Jurkat T cells that have been pre-treated with 100 mM PMA leading to

an increase of granzyme B production (Figure 74E). These Jurkat T cells were analysed, and we were able to show high levels of granzyme B, Tim-3, and VISTA to be found. For the co-culture the medium was changed to not contain any further PMA and the cells were in contact with each other for 16 h in presence or absence of either VISTA neutralizing antibodies, galectin-9 neutralizing antibodies or both. The presence of such neutralizing antibodies clearly inhibited the proper interaction of these cells and therefore lead to a reduced accumulation and activation of granzyme B within Jurkat T cells. This increased the viability of T cells and inhibited the activation of caspase 3 within them (Figure 74F).

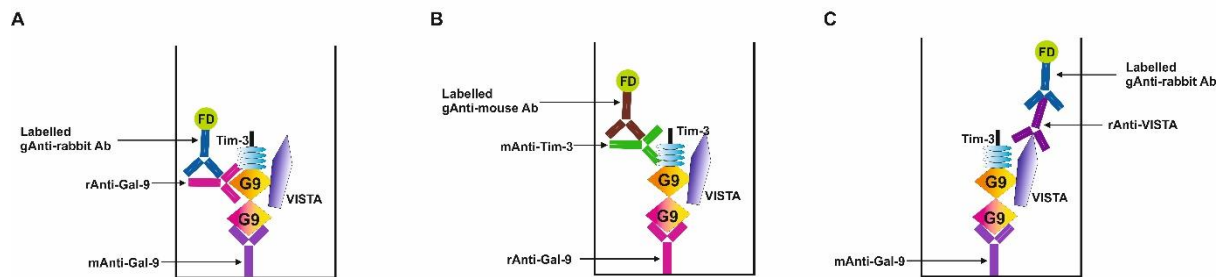


Figure 73 Visual scheme showing the ELISA approach used to determine the binding association of Tim-3 and VISTA to galectin-9 found on human embryonic cells. (A) The binding of galectin-9 to the ELISA plates was measured using mouse anti-galectin-9 capture antibody and rabbit anti-galectin-9 detection antibody. The signal was detectable due to a goat anti-rabbit antibody containing a fluorescent label. (B) For determining Tim-3 binding the capture antibody against galectin-9 has been originating from rabbit and the anti-Tim-3 detection antibody mouse. Signal was achieved by using goat anti-mouse antibody with fluorescent labelling. (C) VISTA was detected using a mouse anti-galectin-9 capture antibody, rabbit anti-VISTA detection antibody and goat anti-rabbit fluorescent labelled antibody.

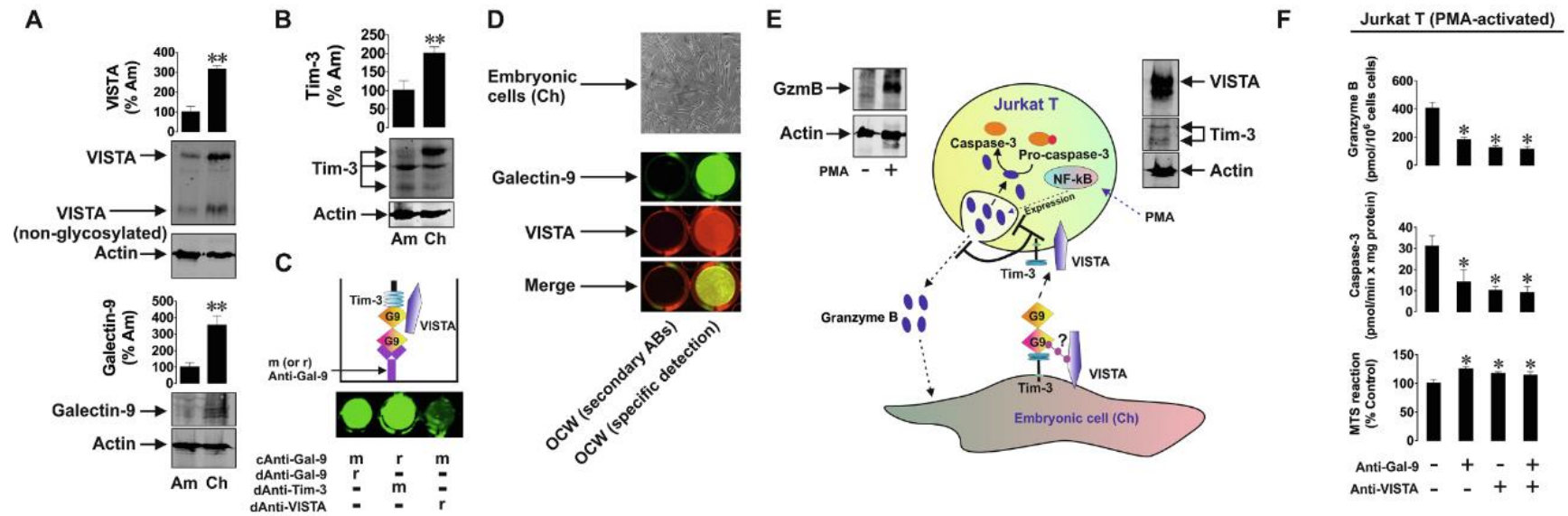


Figure 74 Suppression of immune responses towards embryonic cells are heavily influenced by galectin-9 and VISTA levels. As described in Materials and methods we were able to culture primary human embryonic cells for co-culture purposes. (A, B) These cells were investigated regarding their expression levels of galectin-9, Tim-3, and VISTA in two different developmental stages. The chorion (Ch) stage ranges from 13-14 weeks of development and the samples of the amnion (Am) stage were retrieved at 20 weeks. (C) Association of these proteins with each other were detected by using ELISA approaches and analysing signals gained from proteins at the same time. (D) On embryonic cells the co-localization of VISTA and galectin-9 was determined by on-cell Western Blotting. Close proximity of VISTA and galectin-9 is shown by merging both signals. (E) Jurkat T cells were activated with 100 mM PMA for 24 h and expression levels of Tim-3, VISTA and granzyme B was analysed. (F) Apoptotic activity such as accumulation of granzyme B and increased caspase 3 activity were analysed in co-cultured Jurkat T cells in presence and absence of neutralization antibodies against VISTA, galectin-9, or both. Images shown are representing seven individual experiments. Mean +/- SEM is included. *-p<0.05 and **-p<0.01 vs. control shown.

We were also interested in understanding if galectin-9 bound on the surface of embryonic cells can lead to colonization of such cells by gram-negative bacteria causing an increased risk of bacterial infections of foetal cells. For this investigation, we co-cultured primary embryonic cells from the chorion stage with a stock of 50 μ l of *E. Coli XL10 Gold*® cells in antibiotic-free medium for 16 h to enable the bacteria to form colonies on the foetal cells (Figure 75A). Next, we removed the medium containing non-bound bacteria and added fresh medium containing THP-1 monocytes at a concentration of 10^6 cells/dish in 3 ml. The co-culture has been performed for 16 h in normal cell culture conditions using antibiotic-free medium in presence and absence of 10 mM lactose. After co-incubation we analysed the levels of IL-1 β , IL-6 and TNF- α within the medium. Without exposure to *E. coli* the co-culture did show only very low background levels, while the presence of bacteria in the co-culture increased the levels of all three cytokines significantly. The increase was not reduced by the presence of lactose (Figure 75B). These findings clearly indicate that galectin-9 bound on embryonic cell surface does not associate with bacteria therefore does not lead to colonization. This also indicates that galectin-9 is not included in influencing the innate immune responses against bacteria infecting embryonic cells. Yet, in case of the mother's immune system attacking foetal cells galectin-9 is able to inhibit these unfortunate immune responses.

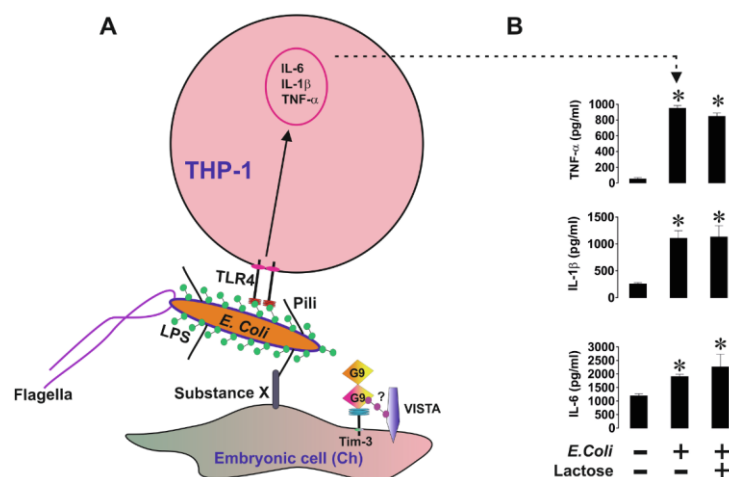


Figure 75 No colonization of galectin-9 expressing embryonic cells by Gram-negative bacteria was detectable. Primary embryonic cells originating from the chorion stage were exposed to *E. coli* cells for 16 h with or without 10 mM lactose. After bacterial colonization these cells were co-cultured with THP-1 cells for 16 h to determine cytokine levels corresponding to an immune response. The levels of IL-1 β , IL-6 and TNF- α were analysed using ELISA approach. Results are representative of four experiments including mean \pm SEM. *- $p < 0.05$ and **- $p < 0.01$ vs. control.

3.4.2.3 Macrophages phagocyte galectin-9 “opsonized” T cells.

With the results gathered during the studies and knowledge so far about the function of galectin-9 we were interested to determine if T cells opsonised with galectin-9 are phagocytosed by macrophages. To investigate this effect, we pre-treated Jurkat T cells for 24 h with 100 mM PMA and exposed them in fresh PMA-free medium to 2.5 µg/ml galectin-9 (Figure 76A). We chose this specific concentration of galectin-9 based on our previous observations, as in case of using recombinant protein we were able to determine that the effects seen are about 250 – 500x less efficient than cell-derived proteins.

We characterized the expression of a certain “eat-me signal” for macrophages expressed on the T cell surface after the exposure to galectin-9, phosphatidylserine (PS). This is done by using annexin V staining of cells as well as determining cell viability and the release of TGF-β and HMGB-1, as both are secreted by stressed, dying or already dead cells. Cell viability was not significantly affected by the exposure to galectin-9 with just a small percentage of apoptotic cells, even though the PS levels on the cell surface were crucially increased as shown by the annexin V staining (Figure 76B). Secretion of both, TGF-β and HMGB-1 were also significantly upregulated. These cells expressing high levels of PS, HMGB-1 and TGF-β were in the next step co-cultured for 3 h with THP-1 macrophages. THP-1 cells were transformed into macrophages by exposing them for 24 h to 100 mM PMA. These macrophages were permeabilized with methanol and accumulation of the T cell marker CD3 was assessed within the cells by in-cell Western approach. Galectin-9 opsonized Jurkat T cells were significantly higher phagocytosed than non-exposed cells (Figure 76C, upper panel), HMGB-1 present in the medium enhanced this effect. As Tim-3 can act as a ligand for both galectin-9 and PS we were also interested in investigating the influence of surface-bound Tim-3 on macrophages in phagocytosis. After co-culturing the galectin-9 pre-treated Jurkat T cells and PMA-differentiated THP-1 for 1 h in presence and absence of Tim-3 neutralizing antibody we were able to determine that neutralization of the Tim-3 binding ability of macrophages reduced phagocytosis of Jurkat T cells (Figure 76C, lower panel).

Lastly, we decided to investigate the physiological indications of the effects seen, this was done by co-culturing PMA-activated Jurkat T cells that were exposed to 10% human blood plasma from healthy donors containing 370 pg/ml galectin-9, or from AML

patients containing 8200 pg/ml galectin-9 for 16 h with PMA-treated THP-1 macrophages. Exposure to blood plasma of AML patients containing very high levels of galectin-9 led to increased phagocytosis, while exposure to healthy donor blood plasma did not inflict any changes in phagocytosis compared to the control. Using Tim-3 neutralizing antibody decreased the effects seen in the co-cultures with AML blood plasma (Figure 76D). To verify the effects seen is dependent on the presence of galectin-9 on the cell surface of Jurkat T cells we investigated these levels after exposure to AML blood plasma, which were significantly increased and confirmed the opsonization (Figure 76E).

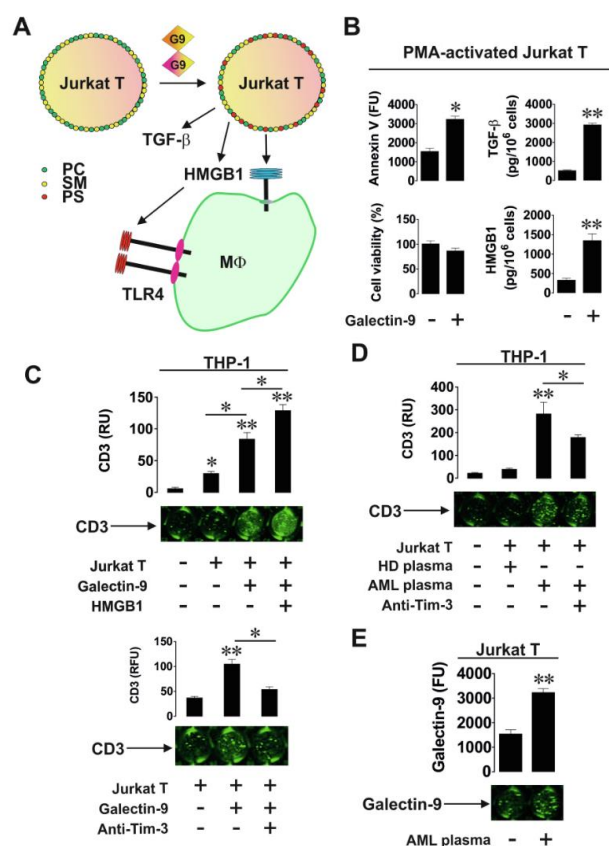


Figure 76 Phagocytosis of T cells by macrophages is triggered by opsonization with secreted galectin-9. (A) PMA-treated Jurkat T cells were exposed to galectin-9 for 16 h and co-cultured with THP-1 macrophages for 3 h. PC- phosphatidylcholine, PS- phosphatidylserine and SM – sphingomyelin. (B) Viability, HMGB-1, TGF-β secretion and PS expression of the Jurkat T cells were analysed. (C) In-cell Western of CD3 in THP-1 cells was used to determine phagocytosis of T cells (top panel). Effects were attenuated with Tim-3 neutralizing antibody (bottom panel). (D) To verify effects in physiological conditions Jurkat T cells were exposed to AML blood plasma containing high levels of galectin-9 for 16 h increasing phagocytosis (top panel). Opsonization by galectin-9 after AML exposure was verified using on-cell Western (bottom panel). Representative images from one out of five experiments shown, including mean +/-SEM. *-p<0.05 and **-p<0.01 vs. control.

For finalizing the studies, we verified that in human primary T cells the opsonization with galectin-9 increases the levels of PS expressed on the cell-surface. We therefore investigated the effects of galectin-9 on T helper cells (CD4⁺) as well as cytotoxic T cells (CD8⁺). Both cell types were exposed to 2.5 µg/ml galectin-9 for 16 h and we measured PS levels by annexin V staining. In each cell type the levels of PS were increased after exposure to galectin-9, while the effects were significantly higher in CD8⁺ cytotoxic T cells (Figure 77). These differences in the cell types might be dependent on the ability to produce granzyme B in case of cytotoxic T cells and the lack thereof in T helper cells.

In summary, the effects seen verify the ability of galectin-9 to increase phagocytosis of T cells by macrophages.

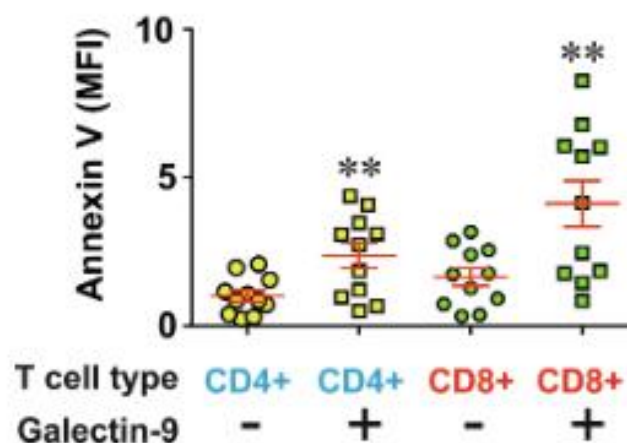


Figure 77 Galectin-9 induce PS expression and translocation on the cell surface in T helper and cytotoxic T cells. CD4⁺ T helper cells and CD8⁺ cytotoxic T cells were exposed for 16 h to 2.5 µg/ml galectin-9. The translocation of PS was determined using annexin V staining. Data include results of eleven independent experiments as well as mean +/- SEM. **-p<0.01 vs. no stimulation.

3.4.2.4 Discussion.

In the tumour microenvironment the effects of galectin-9 on the suppression of immune responses are well known to be achieved by impairing anti-cancer activity of cytotoxic T cells and NK cells leading to cancer growth and immune escape (Yasinska, 2020). In normal immune responses in the human body the exact function of galectin-9 still remains to be understood.

In this chapter we were able to confirm that macrophages and other myeloid cells secrete galectin-9 allowing the opsonization of gram-negative bacteria. This is mainly achieved by the binding of galectin-9 to LPS on the surface of such bacteria (Figure 70 and 71). The binding is due to the interaction of galectin-9 with sugar components found in the LPS structure and can be inhibited by the presence of lactose. Phagocytosis is achieved by interaction of bacteria-bound galectin-9 with the corresponding receptors, Tim-3, and VISTA, similar to the effects seen on T cells. The bound galectin-9 helps to render bacteria barely mobile and acts as a signalling protein for macrophages enabling the bacteria to be easily captured by such cells. The opsonization increases the amount of bacteria to be recognized by innate immune cells and therefore enhances the production of cytokines such as IL-1 β , IL-6 and TNF- α . Interestingly, this effects seems to be solely working on gram-negative bacteria expressing LPS as PGN-expressing gram-positive bacteria are poorly bound by galectin-9 and it does not show any involvement in the phagocytosis of gram-positive bacteria.

On human embryonic cells galectin-9 can be highly expressed on the surface, especially in early stages of development (Figure 74). These high levels of galectin-9 on the cell surface are inhibiting potential cytotoxic immune responses of T cells towards embryonic cells. The effect is caused by, as already described in earlier chapters, the stimulation of granzyme B production and activation within T cells leading to an increase of caspase 3 activity within these cells and therefore inducing apoptosis. The effect is similar to the one seen by AML cells induced by secretion of galectin-9 (Goncalves-Silva, 2017, Yasinska, 2020). Yet, the galectin-9 bound on the surface of embryonic cells does not show any involvement of colonization of these cells by gram-negative bacteria. In general, infection of human cells by bacteria is achieved by using the pili to bind on a variety of substances on the host cells. The pili is the primary structure used by bacteria to bind on such host cells (Ribet, 2015). In *E. coli* this is

achieved by pili using the adhesion structure PapG to bind onto glycosphingolipids found on kidney epithelium. Another form of pili named “Type I pili” is able to interact with D-mannosylated receptors, such as uroplakins in the bladder (Ribet, 2015; Roberts, 1994; Lillington, 2014; Melville, 2013). By investigating cell-bound galectin-9 we were able to show that it is not involved in adhesion of gram-negative bacteria to foetal cells (Figure 75).

Soluble galectin-9 on the other hand is also known to impair the cytotoxic functions of NK and T cells (Yasinska, 2020; Okoye, 2020). In cytotoxic T cells it leads to apoptosis by induction of granzyme B production and also increases the secretion of TGF- β and HMGB-1 (Figure 76B). This release of TGF- β by apoptotic T cells increases the production and secretion of galectin-9 in cancer cells and possibly also in tumour-associated macrophages or in case of the embryonic development in placental macrophages (Chen, 2001; Wu, 2014). The opsonization of galectin-9 on T cells also causes translocation of PS onto the cell surface (Figure 76B and 77). This process is most likely performed by scramblases such as TMEM16F and Xk-related protein 8 (Xkr8). As calcium-dependent scramblase, TMEM16F might be the most prominent to induce translocation of PS on cell surface when galectin-9 leads to calcium mobilization within T cells. On the other hand, Xkr8 is activated by increased caspase 3 activity as seen in cytotoxic T cells after galectin-9 binding via granzyme B-dependent manner (Marino, 2013; Suzuki, 2013 & 2010; Bushell, 2019).

HMGB1 induces the activation of macrophages and their phagocytosis activity as a ligand of TLR2 and TLR4 (Yasinska, 2018; Selno, 2021). Tim-3 has been proven to also increase phagocytosis of T cells by being expressed on macrophage cell surface as a galectin-9 as well as PS receptor (Figure 76). The interaction of Tim-3 expressed on macrophages and galectin-9 and PS expressed on T cells explains the phagocytosis of affected T cells by either placental macrophages in the embryonic development or by tumour-associated macrophages. This effect is furthered by the induction of TGF- β production due to LPS binding. LPS is able to cause innate immune responses, the increase of TGF- β also leads to an upregulation of galectin-9 production (Sun, 2018). High levels of galectin-9 induce opsonization of gram-negative bacteria and therefore furthers innate immune responses towards bacterial infections (Figure 70).

Studies of other galectins, such as galectin-4 and galectin-8 as tandem structures as well as galectin-3 have also recently reported their ability of interaction with gram-negative bacteria via LPS (Campanero-Rhodes, 2021). The exact function of galectins regarding the opsonization of bacteria as well as T cells needs to be unravelled by further research.

Taken together the results in this chapter clearly show an evolutionary traction of galectin-9 in regard to the survival of most species. It enables the protection against bacterial infections as well a regulation of immune responses. Galectin-9 is clearly involved in the opsonization of both gram-negative bacteria leading to an improved anti-bacterial innate immune response as well as opsonisation of T cells to protect the embryonic development by recruitment of placental macrophages leading to the phagocytosis of rogue T cells. This process can be unfortunately also used by malignant cells to protect especially newly formed tumour cells against the immune responses of cytotoxic lymphocytes by recruitment of tumour-associated macrophages leading to suppression of anti-cancer T cell functions.

Galectin-9 also furthers the production of TGF- β and HMGB-1 by T cells leading to an increase in the immunosuppressive environment. These factors are able to contribute either indirectly (HMGB-1) or directly (TGF- β) to the induction of increased galectin-9 production in cancer cells and tumour-associated macrophages. Recent studies indicate that galectin-9 is also able to enhance T cell receptor signalling, the exact function of this effects needs further investigation especially in regard to T cells infiltrating malignant tissues.

In summary we were able to show that galectin-9, secreted or cell-bound, plays a fundamental role in the bacterial defence as well as suppression of immune responses towards embryonic cells and tumour development.

The results of this chapter show that the release of galectin-9 induces anti-bacterial immune response by opsonization as well as suppression of T cells by enhancement of macrophage activity.

3.5 FUNDAMENTAL PATHOLOGICAL FUNCTIONS OF GALECTIN-9 AND VISTA IN IMMUNE EVASION CHECKPOINT PATHWAYS.

The chapters so far show that galectin-9 is a potential target for cancer therapy. The functions of galectin-9 in the normal human body enabling better bacterial innate immune responses as well as its ability to support embryonic cells in their survival against the mother's immune system can be adapted by malignant cells to further inhibit anti-cancer immunity. Understanding exactly how the pathological adaption is performed should be furthered to ease the development of a cancer therapy using galectin-9 and/or its regulatory pathway as the proposed treatment target. In this final chapter we investigate how cancer cells are using galectin-9 to suppress the anti-cancer immune responses of cytotoxic T and NK cells. The galectin-9 secretion by cancer cells is in focus as well as the influence of opsonization of T cells by galectin-9 in tumour-associated macrophage recruitment leading to their phagocytosis.

3.5.1 INTERACTION WITH T LYMPHOCYTES LEADS TO SOLID TUMOUR SECRETING GALECTIN-9 AND THEREFORE INDUCES IMMUNOSUPPRESSION BY INTERACTION WITH OTHER CHECKPOINT PROTEINS.

As major contributor regulating immune responses galectin-9 is able to suppress functions of cytotoxic T cells and natural killer cells by interacting with receptors such as Tim-3, VISTA as well as programmed cell death protein 1 (PD-1) (Yang, 2021). In NK cells as mentioned in chapter 3 galectin-9 mainly interacts with Tim-3 as a receptor and solely suppresses their functionality, while in cytotoxic T cells it can lead to programmed cell death by interacting with both Tim-3 and VISTA via increased granzyme B production and inducing its leakage in the T cells themselves. These effects allow cancer cells to escape immune surveillance of lymphocytes.

Galectin-9 is found to be highly expressed on a variety of human malignancies including severely aggressive ones such as high-grade glioblastomas and pancreatic ductal adenocarcinomas (Yasinska, 2019; Seifert, 2020). Other more common malignancies include colorectal, lung and breast cancers as well as haematological malignancies (Selno, 2020). In acute myeloid leukaemia galectin-9 is used as a crucial way to induce immune evasion (Goncalves-Silva, 2017). Hereby, it is secreted in high levels interacting with immune cells in the blood stream. Studies of solid tumours such

as breast cancer cell lines showed that the secreted levels of galectin-9 were either low or non-detectable, yet high levels were found based on cell surface to protect against T cells (Yasinska, 2019).

While galectin-9 was mainly studied and associated with cancer cells and their function to suppress immune responses, we were able to prove, as explained in the chapter prior, that the primary function of galectin-9 throughout evolution was the protection against infection of gram-negative bacteria, leading to their phagocytosis by macrophages as well as neutrophils (Chapter 6.2; Vega-Carrascal, 2014). Infection by gram-negative bacteria leads to enhancement of galectin-9 production and their opsonization. With these results in mind, it would naturally be more productive for solid cancer cells to also secrete high levels of galectin-9 for suppression against immune response by T and NK cells. Therefore, the hypothesis in this chapter is interactions between solid cancer cells and T cells leads to the secretion of galectin-9 into the microenvironment and to the opsonization of approaching T cells, minimizing further attacks on the growing malignancy by cytotoxic lymphocytes.

In this chapter we are interested to investigate for the very first time that the interactions of T cells and solid tumour growths lead to the release of high levels galectin-9 normally stored in and on these cancer cells. Two mechanisms might be responsible for this release. Galectin-9 can be translocated onto the cell surface and released by proteolytic shedding with its trafficker and carrier such as Tim-3 or it is secreted by lysosome formation also including a trafficker as galectin-9 does not contain any secretion sequence on its own. After release galectin-9 on the one hand causes the opsonization of T cells and on the other interacts with other checkpoint proteins on the immune cells completely attenuating their cytotoxic activities. We mainly focused on one of the most prominent immunosuppressive interaction by galectin-9 and VISTA in human cancer cells. The results in this chapter should clearly show the efficiency of galectin-9 as a potential immune therapy target in a variety of cancer types.

3.5.1.1 Interaction between human solid cancer cells and T cells lead to secretion of galectin-9.

First, we were interested to investigate if T cells interacting with cancer cells leads to secretion of galectin-9 by human solid tumour cells. We were able to verify that most of these cancer cells did not secrete galectin-9 on their own and those that did only released very small amounts. In this study we also included non-malignant cells such as primary human embryonic cells and the rapidly proliferating keratinocyte cell line HaCaT. These different cell types investigated showed all high levels of galectin-9 to be produced, mostly in presence of increased levels of TGF- β . In this study we focused on following cell lines: G401 kidney rhabdoid tumour cell line, LN-18 high grade glioblastoma cell line, MCF-7 breast cancer cell line and WT3ab Wilms tumour cell line.

These cell lines were co-cultured for 16 h with Jurkat T cells at a ratio of 1:1. After the co-culture the Jurkat T cells were removed, the cancer cells washed twice with PBS and fresh medium added again. The cells were kept in the incubator for 4 h and samples taken after 2, 3 and 4 h to investigate galectin-9 levels released by ELISA method. Jurkat T cells were also investigated and did only secrete barely detectable levels of galectin-9. In the study we were able to verify that solid cancer cells secreted high levels of galectin-9 after co-incubation with Jurkat T cells, while non-malignant HaCaT keratinocytes secrete lesser levels and in human embryonic cells no secretion of galectin-9 has been found (Figure 80A). While in previous chapters we were already able to confirm galectin-9 expression levels in MCF-7, HaCaT, embryonic cells as well as in WT3ab cells, in this chapter we also verified the expression of this protein found in G401 and LN-18 cells (Figure 78 and 79).

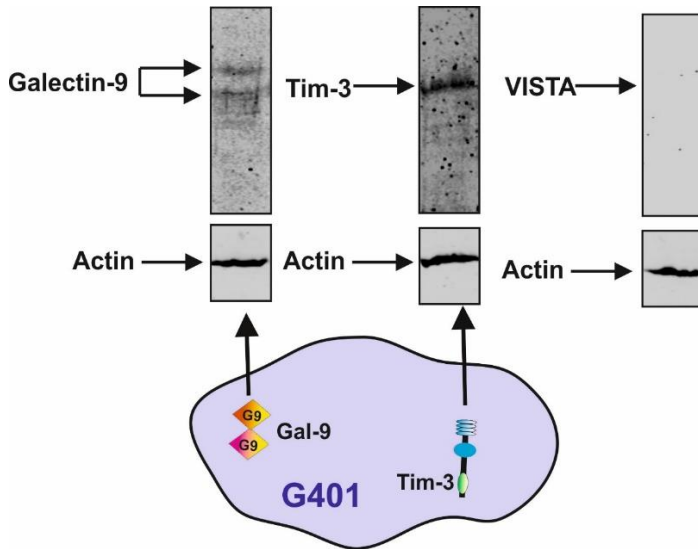


Figure 78 G401 human kidney rhabdoid tumour cell line was investigated regarding its expression levels of galectin-9, VISTA, and Tim-3. Analysis was performed using Western Blot approach. Data was gathered from four independent experiments including representative images, mean +/- SEM.

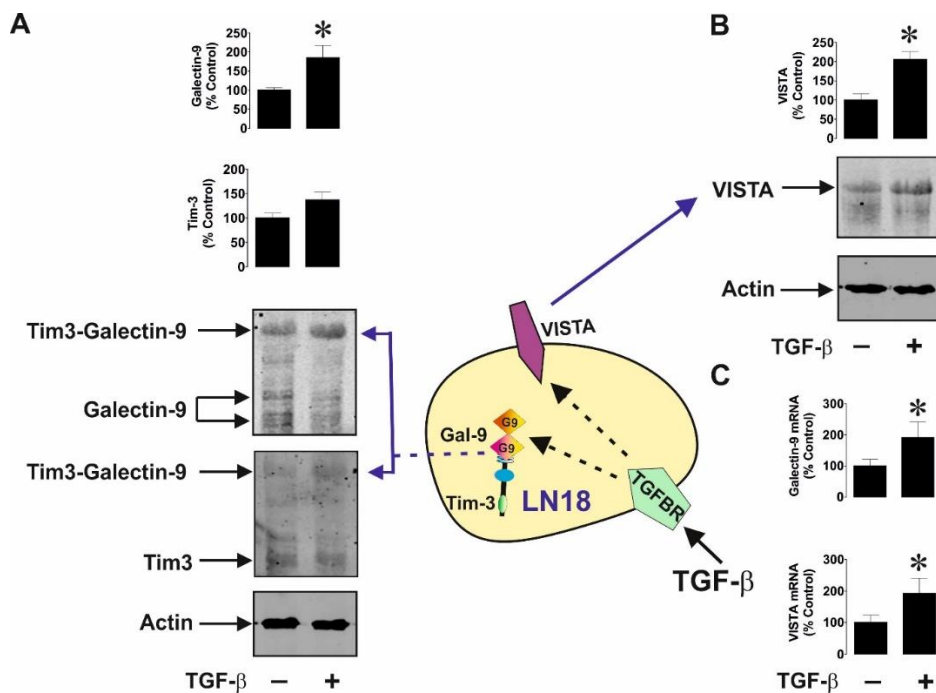


Figure 79 Human glioblastoma cell line LN-18 was studied to determine galectin-9, VISTA, and Tim-3 expression levels after TGF- β induction. After exposure of LN-18 cells to 2 ng/ml TGF- β for 24 h Western Blot analysis was used to determine the expression levels of galectin-9, VISTA, and Tim-3 as well as their mRNA levels. Data include representative images of one out of four experiments with similar results, mean +/- SEM shown.

Next, we investigated if these effects were found to be induced by different types of T cells to ensure it was not Jurkat T cell-dependent. To do so, we co-cultured the MCF-7 breast cancer cell line with either primary human CD3-positive, Jurkat (CD4⁺) or TALL-104 cytotoxic (CD8⁺) T cells. Co-incubation was performed for 24 h at a ratio of 1:1 and samples were taken as described above after changing the medium. No functionally significant levels of galectin-9 have been secreted by any of the T cell types, with Jurkat secreted less than 100 pg/ml as an example. The MCF-7 cell line comparing to others released high levels of galectin-9 in each of the co-cultures (Figure 80B). In regard to other solid, adherent cell lines without contact to T cells only LN-18 glioblastoma cell line was able to secrete low levels of galectin-9 prior (Figure 80C).

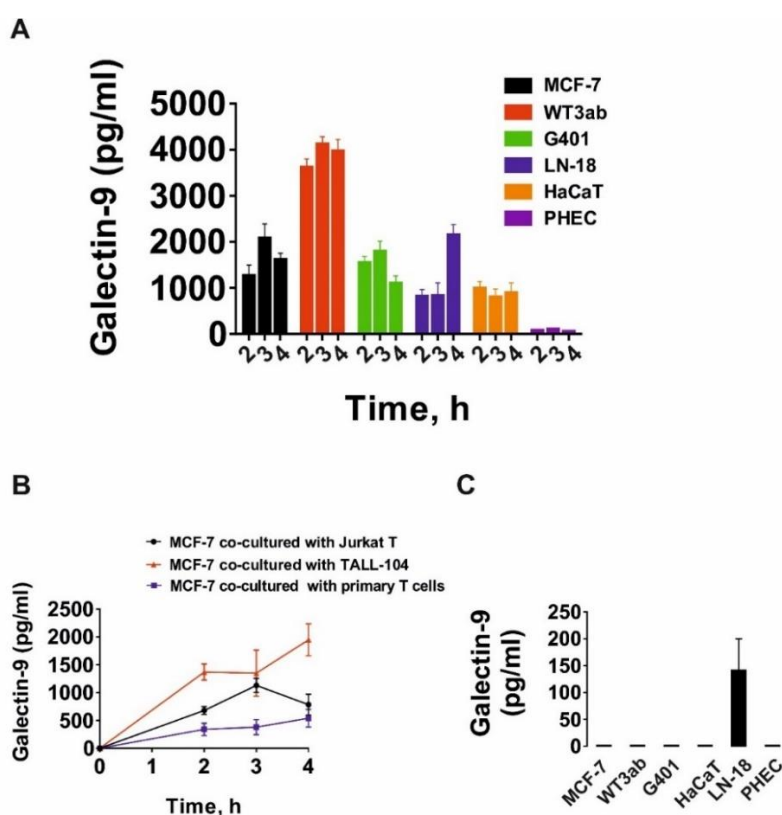


Figure 80 Interaction with T cells leads to secretion of galectin-9 by solid human cancer cells as well as keratinocytes. At a ratio of 1:1 we co-cultured Jurkat T cells and a variety of solid cancer types, keratinocytes, or primary human embryonic cells for 16 h. The cells were separated from each other, and the adherent cells washed twice with PBS before adding again fresh medium culturing them for another 4 h. The release of galectin-9 was measured in samples taken at 2, 3 and 4 h. Jurkat T cells themselves did not release significant levels of galectin-9 on their own (A). To determine if these effects are seen while contact with any type of T cell, we used MCF-7 breast cancer cells and co-incubated them with either primary CD3-positive T cells, Jurkat (CD4⁺) or TALL-104 cytotoxic (CD8⁺) T cells for 16 h again at a ratio of 1:1 (B). Adherent cells were investigated regarding galectin-9 release in resting state (C). Data includes mean \pm SEM of four independent experiments.

We were able to confirm during our studies that MCF-7 express only Tim-3 as a galectin-9 binding receptor, while WT3ab express mostly VISTA and only a very low amount of Tim-3 and LN-18 does express both receptors – VISTA and Tim-3 (LN-18 seen in Figure 79). Galectin-9 lacks secretory sequences on its own, therefore we assessed which carrier/ trafficker fragments it was released with as a complex. The secreted galectin-9 from co-cultures was immunoprecipitated, verified by using Western blot approaches without boiling the sample used. In case of MCF-7 the co-culture with Jurkat T cells led to secretion of galectin-9 in complex with Tim-3 fragments (Figure 81A). In the WT3ab cell line which does not express detectable amounts of Tim-3 galectin-9 was released in complex with VISTA fragments (Figure 81B). The Western Blot analysis caused the dissociation of galectin-9 from the VISTA fragments, which verifies results gathered in prior galectin-9 studies that Tim-3 had a higher binding affinity to galectin-9 than VISTA.

In case of the LN-18 glioblastoma cell line both types of known carriers/traffickers for galectin-9 were expressed in high levels. In such case the preferred carrier for galectin-9 is as seen in prior findings with primary human embryonic cells Tim-3 rather than VISTA (Figure 81C).

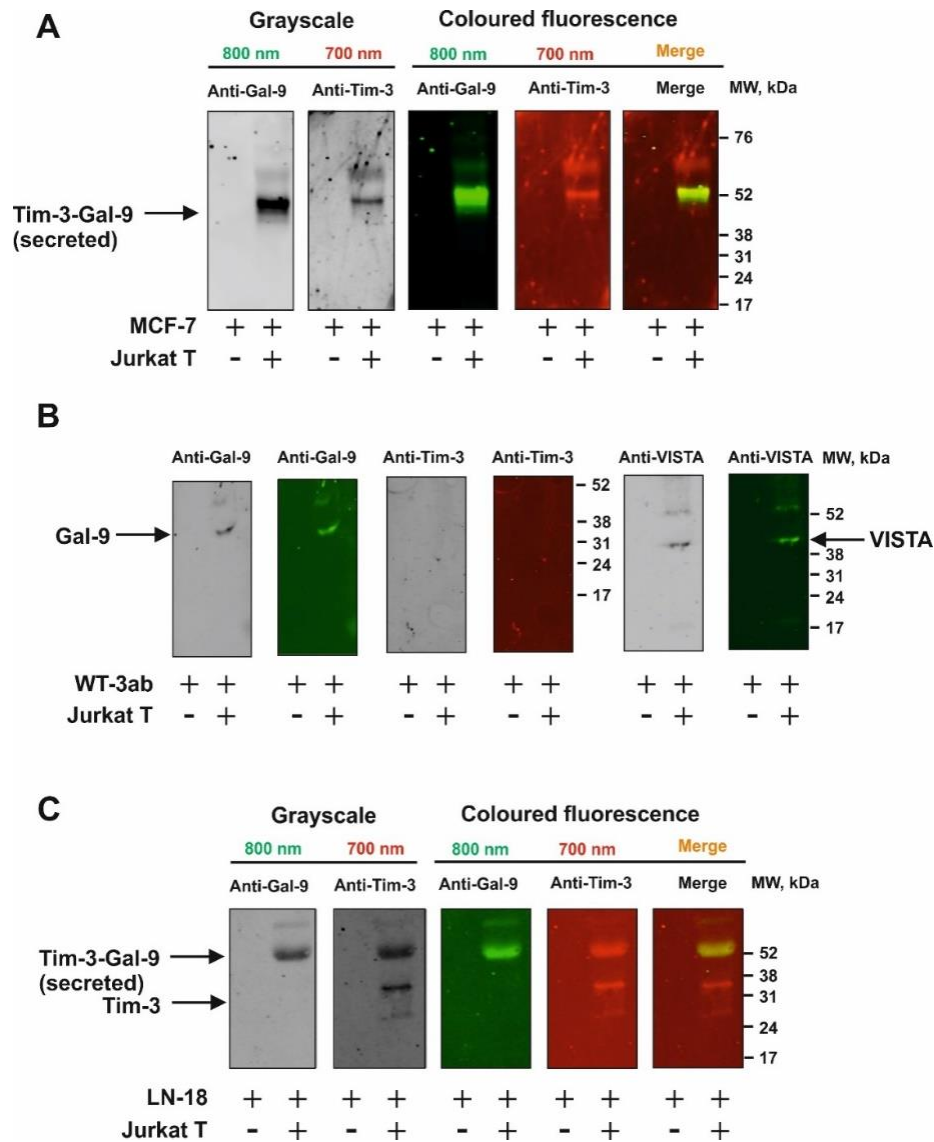


Figure 81 Investigation of trafficker protein for galectin-9 in different cell lines. After co-culture with Jurkat T cells at a ratio of 1:1 for 16 h we investigated with which potential carrier/trafficker – VISTA or Tim-3 – was used to secrete galectin-9 by MCF-7 breast cancer cells (A), WT3ab paediatric kidney cancer cells (B) or LN-18 glioblastoma cells (C). The cells were washed after co-culture and the solid cells kept in fresh medium before immunoprecipitation of secreted galectin-9. The analysis was performed using Western Blotting with non-boiled samples. Images are used to visualize effects seen and are representative for four independent experiments.

As a next step, we decided to investigate if the galectin-9 derived from the interactions of cytotoxic TALL-104 cells and MCF-7 breast cancer cell line is able to opsonize such cytotoxic T cells. The cells – MCF-7 and TALL-104 – were co-cultured at a ratio of 1:1 and separated as described prior. As TALL-104 express only very low levels of galectin-9 and Tim-3 we then lysed these cells and loaded about 50 – 60 µg/ml cellular protein of resting cells and about 15 µg/well of TALL-104 lysates co-cultured with MCF-

7 cells on an ELISA plate for galectin-9 detection. In both cases the samples were not boiled to avoid breaking binding abilities of Tim-3 to the fixed galectin-9. In the TALL-104 lysates originating from the co-culture we were able to detect a band at a size of ca. 52 kDa with both Tim-3 and galectin-9 antibodies (Figure 82A). A similar band can be found by immunoprecipitation of galectin-9 secreted by MCF-7 into the medium after co-culture (Figure 82B). The detected complex is corresponding to the secreted version of galectin-9 bound to a single Tim-3 protein as a trafficker and therefore indicates that galectin-9 is more prone to bind to the trafficker and stay bound to it than to its receptors found on the TALL-104 cells. We were able to rule out that this complex originates from within the TALL-104 T cells as these complexes would still be bigger in size before the shedding from the surface and are known to have a size of 70 kDa.

Interestingly is also the fact that according to the galectin-9 mRNA levels analysed in the TALL-104 lysates, these cells were significantly downregulating its own galectin-9 produced after the interaction with MCF-7 cells. VISTA mRNA levels were also downregulated while the Tim-3 mRNA levels were higher after co-culture (Figure 82C). According to the secretion levels detected of galectin-9 and Tim-3 by MCF-7 cells, we were also able to verify significantly upregulated mRNA levels in these cells (Figure 82D). Corresponding to the results gathered in prior chapters the TALL-104 cells co-cultured with MCF-7 breast cancer cells were unable to release granzyme B to the cancer cells (Figure 82E and F).

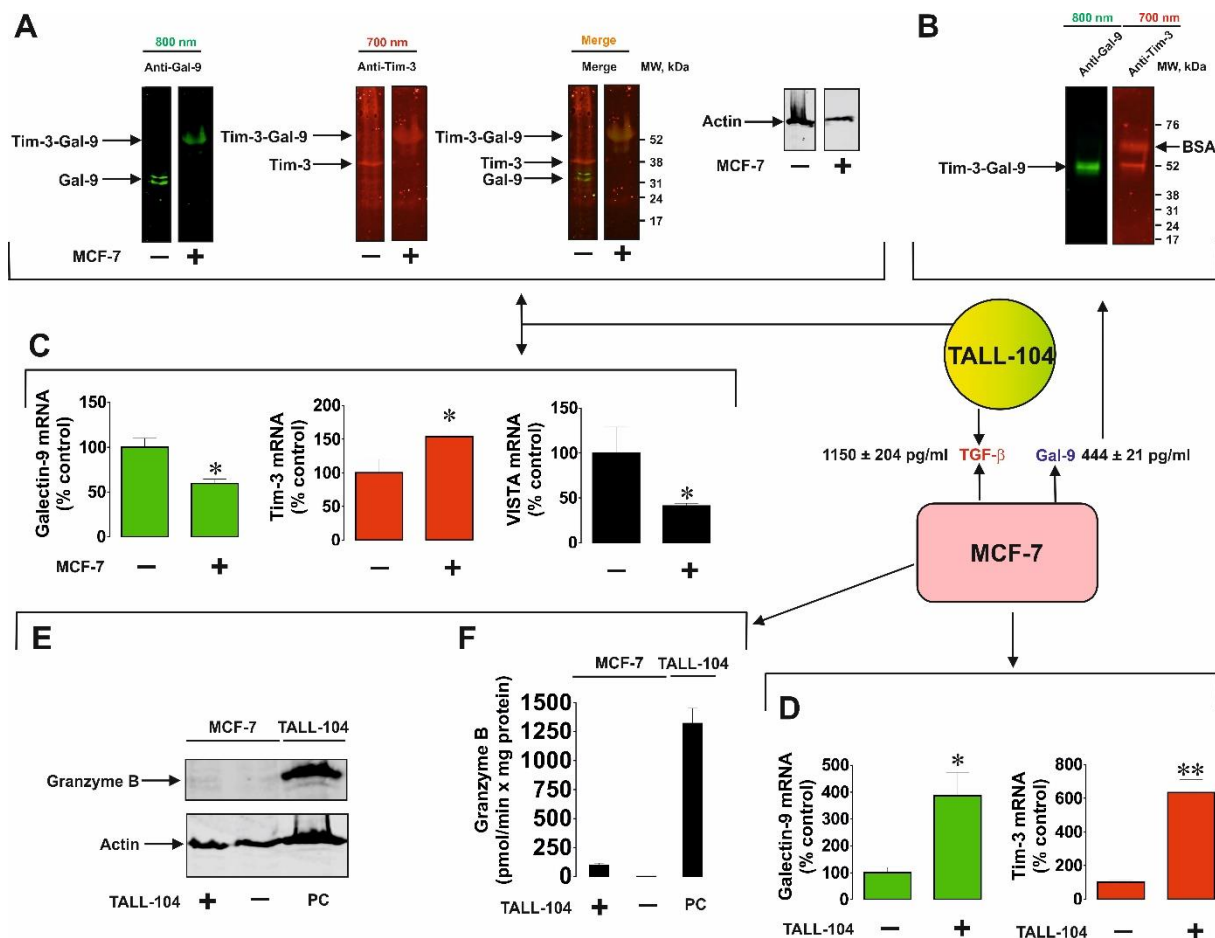


Figure 82 Galectin-9 derived from solid cancer cells leads to opsonization of cytotoxic T cells.

We co-cultured for 16 h at a ratio of 1:1 MCF-7 breast cancer cells with TALL-104 T cells (A). As control resting TALL-104 cells were used, both co-cultured and resting were lysed, and samples were analysed using Western Blot approach without boiling to detect galectin-9 and Tim-3 in these samples (B). Medium was collected after co-culture and galectin-9 immunoprecipitated. The amount of released galectin-9 as well as TGF- β mRNA levels were analysed in samples from TALL-104 (C) and MCF-7 (D) using qRT-PCR. Granzyme B found in both TALL-104 and MCF-7 were analysed quantitative (E) and its activity (F). Representative images were chosen from one out of four independent experiments, mean \pm SEM included.

3.5.1.2 Secretion of galectin-9 is performed by solid tumour cells using two different mechanisms after induction by T cells.

For the secretion of galectin-9 we considered the possibility of two mechanisms used by cancer cells. To investigate these mechanisms, we co-cultured MCF-7 breast cancer cells with Jurkat T cells for 16 h at a ratio of 1:1 as described prior in this chapter. After co-culture the MCF-7 cells were kept for 4 h in fresh medium and samples were taken at 2, 3, 4 h. To analyse the influence of which mechanisms are used we added a variety of inhibitors to these cells, included are the inhibitors U73122 against PLC (phospholipase C), Gö6083 against PKC (protein kinase C), vacuolin-1 against lysosomal exocytosis, AZD2014 against mTOR, EDTA against matrix metalloproteinase and a proteinase inhibitor cocktail (PIC) against lysosomal proteases and matrix metalloproteinases (Figure 83A).

Our results show that galectin-9 secretion was downregulated by EDTA, Gö6983, PIC and vacuolin-1 (Figure 83B). Interestingly, AZD2014 usage led to an upregulation of galectin-9 secretion suggesting an autophagy-dependent lysosomal secretion, which was confirmed by the effects seen with vacuolin-1. In comparison AML cells secrete galectin-9 independent from autophagy. As a variety of inhibitors suppressed the secretion of galectin-9 it is most likely that at least two mechanisms are involved. Firstly, translocation of galectin-9 onto the cell surface in PLC-independent, PKC-dependent manner which is followed by shedding off of the Tim-3 – galectin-9 complex by matrix metalloproteinases, similar to AML cells. Secondly, the formation of autophagosome followed by lysosomal exocytosis might be used to in which the galectin-9 protein will be also ultimately shed off. This process is verified by the fact that galectin-9 secretion was attenuated after blocking of lysosomal proteases and matrix metalloproteinases using PIC.

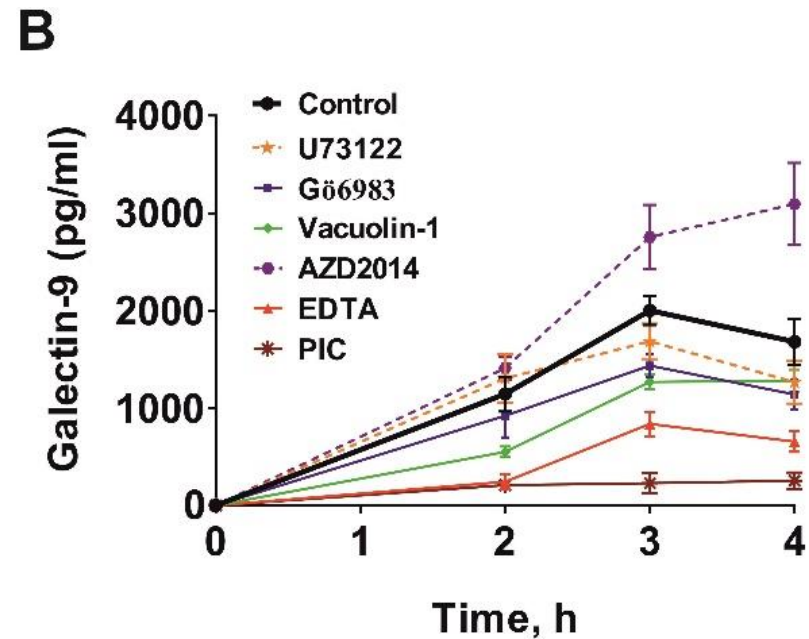
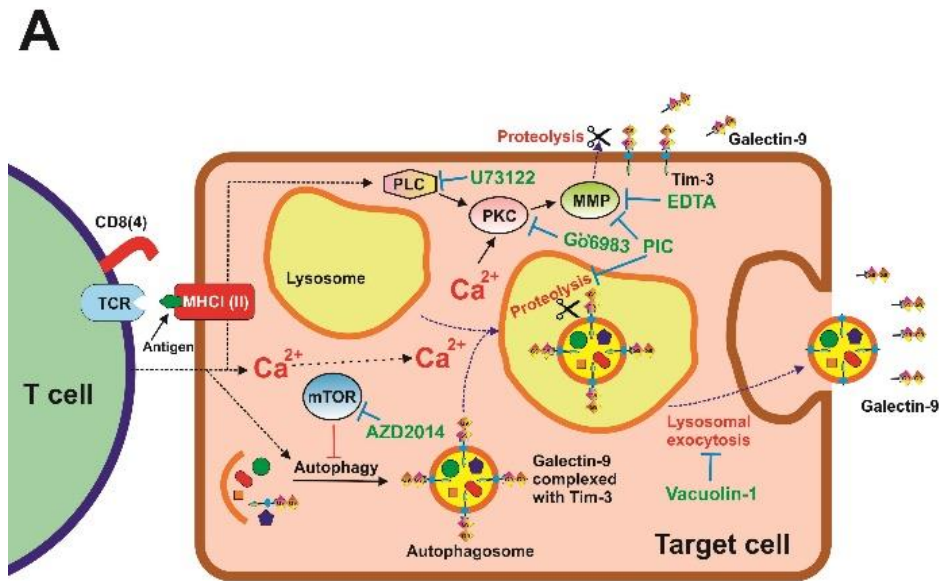


Figure 83 Two mechanisms are involved in galectin-9 secretion by MCF-7 human breast cancer cells after induction by T cells. Scheme shown including a variety of biochemical mechanisms involved in the galectin-9 secretion by cancer cells induced by interaction with T cells. We investigated two most prominent mechanisms in our studies. One mechanism is the calcium/PKC-dependent translocation of the galectin-9 – Tim-3 complex onto the cell surface followed by matrix metalloproteinases causing proteolytic shedding. Another possibility is by galectin-9 in complex with a trafficker being integrated into an autophagosome, which then merge with lysosomes. In such the galectin-9 protein is shed and secretion is performed by lysosomal exocytosis (A). To investigate this MCF-7 human breast cancer cells were co-cultured with Jurkat T cells at a ratio of 1:1 for 16 h. As described before, the adherent breast cancer cells were washed and given fresh medium, which was kept for 4 h and samples were taken after 2, 3, 4 h. The medium we used as replacement would contain certain inhibitors for specific processes needed for shedding galectin-9 in regard to the two mechanisms investigated. The inhibitors used were: AZD2014 – 10 μ M, EDTA – 200 μ M, Gö6983 – 70 nM, PIC – 30 μ M, U73122 – 30 μ M, and Vacuolin-1. Data included are mean \pm SEM of five independent experiments.

PKC influence is most likely dependent on calcium while being diacyl glycerol (DAG) - independent. To verify this, we investigated the intracellular calcium levels after co-culture of cells. Hereby, we kept the MCF-7 and Jurkat cells together in culture for 2 h again at a ratio of 1:1 and analysed the intracellular calcium levels using the Fluo4 reactive dye. In the co-culture we were able to find significantly high levels of calcium in MCF-7 cells in contact with Jurkat T cells compared to no co-cultured, resting MCF-7 cells (Figure 84). These results clearly suggest that the environment influences the activation of Ca^{2+} -dependent PKC isoforms, which were suppressed by using Gö6983 in connection with DAG/ Ca^{2+} -dependent isoforms of this enzyme.

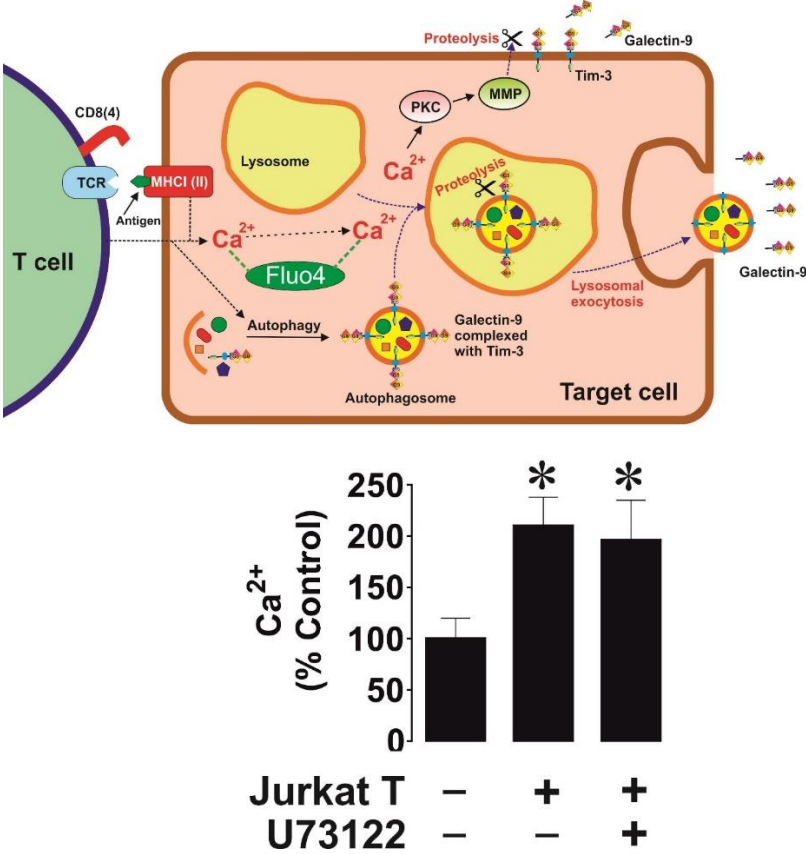


Figure 84 Interactions with T cells led to increased calcium levels in MCF-7 human breast cancer cells. We co-cultured MCF-7 cells with Jurkat T cells for 2 h at a ratio of 1:1 and investigated calcium levels found within using Fluo4 reactive dye. Data include mean +/- SEM of six independent experiments.

3.5.1.3 Secreted galectin-9 interacts with VISTA expressed on T cells to suppress their anti-cancer activity.

We next investigated the function of the galectin-9 proteins released by solid tumours and how this immunosuppressive activity interacts with other immune checkpoint proteins or mechanisms leading to T cell inactivation. We used a co-culture of MCF-7 breast cancer cells and CD4⁺ Jurkat T cells, exhibiting T helper cell activity, for 16 h at a ratio of 1:1 with or without galectin-9 neutralizing antibodies as well as an isotype control. After co-culturing these cells, we investigated the release of IL-2, a cytokine responsible to induce cytotoxic T cell activity, within the medium and lysate of the incubated Jurkat T cells.

We also determined the activity of phosphatidylinositol 3 kinase (PI3K) in the Jurkat T cells as this kinase and its corresponding pathway are contributing to the IL-2 expression and therefore indicate further activation of TCR signalling. In resting Jurkat T cells we were unable to detect any physiological relevant levels of IL-2 to be secreted, furthermore the MCF-7 cancer cells did not secrete any on their own. Our results show that secretion of IL-2 and the total amount produced by the Jurkat T cells was clearly decreased after interacting with the breast cancer cells if a galectin-9 neutralizing antibody was present in the medium, an effect not seen in the isotype control (Figure 85). Similar changes were detectable regarding the PI3K activity. Therefore, we were able to verify that interaction of galectin-9 does lead to increased IL-2 secretion as well as PI3K activity by Jurkat T cells.

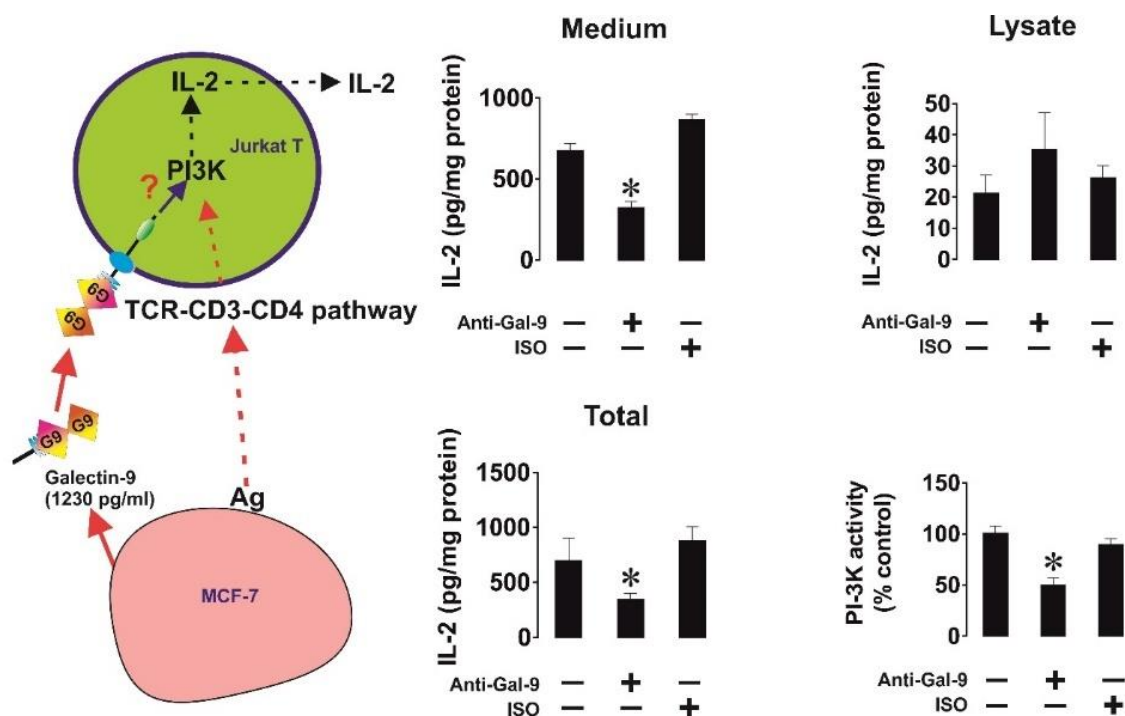


Figure 85 Galectin-9 derived from solid tumours can induce increased IL-2 secretion and PI3K activity in T helper cells. MCF-7 cells were co-cultured with CD4⁺ Jurkat T cells at a ratio of 1:1 with or without galectin-9 neutralizing antibodies or isotype control for 16 h. We measured IL-2 levels with ELISA in medium and within T cell lysates, as well as PI3K activity within the lysates. Five independent experiments were performed, mean +/- SEM included.

Next, we decided to repeat the experiment using the LN-18 glioblastoma cancer cell line instead of the MCF-7 breast cancer cell line. These cells express VISTA as a galectin-9 receptor which is not found on MCF-7 cells. We co-cultured them as described above with Jurkat T cells for 16 h at a ratio of 1:1. This co-culture did not induce an increased secretion of IL-2 by Jurkat T cells compared to resting cells, yet the levels of TGF- β and galectin-9 were significantly increased in accordance with findings of chapters before with other cancer cell lines (Figure 86A). As seen with prior studies did TGF- β also increase in the LN-18 cells galectin-9 and VISTA expression both on protein and mRNA levels (Figure 87).

We verified the results by co-culturing the LN-18 cells with CD3⁺ primary human T cells and analysed the release of galectin-9, granzyme B, IL-2 and TGF- β found in the medium. Both IL-2 and granzyme B levels stayed unchanged in comparison to control samples, yet TGF- β and galectin-9 were significantly increased. (Figure 86B).

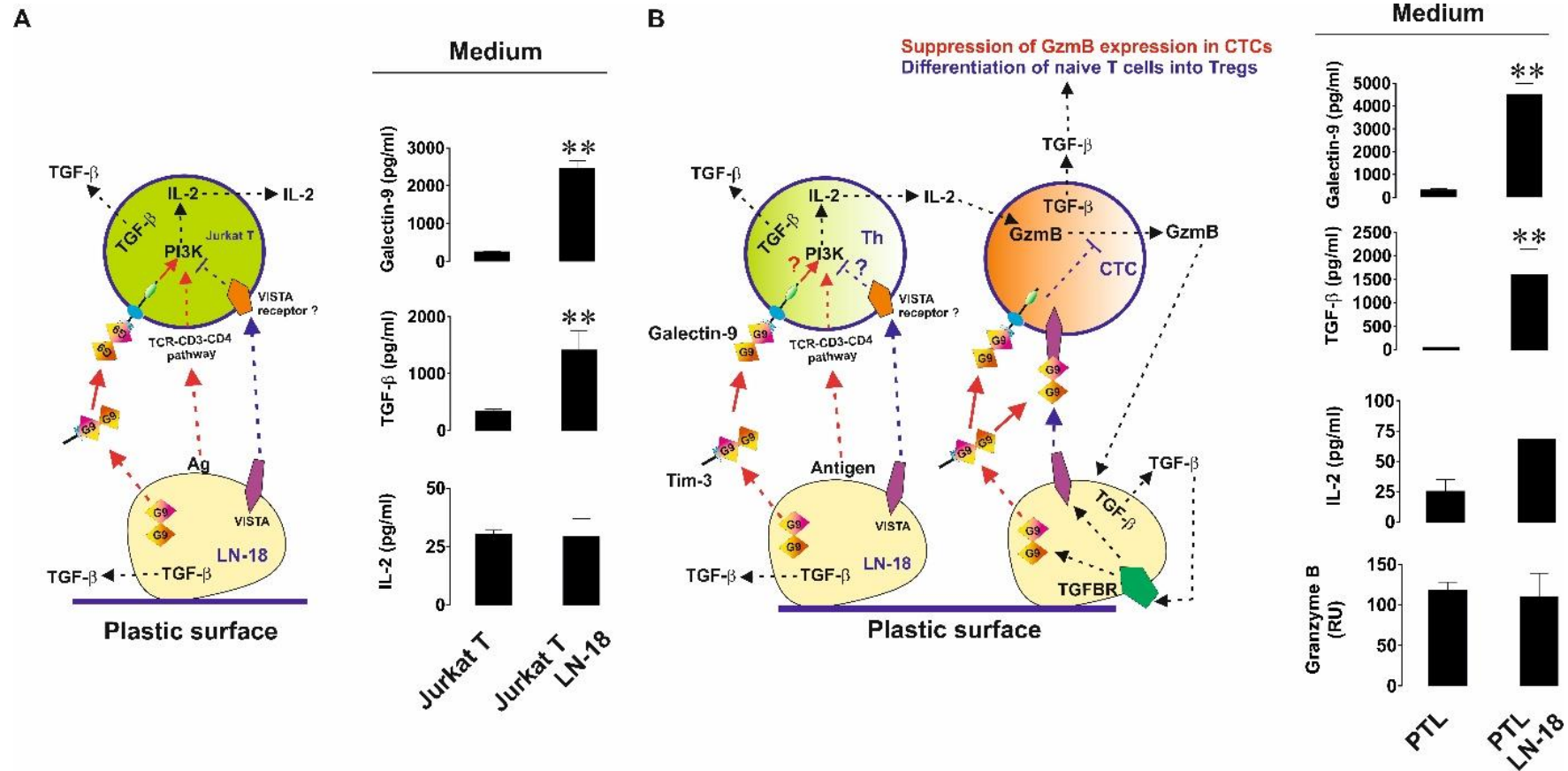


Figure 86 Expressing both galectin-9 and VISTA enables cancer cells to inhibit anti-cancer immunity of T helper and cytotoxic T cells. We cultured LN-18 glioblastoma cancer cells with Jurkat T cells (A) or primary CD3⁺ human T cells (B) for 16 h at a ratio of 1:1. We analysed the secreted levels of galectin-9, (if applicable) granzyme B, IL-2 and TGF- β using ELISA. The Data are acquired in six independent experiments, mean +/- SEM are shown.

The co-culture of LN-18 cells with Jurkat T cells as well as primary T cells lead to increased levels of VISTA on the cell surface (Figure 87), yet ELISA approaches did not show any increased secretion of VISTA.

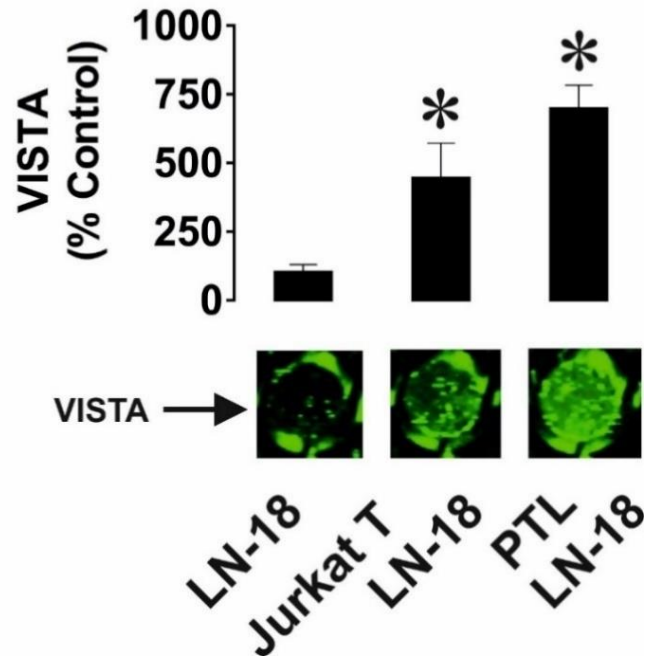


Figure 87 VISTA translocated onto the surface of LN-18 cells after induction by T cells. The glioblastoma cell line was kept in culture with either Jurkat T cells or primary T cells at a ratio of 1:1 for 16 h. We analysed the levels of VISTA on the cell surface using on-cell Western. Images shown are representatives of five independent experiments with similar results, mean +/- SEM shown.

To determine the influence of VISTA in triggering apoptotic events in T cells by interacting with galectin-9 we used a co-culture of LN-18 glioblastoma cells with Jurkat T cells and added either galectin-9 or VISTA neutralizing antibodies. In comparison to MCF-7 the IL-2 secretion levels in this co-culture did not change in presence of galectin-9 neutralizing antibody, neutralizing VISTA on the other hand led to an upregulation of IL-2 levels in the medium (Figure 88A). Investigating the Jurkat T cells we were able to also detect an increase in PI3K activity after neutralizing VISTA, clearly indicating a suppressive effect VISTA contributes to in T helper cells.

For in vivo confirmation of observed effects, we used xenograft models. We were interested to verify if the effects of LN-18 cells seen are also able to suppress primary T cell activities within mice. First, we decided to investigate the ability of LN-18 cells to inhibit the immune responses of mouse cytotoxic T cells by co-culturing LN-18 cells with mouse T cells for 16 h at a ratio of 1:1 with or without VISTA and galectin-9

neutralizing antibodies. We were able to detect a significant increase in release of granzyme B into the cell culture medium (Figure 88B). These levels were even further increased in case of galectin-9 neutralization present and high levels were detected in case of VISTA neutralization (Figure 88B). According to these results the viability of the cancer cells was clearly reduced while neutralizing either VISTA or galectin-9 (Figure 88B).

In the xenograft studies we were also able to verify that IL-2 levels were only upregulated if VISTA was neutralized as seen with the Jurkat co-culture studies (Figure 88A). Next, we studied total cell-associated human galectin-9 levels using lysates of mouse T cells by ELISA, as this method does not have a cross-reactivity with mouse galectin-9. While using the galectin-9 neutralizing antibody we were nearly unable to detect any galectin-9 levels in the T cells. In case of using VISTA neutralizing antibody these levels were significantly reduced (Figure 88B), as the inhibition of VISTA being available leads to galectin-9 lacking binding partners on the mouse T cells.

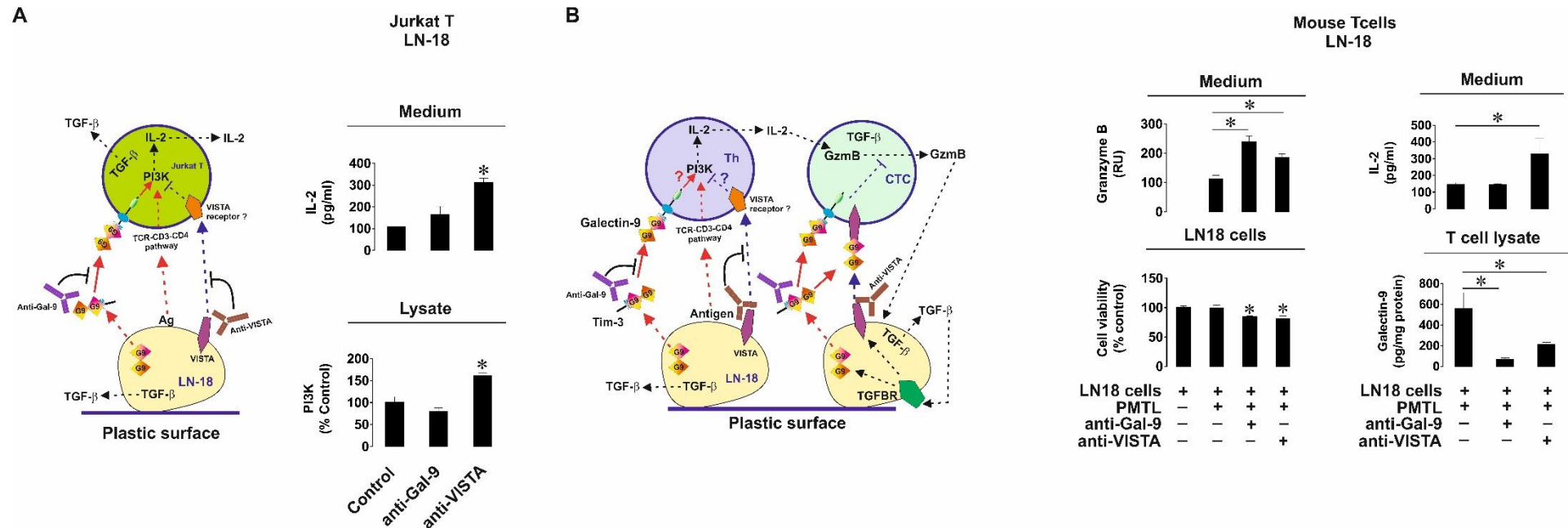


Figure 88 *Suppression of T helper and cytotoxic T cells activity is achieved by interaction between VISTA and galectin-9 on T cell surface.* We used a co-culture of LN-18 glioblastoma cancer cells with Jurkat T cells at a ratio of 1:1 for 16 h with or without VISTA and galectin-9 neutralizing antibody to study the effects of VISTA and galectin-9 on cell responses. We measured the PI3K activity within T cell lysates and the release of IL-2 in medium (A). Next, we repeated the experiment using primary mouse T cells instead of Jurkat T cells using also neutralizing antibodies. In cell culture medium we measured the release of granzyme B and IL-2 levels. LN-18 viability was measured using MTS assays, cell-associated human galectin-9 on mouse T cells was measured using the ELISA method. Data are included of six independent experiments, with mean +/- SEM shown.

3.5.1.4 In vivo studies confirm the ability of solid cancer cells to secrete galectin-9 to suppress the activity of cytotoxic T cells.

For confirming these results *in vivo*, we used the C57 BL16 mice, which are wild type and are not immunocompromised, we separated them in groups of five either receiving no injection as a control group or LN-18 cells being injected at a rate of 2×10^6 cells per mouse. After injection we waited five hours to take blood samples.

Next, we gathered the injection sites of each mouse and created soft homogenates with cell lysis buffer, consisting of 5 mM EDTA, 150 mM NaCl, 0.5% NP-40 and 50 mM Tris pH 7.5. This was performed to gather proteins secreted into the injection side's microenvironment as well as lyse the haematopoietic cells gathered there. In the injection side we found high levels of human galectin-9 secreted but no detectable levels of human VISTA. No amount of either was detectable in the control group. We were able to verify that in both groups the chosen area of injection contained T cells as we clearly detected CD3 proteins within the homogenates (Figure 89A). In the mice injected with LN-18 cells we found high levels of human galectin-9 within the blood plasma; no signals found in the control group as comparison. The lysates of primary mouse T cells also contained significant levels of human galectin-9, which could not be found in the control group (Figure 89B). In addition to that, TGF- β levels in the LN-18 cohort was also highly upregulated (Figure 89B).

Lastly, we investigated if the human galectin-9 is able to inhibit anti-cancer activity of the mouse T lymphocytes. To do so, we co-cultured at a ratio of 1:1 the T cells originating either from the mouse control group or the mouse with LN-18 injected with K562 cells that were pre-treated with 100 nM PMA for 24 h. The cells were kept together in culture for 24 h followed by analysing the viability of K562 cells. In case of using the control group mouse T cells, the viability of the K562 cells was clearly lower than in cells with no co-culture as well as those in culture with mouse T cells from the LN-18 group (Figure 89C). Therefore, we are able to verify that the interaction of cancer cells with T cells leads to a downregulation of immune responses against cancer cells.

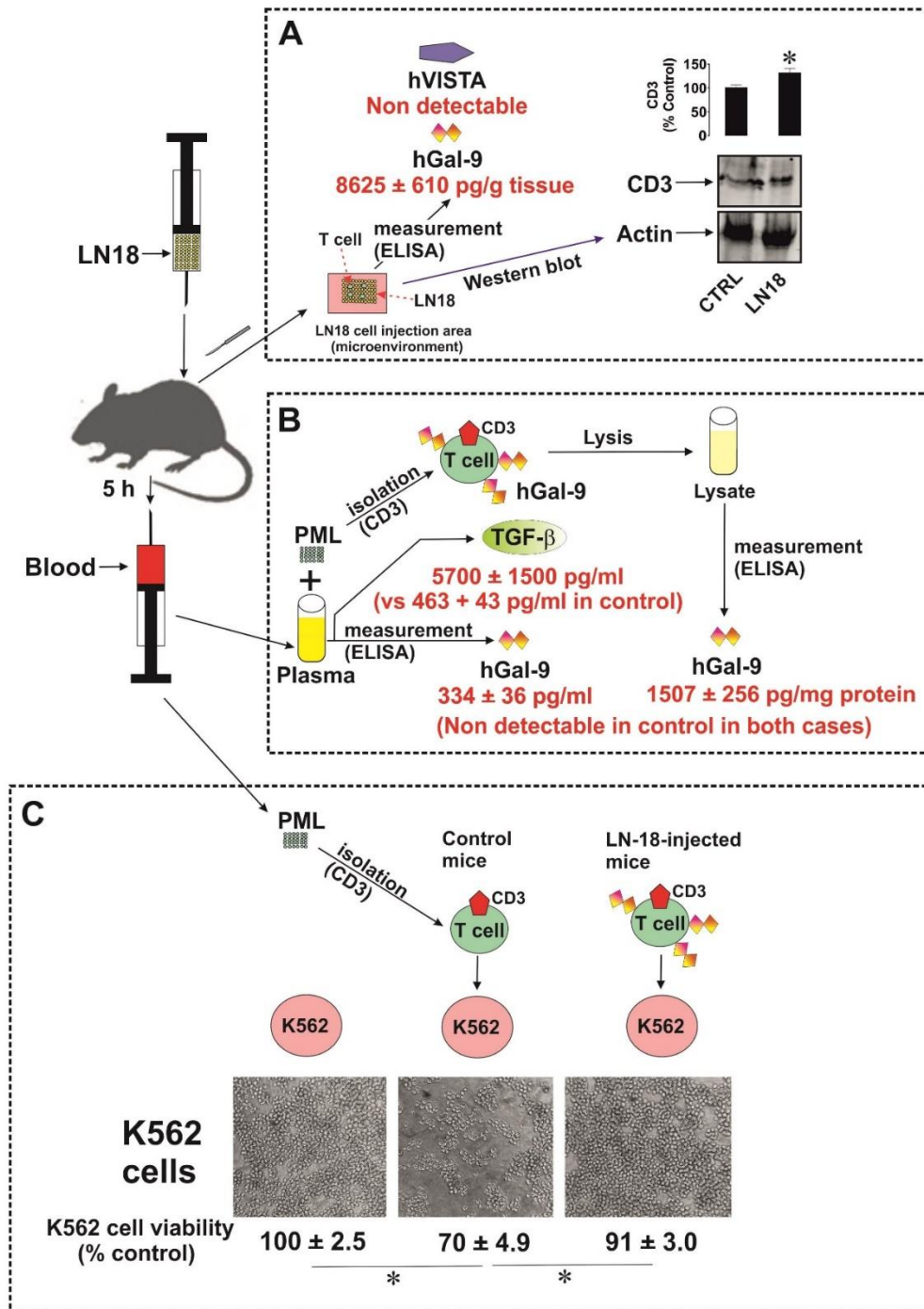


Figure 89 Detection of in vivo secretion of galectin-9 by solid cancer cells We used C57 BL16 mouse, which had tumorigenic LN-18 cells injected subcutaneously at 2×10^6 cells per mouse. We measured the presence of CD3 proteins as well as human galectin-9 and VISTA in the direct microenvironment of the injection site (A). We also investigated the levels of human galectin-9 and TGF- β in the blood plasma of these mice and the presence of human galectin-9 on the primary mouse T cell lysates (B). Lastly, we used a co-culture of K562 cells with primary mouse T lymphocytes taken from both control and LN-18 injected mice to determine their efficiency. We analysed the viability of these K562 cells using MTS assay, including images taken (C). Shown are images from five independent experiments, included are also mean +/- SEM values of these experiments.

3.5.1.5 Discussion.

The focus of our research in this chapter was to determine which mechanisms are used by cancer cells to secrete galectin-9 and suppress anti-cancer immune responses of T cells. In the previous chapters we did not see significant secretion of galectin-9 by resting solid tumour cells, yet the opsonization of T cells by secreted galectin-9 lead to inhibition of cytotoxic T cell responses. This leads to the expression of an “eat-me” signal by phosphatidyl serine externalisation. We therefore were interested in determining if interactions between T cells and solid cancer cells leads to a triggering of galectin-9 secretion. In this study, we were able to show that using T cell lines such as Jurkat T cells (helper cells) and TALL-104 cells (cytotoxic T cells) as well as primary human CD3⁺ T cells led to an induction of galectin-9 secretion in a variety of solid cancer cells including kidney, breast, and high-grade glioblastoma cancer cells. Important to note is that also in non-malignant keratinocytes (HaCaT cell line) the contact to T cells induced a secretion of high levels of galectin-9 (Figure 80), though lesser amount than in cancer cells. In case of primary human foetal cells, which as mentioned in the chapter prior express high galectin-9 levels on the cell surface, no secretion of galectin-9 was detectable after exposure to T cells (Figure 80).

Galectin-9 itself does not express any secretion sequences, therefore a carrier/trafficker protein is required, as seen in the AML cancer cell study. In case of Tim-3 being available this protein was preferred as a carrier due to a higher binding affinity to galectin-9 than others, for example VISTA (Yasinska, 2020; Prokhorov, 2015). Yet, in cell types such as the WT3ab cell line (Wilms' tumour) with no detectable amount of Tim-3 is expressed, VISTA was used as a corresponding carrier for galectin-9.

Seemingly, galectin-9 secretion can be adapted by healthy cells such as keratinocytes too to induce immune evasion as seen in cancer cells (Figure 80). This might be corresponding with the possibility of galectin-9 being responsible for certain events in disorders such as psoriasis, in which an increased immune response of T cells against keratinocytes is detectable, while in this case keratinocytes are able to suppress T cell responses by high galectin-9 levels present and do proliferate excessively (Casciano, 2018). Therefore, our results propose a possible influence of galectin-9 levels regarding the suppressive functions lacking in cases of autoimmunity. Embryonic cells do not aim to actively suppress T cell responses in general as the immune system is

needed to protect both the mother's body as well as the embryo against infections and stress. These cells do have galectin-9 translocated onto the surface in case of T cells attempting to attack the foetus directly. Cancer cells on the other hand depend on suppressing T cells approaching the tumour cells in the microenvironment and high numbers of T cells found in the circulatory system if galectin-9 is being secreted into the blood stream.

By addition of pharmacological inhibitors to the cell culture we were able to verify that cancer cells use matrix metalloproteinases to shed galectin-9 from the cell surface after translocation by carriers such as Tim-3 and VISTA. In our studies we were able to determine that these mechanisms are PKC-dependent and PLC-independent. Within cancer cells we were able to detect high levels of intracellular calcium if these cells were engaging with T cells. As Gö6983 can inhibit this process Ca²⁺-dependent and DAG-independent PKC isoforms might play a role in this mechanism. The levels of intracellular Ca²⁺ were most likely elevated in a PLC-independent manner as the use of the PLC inhibitor U73122 did not lead to any changes of the intracellular calcium levels (Figure 84) and no changes in the galectin-9 secretion (Figure 83B).

Another possible mechanism recruits the formation of autophagosomes to induce secretion of galectin-9 by autophagy in complex with Tim-3 or VISTA localized onto the cell surface. Secretion is done by fusion with a lysosome inducing lysosomal exocytosis. Hereby, galectin-9 is shed off by proteases within the lysosome followed by release by exocytosis (Buratta, 2020).

The results gathered demonstrate that galectin-9 can suppress the activities of both T helper and cytotoxic T cells while cooperating with other immune checkpoint proteins. It is already known that the interaction with Tim-3 on the surface of T cells can induce the activation of PI3K and its downstream pathway. In T helper cells this mechanism is verified by using galectin-9 derived from MCF-7 breast cancer cells (Figure 85). The activation of the PI3K pathway also led to an increase in IL-2 expression and production within the T helper cells. We were able to verify this in the Jurkat T cells which were co-cultured with MCF-7 breast cancer cells (Figure 85). Therefore, in order to block the production of IL-2 and its function to recruit an immune response towards the cancer cells another checkpoint protein able to interact with galectin-9 is needed. One of such proteins known to suppress the activation of IL-2 production is PDL1 which can upregulate SHP2 phosphatase activity leading to the blockage of PI3K and MAP

kinase pathways (Wu, 2021). This can also attenuate the activation of anti-apoptosis protein BCL-XL, enabling the death of cytotoxic T cells by granzyme B leakage due to increased binding of galectin-9. Yet, the MCF-7 cells we used for our studies do not produce PD-L1 as well as VISTA which is a member of the B7 family of proteins similar to PD-L1. We determined that VISTA is able to suppress the PI3K pathway and IL-2 production and therefore enhance the effects of galectin-9 to induce killing of cytotoxic T cells as well as suppressing the overall activity of both T helper and cytotoxic T cells. By co-culturing of LN-18 high-grade glioblastoma cells with either Jurkat T or primary human or mouse CD3⁺ T cells we were able to confirm this effect. If a VISTA neutralization antibody was added to the co-culture both IL-2 production and PI3K activity were upregulated, suggesting that VISTA is used to block this pathway, LN-18 express barely detectable levels of PD-L1 (Tong, 2020). Similar to this study did the addition of VISTA or galectin-9 neutralizing antibody to a co-culture of LN-18 cells with primary mouse T cells lead to a decreased viability of the cancer cells and an increase in granzyme B release by the T cells (Figure 88B). The increase in granzyme B release after neutralization of VISTA has already been determined in prior studies focussing on VISTA as galectin-9 receptor expressed on T cells and its inhibitory effects of PI3K activity and IL-2 production in different T cell types.

We also investigated the effects of galectin-9 secretion by solid cancer cells *in vivo*, by injecting LN-18 cells into mice subcutaneously which led to a release of galectin-9 into the environment after interacting with mouse T cells (Figure 89). In these mice we were also able to detect human galectin-9 within the blood stream, which was able to opsonize the mouse T cells. TGF- β levels were also highly upregulated in the LN-18-injected mice compared to control mice, the ELISA approach hereby detected both mouse and human TGF- β , while in the galectin-9 studies we were able to detect only human derived. The TGF- β detected was most likely produced in a para- and autocrine way by mouse T cells after human galectin-9 bound. As confirmed by the data seen in Figure 88B does galectin-9 affect the function of mouse T cells. We decided to confirm this by co-culturing T cells derived from the control and LN-18-injected mice with K562 cells as they do not engage in studied immune evasion methods (Goncalves-Silva, 2017). If the K562 were co-cultured with control group T cells viability was significantly reduced, an effect we were not able to detect in the LN-18 derived T cell co-culture. These results clearly show that the exposure of T cells to LN-18 cancer cells led to a

decrease in their efficiency to kill other cells due to the opsonisation by galectin-9 (Figure 89).

In summary, we were able to show for the very first time that solid cancer cells are able to release galectin-9 after interacting with T cells. The mechanisms needed are either proteolytic shedding after translocation to the cell surface or the use of lysosomal secretion by autophagy including proteolytic shedding. These mechanisms are also found in non-malignant cells such as keratinocytes after exposure to T cells and might explain the suppressive effects of keratinocytes on T cells during psoriasis development in which it will lead to significant keratinocyte proliferation. On the other hand, embryonic cells expressing high levels of galectin-9 on the cell surface did not secrete it after interacting with T cells, this indicates that here galectin-9 is solely used to inhibit direct attacks of T cells rather than suppressing their efficiency in the environment. The suppressive effect of galectin-9 on T cells such as inhibiting IL-2 production by T helper cells as well as attenuating cytotoxic T cell responses is further potentiated by galectin-9 interacting with VISTA. Hereby, the interaction between VISTA and galectin-9 inhibits the activation of the PI3K pathway as well as BCL-XL anti-apoptotic proteins and leads to the alternation of the membrane potential. These results clearly show that galectin-9 and its corresponding receptors and pathways should be considered as a highly efficient target to develop immunotherapy against a wide range of cancers.

3.5.2 DIFFERENTIATION AND POLARIZATION OF MACROPHAGES ENABLES THEM TO RELEASE VISTA AS A CHECKPOINT IMMUNE PROTEIN

In our studies we have been collaborating with colleagues in a variety of countries. One such collaboration was performed with colleagues of the department of human medicine at the University of Oldenburg. In this study the focus was on where the secreted VISTA proteins detectable in the tumour microenvironment come from. A cell type able to produce VISTA are tumour-associated macrophages. These cells were investigated regarding their ability to secrete the expressed VISTA protein by proteolytic shedding. Macrophages can be separated into two groups, one consists of M1 macrophages, which are activated classically and are able to produce cytokines such as IL6, IL-12 and IL-23 (Shapouri-Moghaddam, 2018).

The second group is named M2 macrophages which are activated in a non-classical way and are able to produce high amounts of TGF- β and cytokines such as IL-10. While these specifications are allowing researchers to differentiate macrophages, the exact way of activation *in vivo* consists of a higher variety of macrophage types being produced allowing the presence of further subtypes as well as tissue-type specific macrophages mostly dependent on the cytokines used to activate them. Subtypes are responsible for different functions such as enabling wound healing (M2a), regulating Th2 responses (M2b), and immunosuppression (M2c). One of such subtypes are associated with tumour cells, M2d, which are enabling angiogenesis, formation of metastasis as well as overall tumour growth. These subtypes are often difficult to separate from each other due to similar functions in for example allergies as well as due to the possibility of forming mixed phenotypes (Martinez-FO, 2014; Viola, 2019). Macrophages are able to highly express VISTA similar to other hematopoietic cells especially myeloid cells such as monocytes. Studies with mouse kidney cells showed that macrophages associated with this tissue type expressed high levels of VISTA, yet during infiltration VISTA expression has been downregulated. Further research also shows that dysregulation of VISTA expression on macrophages can cause issues during ischemic injury repair of kidney tissues as it can lead to impairment of cytokine and chemokine production (Broughton, 2019; Park, 2019).

In prior studies shown in this thesis we were able to find higher levels of released VISTA by acute myeloid cells in comparison to healthy mononuclear leukocytes. The

effect of VISTA on resting and activated macrophages are still unknown as well as the possibility of macrophages releasing soluble VISTA by proteolytic shedding. In this chapter we collaborated with our colleagues to determine the effects of VISTA on monocytes and macrophage types M1 and M2. This study also focussed on understanding the effects of soluble VISTA on the inhibition of cytotoxic T cell activity.

3.5.2.1 Monocytes express high levels of VISTA and release it into the microenvironment by metalloproteinases cleavage.

In cancer cells, as shown prior, the release of VISTA is facilitated by proteolytic cleavage by matrix metalloproteinases after its expression, glycosylation, and translocation onto the cell surface (Figure 90A). Our collaborators in Germany decided to investigate if this mechanism is deployed also by monocytes. They used flow cytometry to analyse VISTA expression on primary isolated monocytes (Figure 90B). These cells were exposed to 50 μ M of batimastat (broadband inhibitor against metalloproteinases) as well as GI254023X (specific inhibitor against ADAM 10 and matrix metalloproteinases 9 (MMP-9)) for 3 days to suppress any proteolytic cleavage. They were able to verify that these inhibitors also led in monocytes to an impairment of release of VISTA (Figure 90C).

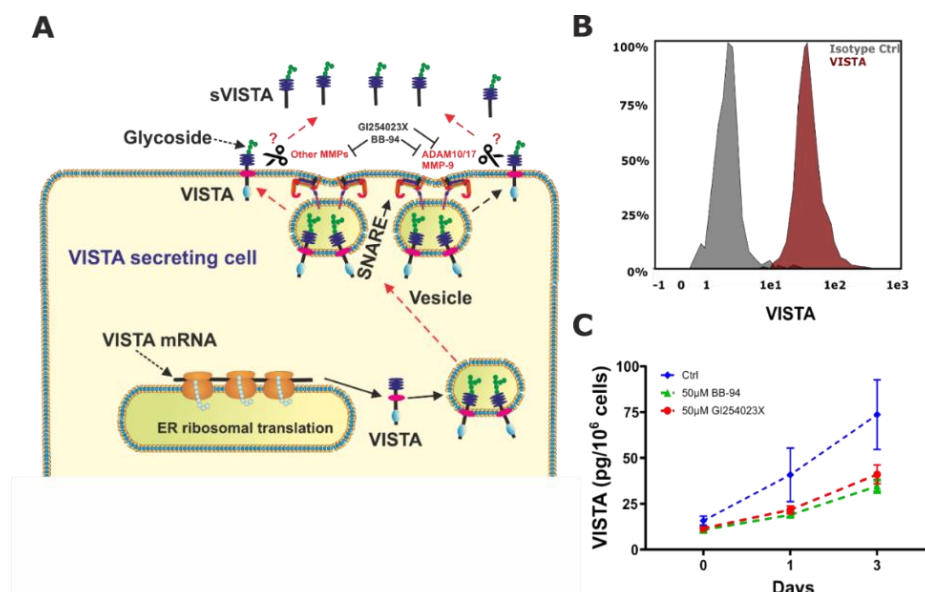


Figure 90 Analysis of monocytes regarding VISTA expression. A scheme was made to show the functions of metalloproteinases in regard of VISTA shedding from monocytes and the position on which the inhibitors used act (A). Primary human monocytes were investigated by our collaborators regarding their VISTA expression by flow cytometry (B). Our collaborators were able to verify the release of VISTA is dependent on metalloproteinases by incubating monocytes with inhibitors (C).

3.5.2.2 VISTA secretion can be detected in differentiating macrophages but not fully differentiated ones.

Important for this study is that our collaborators were also able to analyse VISTA expression in both M1 and M2 macrophages by using immunofluorescence microscopy, as such the VISTA protein has been found within the unstimulated cells, most likely in intracellular vesicles (Figure 91).

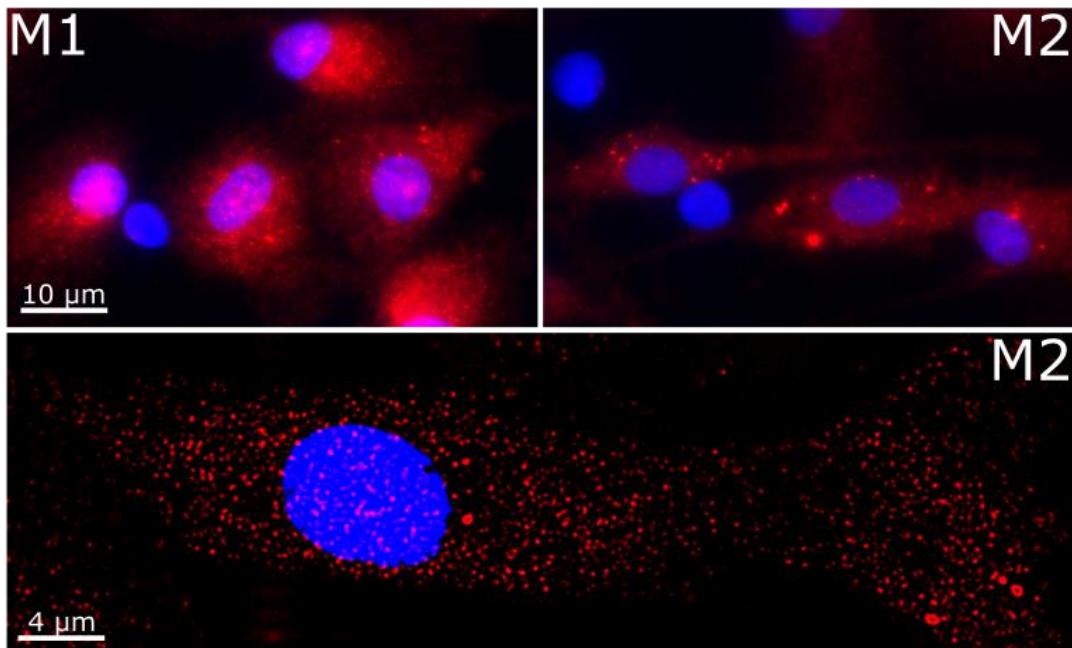


Figure 91 Determination of VISTA within M1 and M2 macrophages. Analysis was performed by our collaborators. Staining was performed by using monoclonal anti-human VISTA antibody (mouse) and secondary Alexa Fluor 594-coupled antibody. The lower part shows deconvolution of a z-stack.

3.5.2.3 VISTA released into the microenvironment is able to inhibit the functions in TALL-104 and Jurkat T cells but does not induce apoptosis.

We decided then to investigate the effects of this soluble VISTA as found by our collaborators and determine its suppressive effects on cytotoxic T cells. We hereby exposed first TALL104 T cells (CD8⁺) for 16 h to 5 µg/ml VISTA-Fc proteins or as an isotype control of just Fc proteins. After incubation we analysed in-cell activity of granzyme B and viability of these cells. VISTA itself was unable to upregulate granzyme B within the T cells and did not cause changes in their viability (Figure 91A-C) as seen in previous studies with PMA-activated, granzyme B expressing Jurkat T cells.

Next, we repeated this experiments using T helper cells instead and investigated the effects of soluble VISTA on these. To do so, we cultured Jurkat T cells (CD4⁺) with K562 which are able to stimulate Jurkat T cells by interacting with TCR (Figure 91D-H). As comparison we used PMA-activated Jurkat T cells (granzyme B-producing). In both co-cultures we were able to detect a decrease in IL-2 release in presence of soluble VISTA, most likely caused by the downregulation of PI3K activity in the Jurkat T cells.

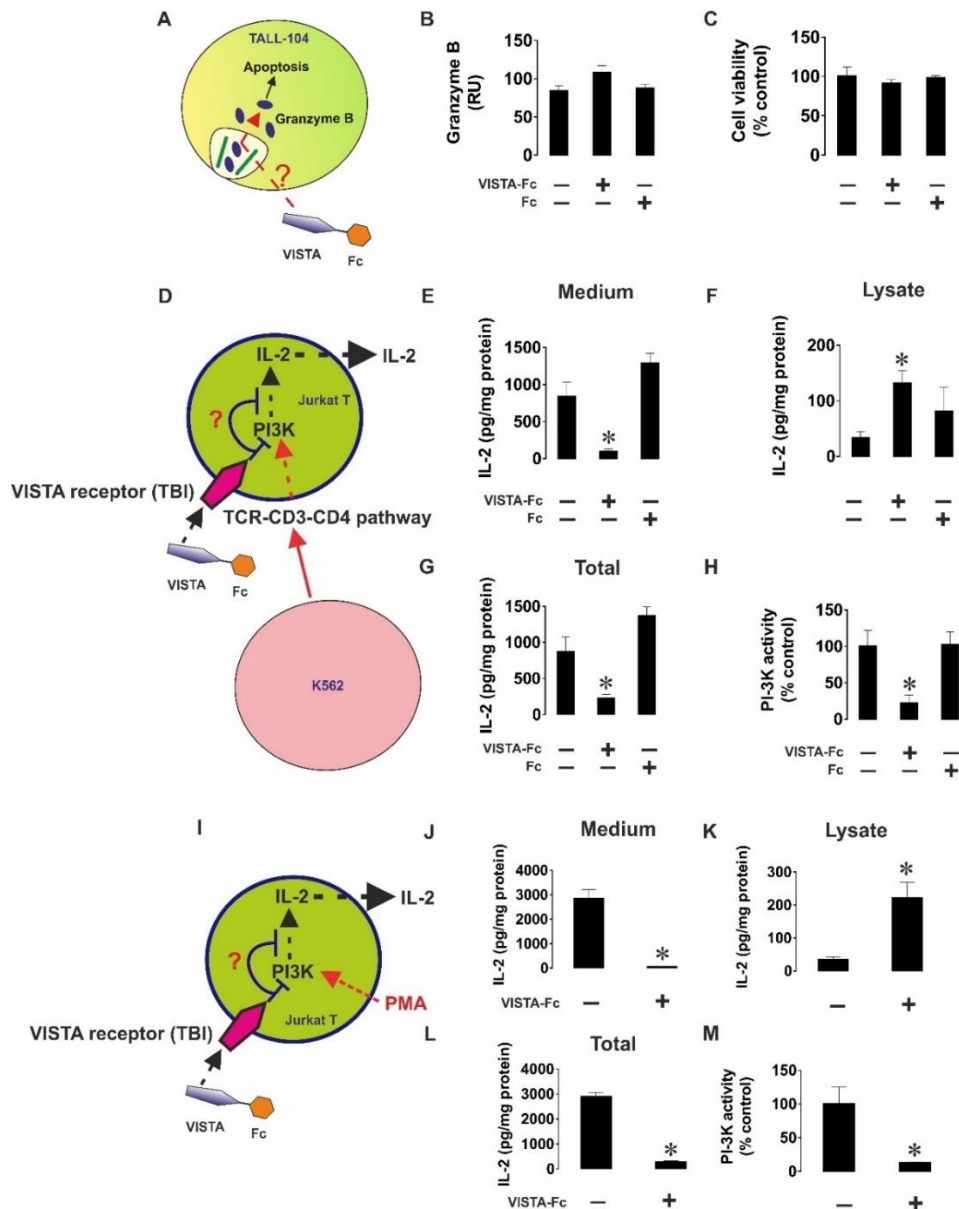


Figure 92 Soluble VISTA released into the microenvironment does not lead to activation of intracellular granzyme B activity in cytotoxic T cells and prevents T helper cells from releasing IL-2. (A) TALL-104 cells were kept in culture with either 5 $\mu\text{g/ml}$ VISTA-Fc or as control solely Fc for 16 h. (B) Viability of TALL-104 was determined after exposure. (C) For further studies we used K562 human chronic myeloid leukaemia cells, which do not express and release detectable amounts of VISTA and IL-2. These cells were treated with 100 nM PMA for 24 h to immobilize them onto wells of a Maxisorb plates followed by a co-culture with Jurkat T cells at a ratio of 1:1. (D) In some of the Jurkat co-culture wells we added either 5 $\mu\text{g/ml}$ VISTA-Fc or control Fc for 24 h before being separated. In these co-cultures, IL-2 secretion was measured (E) within the medium and (F) within cell lysates by ELISA approach. (G) Total amount of IL-2 found within the cells were calculated. (H) Measurement of PI3K activity was performed. (I) Jurkat T cells pre-treated with 100 nM PMA were exposed to either VISTA-Fc or control Fc for 24 h. Again IL-2 was measured in (J) medium and (K) cell lysates. (L) Total amount of IL-2 detectable was calculated and (M) PI3K activity analysed within these cells. The data shown include mean \pm SEM of four independent experiments. * $p < 0.05$ vs. control samples.

Lastly, to determine the ability of soluble VISTA to suppress activity of cytotoxic T cells we co-cultured K562 chronic myeloid leukaemia cells, with low amounts of VISTA and galectin-9 present, with TALL-104 cells in presence or absence of 5 $\mu\text{g/ml}$ VISTA-Fc or isotype control. In each of these cultured experiments the cell viability and in-cell granzyme B activity was assessed. In presence of VISTA K562 cells were not injected with granzyme B therefore preventing the induction of cell death (Figure 92). VISTA was not able to activate granzyme B within the TALL-104 cells (Figure 92). These results clearly indicate that while VISTA is able to prevent injection of granzyme B within the targeted cells, such as cancer cells, the presence of VISTA alone does not lead to an activation of granzyme B within the T cells themselves.

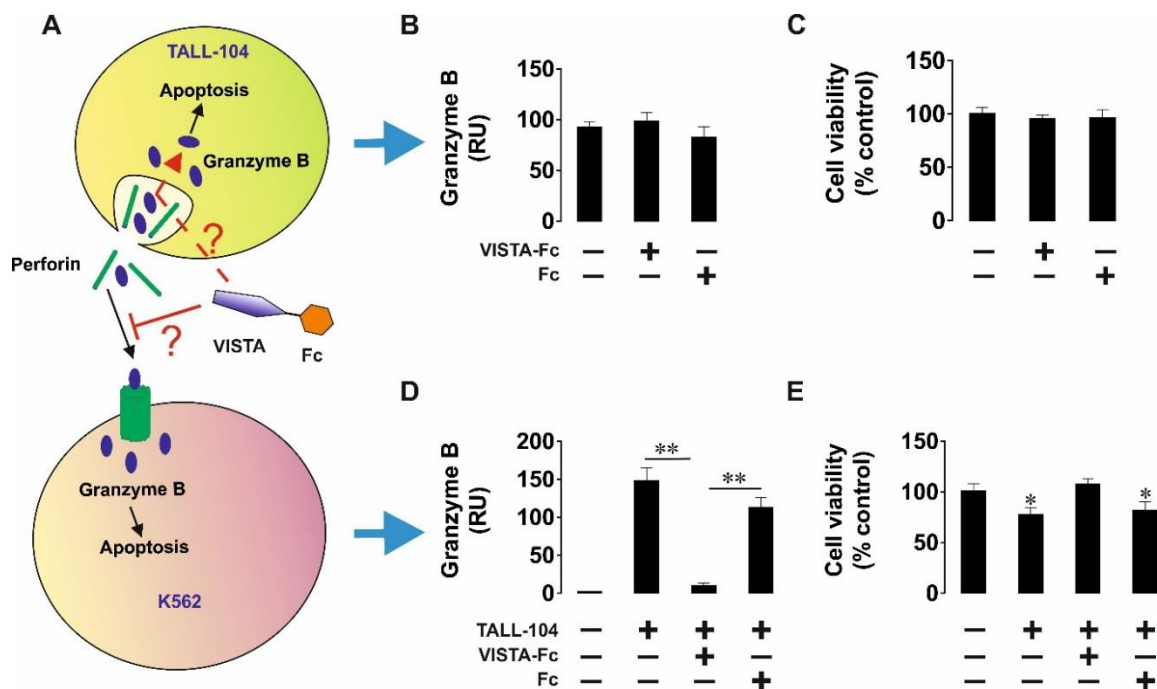


Figure 93 Soluble VISTA influences the granzyme B release into target cells (e.g. chronic myeloid leukaemia cells) but does not induce cell death in cytotoxic T cells. (A) K562 cells were immobilized onto wells of a maxisorp plate by exposure to 100 nM PMA for 24 h. These cells are known to not express and release any significant levels of galectin-9. After immobilization the medium in each well was replaced with Iscove's Modified Dulbecco's medium formulated by ATCC containing 2.5 $\mu\text{g/ml}$ human albumin, 0.5 $\mu\text{g/ml}$ D-mannitol and foetal bovine serum as well as 100 units/ml recombinant human IL-2. To some of these wells TALL-104 cells were added at a ratio of 1:1. Some co-cultured wells were supplied with either VISTA-Fc or control Fc for 16 h. (B) In co-cultured TALL-104 cells in-cell granzyme B activity was measured, and (C) cell viability was analysed. (D) In K562 cells in-cell activity of granzyme B was determined as well as (E) cell viability. Data set includes mean \pm SEM of four independent experiments. * $p < 0.05$, ** $p < 0.01$ vs. control.

3.5.2.4 Discussion.

The production and specific activity of VISTA is important to understand for determining the effects of the galectin-9 interaction with VISTA in presence of cancer cells. In previous studies, VISTA has been found on the surface of a variety of cell types including monocytes. The results gathered by our collaborators and us demonstrate that soluble VISTA can be released by monocytes and to a certain extent by macrophages within the tumour-microenvironment by proteolytic shedding. These processes are attenuated by inhibitors against either matrix metalloproteinases in general or against specific proteinases such as ADAM 10 and MMP-9 (Figure 89C) (Yasinska, 2020). The findings are verifying results from experiments performed with plasma from primary human acute myeloid leukaemia samples in which levels of truncated forms of VISTA were detectable. Cleavage on THP-1 AML cells was inhibited targeting metalloproteinases by proteinase inhibitor GI254023X. As VISTA is also seen as a homolog protein to PD-L1 and such exosomal PD-L1 leads to immunosuppression, we were interested to study VISTA regarding a potential of inducing the suppression of immune responses in cancer patients. Our collaborators were able to find that shedding of VISTA was mainly detectable in monocytes that have yet to be differentiated while fully differentiated monocytes indicated lowered ability to release VISTA (Figure 90). VISTA release from macrophages seems to be determined by stimulation with cytokines depending on if the stimulation is pro- or anti-inflammatory. This indicates that VISTA is crucial for regulation of adaptive and innate immune responses.

While VISTA deficiency in macrophages has been found to lead to high levels of inflammatory cytokines being produced understanding the exact mechanisms of VISTA release by macrophages is important to determine its influence in regard to immune regulation and potentially macrophage polarization. In studies prior it was also shown that macrophages in mice downregulated VISTA production after LPS stimulation (Borggrewe, 2018, Rodrigez-Garcia, 2011). Further studies are needed to understand if prolonged exposure to LPS can lead to constant decrease of VISTA in macrophages and may induce depletion of VISTA produced.

Studies performed so far indicate that VISTA can generally downregulate immune responses by cytotoxic T cells and might inhibit cytokine production (Wag, 2011 & 2014). The exact role of soluble VISTA has yet to be understood. In the experiments

performed by us in this study we were able to determine that soluble VISTA leads to a suppression of cytotoxic T cell activity yet does not lead to an increase in in-cell activity of granzyme B and therefore does not induce apoptosis of T cells. Altogether the findings in our studies indicate that the interaction between galectin-9 and VISTA is needed to induce cell death of approaching cytotoxic T cells within tumour-microenvironment. Soluble VISTA does inhibit the release of granzyme B into targeted cancer cells by T cells but does not induce cell death of such T lymphocytes. This clearly indicates an important mechanism regarding granzyme B within negative T cell malignancies as T cells normally do not tend to release high levels of galectin-9 and therefore malignancies use it to evade targeted attacks by cytotoxic T cells. Malignant T cells are also able to produce and release soluble VISTA, a combination of high galectin-9 and VISTA can be used by these malignancies to evade immune responses.

In summary, in this study performed by our collaborators and us, we were able to detect soluble VISTA released by monocytes. Furthermore, soluble VISTA is able to suppress cytotoxic T cell activity but does not lead to increased apoptosis of such cells. While monocytes are able to release VISTA into the blood stream to suppress the activation of resting T cells, once they are interacting with infections by pathogens these cells differentiate into macrophages and downregulate their ability to release VISTA. Altogether we provided more insight into the role of VISTA regulating innate and adaptive immune responses.

4 FUTURE OUTLOOK

These results gathered clearly verify a complex mechanism used during the cancer immune suppression, which has been originating from the embryonic development. As such it is a target to modulate with a high potential to efficiently manipulate the immune system against malignancies. As all these pathways are highly regulated by TGF- β , attempting to externally regulate the amount of such being available has a high potential to further manipulate each of these proteins being produced. The next steps therefore should be to investigate the exact cell-internal mechanisms induced by the interaction of galectin-9 with both VISTA and Tim-3 on T cells and determine which of these components is potentially the main activator of anti-cancer immunity. If the corresponding protein is mostly upregulated by TGF- β an inhibitor against this specific component should be the best approach to regulate the interaction between T cells and cancer cells. Furthermore, suppression of VISTA and galectin-9 production by other cells recruited by cancer cells, such as macrophages should also be aimed for.

By understanding the origin of these pathways we can further clarify how exactly it can be manipulated. The further down in evolution we are able to find it the more likely it is a very stable target, which is not easily manipulated by cancer cells using mutations. Also, investigating it in healthy organisms and healthy tissue enables us to determine its influence on miscarriages or autoimmunity as our data clearly indicates that this mechanism seem to correlate with severe complications leading to both of these issues.

Lastly, future research should also be invested in understanding the internal mechanisms within both cancer cells and lymphocytes activated after the binding of VISTA/Tim-3 with galectin-9. Determining which immunoregulatory pathways are induced after the interaction will lead to further understanding how the cancer cells are able to efficiently suppress anti-cancer immunity.

Mapping these pathways accordingly will enable the identification of key factors detectable within human blood samples permitting the recognition of immune evasion machinery operated by each individual tumour type. This allows the development of personalized targeted immunotherapy in the future, which will include the investigated proteins and their activation pathways.

5 BIBLIOGRAPHY

Merlo, L., Pepper, J., Reid, B. *et al.* Cancer as an evolutionary and ecological process. *Nat Rev Cancer* 6, 924–935 (2006).

Tak W. Mak, Mary E. Saunders, Bradley D. Jett, Chapter 20 - Hematopoietic Cancers, Editor(s): Primer to the Immune Response (Second Edition), Academic Cell, 2014, Pages 553-585,

Shao C, Li G, Huang L, et al. Prevalence of High Tumor Mutational Burden and Association With Survival in Patients With Less Common Solid Tumors. *JAMA Netw Open*. 2020;3(10):e2025109. doi:10.1001/jamanetworkopen.2020.25109

The Global Cancer Observatory - All Rights Reserved, December, 2020. WHO website <https://gco.iarc.fr/today/home>

Hanahan D. Hallmarks of Cancer: New Dimensions. *Cancer Discov*. 2022 Jan;12(1):31-46.

Das SK, Menezes ME, Bhatia S, Wang XY, Emdad L, Sarkar D, Fisher PB. Gene Therapies for Cancer: Strategies, Challenges and Successes. *J Cell Physiol*. 2015 Feb;230(2):259-71.

Maccalli C, Volontè A, Cimminiello C, Parmiani G. Immunology of cancer stem cells in solid tumours. A review. *Eur J Cancer*. 2014 Feb;50(3):649-55.

Anand P, Kunnumakkara AB, Sundaram C, Harikumar KB, Tharakan ST, Lai OS, Sung B, Aggarwal BB. Cancer is a preventable disease that requires major lifestyle changes. *Pharm Res*. 2008 Sep;25(9):2097-116.

Preetha Anand, Ajai Kumar B. Kunnumakara, Chitra Sundaram, Kuzhuvilil B. Harikumar, Sheeja T. Tharakan, Oiki S. Lai, Bokyung Sung, and Bharat B. Aggarwal, Cancer is a Preventable Disease that Requires Major Lifestyle Changes, *Pharm Res*. 2008 Sep; 25(9): 2097–2116

Mroz EA, Rocco JW. The challenges of tumor genetic diversity. *Cancer*. 2017 May 15;123(6):917-927. doi: 10.1002/cncr.30430. Epub 2016 Nov 8. PMID: 27861749; PMCID: PMC5370554.

Eisenhauer EA, Therasse P, Bogaerts J, Schwartz LH, Sargent D, Ford R, Dancey J, Arbuck S, Gwyther S, Mooney M, Rubinstein L, Shankar L, Dodd L, Kaplan R, Lacombe D, Verweij J. New response evaluation criteria in solid tumours: revised RECIST guideline (version 1.1). *Eur J Cancer*. 2009 Jan;45(2):228-47.

Ma Y, Wang Q, Dong Q, Zhan L, Zhang J. How to differentiate pseudoprogression from true progression in cancer patients treated with immunotherapy. *Am J Cancer Res*. 2019 Aug 1;9(8):1546-1553.

Kamińska M, Ciszewski T, Łopacka-Szatan K, Miotła P, Starosławska E. Breast cancer risk factors. *Prz Menopauzalny*. 2015 Sep;14(3):196-202.

Giuliano, A.E., Edge, S.B. & Hortobagyi, G.N. Eighth Edition of the AJCC Cancer Staging Manual: Breast Cancer. *Ann Surg Oncol* 25, 1783–1785 (2018)

<https://www.cancerresearchuk.org/about-cancer/breast-cancer/survival>

Stieglitz E, Loh ML. Genetic predispositions to childhood leukemia. *Ther Adv Hematol*. 2013 Aug;4(4):270-90.

Forman WB. Cancer in persons with inherited blood coagulation disorders. *Cancer*. 1979 Sep;44(3):1059-61.

Cai SF, Levine RL. Genetic and epigenetic determinants of AML pathogenesis. *Semin Hematol*. 2019 Apr;56(2):84-89.

Czeh M, Rosenbauer F. Uncovering a new cellular origin for acute myeloid leukemia with lineage plasticity. *Mol Cell Oncol*. 2016 Dec 14;4(2):e1268241.

Kumar CC. Genetic abnormalities and challenges in the treatment of acute myeloid leukemia. *Genes Cancer*. 2011 Feb;2(2):95-107.

Welch JS, Ley TJ, Link DC, Miller CA, Larson DE, Koboldt DC, Wartman LD, Lamprecht TL, Liu F, Xia J, Kandoth C, Fulton RS, McLellan MD, Dooling DJ, Wallis JW, Chen K, Harris CC, Schmidt HK, Kalicki-Veizer JM, Lu C, Zhang Q, Lin L, O'Laughlin MD, McMichael JF, Delehaunty KD, Fulton LA, Magrini VJ, McGrath SD, Demeter RT, Vickery TL, Hundal J, Cook LL, Swift GW, Reed JP, Alldredge PA, Wylie TN, Walker JR, Watson MA, Heath SE, Shannon WD, Varghese N, Nagarajan R, Payton JE, Baty JD, Kulkarni S, Klco JM, Tomasson MH, Westervelt P, Walter MJ, Graubert TA, DiPersio JF, Ding L, Mardis ER, Wilson RK. The origin and evolution of mutations in acute myeloid leukemia. *Cell*. 2012 Jul 20;150(2):264-78.

Hwang SM. Classification of acute myeloid leukemia. *Blood Res*. 2020 Jul 31;55(S1):S1-S4.

Lynch HT, Follett KL, Lynch PM, Albano WA, Mailliard JL, Pierson RL. Family History in an Oncology Clinic: Implications for Cancer Genetics. *JAMA*. 1979;242(12):1268-1272.

Conklin KA. Chemotherapy-associated oxidative stress: impact on chemotherapeutic effectiveness. *Integr Cancer Ther*. 2004 Dec;3(4):294-300.

Wu J, Waxman DJ. Immunogenic chemotherapy: Dose and schedule dependence and combination with immunotherapy. *Cancer Lett*. 2018 Apr 10;419:210-221.

Tormey DC. Combined chemotherapy and surgery in breast cancer: a review. *Cancer*. 1975 Sep;36(3):881-92.

Muhammad Raza, Muhammad Imran, Shafi Ullah, Nanocarriers for Cancer Diagnosis and Targeted Chemotherapy, Chapter 1: Potential physical and biological barriers leading to failure of cancer chemotherapy, 2019

Kennedy LB, Salama AKS. A review of cancer immunotherapy toxicity. *CA Cancer J Clin*. 2020 Mar;70(2):86-104. doi: 10.3322/caac.21596. Epub 2020 Jan 16. PMID: 31944278.

Biotechnne CURRENT AND EMERGING IMMUNE CHECKPOINT TARGETS FOR IMMUNO-ONCOLOGY RESEARCH

John L. Marshall, Lee M. Ellis . Edward P. Gelmann, Howard L. Kaufman . Louis M. Weiner, Emanuel F. Petricoin, Cancer Therapeutic targets, Springer (2017)

Zhu H, Bengsch F, Svoronos N, Rutkowski MR, Bitler BG, Allegranza MJ, Yokoyama Y, Kossenkov AV, Bradner JE, Conejo-Garcia JR, Zhang R. BET Bromodomain Inhibition Promotes Anti-tumor Immunity by Suppressing PD-L1 Expression. *Cell Rep.* 2016 Sep 13;16(11):2829-2837.

Huang Q, Zheng Y, Gao Z, Yuan L, Sun Y, Chen H. Comparative Efficacy and Safety of PD-1/PD-L1 Inhibitors for Patients with Solid Tumors: A Systematic Review and Bayesian Network Meta-analysis. *J Cancer.* 2021 Jan 1;12(4):1133-1143.

Migden MR, Khushalani NI, Chang ALS, Lewis KD, Schmults CD, Hernandez-Aya L, Meier F, Schadendorf D, Guminski A, Hauschild A, Wong DJ, Daniels GA, Berking C, Jankovic V, Stankevich E, Booth J, Li S, Weinreich DM, Yancopoulos GD, Lowy I, Fury MG, Rischin D. Cemiplimab in locally advanced cutaneous squamous cell carcinoma: results from an open-label, phase 2, single-arm trial. *Lancet Oncol.* 2020 Feb;21(2):294-305.

Madore J, Vilain RE, Menzies AM, Kakavand H, Wilmott JS, Hyman J, Yearley JH, Kefford RF, Thompson JF, Long GV, Hersey P, Scolyer RA. PD-L1 expression in melanoma shows marked heterogeneity within and between patients: implications for anti-PD-1/PD-L1 clinical trials. *Pigment Cell Melanoma Res.* 2015 May;28(3):245-53.

Zetter BR. Angiogenesis and tumor metastasis. *Annu Rev Med.* 1998;49:407-24. doi: 10.1146/annurev.med.49.1.407. PMID: 9509272.

López ÁG, Sabuco J, Seoane JM, Duarte J, Januário C, Sanjuán MA. Avoiding healthy cells extinction in a cancer model. *J Theor Biol.* 2014 May 21;349:74-81.

Maas JW, Groothuis PG, Dunselman GA, de Goeij AF, Struyker Boudier HA, Evers JL. Endometrial angiogenesis throughout the human menstrual cycle. *Hum Reprod.* 2001 Aug;16(8):1557-61.

Sullivan LA, Brekken RA. The VEGF family in cancer and antibody-based strategies for their inhibition. *MAbs.* 2010 Mar-Apr;2(2):165-75.

Venepureddy A, Singh P, Rastogi R, Atallah JP, Terjanian T. Evolution of ramucirumab in the treatment of cancer - A review of literature. *J Oncol Pharm Pract.* 2017 Oct;23(7):525-539.

Ferrara N. VEGF as a therapeutic target in cancer. *Oncology.* 2005;69 Suppl 3:11-6.

Zirlik K, Duyster J. Anti-Angiogenics: Current Situation and Future Perspectives. *Oncol Res Treat.* 2018;41(4):166-171.

Madhunapantula SV, Mosca PJ, Robertson GP. The Akt signaling pathway: an emerging therapeutic target in malignant melanoma. *Cancer Biol Ther.* 2011 Dec 15;12(12):1032-49. doi: 10.4161/cbt.12.12.18442. Epub 2011 Dec 15. PMID: 22157148; PMCID: PMC3335938.

Nitulescu GM, Van De Venter M, Nitulescu G, Ungurianu A, Juzenas P, Peng Q, Olaru OT, Grădinaru D, Tsatsakis A, Tsoukalas D, Spandidos DA, Margina D. The Akt pathway in oncology therapy and beyond (Review). *Int J Oncol.* 2018 Dec;53(6):2319-2331.

Dillon LM, Miller TW. Therapeutic targeting of cancers with loss of PTEN function. *Curr Drug Targets*. 2014 Jan;15(1):65-79.

Yang, J., Nie, J., Ma, X. et al. Targeting PI3K in cancer: mechanisms and advances in clinical trials. *Mol Cancer* 18, 26 (2019).

Lazaro G, Kostaras E, Vivanco I. Inhibitors in AKTion: ATP-competitive vs allosteric. *Biochem Soc Trans*. 2020 Jun 30;48(3):933-943.

Zhang C, Liu J, Zhong JF, Zhang X. Engineering CAR-T cells. *Biomark Res*. 2017 Jun 24;5:22.

Magnani, C.F.; Tettamanti, S.; Alberti, G.; Pisani, I.; Biondi, A.; Serafini, M.; Gaipa, G. Transposon-Based CAR T Cells in Acute Leukemias: Where Are We Going? *Cells* 2020,

Sterner, R.C., Sterner, R.M. CAR-T cell therapy: current limitations and potential strategies. *Blood Cancer J*. 11, 69 (2021).

Haslauer T, Greil R, Zaborsky N, Geisberger R. CAR T-Cell Therapy in Hematological Malignancies. *Int J Mol Sci*. 2021 Aug 20;22(16):8996.

He Y, Cao J, Zhao C, Li X, Zhou C, Hirsch FR. TIM-3, a promising target for cancer immunotherapy. *Onco Targets Ther*. 2018 Oct 16;11:7005-7009.

Kane LP. T cell Ig and mucin domain proteins and immunity. *J Immunol*. 2010 Mar 15;184(6):2743-9.

Anderson AC, Anderson DE. TIM-3 in autoimmunity. *Curr Opin Immunol*. 2006 Dec;18(6):665-9.

Hu XH, Tang MX, Mor G, Liao AH. Tim-3: Expression on immune cells and roles at the maternal-fetal interface. *J Reprod Immunol*. 2016 Nov;118:92-99.

Wolf, Y., Anderson, A.C. & Kuchroo, V.K. TIM3 comes of age as an inhibitory receptor. *Nat Rev Immunol* 20, 173–185 (2020)

Das M, Zhu C, Kuchroo VK. Tim-3 and its role in regulating anti-tumor immunity. *Immunol Rev*. 2017 Mar;276(1):97-111.

Banerjee H, Kane LP. Immune regulation by Tim-3. *F1000Res*. 2018 Mar 14;7:316.

Gandhi, A.K., Kim, W.M., Sun, ZY.J. et al. High resolution X-ray and NMR structural study of human T-cell immunoglobulin and mucin domain containing protein-3. *Sci Rep* 8, 17512 (2018)

Huang YH, Zhu C, Kondo Y, Anderson AC, Gandhi A, Russell A, Dougan SK, Petersen BS, Melum E, Pertel T, Clayton KL, Raab M, Chen Q, Beauchemin N, Yazaki PJ, Pyzik M, Ostrowski MA, Glickman JN, Rudd CE, Ploegh HL, Franke A, Petsko GA, Kuchroo VK, Blumberg RS. CEACAM1 regulates TIM-3-mediated tolerance and exhaustion. *Nature*. 2015 Jan 15;517(7534):386-90..

Yasinska IM, Gonçalves Silva I, Sakhnevych SS, Ruegg L, Hussain R, Siligardi G, Fiedler W, Wellbrock J, Bardelli M, Varani L, Raap U, Berger S, Gibbs BF, Fasler-Kan E, Sumbayev VV. High mobility group box 1 (HMGB1) acts as an "alarmin" to promote acute myeloid leukaemia progression. *Oncoimmunology*. 2018 Feb 27;7(6)

Liu Y, Gao LF, Liang XH, Ma CH. Role of Tim-3 in hepatitis B virus infection: An overview. *World J Gastroenterol*. 2016 Feb 21;22(7):2294-303.

Boenisch O, D'Addio F, Watanabe T, Elyaman W, Magee CN, Yeung MY, Padera RF, Rodig SJ, Murayama T, Tanaka K, Yuan X, Ueno T, Jurisch A, Mfarrej B, Akiba H, Yagita H, Najafian N. TIM-3: a novel regulatory molecule of alloimmune activation. *J Immunol*. 2010 Nov 15;185(10):5806-19.

Zhao L, Yu G, Han Q, Cui C, Zhang B. TIM-3: An emerging target in the liver diseases. *Scand J Immunol*. 2020 Apr;91(4):e12825.

Sun, Q., Zhang, Y., Liu, M. et al. Prognostic and diagnostic significance of galectins in pancreatic cancer: a systematic review and meta-analysis. *Cancer Cell Int* 19, 309 (2019).

Blois SM, Verlohren S, Wu G, Clark G, Dell A, Haslam SM, Barrientos G. Role of galectin-glycan circuits in reproduction: from healthy pregnancy to preterm birth (PTB). *Semin Immunopathol*. 2020 Aug;42(4):469-486.

Hara A, Niwa M, Noguchi K, Kanayama T, Niwa A, Matsuo M, Hatano Y, Tomita H. Galectin-3 as a Next-Generation Biomarker for Detecting Early Stage of Various Diseases. *Biomolecules*. 2020 Mar 3;10(3):389.

Kopcow HD, Rosetti F, Leung Y, Allan DS, Kutok JL, Strominger JL. T cell apoptosis at the maternal-fetal interface in early human pregnancy, involvement of galectin-1. *Proc Natl Acad Sci U S A*. 2008 Nov 25;105(47):18472-7

Özlem Türeci, Holger Schmitt, Natalie Fadle, Michael Pfreundschuh, Ugur Sahin, Molecular Definition of a Novel Human Galectin Which Is Immunogenic in Patients with Hodgkin's Disease*, *Journal of Biological Chemistry*, Volume 272, Issue 10, 1997, Pages 6416-6422,

Yu J, Zhu R, Yu K, Wang Y, Ding Y, Zhong Y, Zeng Q. Galectin-9: A Suppressor of Atherosclerosis? *Front Immunol*. 2020 Nov 4;11:604265. doi: 10.3389/fimmu.2020.604265. Erratum in: *Front Immunol*. 2021 Apr 13;12:686592.

Zhang, Ab., Peng, Yf., Jia, Jj. et al. Exosome-derived galectin-9 may be a novel predictor of rejection and prognosis after liver transplantation. *J. Zhejiang Univ. Sci. B* 20, 605–612 (2019).

Yang, R., Sun, L., Li, CF. et al. Galectin-9 interacts with PD-1 and TIM-3 to regulate T cell death and is a target for cancer immunotherapy. *Nat Commun* 12, 832 (2021).

Roy Heusschen, Arjan W. Griffioen, Victor L. Thijssen, Galectin-9 in tumor biology: A jack of multiple trades, *Biochimica et Biophysica Acta (BBA) - Reviews on Cancer*, Volume 1836, Issue 1, 2013, Pages 177-185,

Klibi J, Niki T, Riedel A, Pioche-Durieu C, Souquere S, Rubinstein E, Le Moulec S, Guigay J, Hirashima M, Guemira F, Adhikary D, Mautner J, Busson P. Blood diffusion and Th1-suppressive effects of galectin-9-containing exosomes released by Epstein-Barr virus-infected nasopharyngeal carcinoma cells. *Blood*. 2009 Feb 26;113(9):1957-66.

Wiersma VR, de Bruyn M, Helfrich W, Bremer E. Therapeutic potential of Galectin-9 in human disease. *Med Res Rev.* 2013 Jun;33 Suppl 1:E102-26.

Golden-Mason L, Rosen HR. Galectin-9: Diverse roles in hepatic immune homeostasis and inflammation. *Hepatology.* 2017 Jul;66(1):271-279. doi: 10.1002/hep.29106. Epub 2017 May 27.

Wu C, Thalhamer T, Franca RF, Xiao S, Wang C, Hotta C, Zhu C, Hirashima M, Anderson AC, Kuchroo VK. Galectin-9-CD44 interaction enhances stability and function of adaptive regulatory T cells. *Immunity.* 2014 Aug 21;41(2):270-82.

Li, YH., Zhou, WH., Tao, Y. et al. The Galectin-9/Tim-3 pathway is involved in the regulation of NK cell function at the maternal–fetal interface in early pregnancy. *Cell Mol Immunol* 13, 73–81 (2016).

Mohamed A. ElTanbouly, Walburga Croteau, Randolph J. Noelle, J. Louise Lines, VISTA: A novel immunotherapy target for normalizing innate and adaptive immunity,, *Seminars in Immunology*, Volume 42, 2019, 101308

Yuan L, Tatineni J, Mahoney KM, Freeman GJ. VISTA: A Mediator of Quiescence and a Promising Target in Cancer Immunotherapy. *Trends Immunol.* 2021 Mar;42(3):209-227.

Collins M, Ling V, Carreno BM. The B7 family of immune-regulatory ligands. *Genome Biol.* 2005;6(6):223.

Lines JL, Pantazi E, Mak J, Sempere LF, Wang L, O'Connell S, Ceeraz S, Suriawinata AA, Yan S, Ernstoff MS, Noelle R. VISTA is an immune checkpoint molecule for human T cells. *Cancer Res.* 2014 Apr 1;74(7):1924-32.

Nowak EC, Lines JL, Varn FS, Deng J, Sarde A, Mabaera R, Kuta A, Le Mercier I, Cheng C, Noelle RJ. Immunoregulatory functions of VISTA. *Immunol Rev.* 2017 Mar;276(1):66-79.

Gao J, Ward JF, Pettaway CA, Shi LZ, Subudhi SK, Vence LM, Zhao H, Chen J, Chen H, Efsthathiou E, Troncoso P, Allison JP, Logothetis CJ, Wistuba II, Sepulveda MA, Sun J, Wargo J, Blando J, Sharma P. VISTA is an inhibitory immune checkpoint that is increased after ipilimumab therapy in patients with prostate cancer. *Nat Med.* 2017 May;23(5):551-555.

Kakavand H, Jackett LA, Menzies AM, et al. Negative immune checkpoint regulation by VISTA: a mechanism of acquired resistance to anti-PD-1 therapy in metastatic melanoma patients. *Mod Pathol.* 2017;30(12):1666-1676.

Mulati K, Hamanishi J, Matsumura N, Chamoto K, Mise N, Abiko K, Baba T, Yamaguchi K, Horikawa N, Murakami R, Taki M, Budiman K, Zeng X, Hosoe Y, Azuma M, Konishi I, Mandai M. VISTA expressed in tumour cells regulates T cell function. *Br J Cancer.* 2019 Jan;120(1):115-127.

Nishant Mehta, Sainiteesh Maddineni, Irimpan I. Mathews, R. Andres Parra Sperberg, Po-Ssu Huang, Jennifer R. Cochran, Structure and Functional Binding Epitope of V-domain Ig Suppressor of T Cell Activation, *Cell Reports*, Volume 28, Issue 10, 2019, Pages 2509-2516.e5,

ElTanbouly MA, Zhao Y, Nowak E, Li J, Schaafsma E, Le Mercier I, Ceeraz S, Lines JL, Peng C, Carriere C, Huang X, Day M, Koehn B, Lee SW, Silva Morales M, Hogquist KA, Jameson SC, Mueller D, Rothstein J, Blazar BR,

Cheng C, Noelle RJ. VISTA is a checkpoint regulator for naïve T cell quiescence and peripheral tolerance. *Science*. 2020 Jan 17;367(6475):eaay0524.

Long Yuan, Jahnvi Tatineni, Kathleen M. Mahoney, Gordon J. Freeman, VISTA: A Mediator of Quiescence and a Promising Target in Cancer Immunotherapy, *Trends in Immunology*, Volume 42, Issue 3, 2021, Pages 209-227,

Wang J, Wu G, Manick B, Hernandez V, Renelt M, Erickson C, Guan J, Singh R, Rollins S, Solorz A, Bi M, Li J, Grabowski D, Dirx J, Tracy C, Stuart T, Ellinghuysen C, Desmond D, Foster C, Kalabokis V. VSIG-3 as a ligand of VISTA inhibits human T-cell function. *Immunology*. 2019 Jan;156(1):74-85.

Sarah A. Robertson, Immune regulation of conception and embryo implantation—all about quality control?, *Journal of Reproductive Immunology*, Volume 85, Issue 1, 2010, Pages 51-57,

Jaume Alijotas-Reig, Taisiia Melnychuk, Josep Maria Gris, Regulatory T cells, maternal–foetal immune tolerance and recurrent miscarriage: New therapeutic challenging opportunities, *Medicina Clínica*, Volume 144, Issue 6, 2015, Pages 265-268,

Tavian M, Péault B. Embryonic development of the human hematopoietic system. *Int J Dev Biol*. 2005;49(2-3):243-50.

Tavian M, Biasch K, Sinka L, Vallet J, Péault B. Embryonic origin of human hematopoiesis. *Int J Dev Biol*. 2010;54(6-7):1061-5.

Dekel N, Gnainsky Y, Granot I, Racicot K, Mor G. The role of inflammation for a successful implantation. *Am J Reprod Immunol*. 2014 Aug;72(2):141-7.

Li, Y., Li, D. & Du, M. TIM-3: a crucial regulator of NK cells in pregnancy. *Cell Mol Immunol* 14, 948–950 (2017).
Li YH, Zhou WH, Tao Y, Wang SC, Jiang YL, Zhang D, Piao HL, Fu Q, Li DJ, Du MR. The Galectin-9/Tim-3 pathway is involved in the regulation of NK cell function at the maternal-fetal interface in early pregnancy. *Cell Mol Immunol*. 2016 Jan;13(1):73-81.

Laura Ridolfi, Massimiliano Petrini, Laura Fiammenghi, Angela Riccobon, Ruggero Ridolfi, Human embryo immune escape mechanisms rediscovered by the tumor, *Immunobiology*, Volume 214, Issue 1, 2009, Pages 61-76,

Kim, J., Kim, J. & Bae, JS. ROS homeostasis and metabolism: a critical liaison for cancer therapy. *Exp Mol Med* 48, e269 (2016)

Brahimi-Horn, M.C., Chiche, J. & Pouyssegur, J. Hypoxia and cancer. *J Mol Med* 85, 1301–1307 (2007).
Dunwoodie SL. The role of hypoxia in development of the Mammalian embryo. *Dev Cell*. 2009 Dec;17(6):755-73.
Berra, E., Pagès, G. & Pouyssegur, J. MAP Kinases and Hypoxia in the Control of VEGF Expression. *Cancer Metastasis Rev* 19, 139–145 (2000).

De Falco, S. The discovery of placenta growth factor and its biological activity. *Exp Mol Med* 44, 1–9 (2012).

Jiang, X., Wang, H. Macrophage subsets at the maternal-fetal interface. *Cell Mol Immunol* 17, 889–891 (2020).

Miwa N, Hayakawa S, Miyazaki S, Myojo S, Sasaki Y, Sakai M, Takikawa O, Saito S. IDO expression on decidual and peripheral blood dendritic cells and monocytes/macrophages after treatment with CTLA-4 or interferon-gamma increase in normal pregnancy but decrease in spontaneous abortion. *Mol Hum Reprod.* 2005 Dec;11(12):865-70.

Chen L, Shi Y, Zhu X, Guo W, Zhang M, Che Y, Tang L, Yang X, You Q, Liu Z. IL-10 secreted by cancer-associated macrophages regulates proliferation and invasion in gastric cancer cells via c-Met/STAT3 signaling. *Oncol Rep.* 2019 Aug;42(2):595-604.

Alex Friedlaender, Alfredo Addeo, Giuseppe Banna, New emerging targets in cancer immunotherapy: the role of TIM3, *ESMO Open*, Volume 4, Supplement 3, 2019,

Nakajima R, Miyagaki T, Kamijo H, Oka T, Shishido-Takahashi N, Suga H, Sugaya M, Sato S. Possible therapeutic applicability of galectin-9 in cutaneous T-cell lymphoma. *J Dermatol Sci.* 2019 Dec;96(3):134-142.

MadhuKalia, Biomarkers for personalized oncology: recent advances and future challenges, *Metabolism*, Volume 64, Issue 3, Supplement 1, March 2015, Pages S16-S21

Gonçalves Silva I, Yasinska IM, Sakhnevych SS, Fiedler W, Wellbrock J, Bardelli M, Varani L, Hussain R, Siligardi G, Ceccone G, Berger SM, Ushkaryov YA, Gibbs BF, Fasler-Kan E, Sumbayev VV. The Tim-3-galectin-9 Secretory Pathway is Involved in the Immune Escape of Human Acute Myeloid Leukemia Cells. *EBioMedicine.* 2017 Aug;22:44-57.

Qin, S., Xu, L., Yi, M. et al. Novel immune checkpoint targets: moving beyond PD-1 and CTLA-4. *Mol Cancer* 18, 155 (2019).

Hypoxia Deng J, Li J, Sarde A, Lines JL, Lee YC, Qian DC, Pechenick DA, Manivanh R, Le Mercier I, Lowrey CH, Varn FS, Cheng C, Leib DA, Noelle RJ, Mabaera R. Hypoxia-Induced VISTA Promotes the Suppressive Function of Myeloid-Derived Suppressor Cells in the Tumor Microenvironment. *Cancer Immunol Res.* 2019 Jul;7(7):1079-1090.

TGF- β Ungefroren H. Autocrine TGF- β in Cancer: Review of the Literature and Caveats in Experimental Analysis. *Int J Mol Sci.* 2021 Jan 19;22(2):977.

Yin J, Ren W, Huang X, Deng J, Li T, Yin Y. Potential Mechanisms Connecting Purine Metabolism and Cancer Therapy. *Front Immunol.* 2018 Jul 30;9:1697.

Wang L, Rubinstein R, Lines JL, Wasiuk A, Ahonen C, Guo Y, et al. VISTA, a novel mouse Ig superfamily ligand that negatively regulates T cell responses. *J Exp Med* (2011) 208:577–92.

Wada J, Kanwar YS. Identification and characterization of galectin-9, a novel beta-galactoside-binding mammalian lectin. *J Biol Chem* (1997) 272:6078–86.

Goncalves Silva I, Ruegg L, Gibbs BF, Bardelli M, Fruehwirth A, Varani L, et al. The immune receptor Tim-3 acts as a trafficker in a Tim-3/galectin-9autocrine loop in human myeloid leukemia cells. *Oncolimmunology* (2016) 5:e1195535.

Lines JL, Pantazi E, Mak J, Sempere LF, Wang L, O'Connell S, et al. VISTA is an immune checkpoint molecule for human T cells. *Cancer Res* (2014)74:1924–32

Lines JL, Sempere LF, Broughton T, Wang L, Noelle R. VISTA is a novel broad-spectrum negative checkpoint regulator for cancer immunotherapy. *Cancer Immunol Res* (2014) 2:510–717

Huang C, Bi E, Hu Y, Deng W, Tian Z, Dong C, et al. A Novel NF- κ B Binding Site Controls Human Granzyme B Gene Transcription. *J Immunol* (2006)176:4173–81.

Sumbayev VV, Jensen JK, Hansen JA, Andreasen PA. Novel modes of oestrogen receptor agonism and antagonism by hydroxylated and chlorinated biphenyls, revealed by conformation-specific peptide recognition patterns. *Mol Cell Endocrinol* (2008) 287:30–9.

Kurschus FC, Jenne DE. Delivery and therapeutic potential of human granzyme B. *Immunol Rev* (2010) 235:159–71.

Prokhorov A, Gibbs BF, Bardelli M, Ruegg L, Fasler-Kan E, Varani L, et al. The immune receptor Tim-3 mediates activation of PI3 kinase/mTOR and HIF-1 pathways in human myeloid leukaemia cells. *Int J Biochem Cell Biol*(2015) 59:11–20.

Kashio Y, Nakamura K, Abedin MJ, Seki M, Nishi N, Yoshida N, et al. Galectin-9 induces apoptosis through the calcium-calpain-caspase-1 pathway. *J Immunol* (2003) 170:3631–6.

Lhuillier C, Barjon C, Niki T, Gelin A, Praz F, Morales O, et al. Impact of Exogenous Galectin-9 on Human T Cells: CONTRIBUTION OF THE T CELLRECEPTOR COMPLEX TO ANTIGEN-INDEPENDENT ACTIVATIONBUT NOT TO APOPTOSIS INDUCTION. *J Biol Chem* (2015) 290:16797–811.

Bird CH, Christensen ME, Mangan MSJ, Prakash MD, Sedelies KA, Smyth MJ, et al. The granzyme B-Serpinb9 axis controls the fate of lymphocytes after lysosomal stress. *Cell Death Differ* (2014) 21:876–87

Yasinska et al. Galectin-9 and VISTA Ligand-Receptor Interactions *Frontiers in Immunology* | www.frontiersin.org November 2020 | Volume 11 | Article 58055715

Zhang M, Park S-M, Wang Y, Shah R, Liu N, Murmann AE, et al. Serine Protease Inhibitor 6 Protects Cytotoxic T Cells from Self-Inflicted Injury by Ensuring the Integrity of Cytotoxic Granules. *Immunity* (2006) 24:451–61.

Yasinska IM, Sakhnevych SS, Pavlova L, Teo Hansen Selnø A, Teuscher Abeleira AM, Benlaouer O, Gonçalves Silva I, Mosimann M, Varani L, Bardelli M, Hussain R, Siligardi G, Cholewa D, et al. The Tim-3-Galectin-9 pathway and its regulatory mechanisms inhuman breast cancer. *Front Immunol*. 2019; 10:1594

Cooper DN. Galectinomics: finding themes in complexity. *Biochim Biophys Acta*. 2002 Sep 19;1572(2-3):209-31.

Yasinska IM, Gonçalves Silva I, Sakhnevych S, Gibbs BF, Raap U, Fasler-Kan E, Sumbayev VV. Biochemical mechanisms implemented by human acute myeloid leukemia cells to suppress host immune surveillance. *Cell Mol Immunol*. 2018; 15:989–91

Lhuillier C, Barjon C, Niki T, Gelin A, Praz F, Morales O, Souquere S, Hirashima M, Wei M, Dellis O, Busson P. Impact of Exogenous Galectin-9 on Human T Cells: Contribution of the t cell receptor complex to antigen-independent activation but not to apoptosis induction. *J Biol Chem*. 2015; 290:16797–811.

Gonçalves Silva I, Yasinska IM, Sakhnevych SS, Fiedler W, Wellbrock J, Bardelli M, Varani L, Hussain R, Siligardi G, Ceccone G, Berger SM, Ushkaryov YA, Gibbs BF, et al. The Tim-3-galectin-9 secretory pathway is involved in the immune escape of human acute myeloid leukemia cells. *EBioMedicine*. 2017; 22:44–57.

Lhuillier C, Barjon C, Niki T, Gelin A, Praz F, Morales O, Souquere S, Hirashima M, Wei M, Dellis O, Busson P. Impact of Exogenous Galectin-9 on Human T Cells: Contribution of the t cell receptor complex to antigen-independent activation but not to apoptosis induction. *J Biol Chem*. 2015; 290:16797–811.

Gonçalves Silva I, Rüegg L, Gibbs BF, Bardelli M, Fruehwirth A, Varani L, Berger SM, Fasler-Kan E, Sumbayev VV. The immune receptor Tim-3 acts as a trafficker in a Tim-3/galectin-9 autocrine loop in human myeloid leukemia cells. *Oncoimmunology*. 2016; 5:e1195535.

St-Pierre Y. Galectins in hematological malignancies. *Am J Blood Res*. 2011;1(2):119-29. Epub 2011 Sep 7.

Prokhorov A, Gibbs BF, Bardelli M, Rüegg L, Fasler-Kan E, Varani L, Sumbayev VV. The immune receptor tim-3 mediates activation of PI3 kinase/mTOR and HIF-1 pathways in human myeloid leukaemia cells. *Int J Biochem Cell Biol*. 2015; 59:11–20.

Gonçalves Silva I, Gibbs BF, Bardelli M, Varani L, Sumbayev VV. Differential expression and biochemical activity of the immune receptor Tim-3 in healthy and malignant human myeloid cells. *Oncotarget*. 2015;6:33823–33.

Kikushige Y, Miyamoto T, Yuda J, Jabbarzadeh-Tabrizi S, Shima T, Takayanagi S, Niino H, Yurino A, Miyawaki K, Takenaka K, Iwasaki H, Akashi K. A TIM-3/Gal-9 autocrine stimulatory loop drives self-renewal of human myeloid leukemia stem cells and leukemic progression. *Cell Stem Cell*. 2015; 17:341–52.

Kim SJ, Angel P, Lafyatis R, Hattori K, Kim KY, Sporn MB, Karin M, Roberts AB. Autoinduction of transforming growth factor beta 1 is mediated by the AP-1 complex. *Mol Cell Biol*. 1990; 10:1492–97.

Duan D, Derynck R. Transforming growth factor- β (TGF- β)-induced up-regulation of TGF- β receptors at the cell surface amplifies the TGF- β response. *J Biol Chem*. 2019; 294:8490–504.

Massagué J, Seoane J, Wotton D. Smad transcription factors. *Genes Dev*. 2005; 19:2783–810.

Sumbayev VV, Nicholas SA. Hypoxia-inducible factor 1 as one of the "signaling drivers" of toll-like receptor-dependent and allergic inflammation. *Arch Immunol Ther Exp (Warsz)*. 2010; 58:287–94.

Abooli M, Lall GS, Coughlan K, Lall HS, Gibbs BF, Sumbayev VV. Crucial involvement of xanthine oxidase in the intracellular signalling networks associated with human myeloid cell function. *Sci Rep*. 2014; 4:6307.

Sumbayev VV, Yasinska IM. Regulation of MAP kinase-dependent apoptotic pathway: implication of reactive oxygen and nitrogen species. *Arch Biochem Biophys*. 2005; 436:406–12.

Manzo G. Similarities between embryo development and cancer process suggest new strategies for research and therapy of tumors: a new point of view. *Front Cell Dev Biol.* 2019; 7:20

Birchenall-Roberts MC, Ruscetti FW, Kasper J, Lee HD, Friedman R, Geiser A, Sporn MB, Roberts AB, Kim SJ. Transcriptional regulation of the transforming growth factor beta 1 promoter by v-src gene products is mediated through the AP-1 complex. *Mol Cell Biol.*1990; 10:4978–83.

Yasinska IM, Gonçalves Silva I, Sakhnevych SS, Ruegg L, Hussain R, Siligardi G, Fiedler W, Wellbrock J, Bardelli M, Varani L, Raap U, Berger S, Gibbs BF, et al. High mobility group box 1 (HMGB1) acts as an "alarmin" to promote acute myeloid leukaemia progression. *Oncoimmunology.* 2018; 7:e1438109.

Battaglia V, Compagnone A, Bandino A, Bragadin M, Rossi CA, Zanetti F, Colombatto S, Grillo MA, Toninello A. Cobalt induces oxidative stress in isolated liver mitochondria responsible for permeability transition and intrinsic apoptosis in hepatocyte primary cultures. *Int J Biochem Cell Biol.* 2009; 41:586–94.

Stenger C, Naves T, Verdier M, Ratinaud MH. The cell death response to the ROS inducer, cobalt chloride, in neuroblastoma cell lines according to p53 status. *Int J Oncol.* 2011; 39:601–09.

Kubiczkova L, Sedlarikova L, Hajek R, Sevcikova S. TGF- β - an excellent servant but a bad master. *J Transl Med.*2012; 10:183.

He W, Dorn DC, Erdjument-Bromage H, Tempst P, Moore MA, Massagué J. Hematopoiesis controlled by distinct TIF1 γ and Smad4 branches of the TGF β pathway. *Cell.* 2006; 125:929–41.

Buckle I, Guillerey C. Inhibitory Receptors and Immune Checkpoints Regulating Natural Killer Cell Responses to Cancer. *Cancers.* (2021)13:4263.

Yoo MJ, Long B, Brady WJ, Holian A, Sudhir A, Gottlieb M. Immune checkpoint inhibitors: An emergency medicine focused review. *Am J Emerg Med.* (2021) 50:335–44.

Selno ATH, Schlichtner S, Yasinska IM, Sakhnevych SS, Fiedler W, Wellbrock J, et al. Transforming growth factor beta type 1 (TGF- β) and hypoxia-inducible factor 1 (HIF-1) transcription complex as master regulators of the immunosuppressive protein galectin-9 expression in human cancer and embryonic cells. *Aging.* (2020) 12:23478–96.

Xie X, Chen C, Chen W, Jiang J, Wang L, Li T, et al. Structural basis of VSIG3: the ligand for VISTA. *Front Immunol.* (2021)12:625808.

Yasinska IM, Meyer NH, Schlichtner S, Hussain R, Siligardi G, Casely-Hayford M, et al. Ligand-receptor interactions of galectin-9 and VISTA suppress human T lymphocyte cytotoxic activity. *Front Immunol.* (2020)11:580557.

Im E, Sim DY, Lee HJ, Park JE, Park WY, Ko S, et al. Immune functions as a ligand or a receptor, cancer prognosis potential, clinical implication of VISTA in cancer immunotherapy. In: *Seminars in cancer biology.*(2021).

Popp FC, Capino I, Bartels J, Damanakis A, Li J, Datta RR, et al. Expression of immune checkpoint regulators IDO, VISTA, LAG3, andTIM3 in resected pancreatic ductal adenocarcinoma. *Cancers.* (2021)13:2689.

Thomas DA, Massague J. TGF-beta directly targets cytotoxic T cell functions during tumor evasion of immune surveillance. *Cancer Cell*. (2005) 8:369–80.

Teo Hansen Selno A, Schlichtner S, Yasinska IM, Sakhnevych SS, Fiedler W, Wellbrock J, et al. High mobility group box 1 (HMGB1) induces toll-like receptor 4-mediated production of the immunosuppressive protein galectin-9 in human cancer cells. *Front Immunol*. (2021)12:675731.

Guglielmo GMDi, Le Roy C, Goodfellow AF, Wrana JL. Distinct endocytic pathways regulate TGF- β receptor signalling and turnover. *Nature CellBiology*. (2003) 5:410–21.

Mitchell H, Choudhury A, Pagano RE, Leof EB. Ligand-dependent and -independent transforming growth factor- β receptor recycling regulated by clathrin-mediated endocytosis and Rab11. *Molec Biol Cell*. (2004) 15:4166–78.

Barton GM, Kagan JC. A cell biological view of Toll-like receptor function: regulation through compartmentalization. *Nat Rev Immunol*. (2009) 9:535–42.

Meldi L, Brickner JH. Compartmentalization of the nucleus. *Trends Cell Biol*.(2011) 21:701–8.

Chen W, Frank ME, Jin W, Wahl SM. TGF-beta released by apoptotic T cells contributes to an immunosuppressive milieu. *Immunity*. (2001) 14:715–25.

Kang R, Zhang Q, Zeh HJ, Lotze MT, Tang D. HMGB1 in Cancer: Good, Bad, or Both? *Clin Cancer Res* (2013) 19:4046–57.

He SJ, Cheng J, Feng X, Yu Y, Tian L, Huang Q. The Dual Role and Therapeutic Potential of High-Mobility Group Box 1 in Cancer. *Oncotarget*(2017) 8:64534–50

Chiba S, Baghdadi M, Akiba H, Yoshiyama H, Kinoshita I, Dosaka-Akita H, et al. Tumor-Infiltrating DCs Suppress Nucleic Acid-Mediated Innate Immune Responses Through Interactions Between the Receptor TIM-3 and the Alarmin HMGB1. *Nat Immunol* (2012) 13:832–42.

Suga H, Sugaya M, Fujita H, Asano Y, Tada Y, Kadono T, et al. TLR4, Rather Than TLR2, Regulates Wound Healing Through TGF-b and CCL5 Expression. *J Dermatol Sci* (2014) 73:117–24.

Vega-Carrascal, D.A. Bergin, O.J. McElvaney, C. McCarthy, N. Banville, K. Pohl, M. Hirashima, V.K. Kuchroo, E.P. Reeves, N.G. McElvaney, Galectin-9 signaling through TIM-3 is involved in neutrophil-mediated Gram-negative bacterial killing: an effect abrogated within the cystic fibrosis lung, *J. Immunol*. 192 (5) (2014) 2418–2431.

W. Chen, M.E. Frank, W. Jin, S.M. Wahl, TGF-beta released by apoptotic T cells contributes to an immunosuppressive milieu, *Immunity* 14 (2001) 715–725.

D. Ribet, P. Cossart, How bacterial pathogens colonize their hosts and invade deeper tissues, *Microbes Infect*. 17 (3) (2015) 173–183.

J.A. Roberts, B.I. Marklund, D. Ilver, D. Haslam, M.B. Kaack, G. Baskin, M. Louis, R. Mollby, J. Winberg, S. Normark, The Gal(alpha 1–4)Gal-specific tip adhesin of *Escherichia coli* P-fimbriae is needed for pyelonephritis to occur in the normal urinary tract, *PNAS* 91 (25) (1994) 11889–11893.

- J. Lillington, S. Geibel, G. Waksman, Biogenesis and adhesion of type 1 and P pili, *BBA* 1840 (9) (2014) 2783–2793.
- S. Melville, L. Craig, Type IV pili in Gram-positive bacteria, *Microbiology and molecular biology reviews* : MMBR. 77 (3) (2013) 323–341.
- Okoye, L. Xu, M. Motamedi, P. Parashar, J.W. Walker, S. Elahi, Galectin-9 expression defines exhausted T cells and impaired cytotoxic NK cells in patients with virus-associated solid tumors, *J. ImmunoTher. Cancer* 8 (2) (2020) e001849,
- C. Wu, T. Thalhamer, R. Franca, S. Xiao, C. Wang, C. Hotta, C. Zhu, M. Hirashima, A. Anderson, V. Kuchroo, Galectin-9-CD44 interaction enhances stability and function of adaptive regulatory T cells, *Immunity* 41 (2) (2014) 270–282.
- G. Marino, G. Kroemer, Mechanisms of apoptotic phosphatidylserine exposure, *Cell Res.* 23 (11) (2013) 1247–1248.
- J. Suzuki, D.P. Denning, E. Imanishi, H.R. Horvitz, S. Nagata, Xk-related protein 8 and CED-8 promote phosphatidylserine exposure in apoptotic cells, *Science* 341 (6144) (2013) 403–406.
- J. Suzuki, M. Umeda, P.J. Sims, S. Nagata, Calcium-dependent phospholipid scrambling by TMEM16F, *Nature* 468 (7325) (2010) 834–838.
- S.R. Bushell, A.C.W. Pike, M.E. Falzone, N.J.G. Rorsman, C.M. Ta, R.A. Corey, T. D. Newport, J.C. Christianson, L.F. Scofano, C.A. Shintre, A. Tessitore, A. Chu, Q. Wang, L. Shrestha, S.M.M. Mukhopadhyay, J.D. Love, N.A. Burgess-Brown, R. Sitsapesan, P.J. Stansfeld, J.T. Huiskonen, P. Tammara, A. Accardi, E. P. Carpenter, The structural basis of lipid scrambling and inactivation in the endoplasmic reticulum scramblase TMEM16K, *Nat. Commun.* 10 (2019) 3956.
- M.A. Campanero-Rhodes, I. Kalograiaki, B. Euba, E. Llobet, A. Arda, J. JimenezBarbero, J. Garmendia, D. Solís, Exploration of Galectin Ligands Displayed on Gram-Negative Respiratory Bacterial Pathogens with Different Cell Surface Architectures, *Biomolecules.* 11 (4) (2021) 595,
- A.M. Seifert, C. Reiche, M. Heiduk, A. Tannert, A.C. Meinecke, S. Baier, J. von Renesse, C. Kahlert, M. Distler, T. Welsch, C. Reissfelder, D.E. Aust, G. Miller, J. Weitz, and L. Seifert, Detection of pancreatic ductal adenocarcinoma with galectin-9 serum levels. *Oncogene* 39 (2020) 3102-3113.
- S. Schlichtner, N.H. Meyer, I.M. Yasinska, N. Aliu, S.M. Berger, B.F. Gibbs, E. Fasler-Kan, and V.V. Sumbayev, Functional role of galectin-9 in directing human innate immune reactions to Gram-negative bacteria and T cell apoptosis. *International immunopharmacology* 100 (2021) 108155.
- Vega-Carrascal, D.A. Bergin, O.J. McElvaney, C. McCarthy, N. Banville, K. Pohl, M. Hirashima, V.K. Kuchroo, E.P. Reeves, and N.G. McElvaney, Galectin-9 signaling through TIM-3 is involved in neutrophil-mediated Gram-negative bacterial killing: an effect abrogated within the cystic fibrosis lung. *Journal of immunology* 192 (2014) 2418-31.

Prokhorov, B.F. Gibbs, M. Bardelli, L. Ruegg, E. Fasler-Kan, L. Varani, and V.V. Sumbayev, The immune receptor Tim-3 mediates activation of PI3 kinase/mTOR and HIF-1 pathways in human myeloid leukaemia cells. *The international journal of biochemistry & cell biology* 59 (2015) 11-20.

F. Casciano, P.D. Pigatto, P. Secchiero, R. Gambari, and E. Reali, T Cell Hierarchy in the Pathogenesis of Psoriasis and Associated Cardiovascular Comorbidities. *Frontiers in immunology* 9 (2018) 1390.

S. Buratta, B. Tancini, K. Sagini, F. Delo, E. Chiaradia, L. Urbanelli, and C. Emiliani, Lysosomal Exocytosis, Exosome Release and Secretory Autophagy: The Autophagic- and Endo-Lysosomal Systems Go Extracellular. *International journal of molecular sciences* 21 (2020).

Yang, R., Sun, L., Li, CF. et al. Galectin-9 interacts with PD-1 and TIM-3 to regulate T cell death and is a target for cancer immunotherapy. *Nat Commun* 12, 832 (2021).

Q. Wu, L. Jiang, S.C. Li, Q.J. He, B. Yang, and J. Cao, Small molecule inhibitors targeting the PD-1/PD-L1 signaling pathway. *Acta pharmacologica Sinica* 42 (2021) 1-9.

L. Tong, J. Li, Q. Li, X. Wang, R. Medikonda, T. Zhao, T. Li, H. Ma, L. Yi, P. Liu, Y. Xie, J. Choi, S. Yu, Y. Lin, J. Dong, Q. Huang, X. Jin, M. Lim, and X. Yang, ACT001 reduces the expression of PD-L1 by inhibiting the phosphorylation of STAT3 in glioblastoma. *Theranostics* 10 (2020) 5943-5956.

Shapouri-Moghaddam A, Mohammadian S, Vazini H, Taghadosi M, Esmaeili SA, Mardani F, et al. Macrophage Plasticity, Polarization, and Function in Health and Disease. *J Cell Physiol* (2018) 233:6425–40.

Martinez FO, Gordon S. The M1 and M2 Paradigm of Macrophage Activation: Time for Reassessment. *F1000Prime Rep* (2014) 6:13.

Viola A, Munari F, Sanchez-Rodriguez R, Scolaro T, Castegna A. The Metabolic Signature of Macrophage Responses. *Front Immunol* (2019) 10:1462.

Broughton TWK, Eltanbouly MA, Schaafsma E, Deng J, Sarde A, Croteau W, et al. Defining the Signature of VISTA on Myeloid Cell Chemokine Responsiveness. *Front Immunol* (2019) 10:2641–53.

Park JG, Lee CR, Kim MG, Kim G, Shin HM, Jeon YH, et al. Kidney Residency of VISTA-Positive Macrophages Accelerates Repair From Ischemic Injury. *Kidney Int* (2019) 97:980–94.

Wang L, Le Mercier I, Putra J, Chen W, Liu J, Schenk AD, et al. Disruption of the Immune-Checkpoint VISTA Gene Imparts a Proinflammatory Phenotype With Predisposition to the Development of Autoimmunity. *Proc Natl Acad Sci USA* (2014) 111:14846–51

Borggrewe M, Grit C, Den Dunnen WFA, Burm SM, Bajramovic JJ, Noelle RJ, et al. VISTA Expression by Microglia Decreases During Inflammation and Is Differentially Regulated in CNS Diseases. *Glia* (2018) 66:2645–58.

Rodriguez-Garcia M, Porichis F, De Jong OG, Levi K, Diefenbach TJ, Lifson JD, et al. Expression of PD-L1 and PD-L2 on Human Macrophages Is Up-Regulated by HIV-1 and Differentially Modulated by IL-10. *J Leukoc Biol*(2011) 89:507–15.

6 PUBLICATION LIST



Ligand-Receptor Interactions of Galectin-9 and VISTA Suppress Human T Lymphocyte Cytotoxic Activity

OPEN ACCESS

Edited by:

Dianwen Ju,
Fudan University, China

Reviewed by:

Illa Voskoboinik,
Peter MacCallum Cancer Centre,
Australia
Eva Rettinger,
University Hospital Frankfurt, Germany

***Correspondence:**

Vadim V. Sumbayev
V.Sumbayev@kent.ac.uk
Elizaveta Fasler-Kan
elizaveta.fasler@insel.ch
Bernhard F. Gibbs
bernhard.gibbs@uni-oldenburg.de
Inna M. Yasinska
innayas1975@gmail.com

[†]These authors have contributed
equally to this work

Specialty section:

This article was submitted to
Cancer Immunity
and Immunotherapy,
a section of the journal
Frontiers in Immunology

Received: 06 July 2020

Accepted: 23 October 2020

Published: 20 November 2020

Citation:

Yasinska IM, Meyer NH,
Schlichtner S, Hussain R, Siligardi G,
Casely-Hayford M, Fiedler W,
Wellbrock J, Desmet C, Calzolari L,
Varani L, Berger SM, Raap U,
Gibbs BF, Fasler-Kan E and
Sumbayev VV (2020) Ligand-Receptor
Interactions of Galectin-9 and VISTA
Suppress Human T Lymphocyte
Cytotoxic Activity.
Front. Immunol. 11:580557.
doi: 10.3389/fimmu.2020.580557

Inna M. Yasinska^{1*†}, N. Helge Meyer^{2†}, Stephanie Schlichtner^{1†}, Rohanah Hussain³,
Giuliano Siligardi³, Maxwell Casely-Hayford¹, Walter Fiedler⁴, Jasmin Wellbrock⁴,
Cloe Desmet⁵, Luigi Calzolari⁵, Luca Varani⁶, Steffen M. Berger⁷, Ulrike Raap²,
Bernhard F. Gibbs^{1,2*}, Elizaveta Fasler-Kan^{7,8*} and Vadim V. Sumbayev^{1*}

¹ Medway School of Pharmacy, Universities of Kent and Greenwich, Chatham Maritime, United Kingdom, ² Division of Experimental Allergology and Immunodermatology, University of Oldenburg, Oldenburg, Germany, ³ Beamline 23, Diamond Light Source, Didcot, United Kingdom, ⁴ Department of Oncology, Hematology and Bone Marrow Transplantation with Section Pneumology, Hubertus Wald University Cancer Center, University Medical Center Hamburg-Eppendorf, Hamburg, Germany, ⁵ European Commission Joint Research Centre, Ispra, Italy, ⁶ Institute for Research in Biomedicine, Università della Svizzera Italiana (USI), Bellinzona, Switzerland, ⁷ Department of Pediatric Surgery, Department of Biomedical Research, Children's Hospital, Inselspital, University of Bern, Bern, Switzerland, ⁸ Department of Biomedicine, University Hospital Basel and University of Basel, Basel, Switzerland

Acute myeloid leukemia (AML), a blood/bone marrow cancer, is a severe and often fatal malignancy. AML cells are capable of impairing the anti-cancer activities of cytotoxic lymphoid cells. This includes the inactivation of natural killer (NK) cells and killing of T lymphocytes. Here we report for the first time that V-domain Ig-containing suppressor of T cell activation (VISTA), a protein expressed by T cells, recognizes galectin-9 secreted by AML cells as a ligand. Importantly, we found that soluble VISTA released by AML cells enhances the effect of galectin-9, most likely by forming multiprotein complexes on the surface of T cells and possibly creating a molecular barrier. These events cause changes in the plasma membrane potential of T cells leading to activation of granzyme B inside cytotoxic T cells, resulting in apoptosis.

Keywords: Galectin-9, VISTA, T cells, NK cells, acute myeloid leukemia, immune escape

INTRODUCTION

Acute myeloid leukemia (AML) is a blood/bone marrow cancer originating from myeloid precursors, which rapidly progresses into a systemic and often a fatal malignancy. Human AML cells operate a variety of biochemical mechanisms which allow them to escape host immune surveillance (1). These molecular pathways cause impairment of the anti-cancer activities of natural killer (NK) cells and cytotoxic T cells which could otherwise attack and kill AML cells (1, 2). It has recently been reported that one of these immune evasion pathways includes high expression/secretion of the protein galectin-9, its receptor and its possible trafficker/carrier (as with all galectins, galectin-9 requires a carrier protein-trafficker to be secreted) - the T cell immunoglobulin and

mucin domain containing protein 3 (Tim-3) (3–6). Galectin-9 has two similar ligand/sugar-binding domains (7, 8). These domains are fused together by a peptide linker, which could be of three different sizes (due to alternative splicing), that determines the presence of three isoforms of galectin-9 in human cells (7, 8).

Galectin-9 is actively engaged in impairing the cytotoxic activities of NK cells and can, in addition to suppression, induce apoptotic death of cytotoxic T cells (5, 9–12). However, the mechanisms underlying these differential effects remain unknown. It has been reported that cytotoxic lymphoid cell-based Tim-3 is involved in these effects as a receptor. Tim-3 is expressed by both T cells and NK cells, however, immunosuppressive effects of galectin-9 vary in these cells, suggesting that some additional factors determine the differential responses of NK and T cells to galectin-9 (2, 5). We hypothesized that one of these additional factors could be another immunoglobulin (Ig) superfamily member, known as V-domain Ig-containing suppressor of T cell activation (VISTA), which is expressed in both myeloid and T cells, while NK cells express barely detectable amounts of VISTA (13–15). VISTA has been reported to display both receptor and ligand properties (13–15). Given the similarities between Tim-3 and VISTA structural organizations, we proposed that galectin-9 can interact with T cell-based VISTA causing downstream effects and thus might determine differences in NK and T cell responses to galectin-9.

Here we report for the first time that galectin-9 binds VISTA, most likely as a ligand. Binding was verified using co-immunoprecipitation assays and biophysical methods – synchrotron radiation circular dichroism (SRCD) spectroscopy and surface plasmon resonance (SPR). We confirmed that human T cells, but not NK cells (no VISTA protein was detected by Western blot), express VISTA protein. Both VISTA and Tim-3 mediate galectin-9-induced downregulation of granzyme B (pro-apoptotic protease) release from T cells, increasing the presence of this enzyme inside the T cells which produce it and possibly causing activation of the caspase-3 pro-apoptotic pathway. Furthermore, we found that primary human AML cells secrete high amounts of VISTA compared to healthy mononuclear leukocytes. Exposure of phorbol 12-myristate 13-acetate (PMA – an activator of granzyme B production and release)-activated Jurkat T cells to human galectin-9 and soluble VISTA significantly affects their polarization/membrane potential thus preventing granzyme B release. The same effect was observed in primary human T cells but not in NK cells. We hypothesized that galectin-9 and soluble VISTA can form multiprotein agglomerates engaging with Tim-3 and VISTA on the surface of T cells (but not NK cells which did not show expression of detectable amounts of VISTA protein in Western blot analysis) thus affecting the cell polarity/plasma membrane potential and leading to granzyme B-mediated self-killing.

MATERIALS AND METHODS

Materials

RPMI-1640 cell culture medium, fetal bovine serum and supplements as well as basic laboratory chemicals were purchased from Sigma (Suffolk, UK). Microtitre plates for

Enzyme-Linked Immunosorbent Assay (ELISA) were provided by Oxley Hughes Ltd (London, UK). Rabbit antibodies against VISTA, galectin-9, granzyme B and CD3 were purchased from Abcam (Cambridge, UK). Goat antibody against VISTA was purchased from Santa Cruz Biotechnology (Heidelberg, Germany). Antibodies against actin were purchased from Abcam (Cambridge, UK) and Proteintech (Manchester, UK). Mouse antibody against PARP was obtained from Enzo Life Sciences (Exeter, UK). Goat anti-mouse, anti-rabbit and donkey anti-goat fluorescence dye-labeled antibodies were obtained from Li-COR (Lincoln, Nebraska USA). ELISA-based assay kits for detection of galectin-9, Tim-3 and VISTA as well as human recombinant galectin-9 and anti-VISTA antibody reacting to native protein were purchased from Bio-Techne (R&D Systems, Abingdon, UK). VISTA-Fc and Fc human recombinant proteins were obtained from Sino Biological US Inc (Wayne, PA, USA). Anti-Tim-3 mouse monoclonal antibodies (detection and neutralizing) as well as human Ig-like V-type domain of Tim-3 (amino acid residues 22-124), expressed and purified from *E. coli* (16) were used in our work. Antibodies for fluorescent microscopy and flow cytometry as well as annexin V/propidium iodide apoptosis assay kits were from Invitrogen (Carlsbad, USA). All other chemicals purchased were of the highest grade of purity commercially available.

Cell Lines and Primary Human Samples

THP-1 human myeloid leukemia monocytes, Jurkat T cells and MCF-7 human breast cancer cells were obtained from the European Collection of Cell Cultures (Salisbury, UK). HaCaT keratinocytes were purchased from CLS (Cell Line Service, Germany) and cultured according to the CLS recommendations.

Blood plasma of healthy human donors was obtained as described (17) from buffy coat blood (purchased from healthy donors undergoing routine blood donation) which was purchased from the National Health Blood and Transfusion Service (NHSBT, UK) following ethical approval (REC reference: 16-SS-033). Mononuclear-rich leukocytes were isolated using Ficoll-density centrifugation according to the manufacturer's protocol. Cell numbers were determined using haemocytometers and then diluted with HEPES-buffered Tyrode's solution before treatment as indicated in the text. NK cells were purified as previously described (5). Primary human T cells were purified using a commercial T cell purification kit (EasySep Human T Cell Isolation Kit, StemCell Technologies, Cologne, Germany). Primary human AML plasma samples and cells obtained from newly diagnosed AML patients were provided by the sample bank of University Medical Centre Hamburg-Eppendorf (Ethik-Kommission der Ärztekammer Hamburg, reference: PV3469). Cells were kept in IMDM medium containing 15% BIT 9500 serum substitute, 100 μ M mercaptoethanol, 100 ng/ml stem cell factor (SCF), 50 ng/ml FLT3, 20 ng/ml G-CSF, 20 ng/ml IL-3, 1 μ M UM729 and 500 nM stemregenin 1 (SR1).

Western Blot Analysis

VISTA, Tim-3, PARP cleavage and CD3 levels were analyzed by Western blot and compared to the amounts of β -actin (protein

loading control), as previously described (18). Briefly, cells were lysed in using the buffer (50 mM Tris-HCl, 5 mM EDTA, 150 mM NaCl, 0.5% Nonidet-40, 1 mM PMSF, pH 8.0). After centrifugation, protein content in supernatants was analyzed using Bradford assay. Proteins were resolved using SDS-polyacrylamide gels followed by blotting onto nitrocellulose membranes. Molecular weights were calibrated in proportion to the running distance of rainbow markers. All primary antibodies were diluted 1:1000. Li-COR goat secondary antibodies (dilution 1:2000), conjugated with fluorescent dyes, were used in accordance with manufacturer's protocol to visualize target proteins (using a Li-COR Odyssey imaging system). Western blot data were analyzed using Odyssey software and values were subsequently normalized against those of β -actin (loading control).

In Vitro Assay of VISTA-Galectin-9 Interactions

This assay was performed as described before for Tim-3-galectin-9 interactions. Briefly, VISTA protein from Jurkat T cell lysates was first precipitated on Maxisorp ELISA plates. For this purpose ELISA plates were coated overnight with goat antibody against VISTA. Plates were then blocked with 2% BSA. Tissue culture medium obtained from culturing PMA-treated THP-1 or MCF 7 (negative control) cells was then applied for 2 h at room temperature, followed by extensive washing with TBST buffer. Proteins were then extracted using 0.2 M glycine-HCl buffer (pH 2.0). Extracts were neutralized using lysis buffer and subjected to Western blot analysis (samples were not boiled in this case) using rabbit anti-galectin-9 and mouse anti-Tim-3 antibodies as described before (4) and above. Alternatively, the format was subjected to measurement of bound galectin-9 using an ELISA kit according to the manufacturer's protocol.

Enzyme-Linked Immunosorbent Assays (ELISAs)

Secreted galectin-9 and soluble VISTA, were measured either in cell culture medium or in blood plasma by ELISA using R&D Systems kits according to manufacturer's protocols.

On-Cell Western Analysis

We employed LI-COR on-cell Western (OCW) assay to analyze total Tim-3 and VISTA expressions in the studied cells using the Li-COR Odyssey imaging system as previously described (4, 19).

Fluorescent Microscopy and Flow Cytometry

Cells were cultured overnight on 12 mm cover slips in 24-well plates and then fixed/permeabilised for 20 min with ice-cold MeOH/acetone (1:1). Alternatively cells were fixed in a freshly prepared 2% paraformaldehyde, washed three times with PBS and then permeabilised with 0.1% TX-100. Cover slips were blocked for 1h at RT with 10% goat serum in PBS. Cells were stained with anti-VISTA antibody overnight at 4°C. As secondary antibodies were used goat-anti-mouse Alexa Fluor

488 for 45 min at RT. The nuclei were stained with 4',6-diamidino-2-phenylindole (DAPI). The preparations were analyzed using Olympus microscope as described previously (16, 20). Images were collected and analyzed using proprietary image acquisition software.

Flow cytometry experiments were performed in accordance with a previously described protocol (21). Briefly, cells were collected and fixed with 2% paraformaldehyde and permeabilised with 0.1% TX-100. Cells were stained with mouse anti-VISTA antibodies conjugated with Alexa Fluor 488 o/n at 4°C. Mean fluorescence intensity of stained cells was measured and analyzed using a FACSCalibur analyzer and the CELLQuest Pro Software (Becton Dickinson, USA).

Measurement of Granzyme B and Caspase-3 Activities

Granzyme B activity in cell lysates was measured using a fluorometric assay based on the ability of the enzyme to cleave the fluorogenic substrate Ac-IEPD-AFC (Sigma). Caspase-3 activity was measured spectrophotometrically based on its ability to cleave its specific substrate Ac-DEVD-pNA. Both assays were performed according to the manufacturers' protocol. In-cell activity of granzyme B (granzyme B catalytic activity in living cells) was measured by incubation of living cells with 150 μ M Ac-IEPD-AFC (granzyme B substrate) for 1 h at 37°C in sterile PBS. This did not affect viability of the cells as measured by MTS assay (Promega kit, measurements were performed according to the manufacturer's protocol). Total cell fluorescence was then measured in living cells (22) using excitation and emission wavelengths recommended in the Ac-IEPD-AFC manufacturer's (Sigma) protocol. An equal number of cells, which were not exposed to granzyme B substrate, were used as a control.

Apoptosis and Cell Viability Assays

The percentage of apoptotic cells was measured using an annexin V/propidium iodide assay kit by flow cytometry according to the manufacturer's (Invitrogen) instructions. Cell viability was assessed using an MTS assay kit (Promega) according to the manufacturer's protocol.

Characterization of Cell Membrane Potential

This was performed using a DiBAC₄(3) fluorescent probe where the intensity of accumulation in a cell is proportional to its depolarization. This assay was performed as recommended by the manufacturer and described before (23).

Synchrotron Radiation Circular Dichroism Spectroscopy

Human recombinant VISTA, galectin-9 and Tim-3 as well as VISTA-galectin-9 or VISTA-galectin-9-Tim-3 complexes were characterized using SRCD spectroscopy at beam line 23, Diamond Light Source (Didcot, UK). SRCD measurements were performed with 0.2 μ g/ml of samples using a 1 cm path length cell, 3 mm aperture diameter and 40 μ l capacity using

Module B with a 1 nm increment, 1s integration time, 1.2 nm bandwidth at 23°C (24–26). The obtained results were analyzed with the help of CDApps (25) and OriginPro™.

Surface Plasmon Resonance

This assay was performed using a CM5 sensor chip. A Biacore amino coupling kit was employed to immobilize galectin-9 on the chip surface and VISTA (as a fusion protein with Fc) as well as Fc alone were flowed through in order to assess interactions using a Biacore T200 instrument. Data analysis was performed using Biacore T200 software and also using exponential decay (GraphPad Prism), taking into account both association and dissociation (27).

Statistical Analysis

Each experiment was performed at least three times and statistical analysis when comparing two events at a time was conducted using a two-tailed Student's *t*-test. Multiple comparisons were performed by ANOVA. Post-hoc Bonferroni correction was applied. Statistical probabilities (*p*) were expressed as * when *p*<0.05; **, *p*<0.01 and *** when *p*<0.001.

RESULTS

Galectin-9 Specifically Binds VISTA With High Affinity

In order to assess the possible interactions of VISTA with galectin-9 we used 96 well ELISA plates coated with goat anti-VISTA antibody. We then immunoprecipitated VISTA from Jurkat T cells by exposing the plate to Jurkat T cell lysates (Figures 1A, B) as previously described (4). We found that these cells express VISTA protein, while we could not detect any VISTA in primary NK cell lysates (Figure 1C; a full comparison of fluorescence observed for VISTA in Western blot analysis conducted in Jurkat T, primary human NK, THP-1, primary human AML and primary human T cells is presented in Supplementary Figure 1). When VISTA was captured and attached to an ELISA plate surface through the antibody, we exposed this di-protein complex to medium obtained from culturing THP-1 human AML cells for 24 h in the presence of 100 nM PMA (in order to maximize galectin-9 secretion (5)), which triggered the cells to produce around 6 ng of galectin-9 per 10⁶ cells (as measured by ELISA). As a negative control we used medium obtained from culturing MCF-7 breast cancer cells for 24 h in the presence of 100 nM PMA. MCF-7 cells express but don't secrete any galectin-9 (6) that was also confirmed here by ELISA where no release of galectin-9 was detected). After 2 h of exposure we either eluted bound proteins using glycine-HCl buffer (pH 2.0) and subjected the extract to Western blot analysis (4) (Figure 1A) or assessed galectin-9 concentrations by ELISA (Figure 1B). Western blot analysis demonstrated that galectin-9 was present in samples exposed to the medium from THP-1 but not MCF-7 cells (Figure 1A). ELISA analysis also confirmed the presence of galectin-9 in samples exposed to the medium from THP-1 but not MCF-7 cells (Figure 1B). Importantly, exposure

of the ELISA plate coated with anti-VISTA antibody (and BSA-blocked) to galectin-9 containing medium did not result in any signal, also confirming specific interaction of galectin-9 with VISTA (data not shown). SRCD spectroscopy showed that human recombinant galectin-9 binds VISTA causing conformational changes (Figure 1D) and titration showed that the K_d of this binding is 18 nM which confirms a relatively high binding affinity (Figure 1E). Since VISTA was used as an immunoglobulin fragment crystallisable region (VISTA-Fc) fusion protein, we checked if Fc can bind galectin-9, but the result was negative, suggesting that there is no specific interaction between these two proteins (Figure 1F). For the experiment shown in Figure 1D the observed spectra of Fc protein were subtracted from those of VISTA-Fc.

In order to further confirm specific interactions between galectin-9 and VISTA, we performed SPR analysis with galectin-9 immobilized on a CM5 Biacore sensor chip with either VISTA-Fc or Fc flowing through the cell. The binding of VISTA but not Fc was confirmed and we used three different approaches to calculate the K_d – a Lineweaver-Burk type plot, Biacore T200 software and GraphPad prism (exponential decay, association and dissociation approach), see Supplementary Figure 2. The K_d in all cases was approximately 100 nM (specific values for each method are shown in Supplementary Figure 2). These results confirmed specific binding of galectin-9 to VISTA.

VISTA Mediates Galectin-9-Induced Suppression of Granzyme B Release and Pro-Apoptotic Processes in T Cells

To assess the possible role of granzyme B, a pro-apoptotic proteolytic enzyme produced mainly by cytotoxic T cells and NK cells, in galectin-9-induced killing of T cells, we co-cultured THP-1 human AML cells and Jurkat T cells (at a ratio 1:1; Jurkat T cells express high amounts of VISTA and can express granzyme B and release this enzyme upon stimulation with PMA (28, 29), which activates granzyme B expression through NF-κB (29)). Both cell types were pre-treated for 24 h with 100 nM PMA before being co-cultured in PMA-free medium. Induction of granzyme B expression by PMA in Jurkat T cells was confirmed by Western blot analysis (Supplementary Figure 3). This led to the adhesion of THP-1 cells and caused them to release high levels of galectin-9 (>6 ng per 10⁶ cells over 16 h of incubation in PMA-free medium after pre-treatment) and activation of granzyme B in Jurkat T cells (these cells did not adhere to the surface and remained in suspension) as well as upregulating their capability to release this enzyme. Equal amounts of cells were co-cultured for 16 h (Figure 2A) and galectin-9 release (Figure 2B) as well as granzyme B activity (Figure 2C) were measured in both cell types. Importantly, PMA-pre-treated THP-1 cells released around 250 pg of soluble VISTA per 10⁶ cells during 16 h of post-PMA incubation (as measured by ELISA).

We found that PMA-treated THP-1 cells produced high levels of galectin-9 which were slightly reduced in the presence of Jurkat T cells (Figure 2B), suggesting most likely the interaction of galectin-9 with surface receptors of Jurkat T cells. Importantly, resting Jurkat T cells, pre-treated for 24 h with 100 nM PMA,

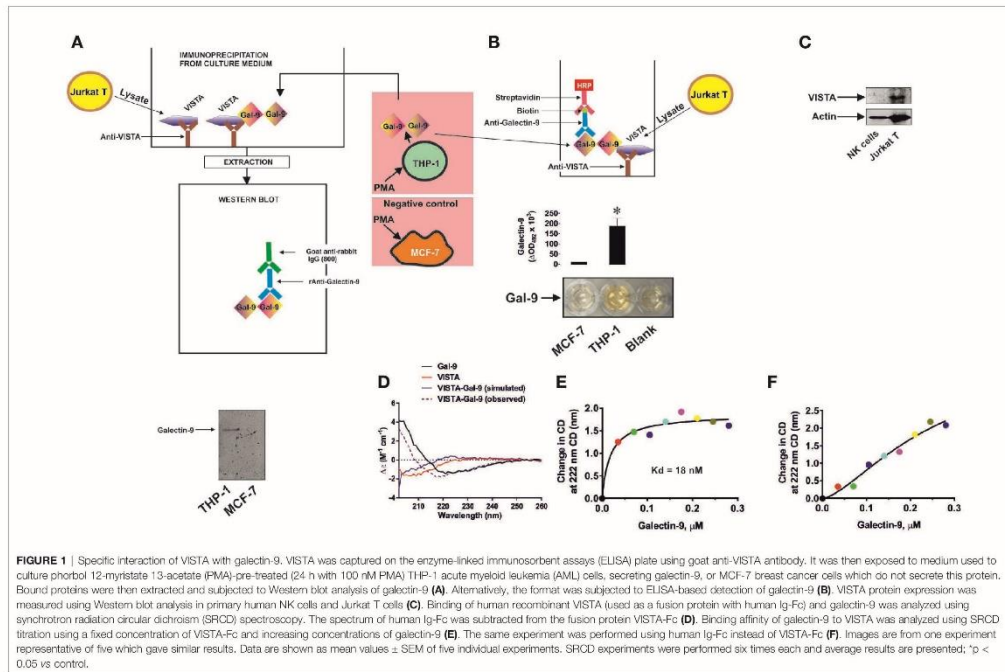
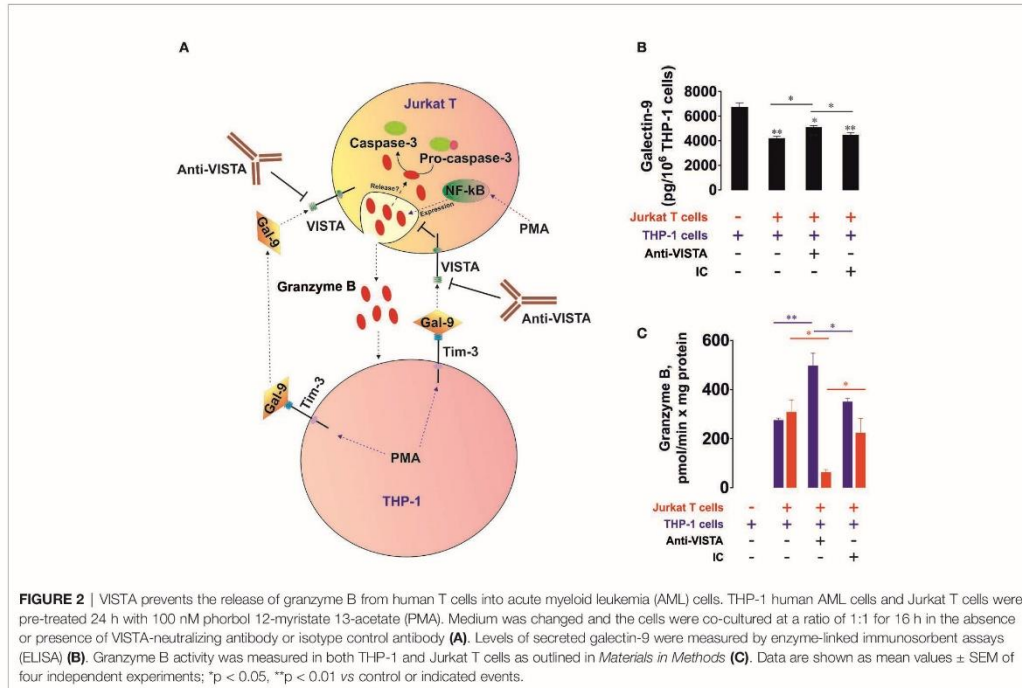


FIGURE 1 | Specific interaction of VISTA with galectin-9. VISTA was captured on the enzyme-linked immunosorbent assays (ELISA) plate using goat anti-VISTA antibody. It was then exposed to medium used to culture phorbol 12-myristate 13-acetate (PMA)-pre-treated (24 h with 100 nM PMA) THP-1 acute myeloid leukemia (AML) cells, secreting galectin-9, or MCF-7 breast cancer cells which do not secrete this protein. Bound proteins were then extracted and subjected to Western blot analysis of galectin-9 (A). Alternatively, the format was subjected to ELISA-based detection of galectin-9 (B). VISTA protein expression was measured using Western blot analysis in primary human NK cells and Jurkat T cells (C). Binding of human recombinant VISTA (used as a fusion protein with human Ig-Fc) and galectin-9 was analyzed using synchrotron radiation circular dichroism (SRCD) spectroscopy. The spectrum of human Ig-Fc was subtracted from the fusion protein VISTA-Fc (D). Binding affinity of galectin-9 to VISTA was analyzed using SRCD titration using a fixed concentration of VISTA-Fc and increasing concentrations of galectin-9 (E). The same experiment was performed using human Ig-Fc instead of VISTA-Fc (F). Images are from one experiment representative of five which gave similar results. Data are shown as mean values \pm SEM of five individual experiments. SRCD experiments were performed six times each and average results are presented; * p < 0.05 vs control.



during 16 h of post-PMA incubation in PMA-free medium released *ca.* 300 pg galectin-9 per 10^6 cells and did not release detectable amounts of soluble VISTA (as measured by ELISA). Resting PMA-pre-treated THP-1 cells did not show detectable granzyme B activity. In the presence of Jurkat T cells granzyme B was almost equally distributed between THP-1 and Jurkat T cells (Figure 2C). Importantly, Ac-IEPD-AFC has a similar amino acid sequence to the caspase 8-specific substrate, IETD (often derivative of type Ac-IETD is used). Therefore, caspase 8 has lower affinity to Ac-IEPD-AFC and can thus cleave it. To rule out the involvement of caspase 8 in the effects observed, we measured Ac-IEPD-AFC cleavage in the presence of the 100 μ M granzyme B inhibitor benzyloxycarbonyl-ala-ala-asph-chloromethylketone (Z-AAD-CMK) in the reaction mixture. The presence of this inhibitor completely abolished the observed proteolytic activities which allowed us to conclude that the effects seen were caused by granzyme B and not by caspase 8 or other proteolytic enzymes (Supplementary Figure 4). When the co-culture was performed in the presence of 5 μ g/ml anti-VISTA neutralizing antibody (R&D Systems), granzyme B activity was mainly detectable in Jurkat T cells. The presence of isotype control antibody didn't cause any changes compared to co-culture in the absence of antibodies. The differences in effects were also observed in THP-1 cells (Supplementary Figure 5A). Importantly, granzyme B in T cells is located in acidic granules, where it doesn't display catalytic activity since this requires

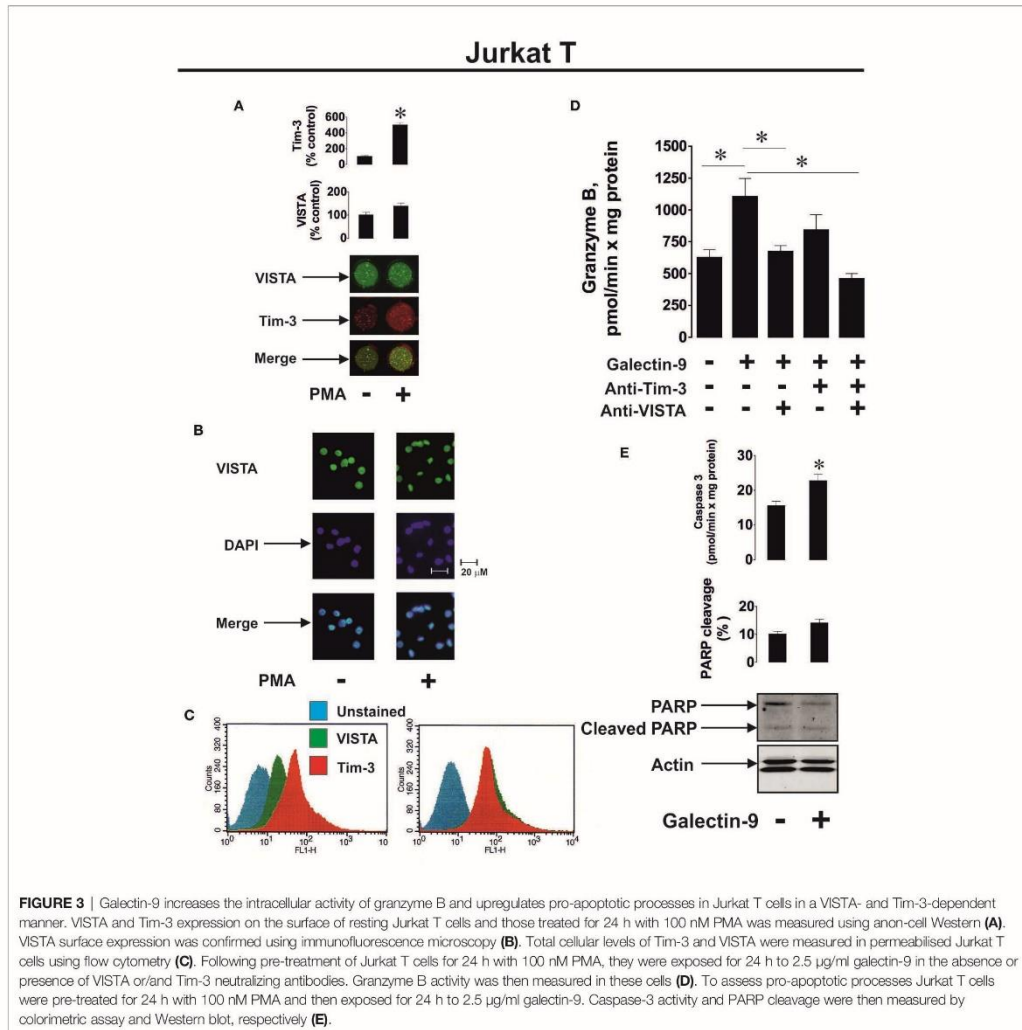
neutral (cytosolic) pH (30). By lysing the cells, granzyme B is co-extracted from the granules, thus enabling the measurement of its total activity. To confirm that granzyme B displays increased activity inside living Jurkat T cells in the presence of THP-1 cells, we measured in-cell activity of the enzyme in resting PMA (100 nM, 24 h) pre-treated Jurkat T cells after 16 h of incubation in PMA free medium and in Jurkat T cells (also pre-treated 24 h with 100 nM PMA) co-cultured for 16 h with PMA-pre-treated THP-1 cells. Then Jurkat T cells (in suspension) were separated from THP-1 cells (adherent) and incubated for 1 h at 37°C in the presence of 150 μ M Ac-IEPD-AFC (granzyme B substrate). Cells were then precipitated and fluorescence was measured against equal amounts of the same cells not exposed to the substrate. We found that in-cell activity of granzyme B was significantly increased in Jurkat T cells co-cultured with THP-1 cells (Supplementary Figure 5B).

Our observations suggest that VISTA protein is involved in galectin-9-induced suppression of granzyme B release from T cells. Importantly, both VISTA and Tim-3 neutralizing antibodies used in this study were tested and it was found that they blocked the effects of the target proteins, but did not induce any of the downstream effects of their target proteins suggesting no agonistic properties (data not shown). When recombinant Tim-3 or VISTA were immobilized on the surface of the ELISA plate and exposed to galectin-9 for 2 h, galectin-9 was detectable using ELISA detection antibody. When, before exposure to

galectin-9, immobilized proteins were pre-incubated with corresponding neutralizing antibodies, galectin-9 was no longer detectable. Neither of the antibodies induced Tim-3 signaling reported earlier for agonistic anti-Tim-3 antibody (16) or pro-apoptotic effects in Jurkat T cells expressing VISTA.

We then verified whether human recombinant galectin-9 causes the same effects in PMA-activated Jurkat T cells. We found that VISTA was present on the surface of Jurkat T cells regardless of PMA treatment, while Tim-3 mainly appeared on the cell surface after 24 h of exposure to 100 nM PMA (Figure

3A, importantly, expression levels of Tim-3 in Jurkat T cells are lower compared to AML cells, for example THP-1). The presence of VISTA was confirmed using immunofluorescent microscopy (Figure 3B) and the total amounts of both VISTA and Tim-3 were analyzed using FACS (Figure 3C). Exposure of Jurkat T cells (following 24 h pre-treatment with 100 nM PMA) to 2.5 µg/ml galectin-9 induced the activation of cell-associated granzyme B and the effect was downregulated when cells were pre-exposed (before treatment with galectin-9) to 5 µg/ml Tim-3-neutralizing or VISTA-neutralizing antibody. The presence of both



antibodies attenuated the galectin-9-induced effect (Figure 3D). Importantly, this experiment confirmed the role of Jurkat T-associated VISTA/Tim-3 in galectin-9-induced effects (in this experiment soluble VISTA/Tim-3 were not present in the medium but they were present on the surface of Jurkat T cells).

To investigate if galectin-9 induces pro-apoptotic effects in PMA-activated Jurkat T cells, we exposed them to 2.5 µg/ml galectin-9 for 16 h and measured caspase-3 activity (colorimetric assay) as well as poly-ADP-ribose polymerase (PARP) cleavage (Western blot). We found that caspase-3 activity was significantly upregulated by galectin-9 and this resulted in a tendency for increased PARP cleavage (Figure 3E).

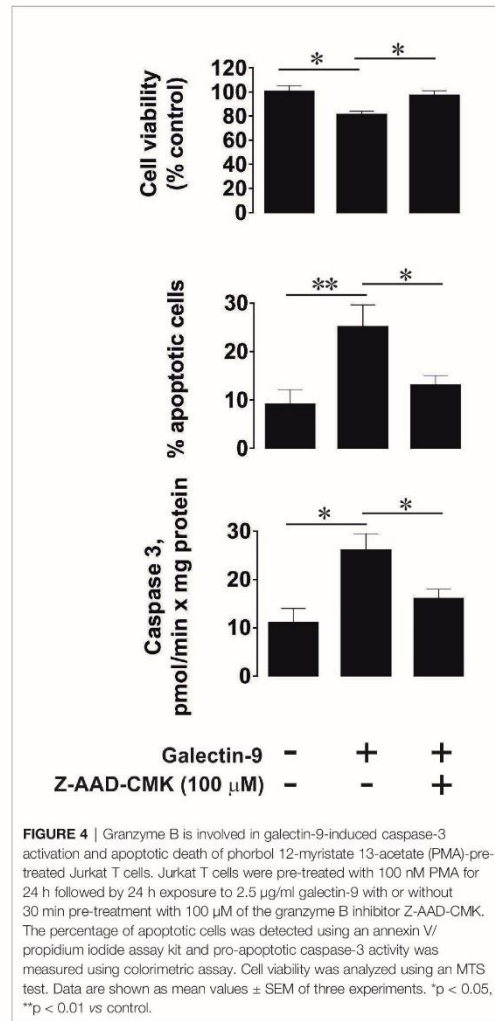
To confirm that caspase-3 activation followed by apoptotic cell death in PMA pre-treated (100 nM, 24 h) Jurkat T cells are granzyme B-dependent, we exposed these cells to 2.5 µg/ml galectin-9 for 24 h with or without 30 min pre-treatment with 100 µM Z-AAD-CMK (granzyme B inhibitor). We then assessed the percentage of apoptotic cells by measuring caspase 3 activity, using a colorimetric assay, in combination with an annexin V/propidium iodide assay. In addition, we measured cell viability using an MTS test. We found that galectin-9-induced caspase-3 activation and apoptotic death were attenuated by the granzyme B inhibitor (Figure 4).

To further confirm the role of granzyme B in galectin-9-induced pro-apoptotic processes we used HaCaT cells (non-malignant human keratinocytes), which express both Tim-3 and VISTA (Figures 5A–C), but their granzyme B activity was almost undetectable (Figure 5D). Exposure of HaCaT cells to 2.5 µg/ml galectin-9 did not result in any further pro-apoptotic effects (Figures 5D, E). However, caspase-3 activity was slightly increased after galectin-9 treatment, but the activity level (only 2.67 ± 0.45 pmol/min per mg protein) was still too low to induce pro-apoptotic processes (approx. 10-fold higher activity is required for this to occur), which is most likely a result of an absence of granzyme B activity in HaCaT cells.

To assess differences in the reactivity of T cells and NK cells to galectin-9 produced by AML cells, we co-cultured 24 h 100 nM PMA-pre-treated THP-1 AML cells with 24 h 100 nM PMA-pre-treated Jurkat T cells (co-culture was performed in PMA-free medium) or primary human NK cells in the absence or presence of anti-galectin-9 antibody for 16 h. In both cases, secreted galectin-9 levels were similar when THP-1 and Jurkat T cells were co-cultured (4.2 ± 0.3 ng/ml) compared to THP-1 cells co-cultured with primary human NK cells (3.9 ± 0.2 ng/ml). We found that the presence of THP-1 cells upregulated PARP cleavage in Jurkat T cells but not in NK cells. This effect was significantly reduced by the presence of anti-galectin-9 antibody in Jurkat T cells (as well as caspase-3 activity) and did not have any influence on the NK cells, which did not produce detectable amounts of VISTA protein (Figure 6).

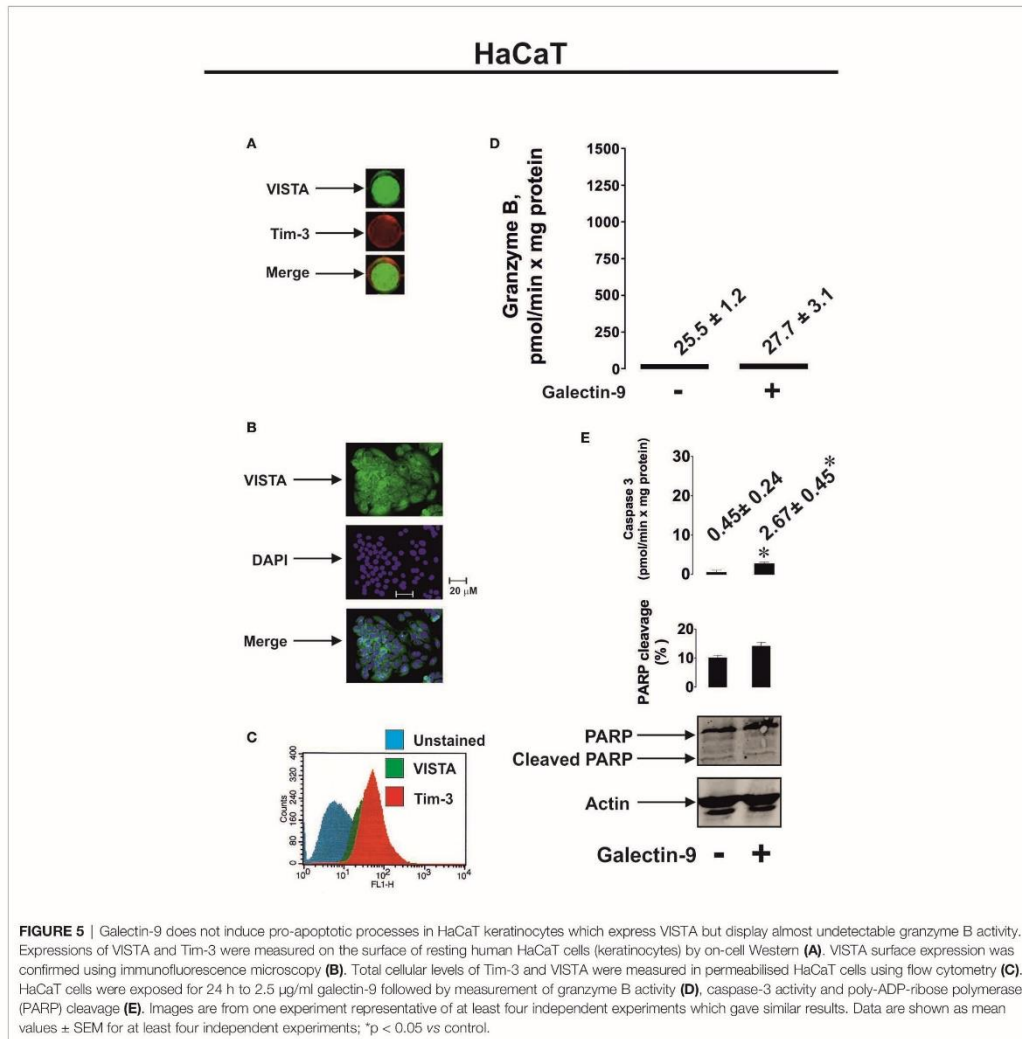
Soluble VISTA Induces Apoptotic Signaling Cascades in T Cells in Association With Galectin-9

Since recent evidence has clearly demonstrated that VISTA protein can be secreted by human myeloid cells, we asked whether human



AML cells produce soluble VISTA. We measured VISTA and galectin-9 proteins in the blood plasma of 5 newly diagnosed AML patients and 5 healthy donors. We found that in AML patients, the levels of both proteins were significantly upregulated (Figures 7A, B). Furthermore, there was a clear correlation between the levels of both proteins (Figure 7C).

We found that isolated primary human healthy leukocytes produce around 220 ± 24 pg of galectin-9 per 10^6 cells and 89 ± 12 pg of soluble VISTA, while primary human AML cells produced 5980 ± 626 pg of galectin-9 per 10^6 cells and 707 ± 154 pg of soluble VISTA during 24 h when cultured *in vitro* (Supplementary Figure 6A). Using Western blot analysis we



determined the molecular weight of soluble VISTA in blood plasma of AML patients, which was observed at 40 kDa (Supplementary Figure 6B). This is likely to correspond to the glycosylated extracellular domain of the protein, because deglycosylation performed using a deglycosylation kit (Promega) led to a reduction in molecular weight and the appearance of two new bands at around 36 and 28 kDa (Supplementary Figure 6B). Incubation of the samples with deglycosylation enzymes was performed for 3 h in order to observe the deglycosylation path. A longer incubation period (18 h) led to the appearance of a 28 kDa band only (data not shown). Respectively, the bands observed most

likely correspond to partially and fully deglycosylated protein. The smallest molecular weight protein is close to that of extracellular protein domain (31). Soluble VISTA is most likely to be produced in a similar manner to soluble Tim-3 and other Ig-type proteins – *via* proteolytic shedding. To confirm this we exposed THP-1 cells (following 24 h pre-treatment with 100 nM PMA) or primary human AML cells to 100 μ M GI254023X (an inhibitor of angiotensin and metalloproteinase domain-containing proteins (ADAM) 10/17) or 100 μ M batimastat (BB-94, matrix metalloproteinase inhibitor) for 24 h. Given the similarities between Tim-3 and VISTA we hypothesized that they may be

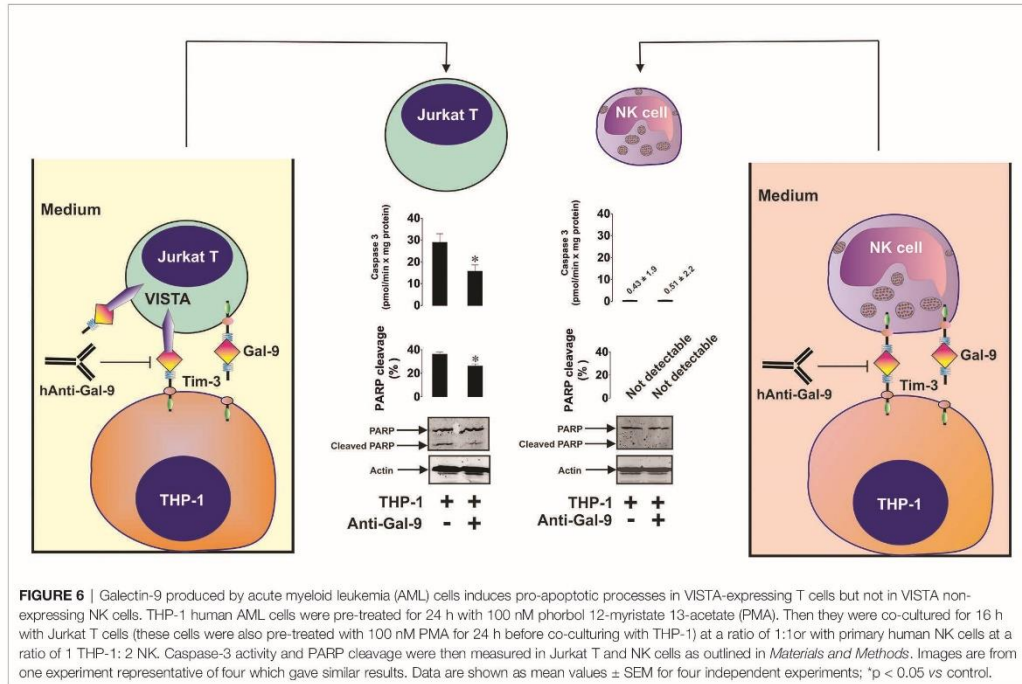


FIGURE 6 | Galectin-9 produced by acute myeloid leukemia (AML) cells induces pro-apoptotic processes in VISTA-expressing T cells but not in VISTA non-expressing NK cells. THP-1 human AML cells were pre-treated for 24 h with 100 nM phorbol 12-myristate 13-acetate (PMA). Then they were co-cultured for 16 h with Jurkat T cells (these cells were also pre-treated with 100 nM PMA for 24 h before co-culturing with THP-1) at a ratio of 1:1 or with primary human NK cells at a ratio of 1 THP-1: 2 NK. Caspase-3 activity and PARP cleavage were then measured in Jurkat T and NK cells as outlined in *Materials and Methods*. Images are from one experiment representative of four which gave similar results. Data are shown as mean values ± SEM for four independent experiments; *p < 0.05 vs control.

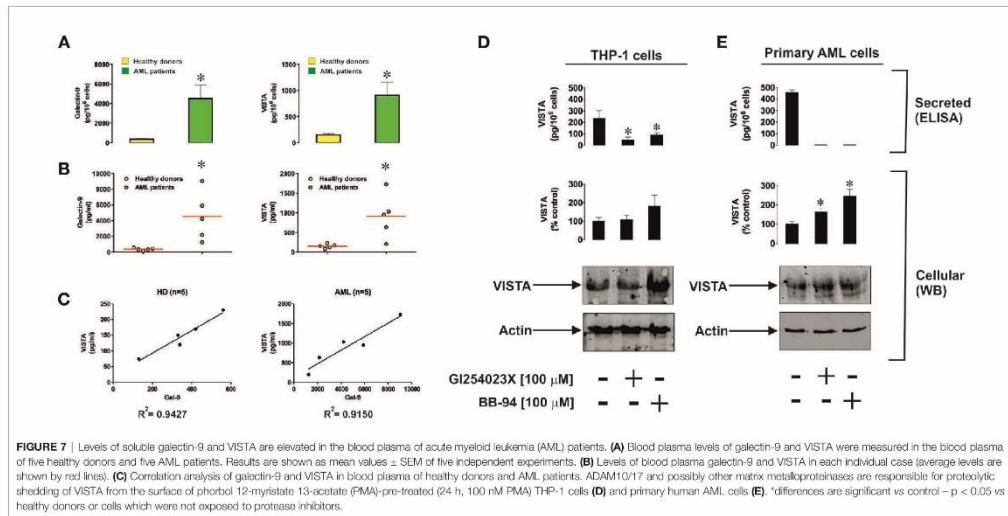
shed by the same proteolytic enzymes and thus used these particular protease inhibitors (5). We found that both inhibitors significantly reduced the release of soluble VISTA by THP-1 cells, where the effect of GI254023X was stronger (Figure 7D) and attenuated the effect in primary AML cells (Figure 7E). These results suggest that, as with Tim-3, VISTA is mainly shed by ADAM10/17 enzymes.

We then exposed 24 h 100 nM PMA pre-treated Jurkat T cells to 2.5 µg/ml galectin-9, 5 µg/ml (to assure use of equimolar amounts of proteins) VISTA or a combination of both proteins in the indicated concentrations for 16 h. Cells clearly expressed both receptors (VISTA and Tim-3) as determined by immunofluorescent microscopy (Figure 8A). We then measured PARP cleavage as a marker of caspase-3 induced pro-apoptotic events and found that a combination of galectin-9 and VISTA significantly increased PARP cleavage and obviously reduced the total amount of PARP (Figure 8B). In-cell activity of granzyme B was also significantly increased in the presence of galectin-9 or VISTA and was further significantly upregulated in the presence of a combination of both proteins (Figure 8C).

To assess if galectin-9 and VISTA could form complexes affecting cell polarity (plasma membrane potential), we exposed 24 h 100 nM PMA pre-treated Jurkat T cells to DiBAC₄ reactive dye which concentrates in depolarised cells as outlined in *Materials and Methods* and described previously (23). Cells were treated with 2.5 µg/ml galectin-9 or 5 µg/ml VISTA or a combination of both proteins at the indicated concentrations

for 30 min. We then measured fluorescence to characterize cell membrane potential over a 10 min period. We found that both galectin-9 and VISTA upregulated fluorescence intensity, however, the effect was substantially greater when cells were exposed to a combination of both proteins (Figure 8D). We hypothesized that soluble VISTA and galectin-9 may form multiprotein complexes on the T cell surface which may affect membrane potential and prevent granzyme B release. We sought to confirm whether the three proteins are capable of forming a complex and thus performed SRCD spectroscopy of human recombinant VISTA-Fc (Fc spectra were subtracted), galectin-9 and Tim-3 as well as an equimolar mixture of all three proteins (Supplementary Figure 7). There was an obvious interaction of the three proteins since conformational changes were seen in the observed spectrum compared to the simulated spectrum.

We then confirmed the observed effect using primary CD3-positive T cells isolated from the blood of healthy donors. These cells expressed both Tim-3 and VISTA as well as CD3 (a T cell-specific biological marker) as measured by Western blot analysis (Figure 8E). Cells were exposed for 16 h to 2.5 µg/ml galectin-9 in the absence or presence of 5 µg/ml VISTA (or 5 µg/ml Fc – the protein fragment to which the recombinant VISTA is fused). We found that, as in PMA-activated Jurkat T cells, a combination of both galectin-9 and VISTA significantly upregulated PARP cleavage, while the presence of galectin-9 alone non-significantly increased it



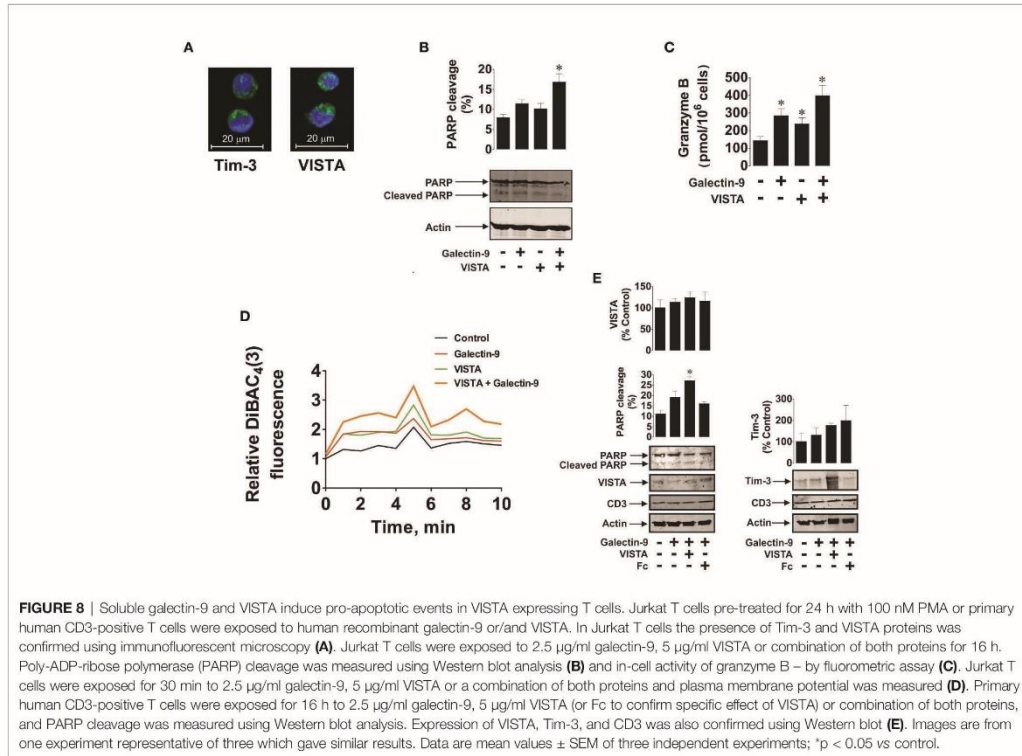


(Figure 8E), which is in line with the observations made in Jurkat T cells (Figures 8B, C).

Taken together, our results suggest that galectin-9 is a ligand for VISTA, which can induce granzyme B-dependent programmed death of T cells, especially in combination with soluble VISTA. The presence of VISTA in cytotoxic lymphoid cells may determine their responsiveness to galectin-9.

DISCUSSION

Elucidating the reasons for the differential responsiveness of human NK and T cells to galectin-9 was the main goal of this study. Our results indicate that human T but not NK cells produce detectable amounts of the protein VISTA (Figures 1C and 8E), which can act as immunosuppressive receptor but can also be present in soluble form and function as a ligand. Immunoprecipitation studies and biophysical assays (SRCD spectroscopy and SPR) indicated specific binding of galectin-9 to VISTA with a relatively high affinity (Kd was 18 nM in surface-free SRCD spectroscopy assay and ~ 100 nM when analyzed by SPR assay involving protein immobilization on the surface). Galectin-9 derived from THP-1 human AML cells was shown to downregulate the release of granzyme B (a pro-apoptotic

proteolytic enzyme) from PMA-activated Jurkat T cells (Figure 2). As shown in Figure 2, PMA led to both activation of granzyme B in Jurkat T cells and its release into THP-1 cells. Exposure of these cells to both PMA and calcium ionophore could have led to a higher level of granzyme B activation, as indicated in previous reports (28), but it would also have led to an artificial increase in cytosolic calcium levels. Such an effect could normally lead to artificially enhanced pro-apoptotic effects (32), whereas the aim of our study was to observe more naturally occurring apoptosis.

Our experiments suggested that pro-apoptotic effects can be induced by galectin-9 only in cells which express both VISTA and also produce active granzyme B. This was applicable to PMA-activated Jurkat T cells (Figures 3 and 4). Furthermore, galectin-9-induced caspase-3 activation and apoptotic death of these cells were attenuated by 100 µM Z-AAD-CMK (granzyme B inhibitor), suggesting the involvement of granzyme B in the process. The pro-apoptotic effects were not observed in HaCaT keratinocytes which express both Tim-3 and VISTA but granzyme B activity in these cells is barely detectable (Figure 5). Primary human NK cells, which express Tim-3, granzyme B but no detectable VISTA, also did not respond pro-apoptotically to galectin-9 released by THP-1 human AML cells (Figure 6). Our results suggest a lack of VISTA expression in NK cells and are in line with previously reported

observations where flow cytometry tests have shown NK cells, to be mostly negative for VISTA expression (13–15). All these results suggest galectin-9-triggered VISTA/Tim-3-mediated prevention of granzyme B release from T cells. It is interesting to note that AML cell-derived galectin-9 induces the same effects as recombinant protein but in much lower concentrations which suggests that galectin-9 produced by AML cells displays higher activity compared to the recombinant one.

AML cells were found to produce high levels of both proteins – galectin-9 and VISTA (Figure 7). In this study we found that both PMA-treated THP-1 and primary human AML cells released soluble forms of galectin-9 and VISTA proteins in high amounts. Blood plasma of newly diagnosed AML patients contains significantly greater levels of soluble VISTA and galectin-9 compared to the blood plasma of healthy donors. There is a clear correlation between the secretion of these two proteins (Figures 7A–C). Western blot analysis (before and after deglycosylation) indicated that blood plasma most likely contains the glycosylated extracellular domain of VISTA protein (as in the case of Tim-3, Supplementary Figure 6B). Furthermore, we found that VISTA (like Tim-3) is shed from the surface of AML cells by ADAM10/17 proteolytic enzymes (Figures 7D, E). Interestingly, simultaneous increases in the expressions of galectin-9, VISTA and Tim-3 were reported for other cancers, for example gastric cancer (33). Our further experiments indicate that soluble VISTA significantly enhances the pro-apoptotic effects of soluble galectin-9 in T cells. This occurs due to changes in cell polarization/membrane potential (Figure 8D), which may attenuate the capability of T cells to release granzyme B from the cell. As a result, granzyme B is released from the acidic granules in the cell which produced it and thus displays a high activity within this cell (Figure 8C, Supplementary Figure 5B). Granzyme B can then induce the classic caspase-3-mediated apoptotic pathway. Furthermore, galectin-9 could possibly upregulate granzyme B expression in T cells in a Tim-3-dependent manner, since presence of the Tim-3-galectin-9 complex on the cell surface leads to activation of NF- κ B, which is known to induce granzyme B expression in these cells (29).

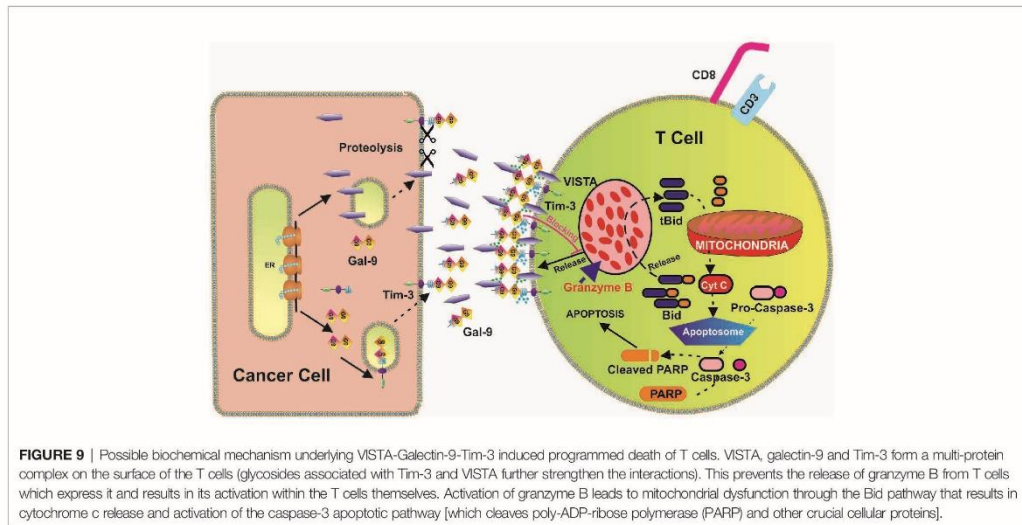
We hypothesized that, given the affinity of Tim-3 and VISTA to galectin-9, these three proteins may form agglomerates on the cell surface thereby affecting cell membrane potential/polarization and the ability to release granzyme B. SRCD experiments confirmed that human recombinant VISTA, galectin-9 and Tim-3 can form agglomerates leading to conformational changes of these proteins. Importantly, granzyme B displays highest catalytic activity at neutral pH. Therefore, in cells producing it, this enzyme is stored in acidic granules to prevent its activation (27, 34). However, when T cells such as Tregs (regulatory T cells) and CD8-positive cytotoxic T cells are ready to release granzyme B (34), formation of the multiprotein barrier by galectin-9, VISTA and Tim-3 could potentially lead to its release (leakage) from the granules, thus resulting in its activation within the cells that produce it. In addition, it has been demonstrated that galectin-9 strongly induces calcium mobilization specifically in T cells (35). Unlike T cells, however, this effect can be either very mild or absent in myeloid cells (16, 35). Forming such a barrier around the T cell by galectin-9, VISTA and

Tim-3 will most likely preserve a high calcium concentration in the T cells, which can then provoke granzyme B release from the granules and lead to apoptosis induction in granzyme B expressing cytotoxic T cells and Tregs. In helper T cells, where granzyme B activity is barely detectable, an increase in intracellular calcium concentration can lead to calcium-calpain-caspase-dependent apoptosis (32). In support of this assumption, our experiments with HaCaT cells showed a slight increase in caspase-3 activity after exposure to galectin-9 (Figure 5E), however the actual caspase-3 activity was substantially lower compared to galectin-9-treated PMA-activated Jurkat T cells, despite granzyme B activity in these cells is almost undetectable. Galectin-9-induced apoptotic effects can be stronger in T helper cells (however, a high concentration of galectin-9 is required (32, 35) than in HaCaT keratinocytes (36), since T cells display strong pro-apoptotic calcium signaling (32, 35).

Serpin B9 is the endogenous inhibitor of granzyme B, which is known to be involved in the protection of cytotoxic lymphoid cells against granzyme B-induced programmed death (37–40). One could hypothesize that if granzyme B is leaking from the intracellular granules of T cells, its concentration is higher than that of serpin B9, similar to the effects observed in NK cells (39). Jurkat T cells, which we studied, almost lack serpin B9 expression (40) and thus we observed proapoptotic events in these cells. In primary T cells, the amount of granzyme B leaking upon exposure to galectin-9 may be higher than those of serpin-9 thus causing proapoptotic events. However, this phenomenon requires further investigation in order to understand the detailed intracellular mechanisms leading to galectin-9-induced programmed death of T lymphocytes. Normally diffusion of granzyme B through transmembrane pores appears to be the dominant mechanism of granzyme delivery into the target cells (41, 42). These pores are formed by the pore-forming protein perforin (41, 42) produced by NK and cytotoxic T cells. However, upon changes in plasma membrane potential induced by galectin-9/VISTA, granzyme B release from T cells is most likely affected. Similar effects were described in regulatory T cells (Tregs) (43) and NK cells (39) where granzyme B was shown to leak from cytotoxic granules and induce self-inflicted damage and programmed cell death.

Our results suggest that intracellular leakage of granzyme B may be involved in galectin-9-induced VISTA-dependent cell death too, although other mechanisms, for example calcium-mediated pro-apoptotic events observed when higher galectin-9 concentrations (1 μ M or 32 μ g/ml) (32), cannot be ruled out. Schematically, our hypothesis of the involvement of granzyme B in VISTA/Tim-3/galectin-9-induced self-killing of T cells is summarized in Figure 9.

Taken together, our findings demonstrate for the first time that VISTA interacts with galectin-9 with relatively high affinity, without preventing the interaction of galectin-9 with Tim-3. Soluble VISTA enhances the immunosuppressive activity of galectin-9. Given the affected plasma membrane potential of the cells exposed to a combination of galectin-9 and VISTA, one could suggest that multiprotein complexes are formed by Tim-3, galectin-9 and VISTA (both T cell surface-based and soluble), thus depolarising the cell and forming a barrier which prevents the release of



granzyme B. On the other hand, it is possible that soluble VISTA additionally, binds to some other T cells receptors, which remain to be identified, supporting galectin-9-induced pro-apoptotic effects. These effects increase granzyme B activity within the cell that produces it, finally leading to suppressed cellular activity and even to cell death.

DATA AVAILABILITY STATEMENT

The datasets used and/or analyzed during the current study are available from the corresponding author on reasonable request.

ETHICS STATEMENTS

The studies involving human participants were reviewed and approved by Blood plasma of healthy human donors was obtained as described from buffy coat blood (purchased from healthy donors undergoing routine blood donation) which was purchased from the National Health Blood and Transfusion Service (NHSBT, UK) following ethical approval (REC reference: 16-SS-033). Written informed consent for participation was not required for this study in accordance with the national legislation and the institutional requirements.

AUTHOR CONTRIBUTIONS

IM, NM, and SS performed majority of the experiments and analysed the data. RH and GS performed SRCD spectroscopy and data analysis. MC-H provided expertise on structural data

analysis and compound characterisation. WF and JW isolated and provided primary AML samples used to obtain crucial data. CD and LC helped with performing SPR analysis. LV designed anti-Tim-3 antibodies used in this study. SB and UR participated in design of the concept and planning the experiments as well as writing the manuscript. BG, EF-K, and VS designed the study, planned all the experiments together with IY, analyzed the data, and wrote the manuscript. All authors contributed to the article and approved the submitted version.

ACKNOWLEDGMENTS

We thank Diamond Light Source for access to B23 beamline (projects numbers SM24509, SM20755, and SM21202) and Charlotte S. Hughes for excellent technical assistance. Surface plasmon resonance experiments were performed through access to the Nanobiotechnology Laboratory under the Framework for open access to the Joint Research Centre Research Infrastructures of the European Commission. BG, NM and UR acknowledge intramural funding support by the school of Medicine and Health Sciences, University of Oldenburg. This work was also supported by the Deutsche Forschungsgemeinschaft consortium FOR 2690 with funding to UR (RA 1026/3-1) and by the Swiss Batzbeär grant (to EF-K and SB).

SUPPLEMENTARY MATERIAL

The Supplementary Material for this article can be found online at: <https://www.frontiersin.org/articles/10.3389/fimmu.2020.580557/full#supplementary-material>

REFERENCES

- Yasinska IM, Gonçalves Silva I, Sakhnevych S, Gibbs BF, Raap U, Fasler-Kan E, et al. Biochemical mechanisms implemented by human acute myeloid leukemia cells to suppress host immune surveillance. *Cell Mol Immunol* (2018) 2018 (15):989–91. doi: 10.1038/s41423-018-0047-6
- Khaznadar Z, Henry G, Setterblad N, Agaoguc S, Raffoux E, Boissel N, et al. Acute myeloid leukemia impairs natural killer cells through the formation of a deficient cytotoxic immunological synapse. *Eur J Immunol* (2014) 44:3068–80. doi: 10.1002/eji.201444500
- Kikushige Y, Miyamoto T, Yuda J, Jabbarzadeh-Tabrizi S, Shima T, Takayanagi S, et al. A TIM-3/Gal-9 Autocrine Stimulatory Loop Drives Self-Renewal of Human Myeloid Leukemia Stem Cells and Leukemic Progression. *Cell Stem Cell* (2015) 17:341–52. doi: 10.1016/j.stem.2015.07.011
- Gonçalves Silva I, Ruegg L, Gibbs BF, Bardelli M, Fruehwirth A, Varani L, et al. The immune receptor Tim-3 acts as a trafficker in a Tim-3/galectin-9 autocrine loop in human myeloid leukemia cells. *Oncotarget* (2016) 5: e1195535. doi: 10.1080/2162402X.2016.1195535
- Gonçalves Silva I, Yasinska IM, Sakhnevych SS, Fiedler W, Wellbrock J, Bardelli M, et al. The Tim-3-galectin-9 Secretory Pathway is Involved in the Immune Escape of Human Acute Myeloid Leukemia Cells. *EBioMedicine* (2017) 22:44–57. doi: 10.1016/j.ebiom.2017.07.018
- Yasinska IM, Sakhnevych SS, Pavlova L, Teo Hansen Selno A, Teuscher Abeleira AM, Benlaouer O, et al. The Tim-3-Galectin-9 Pathway and Its Regulatory Mechanisms in Human Breast Cancer. *Front Immunol* (2019) 10:1594. doi: 10.3389/fimmu.2019.01594
- Delacour D, Koch A, Jacob R. The role of galectins in protein trafficking. *Traffic* (2009) 10:1405–13. doi: 10.1111/j.1600-0854.2009.00960.x
- Wada J, Kanwar YS. Identification and characterization of galectin-9, a novel beta-galactoside-binding mammalian lectin. *J Biol Chem* (1997) 272:6078–86. doi: 10.1074/jbc.272.9.6078
- Golden-Mason L, McMahan RH, Strong M, Reisdorph R, Mahaffey S, Palmer BE, et al. Galectin-9 functionally impairs natural killer cells in humans and mice. *J Virol* (2013) 87:4835–45. doi: 10.1128/JVI.01085-12
- Sehrawat S, Reddy PB, Rajasagi N, Suryawanshi A, Hirashima M, Rouse BT. Galectin-9/TIM-3 interaction regulates virus-specific primary and memory CD8⁺ T cell response. *PLoS Pathog* (2010) 6:e1000882. doi: 10.1371/journal.ppat.1000882
- Kang CW, Dutta A, Chang IY, Mahalingam J, Lin YC, Chiang JM, et al. Apoptosis of tumor infiltrating effector TIM-3+CD8+ T cells in colon cancer. *Sci Rep* (2015) 5:15659. doi: 10.1038/srep15659
- Heusschen R, Griffioen AW, Thijssen VL. Galectin-9 in tumor biology: a jack of multiple trades. *Biochim Biophys Acta* (2013) 1836:177–85. doi: 10.1016/j.bbcan.2013.04.006
- Lines JL, Pantazi E, Mak J, Sempere LF, Wang L, O'Connell S, et al. VISTA is an immune checkpoint molecule for human T cells. *Cancer Res* (2014) 74:1924–32. doi: 10.1158/0008-5472.CCR-13-1504
- Wang L, Rubinstein R, Lines JL, Wasiuk A, Ahonen C, Guo Y, et al. VISTA, a novel mouse Ig superfamily ligand that negatively regulates T cell responses. *J Exp Med* (2011) 208:577–92. doi: 10.1084/jem.20100619
- Lines JL, Sempere LF, Broughton T, Wang L, Noelle R. VISTA is a novel broad-spectrum negative checkpoint regulator for cancer immunotherapy. *Cancer Immunol Res* (2014) 2:510–717. doi: 10.1158/2326-6066.CCR-14-0072
- Prokhorov A, Gibbs BF, Bardelli M, Ruegg L, Fasler-Kan E, Varani L, et al. The immune receptor Tim-3 mediates activation of PI3 kinase/mTOR and HIF-1 pathways in human myeloid leukaemia cells. *Int J Biochem Cell Biol* (2015) 59:11–20. doi: 10.1016/j.biocel.2014.11.017
- Gonçalves Silva I, Gibbs BF, Bardelli M, Varani L, Sumbayev VV. Differential expression and biochemical activity of the immune receptor Tim-3 in healthy and malignant human myeloid cells. *Oncotarget* (2015) 6:33823–33. doi: 10.18632/oncotarget.5257
- Yasinska IM, Gibbs BF, Lall GS, Sumbayev VV. The HIF-1 transcription complex is essential for translational control of myeloid hematopoietic cell function by maintaining mTOR phosphorylation. *Cell Mol Life Sci* (2014) 71:699–710. doi: 10.1007/s00018-013-1421-2
- Yasinska IM, Ceccone G, Ojeda-Jimenez I, Ponti J, Hussain R, Siligardi G, et al. Highly specific targeting of human acute myeloid leukaemia cells using pharmacologically active nanoconjugates. *Nanoscale* (2018) 10:5827–33. doi: 10.1039/C7NR09436A
- Fasler-Kan E, Suenderhauf C, Barteneva N, Poller B, Gyga D, Huwyler J. Cytokine signaling in the human brain capillary endothelial cell line hCMEC/D3. *Brain Res* (2010) 1354:15–22. doi: 10.1016/j.brainres.2010.07.077
- Fasler-Kan E, Barteneva N, Ketterer S, Wunderlich K, Huwyler J, Gyga D, et al. Activation of the JAK-STAT intracellular pathway in human retinal pigment epithelial cell line ARPE-19. *Int J Interferon Cytokine Mediator Res* (2010) 2:127–36. doi: 10.2147/IJICMR.S13642
- Thong B, Pilling J, Ainscow E, Beri R, Unitt J. Development and validation of a simple cell-based fluorescence assay for dipeptidyl peptidase 1 (DPP1) activity. *J Biomol Screen* (2011) 16:36–43. doi: 10.1177/1087057110385228
- Yamada A, Gaja N, Ohya S, Muraki K, Narita H, Ohwada T, et al. Usefulness and limitation of DiBAC4(3), a voltage-sensitive fluorescent dye, for the measurement of membrane potentials regulated by recombinant large conductance Ca²⁺-activated K⁺ channels in HEK293 cells. *Jpn J Pharmacol* (2001) 86:342–50. doi: 10.1254/jip.86.342
- Hussain R, Benning K, Javorfi T, Longo E, Rudd TR, Pulford B, et al. CDApps: integrated software for experimental planning and data processing at beamline B23, Diamond Light Source. *J Synchrotron Radiat* (2015) 22:465–8. doi: 10.1107/S1600577514028161
- Hussain R, Javorfi T, Siligardi G. Circular dichroism beamline B23 at the Diamond Light Source. *J Synchrotron Radiat* (2012) 19:132–5. doi: 10.1107/S0909049511038982
- Siligardi G, Hussain R. CD spectroscopy: an essential tool for quality control of protein folding. *Methods Mol Biol* (2015) 1261:255–76. doi: 10.1007/978-1-4939-2230-7_14
- Sumbayev VV, Jensen JK, Hansen JA, Andreasen PA. Novel modes of oestrogen receptor agonism and antagonism by hydroxylated and chlorinated biphenyls, revealed by conformation-specific peptide recognition patterns. *Mol Cell Endocrinol* (2008) 287:30–9. doi: 10.1016/j.mce.2008.02.004
- Viswanathan K, Bot I, Liu L, Dai E, Turner PC, Togonou-Bickersteth B, et al. Viral cross-class serpin inhibits vascular inflammation and T lymphocyte fratricide; a study in rodent models *in vivo* and human cell lines *in vitro*. *PLoS One* (2012) 7:e44694. doi: 10.1371/journal.pone.0044694
- Huang C, Bi E, Hu Y, Deng W, Tian Z, Dong C, et al. A Novel NF-κB Binding Site Controls Human Granzyme B Gene Transcription. *J Immunol* (2006) 176:4173–81. doi: 10.4049/jimmunol.176.7.4173
- Peters PJ, Borst J, Oorschot V, Fukuda M, Krahenbuhl O, Tschopp J, et al. Cytotoxic T lymphocyte granules are secretory lysosomes, containing both perforin and granzymes. *J Exp Med* (1991) 173:1099–109. doi: 10.1084/jem.173.5.1099
- Mehta N, Maddineni S, Mathews II, Andres Parra Sperberg R, Huang PS, Cochran JR. Structure and Functional Binding Epitope of V-domain Ig Suppressor of T Cell Activation. *Cell Rep* (2019) 28:2509–16. doi: 10.1016/j.celrep.2019.07.073
- Kashio Y, Nakamura K, Abedin MJ, Seki M, Nishi N, Yoshida N, et al. Galectin-9 induces apoptosis through the calcium-calpain-caspase-1 pathway. *J Immunol* (2003) 170:3631–6. doi: 10.4049/jimmunol.170.7.3631
- Wang R, Song S, Harada K, Ghazanfari Amlashi F, Badgwell B, Pizzi MP, et al. Multiplex profiling of peritoneal metastases from gastric adenocarcinoma identified novel targets and molecular subtypes that predict treatment response. *Gut* (2020) 69:18–31. doi: 10.1136/gutjnl-2018-318070
- Kurschus FC, Jenne DE. Delivery and therapeutic potential of human granzyme B. *Immunol Rev* (2010) 235:159–71. doi: 10.1111/j.0105-2896.2010.00894.x
- Lhuillier C, Barjon C, Niki T, Gelin A, Praz F, Morales O, et al. Impact of Exogenous Galectin-9 on Human T Cells: CONTRIBUTION OF THE T CELL RECEPTOR COMPLEX TO ANTIGEN-INDEPENDENT ACTIVATION BUT NOT TO APOPTOSIS INDUCTION. *J Biol Chem* (2015) 290:16797–811. doi: 10.1074/jbc.M115.661272
- Hensleit U, Rosenbach T, Kolde G. Induction of apoptosis in human HaCaT keratinocytes. *Arch Dermatol Res* (1996) 288:676–83. doi: 10.1007/BF02505277
- Bird CH, Christensen ME, Mangan MSJ, Prakash MD, Sedelies KA, Smyth MJ, et al. The granzyme B-Serpins9 axis controls the fate of lymphocytes after lysosomal stress. *Cell Death Differ* (2014) 21:876–87. doi: 10.1038/cdd.2014.7

38. Zhang M, Park S-M, Wang Y, Shah R, Liu N, Murmann AE, et al. Serine Protease Inhibitor 6 Protects Cytotoxic T Cells from Self-Inflicted Injury by Ensuring the Integrity of Cytotoxic Granules. *Immunity* (2006) 24:451–61. doi: 10.1016/j.immuni.2006.02.002
39. Ida H, Nakashima T, Kedersha NL, Yamasaki S, Huang M, Izumi Y, et al. Granzyme B leakage-induced cell death: a new type of activation-induced natural killer cell death. *Eur J Immunol* (2003) 33:3284–92. doi: 10.1002/eji.200324376
40. Fritsch K, Finke J, Grüllich C. Suppression of granzyme B activity and caspase-3 activation in leukaemia cells constitutively expressing the protease inhibitor 9. *Ann Hematol* (2013) 92:1603–9. doi: 10.1007/s00277-013-1846-6
41. Lopez JA, Susanto O, Jenkins MR, Lukoyanova N, Sutton VR, Law RH, et al. Perforin forms transient pores on the target cell plasma membrane to facilitate rapid access of granzymes during killer cell attack. *Blood* (2013) 121:2659–68. doi: 10.1182/blood-2012-07-446146
42. Voskoboinik I, Whisstock JC, Trapani JA. Perforin and granzymes: function, dysfunction and human pathology. *Nat Rev Immunol* (2015) 15:388–400. doi: 10.1038/nri3839
43. Karreci ES, Eskandari SK, Dotiwala F, Routray SK, Kurdi AT, Assaker JP, et al. Human regulatory T cells undergo self-inflicted damage via granzyme pathways upon activation. *JCI Insight* (2017) 2:e91599. doi: 10.1172/jci.insight.91599

Conflict of Interest: The authors declare that the research was conducted in the absence of any commercial or financial relationships that could be construed as a potential conflict of interest.

Copyright © 2020 Yasinska, Meyer, Schlichtner, Hussain, Siligardi, Casely-Hayford, Fiedler, Wellbrock, Desmet, Calzolari, Varani, Berger, Raap, Gibbs, Fasler-Kan and Sumbayev. This is an open-access article distributed under the terms of the Creative Commons Attribution License (CC BY). The use, distribution or reproduction in other forums is permitted, provided the original author(s) and the copyright owner(s) are credited and that the original publication in this journal is cited, in accordance with accepted academic practice. No use, distribution or reproduction is permitted which does not comply with these terms.

Transforming growth factor beta type 1 (TGF- β) and hypoxia-inducible factor 1 (HIF-1) transcription complex as master regulators of the immunosuppressive protein galectin-9 expression in human cancer and embryonic cells

Anette Teo Hansen Selnø¹, Stephanie Schlichtner¹, Inna M. Yasinska¹, Svetlana S. Sakhnevych¹, Walter Fiedler², Jasmin Wellbrock², Elena Klenova³, Ludmila Pavlova³, Bernhard F. Gibbs^{1,4}, Martin Degen⁵, Isabelle Schnyder⁶, Nijas Aliu⁷, Steffen M. Berger⁶, Elizaveta Fasler-Kan^{6,8}, Vadim V. Sumbayev¹

¹Medway School of Pharmacy, Universities of Kent and Greenwich, Chatham Maritime, United Kingdom

²Department of Oncology, Hematology and Bone Marrow Transplantation with Section Pneumology, Hubertus Wald University Cancer Center, University Medical Center Hamburg-Eppendorf, Hamburg, Germany

³School of Biological Sciences, University of Essex, Colchester, United Kingdom

⁴Division of Experimental Allergy and Immunodermatology, University of Oldenburg, Oldenburg, Germany

⁵Dental Research Center, Department of Orthodontics and Dentofacial Orthopedics, University of Bern, Bern, Switzerland

⁶Department of Pediatric Surgery, Children's Hospital, Inselspital Bern, University of Bern and Department of Biomedical Research, University of Bern, Bern, Switzerland

⁷Department of Human Genetics, Children's Hospital, Inselspital, University of Bern, Bern, Switzerland

⁸Department of Biomedicine, University of Basel and University Hospital Basel, Basel, Switzerland

Correspondence to: Vadim V. Sumbayev, Elizaveta Fasler-Kan; email: V.Sumbayev@kent.ac.uk, elizaveta.fasler@insel.ch

Keywords: galectin-9, immune escape, TGF-beta, HIF-1

Received: September 23, 2020 **Accepted:** November 15, 2020 **Published:** December 8, 2020

Copyright: © 2020 Selnø et al. This is an open access article distributed under the terms of the [Creative Commons Attribution License](https://creativecommons.org/licenses/by/3.0/) (CC BY 3.0), which permits unrestricted use, distribution, and reproduction in any medium, provided the original author and source are credited.

ABSTRACT

Galectin-9 is one of the key proteins employed by a variety of human malignancies to suppress anti-cancer activities of cytotoxic lymphoid cells and thus escape immune surveillance. Human cancer cells in most cases express higher levels of galectin-9 compared to non-transformed cells. However, the biochemical mechanisms underlying this phenomenon remain unclear.

Here we report for the first time that in human cancer as well as embryonic cells, the transcription factors hypoxia-inducible factor 1 (HIF-1) and activator protein 1 (AP-1) are involved in upregulation of transforming growth factor beta 1 (TGF- β 1) expression, leading to activation of the transcription factor Smad3 through autocrine action. This process triggers upregulation of galectin-9 expression in both malignant (mainly in breast and colorectal cancer as well as acute myeloid leukaemia (AML)) and embryonic cells. The effect, however, was not observed in mature non-transformed human cells. TGF- β 1-activated Smad3 therefore displays differential behaviour in human cancer and embryonic vs non-malignant cells. This study uncovered a self-supporting biochemical mechanism underlying high levels of galectin-9 expression operated by the human cancer and embryonic cells employed in our investigations. Our results suggest the possibility of using the TGF- β 1 signalling pathway as a potential highly efficient target for cancer immunotherapy.

INTRODUCTION

Galectin-9 is one of the crucial proteins used by various types of cancer cells to suppress cytotoxic immune responses and thus, escape immune surveillance [1]. Some cancer cells (acute myeloid leukaemia (AML) and colorectal cancer) are capable of secreting this protein, while other cancer cells translocate galectin-9 onto the surface [1] and use it to impair anti-cancer activities of cytotoxic lymphoid cells such as cytotoxic T lymphocytes and natural killer (NK) cells [1–6]. Galectin-9 lacks a secretion signal sequence and thus cannot be secreted on its own. Its receptor, the T cell immunoglobulin and mucin domain containing protein 3 (Tim-3), can also act as a possible trafficker for galectin-9 [7]. When complexed with Tim-3 on the cell surface, galectin-9 induces downstream signalling of differential intensity [8–10], depending on the type of human myeloid and lymphoid cells [11]. In myeloid cells, galectin-9 primarily triggers growth factor type responses, while in lymphoid cells it induces pro-apoptotic signalling [10–13]. Galectin-9, together with Tim-3, can be shed from the cell surface by proteolytic enzymes, thus being released into the tumour microenvironment or blood [2].

Human cancer cells express significantly higher levels of galectin-9 compared to healthy human cells [1]. In particular, high amounts of galectin-9 are secreted by AML and colorectal cancer cells [1, 14]. However, the biochemical mechanisms underlying increased galectin-9 expression in human cancer cells are unknown. Understanding these mechanisms will significantly improve our knowledge concerning the biochemistry of malignant tumour immune escape and would facilitate identification of new targets for efficient cancer immunotherapy.

It has been reported that human cancer cells produce transforming growth factor beta type 1 (TGF- β 1, also known as TGF- β), that can display autocrine activity by binding to TGF- β receptors (TGFBR) [15, 16]. TGF- β is known to transduce its signal *via* the Smad3 transcription factor, which triggers the expression of target genes [17]. The galectin-9 gene LGALS9 promoter region has several (at least 5) Smad3 response elements and Smad3 has been reported to induce galectin-9 expression [18, 19]. In addition, the TGF- β encoding gene has at least 9 Smad3 response elements in its promoter region and thus could also upregulate TGF- β expression in an autocrine manner capable of supporting itself without external signals. Initial activation of TGF- β could be induced by the hypoxia-inducible factor 1 (HIF-1) transcription complex, which contains two subunits – a constitutive β subunit and an inducible α subunit. HIF-1 displays high activity in the

early stages of tumour growth and thus could initiate TGF- β expression [20], which can then trigger the autocrine pathway described above leading to galectin-9 overexpression. In addition, the activities of enzymes which generate reactive oxygen species (ROS), such as NADPH oxidase and xanthine oxidase, are elevated in cancer cells compared to healthy cells in corresponding tissues [20, 21]. Increased ROS levels lead to the activation of apoptosis signal regulating kinase 1 (ASK1) and its downstream pathway, resulting in activation of the AP-1 (activator protein 1) [22] transcription complex which could upregulate TGF- β expression.

Importantly, similar events could also occur in human embryonic cells, thus leading to the expression of high levels of galectin-9 and preventing embryo rejection by mother's immune system [23]. Experimental investigation of this complex hypothesis became the aim of this study.

Here we report for the first time that in human breast cancer, AML and embryonic cells, HIF-1 and AP-1 upregulate the expression of TGF- β , leading to the activation of Smad3 through autocrine action. This process subsequently upregulates galectin-9 expression in both malignant and embryonic cells, but not in mature healthy human cells. Activated Smad3 therefore displays differential behaviour in cancer/embryonic *vs* healthy cells.

RESULTS

HIF-1, TGF- β , Smad3 and galectin-9 are highly upregulated in primary human cancer and embryonic cells

In order to investigate the hypothesis of self-sustaining upregulation of TGF- β and galectin-9 expression in human cancer and embryonic cells we tested primary human breast tumours, primary AML cells as well as primary embryonic cells.

We found that all five tested breast cancer patients showed very high levels of xanthine oxidase and NADPH oxidase activities as well as thiobarbiturate-reactive species (TBRS, products of lipid peroxidation indicating increased oxidative burst) levels in tumour tissues compared to healthy tissues (Figure 1A, 1B). Respectively, levels of HIF-1 α were also significantly higher in tumour samples (Figure 1C). This was in line with the highly increased amounts of tumour-associated TGF- β and intracellular levels of phospho-S423/S425-Smad3 (active form, Figure 1C). In line with our previous observations [1], levels of both Tim-3 and galectin-9 were substantially increased in

tumour tissues compared to non-malignant samples (Figure 1D).

Similar observations were seen in AML, a non-solid malignancy. AML cells isolated from newly diagnosed patients were compared with primary leukocytes isolated from healthy donors upon culturing them for 24 h. AML cells showed significantly upregulated xanthine oxidase and NADPH oxidase activities as well as TBRS levels (Figure 2A), which suggests a higher level of oxidative stress in AML cells. HIF-1 α and phospho-S423/S425-Smad3 were almost undetectable in primary healthy leukocytes, but were clearly detectable in AML cells (Figure 2B). AML cells released significantly higher amounts of TGF- β compared to healthy leukocytes. Respectively, AML cells secreted much higher amounts of both Tim-3 and galectin-9 (Figure 2C; secreted levels were measured since over 24 h AML cells release much higher amounts of these proteins compared to those present in the cells at a single moment of time, when the cells are harvested).

To understand the role of TGF- β we analysed blood plasma of six healthy donors, six primary breast cancer patients, six metastatic breast cancer patients and six AML patients. In cases of primary and metastatic breast cancers, blood plasma levels of TGF- β were similar to those in healthy donors. However, in AML patients they were strikingly and significantly elevated (Figure 3). These results suggest that in solid tumours, like primary and metastatic breast tumours, produced TGF- β most likely remains in the tumour microenvironment while in the case of AML, this growth factor is secreted into the peripheral blood and can be employed by circulating AML cells.

Intriguingly, primary human embryonic cells obtained from chorion (around week 13 of pregnancy) of seven pregnant patients and amniotic liquid obtained from another seven patients (between weeks 20 and 25) had clearly detectable activities of xanthine oxidase, NADPH oxidase and TBRS (Figure 4A). The earlier the stage was, the higher was the level of oxidative burst. A

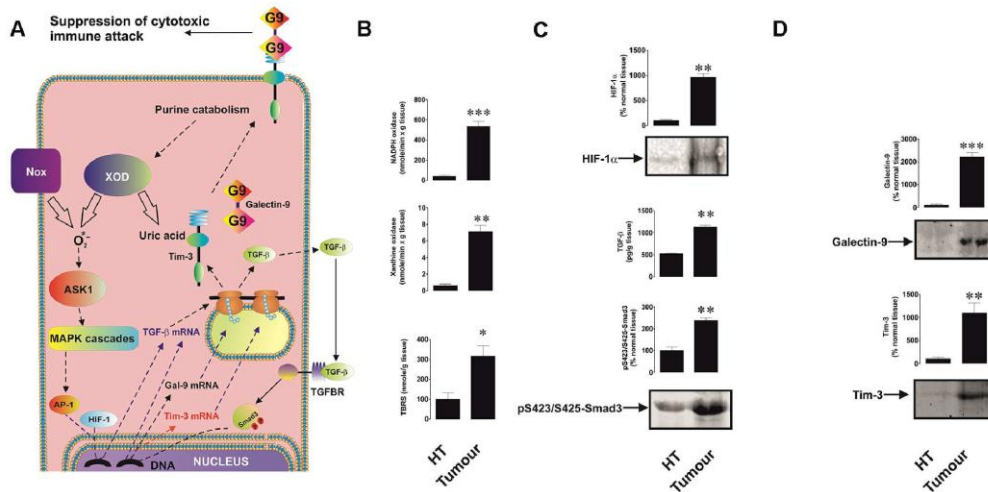


Figure 1. Increased redox status, upregulated HIF-1 α and TGF- β /Smad3 pathways as well as Tim-3 and galectin-9 expression in breast tumour tissues compared to non-transformed peripheral tissues. The proposed pathway studied is summarised in panel (A), where it is indicated that xanthine oxidase (XOD) and NADPH oxidase (Nox) produce ROS which activate AP-1 transcription factor through ASK1-controlled MAP kinase cascades. HIF-1 and AP-1 contribute to the activation of TGF- β expression, which then displays autocrine activity and stimulates the activation of galectin-9 and possibly Tim-3 expression through Smad3 transcription factor. Tissue lysates were subjected to measurement of xanthine oxidase and NADPH oxidase activities as well as TBRS levels (B). HIF-1 α accumulation, tissue-associated TGF- β and phospho-S423/S425-Smad3 levels (C) as well as levels of tissue-associated Tim-3 and galectin-9 (D) were analysed in tissue lysates. All quantities are expressed in respective units per 1 gram of the tissue. Normalisations against total protein loaded (for Western blot; measured by Li-Cor protein assay kit) and per mg of the total protein for enzyme activities and TBRS assays were also performed. These results are presented in the Supplementary Figure 1. Images are from one experiment representative of five which gave similar results. Data are shown as mean values \pm SEM of five independent experiments. * - $p < 0.05$ and ** - $p < 0.01$ vs non-transformed peripheral tissue abbreviated as HT (healthy tissue).

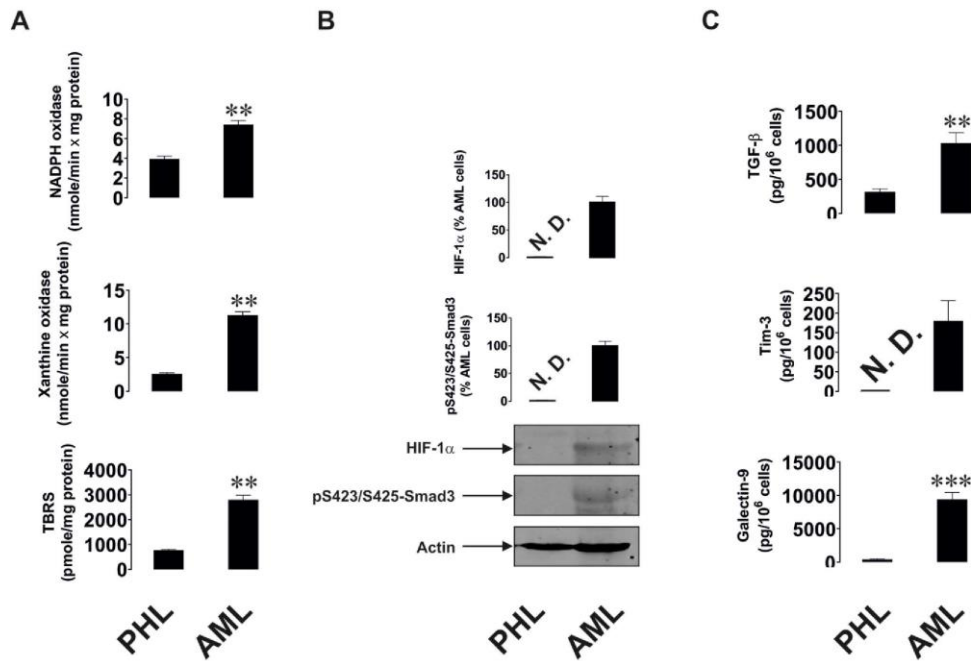


Figure 2. Increased redox status, upregulated HIF-1 α and TGF- β /Smad3 pathways as well as Tim-3 and galectin-9 expression in primary human AML cells compared to non-transformed mononuclear leukocytes. Measurements were conducted in primary human AML cells vs primary mononuclear leukocytes obtained from healthy donors. Activities of xanthine oxidase, NADPH oxidase and TBRS levels (A). Levels of accumulated HIF-1 α protein and phospho-S423/S425-Smad3 (B). Levels of secreted TGF- β , Tim-3 and galectin-9 measured in cell culture medium (C). Images are from one experiment representative of five which gave similar results. Data are shown as mean values \pm SEM of five independent experiments. * - $p < 0.05$ and ** - $p < 0.01$ vs non-transformed ("healthy") primary human mononuclear leukocytes (abbreviated as PHL – "primary healthy leukocytes").

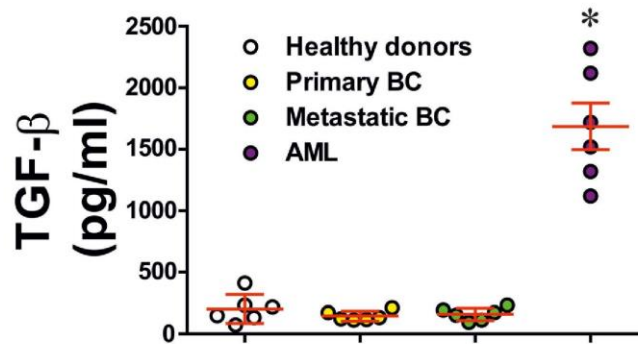


Figure 3. Levels of secreted TGF- β in blood plasma of healthy donors, primary and metastatic breast cancer patients and AML patients. TGF- β concentrations were measured in blood plasma of healthy donors, patients with primary breast tumours, patients with metastatic breast solid tumours and AML patients (n=6 for all donor types). Data are shown as mean values \pm SEM (data for each patient are shown). * - $p < 0.05$ vs healthy donors.

similar pattern was observed for HIF-1 α , secreted TGF- β and phospho-S423/S425-Smad3 levels (Figure 4B, 4C). Respectively, Tim-3 and galectin-9 were clearly detectable in both cell types, although not secreted, and were significantly higher at earlier pregnancy stages (Figure 4D, 4E).

Redox-dependent mechanisms contribute to TGF- β and galectin-9 expression

In order to understand the ability of redox-dependent ASK1-mediated activation of AP-1 in TGF- β and galectin-9 production, we used THP-1 human acute myeloid leukaemia cells which express Toll-like receptor 4 (TLR4; Figure 5A). Cells were exposed for 24 h to 1 μ g/ml high mobility group box 1 (HMGB1) protein. We found that HMGB1 induced the secretion of TGF- β and galectin-9 by THP-1 cells (Figure 5B). To investigate the contribution of the NADPH oxidase-ASK1-AP-1 redox-dependent pathway to TGF- β expression we pre-treated the cells with 30 μ M DPI (Diphenyleneiodonium chloride, NADPH oxidase inhibitor) or 1 μ M SR11302 (AP-1 inhibitor) for 1 h before exposing them for 24 h to HMGB1. Another set of cells was subjected to transfection with dominant-negative ASK1 (Δ N-ASK1), to block the activity of this enzyme prior to the 24 h exposure to HMGB1. We found that HMGB1 induced TGF- β and galectin-9 secretion (Figure 5B). DPI, SR11302 and Δ N-ASK1 attenuated the effect, suggesting that redox-induced ASK1-mediated AP-1 activation leads to increased TGF- β and galectin-9 production by THP-1 cells.

We then studied the ability of xanthine oxidase to upregulate TGF- β production. We used MCF-7 breast cancer cells, which express xanthine oxidase [21] and induced its activity by ammonium molybdate. Xanthine oxidase is a molybdenum-containing enzyme, so excess of molybdenum converts all the available xanthine oxidase molecules into their active form. To confirm the specificity of the effect we exposed MCF-7 cells to 100 μ g/ml ammonium molybdate for 24 h in the absence or presence of 250 μ g/ml allopurinol, a specific xanthine oxidase inhibitor. We found that xanthine oxidase activity was significantly upregulated by molybdate in MCF-7 cells (Figure 6A). This led to increased oxidative burst based on significantly increased TBRS levels. Xanthine oxidase activation was not able to induce HIF-1 α accumulation but the level of secreted TGF- β was significantly increased (Figure 6A). This resulted in a significant upregulation of Smad3 S423/S425 phosphorylation (Figure 6B). As a result, galectin-9 expression was also significantly increased (Figure 6B). Allopurinol attenuated all these effects (Figure 6A, B), indicating a specific role for xanthine oxidase in the processes outlined above.

The HIF-1 transcription complex triggers galectin-9 expression by inducing TGF- β production; Smad3 is involved in both TGF- β and galectin-9 expression

We then considered the effect of HIF-1 activation on TGF- β production and its subsequent effect on galectin-9 expression. We exposed wild type and HIF-1 α knockdown (achieved by transfection of HIF-1 α siRNA) MCF-7 cells as well as those transfected with random siRNA to 50 μ M cobalt chloride (CoCl₂) for 6 h (Co cations directly inhibit degradative hydroxylation of HIF-1 α [24]), followed by measurement of HIF-1 DNA-binding activity, cell-associated and secreted TGF β (ELISA) as well as cellular galectin-9 levels (Western blot – MCF-7 cells do not secrete galectin-9). We found that CoCl₂ induced significant upregulation of HIF-1 DNA-binding activity in wild type and random siRNA-transfected MCF-7 cells (Figure 7A). No effect was observed in HIF-1 α knockdown cells (Figure 7A). In wild type cells CoCl₂ induced significant upregulation of secreted and total levels of TGF- β . The effect was not observed in HIF-1 α knockdown cells (Figure 7A). In MCF-7 cells transfected with random siRNA, the level of total TGF- β was upregulated to the one observed in wild type cells exposed to CoCl₂. However, the application of DOTAP to transfect these cells with random siRNA together with CoCl₂ slowed down the process of TGF- β secretion. As a result, the level of galectin-9 was only upregulated in wild type MCF-7 cells treated with CoCl₂ (Figure 7). These results suggest that HIF-1 induces the expression of TGF- β , which then facilitates the upregulation of galectin-9 expression. To further investigate this assumption we studied the dynamics of the process. We exposed wild type MCF-7 cells to 50 μ M CoCl₂ for 1, 2, 3, 4, 5 and 6 h time points and detected HIF-1 DNA-binding activity, levels of secreted TGF- β and cellular galectin-9 expressions. We found that HIF-1 DNA-binding activity was increased after 1 h of exposure to CoCl₂, while the levels of secreted TGF- β were significantly increased following 3 h of exposure (Figure 7B). Cellular galectin-9 level was significantly upregulated only in 6 h of exposure to CoCl₂ (Figure 7B). To specifically confirm the contribution of TGF- β in regulating galectin-9 expressions, we exposed wild type MCF-7 cells to 50 μ M CoCl₂ for 6 h in the absence or presence of TGF- β neutralising antibody or isotype control antibody. We found that TGF- β neutralising antibody but not the isotype control attenuated CoCl₂-induced galectin-9 upregulation in MCF-7 cells (Figure 7C). All these findings clearly demonstrated that HIF-1 induces TGF- β production which displays autocrine activity and triggers galectin-9 expression.

In order to confirm the role of Smad3 in both TGF- β and galectin-9 expression we used wild type and Smad3

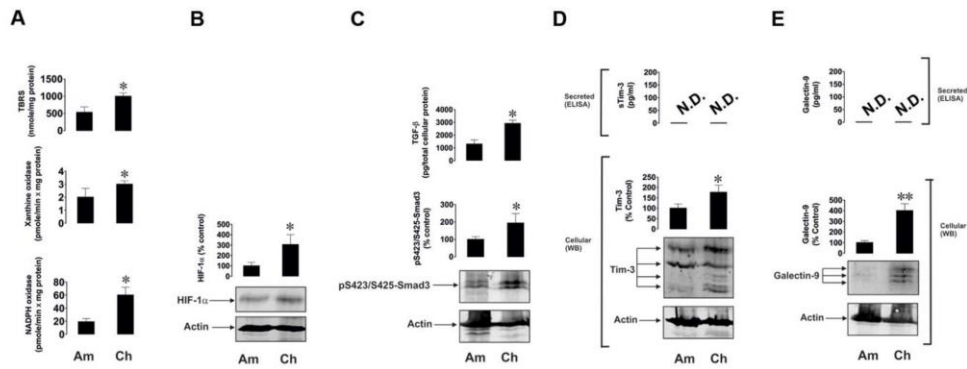


Figure 4. Oxidative burst, HIF-1 α accumulation, TGF- β /Smad3 pathway and Tim-3/galectin-9 levels are highly upregulated in primary human embryonic cells at early pregnancy stages. Primary human embryonic cells, obtained from amniotic fluid (Am, around 20-25 weeks of pregnancy) and chorion (Ch, around 13 weeks of pregnancy), were subjected to measurement of xanthine oxidase and NADPH oxidase activities as well as TBRS levels (A). HIF-1 α accumulation (B), secreted TGF- β and cell-associated phospho-S423/S425-Smad3 levels were also analysed (C), as well as levels of cell-associated and secreted Tim-3 (D) and galectin-9 (E). Images are from one experiment representative of seven, which gave similar results. Data are shown as mean values \pm SEM of seven independent experiments. * - $p < 0.05$ vs amniotic cells.

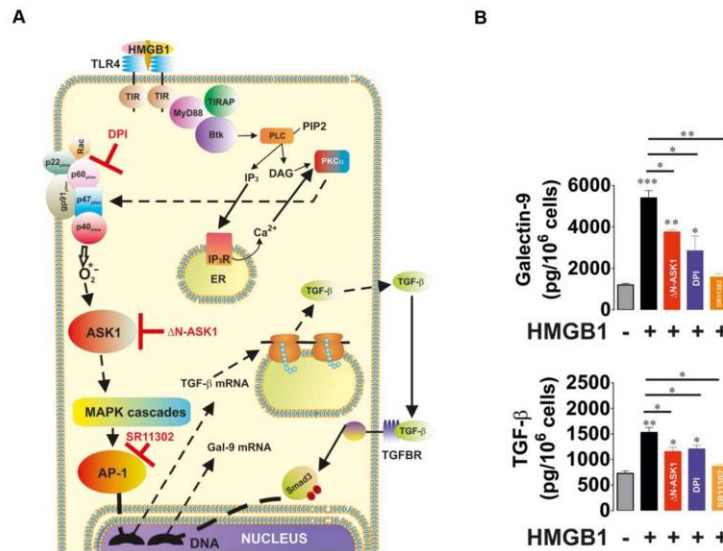


Figure 5. Oxidative stress-induced activation of AP-1 in an ASK1-dependent manner induces TGF- β and galectin-9 expression. THP-1 cells were treated with the Toll-like receptor 4 (TLR4) ligand, high mobility group box 1 (HMGB1), for 24 h. TLR4 mediates activation of NADPH oxidase using myeloid differentiation factor 88 (MyD88), TLR4 TIR domain-associated protein (TIRAP) and Bruton's tyrosine kinase (Btk). Activation of Btk by MyD88 and TIRAP leads to Btk-dependent phosphorylation of phospholipase C (PLC, mainly isoform 1 γ), which triggers activation of protein kinase C alpha (PKC α). PKC α activates NADPH oxidase which produces superoxide anion radical, activating the ASK1 pathway and activation of AP-1 transcription factor. The scheme is shown in panel (A). THP-1 cells were exposed for 24 h to 1 μ g/ml HMGB1 with or without pre-treatment with 30 μ M DPI (NADPH oxidase inhibitor), 1 μ M SR11302 (AP-1 inhibitor) or transfection with dominant-negative isoform of ASK1 (Δ N-ASK1). Levels of secreted TGF- β and galectin-9 were measured by ELISA (B). Data are shown as mean values \pm SEM of four independent experiments. * - $p < 0.05$ and ** - $p < 0.01$ vs control.

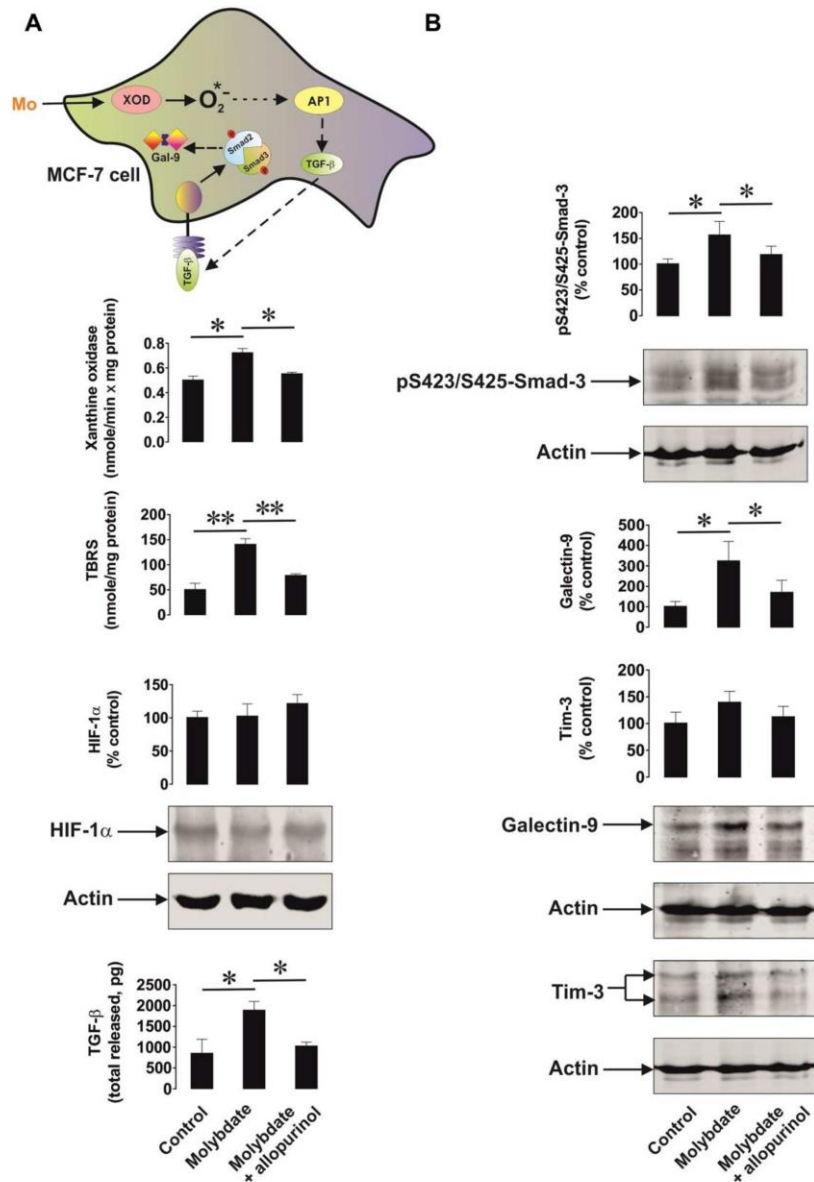


Figure 6. Xanthine oxidase activation leads to increased oxidative stress and upregulation of the TGF- β /Smad3 pathway as well as galectin-9 expression. MCF-7 human breast cancer cells were exposed to ammonium molybdate for 24 h to induce xanthine oxidase activity in the absence or presence of the xanthine oxidase inhibitor allopurinol. Xanthine oxidase activity, TBRS levels, HIF-1 α accumulation, secreted TGF- β (A), and cell-associated phospho-S423/S425-Smad3, Tim-3 and galectin-9 (B) were analysed as outlined in the Materials and Methods. Images are from one experiment representative of four which gave similar results. Data are shown as mean values \pm SEM of four independent experiments. * - $p < 0.05$ and ** - $p < 0.01$ vs indicated events.

knockdown MCF-7 cells. As a control for reagents, we used MCF-7 cells transfected with random siRNA as outlined in Materials and Methods. Cells were exposed to 2 ng/ml TGF- β for 24 h and cell-associated (in cell lysates) and the levels of secreted (in cell culture medium) TGF- β were measured by ELISA. Phospho-S423/S425-Smad3 and galectin-9 were measured in cell lysates to confirm successful knockdown and to assess the effects on galectin-9 expression (Figure 7D). We found that the presence of TGF- β led to an increase in secreted TGF- β levels (Figure 7E). This increase did not take place in Smad3 knockdown cells. The same was applicable to the levels of galectin-9 (Figure 7E). MCF-7 cells transfected with random siRNA displayed increased levels of cell-associated as well as secreted TGF- β . This resulted in upregulation of galectin-9 expression as well (Figure 7E). However, MCF-7 cells transfected with random siRNA in the presence of CoCl₂ displayed higher levels of cell-associated TGF- β and lower levels of secreted protein compared to similar cells treated with TGF- β . This means that the presence of DOTAP reagent and cobalt cations reduces the ability of MCF-7 cells to secrete *de novo* produced TGF- β .

TGF- β induces galectin-9 expression in human cancer and embryonic cells

To confirm and study the differential effects of TGF- β on galectin-9 expression we treated THP-1 human AML cells, Colo205 human colorectal cancer cells, MCF-7 human breast cancer cells, HaCaT human keratinocytes (non-malignant cells), primary healthy human keratinocytes as well as HEK293 human embryonic kidney cells, with 2 ng/ml human recombinant TGF- β (specifically TGF- β type 1 was used) for 24 h. Cellular and secreted levels of galectin-9 and Tim-3 were then determined. We found that in all types of human cancer cells and in HEK293, TGF- β upregulated the amounts of expressed galectin-9 but not Tim-3. However, in non-malignant cells (both types of keratinocytes), no upregulation of either galectin-9 or Tim-3 expression was observed (Figure 8). Both types of keratinocytes expressed barely detectable levels of galectin-9 and this was not inducible by TGF- β . To find out whether such a phenomenon (the absence of induction of galectin-9 expression by TGF- β) applies also to cancer cells we used K562 chronic myeloid leukaemia cells which express only traces of galectin-9 protein [1] compared to for example THP-1 or other AML cells. Exposure of these cells to increasing concentrations of TGF- β for 24 h led to a clear induction of galectin-9 expression (Supplementary Figure 2), suggesting differential responses of cancer/embryonic and non-malignant mature human cells. Importantly, levels of phospho-S423/S425 Smad-3 were undetectable in resting K562

cells and were clearly detectable in TGF- β -treated cells (Supplementary Figure 2). Regardless the treatment, K562 cells did not release detectable amounts of galectin-9 (Supplementary Figure 2).

Since Smad3 is the transcription factor activated by TGF- β , which then induces galectin-9 expression, we compared TGF- β -induced S423/S425 Smad3 phosphorylation in malignant and non-malignant human cells. MCF-7 breast cancer cells as well as non-malignant HaCaT cells and primary keratinocytes were exposed for 24 h to 2 ng/ml TGF- β followed by measurement of phospho-S423/S425 Smad3. We detected significant upregulation of phospho-S423/S425-Smad3 levels only in MCF-7 cells but not in non-malignant keratinocytes. In addition, the profile of the phospho-S423/S425-Smad3 band was different in malignant and non-malignant cells (Figure 9). Taken together these results suggest that TGF- β -induced Smad3-mediated galectin-9 expression takes place mainly in human cancerous and embryonic cells. The responses associated with TGF- β -induced S423/S425 Smad3 phosphorylation are clearly different in cancer/embryonic and mature non-malignant human cells.

DISCUSSION

Galectin-9 plays a crucial role in determining the ability of cancer cells to escape host immune surveillance [1, 2]. As with all galectins, galectin-9 lacks a secretion signal sequence and thus requires trafficking in order to be externalised onto the cell surface or secreted [1, 7]. Cell surface-based or secreted galectin-9 can impair anti-cancer activities of NK and cytotoxic T cells [1, 2, 6, 7]. Tim-3 acts as a receptor and possible trafficker for galectin-9 and also participates in the transduction of moderate growth signals from galectin-9 into cancer cells (for example AML cells) as well as pro-apoptotic signals into cytotoxic T cells [3].

Many types of cancer cells express significantly higher amounts of galectin-9 compared to non-malignant cells of similar origin [1]. However, the biochemical mechanisms underlying this phenomenon remain unclear and thus investigation of galectin-9 expression control pathways was the main goal of this study.

We hypothesised that TGF- β , a growth factor with autocrine activity, is responsible for the upregulation of galectin-9 expression in cancer cells. We found that human breast tumour cells and AML cells produced significantly higher levels of TGF- β compared to non-transformed cells of similar origin. Interestingly, the levels of oxidative stress and activities of ROS producing enzymes (xanthine oxidase and NADPH

oxidase) were significantly higher in cancer cells/tissues. Oxidative stress normally leads to activation of the AP-1 transcription complex [22], which contributes to TGF- β expression [25]. In addition, the levels of HIF-1 α accumulation were much higher in cancer samples. HIF-1 α determines transcriptional activity of the HIF-1 complex, which directly activates the expression of TGF- β . As a result of increased TGF- β activity, the levels of phosphorylated (active, when phosphorylated at S423/S425) Smad3, which is a TGF- β transcription factor, were significantly upregulated in the studied cancer cells/tissues. The levels of galectin-9 and its receptor Tim-3 were upregulated in all the studied cancer cell types (these results are shown in Figures 1 and 2). Interestingly, AML but not breast cancer

patients showed significantly increased blood plasma levels of TGF- β (Figure 3), which suggests that in breast (solid) tumours TGF- β remains within tumour microenvironment, while in AML it is secreted into the blood thus having the opportunity to systemically act on AML cells in circulation.

Importantly, primary human embryonic cells showed the same pattern as breast cancer and AML cells (Figure 4). The earlier the stage the pregnancy was, the higher were the levels of galectin-9 and Tim-3 and components of the possible upstream pathway outlined above. Embryonic cells were similar to breast and other solid tumour cells and not like AML cells in terms of galectin-9 and Tim-3 secretion and where unable to secrete detectable amounts of these proteins (Figure 4).

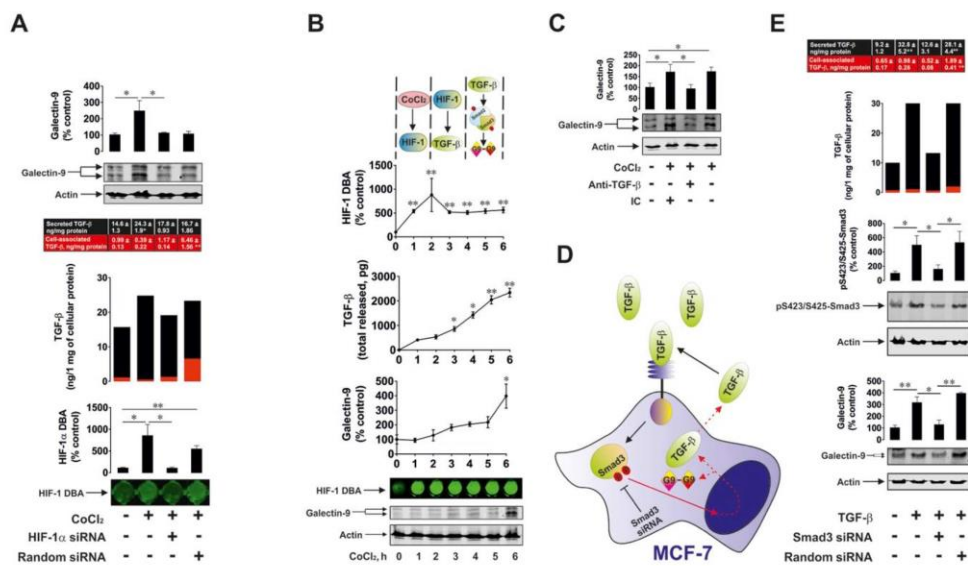


Figure 7. HIF-1 and Smad3 are involved in the production of TGF- β and galectin-9. (A) Cobalt chloride induces HIF-1 activation, TGF- β and galectin-9 production. Wild type, HIF-1 α knockdown and random siRNA-transfected MCF-7 cells were exposed to 50 μ M cobalt chloride for 6 h followed by measurement of HIF-1 DBA, secreted (in cell culture medium) and cell-associated (in cell lysates) TGF- β as well as cell-associated galectin-9. Images are from one experiment representative of three which gave similar results. (B) Dynamics of cobalt chloride-induced HIF-1 activation, TGF- β and galectin-9 accumulation in MCF-7 human breast cancer cells. MCF-7 cells were exposed to 50 μ M cobalt chloride for 1, 2, 3, 4, 5 and 6 h followed by measurement of HIF-1 DBA, secreted and cell-associated TGF- β as well as cell-associated galectin-9. Images are from one experiment representative of three which gave similar results (in the case of TGF- β – vs 1 h time-point since at zero point cells can't release any TGF- β . At this time-point, fresh medium has just been supplied and measurement was taken immediately to confirm zero TGF- β level). (C) HIF-1-induced galectin-9 expression is mediated by TGF- β . MCF-7 cells were exposed to 50 μ M cobalt chloride for 6 h with or without presence of TGF- β neutralising or isotype control antibody. Galectin-9 expression was then assessed by Western blot. Images are from one experiment representative of three, which gave similar results. (D), (E) Smad3 is involved in TGF- β and galectin-9 expression. (D) Scheme of the experiment performed showing studied effects. (E) Wild type, Smad3 knockdown and random siRNA-transfected MCF-7 cells were exposed to 2 ng/ml TGF- β for 24 h followed by measurement of secreted (in cell culture medium) and cell-associated (in cell lysates) TGF- β as well as cell-associated galectin-9 and phospho-S423/S425 Smad3. Images are from one experiment representative of three, which gave similar results. All quantitative data are shown as mean values \pm SEM (n=3-4) * - p < 0.05 and ** - p < 0.01 vs indicated events.

We have confirmed that upregulation of both NADPH oxidase and xanthine oxidase are capable of increasing TGF- β production. HMGB1-induced NADPH oxidase activation led to upregulated TGF- β and galectin-9 production by THP-1 human AML cells. Blockade of NADPH oxidase activity, ASK1 kinase activity or AP-1 transcriptional activity

decreased HMGB1-induced effects (Figure 5). Importantly, from our previous work we know that HMGB1 acts through Toll-like receptors (TLRs) 2 and 4 causing oxidative stress and also inducing HIF-1 activation [26]. AP-1 is known to be required for TGF- β expression although it might not directly act on the TGF- β gene [25],

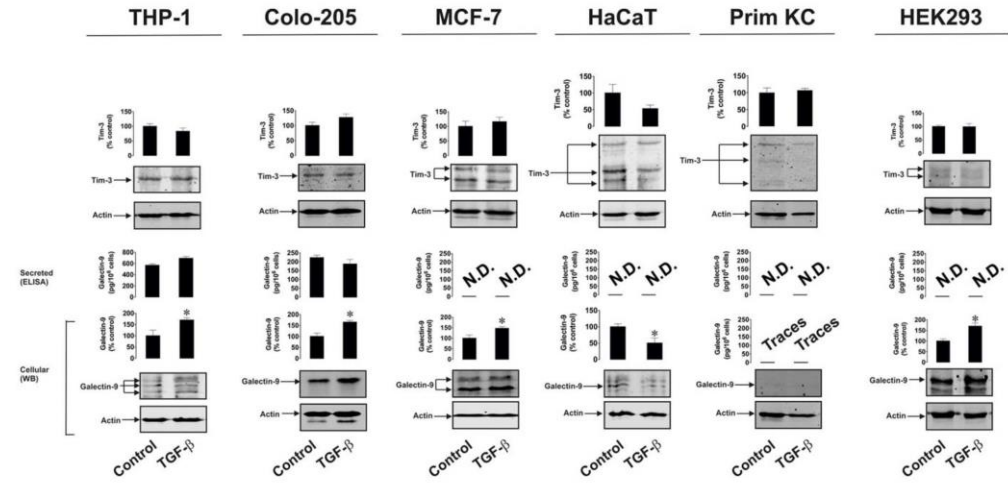


Figure 8. TGF- β induces galectin-9 expression in human cancer and embryonic but not healthy cells. THP-1 (AML), Colo-205 (colorectal cancer), MCF-7 (breast cancer) HaCaT (keratinocytes), primary human keratinocytes (Prim KC) as well as HEK293 (human embryonic kidney cells) were exposed for 24 h to 2 ng/ml human recombinant TGF- β . Levels of cell-associated Tim-3 and galectin-9 as well as secreted galectin-9 were measured. Images are from one experiment representative of four which gave similar results. Data are shown as mean values \pm SEM of four independent experiments. * - $p < 0.05$ vs control.

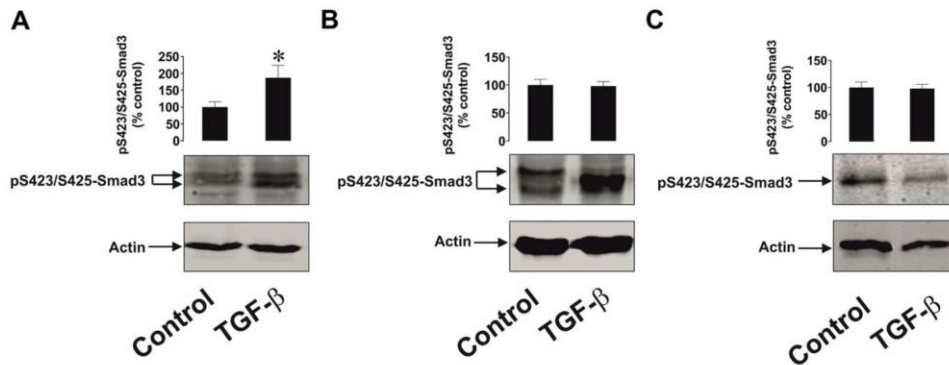


Figure 9. The effects of TGF- β on Smad3 phosphorylation in human cancer and non-malignant cells. (A) MCF-7 (breast cancer), (B) HaCaT (keratinocytes) and (C) primary human keratinocytes were exposed for 24 h to 2 ng/ml TGF- β followed by Western blot analysis of phospho-S423/S425-Smad3 levels. Images are from one experiment representative of four which gave similar results. Data are shown as mean values \pm SEM of four independent experiments. * - $p < 0.05$ vs control.

However, blocking AP-1 attenuates any HMGB1-induced increase in TGF- β and subsequent galectin-9 production. Specific activation of xanthine oxidase in MCF-7 human breast cancer cells also upregulated the level of oxidative burst, however it was not sufficient to induce HIF-1 α accumulation (Figure 6A). Despite this, TGF- β /phospho-S423/425-Smad3 and galectin-9 levels were significantly upregulated suggesting contribution of the AP-1 pathway (Figure 6B).

We also confirmed the role of HIF-1 in TGF- β expression by exposing MCF-7 breast cancer cells to CoCl₂, which inhibits degradative hydroxylation of HIF-1 α thus causing its stabilisation, leading to HIF-1 activation. Importantly, CoCl₂ is known to induce oxidative stress by increasing ROS generation which is achieved through acting on the mitochondrial transition pore [27, 28]. As a result, it leads to formation of free oxygen containing radicals which trigger ASK1-mediated AP-1 activation [22]. These experiments demonstrated the importance of HIF-1 in regulating TGF- β expression. While AP-1 is required but does not seem to control TGF- β gene expression directly, HIF-1 acts as a direct regulator. We found that CoCl₂ induced TGF- β and galectin-9 expression in wild type but not in HIF-1 α knockdown MCF-7 cells. This confirms the involvement of HIF-1 in CoCl₂-induced TGF- β expression. Interestingly, in MCF-7 cells transfected with random siRNA, TGF- β expression was upregulated, although DOTAP transfection and the presence of CoCl₂, but not TGF- β , slowed down the secretion process and galectin-9 expression was not increased, suggesting that it might depend on the autocrine activity of secreted TGF- β (Figure 7A). When studying the process in dynamics we found that CoCl₂ rapidly induces HIF-1 activation in MCF-7 cells (after 1 h of exposure, a significant increase in HIF-1 DNA-binding activity was clearly detectable, Figure 7B). Secreted TGF- β levels were significantly increased after 3-4 h of cell exposure to CoCl₂ whereas galectin-9 levels were only significantly upregulated after 6 h. This supports the notion that CoCl₂-induced galectin-9 expression depends on the autocrine activity of TGF- β , the expression of which is induced by the HIF-1 transcription complex. We specifically confirmed the role of HIF-1-induced TGF- β production in upregulating the expression of galectin-9 in MCF-7 cells. Wild type MCF-7 cells were exposed to 50 μ M CoCl₂ in the absence or presence of TGF- β -neutralising antibody or isotype control antibody (Figure 7C). Since TGF- β -neutralising antibody but not isotype control attenuated CoCl₂-induced galectin-9 expression, it demonstrates that the autocrine activity of this growth factor crucially controls the expression of galectin-9. The whole pathway includes activation of HIF-1 which upregulates TGF- β expression; TGF- β is then secreted

and displays autocrine activity leading to the induction of galectin-9 expression in MCF-7 breast cancer cells. The role of Smad3 in both TGF- β self-induced expression and production of galectin-9 was confirmed using Smad3 knockdown MCF-7 cells.

Our study further demonstrated that TGF- β induces galectin-9 expression in human AML, breast and colorectal cancer as well as embryonic cells but not in the studied healthy (non-malignant) human cells. Importantly, in healthy human cells (keratinocytes) expressing barely detectable amounts of galectin-9, TGF- β cannot induce galectin-9 expression, while if cancer cells (for example K562 chronic myeloid leukaemia cells) express only traces of galectin-9, TGF- β can induce expression of this protein (Figure 8 and Supplementary Figure 2). This is in line with previous observations suggesting differential Smad3-dependent TGF- β signalling effects in malignant and non-malignant cells [17, 29]. Our investigations further confirmed that TGF- β induces S423/S425-phosphorylation of Smad3 in the studied cancer cells but not in healthy human cells. In addition, phospho-S423/S425-Smad3 Western blot band profiles vary between malignant and non-malignant human cells (Figure 9). This suggests differential responses of the investigated malignant/embryonic and non-malignant mature human cells to TGF- β in terms of their ability to react by significantly increasing galectin-9 expression. One could hypothesise that another reason for these differences in responses could be in differential reactivity of the cells in terms of TGFBR expression or their downstream signalling. Cancer/embryonic cells may retain high levels of TGFBRs on their surface while non-transformed cells may decrease these levels in response to the presence of high levels of TGF- β in the microenvironment. Another possibility is the involvement of differential co-activator proteins recruited by Smad3 in different cell types [30]. There are two main co-activators of Smad3 – transcription intermediary factor 1-gamma (TIF-1 γ) also known as TRIM33 (tripartite motif-containing factor 33) and Smad4 [30]. Both co-activators and also some other binding partners (for example Smad2) are known to interact with Smad3 which influences the response Smad3 is going to trigger. In future work it will be important to understand which of co-activators/chaperons are involved in galectin-9 expression in different cell types.

Interestingly, in support of our observations, a previous clinical study has demonstrated that high expression levels of TGF- β receptors (TGFBRs) are associated with poor prognosis for AML patients and have a significant negative impact on complete

remission achievement and long-term survival of these patients [31].

Our observations suggest, that during early stages of tumour growth or embryonic development, when the cells pass through a low oxygen availability stage, activation of HIF-1 induces TGF- β expression. TGF- β can then display autocrine activity and induce galectin-9 expression (a summary is shown in Figure 10). At later stages, when angiogenesis addresses the issue of low oxygen availability and normalises it, TGF- β can induce its own expression through the Smad3 transcription factor. At the same time, Smad3 can induce the expression of galectin-9 (see Figure 10). Therefore, cancer and embryonic cells studied here operate a self-supporting autocrine mechanism which is a two-stage

process. During the early stage, initial TGF- β expression is, most likely, induced by the HIF-1 transcription complex and at later stages, TGF- β triggers self-expression. At both stages, TGF- β induces galectin-9 expression through the Smad3 pathway. Interestingly, TGF- β can display both tumour promoting and tumour suppressing biochemical activities [29]. However, tumour suppressive activities of the TGF- β are often avoided by tumours through acquiring mutations in critical signalling proteins or by just inhibiting TGF- β -induced anti-proliferative responses [29].

These finding demonstrate a self-supporting mechanism of galectin-9 expression operated by human AML, breast and colorectal cancer as well as embryonic cells.

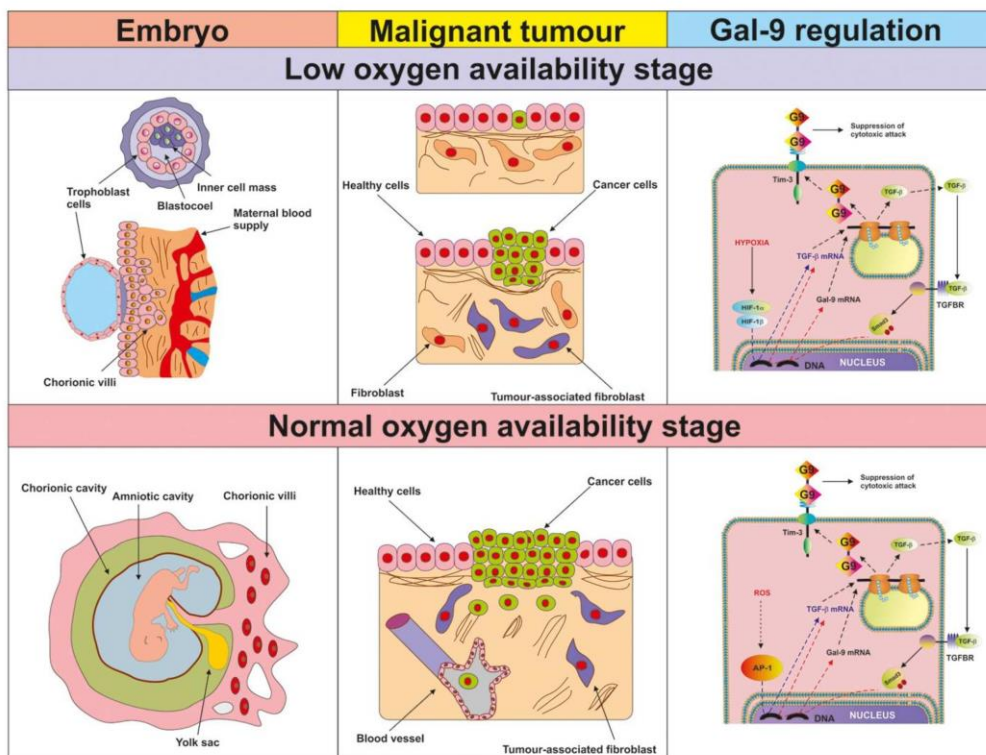


Figure 10. Proposed mechanism of the regulation of galectin-9 expression in human cancer and embryonic stage at low and normal oxygen availability stages. The figure depicts the key processes taking place in embryonic development and malignant tumour growth during the initial low oxygen availability (hypoxic) stage and later (normal oxygen availability) stages. The studied biochemical events are demonstrated in the right-hand panel. During the hypoxic stage, HIF-1 induces TGF- β expression, which then displays autocrine activity and triggers galectin-9 expression in a Smad3-dependent manner. During the normal oxygen availability stage, AP-1 contributes to TGF- β expression but it is also self-triggered by TGF- β . Galectin-9 upregulation is perpetually induced by the TGF- β -Smad3 pathway.

Our results suggest the possibility of using TGF- β signalling as a potential highly efficient target for cancer immunotherapy.

MATERIALS AND METHODS

Materials

RPMI-1640 cell culture medium, foetal bovine serum and supplements as well as basic laboratory chemicals were purchased from Sigma (Suffolk, UK). Microtitre plates for ELISA were obtained from Oxley Hughes Ltd (London, UK). Rabbit antibodies against galectin-9 and phospho-S423/S425-Smad3 as well as mouse antibody against HIF-1 α were purchased from Abcam (Cambridge, UK). Antibodies against β -actin were purchased from Abcam (Cambridge, UK) and Proteintech (Manchester, UK). Goat anti-mouse and anti-rabbit fluorescently-labelled dye secondary antibodies were obtained from Li-COR (Lincoln, Nebraska USA). ELISA-based assay kits for the detection of galectin-9, Tim-3 and TGF- β as well as human recombinant TGF- β 1 protein were purchased from Bio-Techne (R&D Systems, Abingdon, UK). Anti-Tim-3 mouse monoclonal antibody was described before [8]. All other chemicals purchased were of the highest grade of purity commercially available.

Cell lines and primary human samples

Cell lines used in this work were purchased from either the European Collection of Cell Cultures (THP-1, Colo-205 and MCF-7), the American Tissue Culture Collection (ATCC, - HEK293) or CLS Cell Lines Service GmbH (HaCaT keratinocytes). Cell lines were accompanied by identification test certificates and were grown according to corresponding tissue culture collection protocols.

Blood plasma of healthy human donors was obtained, as previously described [9], from buffy coat blood (purchased from healthy donors undergoing routine blood donation) which was bought from the National Health Blood and Transfusion Service (NHSBT, UK) following ethical approval (REC reference: 16-SS-033). Mononuclear-rich leukocytes were isolated using Ficoll-density centrifugation according to the manufacturer's protocol [9]. Cell numbers were determined using a haemocytometer and then diluted with HEPES-buffered Tyrode's solution before treatment as indicated. Primary human AML plasma samples and cells (cultured as described before) [32] were obtained from the sample bank of University Medical Centre Hamburg-Eppendorf (Ethik-Kommission der Ärztekammer Hamburg, reference: PV3469).

Primary human breast tumour tissue samples, together with paired corresponding peripheral non-transformed tissues of the same patients, were collected through surgery from breast cancer patients at the Colchester General Hospital, following informed written consent obtained before surgery [1]. Tissue specimens were visually examined by an experienced pathologist and fresh tumour tissues were selected using conventional pathologic criteria and further confirmed by subsequent histopathological examination. Normal (non-transformed) peripheral tissues (also called "normal" or "healthy" tissues and abbreviated as HT in the figures) were selected at a distance from the site of the matching primary tumour; these tissues were microscopically inspected to confirm normal histology.

Blood samples were collected before breast surgery from patients with primary breast cancer (PBC) and before treatment of patients who had metastatic breast cancer (MBC). Samples were also collected from healthy donors (individuals with no diagnosed pathology). Blood separation was performed using a buoyancy density method employing Histopaque 1119-1 (Sigma, St. Louis, MO) according to the manufacturer's protocol [1]. Ethical approval for these studies was obtained from the NRES Essex Research Ethics Committee and the Research and Innovation Department of the Colchester Hospitals University, NHS Foundation Trust [MH 363 (AM03) and 09/H0301/37].

Placental tissues (CVS, *chorionic villus sampling*) and amniotic fluids were collected after obtaining informed written consent from pregnant women at the University Hospital Bern. Cells were prepared and propagated as described before [33]. CVS was washed with PBS, treated with 270 U/ml of collagenase type 2 (Sigma, Buchs, Switzerland) for 50 min at 37° C, washed twice with PBS and cells were then re-suspended and cultured in CHANG medium (Irvine Scientific, Irvine, USA) according to the manufacturer's instructions. Amniotic fluid samples were centrifuged and cell pellets were then re-suspended in CHANG medium. The first medium change was performed after 5 days of incubation at 37° C. The medium was then changed every second day until the number of cells was sufficient.

Primary keratinocytes from cleft lip palate patients were cultured in keratinocyte medium as described previously [34]. Briefly, fresh tissue samples were placed into sterile tubes containing Dulbecco's modified Eagles medium (DMEM, Gibco/Life Technologies; Thermo Fischer Scientific, Lucerne, Switzerland) supplemented with 10% FCS. The tissue was chopped into small pieces (< 1 mm³) and placed into 6-well

plates in 800 μ l DMEM, 10% FCS, 1xAmphotericin B. In mixed cell-type outgrowths, fibroblasts were separated from keratinocytes by differential trypsinization. Keratinocytes were then cultured in keratinocyte basal serum-free medium (KSFM, Gibco), supplemented with 25 mg/ml bovine pituitary extract, 0.2 ng/ml epidermal growth factor, and CaCl_2 to a final concentration of 0.4 mM, as previously described [35]. Primary cells were tested for their purity by qPCR and immunofluorescent staining [34]. Isolation of human cells was approved by the Kantonale Ethikkommission of Bem, Switzerland, protocol number 2017-01394). Written informed consent was obtained from the parents of the children involved.

Plasmids

Plasmid encoding hemagglutinin (HA)-tagged human ASK1 with kinase-dead domain (dominant-negative form), $\Delta\text{N-ASK1}$, was a kind gift of Professor Ichijo (University of Tokyo, Tokyo, Japan). Plasmid was amplified using E. Coli XL10 Gold® (Stratagene Europe, Amsterdam, The Netherlands) and isolated/purified using the GenElute™ plasmid purification kit according to the manufacturer's protocol. Purified plasmids were transfected into THP-1 cells using DOTAP transfection reagent according to the manufacturer's protocol [24].

Transfection of HIF-1 α siRNA into MCF-7 cells

siRNA specific to HIF-1 α was selected as described previously and purchased from Sigma (Suffolk, UK) together with a mutated form of siRNA (called random siRNA, which was used as negative control) [24]. We employed a HIF-1 α -specific siRNA target sequence (ugu gag uuc gca ucu uga u dtdt) localised at position 146 bases downstream of the HIF-1 α start codon. Smad3 siRNA was a commercially available reagent purchased from Ambion (ID 107876) through Thermo Fisher Scientific. Random (mutated) siRNA used as a negative control in all the knockdown experiments had the following sequence: uac acc guu agc aga cac c dtdt. siRNAs were transfected into THP-1 cells using DOTAP transfection reagent according to the manufacturer's protocol. Successful HIF-1 α knockdown was verified by assessing HIF-1 DNA-binding activity.

Western blot analysis

Galectin-9, Tim-3, HIF-1 α and phospho-S423/S425 Smad-3 were measured by Western blot and compared to the amounts of β -actin (protein loading control), as previously described [1]. Cells were lysed in 50 mM Tris-HCl, 5 mM EDTA, 150 mM NaCl, 0.5% Nonidet-40, 1 mM PMSF, pH 8.0. Tissue lysates for Western blot

analysis were prepared as described previously. Briefly, 100 mg of frozen tissues were grounded into a powder in dry ice, followed by the addition of 100 μ l of tissue lysis buffer (20 mM Tris/HEPES pH 8.0, 2 mM EDTA, 0.5 M NaCl, 0.5% sodium deoxycholate, 0.5% Triton X-100, 0.25 M sucrose, supplemented with 50 mM 2-mercaptoethanol, 50 μ M PMSF, and 1 μ M pepstatin which was supplied just before use). Tissues were homogenised using a Polytron homogenizer (Capitol Scientific, USA) and a syringe was applied in order to acquire a homogenous tissue suspension. These tissue suspensions were then filtered through medical gauzes and centrifuged at +4° C at 10,000 g for 15 min. Proteins present in supernatants were precipitated by incubation of the samples on ice for 30 min with equal volumes of ice-cold acetone. Protein pellets were obtained by centrifugation at +4° C, 10,000 g for 15 min followed by air drying at room temperature and then mixed with the SDS-lysis buffer described above. When measuring transcription factors, cell lysis buffer described above was also applied.

Li-Cor goat secondary antibodies conjugated with infrared fluorescent dyes, were used as described in the manufacturer's protocol in order to visualise specific proteins (Li-Cor Odyssey imaging system was employed). Western blot data were quantitatively analysed using Odyssey software and values were subsequently normalised against those of β -actin or total protein loaded.

Detection of HIF-1 DNA-binding activity

HIF-1 DNA-binding activity was measured using the method similar to the one we recently described, with some modifications [36]. A 96-well Maxisorp™ microtitre plate was coated with streptavidin and blocked with BSA as described before. A volume of 2 pmol/well biotinylated 2HRE-containing oligonucleotide was immobilised by 1 h incubation at room temperature. The plate was then washed five times with TBST buffer (10 mM Tris-HCl, pH 8.0, 150 mM NaCl, 0.05% Tween-20), followed by 1 h incubation with 20 μ l/well of cell lysate at room temperature. The plate was again washed with TBST buffer and mouse anti-HIF-1 α antibody (1:1 000 in TBS with 2% BSA) was added. After 1 h of incubation at room temperature the plate was washed with TBST buffer and then incubated with 1:1 000 Li-Cor goat anti-mouse secondary antibody labelled with infrared fluorescent dye. After extensive washing with TBST, the bound secondary antibody was detected using Li-Cor fluoroimager.

Enzyme-linked immunosorbent assays (ELISAs)

Secreted TGF- β , galectin-9 and Tim-3 were measured, either in cell culture medium or in blood plasma, by

ELISA using R&D Systems kits according to manufacturer's protocols.

Detection of xanthine oxidase and NADPH oxidase activities as well as quantitation of thiobarbiturate reactive species (TBRS)

Xanthine oxidase activity was measured using a spectrophotometric assay described previously [21]. NADPH oxidase activity was measured based on the ability of this enzyme to produce superoxide anion radical [36]. TBRS were quantified using a previously described colorimetric assay [37].

Statistical analysis

Each experiment was performed at least three times and statistical analysis, when comparing two normally distributed events at a time, was conducted using a two-tailed Student's *t*-test. In cases when multiple comparisons (more than two groups) were performed, we used an ANOVA test. Post-hoc Bonferroni correction was used where applicable. Statistical probabilities (p) were expressed as * when $p < 0.05$; **, $p < 0.01$ and *** when $p < 0.001$.

AUTHOR CONTRIBUTIONS

ATHS, SS, IMY and SSS performed majority the experiments and analysed data. WF and JW isolated and provided primary AML samples used to obtain crucial data. EK and LP provided primary breast cancer samples and performed several reported experiments with these samples. BFG did the experiments with primary healthy leukocytes. MD, IS and EFK performed the reported studies on primary keratinocytes. NA, EFK and SB completed the work with primary embryonic cells. VVS designed the study, planned all the experiments together with EFK, analysed the data. VVS, EFK and BFG wrote the manuscript.

CONFLICTS OF INTEREST

The authors declare that they have no conflicts of interest.

FUNDING

This work was supported in part by the Batzebär grant (to EFK and SB). The funders had no role in study design, data collection, data analysis, interpretation, or writing of the report. We thank Diamond Light Source for access to B23 beamline (projects numbers are SM24509, SM20755 and SM21202). We are most grateful to Dr Luca Varani from the Institute for Research in Biomedicine (IRB), Bellinzona,

Switzerland for the gift of anti-Tim-3 antibody and to Prof Hidenori Ichijo from the University of Tokyo, Japan for the kind gift of the plasmid encoding hemagglutinin (HA)-tagged human ASK1 with kinase-dead domain (dominant-negative form), Δ N-ASK1.

REFERENCES

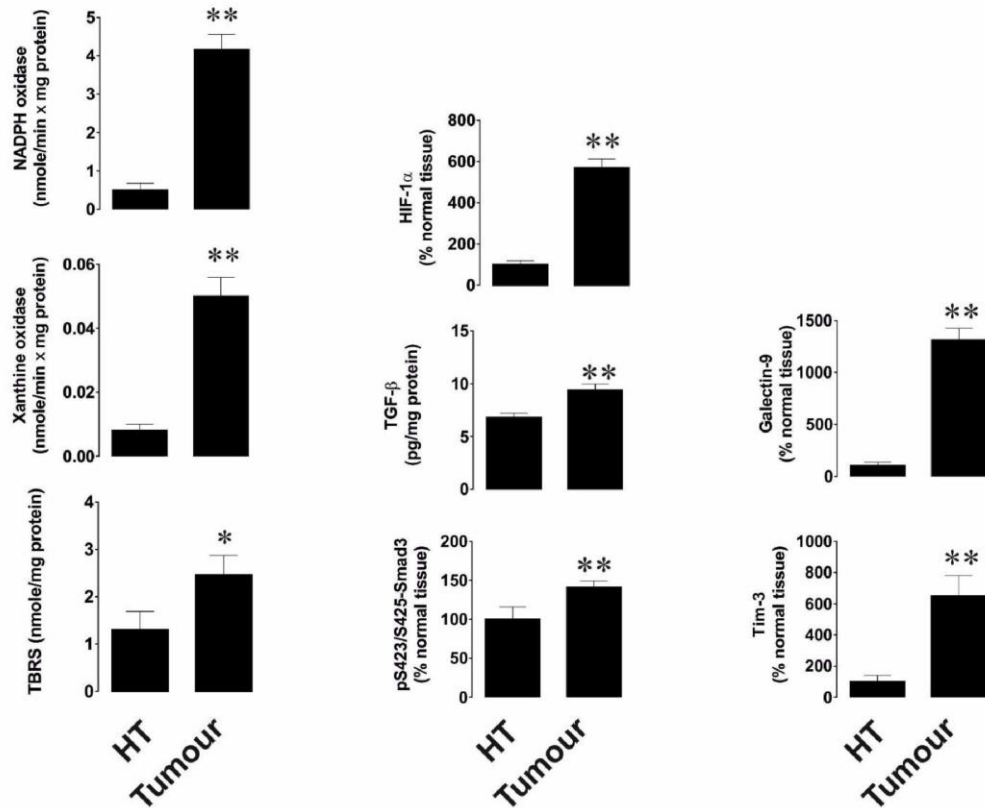
1. Yasinska IM, Sakhnevych SS, Pavlova L, Teo Hansen Selnø A, Teuscher Abeleira AM, Benlaouer O, Gonçalves Silva I, Mosimann M, Varani L, Bardelli M, Hussain R, Siligardi G, Cholewa D, et al. The Tim-3-Galectin-9 pathway and its regulatory mechanisms in human breast cancer. *Front Immunol*. 2019; 10:1594. <https://doi.org/10.3389/fimmu.2019.01594> PMID:31354733
2. Gonçalves Silva I, Yasinska IM, Sakhnevych SS, Fiedler W, Wellbrock J, Bardelli M, Varani L, Hussain R, Siligardi G, Ceccone G, Berger SM, Ushkaryov YA, Gibbs BF, et al. The Tim-3-galectin-9 secretory pathway is involved in the immune escape of human acute myeloid leukemia cells. *EBioMedicine*. 2017; 22:44–57. <https://doi.org/10.1016/j.ebiom.2017.07.018> PMID:28750861
3. Yasinska IM, Gonçalves Silva I, Sakhnevych S, Gibbs BF, Raap U, Fasler-Kan E, Sumbayev VV. Biochemical mechanisms implemented by human acute myeloid leukemia cells to suppress host immune surveillance. *Cell Mol Immunol*. 2018; 15:989–91. <https://doi.org/10.1038/s41423-018-0047-6> PMID:29872115
4. Sehrawat S, Reddy PB, Rajasagi N, Suryawanshi A, Hirashima M, Rouse BT. galectin-9/TIM-3 interaction regulates virus-specific primary and memory CD8 T cell response. *PLoS Pathog*. 2010; 6:e1000882. <https://doi.org/10.1371/journal.ppat.1000882> PMID:20463811
5. Lhuillier C, Barjon C, Niki T, Gelin A, Praz F, Morales O, Souquere S, Hirashima M, Wei M, Dellis O, Busson P. Impact of Exogenous Galectin-9 on Human T Cells: Contribution of the t cell receptor complex to antigen-independent activation but not to apoptosis induction. *J Biol Chem*. 2015; 290:16797–811. <https://doi.org/10.1074/jbc.M115.661272> PMID:25947381
6. Golden-Mason L, McMahan RH, Strong M, Reisdorph R, Mahaffey S, Palmer BE, Cheng L, Kulesza C, Hirashima M, Niki T, Rosen HR. Galectin-9 functionally impairs natural killer cells in humans and mice. *J Virol*. 2013; 87:4835–45. <https://doi.org/10.1128/JVI.01085-12> PMID:23408620
7. Gonçalves Silva I, Rüegg L, Gibbs BF, Bardelli M, Fruehwirth A, Varani L, Berger SM, Fasler-Kan E,

- Sumbayev VV. The immune receptor Tim-3 acts as a trafficker in a Tim-3/galectin-9 autocrine loop in human myeloid leukemia cells. *Oncoimmunology*. 2016; 5:e1195535.
<https://doi.org/10.1080/2162402X.2016.1195535>
PMID:27622049
8. Prokhorov A, Gibbs BF, Bardelli M, Rüegg L, Fasler-Kan E, Varani L, Sumbayev VV. The immune receptor tim-3 mediates activation of PI3 kinase/mTOR and HIF-1 pathways in human myeloid leukaemia cells. *Int J Biochem Cell Biol*. 2015; 59:11–20.
<https://doi.org/10.1016/j.biocel.2014.11.017>
PMID:25483439
 9. Gonçalves Silva I, Gibbs BF, Bardelli M, Varani L, Sumbayev VV. Differential expression and biochemical activity of the immune receptor Tim-3 in healthy and malignant human myeloid cells. *Oncotarget*. 2015; 6:33823–33.
<https://doi.org/10.18632/oncotarget.5257>
PMID:26413815
 10. Kikushige Y, Miyamoto T, Yuda J, Jabbarzadeh-Tabrizi S, Shima T, Takayanagi S, Niuro H, Yurino A, Miyawaki K, Takenaka K, Iwasaki H, Akashi K. A TIM-3/Gal-9 autocrine stimulatory loop drives self-renewal of human myeloid leukemia stem cells and leukemic progression. *Cell Stem Cell*. 2015; 17:341–52.
<https://doi.org/10.1016/j.stem.2015.07.011>
PMID:26279267
 11. Acharya N, Sabatos-Peyton C, Anderson AC. Tim-3 finds its place in the cancer immunotherapy landscape. *J Immunother Cancer*. 2020; 8:e000911.
<https://doi.org/10.1136/jitc-2020-000911>
PMID:32601081
 12. Kang CW, Dutta A, Chang LY, Mahalingam J, Lin YC, Chiang JM, Hsu CY, Huang CT, Su WT, Chu YY, Lin CY. Apoptosis of tumor infiltrating effector TIM-3+CD8+ T cells in colon cancer. *Sci Rep*. 2015; 5:15659.
<https://doi.org/10.1038/srep15659> PMID:26493689
 13. Kashio Y, Nakamura K, Abedin MJ, Seki M, Nishi N, Yoshida N, Nakamura T, Hirashima M. Galectin-9 induces apoptosis through the calcium-calpain-caspase-1 pathway. *J Immunol*. 2003; 170:3631–36.
<https://doi.org/10.4049/jimmunol.170.7.3631>
PMID:12646627
 14. Heusschen R, Griffioen AW, Thijssen VL. Galectin-9 in tumor biology: a jack of multiple trades. *Biochim Biophys Acta*. 2013; 1836:177–85.
<https://doi.org/10.1016/j.bbcan.2013.04.006>
PMID:23648450
 15. Kim SJ, Angel P, Lafyatis R, Hattori K, Kim KY, Sporn MB, Karin M, Roberts AB. Autoinduction of transforming growth factor beta 1 is mediated by the AP-1 complex. *Mol Cell Biol*. 1990; 10:1492–97.
<https://doi.org/10.1128/mcb.10.4.1492> PMID:2108318
 16. Duan D, Derynck R. Transforming growth factor- β (TGF- β)-induced up-regulation of TGF- β receptors at the cell surface amplifies the TGF- β response. *J Biol Chem*. 2019; 294:8490–504.
<https://doi.org/10.1074/jbc.RA118.005763>
PMID:30948511
 17. Brown KA, Ham AJ, Clark CN, Meller N, Law BK, Chytil A, Cheng N, Pietenpol JA, Moses HL. Identification of novel Smad2 and Smad3 associated proteins in response to TGF-beta1. *J Cell Biochem*. 2008; 105:596–611.
<https://doi.org/10.1002/jcb.21860> PMID:18729074
 18. Massagué J, Seoane J, Wotton D. Smad transcription factors. *Genes Dev*. 2005; 19:2783–810.
<https://doi.org/10.1101/gad.1350705>
PMID:16322555
 19. Wu C, Thalhamer T, Franca RF, Xiao S, Wang C, Hotta C, Zhu C, Hirashima M, Anderson AC, Kuchroo VK. Galectin-9-CD44 interaction enhances stability and function of adaptive regulatory T cells. *Immunity*. 2014; 41:270–82.
<https://doi.org/10.1016/j.immuni.2014.06.011>
PMID:25065622
 20. Sumbayev VV, Nicholas SA. Hypoxia-inducible factor 1 as one of the “signaling drivers” of toll-like receptor-dependent and allergic inflammation. *Arch Immunol Ther Exp (Warsz)*. 2010; 58:287–94.
<https://doi.org/10.1007/s00005-010-0083-0>
PMID:20502970
 21. Aboali M, Lall GS, Coughlan K, Lall HS, Gibbs BF, Sumbayev VV. Crucial involvement of xanthine oxidase in the intracellular signalling networks associated with human myeloid cell function. *Sci Rep*. 2014; 4:6307.
<https://doi.org/10.1038/srep06307> PMID:25200751
 22. Sumbayev VV, Yasinska IM. Regulation of MAP kinase-dependent apoptotic pathway: implication of reactive oxygen and nitrogen species. *Arch Biochem Biophys*. 2005; 436:406–12.
<https://doi.org/10.1016/j.abb.2005.02.021>
PMID:15797253
 23. Manzo G. Similarities between embryo development and cancer process suggest new strategies for research and therapy of tumors: a new point of view. *Front Cell Dev Biol*. 2019; 7:20.
<https://doi.org/10.3389/fcell.2019.00020>
PMID:30899759
 24. Nicholas SA, Sumbayev VV. The involvement of hypoxia-inducible factor 1 alpha in toll-like receptor 7/8-mediated inflammatory response. *Cell Res*. 2009; 19:973–83.

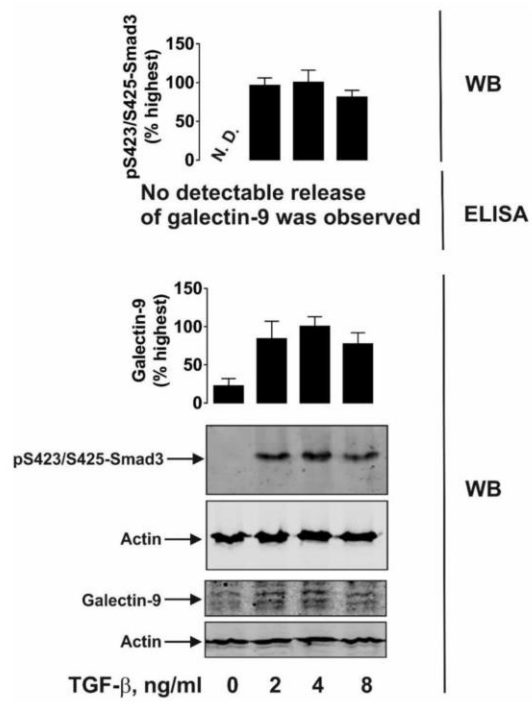
- <https://doi.org/10.1038/cr.2009.44>
PMID:19381167
25. Birchenall-Roberts MC, Ruscetti FW, Kasper J, Lee HD, Friedman R, Geiser A, Sporn MB, Roberts AB, Kim SJ. Transcriptional regulation of the transforming growth factor beta 1 promoter by v-src gene products is mediated through the AP-1 complex. *Mol Cell Biol.* 1990; 10:4978–83.
<https://doi.org/10.1128/mcb.10.9.4978>
PMID:2117705
26. Yasinska IM, Gonçalves Silva I, Sakhnevych SS, Ruegg L, Hussain R, Siligardi G, Fiedler W, Wellbrock J, Bardelli M, Varani L, Raap U, Berger S, Gibbs BF, et al. High mobility group box 1 (HMGB1) acts as an "alarmin" to promote acute myeloid leukaemia progression. *Oncoimmunology.* 2018; 7:e1438109.
<https://doi.org/10.1080/2162402X.2018.1438109>
PMID:29872582
27. Battaglia V, Compagnone A, Bandino A, Bragadin M, Rossi CA, Zanetti F, Colombatto S, Grillo MA, Toninello A. Cobalt induces oxidative stress in isolated liver mitochondria responsible for permeability transition and intrinsic apoptosis in hepatocyte primary cultures. *Int J Biochem Cell Biol.* 2009; 41:586–94.
<https://doi.org/10.1016/j.biocel.2008.07.012>
PMID:18708157
28. Stenger C, Naves T, Verdier M, Ratinaud MH. The cell death response to the ROS inducer, cobalt chloride, in neuroblastoma cell lines according to p53 status. *Int J Oncol.* 2011; 39:601–09.
<https://doi.org/10.3892/ijo.2011.1083> PMID:21687937
29. Kubiczkova L, Sedlarikova L, Hajek R, Sevcikova S. TGF- β - an excellent servant but a bad master. *J Transl Med.* 2012; 10:183.
<https://doi.org/10.1186/1479-5876-10-183>
PMID:22943793
30. He W, Dorn DC, Erdjument-Bromage H, Tempst P, Moore MA, Massagué J. Hematopoiesis controlled by distinct TGF β and Smad4 branches of the TGF β pathway. *Cell.* 2006; 125:929–41.
<https://doi.org/10.1016/j.cell.2006.03.045>
PMID:16751102
31. Otten J, Schmitz L, Vettorazzi E, Schultze A, Marx AH, Simon R, Krauter J, Loges S, Sauter G, Bokemeyer C, Fiedler W. Expression of TGF- β receptor ALK-5 has a negative impact on outcome of patients with acute myeloid leukemia. *Leukemia.* 2011; 25:375–79.
<https://doi.org/10.1038/leu.2010.273>
PMID:21304536
32. Yasinska IM, Ceccone G, Ojea-Jimenez I, Ponti J, Hussain R, Siligardi G, Berger SM, Fasler-Kan E, Bardelli M, Varani L, Fiedler W, Wellbrock J, Raap U, et al. Highly specific targeting of human acute myeloid leukaemia cells using pharmacologically active nanoconjugates. *Nanoscale.* 2018; 10:5827–5833.
<https://doi.org/10.1039/c7nr09436a>
PMID:29538473
33. The AGT Cytogenetics Laboratory Manual. Third edition. Editors: Barch MJ, Knutsen T, Spurbeck J. Lippincott Publishe, 1997, ISBN: 0-397-51651-7.
34. Degen M, Wiederkehr A, La Scala GC, Carmann C, Schnyder I, Katsaros C. Keratinocytes isolated from individual cleft Lip/palate patients display variations in their differentiation potential in vitro. *Front Physiol.* 2018; 9:1703.
<https://doi.org/10.3389/fphys.2018.01703>
PMID:30555344
35. Degen M, Natarajan E, Barron P, Widlund HR, Rheinwald JG. MAPK/ERK-dependent translation factor hyperactivation and dysregulated laminin γ 2 expression in oral dysplasia and squamous cell carcinoma. *Am J Pathol.* 2012; 180:2462–78.
<https://doi.org/10.1016/j.ajpath.2012.02.028>
PMID:22546478
36. Vokurková M, Rauchová H, Řezáčová L, Vaněčková I, Zicha J. NADPH oxidase activity and reactive oxygen species production in brain and kidney of adult male hypertensive Ren-2 transgenic rats. *Physiol Res.* 2015; 64:849–56.
<https://doi.org/10.33549/physiolres.933254>
PMID:26713567
37. Nicholas SA, Bubnov VV, Yasinska IM, Sumbayev VV. Involvement of xanthine oxidase and hypoxia-inducible factor 1 in toll-like receptor 7/8-mediated activation of caspase 1 and interleukin-1 β . *Cell Mol Life Sci.* 2011; 68:151–58.
<https://doi.org/10.1007/s00018-010-0450-3>
PMID:20632067

SUPPLEMENTARY MATERIALS

Supplementary Figures



Supplementary Figure 1. Values presented in Figure 1 normalised against total protein loaded for Western blot data and per 1 mg of total tissue protein for enzyme activity and TBRS assays. Data are shown as mean values \pm SEM of five independent experiments. * - $p < 0.05$ and ** - $p < 0.01$ vs non-transformed peripheral tissue abbreviated as HT (healthy tissue).



Supplementary Figure 2. TGF- β induces galectin-9 expression in K562 human cancer cells. K562 human chronic myeloid leukaemia cells were exposed for 24 h to 2, 4 or 8 ng/ml TGF- β followed by detection of phospho-S423/S425-Smad3 and galectin-9 expression by Western blot. Galectin-9 release was analysed by ELISA. Images are from one experiment representative of three which gave similar results. Data are shown as mean values \pm SEM of three independent experiments.



High Mobility Group Box 1 (HMGB1) Induces Toll-Like Receptor 4-Mediated Production of the Immunosuppressive Protein Galectin-9 in Human Cancer Cells

OPEN ACCESS

Edited by:

Brian J. Czerniecki,
Moffitt Cancer Center, United States

Reviewed by:

Hai Huang,
The Ohio State University,
United States
Nabiha Yusuf,
University of Alabama at Birmingham,
United States

*Correspondence:

Bernhard F. Gibbs
bernhard.gibbs@uni-oldenburg.de
Elizaveta Faslser-Kan
elizaveta.faslser@insel.ch
Vadim V. Sumbayev
V.Sumbayev@kent.ac.uk

[†]These authors have contributed
equally to this work

Specialty section:

This article was submitted to
Cancer Immunity and Immunotherapy,
a section of the journal
Frontiers in Immunology

Received: 03 March 2021

Accepted: 27 May 2021

Published: 21 June 2021

Citation:

Teo Hansen Selno A, Schlichtner S,
Yasinska IM, Sakhnevych SS,
Fiedler W, Wellbrock J, Berger SM,
Klenova E, Gibbs BF, Faslser-Kan E
and Sumbayev VV (2021) High Mobility
Group Box 1 (HMGB1) Induces Toll-
Like Receptor 4-Mediated Production
of the Immunosuppressive Protein
Galectin-9 in Human Cancer Cells.
Front. Immunol. 12:675731.
doi: 10.3389/fimmu.2021.675731

Anette Teo Hansen Selno^{1†}, Stephanie Schlichtner^{1†}, Inna M. Yasinska^{1†},
Svetlana S. Sakhnevych^{1†}, Walter Fiedler², Jasmin Wellbrock², Steffen M. Berger^{3,4},
Elena Klenova⁵, Bernhard F. Gibbs^{1,6*}, Elizaveta Faslser-Kan^{3,7*} and Vadim V. Sumbayev^{1*}

¹Medway School of Pharmacy, Universities of Kent and Greenwich, Chatham Maritime, United Kingdom, ²Department of Oncology, Hematology and Bone Marrow Transplantation With Section Pneumology, Hubertus Wald University Cancer Center, University Medical Center Hamburg-Eppendorf, Hamburg, Germany, ³Department of Pediatric Surgery, Department of Biomedical Research, Children's Hospital, Inselspital, University of Bern, Bern, Switzerland, ⁴Department of Biomedical Research, University of Bern, Bern, Switzerland, ⁵School of Biological Sciences, University of Essex, Colchester, United Kingdom, ⁶Division of Experimental Allergy and Immunodermatology, University of Oldenburg, Oldenburg, Germany, ⁷Department of Biomedicine, University of Basel and University Hospital Basel, Basel, Switzerland

High mobility group box 1 (HMGB1) is a non-histone protein which is predominantly localised in the cell nucleus. However, stressed, dying, injured or dead cells can release this protein into the extracellular matrix passively. In addition, HMGB1 release was observed in cancer and immune cells where this process can be triggered by various endogenous as well as exogenous stimuli. Importantly, released HMGB1 acts as a so-called “danger signal” and could impact on the ability of cancer cells to escape host immune surveillance. However, the molecular mechanisms underlying the functional role of HMGB1 in determining the capability of human cancer cells to evade immune attack remain unclear. Here we report that the involvement of HMGB1 in anti-cancer immune evasion is determined by Toll-like receptor (TLR) 4, which recognises HMGB1 as a ligand. We found that HGMB1 induces TLR4-mediated production of transforming growth factor beta type 1 (TGF- β), displaying autocrine/paracrine activities. TGF- β induces production of the immunosuppressive protein galectin-9 in cancer cells. In TLR4-positive cancer cells, HMGB1 triggers the formation of an autocrine loop which induces galectin-9 expression. In malignant cells lacking TLR4, the same effect could be triggered by HMGB1 indirectly through TLR4-expressing myeloid cells present in the tumour microenvironment (e. g. tumour-associated macrophages).

Keywords: galectin-9, TGF-beta 1, HMGB1 (high mobility group box 1), immune surveillance, Toll-like receptors

INTRODUCTION

High mobility group box 1 (HMGB1) is a non-histone protein predominantly localised in the cell nucleus where it promotes nuclear transcription processes by interacting with DNA (1–4). However, HMGB1 can be passively released into the extracellular matrix by dead, dying or injured cells (1–4). It can also be secreted by cancer and immune cells in response to various exogenous or endogenous stimuli (1–4). Secreted HMGB1 acts as a “danger signal” or “alarmin” which may also trigger malignant tumour progression (1–4). We have recently reported that HMGB1 promotes the generation and secretion of interleukin-1beta (IL-1 β), which induces production of stem cell factor (SCF) by competent cells (5, 6). As such, it could facilitate progression of malignancies such as acute myeloid leukaemia (AML) (6–8).

HMGB1 was reported to act as a ligand for various immune receptors including toll-like receptors (TLRs) 2 and 4, which normally recognise pathogen-associated molecular patterns shared by Gram-negative and Gram-positive bacteria respectively (6). HMGB1 receptors also include receptor of advanced glycation end products (RAGE) and the immune receptor Tim-3 (T cell immunoglobulin and mucin domain containing protein 3) (4, 6). Through these receptors HMGB1 in its immunogenic form could trigger both pro-inflammatory and pro-angiogenic responses (6). Our recent work also suggested that, in Toll-like receptor 4 (TLR4)-expressing cells, HMGB1 induces the production and secretion of transforming growth factor beta type 1 (TGF- β) (9). TGF- β displays both autocrine and paracrine activities and, through the transcription factor Smad3, induces expression of galectin-9, an immunosuppressive protein which impairs the anti-cancer activities of natural killer and cytotoxic T cells (9, 10). Galectin-9 is known as a so-called “tandem protein” which contains two ligand/sugar-binding domains fused together by a linker peptide. As a result of alternative splicing, galectin-9 may be present in three main isoforms which differ because of the length of their linker peptide: long (49 amino acids), medium (27 amino acids) and short (15 amino acids) isoforms (11–13).

Currently, the molecular mechanisms underlying the role of the immunogenic form of HMGB1 in determining the capability of human cancer cells to escape host immune surveillance remain unclear. We hypothesised that HMGB1 could upregulate galectin-9 expression in cancer cells through the activation of TGF- β production induced in a TLR4-dependent manner. Here we report for the first time that the role of HMGB1 in anti-cancer immune evasion is determined by the TLR4. Cancer cells expressing TLR4 release TGF- β in response to stimulation with HMGB1 followed by TGF- β -induced upregulation of galectin-9 expression, forming such an HMGB1-triggered autocrine loop. Galectin-9 expression in cancer cells lacking functional TLR4 could still be triggered by HMGB1 indirectly *via* induction of TGF- β expression in TLR4-positive myeloid cells (e.g. tumour-associated macrophages) present in the tumour microenvironment. Importantly, other

HMGB1 receptors did not demonstrate any involvement in the process of induction of TGF- β expression by this danger signal and its follow-up events.

MATERIALS AND METHODS

Materials

RPMI-1640 medium for culturing the cells, foetal bovine serum, supplements and basic laboratory chemicals were purchased from Sigma (Suffolk, UK). Microtiter plates for ELISA were obtained from Oxley Hughes Ltd (London, UK). Rabbit antibodies against galectin-9, RAGE and phospho-S423/S425-Smad3 as well as mouse antibodies against TLRs 2 and 4 were purchased from Abcam (Cambridge, UK). Antibodies against β -actin were purchased from Abcam (Cambridge, UK) and Proteintech (Manchester, UK). Goat anti-mouse and anti-rabbit fluorescently-labelled dye secondary antibodies were obtained from Li-COR (Lincoln, Nebraska USA). ELISA-based assay kits for the detection of galectin-9, Tim-3 and TGF- β as well as human recombinant TGF- β 1 protein were purchased from Bio-Techne (R&D Systems, Abingdon, UK). ELISA kits for the detection of HMGB1 were purchased from MyBioSource (San Diego, CA, USA). Human HMGB1 and anti-Tim-3 mouse monoclonal antibody were described before (6, 14). All other chemicals purchased were of the highest grade of purity commercially available.

Cell Lines and Primary Human Samples

Cell lines used in this work were purchased from either the European Collection of Cell Cultures (THP-1, Colo-205 and MCF-7) or the American Tissue Culture Collection (ATCC – HEK293). Cell lines were accompanied by identification test certificates and were grown according to corresponding tissue culture collection protocols.

For description of primary cells (9, 15–17) please see the Ethics statement.

Plasmids

Plasmid encoding constitutively active human TLR4 (murine CD4 fused to human TLR4) (18) was generously provided by Professor Medzhitov (Yale University, New Haven, USA).

Cell Transfection

mCD-hTLR4 expression plasmid or empty expression vector were transfected into Colo 205 cells using DOTAP transfection reagent according to the manufacturer’s protocol.

Western Blot Analysis

Galectin-9, Tim-3, phospho-S423/S425 Smad-3, RAGE, TLRs 2 and 4 were measured by Western blot and compared to the amounts of β -actin (protein loading control), as previously described (18).

Li-Cor goat secondary antibodies conjugated with infrared fluorescent dyes, were used as described in the manufacturer’s protocol in order to visualise specific proteins (Li-Cor Odyssey

imaging system was employed). Western blot data were quantitatively analysed using Odyssey software and values were subsequently normalised against those of β -actin or total protein loaded.

Enzyme-Linked Immunosorbent Assays (ELISAs)

Secreted HMGB1, TGF- β , galectin-9 and Tim-3 were measured, either in cell culture medium or in blood plasma (galectin-9 was also measured in some of the cell lysates), by ELISA using MyBioSource or R&D Systems kits (see *Materials* section) according to manufacturer's protocols.

Design of Nanocomplexes For Immunoprecipitation Containing Anti-HMGB1 and Anti-TGF- β Antibodies

Nanoconjugates (nanocomplexes) were designed using 30 nm gold nanoparticles (AuNPs). The synthesis of 30 nm AuNPs was performed essentially as described previously (16, 19). Briefly, 5 ml of aqueous gold (III) chloride trihydrate (10 mM) and 2.5 ml of aqueous sodium citrate (100 mM) were added to 95 ml of MilliQ-water in a round bottom flask supplied with a magnetic stirrer, and the resulting pale-yellow solution was allowed to cool to 1–2°C. Under vigorous stirring, 1 ml of chilled (4°C) aqueous 0.1 M sodium borohydride was added and the dark red solution obtained was then stirred for further 10 min in an ice bath before being allowed to warm to room temperature. The obtained AuNPs were characterised using transmission electron microscopy (TEM) as previously described (16, 20). TEM image of the AuNP is presented in the **Supplementary Figure 1**. Antibody molecules were attached as described before in the ratio of 1 AuNP: 6 antibody molecules in both cases. A sample scheme of the nanoconjugate and its action are presented in **Supplementary Figure 2**. Briefly, the antibody (biotinylated anti-HMGB1 or anti-TGF- β) was coupled to 30 nm AuNPs using glutathione (GSH, tripeptide containing γ -glutamate, cysteine-SH and glycine) as a linker. A 0.05 M solution of GSH was incubated for 2 h at room temperature with a 1 : 1 mixture of aqueous solutions of 0.4 M 1-ethyl-3-(3-dimethylpropyl)-carbodiimide (EDC) and 0.1 M N-hydroxysuccinimide (NHS) to allow the activation of GSH –COOH groups, thus enabling them to interact with antibody amino groups. Activated GSH was then mixed with an antibody in an equimolar ratio and incubated for at least 2 h at 37°C. The antibody was then mixed with 30 nm AuNPs (0.5 mM) at a ratio of 1 AuNP: 6 antibody molecules. This mixture was incubated for at least 18 h at room temperature.

The available amount of AuNPs was calculated using the following equations:

$$N_{AuNP} = m_{totalAu} / m_{AuNP} (m = mass; N = quantity);$$

$$m_{totalAu} = C_{Au} (mol \times l^{-1}) \times MW_{Au} (g \times mol^{-1}) \times V_{AuNP}$$

$$(C = molar concentration, MW = molecular weight, V_{AuNP} = the volume of the AuNP suspension used);$$

$$m_{1AuNP} = \rho_{Au} \times V_{1AuNP}; (\rho = density, V = volume; \rho_{Au} = 19.3 g cm^{-3});$$

$$V_{1AuNP} = 4/3 \pi R^3; (R = radius of a AuNP)$$

$$R = d_{1AuNP} / 2; (d = diameter of 1 AuNP expressed in cm)$$

The amount of antibody molecules was calculated from the molar weight of the antibodies ($150,000 g \times mol^{-1}$) and the Avogadro constant so that 1 mole of an antibody contained 6.02×10^{23} antibody molecules.

In order to confirm successful conjugation of antibodies to the nanoparticles we used the following approaches.

Anti-HMGB1 antibody-conjugated and naked (control) AuNPs were exposed to HRP-conjugated streptavidin for 30 min followed by precipitation by centrifugation (16). Nanomaterials were washed three times with bi-distilled water and exposed for 2 min exposure to 6 mg/ml o-Phenylenediamine (OPD) in the presence of hydrogen peroxide. The reaction was stopped using 10% sulfuric acid. Nanomaterials were precipitated by centrifugation (16) and the absorbance of supernatants was analysed at 492 nm (**Supplementary Figure 3**).

Mouse anti-human TGF- β 1-conjugated AuNPs were exposed for 1 h to anti-mouse or anti-rabbit (control) fluorescent dye-labelled Li-Cor secondary antibodies. nanomaterials were then precipitated by centrifugation (16), washed three times with bi-distilled water and analysed using Li-Cor Odyssey C_{LX} imager (**Supplementary Figure 4**).

Statistical Analysis

Each experiment was performed at least three times and statistical analysis, when comparing two normally distributed events at a time, was conducted using a two-tailed Student's *t*-test. In cases when multiple comparisons (more than two groups) were performed, we used an ANOVA test. Post-hoc Bonferroni correction was used where applicable. Statistical probabilities (p) were expressed as * when $p < 0.05$; **, $p < 0.01$ and *** when $p < 0.001$.

RESULTS

Firstly, we investigated human monocytic AML THP-1 cells and exposed them for 24 h to 1 μ g/ml of immunogenic form of human recombinant HMGB1 (6). We found that exposure to HMGB1 upregulated TGF- β secretion, which subsequently triggered Smad3 phosphorylation (**Figure 1A**). This led to a substantial increase in galectin-9 secretion and reduced levels of total cell-associated and cell surface-based galectin-9 (**Figures 1B, C**). Overall, an increase in total amounts of galectin-9 produced by THP-1 cells was observed and also confirmed by measuring the total quantities of galectin-9 present in cell lysates and secreted protein in cell culture medium by ELISA. Resting cells produced $890 \pm 48 pg/10^6$ cells galectin-9 in total and this rose to 2110 ± 93

pg/10⁶ cells in HMGB1-treated cells. The reduction in cell surface galectin-9 expression suggests its proteolytic shedding off the cell surface together with Tim-3 (which acts both as a receptor and possible trafficker for galectin-9) (21). An increase in Tim-3 secretion was also observed (Figure 1D), which is known to be governed by proteolytic shedding triggered by TLR4 signalling (22). THP-1 cells express four HMGB1 receptors (6) – TLRs 2 and 4, receptor of advanced glycation end products (RAGE) and Tim-3 (Supplementary Figure 5). To confirm the role of the TLRs 2 and 4 in observed responses we studied primary human AML cells obtained from newly diagnosed patients. We selected patients where AML cells expressed Tim-3 and RAGE, but did not express (as determined by Western blotting) detectable amounts of TLRs 2 and 4 proteins, and exposed these AML cells to 2.5 µg/ml HMGB1 for 16 h. None of the effects observed in THP-1 cells were detected in these primary AML cells (Figure 2). These results suggest that TLRs and not RAGE or Tim-3 are mediating HMGB1-induced TGF-β secretion and follow-up events.

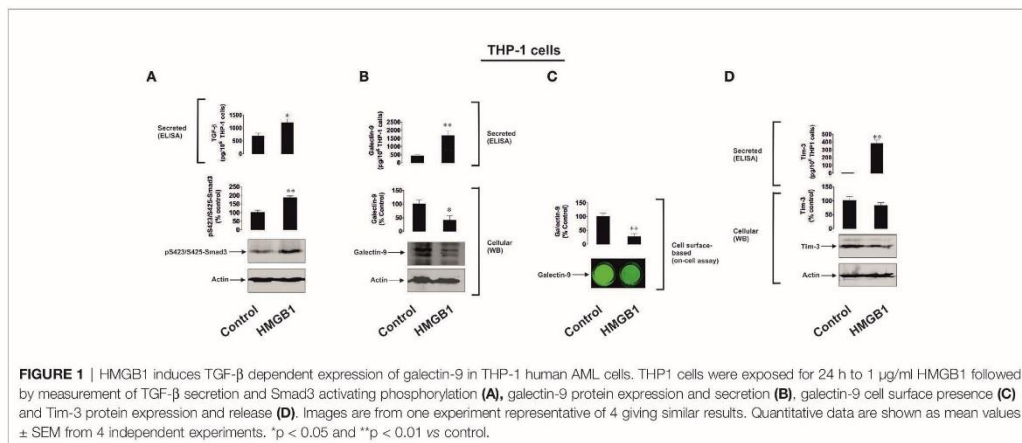
Interestingly, primary human AML cells expressing TLR4 responded to 16 h exposure to 2.5 µg/ml HMGB1 in a similar manner to that observed for THP-1 cells – where the secretion of both galectin-9 and Tim-3 was significantly upregulated (Supplementary Figure 6).

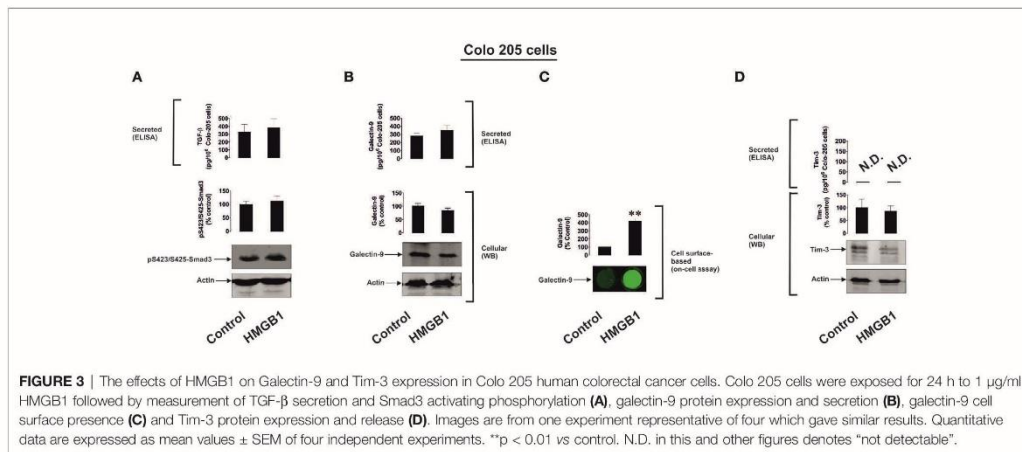
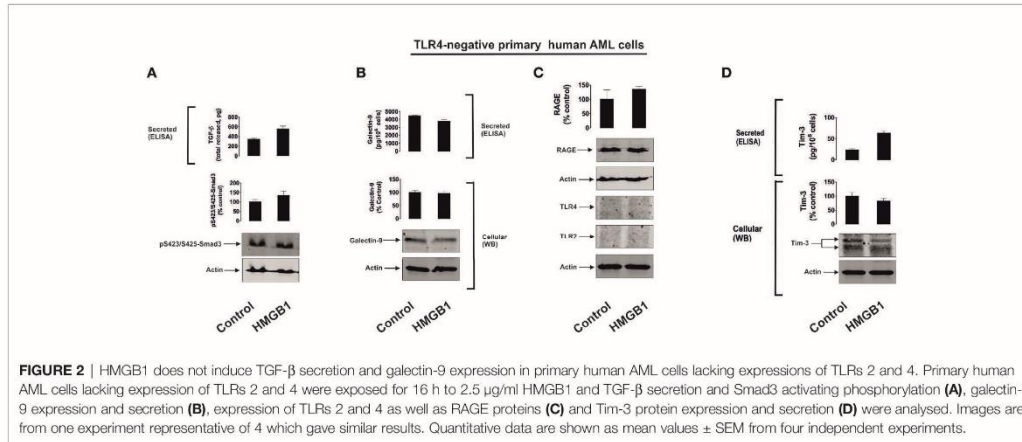
To further investigate the differential roles of TLRs 2 and 4 in the observed effects of HMGB1, we studied human colorectal cancer cells (Colo 205), human breast cancer cells (MCF-7) and human embryonic kidney cells (HEK293). Colo 205 expressed TLR2, RAGE and Tim-3, whereas the other cell types investigated expressed RAGE and Tim-3, but not the other HMGB1 receptors – TLR4 and TLR2 (Supplementary Figure 5). Of all the different cell types investigated, upregulation of galectin-9 translocation onto the cell surface was only observed in Colo 205 cells (these cells express TLR2) upon exposure to 1 µg/ml HMGB1 for 24 h, but neither total galectin-9 levels nor its secretion were upregulated in these cells (Figure 3). Other effects which were observed in THP-1 cells, e.g.

activation of TGF-β production, Smad-3 phosphorylation and upregulated Tim-3 secretion, were undetectable in Colo 205 cells (Figure 3). In other cell types – MCF-7 (Figure 4) and HEK293 (Figure 5) HMGB1 did not trigger any changes observed in THP-1 cells. Taken together, these results suggest that TLR4 mediates HMGB1-induced TGF-β production followed by its autocrine and paracrine effects.

We then tested if naturally occurring, dying cell-derived HMGB1 can induce similar effects in TLR4 expressing cells. We exposed several types of human cancer cell lines (THP-1, Colo 205 and MCF-7) for 24 h to 100 µM BH3I-1 (5-[(4-bromophenyl)methylene]-a-(1-methylethyl)-4-oxo-2-thioxo-3-thiazolidineacetic acid), which is a synthetic cell-permeable Bcl-XL antagonist that induces apoptosis (by inhibiting the interactions between the BH3 domain and Bcl-XL thus defunctionalising mitochondria) (23). We found that upon stimulation with BH3I-1 THP-1 released the highest amounts of HMGB1 (Supplementary Figure 7). To confirm the physiological relevance of this observation, we compared HMGB1 levels in the blood plasma of healthy donors, primary breast cancer patients (a solid tumour where HMGB1 release was assessed in breast cancer-derived MCF-7 cell lines) and AML patients (a “liquid” tumour which was also tested using the THP-1 cell line). We tested the blood plasma of 5 healthy donors, 5 AML patients and 5 patients with primary breast cancer. Here, we observed that AML patients had significantly higher levels of HMGB1 in their blood plasma compared to healthy donors and primary breast cancer patients (Figure 6). These results suggest that in the studied solid tumours HMGB1, if released, most likely stays within the tumour microenvironment.

Given the results described above, THP-1 monocytic cells were chosen to act as HMGB1 releasers and were exposed to 1 mM hydrogen peroxide for 24 h and released 13.14 ± 0.37 ng/ml HMGB1 (Figure 7A). We used this medium (H₂O₂ was degraded using 5 mg/ml horseradish peroxidase) to treat THP-1 cells, which were pre-treated for 24 h with 100 nM

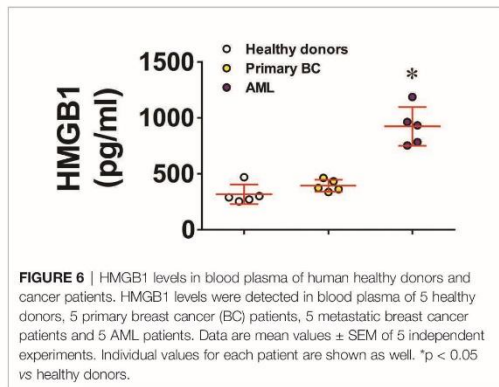
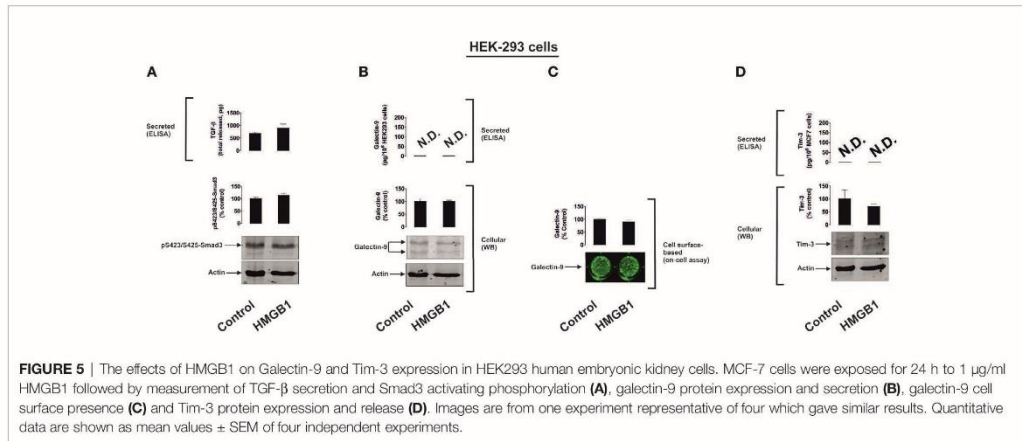
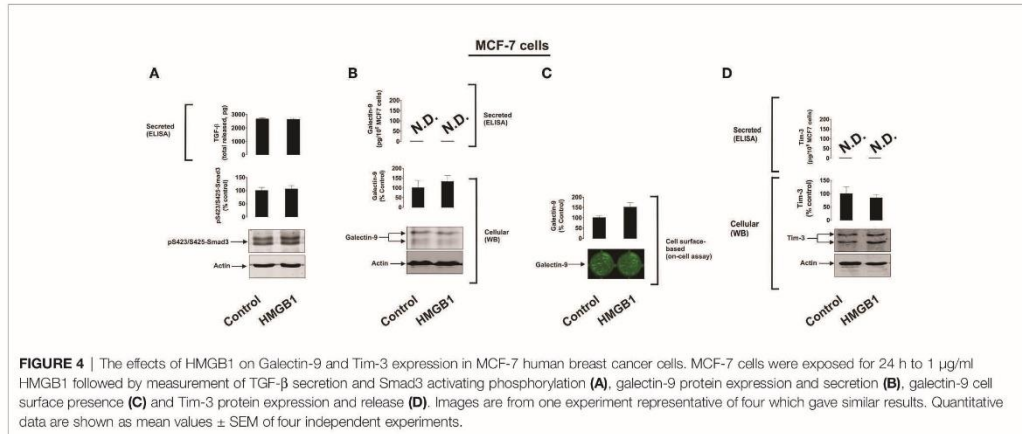




phorbol 12-myristate 13-acetate (PMA), in order to differentiate them into macrophages which express high levels of TLR4 (24). As a control, we exposed PMA-pre-treated THP-1 cells to the same medium but depleted from HMGB1 by immunoprecipitating HMGB1 using nanoconjugates (NCJ, 30 nm gold nanoparticles carrying antibodies against HMGB1) as outlined in Materials and Methods. We found that HMGB1-containing medium led to the production of *ca.* 15 ng/ml TGF- β . This result suggests that naturally produced cell-derived HMGB1 displays higher biological activity than the recombinant protein. The effect was not observed in the cells treated with medium where HMGB1 was removed (Figure 7A). TGF- β -containing medium was then used to treat MCF-7 human breast cancer cells. As a control, we exposed MCF-7 cells to the same medium where TGF- β was immunoprecipitated

using NCJ (30 nm gold nanoparticles carrying antibody against TGF- β) as described in Materials and Methods. We found that TGF- β -containing medium significantly upregulated galectin-9 levels in MCF-7 cells (Figure 7A).

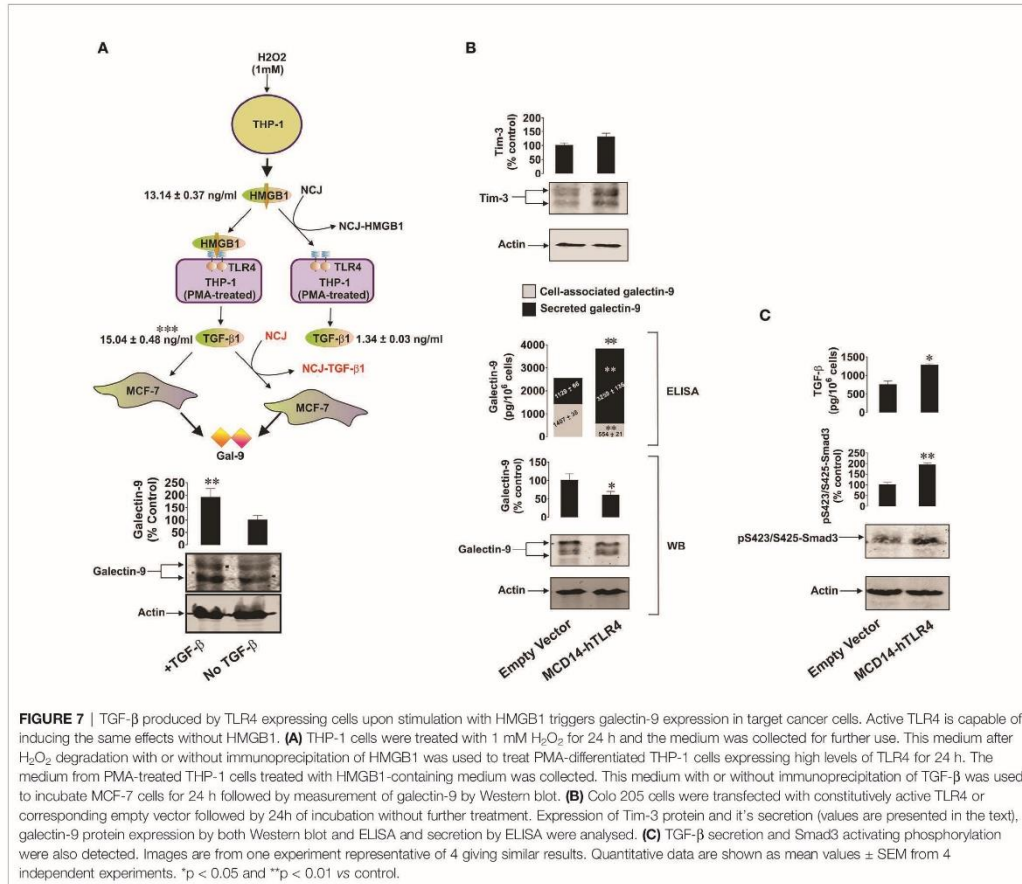
We then sought to further confirm the ability of the TLR4 to mediate the observed effects. For this purpose we transfected Colo 205 cells, where we could not detect TLR4 protein by Western blot (Supplementary Figure 5), with constitutively active TLR4 (mCD4-hTLR4, the construct which consists of the human transmembrane and intracellular domains of TLR4 fused to the extracellular domain of mouse CD4, kindly provided by Prof Ruslan Medzhitov, Yale University, USA) (18). The presence of mCD4-hTLR4 resulted in the upregulation of galectin-9 secretion and reduced its cell-associated levels. We additionally measured cell-associated galectin-9 by ELISA and



observed that it was significantly downregulated in the cells transfected with mCD4-hTLR4, while total galectin-9 levels (secreted + cell-associated) were significantly upregulated in mCD4-hTLR4-transfected cells (Figure 7B). Tim-3 secretion of $95 \pm 9 \text{ pg}/10^6 \text{ cells}$ was also observed in the presence of mCD4-hTLR4 (Figure 7B) while in the cells which did not contain mCD4-hTLR4 it was undetectable. Furthermore, mCD4-hTLR4 upregulated TGF-β secretion, which led to the upregulation of activating Smad3 phosphorylation in these cells (Figure 7C).

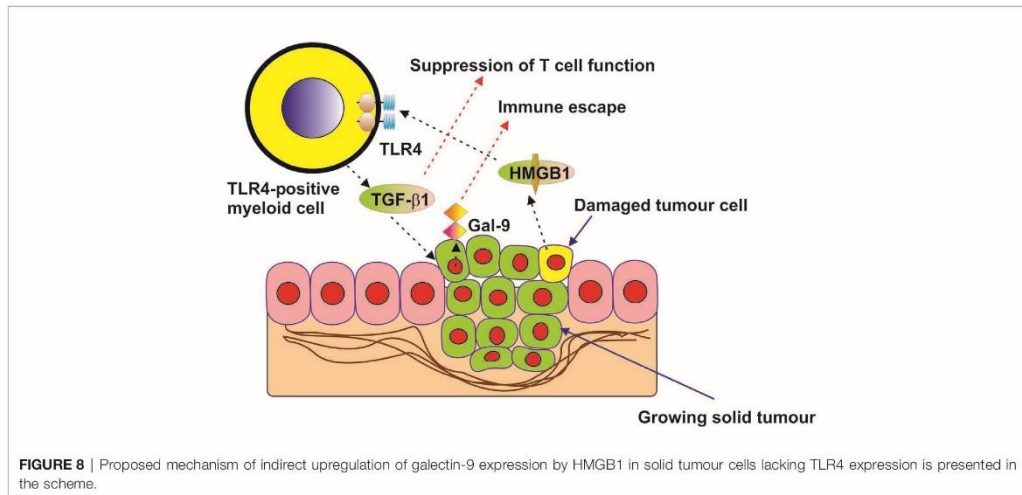
DISCUSSION

The role of HMGB1 as a “danger signal” or alarmin in cancer progression has been extensively studied in the last decade (1–4,



6–8). It has become increasingly evident that it could play a role in anti-cancer immune evasion but the biochemical mechanisms underlying this phenomenon remain unclear. In this work we discovered that in cancer cells expressing TLR4, HMGB1 can induce TGF- β production and secretion (Figure 1). Interestingly, TLR4 has recently been shown to mediate TGF- β production when activated by lipopolysaccharide (LPS), its pathogen-associated ligand, and some endogenous stimuli such as hyaluronic acid (25, 26). It was also demonstrated that HMGB1-induced activation of TGF- β production in TLR4-expressing cells takes place through the activator protein 1 (AP-1) transcription factor and its upstream pathway (9). HMGB1 displays TLR4 ligand properties and could act in TLR4-expressing cells similarly to that observed for LPS (6, 9). An additional factor which could mediate HMGB1-induced TGF- β expression in TLR4 expressing cells could be the

hypoxia-inducible factor 1 (HIF-1) transcription complex, which is upregulated by TLR4-mediated downstream signalling (24). HIF-1 was shown to trigger the expression of TGF- β (9). TGF- β secreted by TLR4-expressing cancer cells (in our case THP-1 human AML cells), displays autocrine/paracrine activities, and thus acts on the malignant cells which have produced it. As a result, TGF- β induces galectin-9 production by these cells in a Smad3-dependent manner, the effect which has recently been reported (9) and confirmed in the present study. Galectin-9 subsequently displays immunosuppressive activities on cytotoxic and helper T cells in the tumour microenvironment as well as on NK cells (10, 17). The effects of HMGB1-induced galectin-9 expression were observed in the TLR4-expressing THP-1 human AML cell line (Figure 1) as well as in primary human AML cells expressing this receptor (Supplementary Figure 6). Our further experiments demonstrated that if cells



do not express TLR4, but express other HMGB1 receptors (TLR2, Tim-3 and RAGE), no induction of TGF- β secretion takes place in these cells when exposed to HMGB1. This was the case in primary human AML cells lacking TLR4 expression (Figure 2), Colo 205 (Figure 3), MCF-7 (Figure 4) and HEK293 cells (Figure 5) and, as a result, no subsequent upregulation of galectin-9 expression was observed in these cells. However, HMGB1 can still upregulate TGF- β production in TLR4-expressing cells (e. g. tumour-associated macrophages) present in the tumour microenvironment where the released TGF- β may activate galectin-9 expression in cancer cells. Furthermore, increased TGF- β in the tumour microenvironment contributes to the creation of an immunosuppressive milieu (27). TGF- β suppresses granzyme B expressions in cytotoxic T cells, thus reducing their cell-killing potential and impairing their anti-cancer activity (28). Furthermore, TGF- β is known to contribute to the differentiation of naïve T cells entering the tumour microenvironment into regulatory T cells (Tregs) which suppress the cytotoxic activities of T cells (29). This proposed pathway is demonstrated using the example of a solid tumour in Figure 8.

Taken together, our results suggest that HMGB1 potentially plays a critical role in anti-cancer immune evasion and these effects are facilitated by TLR4.

DATA AVAILABILITY STATEMENT

The original contributions presented in the study are included in the article/Supplementary Material. The datasets used and/or

analyzed during the current study are available from the corresponding author on reasonable request.

ETHICS STATEMENT

Blood plasma of healthy human donors was obtained, from buffy coat blood (from healthy donors undergoing routine blood donation) (15) which was purchased from the National Health Blood and Transfusion Service (NHSBT, UK) following ethical approval (REC reference: 16-SS-033). Primary human AML plasma samples and cells [cultured as described before (16)] were obtained from the sample bank of University Medical Centre Hamburg-Eppendorf (Ethik Kommission der Ärztekammer Hamburg, reference: PV3469). Primary human AML mononuclear blasts (AML-PB001F, newly diagnosed/untreated) were also purchased from AllCells (Alameda, CA, USA) and handled in accordance with the manufacturer's recommendations. The studies were performed following ethical approval (REC reference: 16-SS-033). Blood samples were collected before breast surgery from patients with primary breast cancer (PBC) and before treatment of patients who had metastatic breast cancer (MBC). Samples were also collected from healthy donors (individuals with no diagnosed pathology – see above). Blood separation was performed using a buoyancy density method employing Histopaque 1119-1 (Sigma, St. Louis, MO) according to the manufacturer's protocol (9, 17). Ethical approval for these studies was obtained from the NRES Essex Research Ethics Committee and the Research & Innovation Department of the Colchester Hospitals University, NHS Foundation Trust [MH 363 (AM03) and 09/H0301/37]. Written informed consent for participation was not required for this study in accordance with the national legislation and the institutional requirements.

AUTHOR CONTRIBUTIONS

AT, SS, IY and SSS performed all the reported experiments with equal contributions. WF and JW isolated and provided primary AML samples used to obtain crucial data and shared expertise on handling primary human AML cells. EK provided primary blood samples from breast cancer patients and shared expertise on their handling. SB participated in design of the concept and planning the experiments. BG, EF-K, and VS designed the study, planned all the experiments, analyzed the data, and wrote the manuscript. All authors contributed to the article and approved the submitted version.

FUNDING

This work was supported in part by the Batzebär grant (to EF-K and SB). The funders had no role in study design, data collection, data analysis, interpretation, or writing of the report.

REFERENCES

- Kang R, Zhang Q, Zeh HJ3rd, Lotze MT, Tang D. HMGB1 in Cancer: Good, Bad, or Both? *Clin Cancer Res* (2013) 19:4046–57. doi: 10.1158/1078-0432.CCR-13-0495
- He SJ, Cheng J, Feng X, Yu Y, Tian L, Huang Q. The Dual Role and Therapeutic Potential of High-Mobility Group Box 1 in Cancer. *Oncotarget* (2017) 8:64534–50. doi: 10.18632/oncotarget.17885
- Krysko O, Love Aes T, Bachert C, Vandenabeele P, Krysko DV. Many Faces of DAMPs in Cancer Therapy. *Cell Death Dis* (2013) 4:e631. doi: 10.1038/cddis.2013.156
- Chiba S, Baghdadi M, Akiba H, Yoshiyama H, Kinoshita I, Dosaka-Akita H, et al. Tumor-Infiltrating DCs Suppress Nucleic Acid-Mediated Innate Immune Responses Through Interactions Between the Receptor TIM-3 and the Alarmin HMGB1. *Nat Immunol* (2012) 13:832–42. doi: 10.1038/ni.2376
- Wyszynski RW, Gibbs BF, Varani L, Iannotta D, Sumbayev VV. Interleukin-1 Beta Induces the Expression and Production of Stem Cell Factor by Epithelial Cells: Crucial Involvement of the PI-3K/mTOR Pathway and HIF-1 Transcription Complex. *Clin Immunol Immunopathol* (2016) 134:7–56. doi: 10.1038/cmi.2014.113
- Yasinska IM, Goncalves Silva I, Sakhnevych SS, Ruegg L, Hussain R, Siligardi G, et al. High Mobility Group Box 1 (HMGB1) Acts as an “Alarmin” to Promote Acute Myeloid Leukemia Progression. *Oncotarget* (2018) 7: e1438109. doi: 10.1080/2162402X.2018.1438109
- Liu L, Zhang J, Zhang X, Cheng P, Liu L, Huang Q, et al. HMGB1: An Important Regulator of Myeloid Differentiation and Acute Myeloid Leukemia as Well as a Promising Therapeutic Target. *J Mol Med (Berl)* (2021) 99:107–18. doi: 10.1007/s00109-020-01998-5
- Liu N, Wu Y, Wen X LP, Lu F, Shang H. Chronic Stress Promotes Acute Myeloid Leukemia Progression Through HMGB1/NLRP3/IL-1 β Signaling Pathway. *J Mol Med (Berl)* (2021) 99:402–14. doi: 10.1007/s00109-020-02011-9
- Teo Hansen Selno A, Schlichtner SS, Yasinska IM, Sakhnevych SS, Fiedler W, Wellbrock J, et al. Transforming Growth Factor Beta Type 1 (TGF- β) and Hypoxia-Inducible Factor 1 (HIF-1) Transcription Complex as Master Regulators of the Immunosuppressive Protein Galectin-9 Expression in Human Cancer and Embryonic Cells. *Aging (Albany NY)* (2020) 12:23478–96. doi: 10.18632/aging.202343
- Yasinska IM, Meyer NH, Schlichtner S, Hussain R, Siligardi G, Casely-Hayford M, et al. Ligand-Receptor Interactions of Galectin-9 and VISTA Suppress Human T Lymphocyte Cytotoxic Activity. *Front Immunol* (2020) 11:580557. doi: 10.3389/fimmu.2020.580557
- Delacour D, Koch A, Jacob R. The Role of Galectins in Protein Trafficking. *Traffic* (2009) 10:1405–13. doi: 10.1111/j.1600-0854.2009.00960.x
- Wada J, Kanwar YS. Identification and Characterization of Galectin-9, a Novel Beta-Galactoside-Binding Mammalian Lectin. *J Biol Chem* (1997) 272:6078–86. doi: 10.1074/jbc.272.9.6078

ACKNOWLEDGMENTS

We are most grateful to Dr Luca Varani from the Institute for Research in Biomedicine (IRB), Bellinzona, Switzerland for the gift of anti-Tim-3 antibody and to Prof Ruslan Medzhitov, Yale University, USA for the gift of the plasmid encoding constitutively active TLR4 (mCD4-hTLR4). We thank Dr Jessica Ponti from the European Commission Joint Research Centre, Ispra, Italy for the gift of gold nanoparticles and their characterisation with transmission electron microscopy.

SUPPLEMENTARY MATERIAL

The Supplementary Material for this article can be found online at: <https://www.frontiersin.org/articles/10.3389/fimmu.2021.675731/full#supplementary-material>

- Nagae M, Nishi N, Nakamura-Tsuruta S, Hirabayashi J, Wakatsuki S, Kato R, et al. Structural Analysis of the Human Galectin-9 N-terminal Carbohydrate Recognition Domain Reveals Unexpected Properties That Differ from the Mouse Orthologue. *J Mol Biol* (2008) 375:119–35. doi: 10.1016/j.jmb.2007.09.060
- Prokhorov A, Gibbs BF, Bardelli M, Ruegg L, Fasler-Kan E, Varani L, et al. The Immune Receptor Tim-3 Mediates Activation of PI3 Kinase/mTOR and HIF-1 Pathways in Human Myeloid Leukemia Cells. *Int J Biochem Cell Biol* (2015) 59:11–20. doi: 10.1016/j.biocel.2014.11.017
- Goncalves Silva I, Gibbs BF, Bardelli M, Varani L, Sumbayev VV. Differential Expression and Biochemical Activity of the Immune Receptor Tim-3 in Healthy and Malignant Human Myeloid Cells. *Oncotarget* (2015) 6 (32):33823–33. doi: 10.18632/oncotarget.5257
- Yasinska IM, Ceppone G, Ojea-Jimenez I, Ponti J, Hussain R, Siligardi G, et al. Highly Specific Targeting of Human Acute Myeloid Leukemia Cells Using Pharmacologically Active Nanoconjugates. *Nanoscale* (2018) 10(13):5827–33. doi: 10.1039/C7NR09436A
- Yasinska IM, Sakhnevych SS, Pavlova I, Teo Hansen Selno A, Teuscher Abeleira AM, Benlaouer O, et al. The Tim-3-Galectin-9 Pathway and Its Regulatory Mechanisms in Human Breast Cancer. *Front Immunol* (2019) 10:1594. doi: 10.3389/fimmu.2019.01594
- Medzhitov R, Preston-Hurlburt P, Janeway CA Jr. A Human Homologue of the Drosophila Toll Protein Signals Activation of Adaptive Immunity. *Nature* (1997) 388(6640):394–7. doi: 10.1038/41131
- Gibbs BF, Yasinska IM, Calzolari L, Gilliland D, Sumbayev VV. Highly Specific Targeting of Human Leukocytes Using Gold Nanoparticle-Based Biologically Active Conjugates. *J BioMed Nanotechnol* (2014) 10(7):1259–66. doi: 10.1166/jbnn.2014.1807
- Sumbayev VV, Yasinska IM, Garcia CP, Gilliland D, Lall GS, Gibbs BF, et al. Gold Nanoparticles Downregulate Interleukin-1-Induced Pro-Inflammatory Responses. *Small* (2013) 9(3):472–7. doi: 10.1002/smll.201201528
- Goncalves Silva I, Ruegg L, Gibbs BF, Bardelli M, Fruehwirth A, Varani L, et al. The Immune Receptor Tim-3 Acts as a Trafficker in a Tim-3/galectin-9 Autocrine Loop in Human Myeloid Leukemia Cells. *Oncotarget* (2016) 5:e1195535. doi: 10.1080/2162402X.2016.1195535
- Moller-Hackbarth K, Dewitz C, Schweigert O, Trad A, Garbers C, Rose-John S, et al. A Disintegrin and Metalloprotease (ADAM) 10 and ADAM17 are Major Shedders of T Cell Immunoglobulin and Mucin Domain 3 (Tim-3). *J Biol Chem* (2013) 288(48):34529–44. doi: 10.1074/jbc.M113.488478
- Sakhnevych SS, Yasinska IM, Fasler-Kan E, Sumbayev VV. Mitochondrial Defunctionalization Suppresses Tim-3-Galectin-9 Secretory Pathway in Human Colorectal Cancer Cells and Thus can Possibly Affect Tumor Immune Escape. *Front Pharmacol* (2019) 10:342. doi: 10.3389/fphar.2019.00342

24. Frede S, Stockmann C, Freitag P, Fandrey J. Bacterial Lipopolysaccharide Induces HIF-1 Activation in Human Monocytes Via P44/42 MAPK and NF- κ B. *Biochem J* (2006) 396:517–27. doi: 10.1042/BJ20051839
25. Sun L, Xiu M, Wang S, Brigstock DR, Li H, Qu L, et al. Lipopolysaccharide Enhances TGF- β 1 Signalling Pathway and Rat Pancreatic Fibrosis. *J Cell Mol Med* (2018) 22:2346–56. doi: 10.1111/jcmm.13526
26. Suga H, Sugaya M, Fujita H, Asano Y, Tada Y, Kadono T, et al. TLR4, Rather Than TLR2, Regulates Wound Healing Through TGF- β and CCL5 Expression. *J Dermatol Sci* (2014) 73:117–24. doi: 10.1016/j.jdermsci.2013.10.009
27. Chen WJ, Frank ME, Jin W, Wahl SM. TGF- β Released by Apoptotic T Cells Contributes to an Immunosuppressive Milieu. *Immunity* (2001) 14:715–25. doi: 10.1016/S1074-7613(01)00147-9
28. Thomas DA, Massague J. TGF- β Directly Targets Cytotoxic T Cell Functions During Tumor Evasion of Immune Surveillance. *Cancer Cell* (2005) 8:369–80. doi: 10.1016/j.ccr.2005.10.012
29. Wang Y, Li XL, Mo YZ, Fan CM, Tang L, Xiong F, et al. Effects of Tumor Metabolic Microenvironment on Regulatory T Cells. *Mol Cancer* (2018) 17:168. doi: 10.1186/s12943-018-0913-y

Conflict of Interest: The authors declare that the research was conducted in the absence of any commercial or financial relationships that could be construed as a potential conflict of interest.

Copyright © 2021 Teo Hansen Selno, Schlichtner, Yasinska, Sakhnevych, Fiedler, Wellbrock, Berger, Klenova, Gibbs, Fasler-Kan and Sumbayev. This is an open-access article distributed under the terms of the Creative Commons Attribution License (CC BY). The use, distribution or reproduction in other forums is permitted, provided the original author(s) and the copyright owner(s) are credited and that the original publication in this journal is cited, in accordance with accepted academic practice. No use, distribution or reproduction is permitted which does not comply with these terms.



Contents lists available at ScienceDirect

International Immunopharmacology

journal homepage: www.elsevier.com/locate/intimp

Functional role of galectin-9 in directing human innate immune reactions to Gram-negative bacteria and T cell apoptosis

Stephanie Schlichtner^a, N. Helge Meyer^{b,c}, Inna M. Yasinska^a, Nijas Aliu^d, Steffen M. Berger^e, Bernhard F. Gibbs^b, Elizaveta Fasler-Kan^{e,f,*}, Vadim V. Sumbayev^{a,*}

^a Medway School of Pharmacy, Universities of Kent and Greenwich, Chatham Maritime, United Kingdom

^b Division of Experimental Allergy and Immunodermatology, Department of Human Medicine, University of Oldenburg, Oldenburg, Germany

^c Division of General and Visceral Surgery, Department of Human Medicine, University of Oldenburg, Oldenburg, Germany

^d Department of Human Genetics, Inselspital Bern, University of Bern, Bern, Switzerland

^e Department of Pediatric Surgery, Children's Hospital, Inselspital Bern, University of Bern, Bern, Switzerland

^f Department of Biomedicine, University of Basel and University Hospital Basel, Basel, Switzerland

ARTICLE INFO

Keywords:

Galectin-9
Phagocytosis
Anti-bacterial immune defence
Embryonic development
Anti-cancer immune evasion

ABSTRACT

Galectin-9 is a member of the galectin family of proteins, which were first identified to specifically bind to carbohydrates containing β -galactosides. Galectin-9 is conserved through evolution and recent evidence demonstrated its involvement in innate immune reactions to bacterial infections as well as the suppression of cytotoxic immune responses of T and natural killer cells. However, the molecular mechanisms underlying such differential immunological functions of galectin-9 remain largely unknown. In this work we confirmed that soluble galectin-9 derived from macrophages binds to Gram-negative bacteria by interacting with lipopolysaccharide (LPS), which forms their cell wall. This opsonisation effect most likely interferes with the mobility of bacteria leading to their phagocytosis by innate immune cells. Galectin-9-dependent opsonisation also promotes the innate immune reactions of macrophages to these bacteria and significantly enhances the production of pro-inflammatory cytokines – interleukin (IL) 6, IL-1 β and tumour necrosis factor alpha (TNF- α). In contrast, galectin-9 did not bind peptidoglycan (PGN), which forms the cell wall of Gram-positive bacteria. Moreover, galectin-9 associated with cellular surfaces (studied in primary human embryonic cells) was not involved in the interaction with bacteria or bacterial colonisation. However, galectin-9 expressed on the surface of primary human embryonic cells, as well as soluble forms of galectin-9, were able to target T lymphocytes and caused apoptosis in T cells expressing granzyme B. Furthermore, “opsonisation” of T cells by galectin-9 led to the translocation of phosphatidylserine onto the cell surface and subsequent phagocytosis by macrophages through Tim-3, the receptor, which recognises both galectin-9 and phosphatidylserine as ligands.

1. Introduction

Galectin-9 is a member of the galectin family of proteins which were first identified to specifically bind to carbohydrates containing β -galactosides [1–5]. Galectins vary in their structural organisation and, so far, three different forms of galectin structure were discovered. Galectins can display dimeric, chimeric or tandem structures [1–3]. Galectin-9 has a tandem structure and contains two distinct carbohydrate recognition domains (CRDs) within one polypeptide [1–5]. The CRDs are fused together by a peptide linker. Galectin-9 may be present in three main isoforms characterised by the length of their linker peptide which can be

long (49 amino acids), medium (27 amino acids) and short (15 amino acids) [1–5].

Galectins are conserved through evolution and have various intracellular and extracellular functions including both normal and pathological processes [1,2]. Galectin-9 is one of the most important galectins and is a major contributor to human immune reactions [6,7], particularly because of its ability to suppress the cytotoxic activities of T and natural killer (NK) cells. In cytotoxic T cells galectin-9 acts through receptors such as Tim-3 (T cell immunoglobulin and mucin-containing protein 3) and VISTA (V-domain Ig-containing suppressor of T cell activation) [7]. Galectin-9 can induce leakage of granzyme B proteolytic

* Corresponding authors.

E-mail addresses: elizaveta.fasler@insel.ch (E. Fasler-Kan), V.Sumbayev@kent.ac.uk (V.V. Sumbayev).

<https://doi.org/10.1016/j.intimp.2021.108155>

Received 14 June 2021; Received in revised form 9 September 2021; Accepted 10 September 2021

Available online 17 September 2021

1567-5769/© 2021 Elsevier B.V. All rights reserved.

enzyme from the intracellular granules of cytotoxic T cells thus leading to their programmed death [7]. In NK cells, galectin-9 acts mainly through Tim-3 and impairs their cytotoxic activities [6]. As such, galectin-9 is used by cancer cells to escape immune surveillance and also by foetus cells where it protects the embryo against rejection by the mother's immune system [8]. Furthermore, galectin-9 was found to participate in neutrophil-mediated killing of Gram-negative bacteria by opsonisation, thus promoting their phagocytosis by neutrophils [9].

However, the actual biochemical role of galectin-9 in anti-bacterial immune defence and suppression of T cell functions remains to be comprehensively understood. Here we report that galectin-9 binds Gram-negative bacteria (*E. Coli XL10 Gold*) by interacting with lipopolysaccharide (LPS), which is a crucial cell wall component. This opsonisation effect renders the bacteria less mobile thus facilitating their capture and phagocytosis by macrophages. Opsonisation also promotes the innate immune reactions of macrophages to Gram-negative bacteria and significantly enhances the production of pro-inflammatory cytokines – interleukin (IL) 6, IL-1 β and tumour necrosis factor alpha (TNF- α). Galectin-9 was almost incapable of binding peptidoglycan (PGN), which forms the cell wall of Gram-positive bacteria. Galectin-9 associated with the cell surface (studied in primary human embryonic cells) was not involved in the interaction with bacteria or bacterial colonisation. However, cell-surface-based galectin-9 on human embryonic cells, as well as secreted galectin-9, targeted T lymphocytes and caused apoptosis in T cells expressing granzyme B. T cells “opsonised” by galectin-9 were phagocytosed by macrophages through Tim-3. Furthermore, galectin-9 induced the release of transforming growth factor beta type 1 (TGF- β) and high mobility group box 1 (HMGB1) from T cells. TGF- β induces the expression of galectin-9 in cancer and embryonic cells and HMGB1 enhances the ability of macrophages to phagocytose apoptotic T cells.

Taken together our results suggest that galectin-9 is capable of opsonising LPS-containing bacteria and T cells triggering their phagocytosis by macrophages. Moreover, galectin-9 provokes the activation of anti-bacterial innate immune reactions and, in the case of T cell suppression, indirectly enhances the phagocytic activity of macrophages.

2. Materials and methods

2.1. Materials

RPMI-1640 cell culture medium, foetal bovine serum and supplements as well as basic laboratory chemicals were obtained from Sigma (Suffolk, UK). Microtitre plates for Enzyme-Linked Immunosorbent Assay (ELISA) were provided by Oxley Hughes Ltd (London, UK). Rabbit antibodies against VISTA (ab243891, BLR035F), galectin-9 (ab69630), granzyme B ab134933, EPR8260), CD3 (ab21703, SP7 and LPS (lipid A, ab8467, 26–5), as well as mouse antibody against Toll-like receptor 2 (TLR2, ab9100, TL2.1), were purchased from Abcam (Cambridge, UK). Antibody against actin (66009-I-Ig) was purchased from and Proteintech (Manchester, UK). Goat anti-mouse (925–32210 and 926–68070) and anti-rabbit (926–3211 and 926–68071) fluorescence dye-labelled antibodies were obtained from Li-COR (Lincoln, Nebraska USA). ELISA-based assay kits/antibodies for the detection of galectin-9 (DY2045), Tim-3 (DY2365), VISTA (DY7126), IL-6 (DY206), IL-1 β (DY201) and TNF- α (DY210) were purchased from Bio-Techne (R&D Systems, Abingdon, UK). Anti-Tim-3 mouse monoclonal antibodies (detection (3B1) and neutralising (4BS)) were generated by Dr Luca Varani and were used in this work [7,10]. Human recombinant VISTA protein was obtained from Sino Biological US Inc (Wayne, PA, USA). Human recombinant Ig-like V-type domain of Tim-3 (amino acid residues 22–124) was described before [7]. Annexin V/propidium iodide apoptosis assay kits were purchased from Invitrogen (Carlsbad, USA). All other chemicals purchased were of the highest grade of purity commercially available.

2.2. Cell lines and primary human cells/samples

Cell lines used in this work were purchased from the European Collection of Cell Cultures (Porton Down, UK). Cell lines were accompanied by identification test certificates and were grown according to corresponding tissue culture collection protocols. *Escherichia coli* (*E. Coli*) XL10 Gold® bacteria were purchased from Stratagene Europe (Amsterdam, The Netherlands).

Blood plasma of healthy human donors was obtained from buffy coat blood (purchased from healthy donors undergoing routine blood donation) which was procured from the National Health Blood and Transfusion Service (NHSBT, UK) following ethical approval (REC reference: 16-SS-033). The procedure was completed as described previously [6,7]. Primary human AML plasma samples were obtained from the sample bank of University Medical Centre Hamburg-Eppendorf (Ethik-Kommission der Ärztekammer Hamburg, reference: PV3469) and kindly provided by Professor Walter Fiedler and Dr Jasmin Wellbrock.

Placental tissues (CVS, chorionic villus sampling) and amniotic fluids were collected after obtaining informed written consent from pregnant women at the University Hospital Bern. Cells were prepared and cultured as described before [8,11]. CVS was washed with PBS, treated with 270 U/ml of collagenase type 2 (Sigma, Buchs, Switzerland) for 50 min at 37° C, washed twice with PBS and cells were then re-suspended and cultured in CHANG medium (Irvine Scientific, Irvine, USA) according to the manufacturer's instructions. Amniotic fluid samples were centrifuged and cell pellets were then re-suspended in CHANG medium. The first medium change was performed after 5 days of incubation at 37° C. The medium was then changed every second day until the number of cells was sufficient.

Primary human T cells were isolated from PBMCs with a CD3 T cell negative isolation kit (Biolegend). Ethical approval of this study was issued by the “Medizinische Ethikkommission der Carl von Ossietzky Universität Oldenburg”. 200,000 T cells per 200 μ l were incubated with and without Gal-9 at a final concentration of 2.5 μ g/ml in RPMI medium. After 16 h cells were stained with anti-CD4, anti-CD-8, anti-CD3 and AnnexinV (Miltenyi Biotec) according to manufacturer's recommendation and analysed on a MacsQuant 16 Analyzer (Miltenyi Biotec).

2.3. In-cell and on-cell Western analysis

In order to detect phagocytosis of bacterial cells or Jurkat T cells by THP-1 macrophages, we analysed these cells by employing the use of specific markers following co-culturing of the respective cells. We used a standard Li-COR in-cell Western assay (methanol was used as a permeabilisation agent) [12] to detect bacterial LPS or T cell-associated CD3 in THP-1 macrophages. Rabbit anti-LPS (which recognises lipid A) and anti-CD3 antibodies were used to detect specific targets and a goat anti-rabbit Li-Cor secondary antibody was employed for visualisation purposes.

In order to characterise the presence of galectin-9 and VISTA on the surface of human embryonic cells or Jurkat T cells (galectin-9 only) we used a standard Li-COR on-cell Western assay [12] where the cells were not permeabilised thus measuring only the proteins present on the cell surface.

2.4. Preparation of bacterial cell extracts and measuring galectin-9 in cytoplasmic and cell wall fractions

E. Coli XL10 Gold® bacterial cells were collected and lysed as described before by sonication on ice in a buffer containing 20 mM Tris-HCl (pH 8.0), 100 mM NaCl, 10 μ M ZnCl₂, 0.5% NP-40, 0.5 mM dithiothreitol and 1 mM phenyl-methyl-sulfonyl-fluoride. Lysates were then centrifuged and both supernatant (cytoplasm extract) and pellet (containing cell wall components) were subjected to further analysis. Lysates were used to detect galectin-9 by Western blot analysis (see below). Cell wall pellets were incubated with biotinylated antibodies

against galectin-9, Tim-3 or VISTA for 2 h at room temperature with constant agitation. Pellets were then precipitated by centrifugation (5 min at 13,000 rpm) followed by three washes with TBST buffer and centrifugation after each wash. After this, pellets were re-suspended in PBS containing HRP-labelled streptavidin and incubated for 1 h at room temperature with constant agitation. This was followed by 3 washes (as described above) and development by re-suspending in 6 mg/ml *ortho*-phenyldiamine (OPD) solution containing hydrogen peroxide. After 5 min incubation at room temperature with constant agitation in the darkness, equal amount of 10 % sulfuric acid solution was added to stop the reaction. Mixtures were centrifuged for 5 min at 13,000 rpm, supernatants were transferred to the wells of a 96-well plate and absorbances were measured at 492 nm.

We also measured galectin-9, Tim-3 and VISTA on the surface of bacterial cells using on-cell ELISA. Bacterial pellets were incubated for 1 h at room temperature in PBS containing antibodies against galectin-9, Tim-3 or VISTA for 2 h at room temperature with constant agitation. Bacterial cells were then precipitated by centrifugation (5 min at 13,000 rpm) followed by three washes with TBST buffer and centrifugation after each wash. After this, pellets were re-suspended in PBS containing HRP-labelled streptavidin and incubated for 1 h at room temperature with constant agitation. Visualisation was performed using OPD as described above.

2.5. Measurement of IL-6, IL-1 β , TNF- α , TGF- β and released HMGB1 concentrations

Concentrations of secreted cytokines/growth factors (IL-6, IL-1 β , TNF- α and TGF- β) were measured by ELISA using Bio-technie kits according to the manufacturer's protocols. HMGB1 was measured using a MyBioSource ELISA assay kit according to the manufacturer's protocol.

2.6. Assessment of binding of galectin-9 and associated proteins with LPS and PGN

ELISA plates were coated with anti-LPS antibody and blocked with BSA. 1 μ g/well *Pseudomonas aeruginosa* (*P. aeruginosa*) LPS (Sigma) was immobilised on the plate for 2 h followed by application of human blood plasma. Blood plasma was then washed away 5 times with TBST buffer and biotinylated antibodies against galectin-9, Tim-3 or VISTA were added. Binding was visualised as described above.

In order to assess the interaction of PGN with galectin-9 we coated the ELISA plate with 5 μ g/well *Staphylococcus aureus* (*S. aureus*) PGN and blocked with BSA. Human blood plasma or 500 ng/well human recombinant galectin-9 (dissolved in PBS) were then applied and incubated for 2 h. The presence of galectin-9 was then detected as described above. To confirm that the plate was successfully coated with PGN, we incubated some of the wells with 10 μ l of THP-1 cell lysate (which contains TLR2 – a PGN receptor) followed by extensive washing with TBST. TLR2 binding was measured using rabbit anti-TLR2 antibody (1:500) and visualised using goat anti-rabbit HRP-labelled antibody (1:1000).

2.7. Western blot analysis

Western blot analysis of galectin-9, VISTA, Tim-3 and granzyme B was performed as described before [7]. Actin staining was used as a protein loading control.

2.8. Granzyme B in-cell activity, caspase-3 activity, cell viability and annexin V tests

In-cell activity of granzyme B was measured as described before [7]. Briefly, living cells were incubated with 150 μ M Ac-IEPD-AFC (granzyme B substrate) for 1 h at 37 °C in sterile PBS. This did not affect the cell viability, as described below. Total cell fluorescence was then

measured in living cells using excitation and emission wavelengths recommended by the Ac-IEPD-AFC manufacturer (Sigma). An equal number of cells, which were not exposed to granzyme B substrate were used as a control.

Caspase-3 activity in cell lysates was measured using a colorimetric assay kit based on cleavage of the substrate Ac-DEVD-pNA according to the manufacturer's (Bio-technie) protocol. Cell viability was measured by MTS assay (Promega kit was used); measurements were performed according to the manufacturer's protocol.

An annexin V test was performed [7] using an Invitrogen assay kit according to the manufacturer's protocol.

2.9. Statistical analysis

Each experiment was performed at least three times and statistical analysis, when comparing two events at a time, was performed using a two-tailed Student's *t*-test. Multiple comparisons were conducted by ANOVA. Post-hoc Bonferroni correction was applied. Statistical probabilities (*p*) were expressed as * when *p* < 0.05; and ** when *p* < 0.01.

3. Results

3.1. Galectin-9 opsonises Gram-negative bacteria via binding to LPS, triggering their phagocytosis and enhancing anti-bacterial innate immune reactions

Galectin-9 was found to be able to opsonise Gram-negative bacteria by direct interaction with them. We first investigated the reactions of galectin-9 with Gram-negative bacteria and with LPS (component of their cell wall) as well as the impact of these interactions on phagocytosis of target bacteria and innate immune reactions to them. We used THP-1 cells which were differentiated into macrophages by 24 h exposure to 100 nM PMA. Upon completion of differentiation, medium was then replaced (PMA and antibiotic free). 50 μ l of *E. Coli XL10 Gold*[®] were added to the culture and incubated under normal cell culturing conditions for 16 h in the presence or absence of 10 mM lactose to block the sugar-binding activity of galectin-9 (Fig. 1A). A concentration of 10 mM lactose was sufficient to block the sugar-binding activities of THP-1 cell-derived galectin-9 and neither affected cell viability (when measured by an MTS test) nor proliferation velocity (assessed by counting the cells). Bacterial cells were then washed away with sterile PBS and THP-1 cells were permeabilised with methanol, as outlined in Materials and methods, and the presence of LPS was detected using anti-LPS antibody (specific to lipid A) by in-cell Western (Fig. 1B). We found that LPS was highly present in THP-1 macrophages when co-cultured with bacteria and these levels were substantially attenuated by the presence of lactose in the culture medium (Fig. 1B). Importantly, co-incubation with bacteria provoked high levels of inflammatory cytokine release from THP-1 cells, where secretions of TNF- α , IL-1 β and IL-6 were significantly upregulated (Fig. 1C). The presence of lactose in the medium significantly reduced the levels of secreted cytokines (Fig. 1C). Importantly, upon completion of co-incubation, we measured galectin-9, Tim-3 and VISTA levels by ELISA. In the presence of bacteria, the level of galectin-9 was 8.7 ± 1.1 ng galectin-9 per 10^6 THP-1 cells. Tim-3 and VISTA levels were 1.12 ± 0.2 and 0.91 ± 0.14 ng per 10^6 THP-1 cells, respectively. Bacteria washed away from the co-culture were lysed and the cytoplasmic components then extracted and subjected to Western blot analysis for presence of galectin-9. It was not detectable in bacterial cytoplasm (Fig. 1D left panel). Pellet containing bacterial cell wall was exposed to biotinylated antibody against galectin-9 for 1 h. Then antibody was washed away with PBS 3 times by re-suspension followed by centrifugation. Pellet was exposed to HRP-labelled streptavidin for 1 h followed by washing as described above and measurement of HRP as outlined in Materials and methods. We found that cell wall pellet derived from bacterial cells that were not co-cultured THP-1 cells did not contain galectin-9. In contrast, galectin-9 was present in the

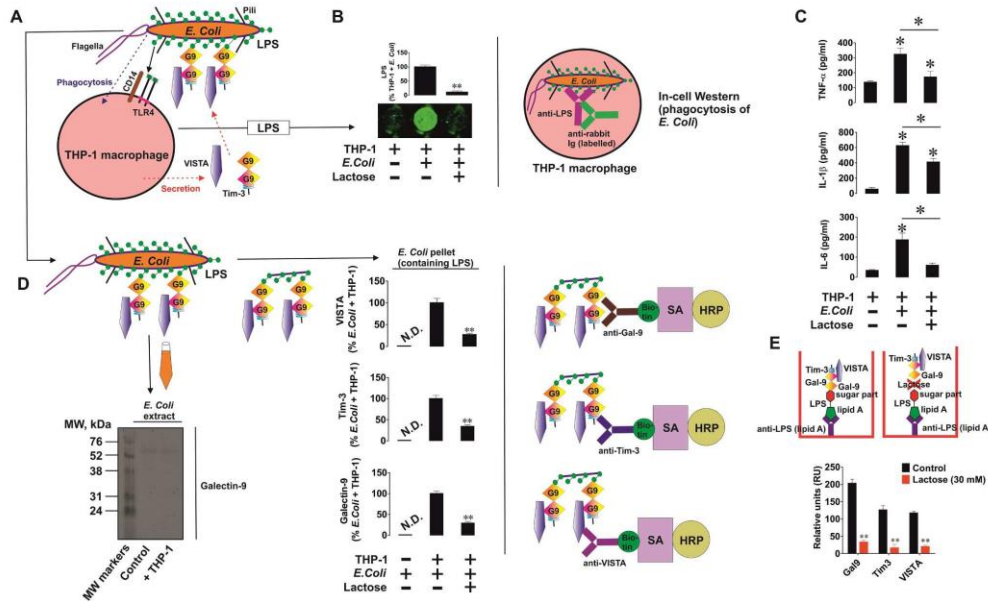


Fig. 1. Opsonisation of Gram-negative bacteria with galectin-9 occurs via LPS binding, triggering phagocytosis of bacterial cells and innate immune cytokine secretion. THP-1 macrophages (obtained by PMA differentiation of monocytes) were co-cultured with *E. Coli XL10 Gold®* for 16 h in the absence or presence of 10 mM lactose (A). Phagocytosis of bacterial cells was then assessed using in-cell Western (B). Concentrations of TNF-α, IL-1β and IL-6 were measured in cell culture medium by ELISA (C). Bacterial cells were lysed and galectin-9 was measured in cytoplasmic extracts by Western blot (D, left panel). Cell wall-containing pellet was subjected to measurement of galectin-9, Tim-3 and VISTA as outlined in Materials and methods (D, right panel). Binding of galectin-9 to LPS and the association of Tim-3 and VISTA with the complex was performed by an ELISA-based method as outlined in Materials and methods (E). Images are from one experiment representative of five which gave similar results. Quantitative data represent mean values ± SEM of five independent experiments. * - p < 0.05 and ** - p < 0.01 vs control.

pellets from bacterial cells co-cultured with THP-1 cells. The presence of lactose reduced the amount of galectin-9 associated with bacteria (Fig. 1D right panel). We also assessed if Tim-3 and VISTA, which were found to associate with galectin-9 in T cells, were attached to bacteria. We used the same approach as for galectin-9 (see above and Fig. 1D right panel for schemes of the assays) and found that both Tim-3 and VISTA were indeed associated with galectin-9 and that their presence, as with galectin-9, was reduced by lactose (Fig. 1D right panel). In order to confirm that Tim-3 and VISTA interact with galectin-9 and not directly with bacteria we exposed bacterial cells (*E. Coli XL10 Gold®*), described above, for 1 h to 0.1 μM human recombinant galectin-9, 0.1 μM human recombinant Tim-3 or 0.1 μM human recombinant VISTA. In addition, we exposed bacterial cells to a mixture of 0.1 μM galectin-9 and 0.1 μM Tim-3 or VISTA (see scheme of the experiment in Supplementary Fig. 1). We found that Tim-3 and VISTA were associated with bacteria only when co-incubated with galectin-9 and not on their own (Supplementary Fig. 2), which provides further confirmation that Tim-3 and VISTA associate with galectin-9 and not with bacteria. Finally, we sought to confirm that galectin-9 interacts with LPS. We coated the ELISA plate with anti-LPS antibody (3 μg/well) and immobilised *P. aeruginosa* LPS on it (1 μg LPS per well), see Materials and methods for further details. We then loaded human blood plasma obtained from healthy donors containing 520 pg/ml galectin-9, 790 pg/ml Tim-3 and 335 pg/ml VISTA with or without 30 mM lactose (this high lactose concentration was used given the viscosity of human blood plasma and the presence of proteins other than galectin-9, which can potentially interact with lactose). We then measured galectin-9 as well as Tim-3 and VISTA associated with LPS. We found that blood plasma galectin-9 was bound to the LPS and

associated with Tim-3 and VISTA (Fig. 1E). The presence of lactose attenuated the association of galectin-9 (and respectively Tim-3 and VISTA) with LPS (Fig. 1E).

To confirm the observed effects with whole bacterial cells we incubated *E. Coli XL10 Gold®* (50 μl stock) with 500 μl of blood plasma obtained from healthy donors containing 460 pg/ml galectin-9, 410 pg/ml Tim-3 and 285 pg/ml VISTA for 1 h in the absence or presence of 30 mM lactose. We then precipitated bacteria and measured galectin-9, Tim-3 and VISTA associated with them as outlined in Materials and methods. We found that galectin-9, as well as Tim-3 and VISTA, were associated with bacteria (Fig. 2) and this association was significantly downregulated by the presence of lactose.

Finally, we sought to confirm that galectin-9 can bind only LPS and not peptidoglycan (PGN), which forms the cell wall of Gram-positive bacteria. For this purpose, we coated the plate with 5 μg/well PGN and applied human blood plasma obtained from healthy donors containing 560 pg/ml galectin-9. For comparison, we applied 500 ng per well of human recombinant galectin-9 (this is approximately 20% of the amount of PGN used to coat the wells of the plate). This high amount was applied alone to assess the possibility of chemical interactions between the two substances – PGN and galectin-9. To confirm the successful immobilisation of PGN on the ELISA plate surface, we loaded cell lysate of THP-1 cells containing TLR2 (PGN receptor [13]) and then measured its presence by ELISA (see Materials and methods for details). We found that PGN did not bind galectin-9 from blood plasma (Fig. 3) but traces of interactions were detectable with recombinant galectin-9 (the concentration here was 1000 times higher than in blood plasma). TLR2 was clearly interacting with PGN, suggesting that it was

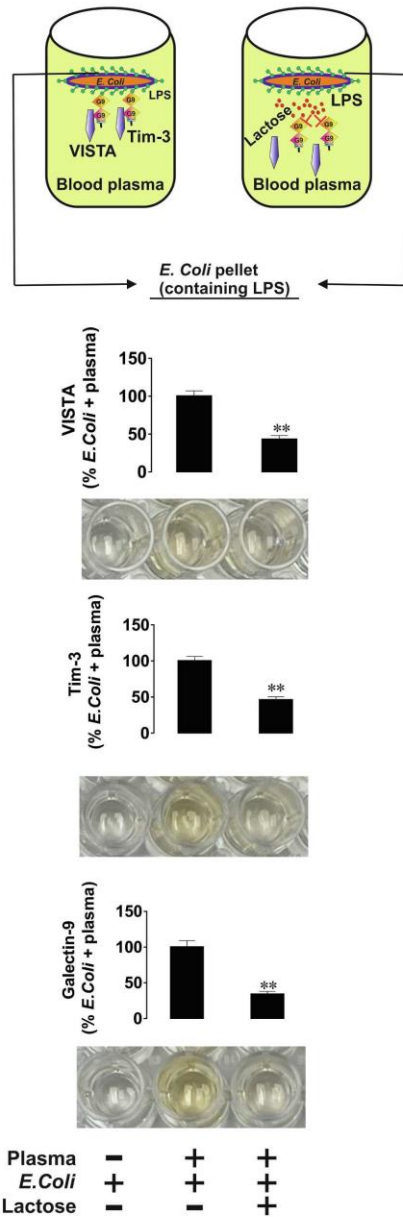


Fig. 2. Galectin-9 from human blood plasma opsonises Gram-negative bacteria. *E. Coli* XL10 Gold® cells were incubated in human blood plasma obtained from healthy donors in the absence or presence of 30 mM lactose. Galectin-9 on the surface of bacteria and its association with Tim-3 and VISTA was detected as outlined in Materials and methods. Images are from one experiment representative of five which gave similar results. Quantitative data represent mean values ± SEM of five independent experiments. ** - p < 0.01 vs control.

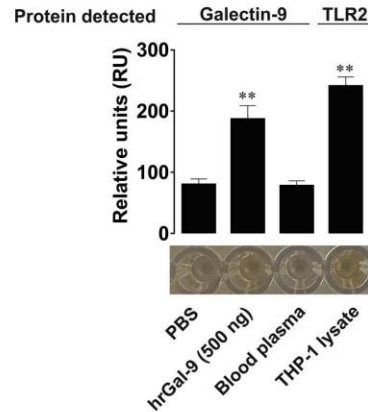
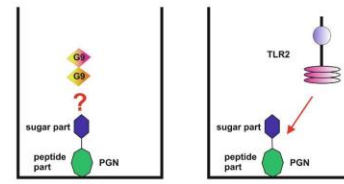


Fig. 3. Galectin-9 from blood plasma does not bind PGN. PGN from *S. aureus* was immobilised on an ELISA plate and exposed to human recombinant galectin-9 (500 ng/well), human blood plasma obtained from healthy donors or THP-1 cell lysate containing TLR2 (PGN receptor) to confirm successful immobilisation of PGN on the plate surface. Images are from one experiment representative of five which gave similar results. Quantitative data represent mean values ± SEM of five independent experiments. ** - p < 0.01 vs control.

successfully immobilised on the ELISA plate. These results indicate that galectin-9 at physiological concentration does not interact with PGN and thus, in line with previous observations, opsonises only Gram-negative bacteria which contain LPS. Opsonisation of Gram-negative bacteria with galectin-9 enhances innate immune reactions to these bacteria and their phagocytosis by macrophages.

3.2. Cell surface-based galectin-9 in human embryonic cells protects them against cytotoxic T cell attack but is not involved in bacterial colonisation

Recently, we reported that human embryonic cells express high levels of galectin-9 at the early stages of pregnancy [8]. We sought to confirm whether embryonic galectin-9 can suppress the cytotoxic activity of T cells. We compared the levels of galectin-9, Tim-3 and VISTA in embryonic cells obtained during the chorion stage (13–14 weeks of pregnancy) and amnion stage (ca 20 weeks). As expected, all of the proteins were expressed at higher levels in the earlier pregnancy stage (Fig. 4 A-C). We asked whether Tim-3 or VISTA, or both proteins, act as traffickers/carriers of galectin-9 in order to translocate it onto the surface. We prepared ELISA formats coating the plate with mouse or rabbit anti-galectin-9 antibody to capture galectin-9 from the cell lysates of embryonic cells obtained at chorion stage (which express high levels of galectin-9). We confirmed successful capturing of galectin-9 by detecting it using rabbit anti-galectin-9 antibody (mouse antibody was used to capture galectin-9 in this case) and visualised the interaction using goat anti-rabbit fluorescently-labelled secondary antibody (Fig. 4 C). We detected Tim-3 and VISTA associated with galectin-9. We found that

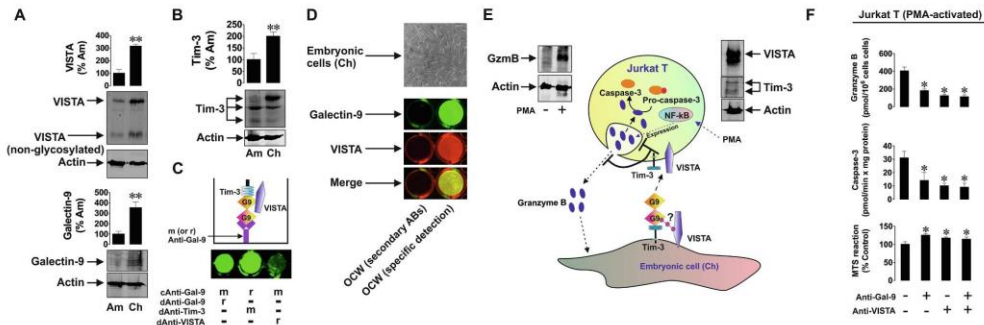


Fig. 4. Galectin-9 and VISTA play a crucial role in suppressing the cytotoxic activities of T cells on human embryonic cells. Primary human embryonic cells were cultured as described in Materials and methods. Levels of galectin-9, VISTA (A) and Tim-3 (B) were measured by Western blot analysis in cells obtained either from 7 patients at chorion stage (weeks 13–14) or 7 patients at amnion stage (ca. week 20). Association of galectin-9 with Tim-3 and VISTA was analysed as described in the text and as shown in Supplementary Fig. 3 (C). The presence of galectin-9 and VISTA on the cell surface was analysed using on-cell Western (D). Cells used for this analysis are also shown on the top of the panel D. Embryonic cells (chorion stage) were then co-cultured for 16 h with Jurkat T cells, which were pre-activated for 24 h with PMA to induce the expression of granzyme B. PMA-activated cells expressed both Tim-3 and VISTA (E). Jurkat T cells were then collected and subjected to measurement of in-cell granzyme B activity, caspase-3 activity in cell lysates and cell viability assay (F). Images are from one experiment representative of seven which gave similar results. Quantitative data represent mean values \pm SEM of seven independent experiments. * - $p < 0.05$ and ** - $p < 0.01$ vs control.

both proteins were detectable but the signal obtained with Tim-3 was much more intense suggesting that Tim-3 is likely to act as carrier/trafficker for galectin-9 in embryonic cells and VISTA possibly associates with the complex. Using on-cell Western, we measured galectin-9 and VISTA on the surface of embryonic cells and found that they were both present and when merging the fluorescence – yellow fluorescence was also detectable suggesting that galectin-9 and VISTA could possibly be located close to each other on the cell surface. Galectin-9 and VISTA

could thus associate when interacting with T cells, as we have recently reported for acute myeloid leukaemia cells [7]. To verify this we co-cultured primary human embryonic cells with Jurkat T cells, which were pre-treated for 24 h with 100 nM PMA [7] in order to activate granzyme B production (Fig. 4E). PMA treated Jurkat T cells expressed granzyme B, Tim-3 and VISTA (Fig. 4 E). Medium was then replaced with PMA-free medium and cells were co-cultured with embryonic cells for 16 h with or without pre-treatment with galectin-9 or/and VISTA

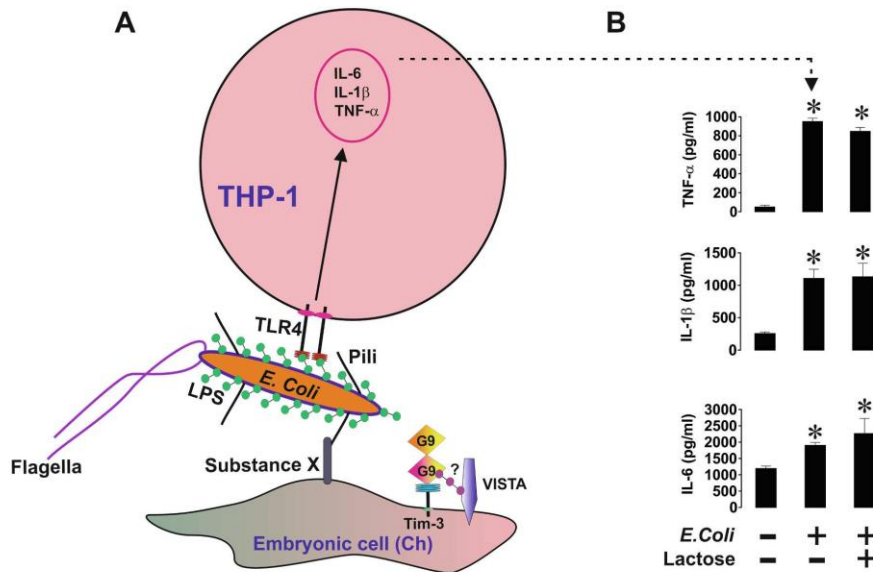


Fig. 5. Galectin-9 is not involved in colonisation of Gram-negative bacteria on embryonic cells. Primary human embryonic cells (chorion stage) were co-cultured with *E. Coli XL10 Gold*® cells for 16 h in the absence or presence of 10 mM lactose. Unbound bacteria were then removed and THP-1 cells (monocytes) were added. The innate immune response to these bacteria was measured by detecting the amounts of IL-6, IL-1 β and TNF- α release using ELISA. Images are from one experiment representative of four which gave similar results. Quantitative data represent mean values \pm SEM of four independent experiments. * - $p < 0.05$ and ** - $p < 0.01$ vs control.

neutralising antibodies. We found that presence of antibodies in the co-culture reduced intracellular activation (most likely caused by leakage) of granzyme B as well as caspase 3 activity and increased the viability of Jurkat T cells (Fig. 4F).

We sought to understand if cell surface-based galectin-9 in human embryonic cells can be involved in the colonisation of Gram-negative bacteria. We co-cultured embryonic cells (chorion stage) with 50 µl stock of *E. Coli XL10 Gold*® for 16 h in antibiotic-free medium allowing bacteria to form colonies on the monolayer of embryonic cells (Fig. 5A). Then we removed the medium containing bacteria and added THP-1 monocytes (10⁶ cells per dish containing 3 ml of culture medium) and incubated for 16 h in antibiotic-free medium under normal cell culture conditions in the absence or presence of 10 mM lactose. We then measured IL-6, IL-1β and TNF-α in cell culture medium (Fig. 5). We found background levels of all three cytokines in the co-culture of embryonic cells with THP-1 cells, which were not exposed to bacteria. However, cytokine levels were significantly upregulated in the presence of bacteria and were not reduced by lactose in the co-cultures (Fig. 5B). These results suggest that cell surface-based galectin-9 in human embryonic cells is not involved in bacterial colonisation and does not influence the association of bacteria with embryonic cells and thus does not determine the innate immune response to bacteria infecting embryonic cells. However, galectin-9 is involved in suppressing the cytotoxic activities of T cells, thus protecting embryonic cells against cytotoxic immune attack.

3.3. Secreted galectin-9 “opsonises” T cells and provokes their phagocytosis by macrophages

Given the results presented above, and the current knowledge on galectin-9-triggered suppression and even apoptosis of T cells, we asked whether T lymphocytes opsonised by galectin-9 can be phagocytosed by macrophages. For this purpose, we used Jurkat T cells activated with 100 nM PMA for 24 h. These cells were then exposed to 2.5 µg/ml galectin-9 in PMA free medium (Fig. 6A). This concentration of galectin-9 was used based on our previous observations. Importantly, recombinant galectin-9, in terms of inducing biological responses, is about 250–500 times less active than myeloid cell-derived protein [7]. After exposure to galectin-9 we characterised the presence of phosphatidylserine (PS, known as an “eat me signal” for macrophages) on the cell surface using annexin V staining, cell viability, as well as the release of TGF-β (known to be released by dying T cells [14]) and HMGB1 (released by damaged, stressed or dying cells). We found that cell viability measured by MTS test was not significantly affected (although some of the cells were apoptotic) despite the significant increase in annexin V staining, indicating increased surface-based PS levels (Fig. 6B). Secreted levels of TGF-β and HMGB1 were significantly upregulated in cells treated with galectin-9. These cells were co-cultured for 3 h with THP-1 macrophages (differentiated for 24 h by exposure to 100 nM PMA). Some of the macrophages were pre-stimulated for 1 h with 1 µg/ml HMGB1 to assess the possibility of phagocytic activity of macrophages being enhanced by HMGB1. We then permeabilised THP-1 cells with methanol and assessed presence of the T cell marker CD3 in THP-1 cells by in-cell Western. We found that galectin-9-treated Jurkat T cells were phagocytosed at significantly higher levels compared to cells which were not pre-exposed to galectin-9 (Fig. 6C, top panel). HMGB1 significantly enhanced the ability of macrophages to phagocytose T cells opsonised with galectin-9. Since, in addition to galectin-9, Jurkat T cells had high amounts of PS on their surface, we asked whether macrophage surface-based Tim-3 is involved in the phagocytosis of T cells as both galectin-9 and PS are Tim-3 ligands. We co-cultured PMA-differentiated THP-1 cells with PMA-activated galectin-9 pre-treated Jurkat T cells (as described above) with or without 1 h pre-exposure of macrophages to 2 µg/ml Tim-3 neutralising antibody. We observed that neutralisation of Tim-3 reduced phagocytosis of T cells (Fig. 6C bottom panel).

To confirm the physiological relevance of this effect we co-cultured

THP-1 macrophages (24 h PMA differentiation was applied) with PMA-activated Jurkat T cells which were first cultured for 16 h in the presence of 10 % human blood plasma obtained either from healthy donors (contained 370 pg/ml galectin-9) or from AML patients (contained 8200 pg/ml galectin-9). In co-cultures where Jurkat T cells were pre-treated with AML patient plasma, the level of phagocytosis was significantly higher, while no significant changes were observed in phagocytosis of cells pre-treated with healthy donor blood plasma. Neutralisation of Tim-3 downregulated phagocytosis of Jurkat T cells pre-treated with blood plasma from AML patients (Fig. 6D). Exposure of Jurkat T cells to blood plasma of AML patients significantly increased galectin-9 levels on their surface (Fig. 6E) confirming an opsonisation effect.

We then sought to confirm that opsonisation of primary human T cells with galectin-9 leads to the appearance of PS on their surface. CD4 and CD8-positive primary human T cells were treated with 2.5 µg/ml galectin-9 for 16 h followed by measurement of PS levels using annexin V staining. We found that, in both cell types, PS levels were significantly upregulated with higher level of upregulation observed in CD8-positive T cells (Fig. 7). The differences in effects are most likely determined by granzyme B levels in both types of T cells (which are higher in CD8-positive cells).

Taken together our results suggest that galectin-9 affects T cells, causing their phagocytosis by macrophages.

4. Discussion

Galectin-9 is known to contribute to immunosuppressive functions in the malignant tumour microenvironment by impairing the anti-cancer activities of cytotoxic lymphoid cells and thus allowing cancer cells to escape immune attack [7]. However, the exact role of galectin-9 in normal human immune reactions remains to be understood.

Here we confirmed that the secreted form of galectin-9, normally produced by macrophages and other cells of myeloid lineage, is capable of opsonising Gram-negative bacteria. The effect takes place through the interaction of galectin-9 with LPS present in the cell wall of these bacteria (Figs. 1 and 2). Galectin-9 most likely interacts with sugar components of LPS since the binding is strongly inhibited by lactose, but occurs when lipid A is occupied by interaction with antibody. Furthermore, during opsonisation of Gram-negative bacteria, the galectin-9 binding partners, Tim-3 and VISTA, form multiprotein associations in a way similar to the one recently reported for T cells [7]. These interactions most likely render the bacteria less mobile. As such, they can be more easily captured by macrophages and phagocytosed. Opsonisation also increases the number of bacteria interacting with innate immune cells and thus enhancing their cytokine production (IL-6, IL-1β and TNF-α). In contrast, PGN, which forms the cell wall of Gram-positive bacteria [13], is poorly recognised by galectin-9 and, as such, galectin-9 cannot be involved in the opsonisation of Gram-positive bacteria (Fig. 3), which is in line with previous observations [9].

Interestingly, galectin-9 is highly expressed in human embryonic cells especially at the early stages of pregnancy (Fig. 4). When present on the cell surface it protects embryonic cells against the cytotoxic activity of T cells by stimulating the upregulation of intracellular granzyme B activity and caspase 3 in attacking T cells, which then undergo apoptosis (Fig. 4). This takes place in the way similar to the one reported for AML cells, which secrete galectin-9 to impair cytotoxic activities of lymphoid cells [6,7].

However, surface-based galectin-9 in embryonic cells is not involved in the interactions of Gram-negative bacteria infecting embryonic cells. When infecting human cells, bacteria normally use their pili and bind various substances on the host cell surface [17]. Pili form a “first class” of organelles involved in the binding of bacteria to host cells [17]. For example, *E. Coli* pili can use the adhesion factor PapG to interact with glycosphingolipids on the kidney epithelium. Another type of pili, called “Type I pili”, binds D-mannosylated receptors (e. g. uroplakins in the

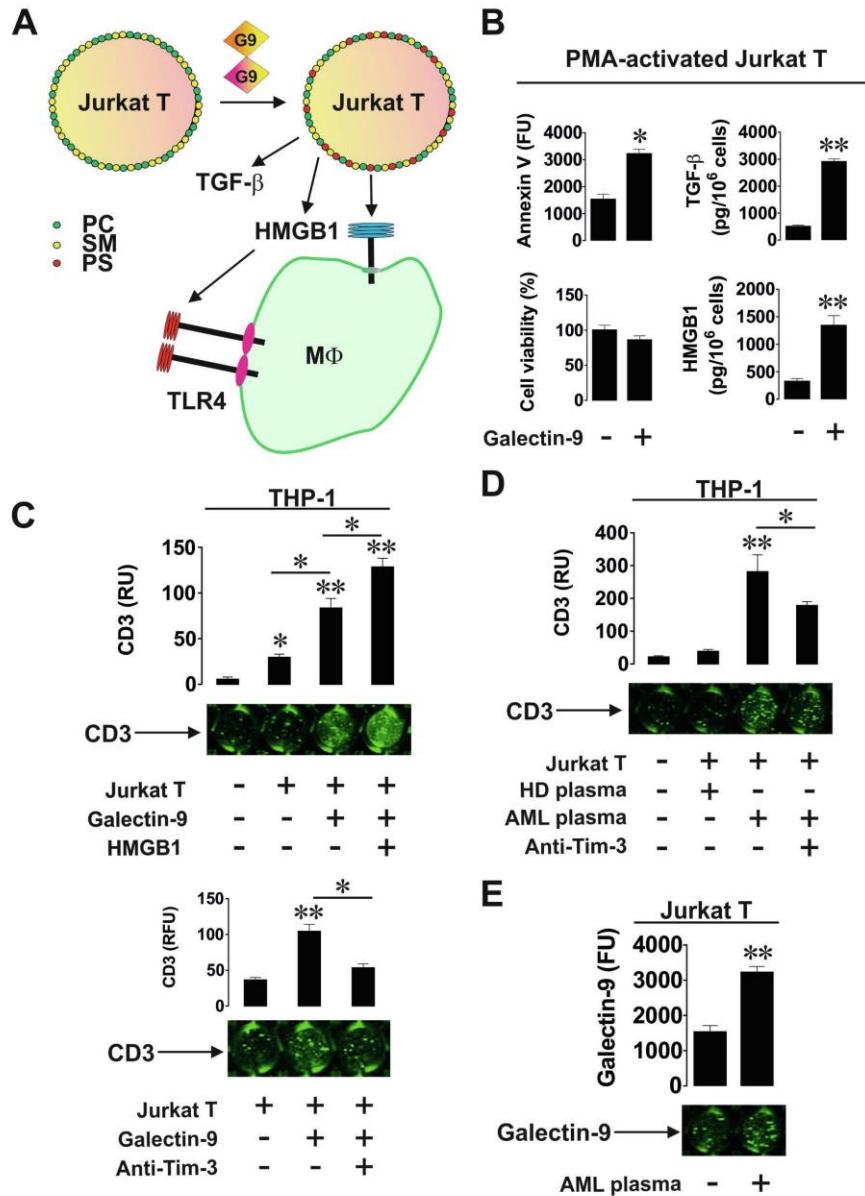


Fig. 6. Galectin-9 opsonises T cells and triggers their phagocytosis by macrophages. PMA-activated Jurkat T cells were exposed to 2.5 µg/ml human recombinant galectin-9 for 16 h followed by co-culturing for 3 h with PMA-differentiated THP-1 macrophages. PC – phosphatidylcholine, SM – sphingomyelin, PS – phosphatidylserine (A). Cell viability, PS (annexin V staining), TGF-β and HMGB1 releases were measured as outlined in Materials and methods (B). Phagocytosis of the T cells was measured in THP-1 cells with or without 1 h pre-activation with HMGB1 (C, top panel) or with or without neutralising Tim-3 (C, bottom panel). PMA-activated Jurkat T cells were first cultured for 16 h in culture medium containing 10 % of blood plasma obtained from healthy human donors or AML patients. This was followed by co-culturing of these cells with THP-1 macrophages for 3 h. Phagocytosis of Jurkat T cells was then analysed using in-cell Western. Cells exposed to blood plasma obtained from AML patients were co-cultured with THP-1 cells with or without 1 h pre-exposure of macrophages to Tim-3 neutralising antibody (D). Given the increased levels of T cell phagocytosis following their exposure to blood plasma obtained from AML patients, these cells were subjected to measurement of galectin-9 on their surface by on-cell Western (E). Images are from one experiment representative of five which gave similar results. Quantitative data represent mean values ± SEM of five independent experiments. * - p < 0.05 and ** - p < 0.01 vs control.

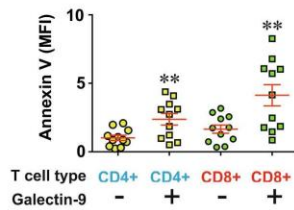


Fig. 7. Exposure of primary human T cells to galectin-9 upregulates PS translocation onto the cell surface. CD4- and CD8-positive T cells isolated from blood of healthy human donors were exposed to 2.5 μ g/ml human recombinant galectin-9 for 16 h followed by PS detection of their surface using annexin V staining. Quantitative data represent mean values \pm SEM of eleven independent experiments. ** - $p < 0.01$ vs control.

bladder [17–20]. From our results, it is clear that cell surface-based galectin-9 does not appear to be involved in adhesion/colonisation of Gram-negative bacteria on the host cell surface (Fig. 5).

In sharp contrast, soluble galectin-9, known to impair cytotoxic activities of T and NK cells [6,7,21], opsonised T cells. This effect leads to activation of granzyme B in T cells expressing this enzyme (e. g. cytotoxic T cells) [7] and can induce apoptosis of T cells and causes the release of TGF- β and HMGB1 (Fig. 6B). Apoptotic T cells are known to release high levels of TGF- β [14], which can upregulate expression of galectin-9 in cancer cells [7,22] and possibly also in malignant tumour-associated macrophages (or placental macrophages involved in protection of the embryo). Galectin-9-dependent opsonisation of T cells leads to the appearance of PS on their surface (Fig. 6B and Fig. 7). This is the process which is most likely triggered by scramblases of types TMEM16F and Xkr-related protein 8 (Xkr8) [23–26]. TMEM16F is also a calcium-dependent scramblase [23–26] and, as such, is most likely involved in the translocation of PS onto the T cells surface since galectin-9 induces intracellular calcium mobilisation in T cells of all types [27]. Xkr8 is a caspase-3-dependent scramblase and can be activated by caspase-3 [23,25,26], the activity of which is significantly upregulated in cytotoxic T cells in a granzyme-B-dependent manner [7].

HMGB1, as a ligand of Toll-like receptors 2 and 4 [15,16], activates macrophages and their ability to phagocytose target cells. Tim-3 present on macrophage cell surfaces is involved in phagocytosis of T cells affected by galectin-9 (Fig. 6), which have two Tim-3 ligands present on their surface, galectin-9 and PS (known as an “eat me” signal [28]). This discovery explains the phenomenon of host T cells being phagocytosed by tumour-associated macrophages or placental macrophages.

Our results demonstrated another reason why LPS induces TGF- β production (the effect which has recently been reported [29]). While LPS directly induces innate immune reactions [13], the upregulation of TGF- β secretion triggers the production of the opsonising protein galectin-9 [8], which significantly enhances innate immune reactions to bacteria (Fig. 1).

Interestingly, other galectins (-4 and -8) with tandem structure and galectin-3 (a chimeric type of galectin) were recently reported to interact with bacterial LPS [30]. Further investigations would have to unravel the role of these galectins in the opsonisation of bacteria and T cells in human immune responses.

Taken together, our results strongly suggest that galectin-9 is involved in the opsonisation of Gram-negative bacteria thus promoting anti-bacterial immune defence, including innate immune reactions and phagocytosis. Opsonisation of T cells by galectin-9 allows it to protect embryos against cytotoxic attack by the mother’s immune system and recruit placental macrophages to phagocytose/remove T cells which potentially pose a threat to the developing embryo. Unfortunately, this phenomenon is also successfully used to protect malignant tumours against cytotoxic T cells and in recruiting tumour-associated macrophages to participate in the suppression of anti-cancer T cell function.

Furthermore, galectin-9 also induces T cells to produce TGF- β and HMGB1 which contribute further to an immunosuppressive milieu. Both factors can either directly (TGF- β) or indirectly (HMGB1, through TLR4-mediated TGF- β expression) induce galectin-9 expression in cancer cells and macrophages [8,16]. Interestingly, recent evidence demonstrated that intracellular galectin-9 expressed by T cells enhances proximal T cell receptor signalling [31], thus further biochemical studies may help to understand the mechanisms of regulation of galectin-9 expression in T cells, especially those infiltrated into malignant tumours.

Taken together, our results have shown that secreted and cell surface-associated galectin-9 plays crucial role both in anti-bacterial immune defence and in the suppression of cytotoxic lymphoid cell function during embryo development and malignant tumour progression.

Author contributions

SS, NHM, IMY and BFG performed majority of the experiments and analysed data (investigation, data curation). NA, EFK and SB completed the work with primary embryonic cells (investigation, methodology, data curation). VVS designed the study, planned all the experiments together with EFK, analysed the data (conceptualisation, data curation, investigation, methodology, supervision). VVS, BFG and EFK wrote the manuscript (writing original draft, review & editing).

Declaration of Competing Interest

The authors declare that they have no known competing financial interests or personal relationships that could have appeared to influence the work reported in this paper.

Acknowledgements

The authors are grateful to Dr Luca Varani from the Institute for Research in Biomedicine, Bellinzona, Switzerland for the gift of anti-Tim-3 antibodies. We sincerely thank Prof Fiedler and Dr Wellbrock from the Department of Oncology, Haematology and Bone Marrow Transplantation with Section Pneumology, Hubertus Wald University Cancer Center, University Medical Center Hamburg-Eppendorf, Germany for providing us with blood plasma obtained from AML patients.

BG and NHM acknowledge intramural funding support by the school of Medicine and Health Sciences, University of Oldenburg.

Appendix A. Supplementary material

Supplementary data to this article can be found online at <https://doi.org/10.1016/j.intimp.2021.108155>.

References

- [1] D. Delacour, A. Koch, R. Jacob, The role of galectins in protein trafficking, *Traffic* 10 (10) (2009) 1405–1413.
- [2] F.T. Liu, G.A. Rabinovich, Galectins: regulators of acute and chronic inflammation, *Ann. N. Y. Acad. Sci.* 1183 (2010) 158–182.
- [3] M. Nagae, N. Nishi, S. Nakamura-Tsuruta, J. Hirabayashi, S. Wakatsuki, R. Kato, Structural analysis of the human galectin-9 N-terminal carbohydrate recognition domain reveals unexpected properties that differ from the mouse orthologue, *J. Mol. Biol.* 375 (1) (2008) 119–135.
- [4] J. Wada, Y.S. Kanwar, Identification and characterization of galectin-9, a novel beta-galactoside-binding mammalian lectin, *J. biological. chem.* 272 (1997) 6078–6086.
- [5] D. Compagno, C. Tiraboschi, J.D. Garcia, Y. Rondon, E. Corapi, C. Velazquez, D. J. Laderach, Galectins as Checkpoints of the Immune System in Cancers, *Their Clinical Relevance, and Implication in Clinical Trials*, *Biomolecules* 10 (2020).
- [6] I. Gonçalves Silva, I.M. Yasinska, S.S. Sakhnevych, W. Fiedler, J. Wellbrock, M. Bardelli, L. Varani, R. Hussain, G. Ciccione, S.M. Berger, Y. A. Ushkaryov, B.F. Gibbs, E. Fasler-Kan, V.V. Sumbayev, The Tim-3-galectin-9 Secretory Pathway is Involved in the Immune Escape of Human Acute Myeloid Leukemia Cells, *EBioMedicine* 22 (2017) 44–57.
- [7] I.M. Yasinska, N.H. Meyer, S. Schlichtner, R. Hussain, G. Siligardi, M. Casely-Hayford, W. Fiedler, J. Wellbrock, C. Desmet, L. Calzolari, L. Varani, S.M. Berger,

- U. Raap, B.F. Gibbs, E. Fasler-Kan, V.V. Sumbayev, Ligand-Receptor Interactions of Galectin-9 and VISTA Suppress Human T Lymphocyte Cytotoxic Activity, *Front. Immunol.* 11 (2020), 580557.
- [8] A.T.H. Selno, S. Schlichtner, I.M. Yasinska, S.S. Sakhnevych, W. Fiedler, J. Wellbrock, E. Klenova, L. Pavlova, B.F. Gibbs, M. Degen, I. Schnyder, N. Aliu, S. M. Berger, E. Fasler-Kan, V.V. Sumbayev, Transforming growth factor beta type 1 (TGF-beta) and hypoxia-inducible factor 1 (HIF-1) transcription complex as master regulators of the immunosuppressive protein galectin-9 expression in human cancer and embryonic cells, *Aging.* 12 (2020) 23478–23496.
- [9] I. Vega-Carrascal, D.A. Bergin, O.J. McElvaney, C. McCarthy, N. Banville, K. Pohl, M. Hirashima, V.K. Kuchroo, E.P. Reeves, N.G. McElvaney, Galectin-9 signaling through TIM-3 is involved in neutrophil-mediated Gram-negative bacterial killing: an effect abrogated within the cystic fibrosis lung, *J. Immunol.* 192 (5) (2014) 2418–2431.
- [10] A. Prokhorov, B.F. Gibbs, M. Bardelli, L. Rüegg, E. Fasler-Kan, L. Varani, V. Sumbayev, The immune receptor Tim-3 mediates activation of PI3 kinase/mTOR and HIF-1 pathways in human myeloid leukaemia cells, *Int. J. Biochem. Cell Biol.* 59 (2015) 11–20.
- [11] *The AGT Cytogenetics Laboratory Manual. Third edition. Editors: Barch MJ, Knutsen T, Spurbeck J. Lippincott Williams, 1997.*
- [12] I.G. Silva, B.F. Gibbs, M. Bardelli, L. Varani, V.V. Sumbayev, Differential expression and biochemical activity of the immune receptor Tim-3 in healthy and malignant human myeloid cells, *Oncotarget.* 6 (32) (2015) 33823–33833.
- [13] S. Akira, K. Takeda, Toll-like receptor signalling, *Nat. Rev. Immunol.* 4 (7) (2004) 499–511.
- [14] W. Chen, M.E. Frank, W. Jin, S.M. Wahl, TGF-beta released by apoptotic T cells contributes to an immunosuppressive milieu, *Immunity* 14 (2001) 715–725.
- [15] I.M. Yasinska, I. Gonçalves Silva, S.S. Sakhnevych, L. Ruegg, R. Hussain, G. Siligardi, W. Fiedler, J. Wellbrock, M. Bardelli, L. Varani, U. Raap, S. Berger, B. F. Gibbs, E. Fasler-Kan, V.V. Sumbayev, High mobility group box 1 (HMGB1) acts as an “alarmin” to promote acute myeloid leukaemia progression, *Oncimmunology.* 7 (6) (2018) e1438109, <https://doi.org/10.1080/2162402X.2018.1438109>.
- [16] A.T.H. Selno, S. Schlichtner, I.M. Yasinska, S.S. Sakhnevych, W. Fiedler, J. Wellbrock, S.M. Berger, E. Klenova, B.F. Gibbs, E. Fasler-Kan, V.V. Sumbayev, High mobility group box 1 (HMGB1) induces Toll-like receptor 4-mediated production of the immunosuppressive protein galectin-9 in human cancer cells, *Front. Immunol.* 21 (12) (2021), 675731.
- [17] D. Ribet, P. Cossart, How bacterial pathogens colonize their hosts and invade deeper tissues, *Microbes Infect.* 17 (3) (2015) 173–183.
- [18] J.A. Roberts, B.I. Marklund, D. Ilver, D. Haslam, M.B. Kaack, G. Baskin, M. Louis, R. Mollby, J. Winberg, S. Normark, The Gal(alpha 1-4)Gal-specific tip adhesin of *Escherichia coli* P-fimbriae is needed for pyelonephritis to occur in the normal urinary tract, *PNAS* 91 (25) (1994) 11889–11893.
- [19] J. Lillington, S. Geibel, G. Waksman, Biogenesis and adhesion of type 1 and P pili, *BBA* 1840 (9) (2014) 2783–2793.
- [20] S. Melville, L. Craig, Type IV pili in Gram-positive bacteria, *Microbiology and molecular biology reviews* : MMBR. 77 (3) (2013) 323–341.
- [21] I. Okoye, L. Xu, M. Motamedi, P. Parashar, J.W. Walker, S. Elahi, Galectin-9 expression defines exhausted T cells and impaired cytotoxic NK cells in patients with virus-associated solid tumors, *J. Immunother. Cancer* 8 (2) (2020) e001849, <https://doi.org/10.1136/jitc-2020-001849>.
- [22] C. Wu, T. Thalhamer, R. Franca, S. Xiao, C. Wang, C. Hotta, C. Zhu, M. Hirashima, A. Anderson, V. Kuchroo, Galectin-9-CD44 interaction enhances stability and function of adaptive regulatory T cells, *Immunity* 41 (2) (2014) 270–282.
- [23] G. Mariño, G. Kroemer, Mechanisms of apoptotic phosphatidylserine exposure, *Cell Res.* 23 (11) (2013) 1247–1248.
- [24] J. Suzuki, D.P. Denning, E. Imanishi, H.R. Horvitz, S. Nagata, Xk-related protein 8 and CED-8 promote phosphatidylserine exposure in apoptotic cells, *Science* 341 (6144) (2013) 403–406.
- [25] J. Suzuki, M. Umeda, P.J. Sims, S. Nagata, Calcium-dependent phospholipid scrambling by TMEM16F, *Nature* 468 (7325) (2010) 834–838.
- [26] S.R. Bushell, A.C.W. Pike, M.E. Falzone, N.J.G. Rorsman, C.M. Ta, R.A. Corey, T. D. Newport, J.C. Christianson, L.F. Scofano, C.A. Shintre, A. Tessitore, A. Chu, Q. Wang, L. Shrestha, S.M.M. Mukhopadhyay, J.D. Love, N.A. Burgess-Brown, R. Sitsapesan, P.J. Stansfeld, J.T. Huiskonen, P. Tammaro, A. Accardi, E. P. Carpenter, The structural basis of lipid scrambling and inactivation in the endoplasmic reticulum scramblase TMEM16K, *Nat. Commun.* 10 (2019) 3956.
- [27] C. Lhuillier, C. Barjon, T. Niki, A. Gelin, F. Praz, O. Morales, S. Souquere, M. Hirashima, M. Wei, O. Dellis, P. Busson, Impact of Exogenous Galectin-9 on Human T Cells: CONTRIBUTION OF THE T CELL RECEPTOR COMPLEX TO ANTIGEN-INDEPENDENT ACTIVATION BUT NOT TO APOPTOSIS INDUCTION, *J. biological. chem.* 290 (27) (2015) 16797–16811.
- [28] Y. Kikushige, T. Miyamoto, TIM-3 as a novel therapeutic target for eradicating acute myelogenous leukemia stem cells, *Int. J. Hematol.* 98 (6) (2013) 627–633.
- [29] L. Sun, M. Xiu, S. Wang, D.R. Brigstock, H. Li, L. Qu, R. Gao, Lipopolysaccharide enhances TGF-beta1 signalling pathway and rat pancreatic fibrosis, *J. Cell Mol. Med.* 22 (2018) 2346–2356.
- [30] M.A. Campanero-Rhodes, I. Kalograiaki, B. Euba, E. Llobet, A. Ardá, J. Jiménez-Barbero, J. Garmendia, D. Solís, Exploration of Galectin Ligands Displayed on Gram-Negative Respiratory Bacterial Pathogens with Different Cell Surface Architectures, *Biomolecules.* 11 (4) (2021) 595, <https://doi.org/10.3390/biom11040595>.
- [31] H.-Y. Chen, Y.-F. Wu, F.-C. Chou, Y.-H. Wu, L.-T. Yeh, K.-I. Lin, F.-T. Liu, H.-K. Sytwu, Intracellular galectin-9 enhances proximal TCR signaling and potentiates autoimmune diseases, *J. Immunol.* 204 (2020) 1158–1172.



OPEN ACCESS

Edited by:

Insan Ullah,
Khyber Medical University, Pakistan

Reviewed by:

Francesca Romana Mariotti,
Bambino Gesù Children's Hospital
(IRCCS), Italy

Michele Bernasconi,
University Children's Hospital
Bern, Switzerland
Oksana Kunduzova,
Institut National de la Santé et de la
Recherche Médicale
(INSERM), France

Dmitri Pchejetski,
University of East Anglia,
United Kingdom
Michael Danilenko,
Ben-Gurion University of the
Negev, Israel

***Correspondence:**

Vadim V. Sumbayev
V.Sumbayev@kent.ac.uk
Elizaveta Faslter-Kan
elizaveta.faslter@insel.ch
Bernhard F. Gibbs
bernhard.gibbs@uni-oldenburg.de

Specialty section:

This article was submitted to
Pathology,
a section of the journal
Frontiers in Medicine

Received: 07 October 2021

Accepted: 17 January 2022

Published: 10 February 2022

Citation:

Schlichtner S, Yasinska IM,
Ruggiero S, Berger SM, Aliu N,
Prunk M, Kos J, Meyer NH, Gibbs BF,
Faslter-Kan E and Sumbayev VV
(2022) Expression of the Immune
Checkpoint Protein VISTA Is
Differentially Regulated by the TGF- β 1
– Smad3 Signaling Pathway in Rapidly
Proliferating Human Cells and T
Lymphocytes. *Front. Med.* 9:790995.
doi: 10.3389/fmed.2022.790995

Expression of the Immune Checkpoint Protein VISTA Is Differentially Regulated by the TGF- β 1 – Smad3 Signaling Pathway in Rapidly Proliferating Human Cells and T Lymphocytes

Stephanie Schlichtner¹, Inna M. Yasinska¹, Sabrina Ruggiero², Steffen M. Berger², Nijas Aliu³, Mateja Prunk⁴, Janko Kos^{4,5}, N. Helge Meyer^{6,7}, Bernhard F. Gibbs^{6*}, Elizaveta Faslter-Kan^{2,8*} and Vadim V. Sumbayev^{1*}

¹ Medway School of Pharmacy, Universities of Kent and Greenwich, Chatham Maritime, United Kingdom, ² Department of Pediatric Surgery, Children's Hospital, Inselspital Bern, University of Bern, Bern, Switzerland, ³ Department of Human Genetics, Inselspital Bern, University of Bern, Bern, Switzerland, ⁴ Department of Biotechnology, Jožef Stefan Institute, Ljubljana, Slovenia, ⁵ Faculty of Pharmacy, University of Ljubljana, Ljubljana, Slovenia, ⁶ Division of Experimental Allergology and Immunodermatology, Department of Human Medicine, University of Oldenburg, Oldenburg, Germany, ⁷ Division of General and Visceral Surgery, Department of Human Medicine, University of Oldenburg, Oldenburg, Germany, ⁸ Department of Biomedicine, University of Basel and University Hospital Basel, Basel, Switzerland

Immune checkpoint proteins play crucial roles in human embryonic development but are also used by cancer cells to escape immune surveillance. These proteins and biochemical pathways associated with them form a complex machinery capable of blocking the ability of cytotoxic immune lymphoid cells to attack cancer cells and, ultimately, to fully suppress anti-tumor immunity. One of the more recently discovered immune checkpoint proteins is V-domain Ig-containing suppressor of T cell activation (VISTA), which plays a crucial role in anti-cancer immune evasion pathways. The biochemical mechanisms underlying regulation of VISTA expression remain unknown. Here, we report for the first time that VISTA expression is controlled by the transforming growth factor beta type 1 (TGF- β)-Smad3 signaling pathway. However, in T lymphocytes, we found that VISTA expression was differentially regulated by TGF- β depending on their immune profile. Taken together, our results demonstrate the differential biochemical control of VISTA expression in human T cells and various types of rapidly proliferating cells, including cancer cells, fetal cells and keratinocytes.

Keywords: immune checkpoint, VISTA, anti-cancer immunity, T lymphocytes, galectin-9

INTRODUCTION

Immune checkpoint proteins play crucial roles in determining the ability of human cancer cells to escape immune surveillance (1, 2). These proteins integrate into a complex machinery which is capable of blocking cytotoxic immune attacks on cancer cells by specialized human lymphoid cells and, in the long run, to fully suppress anti-tumor immunity (1, 2). These pathways can play

fundamental roles and were found to be implemented by human fetal cells in order to protect the embryo against rejection by the mother's immune system (3).

With some immune checkpoint proteins, such as programmed cell death protein 1 (PD-1) and its ligand (PD-L1), cytotoxic T-lymphocyte-associated protein 4 (CTLA4), T cell immunoglobulin and mucin domain containing protein 3 (Tim-3) and its ligand galectin-9, the biochemical mechanisms underlying their expression and regulation of their biological activities have been elucidated (1, 2, 4). Others were only discovered recently and thus such mechanisms remain poorly understood. However, this is a very important issue since identification of the optimal targets for immunotherapy of cancer crucially hinges on our understanding of the biochemistry of immune checkpoint pathways responsible for immune escape. One of such immune checkpoint proteins is V-domain Ig-containing suppressor of T cell activation (VISTA) which plays a crucial role in the suppression of human T cell responses during cancer progression (5–7). VISTA is expressed mainly in blood cells and plays a complex role in regulating immune responses (5–7). Myeloid cells show the highest levels of expression, but lymphoid cells, especially T lymphocytes also express this protein where it can be used as a receptor to suppress their anti-cancer activities (5–7). Interestingly, VISTA has been reported to display both receptor and ligand properties (5–7). However, its receptors (when it acts as a ligand) remain to be identified. One of the VISTA ligands is VSIG3 (V-set and immunoglobulin domain containing 3), which is a member of the immunoglobulin superfamily and is highly expressed in human brain and testis (8). Another VISTA ligand is galectin-9, which is a member of galectin family of proteins conserved throughout evolution (9). Galectin-9 contains two similar, but not identical, subunits bound through a peptide linker, which can be of different size (9, 10). There are three isoforms of galectin-9 which vary in linker size (10). Galectin-9 isoforms can interact with VISTA on the surface of cytotoxic T cells and induce programmed death most likely through prevention of granzyme B release from these cells. Granzyme B is a proteolytic enzyme used to induce apoptotic death of target cells, and its activation inside cytotoxic T cells, which fail to release it, is followed by their programmed death (9). Several types of human cancer cells are known to express VISTA too (11, 12). However, the mechanisms which regulate VISTA expression in human cells remain unknown. By analyzing the promoter region of human VISTA, we noticed that it contains response elements for Smad3 transcription factor which is activated by human transforming growth factor beta type 1 (TGF- β) through specific plasma membrane-associated receptors. Interestingly, we have recently reported that the TGF- β -Smad3 pathway is involved in regulating galectin-9 expression in human cancer and embryonic cells (3). TGF- β displays both autocrine and paracrine activities and is able to induce its own expression, which is also Smad3-dependent as is the expression of galectin-9 (3). Thus, in both cancer and embryonic cells, this pathway is self-controlling and self-sustaining. In this work we aimed to study whether the TGF- β -Smad3 pathway is also involved in VISTA expression.

We discovered for the first time that VISTA expression is controlled by the TGF- β -Smad3 signaling pathway. Interestingly, in T lymphocytes, VISTA is only upregulated by TGF- β if they do not display cytotoxic activity (lack granzyme B expression), while if T cells express this proteolytic enzyme and display cytotoxic activity, VISTA expression is decreased in the presence of TGF- β . We hypothesized that this phenomenon could be possibly triggered by differential nuclear compartmentalisation of VISTA encoding gene (VSIG).

MATERIALS AND METHODS

Materials

RPMI-1640 medium for cell culture, fetal bovine serum, supplements and basic laboratory chemicals were purchased from Sigma (Suffolk, UK). Microtiter plates for ELISA were obtained from Oxley Hughes Ltd (London, UK). Rabbit antibodies against VISTA, galectin-9, granzyme B, phospho-S423/S425-Smad3, Smad4 and TRIM33 as well as goat anti-rabbit horseradish peroxidase (HRP) labeled secondary antibody were purchased from Abcam (Cambridge, UK). Antibodies against β -actin were purchased from Proteintech (Manchester, UK). Goat anti-mouse and anti-rabbit fluorescently-labeled dye secondary antibodies were obtained from Li-COR (Lincoln, NE, USA). Mouse anti-Smad3 antibody, ELISA-based assay kits for the detection of VISTA, galectin-9 (both kits contain mouse capture antibodies against VISTA and galectin-9, respectively) and TGF- β as well as human recombinant TGF- β 1 protein and mouse anti-Smad3 antibody were purchased from Bio-Techne (R&D Systems, Abingdon, UK). Anti-Tim-3 mouse monoclonal antibody was described before (13). All other chemicals employed in this study were of the highest grade of purity commercially available.

Cell Lines and Primary Human Samples

Cell lines used in this work were purchased from either the European Collection of Cell Cultures, American Tissue Culture Collection or CLS Cell Lines Service GmbH. Cell lines were accompanied by identification test certificates. Wilms Tumor cell line WT3ab was kindly provided by Dr. C. Stock (Children's Cancer Research Institute, Vienna, Austria) and cultured as it was previously described (14).

Jurkat T, MCF-7, THP-1, WT-3ab, HaCaT keratinocytes and K562 were cultured in RPMI 1640 media supplemented with 10% fetal bovine serum, penicillin (50 IU/ml), and streptomycin sulfate (50 μ g/ml).

TALL-104 CD8-positive cytotoxic T lymphocytes, derived from human acute lymphoblastic leukemia (TALL), were cultured according to the ATCC instructions. Briefly, ATCC-formulated Iscove's Modified Dulbecco's Medium was used. To make the complete growth medium we added 100 units/ml recombinant human IL-2; 2.5 μ g/ml human albumin; 0.5 μ g/ml D-mannitol and fetal bovine serum to a final concentration of 20% (15). Medium was also supplemented with penicillin (50 IU/ml), and streptomycin sulfate (50 μ g/ml).

Primary human AML mononuclear blasts (AML-PB001F, newly diagnosed/untreated) were also purchased from

AllCells (Alameda, CA, USA) and handled according to the manufacturer's recommendations. The studies were performed following ethical approval (REC reference: 16-SS-033).

Placental tissues (CVS, chorionic villus sampling) and amniotic fluids were collected after obtaining informed written consent from pregnant women at the University Hospital Bern, Inselspital. Fetal cells were handled and cultured as described before (3, 16).

Primary human T cells were isolated from buffy coat blood (purchased from the Deutsches Rotes Kreuz and following ethical approval from the Medizinische Ethikkommission der Carl von Ossietzky Universität Oldenburg) using Ficoll-density centrifugation. PBMCs were collected and T cells purified using a commercial CD3 T cell negative isolation kit (Biolegend) according to the manufacturer's protocol. 200,000 T cells per 200 μ l were incubated for 16 h with and without TGF- β at a final concentration of 2 ng/ml in RPMI medium.

Western Blot Analysis

VISTA, granzyme B, galectin-9, Tim-3, phospho-S423/S425 Smad-3, Smad4 and TRIM33 were measured by Western blot and compared to the amounts of β -actin (protein loading control), as previously described (17).

Li-Cor goat secondary antibodies conjugated with infrared fluorescent dyes, were used as described in the manufacturer's protocol for visualization of specific proteins (Li-Cor Odyssey imaging system was employed). Western blot data were quantitatively analyzed using Odyssey software called Image Studio and values were subsequently normalized against those of β -actin.

Chromatin Immunoprecipitation (ChIP)

ChIP was performed as described recently (18). Resting Jurkat T cells and those treated for 24 h with 2 ng/ml TGF- β were subjected to the study. 5×10^6 cells were used for immunoprecipitation. Cross-linking was performed using 1.42% formaldehyde followed by quenching with 125 mM glycine for 5 min. Cells were then washed twice with PBS and subjected to ChIP in accordance with ChIP-IT high sensitivity kit (Active Motif) protocol. Immunoprecipitation was performed using mouse monoclonal anti-Smad3 antibody (R&D Systems, Abingdon, UK), and IgG isotype control antibody was used for a negative control IP. The Smad3 epitope recognized by this antibody does not overlap with DNA and co-activator binding sites of this protein. Immunoprecipitated DNA was then purified and subjected to quantitative real-time PCR (qRT-PCR) which was performed as outlined below. The following primers were designed using NCBI Primer-Blast primer designing tool: forward - 5'-GCCTACCACATACCAAGCCC-3' and reverse: 5'-ATCGGCAGTTTAAAGCCCGT-3'. These primers allow to amplify the fragment of the promoter region of VSIG (VISTA gene), which surrounds Smad3-binding sites.

qRT-PCR Analysis

To detect VISTA mRNA levels, we used qRT-PCR (15). Total RNA was isolated using a GenEluteTM mammalian total RNA

preparation kit (Sigma-Aldrich) according to the manufacturer's protocol, followed by reverse transcriptase-polymerase chain reaction (RT-PCR) of a target protein mRNA (also performed according to the manufacturer's protocol). This was followed by qRT-PCR. The following primers were used. VISTA: forward - 5'-GATGCACCATCCAACCTGTGT-3', reverse - 5'-GCAGAGGATTCCTACGATGC-3'; actin: forward - 5'-TGACGGGGTCACCCACACTGTGCCCATCTA-3', reverse - 5'-CTAGAAGCATTTGCGGTGCGACGATGGAGGG-3'. Reactions were performed using a LightCycler[®] 480 qRT-PCR machine and SYBR Green I Master kit (Roche, Burgess Hill, UK). The assay was performed according to the manufacturer's protocol. Values representing VISTA mRNA levels were normalized against those of β -actin.

On-Cell Western Analysis

Cell surface levels of VISTA protein were analyzed using on-cell Western analysis performed using a Li-COR Odyssey imager and the assay was performed in line with manufacturer's recommendations as previously described (9).

Enzyme-Linked Immunosorbent Assays (ELISAs)

Secreted VISTA and TGF- β were measured in cell culture medium (VISTA was also measured in some of the cell lysates), by ELISA using R&D Systems kits (see Section Materials) according to manufacturer's protocols. To study recruitment of co-activators Smad4 and TRIM33 by Smad3 we used ELISA-based assay where we applied mouse anti-Smad3 antibody (R&D Systems) as capture. The plate was coated with this antibody (1:500) overnight followed by blocking with 1% BSA (dissolved in phosphate buffered saline, PBS). Then cell lysates were applied and incubated for 2 h followed by 5 times washing with TBS (50 mM Tris-HCl, 140 mM NaCl, pH 7.3) containing 0.1% Tween 20 (TBST). Rabbit anti-TRIM33 or anti-Smad4 antibodies were used (1:1000, 2h incubation) to detect these proteins interacted with Smad3. Finally, the plates were washed 5 times with TBST and horseradish peroxidase (HRP) labeled goat anti-rabbit antibody was applied for 1 h at room temperature. The plates were washed 5 times with TBST followed by visualization through the peroxidase reaction (ortho-phenylenediamine/H₂O₂). The reactions were quenched after 10 min with an equal volume of 1 M H₂SO₄ and the color development was measured in a microplate reader as the absorbance at 492 nm. Schematically both ELISA formats are illustrated in **Supplementary Figure 1**.

Statistical Analysis

Each experiment was performed at least three times and statistical analysis, was conducted using a two-tailed Student's *t*-test. Statistical probabilities (*p*) were expressed as * when *p* < 0.05; ** when *p* < 0.01 and *** when *p* < 0.001.

RESULTS

Firstly, we observed whether TGF- β could induce VISTA expression in human T cells, since this protein was found to mediate galectin-9-induced apoptosis in cytotoxic T lymphocytes (9). We used non-treated Jurkat T cells (CD4-positive), which express just traces of granzyme B protein (9, 16), as well as PMA-activated (activation was performed for 24 h using 100 nM PMA) Jurkat T cells which express granzyme B protein (9, 16). Cells were exposed for 24 h to 2 ng/ml TGF- β followed by detection of VISTA expression by Western blot analysis. We found that TGF- β significantly upregulated VISTA expression in resting Jurkat T cells (**Figure 1A**) while, in PMA-activated cells, VISTA levels were reduced by exposure to TGF- β compared to the non-treated cells (**Figure 1B**). In both cell types TGF- β induced phosphorylation of Smad3 transcription factor (**Supplementary Figure 2A**). We then tested cytotoxic CD8-positive TALL-104 cells. Similarly to granzyme B-expressing PMA-activated Jurkat T cells (**Figure 1B**), TGF- β (2 ng/ml for 24 h) reduced VISTA expression in TALL-104 cells (**Figure 1C**). However, Smad3 phosphorylation was upregulated by TGF- β (**Supplementary Figure 2B right panel**). The expression levels of granzyme B were downregulated by TGF- β in TALL-104 cells (**Supplementary Figure 2B, right panel**), which is in line with a previous observation reporting TGF- β -induced downregulation of granzyme B expression in cytotoxic T cells (19). Importantly, TALL-104 cells expressed Tim-3 and rather small amounts of galectin-9 (**Supplementary Figure 2B, left panel**). Expression of both proteins was not affected by TGF- β (**Supplementary Figure 2B, left panel**). We then isolated primary human T cells (all CD3 positive cells were isolated to allow for the presence of CD8-positive cytotoxic T cells, CD4-positive helper type T cells and CD4-positive cytotoxic cells). These cells were then exposed to 2 ng/ml TGF- β for 16 h (given the higher reactivity of primary T cells compared to T cell lines). Both VISTA and granzyme B expressions were lowered by TGF- β in these cells (**Figure 1D**). Primary human T cells expressed both Tim-3 and galectin-9 (**Supplementary Figure 2C**), but galectin-9 levels were very low (**Supplementary Figure 2C**). Smad3 phosphorylation was highly upregulated by TGF- β in primary T cells. We then tested human myeloid leukemia cells, which are known to express high levels of VISTA. We used the THP-1 cell line (monocytic leukemia) and more premature primary human acute myeloid leukemia (AML) blasts. In THP-1 cells, TGF- β is known to highly upregulate galectin-9 expression in a Smad3-dependent manner (a significant increase in Smad3 phosphorylation induced by TGF- β was also reported for these cells) (3, 20). Furthermore, THP-1 cells do not express detectable amounts of granzyme B protein and do not show detectable catalytic activity of this enzyme (9). However, TGF- β downregulated VISTA expression in THP-1 cells (**Figure 1E**). On the other hand, in primary AML blasts, VISTA expression was significantly upregulated by TGF- β (**Figure 1F**). Given the variation in the effects observed, we investigated whether TGF- β can induce VISTA expression in the cells, which in a resting state do not express this protein. We investigated MCF-7 human epithelial breast cancer

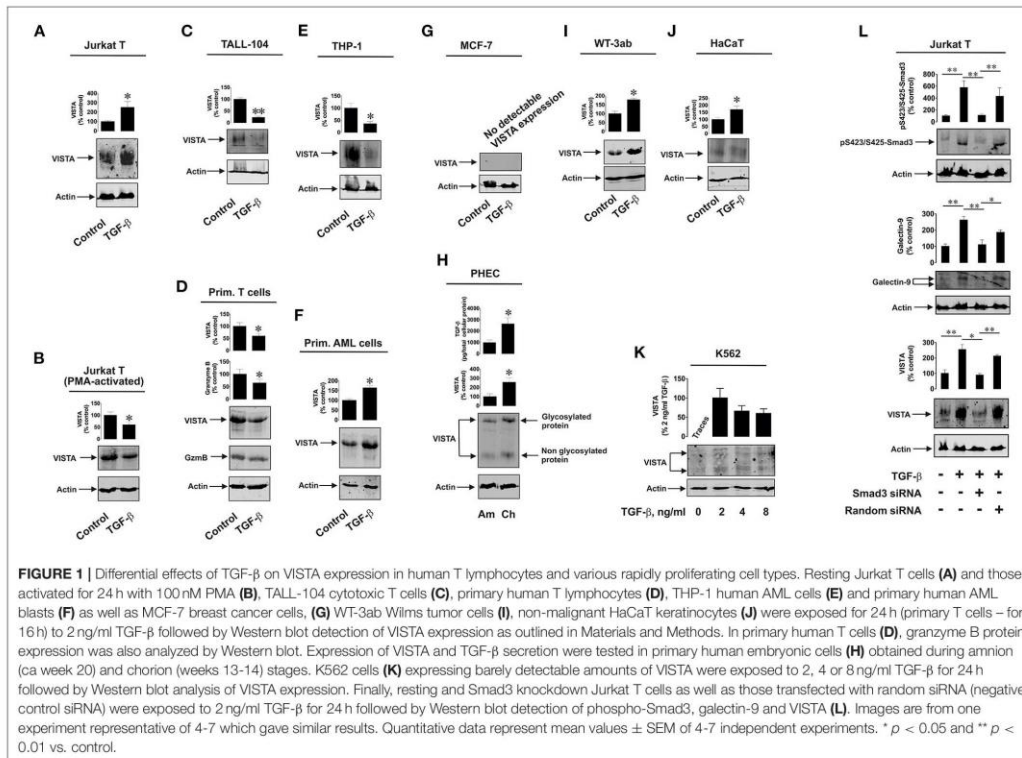
cells, where TGF- β was reported to trigger the expression of galectin-9 (3) and discovered that TGF- β was unable to induce even traces of VISTA expression (**Figure 1G**). VISTA mRNA was also barely detectable in these cells by qRT-PCR (**Supplementary Figure 3**).

Interestingly, primary human embryonic cells express VISTA protein which is also present on their surface (16). The earlier the stage of pregnancy, the more TGF- β fetal cells produce (3). We compared primary human fetal cells taken at the amnion stage (*ca.* week 20) and chorion stage (weeks 13–14). In line with our previously reported results (3, 16), cells obtained at the chorion stage released significantly higher levels of TGF- β and expressed higher VISTA levels (**Figure 1H**). Also, we reported earlier that Smad3 phosphorylation levels are significantly higher in fetal cells obtained at chorion stage (3). Some solid tumor cells also express VISTA, which may be upregulated by TGF- β . We found that in human Wilms tumor (a type of pediatric kidney tumor) cells WT-3ab, which express VISTA, TGF- β significantly upregulated its expression (**Figure 1I**). These cells expressed small amounts of Tim-3 but higher amounts of galectin-9. Galectin-9 expression in these cells was upregulated by TGF- β , as in other cancer cells studied in the past (3), and this correlated with TGF- β -induced Smad3 phosphorylation (**Supplementary Figure 4**).

The same effect applied to non-malignant, rapidly proliferating, human keratinocytes (HaCaT). These cells express VISTA, and this expression was upregulated by 24 h exposure to 2 ng/ml TGF- β [**Figure 1J**; Smad3 activation in these cells takes place as well, though differently from the one reported for cancer and embryonic cells (3)]. Interestingly, in lymphoblasts isolated from human chronic myelogenous leukaemia (K562), which express traces of VISTA, this expression (unlike in MCF-7 cells where no VISTA protein expression is detected at all) can be induced by 24 h of exposure to 2 ng/ml TGF- β where this concentration appears to be the most effective (**Figure 1K**). Higher TGF- β concentrations (4 and 8 ng/ml) also induced VISTA expression, but the expression level was not higher compared to those observed with exposure to 2 ng/ml TGF- β . Resting K562 cells were reported to show undetectable amounts of phospho-Smad3, but this was highly upregulated by TGF- β (3).

Interestingly, most of the investigated cell types display glycosylated VISTA with a molecular weight of *ca.* 52 kDa [this phenomenon was discussed previously (9)], while others have some partially glycosylated (K562, **Figure 1K**) or non-glycosylated (molecular weight *ca.* 30 kDa; primary human embryonic cells, **Figure 1H**) VISTA. Since biologically functional VISTA is known to be glycosylated [52 kDa (9)], these results suggest that the glycosylation velocity of this protein may vary depending on the cell type. It is also possible that primary human embryonic cells store certain amounts of non-glycosylated VISTA, though the reason for this remains to be understood.

We then asked whether TGF- β -induced VISTA expression is Smad3-dependent or not. We used resting Jurkat T cells which we transfected with Smad3 siRNA (or random siRNA – negative control). Successful knockdown (in terms of biological effect) was monitored by Western blot analysis of intracellular levels of



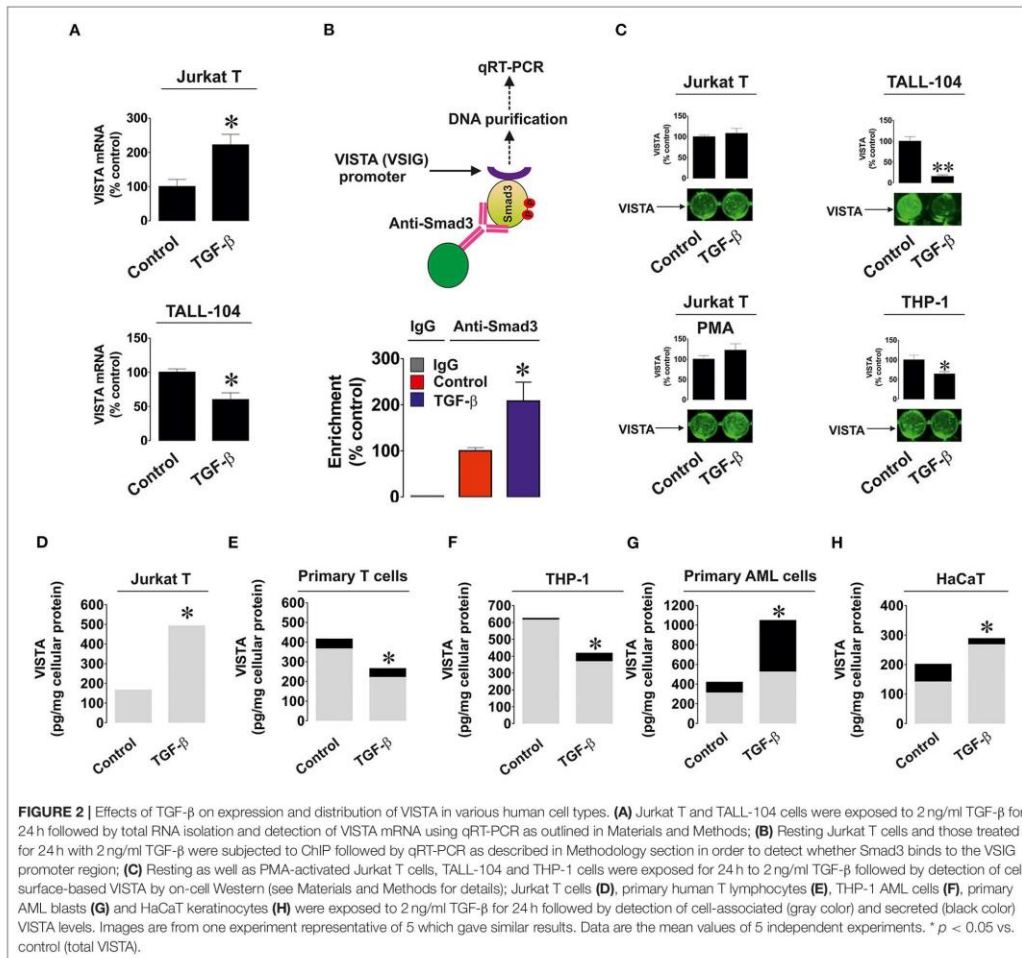
phosphorylated Smad3. Expressions of both VISTA and galectin-9 were induced by TGF- β and attenuated by Smad3 siRNA but not random siRNA (Figure 1L). This suggests that the process is Smad3-dependent.

We investigated whether the observed effects are taking place at mRNA level given the fact that TGF- β -regulated VISTA expression appeared to be Smad3 (transcription factor)-dependent. We used resting and TGF- β -treated (2 ng/ml for 24 h) Jurkat T (where TGF- β upregulates VISTA expression) and TALL-104 cells (where TGF- β treatment downregulated VISTA expression) and measured VISTA mRNA levels as outlined in Materials and Methods. We found that in Jurkat T cells TGF- β significantly upregulated VISTA mRNA levels while in TALL-104 we observed significant downregulation (Figure 2A). To verify that Smad3 binds VSIG (VISTA gene) directly we used ChIP qRT-PCR which confirmed that this process does take place and TGF- β significantly increased the fold of enrichment (Figure 2B) confirming that Smad3 can directly interact with the VSIG promoter region.

Importantly, we tested whether TGF- β impacted the cell surface presence and secretion of VISTA. We detected VISTA on the cell surface of resting and PMA-activated Jurkat T cells,

TALL-104 and THP-1 cells with or without exposure to 2 ng/ml TGF- β for 24 h. The results suggested when the total amounts of VISTA were strongly downregulated (TALL-104 and THP-1 cells), VISTA surface presence was reduced. In other cases, TGF- β did not significantly impact VISTA cell surface presence (Figure 2C), suggesting that this growth factor mainly controls VISTA expression but not its distribution within the cell. We also measured both cell-associated and secreted protein using ELISA. We tested Jurkat T cells (Figure 2D), primary human T cells (Figure 2E), THP-1 cells (Figure 2F), primary human AML cells (Figure 2G), and HaCaT keratinocytes (Figure 2H). Other cell types reported in Figure 1 did not secrete VISTA. The mean values \pm SEM of cell-associated and secreted VISTA are shown in Supplementary Table 1. We observed that TGF- β only significantly affected VISTA secretion (upregulation) in AML cells, whereas total expression levels remained in line with our Western blot observations (Figures 2D–H and see also Figures 1A–K for comparison). This also suggests that TGF- β itself is unlikely to impact VISTA secretion in any of the cell types.

We then assessed if the differential effects observed could be due to involvement of different Smad3 co-activators – TRIM33 (tripartite motif-containing protein 33), also known

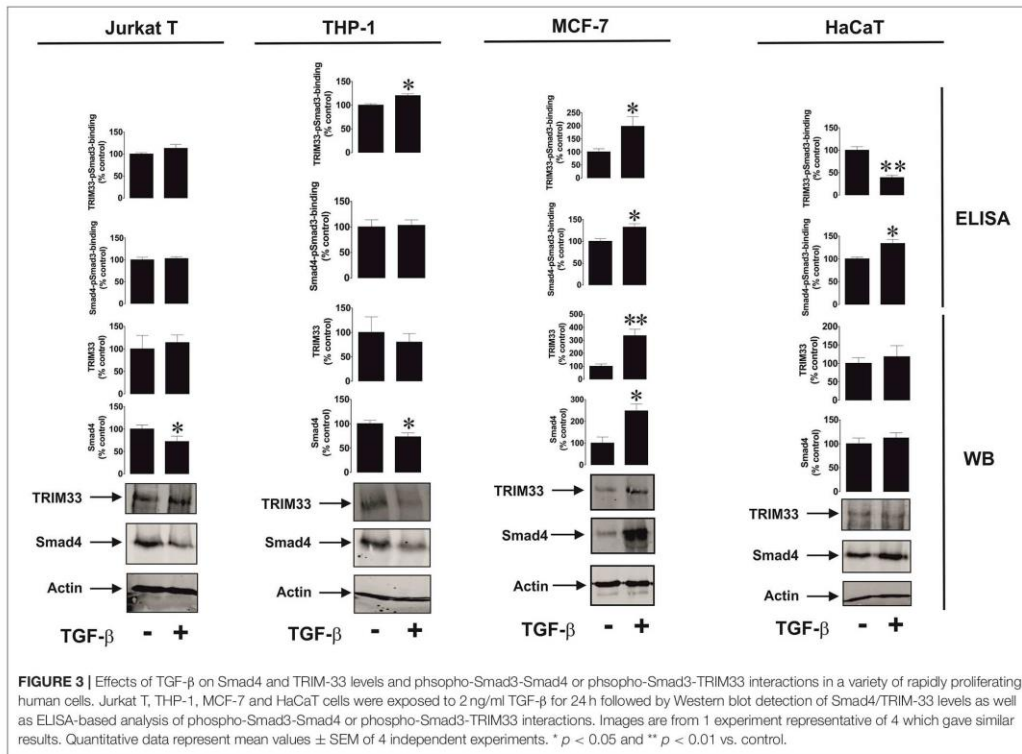


as transcriptional intermediary factor 1 gamma (TIF-1 γ), and Smad4 (21). TRIM33 is known mainly to interact with Smad3 in order to induce expression of repressed genes (21), while Smad4 is used to trigger expression of non-repressed target genes. We tested resting Jurkat T cells (VISTA expression is upregulated by TGF- β), THP-1 (downregulation of VISTA expression by TGF- β), MCF-7 (no effect, since the cells do not express detectable amounts of VISTA) and HaCaT (where VISTA expression is upregulated by TGF- β). We also tested the recruitment of both co-activators by Smad3 using an ELISA-based assay (see Section Materials and Methods and **Supplementary Figure 1** for details). We found that there was no specific correlation between the effect of TGF- β on VISTA expression and the amounts of Smad4/TRIM33 accumulated in the cells or recruited by Smad3

(**Figure 3**). This suggests that the effects observed are unlikely to be due to the involvement of differential co-activators in different cell types.

DISCUSSION

VISTA has recently been reported to actively participate in the suppression of anti-cancer cytotoxic immune responses of T cells (5, 9). However, the mechanisms underlying the expression of this crucial immune checkpoint protein remain unknown. The promoter region of the VISTA gene, VSIR, contains several Smad response elements. As such, we hypothesized that the TGF- β -Smad3 pathway could be responsible for inducing

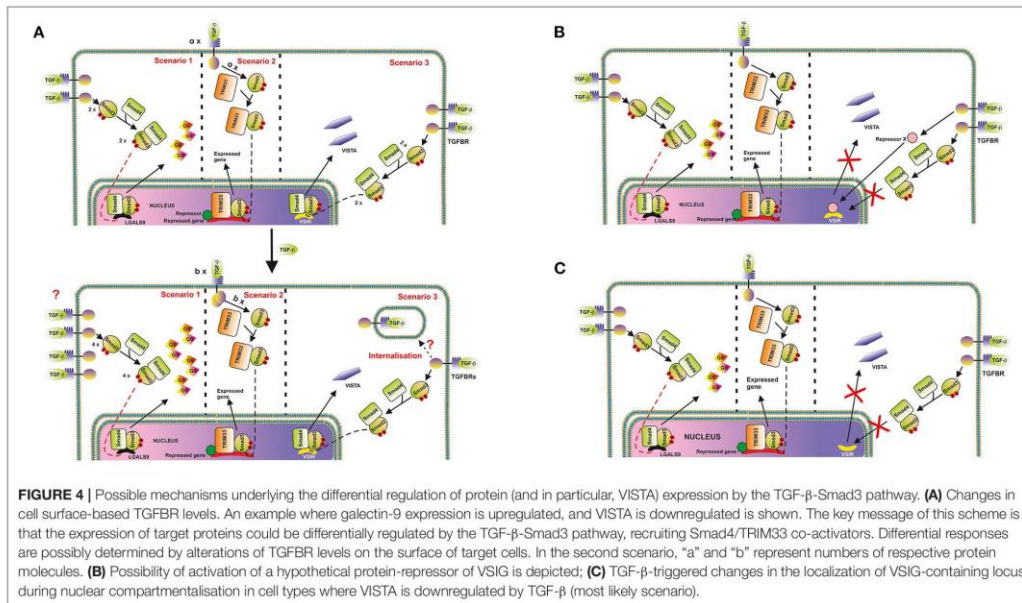


VISTA expression. The experiments showed that TGF- β -induced Smad3 activation led to an increase in VISTA expression in various cell types including resting CD4-positive Jurkat T cells, primary human AML blasts derived from myeloid cell precursors, primary human embryonic cells, Wilms tumor cells, chronic AML cells and HaCaT keratinocytes. In other cell types studied – PMA-activated, granzyme B expressing Jurkat T cells with cytotoxic activity, cytotoxic CD8-positive TALL-104 cells, primary CD3-positive human T lymphocytes (in both cell types, the overall granzyme B expression level is high) and monocytic AML THP-1 cells [which, unlike cytotoxic T cells, do not express detectable amounts of granzyme B protein (9)] – VISTA expression was reduced.

The biological reason for the observed downregulatory effects in various types of T cells described above is most likely their biological function associated with cytotoxic activity (granzyme B expression is used as a marker of their cytotoxic activity). As we have recently reported, galectin-9 interacts with VISTA on the surface of granzyme B-expressing T cells, which leads to leakage of granzyme B from intracellular granules, resulting in its activation (9). As such, these T cells may undergo programmed death mediated by VISTA. As seen in **Figure 1D**

and **Supplementary Figure 2**, granzyme B expression is reduced by exposure of the cells to TGF- β , which is in line with previous observations (19). With monocytic AML cells, which do not express detectable amounts of granzyme B protein (9), this biological response has probably more complex reasons. THP-1 cells secrete high levels of galectin-9, especially when pre-treated with PMA or other triggers of exocytosis (such as latrotoxin, or Toll-like receptor (TLR) ligands) (20). They are also capable of secreting VISTA. Importantly, secretion of both proteins may be required to suppress cytotoxic immune attack conducted by T cells. However, a certain ratio of the amounts of galectin-9 and VISTA secreted is important to achieve the immunosuppressive effect, as we have recently shown (9). TGF- β induces galectin-9 expression in THP-1 cells but not its secretion (3). Upregulation of VISTA expression could potentially lead to increased level of its translocation onto the cell surface with possible shedding, leading to increased levels of soluble VISTA (the evidence of such an effect can be seen in **Figure 2F**). As a result, this kind of response could be required to sustain an effective ratio of secreted galectin-9 and VISTA proteins.

Importantly, TGF- β was only able to induce VISTA expression in cells which already express detectable amounts of this protein.



If cells did not express VISTA (MCF-7), no TGF- β -dependent induction was observed (as it can be seen from **Figure 1G**). Smad3 was obviously responsible for the process of TGF- β -induced VISTA expression. Knock-down of Smad3 expression by siRNA led to attenuation of TGF- β -induced VISTA expression in Jurkat T cells (**Figure 1L**). Further experiments demonstrated that the observed effects take place on both protein and mRNA levels. Furthermore, Smad3 was found to directly bind to the VISTA (VISTA gene) promoter region using ChIP followed by qRT-PCR (**Figures 2A,B**).

However, it is necessary to understand how such a differential effect of TGF- β on VISTA expression can be achieved biochemically. The activities of the Smad3 co-activators Smad4 and TRIM33 did not appear to determine any differences in response (**Figure 3**). Clearly, some cells use more Smad4 leading to reduction in its quantity, without substantially affecting the production and recruitment of TRIM33 by Smad3. This applies to resting Jurkat T cells and THP-1 cells, where the effects of TGF- β on VISTA expression were opposing. MCF-7 upregulate the amounts and usage of both co-activators, while VISTA expression was not induced in these cells. HaCaT cells, which respond to exposure to TGF- β by upregulation of VISTA expression, showed increased Smad3-Smad4 interaction activity and decreased TRIM33 recruitment induced by TGF- β (**Figure 3**).

These results suggest that the differential activities of Smad4 and TRIM33 are unlikely to contribute to achieving responses with TGF- β -induced changes in VISTA expression in various

cell types. Importantly, VISTA expression is most likely to be activated by Smad3 in partnership with Smad4. TRIM33 is involved in Smad3-dependent de-repression of target genes (21). As shown in the **Figure 1G**, in MCF-7 cells, when VISTA gene VSIR is most likely repressed, TGF- β failed to induce its expression. The same is most likely to apply to galectin-9, where the TGF- β -Smad3 pathway was able to upregulate even very low expression levels of this protein (3).

Importantly, the receptors recognizing TGF- β could be internalized by the cell when complexed to its ligand (22–24). Furthermore, the amount of active TGF- β receptor (TGFBR) molecules on the cell surface could be increased in the presence of the ligand. This phenomenon was reported for several types of receptors including TGFBRs (22–24) and Toll-like receptors (TLRs) (25).

Thus, one could hypothesize that in cells where VISTA is upregulated, the respective number of active TGFBR molecules on the cell surface at each time point may either increase upon stimulation with TGF- β or remain unchanged. Conversely, in cells where VISTA is downregulated, the number of appropriate TGFBR molecules may be reduced. As such, the number of VISTA molecules produced will decrease. This proposed regulatory pathway is depicted in **Figure 4A**. However, TGF- β -induced Smad3 activation which took place regardless its effect on VISTA expression, which suggests that the strategy described above is unlikely to be involved.

On the other hand, one cannot rule out the involvement of repressing transcription factors like ATF1, which is known to

participate in TGF- β -induced Smad3-dependent downregulation of granzyme B expression (19). Specifically to ATF1, unlike the granzyme B gene promoter region, the promoter region of VSIR (a gene which encodes VISTA) does not have ATF1 response elements [CREB/ATF response elements ACGTAA or ACGTCC (19)]. If the cells express ATF1, and granzyme B, TGF- β will downregulate expression of this enzyme, however, with VISTA the effect is differential. This mechanism is shown in the **Figure 4B**.

In our view, the most likely molecular mechanism underlying the observed cell function-dependent differential impact of TGF- β on VISTA expression is associated with nuclear compartmentalisation (chromatin re-organization). This phenomenon has recently been investigated and thoroughly discussed as a fundamental molecular mechanism underlying regulation of gene expression (26). Importantly, this kind of regulation approach was reported for T cell development (26, 27). The loci containing genes, the expression of which needs to be downregulated or repressed can be re-located to the periphery of the nucleus, while active genes are normally biased toward the nuclear interior (26). As such, in the cells, which would benefit from downregulation of VISTA expression in response to the presence of TGF- β , respective loci may be re-localized accordingly, while other TGF- β -Smad3 inducible genes [like LGALS9 encoding galectin-9, which is upregulated by TGF- β in THP-1 cells (3) while VISTA is downregulated] can remain active. This kind of re-location to the periphery and possible association with nuclear lamina is sufficient to downregulate expression of respective genes (26). This regulatory strategy is presented in the **Figure 4C**.

The ability of T cell subsets that do not express granzyme B protein to respond to TGF- β by increasing VISTA expression may be the crucial biochemical mechanism used by granzyme B-negative T cell lymphoma/leukemia cells. Apoptotic T cells, which are always present in such cases, release TGF- β (15, 28). TGF- β could then induce VISTA expression which suppresses cytotoxic T lymphocytes trying to attack malignant T cells.

Taken together, our results have uncovered the biochemical phenomenon of differential control of VISTA expression in human T cells and various types of rapidly proliferating cells, including several types of cancer cells, fetal cells and keratinocytes. These results indicate the involvement of a complex molecular mechanism controlling expression of the critical immune checkpoint protein known as VISTA. Activation of this regulatory pathway could lead to differential outcomes which are most likely determined by the specific cell functions and type of interaction with immune and target cells.

REFERENCES

1. Buckle I, Guillerey C. Inhibitory Receptors and Immune Checkpoints Regulating Natural Killer Cell Responses to Cancer. *Cancers*. (2021) 13:4263. doi: 10.3390/cancers13174263
2. Yoo MJ, Long B, Brady WJ, Holian A, Sudhir A, Gottlieb M. Immune checkpoint inhibitors: An emergency medicine focused review. *Am J Emerg Med*. (2021) 50:335–44. doi: 10.1016/j.ajem.2021.08.038

DATA AVAILABILITY STATEMENT

The original contributions presented in the study are included in the article/**Supplementary Material**, further inquiries can be directed to the corresponding author/s.

ETHICS STATEMENT

The studies involving human participants were reviewed and approved by Research Ethics Committee (REC). Primary human AML mononuclear blasts (AML-PB001F, newly diagnosed/untreated) obtained from AllCells (Alameda, CA, USA) were used following ethical approval (REC reference: 16-SS-033). Primary human T cell work received ethical approval from the Medizinische Ethikkommission der Carl von Ossietzky Universität Oldenburg. Placental tissues and amniotic fluids were collected after obtaining informed written consent from pregnant women at the University Hospital Bern, Inselspital following ethical approval. The patients/participants provided their written informed consent to participate in this study.

AUTHOR CONTRIBUTIONS

SS performed majority of the experiments together with IY. EF-K, SR, MP, and JK contributed to performing the experiments on cytotoxic T cells. NM and BG performed isolation and experiments on primary human T cells. NA, EF-K, and SB completed the work with primary embryonic cells. VS designed the study and planned all the experiments together with EF-K and BG and analyzed the data. VS, EF-K, and BG wrote the manuscript. All authors contributed to the article and approved the submitted version.

ACKNOWLEDGMENTS

This work was partly supported by the Swiss Batzebär grant (to EF-K and SB). Also, this project was partly supported by Intramural Funding from the School of Medicine and Health Sciences, University of Oldenburg (FP 2017-013).

SUPPLEMENTARY MATERIAL

The Supplementary Material for this article can be found online at: <https://www.frontiersin.org/articles/10.3389/fmed.2022.790995/full#supplementary-material>

3. Selno ATH, Schlichtner S, Yasinska IM, Sakhnevych SS, Fiedler W, Wellbrock J, et al. Transforming growth factor beta type 1 (TGF-beta) and hypoxia-inducible factor 1 (HIF-1) transcription complex as master regulators of the immunosuppressive protein galectin-9 expression in human cancer and embryonic cells. *Aging*. (2020) 12:23478–96. doi: 10.18632/aging.202343
4. Yasinska IM, Goncalves Silva I, Sakhnevych S, Gibbs BF, Raap U, Fasler-Kan E, et al. Biochemical mechanisms implemented by human acute myeloid leukemia cells to suppress host immune surveillance. *Cell Mol Immunol*. (2018) 15:989–91. doi: 10.1038/s41423-018-0047-6

5. Lines JL, Pantazi E, Mak J, Sempere LF, Wang L, O'Connell S, et al. VISTA is an immune checkpoint molecule for human T cells. *Cancer Res.* (2014) 74:1924–32. doi: 10.1158/0008-5472.CAN-13-1504
6. Wang L, Rubinstein R, Lines JL, Wasiuk A, Ahonen C, Guo Y, et al. VISTA, a novel mouse Ig superfamily ligand that negatively regulates T cell responses. *J Exp Med.* (2011) 208:577–92. doi: 10.1084/jem.20100619
7. Lines JL, Sempere LF, Broughton T, Wang L, Noelle R. VISTA is a novel broad-spectrum negative checkpoint regulator for cancer immunotherapy. *Cancer Immunol Res.* (2014) 2:510–7. doi: 10.1158/2326-6066.CIR-14-0072
8. Xie X, Chen C, Chen W, Jiang J, Wang L, Li T, et al. Structural basis of VSIG3: the ligand for VISTA. *Front Immunol.* (2021) 12:625808. doi: 10.3389/fimmu.2021.625808
9. Yasinska IM, Meyer NH, Schlichtner S, Hussain R, Siligardi G, Casely-Hayford M, et al. Ligand-receptor interactions of galectin-9 and VISTA suppress human T lymphocyte cytotoxic activity. *Front Immunol.* (2020) 11:580557. doi: 10.3389/fimmu.2020.580557
10. Nagae M, Nishi N, Nakamura-Tsuruta S, Hirabayashi J, Wakatsuki S, Kato R. Structural analysis of the human galectin-9 N-terminal carbohydrate recognition domain reveals unexpected properties that differ from the mouse orthologue. *J Mol Biol.* (2008) 375:119–35. doi: 10.1016/j.jmb.2007.09.060
11. Im E, Sim DY, Lee HJ, Park JE, Park WY, Ko S, et al. Immune functions as a ligand or a receptor, cancer prognosis potential, clinical implication of VISTA in cancer immunotherapy. In: *Seminars in cancer biology.* (2021). doi: 10.1016/j.semcancer.2021.08.008
12. Popp FC, Capino I, Bartels J, Damanakis A, Li J, Datta RR, et al. Expression of immune checkpoint regulators IDO, VISTA, LAG3, and TIM3 in resected pancreatic ductal adenocarcinoma. *Cancers.* (2021) 13:2689. doi: 10.3390/cancers13112689
13. Prokhorov A, Gibbs BF, Bardelli M, Ruegg L, Fasler-Kan E, Varani L, et al. The immune receptor Tim-3 mediates activation of PI3 kinase/mTOR and HIF-1 pathways in human myeloid leukaemia cells. *Int J Biochem Cell Biol.* (2015) 59:11–20. doi: 10.1016/j.biocel.2014.11.017
14. Stock C, Ambros IM, Lion T, Zoubek A, Amann G, Gardner H, Ambros PF. Cancer Genetic changes of two Wilms tumors with anaplasia and a review of the literature suggesting a marker profile for therapy resistance. *Genet Cytogenet.* (2002) 135:128–38. doi: 10.1016/S0165-4608(01)00647-1
15. Yasinska IM, Sakhnevych SS, Pavlova L, Teo Hansen Selno A, Teuscher Abeleira AM, Benlaouer O, et al. The tim-3-galectin-9 pathway and its regulatory mechanisms in human breast cancer. *Front Immunol.* (2019) 10:1594. doi: 10.3389/fimmu.2019.01594
16. Schlichtner S, Meyer NH, Yasinska IM, Aliu N, Berger SM, Gibbs BF, et al. Functional role of galectin-9 in directing human innate immune reactions to Gram-negative bacteria and T cell apoptosis. *Int Immunopharmacol.* (2021) 100:108155. doi: 10.1016/j.intimp.2021.108155
17. Goncalves Silva I, Gibbs BF, Bardelli M, Varani L, Sumbayev VV. Differential expression and biochemical activity of the immune receptor Tim-3 in healthy and malignant human myeloid cells. *Oncotarget.* (2015) 6:33823–33. doi: 10.18632/oncotarget.5257
18. Deng J, Li J, Sarde A, Lines JL, Lee YC, Qian DC, et al. Hypoxia-induced VISTA promotes the suppressive function of myeloid-derived suppressor cells in the tumor microenvironment cancer. *Immunol Res.* (2019) 7:1079–90. doi: 10.1158/2326-6066.CIR-18-0507
19. Thomas DA, Massague J. TGF-beta directly targets cytotoxic T cell functions during tumor evasion of immune surveillance. *Cancer Cell.* (2005) 8:369–80. doi: 10.1016/j.ccr.2005.10.012
20. Teo Hansen Selno A, Schlichtner S, Yasinska IM, Sakhnevych SS, Fiedler W, Wellbrock J, et al. High mobility group box 1 (HMGB1) induces toll-like receptor 4-mediated production of the immunosuppressive protein galectin-9 in human cancer cells. *Front Immunol.* (2021) 12:675731. doi: 10.3389/fimmu.2021.675731
21. Massague J, Xi Q. TGF-beta control of stem cell differentiation genes. *FEBS Lett.* (2012) 586:1953–8. doi: 10.1016/j.febslet.2012.03.023
22. Guglielmo GMDi, Le Roy C, Goodfellow AF, Wrana JL. Distinct endocytic pathways regulate TGF-beta receptor signalling and turnover. *Nature Cell Biology.* (2003) 5:410–21. doi: 10.1038/ncb975
23. Mitchell H, Choudhury A, Pagano RE, Leaf EB. Ligand-dependent and -independent transforming growth factor-beta receptor recycling regulated by clathrin-mediated endocytosis and Rab11. *Molec Biol Cell.* (2004) 15:4166–78. doi: 10.1091/mbc.e04-03-0245
24. Miller DS, Bloxham RD, Jiang M, Gori I, Saunders RE, Das D, et al. The dynamics of TGF-beta signaling are dictated by receptor trafficking via the ESCRT machinery. *Cell Reports.* (2018) 25:1841–55.e5. doi: 10.1016/j.celrep.2018.10.056
25. Barton GM, Kagan JC. A cell biological view of Toll-like receptor function: regulation through compartmentalization. *Nat Rev Immunol.* (2009) 9:535–42. doi: 10.1038/nri2587
26. Meldi L, Brickner JH. Compartmentalization of the nucleus. *Trends Cell Biol.* (2011) 21:701–8. doi: 10.1016/j.tcb.2011.08.001
27. Spilianakis CG, Flavell RA. Long-range intrachromosomal interactions in the T helper type 2 cytokine locus. *Nat Immunol.* (2004) 5:1017–27. doi: 10.1038/ni1115
28. Chen W, Frank ME, Jin W, Wahl SM. TGF-beta released by apoptotic T cells contributes to an immunosuppressive milieu. *Immunity.* (2001) 14:715–25. doi: 10.1016/S1074-7613(01)00147-9

Conflict of Interest: The authors declare that the research was conducted in the absence of any commercial or financial relationships that could be construed as a potential conflict of interest.

Publisher's Note: All claims expressed in this article are solely those of the authors and do not necessarily represent those of their affiliated organizations, or those of the publisher, the editors and the reviewers. Any product that may be evaluated in this article, or claim that may be made by its manufacturer, is not guaranteed or endorsed by the publisher.

Copyright © 2022 Schlichtner, Yasinska, Ruggiero, Berger, Aliu, Prunk, Kos, Meyer, Gibbs, Fasler-Kan and Sumbayev. This is an open-access article distributed under the terms of the Creative Commons Attribution License (CC BY). The use, distribution or reproduction in other forums is permitted, provided the original author(s) and the copyright owner(s) are credited and that the original publication in this journal is cited, in accordance with accepted academic practice. No use, distribution or reproduction is permitted which does not comply with these terms.



Macrophage Differentiation and Polarization Regulate the Release of the Immune Checkpoint Protein V-Domain Ig Suppressor of T Cell Activation

Gaetan Aime Noubissi Nzeteu^{1,2}, Stephanie Schlichtner³, Sulamith David², Aylin Ruppenstein², Elizaveta Fasler-Kan^{4,5}, Ulrike Raap^{2,6}, Vadim V. Sumbayev³, Bernhard F. Gibbs² and N. Helge Meyer^{1,2*}

OPEN ACCESS

Edited by:

Antonio Riva,
Foundation for Liver Research,
United Kingdom

Reviewed by:

Reginald Gorczynski,
University of Toronto, Canada
Yunfeng Feng,
Qinghai University Medical College,
China

*Correspondence:

N. Helge Meyer
helge.meyer@uni-oldenburg.de

Specialty section:

This article was submitted to
Immunological Tolerance
and Regulation,
a section of the journal
Frontiers in Immunology

Received: 16 December 2021

Accepted: 12 April 2022

Published: 11 May 2022

Citation:

Noubissi Nzeteu GA, Schlichtner S,
David S, Ruppenstein A, Fasler-Kan E,
Raap U, Sumbayev V, Gibbs BF and
Meyer NH (2022) Macrophage
Differentiation and Polarization
Regulate the Release of the Immune
Checkpoint Protein V-Domain Ig
Suppressor of T Cell Activation.
Front. Immunol. 13:837097.
doi: 10.3389/fimmu.2022.837097

¹ Division of General and Visceral Surgery, Department of Human Medicine, University of Oldenburg, Oldenburg, Germany, ² Division of Experimental Allergy and Immunodermatology, Department of Human Medicine, University of Oldenburg, Oldenburg, Germany, ³ Medway School of Pharmacy, Universities of Kent and Greenwich, Chatham Maritime, United Kingdom, ⁴ Department of Pediatric Surgery, Children's Hospital, Inselspital Bern, University of Bern, Bern, Switzerland, ⁵ Department of Biomedicine, University of Basel and University Hospital Basel, Basel, Switzerland, ⁶ University Clinic of Dermatology and Allergy, University of Oldenburg, Klinikum Oldenburg AöR, Oldenburg, Germany

Recently, the V-domain immunoglobulin suppressor of T-cell activation (VISTA) was identified as a negative immune checkpoint regulator (NCR) that is mainly expressed in hematopoietic cells. Preclinical studies have shown that VISTA blockade results in impeded tumor growth and improved survival. Nevertheless, little is known about the physiological role of VISTA expression in macrophages. This study focused on the differential expression of VISTA in human monocytes and macrophages in order to elucidate a putative role of VISTA regulation upon macrophage polarization and activation. We observed that human peripheral monocytes constitutively release soluble VISTA, which was regulated *via* matrix metalloproteinases. However, monocyte stimulation with cytokines that induce macrophage differentiation, such as granulocyte-macrophage colony-stimulating (GM-CSF) and macrophage colony-stimulating factor (M-CSF), substantially reduced soluble VISTA release. VISTA release was further affected by various pro- and anti-inflammatory stimuli that led to macrophage polarization, where activated M1 macrophages generally released more VISTA than M2 macrophages. Additionally, we observed that stimulation of activated macrophages with the toll-like receptor 4 ligand lipopolysaccharide (LPS) led to a further decrease of soluble VISTA release. Moreover, we found that soluble VISTA impairs T cell cytotoxic activity but did not induce their programmed death. Our results suggest that VISTA is constantly produced and released in the peripheral blood where it may contribute to peripheral tolerance.

Keywords: VISTA, immune checkpoint regulators, macrophage polarization, soluble immune checkpoint proteins, toll-like-receptor 4, antigen-presenting cells, T cell regulation

INTRODUCTION

Macrophages play a crucial role in innate immune responses, inflammation and in antigen presentation. These cells are, however, highly heterogeneous, particularly regarding expression of surface receptors and release of pro-inflammatory and other regulatory cytokines. *In vitro*, two distinct macrophage phenotypes with differential transcriptomic profiles and functions have been intensively described. The first type, M1 macrophages, also called classically activated macrophages, are pro-inflammatory and produce cytokines such as interleukin-1 β (IL-1 β), IL-6, IL-12, IL-23, and tumor necrosis factor alpha (TNF- α). Conversely, the second type, namely M2 macrophages or alternatively activated macrophages, primarily release anti-inflammatory cytokines like IL-10 and the multifunctional transforming growth factor beta type 1 (TGF- β) (1). However, plasticity is a hallmark of macrophage differentiation and *in vivo* a plethora of different macrophage subtypes have been identified. Macrophage activation is favored by the presence of cytokines, where M1 macrophages are activated in the presence of IFN- γ -LPS or TNF- α , while M2 macrophages are activated by either IL-4 for the M2a macrophage subtype, Toll-like receptor (TLR) stimulation in the presence of immune complexes for M2b macrophages, IL-10 for M2c macrophages, or IL-6 for M2d macrophages. Each subtype of M2 macrophages is responsible for specific types of immunogenic function. The M2a phenotype has been mainly associated with tissue remodeling and wound healing. M2b macrophages are immunoregulative and are implicated in a Th2 response. M2c macrophages are immunosuppressive and also involved in tissue remodeling. Various tumors are often infiltrated with M2d macrophages, also called tumor-associated macrophages, that stimulate angiogenesis, tumor growth and metastasis. However, due to their high plasticity regulation of macrophage polarization is much more complex *in vivo* and different macrophage subtypes cannot always be functionally segregated. For example, both M2a and M2b macrophages might have critical roles in allergies and parasitic responses, whereas M2c are also implicated in tumor progression (2, 3). Additionally, mixed phenotypes can occur.

Macrophages, and to a lesser extent monocytes, can serve as antigen-presenting cells (APCs) and present peptide antigens to T cells *via* the major histocompatibility complex (MHC) class II. While antigen binding to the T cell receptor is the basis for a specific immune response, a second signal, which is not antigen-specific, is necessary for full activation of naive T cells. The best characterized co-stimulatory signal is the interaction of cluster of differentiation (CD) 28 on T cells with its ligands B7-1 (CD80) and B7-2 (CD86) on APCs. This second signal promotes clonal expansion, cytokine secretion, and effector function. Absence of this signal, however, facilitates T cell inactivation and induces peripheral tolerance against the respective antigen. In addition, negative signaling can directly counteract the co-stimulatory effects of CD28, thus providing negative checkpoints of T-cell activation.

Cytotoxic T lymphocyte-associated protein (CTLA-4) and Programmed Death-1 (PD-1), which both belong to the CD28/CTLA-4 subfamily of the immunoglobulin (Ig) superfamily, are

key regulatory inhibitors of T cell responses. Consequently, polymorphisms of PD-1 and CTLA-4 are implicated in various autoimmune diseases (4–6). In contrast, blockade of CTLA-4 and PD-1 improves the capacity of immune cells to clear tumor cells (7). Indeed, nivolumab and ipilimumab, which respectively target PD-1 and CTLA-4, have been reported to result in improvement in cancer therapies including melanoma (8).

Besides the prototypic NCRs, CTLA-4 and PD-1, many NCRs of the B7-family and their respective ligands suppress T-cell activity and proliferation. One of these is the V domain-containing immunoglobulin suppressor of T-cell activation (VISTA), also called Differentiation of Embryonic Stem Cells 1 (Dies1), Gi24 and PD-1 homolog (PD-1H). VISTA is a 52000 to 65000 molecular weight type I immunoglobulin membrane protein with an extracellular domain which is homologous to PD-L1 (9, 10). This protein is highly expressed on hematopoietic cells of the myeloid lineage (e.g. monocytes and macrophages). In the mouse kidney it has been shown that resident macrophages (R1) expressed constitutively high levels of VISTA, evenly in homeostatic conditions, whereas infiltrating macrophages (R2) expressed very low levels of VISTA. Furthermore, VISTA may play a major role in the repair process of ischemic injury in the kidney since VISTA dysfunction was reported to impair macrophage cytokine and chemokine production (11, 12).

A soluble form of PD-L1 has been demonstrated to be of significant importance in tumor immunotherapies (13). Moreover, degradation of cell surface protein and molecules of the extracellular matrix (ECM) is essential for different processes such as hemostasis and cell signaling. These degradations are mainly due to the actions of Matrix Metalloproteinase (MMPs). MMP-8 has been identified to play a key role in macrophage differentiation (14), whereas membrane type 1 MMP, along with VISTA, plays a role in tumor growth (15). Recently, we have shown that primary human AML cells secrete high amounts of VISTA compared to healthy mononuclear leukocytes (16). Despite many studies describing a pathological function of VISTA on APCs, little is known regarding its physiological role on resting *versus* activated macrophages, particularly also regarding soluble VISTA that can be released by proteolytic cleavage. Thus, our aim was to analyze the differential expression of VISTA in human monocytes and monocyte-derived M1 and M2 macrophages in order to elucidate the physiological role of VISTA in macrophage polarization. Furthermore, we analyzed VISTA expressions upon TLR4-mediated stimulation of M1 and M2 macrophages. Finally, we elucidated a mechanism by which soluble VISTA impairs cytotoxic activity of human T cells.

MATERIAL AND METHODS

Isolation and Cultivation of Human Monocyte-Derived Macrophages

Human PBMCs were isolated from buffy coats of healthy donors, provided by DRK Blood donation center in Springe (DRK-

Blutspendedienst Niedersachsen, Germany). Isolation of PBMCs was performed by density gradient centrifugation using Histopaque-1119 (Sigma-Aldrich, Germany) as described previously (17). Monocytes were then purified using a commercial immunomagnetic isolation Kit (Miltenyi Biotec, Germany) and resuspended in RPMI 1640 media containing 25mM HEPES and 2.05mM L-glutamine (Biowest SAS, France), supplemented with 10% fetal bovine serum (FBS) – EU-approved, heat-inactivated (Bio-Techne, USA). Cells were seeded at 1×10^5 monocytes per well using 96 well plates. Cells were then incubated at 37°C with 5% CO₂ and differentiated into monocyte-derived macrophages by the addition of either 50ng/mL granulocyte macrophage-colony stimulating factor (GM-CSF, BioLegend, USA), for M1 macrophages, or 50 ng/mL macrophage-colony stimulating factor (M-CSF, BioLegend, USA), for M2 macrophages, to the culture medium. Half of the initial medium was replaced after 5 days. Macrophages were fully differentiated after 7 days and cell supernatant was replaced with fresh differentiation medium.

Metalloproteinase Inhibition Assay

Monocytes were isolated and polarized as described in 2.1. The culture medium was supplemented with either 50 μ M batimastat or 50 μ M GI254023X. Fully differentiated macrophages were cultivated for another 7 days without further activation. Supernatants of monocytes differentiating into macrophages (MoM1 and MoM2) and polarized macrophages (M1 and M2) were collected for soluble VISTA analysis on days 0,1, 3, 5 and 7.

Activation of Polarized Macrophages

Monocytes were isolated and polarized as described in 2.1. After replacement of medium on day 7 polarized macrophages were maintained in culture until day 10. Macrophages were then activated using 200 ng/ml Interferon-gamma (IFN- γ , BioLegend, USA) and 100 ng/ml lipopolysaccharide (VWR, Germany) for M1 polarization. For M2a and M2c phenotypes, macrophages were activated using 40 ng/ml Interleukin-4 (IL-4, BioLegend, USA) or 10 ng/ml Interleukin-10 (IL-10, BioLegend, USA), respectively. After 2 days of activation, cells were further incubated with or without 500 ng/ml LPS for 24 hours.

Cell Lines

Cell lines used in this work were obtained from American Tissue Culture Collection (ATCC, USA) and were accompanied by identification test certificates.

K562 and Jurkat cells were cultured in RPMI 1640 media supplemented with 10% fetal bovine serum, penicillin (50 IU/ml), and streptomycin sulfate (50 μ g/ml).

TALL-104 CD8-positive cytotoxic T lymphocytes, derived from human acute lymphoblastic leukemia (TALL), were cultured according to ATCC instructions. Briefly, ATCC-formulated Iscove's Modified Dulbecco's Medium was supplemented with 100 units/ml recombinant human IL-2, 2.5 μ g/ml human albumin, 0.5 μ g/ml D-mannitol and fetal bovine serum to a final concentration of 20% to make the complete growth medium (18).

K562/TALL-104 and K562/Jurkat Co-Cultures

K562 cells were placed into Maxisorp 96 well plates and 100 nM PMA were added to activate protein kinase C and improve immobilization of these cell onto the plate surface. After 24 h of incubation, medium was removed and either TALL-104 cells (at a ratio of 1 K562:1 TALL-104) or Jurkat cells (at a ratio of 1 K562:1 Jurkat), present in TALL-104 or Jurkat cell culture medium, were added. Cells were co-cultured for 16 h and then separated from each other. Immobilised K562 cells were cultured in TALL-104 culture medium for 16 h as a control.

Flow Cytometry

For flow cytometric analysis, human monocyte-derived macrophages (M1 and M2) were blocked for 30 min at 4°C with 50% FBS in autoMACS Rinsing Solution supplemented with MACS BSA Stock Solution (Miltenyi, Germany) and incubated with fluorescently labeled antibodies directed against, CD68 (Clone: REA886, Miltenyi Germany), CD80 (Clone: REA661, Miltenyi Germany), CD209 (Clone: REA617, Miltenyi Germany), and monoclonal mouse IgG2B anti-human VISTA (Clone: # 730804, R&D Systems, USA) as well as corresponding isotype control antibodies for 30 min at 4°C. Dead cells were stained with Propidium Iodide Solution (Miltenyi Biotec, Germany). The cell suspension was analyzed using a MACS Quant 16 cytometer (Miltenyi Biotec, Germany). Data were evaluated using Flowlogic 7.3 software (Inivai™ Technologies, USA).

Immunofluorescence Microscopy

For immunofluorescence, macrophages were cultivated on cover slides (VWR, Germany). Cells were washed with PBS (Carl Roth, Germany) and fixed with methanol (VWR, Germany) for 10 min at room temperature (RT). Cover slides were then incubated for 30 min with blocking solution (PBS + 0.1% bovine serum albumin, VWR) at RT. Afterwards, cells were incubated with monoclonal mouse anti-human VISTA (R&D Systems, USA) for 1 h at RT. After washing, cells were stained with secondary goat anti-mouse IgG Alexa Fluor 594 (Thermo Scientific, USA), in the dark at RT. Cover slides were mounted with Fluoromount-G Mounting Medium, with DAPI (Thermo Scientific, USA). Image capture was performed using an Olympus BX63 (Olympus, Japan) fluorescence microscope. Images were processed by Olympus cellSense and ImageJ software.

Cytokine and Soluble VISTA Analysis

0.3-1 ml of culture supernatant was collected during macrophage differentiation every 24 h and VISTA concentrations were quantified by ELISA. Each sample was measured in duplicate. After stimulation of macrophages, supernatants were collected in order to quantify VISTA and TNF- α concentrations by ELISA. VISTA and TNF- α levels were analyzed using a Human VISTA/B7-H5/PD-1H DuoSet ELISA, with a minimum detection of 23.4 pg/ml (R&D Systems, USA) and Human TNF- α ELISA MAX Deluxe Set, with a minimum detection 7.8 pg/ml (BioLegend, USA) according to manufacturer's recommendations. Human IL-2 and TGF- β ELISA kits (R&D Systems, USA) were used according to manufacturer's instructions.

In-Cell Granzyme B Activity Assay and Detection of Cell Viability

In-cell activity of granzyme B (granzyme B catalytic activity in living cells) was analyzed by incubation of cells with 150 μ M Ac-IEPD-AFC (granzyme B substrate) for 1 h at 37°C in sterile PBS as described elsewhere (16). Total cell fluorescence was then measured in living cells using excitation and emission wavelengths recommended in the Ac-IEPD-AFC manufacturer's (Sigma) protocol. Equal numbers of cells were subjected to analysis. The activity was expressed in relative units (RU), where 1 RU is equivalent to 1 pmol of cleaved substrate per 10^6 cells. Cell viability was analyzed using an MTS assay kit obtained from Promega (USA) according to the manufacturer's protocol.

Phosphoinositide-3-Kinase (PI3K) Activity

The activity of PI3K was detected as we previously reported (19). Briefly, cell lysates were first incubated with 30 μ l 0.1 mg/ml substrate (PI-4,5-diphosphate) in kinase assay buffer, which was prepared from 20 mM Tris (pH 7.5), 100 mM NaCl, 0.5 mM EDTA, 8 mM MgCl₂ and 40 μ M ATP in a total volume of 100 μ l at 37°C. Reactions were terminated by the addition of 1 ml hexane/isopropanol (13:7, v:v) and 0.2 ml 2 M KCl/HCl conc (8:0.25, v:v). After vortexing the samples, organic phases were washed with HCl (0.5 ml; 0.1 M). Phosphate groups were then detected using molybdenum reagent containing 2 parts of 25 mM (NH₄)₆Mo₇O₂₄, 5 parts of H₂SO₄ (140 ml of H₂SO₄ conc was diluted to 900 ml with bidistilled water), 2 parts of 0.3 M ascorbic acid and 1 part of 2 mM potassium antimonyl-tartrate. The values obtained in control samples of each experiment per 1 mg protein were normalized to 100% of PI3K activity. Other values were then expressed as percentage of control (19).

Statistical Analysis

All data are depicted as mean \pm standard error of the mean (SEM). Samples were tested for normal gaussian distribution using D'Agostino-Pearson and Shapiro-Wilk normality test. As all data was normally distributed, results were analyzed using a parametric paired t-test (for two groups) and a one-way ANOVA mixed test with Holm-Sidak or Sidak post test for multiple comparisons. All calculations were performed using Prism[®] 9.1.2 software (GraphPad Software Inc.). Statistically significance was defined as p<0.05 *, p<0.01 **, p<0.001 ***, p<0.0001 ****.

RESULTS

VISTA Is Expressed in Monocytes and Its Release Is Mediated by Metalloproteinase Cleavage

After its expression and glycosylation, VISTA protein is transported to the cell surface. Soluble VISTA can then be generated from membrane-bound VISTA *via* proteolytic cleavage by MMPs. (Figure 1A) Thus, we asked whether VISTA release from monocytes is facilitated by the same mechanism. Using flow cytometry, VISTA expression was analyzed on the surface of freshly isolated monocytes (Figure 1B). 50 μ M of

batimastat, a broadband matrix metalloproteinases inhibitor (16), and 50 μ M of GI254023X, an inhibitor of ADAM 10 and matrix metalloproteinase 9 (MMP-9) (20), over a period of 3 days was then used to suppress proteolytic cleavage. We observed that the presence of both metalloproteinase inhibitors strongly impaired the release of soluble VISTA into the culture medium (Figure 1C).

Differentiating Monocytes But Not Fully Differentiated Macrophages Secrete Soluble VISTA

We next asked how differentiation into macrophages affects the release of soluble VISTA into the culture medium. Therefore, we determined VISTA concentrations in the supernatant of differentiating monocytes and macrophages differentiated towards an M1 or M2 phenotype by ELISA. Interestingly, monocytes differentiating into M1 (MoM1) and M2 (MoM2) released substantial amounts of soluble VISTA only in the first 3 days of culture (Figures 2A, B). On days five to seven soluble VISTA levels in the culture medium reached a stable plateau. Fully differentiated macrophages (M1 and M2) released significantly less soluble VISTA in comparison to MoM1 and MoM2. Successful polarization of macrophages was assessed by CD163 surface expression (Supplementary Figure 1).

We validated the expression of VISTA in M1 and M2 macrophages using immunofluorescence microscopy. Intriguingly, we found VISTA protein was also localized intracellularly in both unstimulated M1 and M2 macrophages – most likely in intracellular vesicles (Figure 3).

Effect of Different Pro- and Anti-Inflammatory Stimuli on Macrophages Regarding Surface Expression and Release of VISTA

Macrophages play an important role in the activation and modulation of the immune system. Macrophage activation is therefore crucial for the immune response (2). Thus, we investigated whether pro- and anti-inflammatory stimuli could affect VISTA expression as well as its release from macrophages. To this end, macrophages that had been differentiated towards an M1 or M2 phenotype with GM-CSF or M-CSF, respectively, were further maintained in culture and stimulated with IFN- γ +LPS for activated M1 macrophages, IL-4 for activated M2a and IL-10 for M2c macrophages. Successful activation was assessed by CD80, CD163 and CD209 surface expression. (Supplementary Figure 2) Interestingly, VISTA surface expression was only slightly affected in the different M2 macrophage subtypes compared to stimulated M1 macrophages. Additionally, we stimulated M2 macrophages with IFN- γ +LPS to induce a repolarization into an M1 phenotype. Only IL-10-stimulated macrophages, which clearly represent an anti-inflammatory macrophage phenotype, show significantly elevated VISTA surface expression (Figure 4A). Surprisingly, VISTA release was significantly increased in M1 macrophages compared to M2a (IL-4) and M2c (IL-10) macrophages. (Figure 4B) Pro-inflammatory cytokine, i.e. TNF- α release from IFN- γ +LPS stimulated M2 macrophages (Figures 5A, B) and high

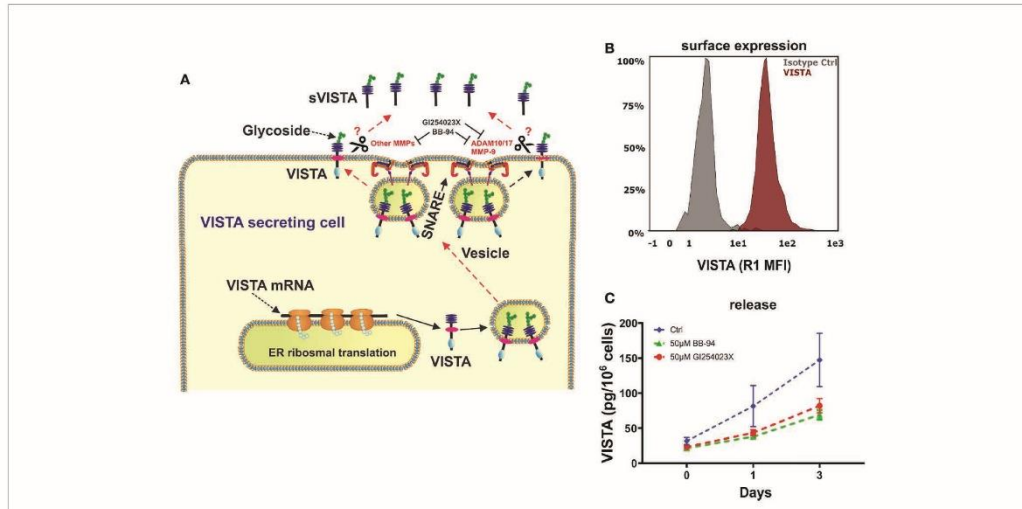


FIGURE 1 | VISTA expression in human monocytes. **(A)** Scheme showing the surface expression of VISTA and proteases involved in shedding and also demonstrating the action of inhibitors. **(B)** Monocytes express VISTA on the Surface (histogram of VISTA expression on monocytes) and **(C)** release soluble VISTA via protease cleavage. VISTA release mediated by cleavage is reduced in the presence of matrix metalloproteinase inhibitors. Data are the mean values \pm SEM (n=6).

surface expression of CD80 (**Supplementary Figure 2**) are indicative of a functional repolarization into an M1 phenotype. At the same time M2(IFN- γ +LPS) macrophages appear to release higher amounts of soluble VISTA compared to M2a(IL-4) and M2c(IL-10) macrophages, rather resembling the activated M1 phenotype (**Figure 4B**).

VISTA Surface Expression and Release of Soluble VISTA After LPS Stimulation of Macrophages

Although cell surface levels of VISTA is only slightly affected by macrophage polarization, M1 macrophages released significantly

more VISTA than M2 macrophages. Thus, we investigated whether further stimulation of macrophages *via* TLR-4 impacted on VISTA production. To this end, we assessed the surface expression of VISTA using flow cytometry and release of soluble VISTA by ELISA from macrophages after stimulation with high concentrations of the TLR4-ligand, LPS. We observed a tendential decrease of cell surface-expressed VISTA by flow cytometry analysis after 24h LPS stimulation (**Figure 5C**). However, only on M2c(IL-10) VISTA surface expression was significantly decreased upon LPS stimulation. Interestingly, VISTA release was reduced in all macrophage phenotypes after LPS stimulation (**Figure 5D**). At the same time soluble TNF- α was upregulated

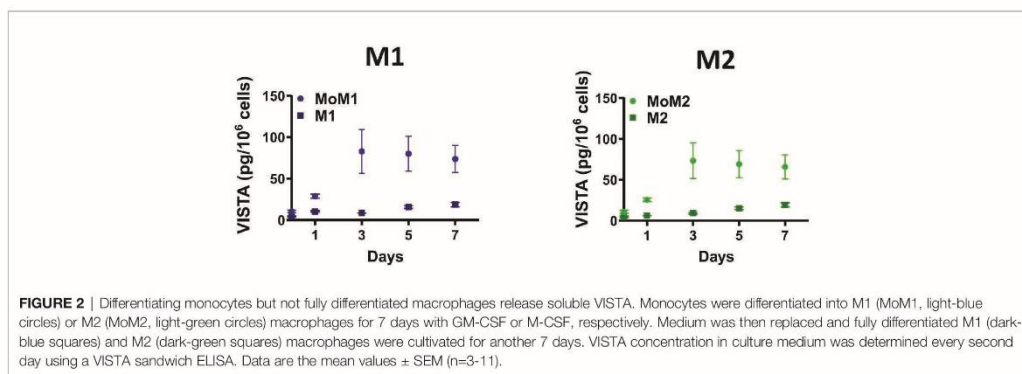


FIGURE 2 | Differentiating monocytes but not fully differentiated macrophages release soluble VISTA. Monocytes were differentiated into M1 (MoM1, light-blue circles) or M2 (MoM2, light-green circles) macrophages for 7 days with GM-CSF or M-CSF, respectively. Medium was then replaced and fully differentiated M1 (dark-blue squares) and M2 (dark-green squares) macrophages were cultivated for another 7 days. VISTA concentration in culture medium was determined every second day using a VISTA sandwich ELISA. Data are the mean values \pm SEM (n=3-11).

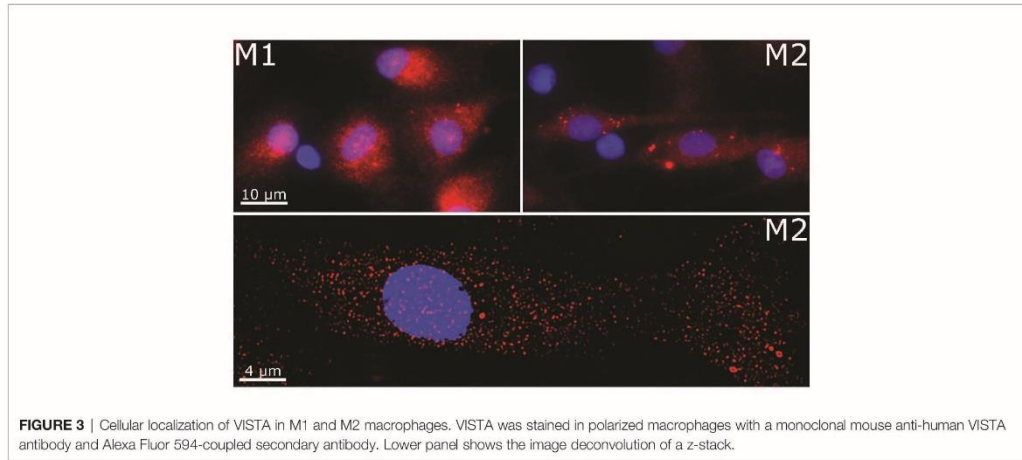


FIGURE 3 | Cellular localization of VISTA in M1 and M2 macrophages. VISTA was stained in polarized macrophages with a monoclonal mouse anti-human VISTA antibody and Alexa Fluor 594-coupled secondary antibody. Lower panel shows the image deconvolution of a z-stack.

following TLR4 ligand stimulation in all phenotypes (**Figure 5B**). Importantly, we investigated whether LPS affects VISTA expression. We have recently shown that transforming growth factor beta type 1 (TGF- β) differentially regulates VISTA expression through the transcription factor Smad3 (21). We tested whether M1 and M2 macrophages produce TGF- β in response to LPS stimulation, as well as measuring VISTA mRNA levels in parallel. (**Figure 5E**) We found that the levels of cell-associated TGF- β were upregulated by LPS in both M1 and M2 macrophages. However, in M1 macrophages, both background and stimulated TGF- β levels were lower compared to those observed in M2, which is most likely related to M2 macrophage function associated with TGF- β production. However, VISTA mRNA levels were significantly upregulated in M1 macrophages after LPS stimulation whilst they were downregulated in M2 macrophages. In both types of macrophages LPS stimulation led to decrease in the release of

soluble VISTA. This suggests that VISTA protein expression and secretion are controlled by differential mechanisms in both type of macrophages. The increased VISTA expression in M1 macrophages may serve as a reservoir of the protein in order to participate in opsonization of LPS-containing Gram-negative bacteria (22). Conversely, the decrease in VISTA expression in M2 macrophages is most likely to be associated with LPS-induced conversion of these cells into an M1 type which would reduce their immunosuppressive potential.

Soluble VISTA Suppresses Activity of Tall-104 and Jurkat T Cells But Does Not Affect Their Viability

We next sought to confirm the cytotoxic T cell suppressive role which soluble VISTA was previously suggested to play. We used

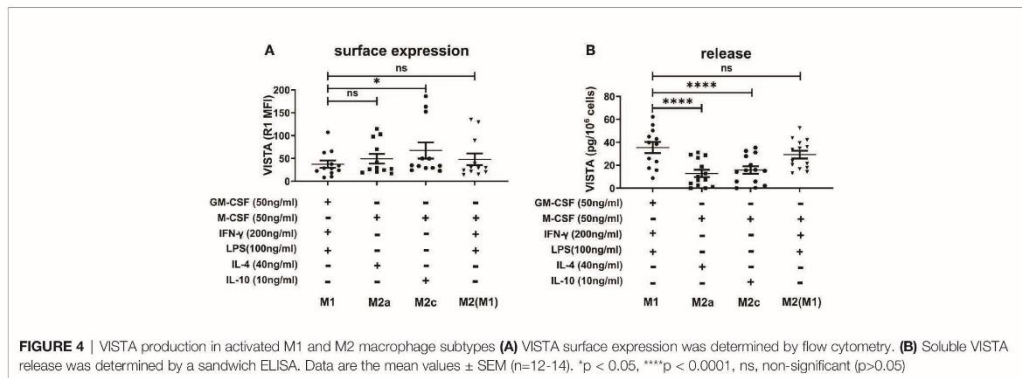
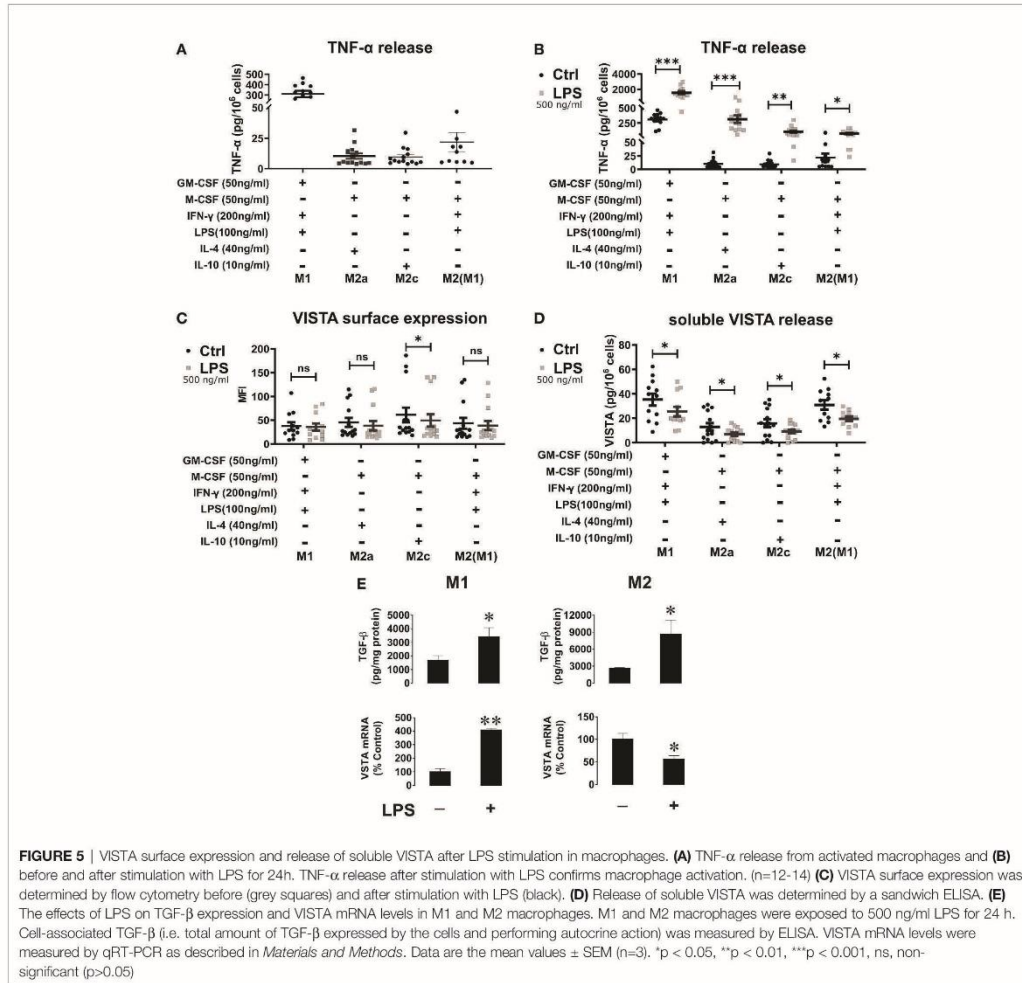


FIGURE 4 | VISTA production in activated M1 and M2 macrophage subtypes **(A)** VISTA surface expression was determined by flow cytometry. **(B)** Soluble VISTA release was determined by a sandwich ELISA. Data are the mean values \pm SEM (n=12-14). *p < 0.05, ****p < 0.0001, ns, non-significant (p>0.05)



TALL-104 CD8-positive cytotoxic T cells and exposed them to 5 μ g/ml (23, 24) VISTA-Fc protein (or an equimolar amount of Fc as a control) for 16 h followed by measurement of in-cell activity of granzyme B in living cells as well as viability of TALL-104 cells. We found that VISTA failed to induce significant upregulation of granzyme B activity in these cells and did not affect their viability (Figures 6A–C), which was in line with our previous observation for PMA-activated (granzyme B expressing) Jurkat T cells. (16)

Next, we wished to elucidate the effect of soluble VISTA on T helper cells. To this end we cultured CD4⁺ Jurkat T cells together with K562 cells, which will stimulate Jurkat cells *via* the T cell receptor. (Figures 6D–H) Alternatively, we stimulated Jurkat T

cells with PMA (Figures 6I–M). In both cases we found that soluble VISTA inhibits the production and the release of IL-2 in Jurkat T cells most likely by downregulating PI3K activity. Finally, in order to assess whether soluble VISTA suppresses the cytotoxic activity of T cells we used K562 chronic myeloid leukemia cells, which express traces of galectin-9 and VISTA but do not release detectable amounts of these proteins. Co-cultures of K562 with TALL-140 cells were performed with or without 5 μ g/ml VISTA-Fc (or an equimolar amount of Fc as control). In-cell activity of granzyme B was measured in both cell types and their viabilities were assessed. We found that VISTA (but not Fc) prevented granzyme B injection into K562 cells, thus preventing their killing

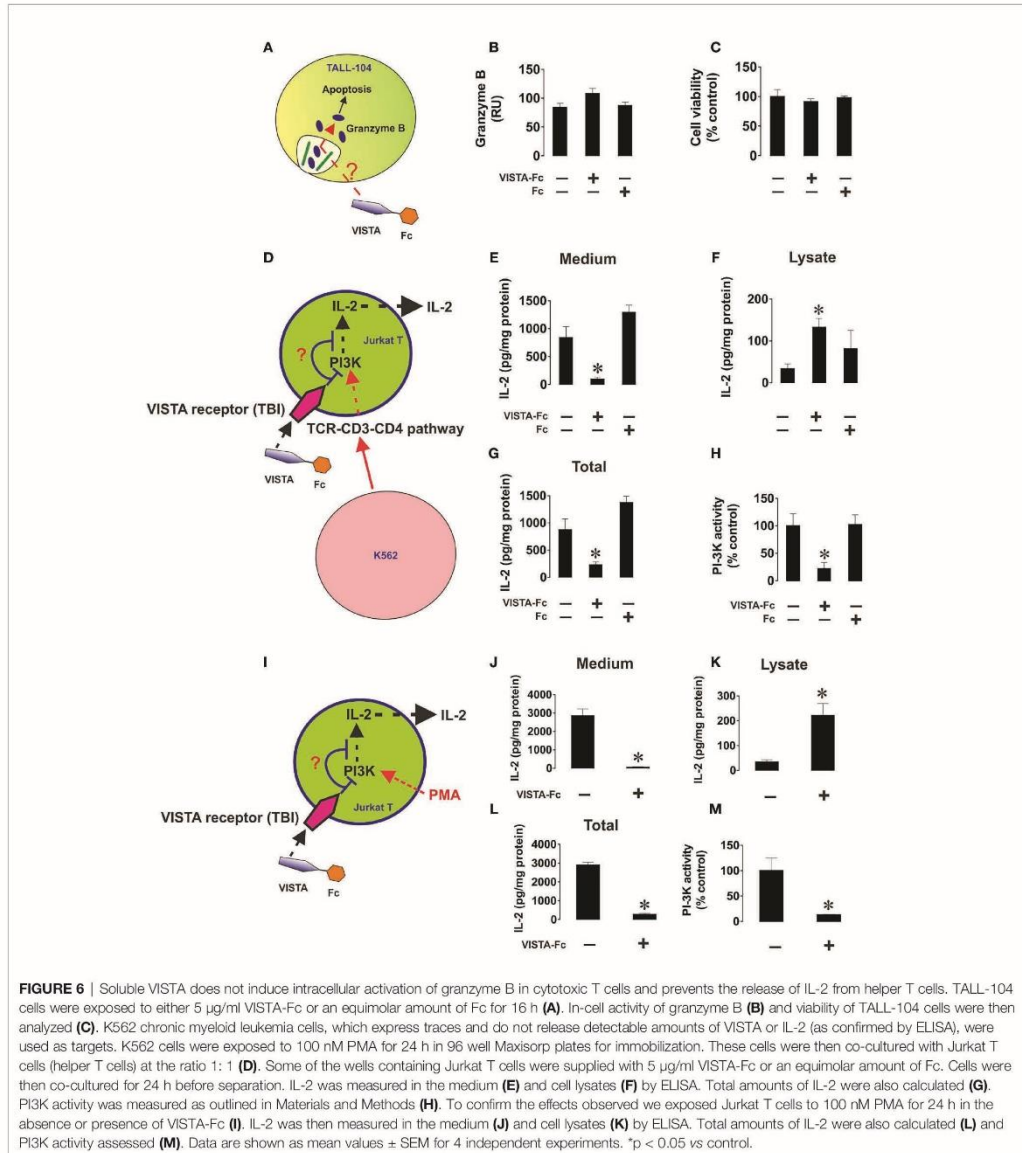
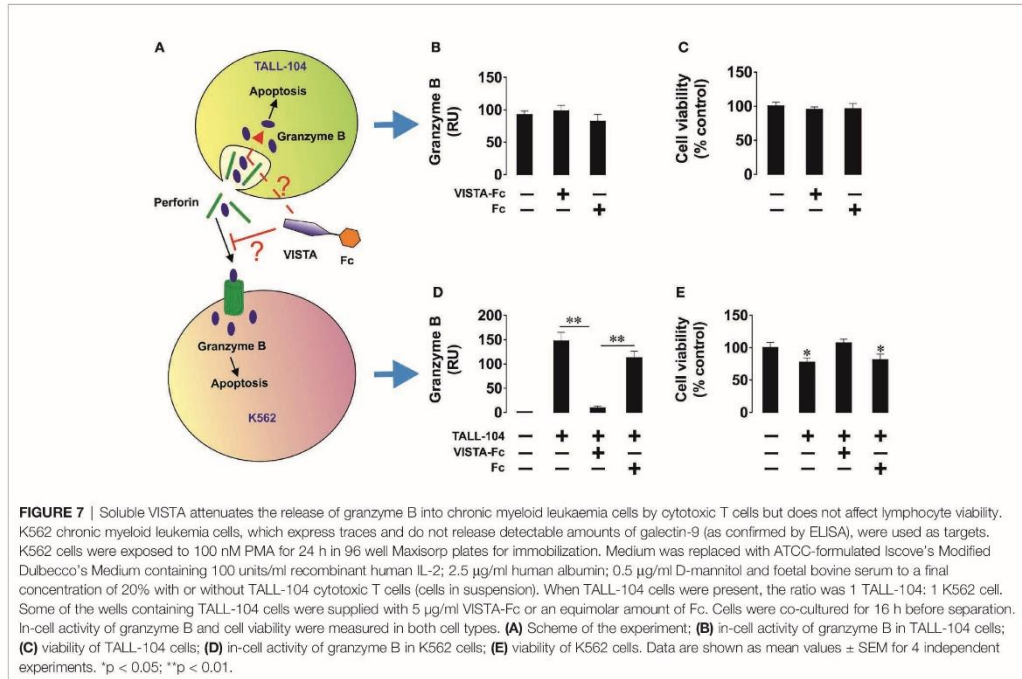


(Figure 7). However, the presence of VISTA did not lead to granzyme B activation inside TALL-104 cells (Figure 7). This suggests that soluble VISTA prevents granzyme B-dependent killing of target cells by cytotoxic T cells but does not lead to programmed death of these T cells.

DISCUSSION

In this study we focused on the expression of VISTA in macrophages during and after polarization as well as activation with various cytokines. (Figure 8A) It has previously been

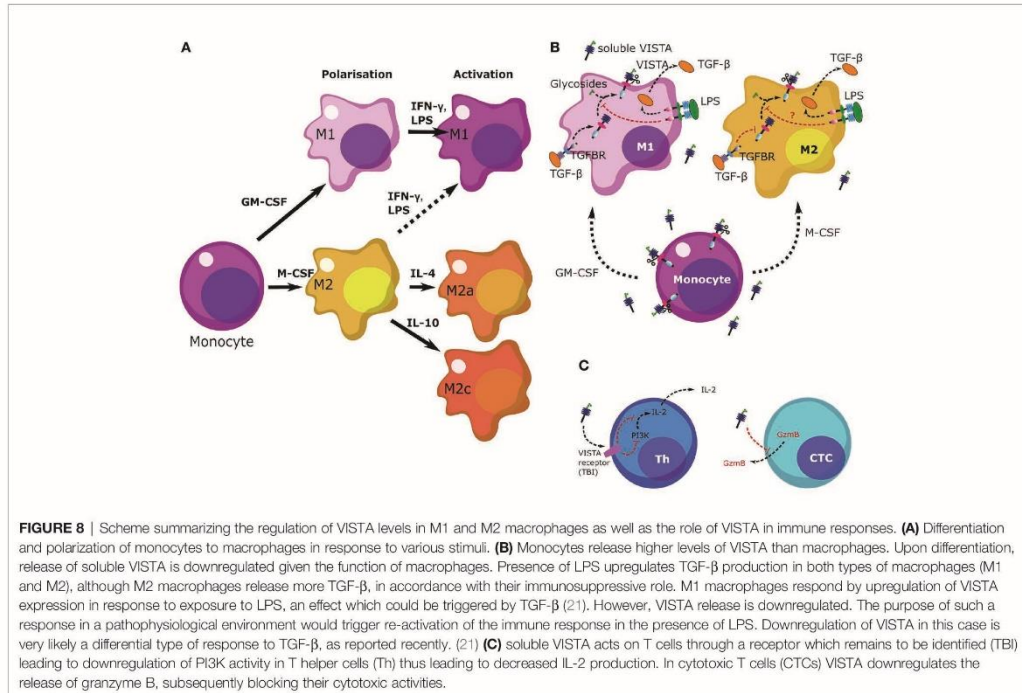


demonstrated that VISTA is expressed as a surface membrane protein on various cell types, including monocytes (9). Here, we demonstrate that VISTA is also released from peripheral blood monocytes and, to a much lower extent, upon differentiating into macrophages. We suggest that soluble VISTA is produced by proteolytic cleavage since protease inhibitors decreased soluble VISTA release from human peripheral monocytes (Figure 1C). This observation is consistent with our previous finding that a truncated form of VISTA is present in the plasma of AML patients and that VISTA cleavage from the surface of THP-1 acute myeloid leukemia (AML) cells is inhibited by the protease inhibitor GI254023X (16). The release of the extracellular domain of the VISTA homolog protein PD-L1 was likewise reported to occur *via* proteolytic cleavage (25). In addition to soluble form, exosomal PD-L1 can contribute to immunosuppression *via* an anti-PD-1 response. (26) A role of exosomal immune checkpoints, including CTLA-4, PD-L1 and Tim-3 is also described in systemic immune suppression and tumor progression. (27) With this regard, it would be interesting to study the potential role of exosomal VISTA in cancer patients. Here, we showed, however, that the protease inhibitors Batimastat and GI254023X largely inhibit the release of VISTA from human monocytes of healthy donors, both to the same extent. Batimastat is an inhibitor of different matrix metalloproteinases, but not ADAM 10, while GI254023X is a specific inhibitor of ADAM 10/17 and matrix metalloproteinase 9

(MMP-9). Further studies are necessary to elucidate whether matrix metalloproteinase mediate direct release of VISTA from human monocytes, i.e. by proteolytic cleavage of its extracellular domain, or indirectly regulate its release, e.g. by modulation of exosomal VISTA.

Interestingly, we found that fully differentiated macrophages showed lower release of soluble VISTA than monocytes (Figure 2). Particularly, fully activated M2a and M2c macrophages show the least amount of VISTA release. We also observed that macrophages stimulated with the Toll-like-receptor 4 ligand LPS generally release less soluble VISTA, while its surface expression is hardly affected. Since VISTA release from monocytes and macrophages by proteolytic cleavage can be differentially regulated by pro- and anti-inflammatory stimuli, this suggests a potential immunomodulatory role for VISTA. We recently reported that soluble VISTA, in association with secreted galectin-9 and Tim-3, plays a role in the opsonization of gram-negative bacteria (22), indicating that VISTA crucially regulates not only adaptive immunity but also innate immune responses.

Thus far, little is known regarding the modulation of immune checkpoints following the activation of macrophage by various inflammatory and anti-inflammatory stimuli. In mice, IL-4 highly promoted the expression of PD-L2 on macrophages (28), whereas PD-L1 surface expressions were increased following stimulation with 500 ng/ml IFN-γ or after *Leishmania* infection (17, 29). In



contrast, we have shown that VISTA surface expression is hardly affected upon the polarization of human macrophages into different phenotypes. Macrophage activation only promoted a slightly higher expression of VISTA in M2 *versus* M1 macrophages (Figure 4A). However, soluble VISTA release was variable in the different activated macrophage subtypes. Activated M1 macrophages generally released more soluble VISTA than the activated M2 macrophages subtypes, albeit moderately, with the exception of M2 stimulated with IFN- γ and LPS (Figure 4B). However, the increased release of TNF- α from these cells indicated a reprogramming into a pro-inflammatory M1 phenotype. In this regard, the intracellular accumulation of VISTA in M1 and M2 macrophages, might represent a dormant reservoir of VISTA protein which can rapidly be expressed on the cell surface and released into the extracellular milieu upon changing stimuli. This is in line with the observation, that VISTA is localized within the endosomal compartment in peritoneal mouse macrophages. (30) This could support the containment of acute inflammation by T-cell inactivation, employing mechanisms similar to other checkpoint molecules e.g. CTLA-4 and PD-1 as well as its ligands PD-L1 and 2. In mice CTLA-4 can be expressed in intracellular compartments and released from the cell surface according to changing conditions (31). Moreover, PD-L1 is expressed in the intracellular

compartment of tumor cells and can be transported to the plasma membrane in certain settings (32). In addition, tumor cell lines and brain tumor cells showed strong constitutive expression of PDL1/2 (33). Storage of VISTA in intracellular vesicles may thus be essential for regulation of VISTA surface expression and release.

VISTA deficiency in macrophages has been previously shown to be associated with a high level of inflammatory chemokine production (11), suggesting a role in innate immune responses. Differential VISTA release from M1 and M2 macrophages indicates that VISTA may be an important immune regulator of inflammatory processes and potentially also in macrophage polarization.

Our findings on human macrophages are supported by recent investigations in mice, where macrophages resident in the CNS produced less VISTA following LPS stimulation (34). This is in contrast to a similar study with PD-L1, whose surface expression increases after LPS stimulation (35). Further studies are necessary to elucidate whether LPS stimulation over longer periods leads to a general decrease in VISTA protein production and a depletion of intracellular VISTA reservoirs in human macrophages.

Previous reports suggested that VISTA, generally downregulates T cell proliferation and cytokine production (23, 24). However, to date the role of soluble VISTA is not fully

understood. It was shown that soluble VISTA-F_C fusion protein can inhibit T-cell proliferation and cytokine production *in vitro*, but in this case, immobilization of VISTA-F_C was necessary (36). In contrast, an engineered pentameric form of the extracellular domain of VISTA was shown to restrain T-cell activation *in vivo* without immobilization, suggesting a possible role of VISTA in the adaptative immune response (37).

Here, we showed that soluble VISTA can play an important role in suppression of the cytotoxic activities of T cells, by suppressing the release of granzyme B from these cells. (Figure 8B) Our recent findings suggested that soluble VISTA could enhance the apoptosis of cytotoxic T cells in conjunction with galectin-9 (16). Here, we confirmed that soluble VISTA on its own (in the absence of galectin-9) prevents release of granzyme B from cytotoxic T cells into target cancer cells. However, this does not lead to a significant activation of these enzyme inside cytotoxic T cells, which would otherwise induce apoptotic death. This highlights an important mechanism which granzyme B negative T cell malignancies - T cells do not normally release high amounts of galectin-9 - might use to evade immune attack by cytotoxic T cells. Since these malignant T cells normally produce VISTA, they could possibly use soluble VISTA, acting on other cytotoxic T cells, to evade immune attack. In addition, we could show that soluble VISTA suppresses the release of IL-2 from CD4+ T cells (Figure 8C).

CONCLUSION

In this study we clearly observed that monocytes constitutively release VISTA. Secretion was markedly reduced upon GM-CSF and M-CSF induced macrophage differentiation and further regulated by macrophage activation. Additionally, we demonstrated that soluble VISTA suppresses T cell activation without inducing apoptosis. Our data support the notion that VISTA plays a role in peripheral tolerance, as has been recently demonstrated by ElTanbouly *et al.* (38). Constant release of soluble VISTA by peripheral blood monocytes into the blood plasma may result in the suppression of resting T cells. However, once monocytes are challenged with a pathogen and differentiate into macrophages, VISTA release may decrease in order to facilitate a more robust immune response. Overall, our study provides further insights into the role of soluble VISTA in innate and adaptive immune responses.

REFERENCES

- Shapouri-Moghaddam A, Mohammadian S, Vazini H, Taghadosi M, Esmaeli SA, Mardani F, et al. Macrophage Plasticity, Polarization, and Function in Health and Disease. *J Cell Physiol* (2018) 233:6425–40. doi: 10.1002/jcp.26429
- Martinez FO, Gordon S. The M1 and M2 Paradigm of Macrophage Activation: Time for Reassessment. *Front Immunol* (2014) 5:1462. doi: 10.3389/fimmu.2014.01462
- Viola A, Munari F, Sanchez-Rodriguez R, Sclaro T, Castegna A. The Metabolic Signature of Macrophage Responses. *Front Immunol* (2019) 10:1462. doi: 10.3389/fimmu.2019.01462
- Zamani MR, Aslani S, Salmaninejad A, Javan MR, Rezaei N. PD-1/PD-L and Autoimmunity: A Growing Relationship. *Cell Immunol* (2016) 310:27–41. doi: 10.1016/j.cellimm.2016.09.009
- Mitsuiki N, Schwab C, Grimbacher B. What did We Learn From CTLA-4 Insufficiency on the Human Immune System? *Immunol Rev* (2019) 287:33–49. doi: 10.1111/imr.12721
- Fathi F, Sadeghi E, Lotfi N, Hafezi H, Ahmadi M, Mozafarpoor S, et al. Effects of the Programmed Cell Death 1 (PDCD1) Polymorphisms in Susceptibility to Systemic Lupus Erythematosus. *Int J Immunogenet* (2020) 47:57–64. doi: 10.1111/iji.12456
- Rosenbaum SR, Knecht M, Mollace M, Zhong Z, Erkes DA, Mccue PA, et al. FOXD3 Regulates VISTA Expression in Melanoma. *Cell Rep* (2020) 30:510–24e516. doi: 10.1016/j.celrep.2019.12.036
- Larkin J, Chiarion-Sileni V, Gonzalez R, Grob JJ, Cowey CL, Lao CD, et al. Combined Nivolumab and Ipilimumab or Monotherapy in Untreated Melanoma. *N Engl J Med* (2015) 373:23–34. doi: 10.1056/NEJMoa1504030

DATA AVAILABILITY STATEMENT

The raw data supporting the conclusions of this article will be made available by the authors, without undue reservation.

ETHICS STATEMENT

Ethical review and approval was not required for the study on human participants in accordance with the local legislation and institutional requirements. The patients/participants provided their written informed consent to participate in this study.

AUTHOR CONTRIBUTIONS

GN, VS, BG and NM conceived the study. GN, SS, E F-K, UR, VS, BG and NM designed experiments. GN, SS, SD, AR, E F-K, VS and NM performed experiments and interpreted the data. GN, VS and NM wrote the manuscript. EF-K, UR, VS, BG and NM revised the manuscript. All authors read and approved the manuscript.

FUNDING

This project was supported by Intramural Funding from the School of Medicine and Health Sciences, University of Oldenburg (FP 2017-013 to UR, BG and NM) and in part by a Swiss Batzebar Grant (to EF-K).

ACKNOWLEDGMENTS

We kindly thank Dr Susanne Mommert, Division of Experimental Immunology and Allergy from the Hanover Medical School, Hanover, for expert advice regarding the culture of macrophages.

SUPPLEMENTARY MATERIAL

The Supplementary Material for this article can be found online at: <https://www.frontiersin.org/articles/10.3389/fimmu.2022.837097/full#supplementary-material>

9. Nowak EC, Lines JL, Varn FS, Deng J, Sarde A, Mabaera R, et al. Immunoregulatory Functions of VISTA. *Immunol Rev* (2017) 276:66–79. doi: 10.1111/immr.12525
10. Villarreal-Espindola F, Yu X, Datar I, Mani N, Sanmamed M, Velcheti V, et al. Spatially Resolved and Quantitative Analysis of VISTA/PD-1H as a Novel Immunotherapy Target in Human Non-Small Cell Lung Cancer. *Clin Cancer Res* (2018) 24:1562–73. doi: 10.1158/1078-0432.CCR-17-2542
11. Broughton TWK, Eltanbouly MA, Schaafsma E, Deng J, Sarde A, Croteau W, et al. Defining the Signature of VISTA on Myeloid Cell Chemokine Responsiveness. *Front Immunol* (2019) 10:2641–53. doi: 10.3389/fimmu.2019.02641
12. Park JG, Lee CR, Kim MG, Kim G, Shin HM, Jeon YH, et al. Kidney Residency of VISTA-Positive Macrophages Accelerates Repair From Ischemic Injury. *Kidney Int* (2019) 97:980–94. doi: 10.1016/j.kint.2019.11.025
13. Tominaga T, Akiyoshi T, Yamamoto N, Taguchi S, Mori S, Nagasaki T, et al. Clinical Significance of Soluble Programmed Cell Death-1 and Soluble Programmed Cell Death-Ligand 1 in Patients With Locally Advanced Rectal Cancer Treated With Neoadjuvant Chemoradiotherapy. *PLoS One* (2019) 14:e0212978. doi: 10.1371/journal.pone.0212978
14. Wen G, Zhang C, Chen Q, Luong Le A, Mustafa A, Ye S, et al. A Novel Role of Matrix Metalloproteinase-8 in Macrophage Differentiation and Polarization. *J Biol Chem* (2015) 290:19158–72. doi: 10.1074/jbc.M114.634022
15. Sakr MA, Takino T, Domoto T, Nakano H, Wong RW, Sasaki M, et al. G124 Enhances Tumor Invasiveness by Regulating Cell Surface Membrane-Type 1 Matrix Metalloproteinase. *Cancer Sci* (2010) 101:2368–74. doi: 10.1111/j.1349-7006.2010.01675.x
16. Yasinska IM, Meyer NH, Schlichtner S, Hussain R, Siligardi G, Casely-Hayford M, et al. Ligand-Receptor Interactions of Galectin-9 and VISTA Suppress Human T Lymphocyte Cytotoxic Activity. *Front Immunol* (2020) 11:580557. doi: 10.3389/fimmu.2020.580557
17. Filippis C, Arens K, Noubissi Nzeteu GA, Reichmann G, Waibler Z, Crauwels P, et al. Nivolumab Enhances *In Vitro* Effector Functions PD-1(+) T-Lymphocytes and Leishmania-Infected Human Myeloid Cells in a Host Cell-Dependent Manner. *Front Immunol* (2017) 8. doi: 10.3389/fimmu.2017.01880
18. Yasinska IM, Sakhnevych SS, Pavlova L, Teo Hansen Selno A, Teuscher Abeleira AM, Benlaouer O, et al. The Tim-3-Galectin-9 Pathway and Its Regulatory Mechanisms in Human Breast Cancer. *Front Immunol* (2019) 10:1594. doi: 10.3389/fimmu.2019.01594
19. Abooli M, Lall GS, Coughlan K, Lall HS, Gibbs BF, Sumbayev VV. Crucial Involvement of Xanthine Oxidase in the Intracellular Signalling Networks Associated With Human Myeloid Cell Function. *Sci Rep* (2014) 4:6307. doi: 10.1038/srep06307
20. Metz VV, Kojro E, Rat D, Postina R. Induction of RAGE Shedding by Activation of G Protein-Coupled Receptors. *PLoS One* (2012) 7:e41823. doi: 10.1371/journal.pone.0041823
21. Schlichtner S, Yasinska IM, Ruggiero S, Berger SM, Aliu N, Prunk M, et al. Expression of the Immune Checkpoint Protein VISTA Is Differentially Regulated by the TGF- β 1 - Smad3 Signaling Pathway in Rapidly Proliferating Human Cells and T Lymphocytes. *Front Med (Lausanne)* (2022) 9:790995. doi: 10.3389/fmed.2022.790995
22. Schlichtner S, Meyer NH, Yasinska IM, Aliu N, Berger SM, Gibbs BF, et al. Functional Role of Galectin-9 in Directing Human Innate Immune Reactions to Gram-Negative Bacteria and T Cell Apoptosis. *Int Immunopharmacol* (2021) 100:108155. doi: 10.1016/j.intimp.2021.108155
23. Wang L, Rubinstein R, Lines JL, Wasiuk A, Ahonen C, Guo Y, et al. VISTA, a Novel Mouse Ig Superfamily Ligand That Negatively Regulates T Cell Responses. *J Exp Med* (2011) 208:577–92. doi: 10.1084/jem.20100619
24. Wang L, Le Mercier I, Putra J, Chen W, Liu J, Schenk AD, et al. Disruption of the Immune-Checkpoint VISTA Gene Imparts a Proinflammatory Phenotype With Predisposition to the Development of Autoimmunity. *Proc Natl Acad Sci USA* (2014) 111:14846–51. doi: 10.1073/pnas.1407447111
25. Khan M, Zhao Z, Arooj S, Fu Y, Liao G. Soluble PD-1: Predictive, Prognostic, and Therapeutic Value for Cancer Immunotherapy. *Front Immunol* (2020) 11:587460. doi: 10.3389/fimmu.2020.587460
26. Chen G, Huang AC, Zhang W, Zhang G, Wu M, Xu W, et al. Exosomal PD-L1 Contributes to Immunosuppression and is Associated With Anti-PD-1 Response. *Nature* (2018) 560:382–6. doi: 10.1038/s41586-018-0392-8
27. Xing C, Li H, Li RJ, Yin L, Zhang HF, Huang ZN, et al. The Roles of Exosomal Immune Checkpoint Proteins in Tumors. *Mil Med Res* (2021) 8:56. doi: 10.1186/s40779-021-00350-3
28. Huber S, Hoffmann R, Muskens F, Voehringer D. Alternatively Activated Macrophages Inhibit T-Cell Proliferation by Stat6-Dependent Expression of PD-L2. *Blood* (2010) 116:3311–20. doi: 10.1182/blood-2010-02-271981
29. Suarez GV, Melucci Ganzarain CDC, Vecchione MB, Trifone CA, Marin Franco JL, Genoula M, et al. PD-1/PD-L1 Pathway Modulates Macrophage Susceptibility to Mycobacterium Tuberculosis Specific CD8(+) T Cell Induced Death. *Sci Rep* (2019) 9:187. doi: 10.1038/s41598-018-36403-2
30. Eltanbouly MA, Croteau W, Noelle RJ, Lines JL. VISTA: A Novel Immunotherapy Target for Normalizing Innate and Adaptive Immunity. *Semin Immunol* (2019) 42:101308. doi: 10.1016/j.smim.2019.101308
31. Alegre ML, Noel PJ, Eisfelder BJ, Chuang E, Clark MR, Reiner SL, et al. Regulation of Surface and Intracellular Expression of CTLA4 on Mouse T Cells. *J Immunol* (1996) 157:4762–70. doi: 10.1046/j.1365-3083.2001.00985.x
32. Zheng B, Yu L, Hu J, Xu H, Wang J, Shi Y, et al. Expression of PD-L1 in Mononuclear Cells, Multinucleated Cells, and Foam Cells in Tenosynovial Giant Cell Tumors. *Int J Clin Exp Pathol* (2019) 12:876–84.
33. Fu Y, Liu CJ, Kobayashi DK, Johanns TM, Bowman-Kirigin JA, Schachtler MO, et al. GATA2 Regulates Constitutive PD-L1 and PD-L2 Expression in Brain Tumors. *Sci Rep* (2020) 10:9027:1–12. doi: 10.1038/s41598-020-65915-z
34. Borggreve M, Grit C, Den Dunnen WFA, Burm SM, Bajramovic JJ, Noelle RJ, et al. VISTA Expression by Microglia Decreases During Inflammation and Is Differentially Regulated in CNS Diseases. *Glia* (2018) 66:2645–58. doi: 10.1002/glia.23517
35. Rodriguez-Garcia M, Porichis F, De Jong OG, Levi K, Diefenbach TJ, Lifson JD, et al. Expression of PD-L1 and PD-L2 on Human Macrophages Is Up-Regulated by HIV-1 and Differentially Modulated by IL-10. *J Leukoc Biol* (2011) 89:507–15. doi: 10.1189/jlb.0610327
36. Lines JL, Pantazi E, Mak J, Sempere LF, Wang L, O'Connell S, et al. VISTA is an Immune Checkpoint Molecule for Human T Cells. *Cancer Res* (2014) 74:1924–32. doi: 10.1158/0008-5472.CAN-13-1504
37. Prodeus A, Abdul-Wahid A, Sparkes A, Fischer NW, Cydzik M, Chiang N, et al. VISTA.COMP - An Engineered Checkpoint Regulator Agonist That Potently Suppresses T Cell-Mediated Immune Responses. *JCI Insight* (2017) 2:94308–9. doi: 10.1172/jci.insight.94308
38. Eltanbouly MA, Zhao Y, Nowak E, Li J, Schaafsma E, Le Mercier I, et al. VISTA is a Checkpoint Regulator for Naive T Cell Quiescence and Peripheral Tolerance. *Science* (2020) 367:264–14. doi: 10.1126/science.aay0524

Conflict of Interest: The authors declare that the research was conducted in the absence of any commercial or financial relationships that could be construed as a potential conflict of interest.

Publisher's Note: All claims expressed in this article are solely those of the authors and do not necessarily represent those of their affiliated organizations, or those of the publisher, the editors and the reviewers. Any product that may be evaluated in this article, or claim that may be made by its manufacturer, is not guaranteed or endorsed by the publisher.

Copyright © 2022 Noubissi Nzeteu, Schlichtner, David, Ruppenstein, Faslser-Kan, Raap, Sumbayev, Gibbs and Meyer. This is an open-access article distributed under the terms of the Creative Commons Attribution License (CC BY). The use, distribution or reproduction in other forums is permitted, provided the original author(s) and the copyright owner(s) are credited and that the original publication in this journal is cited, in accordance with accepted academic practice. No use, distribution or reproduction is permitted which does not comply with these terms.